Annales Academiae Medicae Bialostocensis

http://www.roczniki-amb.com

Volume 49
2004
Suppl. 1

Roczniki Akademii Medycznej w Białymstoku

Proceedings of 40th Symposium
of the Polish Histochemical and Cytochemical Society
16-18 September 2004, BIALYSTOK, POLAND

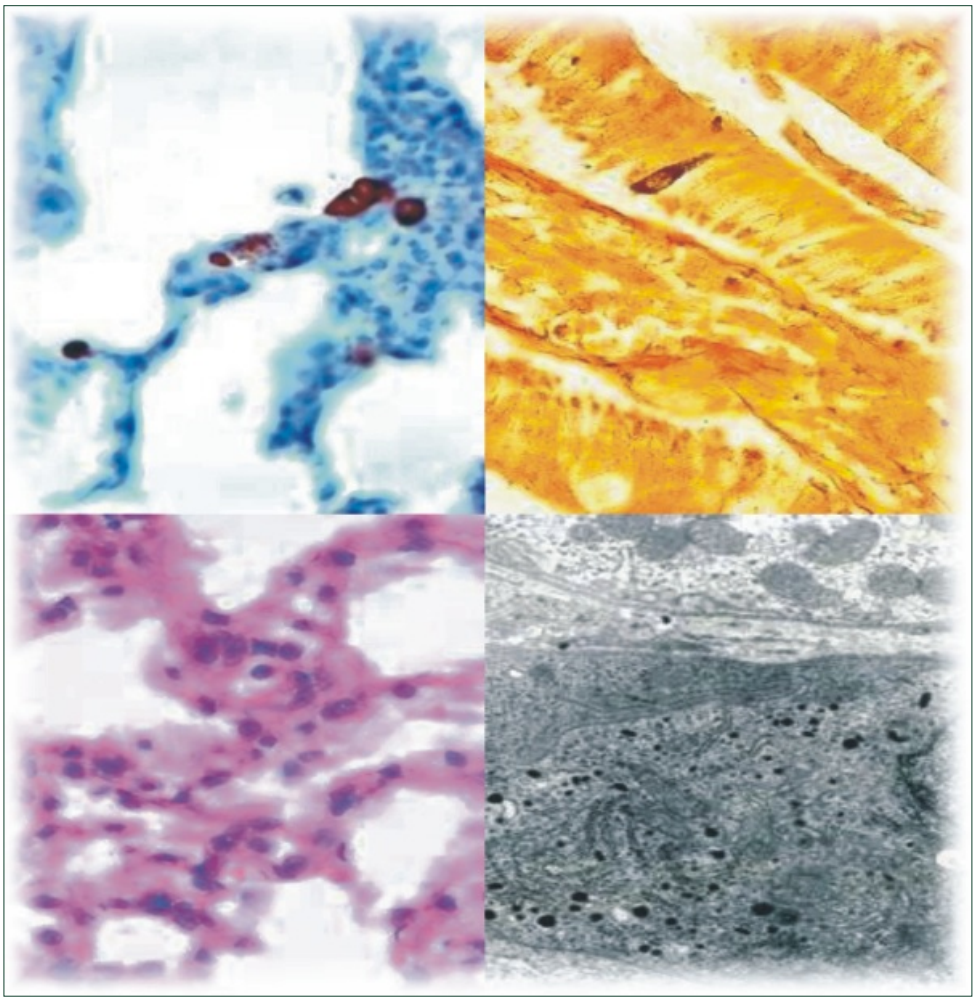

ISSN 0067-6489

Indexed in: Index Medicus/Medline Chemical Abstracts Index Copernicus

Volume 49
2004
Suppl. 1

Roczniki Akademii Medycznej w Białymstoku

Indexed in: Index Medicus/Medline Chemical Abstracts Index Copernicus

Annales Academiae Medicae Bialostocensis
Annual Proceedings of Medical Science

ISSN 0067-6489

Published by: Medical University of Białystok
Kilińskiego 1 Str., 15-089 Białystok, Poland, e-mail: editorial_office@amb.edu.pl

DTP & Print by: ARTICO Artur Rubin, 16-070 Choroszcz, Powstania Styczniowego 18/28 Str., Poland, tel. +48 606 29 66 20, e-mail: a.rubin@wp.pl

Intensity of apoptosis as related to the expression of metallothionein (MT), caspase-3 (cas-3) and Ki-67 antigen and the survival time of patients with primary colorectal adenocarcinomas

Dzięgiel P[1], Dumańska M[1], Forgacz J[2], Wojna A[2], Zabel M[1, 3]

[1]Chair and Department of Histology and Embryology, University School of Medicine in Wrocław; [2]Lower Silesia Centre of Oncology in Wrocław; [3]Chair and Department of Histology and Embryology, University School of Medicine in Poznań, Poland

Abstract

The present study aimed at analysing the intensity of apoptosis, as related to the expression of pro- and anti-apoptotic cellular markers (cas-3, MT, Ki-67 antigen), and at evaluating their expression in relation to the survival time of patients with colorectal adenocarcinoma. Material for the studies was obtained from 40 patients with primary colorectal adenocarcinomas (G2, T3N0M0), treated at the Lower Silesia Centre of Oncology in Wrocław. Tumour samples were fixed in 4% buffered formalin and embedded in paraffin blocks. In obtained paraffin sections, TUNEL reaction (detection of apoptosis) and immunocytochemical reactions were performed (detection of cas-3, MT and Ki-67 antigen expression). The results disclosed a weak correlation between the intensity of apoptosis and the expression of MT, cas-3 and Ki-67 antigen ($r = 0.18$; $r = 0.33$; $r = 0.15$, respectively) in cells of colorectal adenocarcinomas. The survival time of the patients was shorter, when the apoptosis and expression of Ki-67 antigen were highly pronounced. The time periods of the patients' survival showed no correlation with the expression of cas-3 or MT. The obtained results point to the key role of apoptosis and proliferation processes in the clinical course of colorectal adenocarcinomas.

Key words: colorectal adenocarcinoma, metallothionein, apoptosis.

ADDRESS FOR CORRESPONDENCE:
Piotr Dzięgiel
Chair and Department of Histology and Embryology
University School of Medicine
Chałubińskiego 6a; 51-650 Wrocław, Poland
tel. +4871/784-00-81; fax. +4871/784-00-82;
e-mail: piotr@hist.am.wroc.pl

Introduction

The time of survival of patients with neoplastic disease provides the best estimate of aggressiveness, advancement of the disease, as well as of the effectiveness of treatment. Also, in cases of primary colorectal adenocarcinoma, this criterion permits to undertake appropriate therapeutic decisions (chemo- and/or radiotherapy before and/or after surgery) [1]. In colorectal adenocarcinomas, the most important prognostic factors include the morphological traits of the tumours, including its size, histological type, the grade of malignancy G (the extent of cancer cell differentiation, the frequency of mitoses, necrosis) and the depth of infiltration of the intestinal wall [2]. Immunocytochemical indices of tumour growth dynamics include, i.a., proliferation-associated antigens (e.g. Ki-67, PCNA) and, recently, also metallothionein (MT) [3, 4], a low molecular weight (7kDa) protein of a polypeptide chain which consists, depending on the isoform, of 61-68 amino acids [5]. During the recent years, several studies have demonstrated an anti-apoptotic activity of MT, both in normal and in tumour cells [6]. Tumour growth and expansion are known to reflect the proliferative activity and the capacity to eliminate cells by apoptosis and/or necrosis. Therefore, it seemed interesting to examine reciprocal correlations between the intensity of apoptosis and the expression of such pro- and anti-apoptotic cell markers as caspase-3 (cas-3), MT and Ki-67 antigen. The present study aimed at comparing the expression of the above markers and the intensity of apoptosis in cells of primary colorectal adenocarcinomas with the time periods of survival of the affected patients.

Material and Methods

The material for the studies was obtained from 40 patients with primary colorectal adenocarcinoma, treated at the Lower Silesia Centre of Oncology (DCO) in Wrocław between 1993-1994. Clinico-pathological data on the patients, in form of histories of the disease and histopathological diagnoses, were

Figure 1. Apoptosis in cells of primary colorectal carcinoma. x400; background staining with haematoxylin.

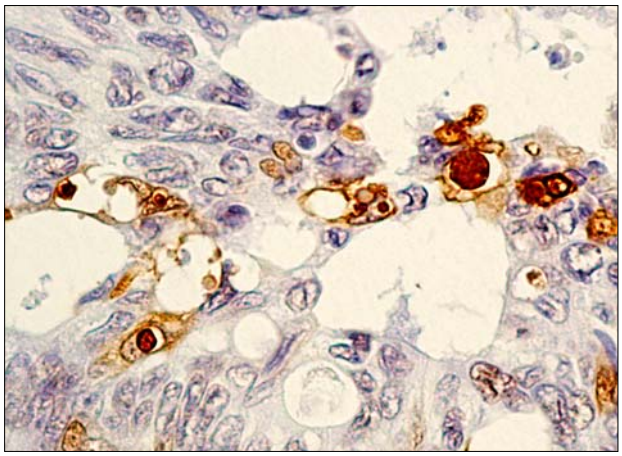

recovered from the DCO archive. Tumour samples were fixed in 4% buffered formalin and embedded in paraffin blocks. Apoptosis was detected, using the TUNEL method and the ApopTag®Plus Peroxidase In situ Apoptosis Detection Kit (Intergen, USA). The expression of MT (isoforms I and II), Ki-67 antigen and the active form of cas-3 were documented by performing immunocytochemical reactions with monoclonal antibodies (respective clones: E9, Ki-S5, CPP32, DakoCytomation, Denmark). Colour reaction was developed, using the EnVision system (DakoCytomation, Denmark). The intensity of apoptosis, the expression of cas-3 and of Ki-67 antigen were quantified, using a three-point scale: 3-5% positive cells - 1 pt, 6-10% positive cells - 2 pts, over 10% positive cells - 3 pts. The expression of MT was quantified, using the IRS scale, according to Remmele (0-12 pts), taking into account both the intensity of the colour reaction and the proportion of positive cells [7]. All the studied tumours showed G2 grade and B2 advancement stage, according to Duke (as modified by Astler and Coller), which corresponded to the clinical classification of T3N0M0 (the 2nd stage of clinical advancement) [2]. The obtained results were subjected to statistical analysis, using the STATISTICA PL software (StatSoft, Poland) and employing Spearman's correlation tests and Kaplan-Meier's survival analysis.

Results

In all the examined tumours, the expression of individual markers was variable as to its site. In the case of MT, a nuclear-cytoplasmatic expression, for cas-3 a cytoplasmatic expression and for Ki-67 antigen - a nuclear expression were disclosed. The intensity of apoptosis in cancer cells was variable in individual tumours (Fig. 1). The analysis of correlation between apoptosis and MT, cas-3 and Ki-67 antigen expression demonstrated that the parameters were poorly related to one another ($r = 0.18$; $r = 0.33$; $r = 0.15$; $p < 0.05$). In turn, the survival times of the patients with either high or moderate intensity of apoptosis were significantly shorter ($p < 0.05$) than those in the patients with a low extent of apoptosis in cancer cells (Fig. 2). Similar results were obtained in the analysis of the patients' survival times, as related to the expression of Ki-67 antigen. The longest survival time was noted at low expression of the antigen, while the shortest survival time was associated with a high and moderate expression of the antigen (Fig. 3). No significant differences in the survival time were associated with varying expressions of cas-3 or MT.

Figure 2. Survival times in patients with primary colorectal adenocarcinoma, the cells of which demonstrated high (d = 3 pts), moderate (s = 2 pts) or low (m = 1 pt) intensity of apoptosis.

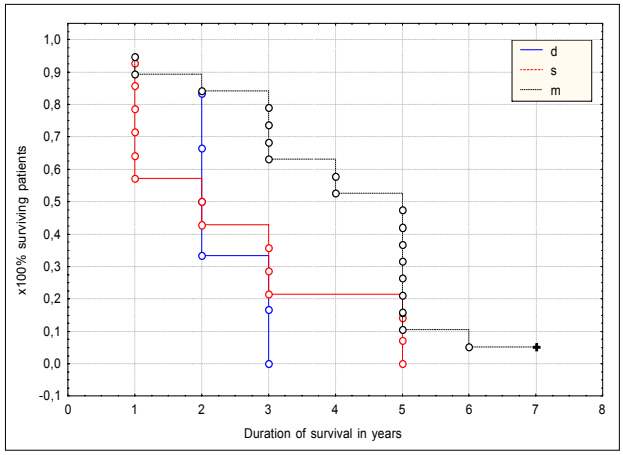

Figure 3. Survival times in patients with primary colorectal adenocarcinoma, the cells of which demonstrated high (d = 3 pts), moderate (s = 2 pts) or low (m = 1 pt) expression of Ki-67 antigen.

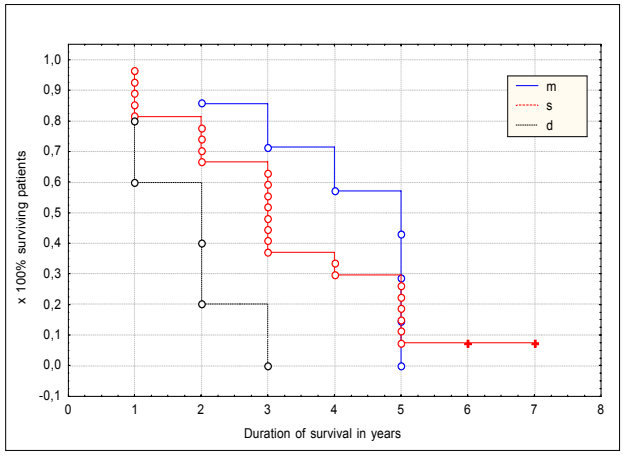

Discussion

The growth and expansion of a tumour are associated with several mechanisms which control cell processes, including cell proliferation and apoptosis. Among the recognized immunocytochemical markers, which reflect the activity of the processes, the expression of MT was also taken into account. The expression of the protein points to an augmented proliferative activity of neoplastic cells and to a less favourable prognosis [3]. Some data are also available, which indicate that MT may act as an anti-apoptotic factor, both in normal and tumour cells [6]. In our studies, an attempt was made to define reciprocal relations between the expression of MT, Ki-67 antigen, the intensity of apoptosis, measured by the TUNEL technique and the expression of cas-3. The significance of the markers was analyzed for the time of survival in patients with primary colorectal adenocarcinoma. In our earlier studies, and in investigations of other

authors, the expression of Ki-67 antigen was found to positively correlate with the expression of MT and with the advancement stage (the depth of intestinal wall infiltration) of colorectal adenocarcinomas [8, 9, 10]. Moreover, augmented expressions of Ki-67 antigen and of MT were observed in patients with tumours of G2 or G3 grade of malignancy and in patients with shorter survival times [8]. In the present studies, a group of patients was selected, uniform in respect to the clinical advancement and G grade. No reciprocal relations were noted between the intensities of expression of the parameters, that pointing out to an extensive heterogeneity of the studied tumours. The analysis of the patients' survival time periods, as related to the expression of Ki-67 antigen, confirmed our earlier reports, indicating a significant prognostic role of the parameter [8]. The marginally positive correlation between the expression of Ki-67 antigen and the intensity of apoptosis demonstrates that proliferation and apoptosis in tumours are not always strictly linked to each other. The principal aim of our studies involved a demonstration of the prognostic significance of apoptosis in cells of colorectal adenocarcinomas. The obtained results are inconsistent with the few earlier results of other authors [11] and indicate higher aggressiveness of colorectal carcinomas in cases with higher intensity of apoptosis. This suggests the need for further studies on apoptosis as a prognostic factor in primary colorectal adenocarcinoma.

References

1. Nowacki MP. Colorectal carcinoma (in Polish). In: Krzakowski M, editor. Onkologia kliniczna. 1st ed. Warszawa: Borgis® Wydawnictwo Medyczne; 2001, p 235-53.

2. Jass JR. Tumors of the small and large intestines (including the anal region). In: Fletcher CDM, editor. Diagnostic histopathology of tumors. 2nd ed. London: Churchill Livingstone; 2000, p 369-409.

3. Dzięgiel P. Expression of metallothioneins in tumor cells. Pol J Pathol, 2004; 55: 3-12.

4. Ioachim EE, Goussia AC, Agnantis NJ, Machera M, Tsianos EV, Kappas AM. Prognostic evaluation of metallothionein expression in human colorectal neoplasms. J Clin Pathol, 1999; 52: 876-9.

5. Coyle P, Philox JC, Carem LC, Rofe AM. Metallothionein: The multipurpose protein. Cell Mol Life Sci, 2002; 59: 627-47.

6. Shimoda R, Achanzar WE, Qu W, Nagamine T, Takagi H, Mori M, Waalkes M. Metallothionein is potential negative regulator of apoptosis. Toxicol Sci, 2003; 73: 294-300.

7. Remmele W, Stegner HE. Recommendation for uniform definition of an immunoreactive score (IRS) for immunohistochemical estrogen receptor detection (ER-ICA) in breast cancer tissue. Pathologe, 1987; 8: 138-40.

8. Dzięgiel P, Forgacz J, Suder E, Surowiak P, Kornafel J, Zabel M. Prognostic significance of metallothionein expression in correlation with Ki-67 expression in adenocarcinomas of large intestine. Histol Histopathol, 2003; 18: 401-7.

9. Dumańska M, Dzięgiel P, Sopel M, Wojnar A, Zabel M. Evaluation of apoptosis, proliferation intensity and metallothionein (MT) expression in comparison with selected clinicopathological variables in primary adenocarcinomas of the large intestine. Folia Morphol, 2004; 63: 107-10.

10. Kuroda K, Aoyama N, Tamura T, Sakashita M, Maekawa S, Inoue T, Wambura C, Shirasaka D, Minami R, Maeda S, Kuroda Y, Kasuga M. Variation in MT expression in early-stage depressed-type and polypoid-type colorectal tunours. Eur J Cancer, 2002; 38: 1879-87.

11. Sinicrope FA, Hart J, Hsu HA, Lemoine M, Michelassi F, Stephens LC. Apoptotic and mitotic indices predict survival rates in lymph node-negative colon carcinomas. Clin Cancer Res, 1999; 5: 1793-1804.

The role of AT1 and AT2 angiotensin receptors in the mechanism of apoptosis in renal tubular cells after physical exercise

Podhorska-Okołów M[1], Dzięgiel P[1], Gomułkiewicz A[1], Dolińska-Krajewska B[1], Murawska-Ciałowicz E[2], Jethon Z[2], Zabel M[1, 3]

[1] Department of Histology and Embryology, Medical University, Wroclaw,
[2] Department of Physiology, University of Physical Education, Wroclaw,
[3] Department of Histology and Embryology, University of Medical Sciences, Poznan, Poland

Abstract

Intensive physical exercise disturbs the entire homeostasis in the body and leads to changes in haemodynamic and metabolic alterations not only in skeletal muscles but also in many distant organs. In response to acute physical exercise, a decrease of the glomerular filtration may occur, followed by stimulation of the renin-angiotensin system (RAS). Recent studies have shown that both AT1 and AT2 angiotensin receptors may play a role in mediating the apoptotic process in the kidney. Our previous studies have demonstrated an occurrence of apoptosis in rat renal tubular cells after an excessive exercise. The aim of the present study was to determine the possible mechanism of exercise-induced apoptosis in rat kidney. The analysis was performed on kidneys of rats, subjected to treadmill running until exhaustion. Apoptosis was detected in paraffin sections by the TUNEL technique. The expression of AT1 and AT2 receptors in renal tubular cells was examined by immunohistochemistry and Western blot. Our results confirmed that apoptosis after physical exercise is present in renal distal tubular cells. Moreover, there was an increased expression of AT1 and AT2 receptors in distal tubular cells. These studies suggest that physical exercise may induce apoptosis by a mechanism, involving the activation of angiotensin AT1 and AT2 receptors.

Key words: angiotensin receptors, apoptosis, kidney, physical exercise.

ADDRESS FOR CORRESPONDENCE:
Marzena Podhorska-Okołów
Department of Histology and Embryology
Medical University of Wroclaw
Chałubinskiego 6a; 51-650 Wroclaw, Poland
tel. 071/784-00-82; fax. 071/784-00-82
e-mail: mapod@hist.am.wroc.pl

Introduction

Intensive physical exercise disturbs the entire homeostasis in the body and leads to changes in haemodynamic and metabolic alterations not only in skeletal muscles but also in many distant organs, such as the kidney or the heart. A decrease of glomerular filtration, sodium depletion and increased blood concentrations of catecholamines (adrenaline, noradrenaline) are among the effects of excessive physical exercise. All of these mechanisms could activate the juxtaglomerular apparatus to renin secretion. Moreover, there are many tissues, including vasculature's endothelial and smooth muscle cells, the heart and the kidney, which have their own local renin-angiotensin (RAS) systems, capable of producing angiotensin II in response to metabolic changes, occurring after physical exercise. Elevated blood renin levels (plasma rennin activity, PRA) stimulate the conversion of angiotensinogen to angiotensin I, which is then converted to active angiotensin II by the angiotensin-converting enzyme within the pulmonary circulation. Angiotensin II acts through its receptor subtypes, type 1 (AT1) and type 2 (AT2) receptors, which involve different molecular mechanisms. Despite the place of secretion, angiotensin II exerts a wide range of actions, including apoptosis promotion. A stimulation of AT1 and AT2 receptors may result in either an increased expression of p53 protein (associated with the activation of the transcriptional nuclear factor kappa B - NF-κB) or in a generation of reactive oxygen species (ROS). Both of them could promote the apoptotic process [1, 2]. Our previous study demonstrated the presence of apoptotic-damaged cells in the kidney after physical exercise [3]. In the present study, we examined the possible role of AT1 and AT2 receptors in the induction of apoptosis of renal tubular cells after an intensive physical exercise.

Material and Methods

Eighteen male Wistar rats, 10-12 weeks of age (200-250 g body weight), formed groups of running (N=12) and not running

Table 1. Apoptosis in kidney tubular cells. Control: notrunning animals. 6h: running animals killed after 6h. 96h: running animals killed after 96h. Significant differences: the control values, as compared to respective values after 6h *p<0.01; the control values, as compared to respective values after 96h **p<0.001.

Apoptotic cell nuclei in 500 examined tubular cells	Control	6h	96h
(%)	1.32 ± 0.3	4.69 ± 0.7 *	5.9 ± 1.2 **

Figure 1. Expression of AT1 receptor in renal distal tubular cells. Immunohistochemical reaction, x200.

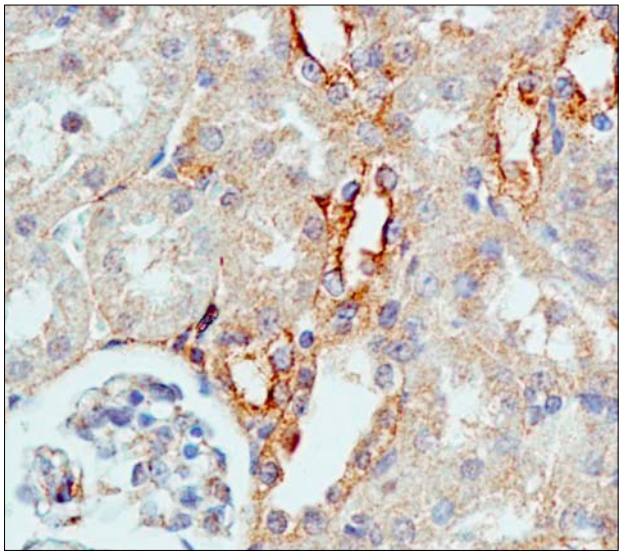

Figure 2. Expression of AT1 receptor protein in kidney cortex homogenate 6h and 96h after exercise. M - molecular marker. Western Blot analysis.

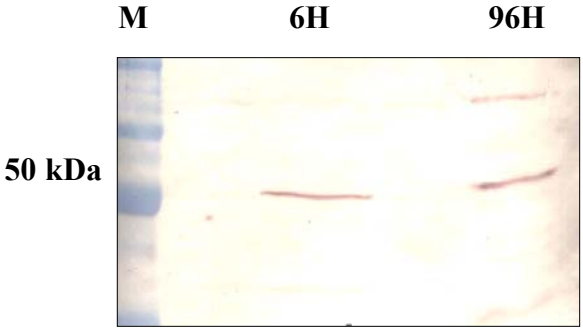

animals (N=6). The animals from the exercise group were subjected to running on a treadmill at 1.0 km/h until exhaustion. After the exercise, the animals returned to their cages and were randomly grouped into animals, killed after 6 hrs (N=6) from the exercise cessation and those, killed after 96 hrs (N=6) from the same time point. Control animals (N=6) remained in their cages throughout the experiment. All the animals were anaesthetized and decapitated. Two kidneys were excised from each rat. The right kidney was fixed in 4% buffered formaldehyde solution for 24 hrs and embedded in paraffin. The left kidney was frozen in liquid nitrogen and stored at -80^{0}C. In paraffin sections, apoptosis was detected by the TUNEL technique, using the ApopTag® Plus Peroxidase In Situ Apoptosis Detection Kit (INTERGEN, Norcross, USA). All the immunocytochemical reactions were performed in paraffin sections. The expression of AT1 and AT2 receptors was demonstrated, using mouse monoclonal antibodies (dilution: 1:200, Santa Cruz Biotechnology, Santa Cruz, CA, USA). All the reactions were accompanied by negative controls in which specific antibodies were substituted by the Primary Negative Control reagent. The investigated antigens were visualised, using biotinylated antibodies and streptavidin-biotinylated peroxidase and diaminobenzidine (LSAB2 kit and DAB, DakoCytomation, Denmark). AT1 receptor protein expression was assessed by the Western blot technique. One block of tissue from each rat was homogenized in a Tris-EDTA buffer. Crude membrane fractions were separated by SDS-PAGE and were electrotransferred to supported nitrocellulose. AT1 receptor protein bands were detected, using a primary antibody (1:500 dilution) from the Santa Cruz Biotechnology (Santa Cruz, CA, USA) and to develop Western blots, we used the chromogenic substrate - BCIP/NBT. Statistical analysis of the results was conducted by using the Chi-square test and the Statistica 5.1 PL software (StatSoft, Cracow, Poland). The differences were considered significant if $p < 0.05$.

Results

A significant increase was observed in the number of apoptotic nuclei in renal tubular cells of all the exercised animals, in comparison to that in the sedentary group (Tab. 1). The distal convoluted tubules displayed a strong expression of both angiotensin AT1 and AT2 receptors after 6, as well as after 96 hours from the exercise (Fig. 1). The obtained results were confirmed by Western blot, which revealed an increased expression of AT1 and AT2 receptor proteins (Fig. 2).

Discussion

It is well known that acute exercise can cause skeletal muscle damage, including apoptosis of myonuclei [4]. The generation of reactive oxygen species (ROS) after an intensive exercise seems to be responsible for exercise-induced changes in many organs. Our previous studies have demonstrated the presence of apoptosis in rat renal tubular cells after excessive exercise; however, the induction of apoptosis in kidney tubular cells was thought to be not associated with oxidative stress [3]. Recent studies suggest that angiotensin II plays a prominent role in the progression of renal injury. Although it was

assumed that angiotensin II stimulates cell proliferation via AT1 receptor and apoptosis via AT2 receptor [5], many authors have recently suggested that both AT1 and AT2 receptors influence the apoptotic process in the kidney [6]. One of the proposed mechanisms of apoptosis induction in kidney mesangial cells damage is the oxidative stress in response to stimulation of AT1 and AT2 receptors [7]. In the present study, we demonstrated an increased expression of AT1 and AT2 receptors in distal renal tubular cells of all the exercised animals. Moreover, there was a strong correlation between the occurrence of apoptosis and the increased expression of AT1 and AT2 receptors only in the cells of distal convoluted tubuli in rat kidneys. Conversely, Bhaskaran et al. [8] demonstrated that angiotensin II promoted apoptosis of renal proximal tubular cells via both AT1 and AT2 receptors *in vitro* and that the angiotensin-induced apoptotic process is mediated through oxidative stress. Nevertheless, we demonstrated in the previous work [3] that an induction of apoptosis in kidney tubular cells was thought to be not associated with the oxidative stress. The different distribution of apoptotic process in renal tubular cells probably depends on the nature of the triggering factor (e.g., oxidative stress, binding of apoptotic factors, DNA damage). We presume that exercise-induced apoptosis of kidney tubular cells could be mediated by both angiotensin AT1 and AT2 receptors, which are expressed in distal tubular cells. The stimulation of both AT1 and AT2 receptors could be associated with an increased expression of angiotensin-induced upregulation of p53, rather than with angiotensin-induced oxidative stress.

Acknowledgements

This study was supported by Grant No 3 PO5D 090 23 from the Polish Ministry of Science.

References

1. Wasilewski J, Gąsior M, Adamowicz-Czoch E, Pogański L. Przeciwmiażdżycowe właściwości inhibitorów enzymu konwertującego i hipotensyjne inhibitorów reduktazy HNG-Co. Folia Cardiol, 2003; 10: 255-63.

2. Morrissey JJ, Klahr S. Effect of AT2 receptor blockade on the pathogenesis of renal fibrosis. Am J Physiol Renal Physiol, 1999; 45: 39-45.

3. Podhorska-Okołów M, Dzięgiel P, Murawska-Ciałowicz E, Krajeńska B, Ciesielska U, Jethon Z, Zabel M. Exercise-induced apoptosis in the renal tubular cells of the rat. Folia Morphol, 2004; 63: 213-16.

4. Podhorska-Okołów M, Sandri M, Zampieri S, Brun B, Rossini K, Carraro U. Apoptosis of myofibers and satellite cells: exercise-induced damage in skeletal muscle of the mouse. Neuropathol Appl Neurobiol, 1998; 24: 518-31.

5. Cao Z, Kelly DR, Cox A, Casley D, Forbes J, Martinello P, Dean R, Gilbert RE, Cooper ME. Angiotensin type 2 receptor is expressed in the adult rat kidney and promotes cellular proliferation and apoptosis. Kidney Int, 2000; 58: 2437-51.

6. Bonnet F, Cao Z, Cooper ME. Apoptosis and angiotensin II: yet another renal regulatory system? Exp Nephrol, 2001; 9: 295-300.

7. Lodha S, Dani D, Mehta R, Bhaskaran M, Reddy K, Ding G, Singhal PC. Angiotensin II-induced mesangial cell apoptosis: role of oxidative stress. Mol Med, 2002; 8: 830-40.

8. Bhaskaran M, Reddy K, Radhakrishanan N, Franki N, Ding G, Singhal PC. Angiotensin II induces apoptosis in renal proximal tubular cells. Am J Physiol Renal Physiol, 2003; 284: 955-65.

Influence of cycloheximide on apoptosis in CHO cells, induced by ethane 1, 2-dimethanesulphonate (EDS)

Polak U, Jankowska A, Warchoł JB

Department of Radiobiology and Cell Biology, K. Marcinkowski University of Medical Sciences, Poznań, Poland

Abstract

Ethane 1, 2-dimethanesulphonate (EDS) causes apoptotic death of Leydig cells. Additionally, EDS causes damage of Chinese Hamster Ovary (CHO) cells but the occurrence of apoptosis is not such plentiful. The present study tested whether the inhibition of protein synthesis by cycloheximide (CHX) would influence apoptosis of CHO cells, induced by EDS. The study compounds induced morphological changes in CHO cell typical for apoptosis. An active form of caspase-9 and an alternation of mitochondrial transmembrane potential were also observed. In our study, a more cumulative effect of the CHX and EDS on apoptosis was observed, when both compounds were simultaneously employed. The obtained results indicated that synthesis of antiapoptotic proteins plays a very important role in the inhibition of apoptosis.

Key words: apoptosis, CHO cells, ethane 1,2-dimethanesulphonate (EDS), cycloheximide (CHX), caspase-9, mitochondrial potential.

Introduction

Cell apoptosis represents a significant phenomenon for cellular homeostasis. It results in self-destruction of cells and plays a reciprocal role to that of cell proliferation. Apoptosis is a genetically controlled death process, where the fate of the cell is determined by the relative abundance of survival and death proteins [1].

Ethane 1,2-dimethanesulphonate (EDS) is an agent that rapidly diffuses across tissues and selectively destroys Leydig cells, which are killed via apoptosis [2, 3, 4]. The influence of EDS on non steroidogenic types of cells was also studied. EDS damages Chinese Hamster Ovary (CHO) cells but the occurrence of apoptosis is not such extensive. The molecular bases of the processes are still not well understood [4]. In this study, we attempted to establish, whether inhibitions of protein synthesis by cycloheximide (CHX) would influence apoptosis of CHO, cells using EDS.

Material and Methods

The experiments were carried on *in vitro* cultured CHO tumour cells, maintained in RPMI 1640 medium, supplemented with 5% FBS, 2 mmol/l L-glutamine, 100 µg/ml streptomycin and 100 U/ml penicillin (37°C; 5% CO_2) [5]. CHO cells were exposed to EDS alone at concentrations of 5-, 10-, 20-, 50- and 100 µmol/l or at constant concentration of CHX [100mmol/l], added together with EDS. Simultaneously, the cells were treated with CHX alone and DMSO at the highest concentration used for dissolving EDS. The effects were observed after 24- and 48h intervals. Apoptotic and necrotic changes were detected by fluorescent microscopy (propidium iodide and Hoechst 33342 staining) and electron microscopy. The cells were incubated for 24h with EDS (10- and 20 mmol/l) and CHX, added at different times points, compared to the addition at EDS. The cells were also treated for 24h with EDS and CHX, added together, and for 24h with EDS, followed by CHX, added 1-, 2-, 3-, 4-, 6-and 12h later. A determination of caspase-9 activity in CHO cells was performed, according to caspase-9 inhibitor Red-LEHD-FMK staining (Oncogene Research Products™). The percentage of caspase-9 positive cells was counted after 12- and 24h incubation

ADDRESS FOR CORRESPONDENCE:
Urszula Polak
Department of Radiobiology and Cell Biology
K. Marcinkowski University of Medical Sciences, Poznań
Święcickiego 6, 60-781 Poznań, Poland
e-mail: ulapo@o2.pl

Fig.1.TheinfluenceofEDSconcentration.
Incubationtime-24h

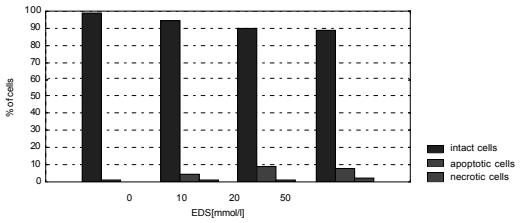

Fig.2.TheinfluenceofEDSconcentration.
Incubationtime-48h

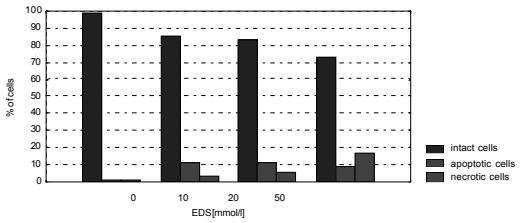

Fig.3.TheinfluenceofEDSandCHX[100umol/l]
Incubationtime-24h

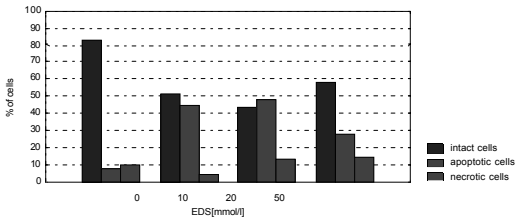

Fig.4.TheinfluenceofEDSandCHX[100umol/l]
Incubationtime-48h

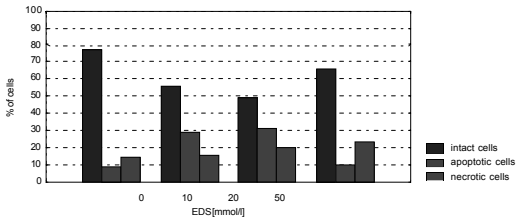

Fig.5.Theactiveformofcaspase-9incubated12h
withEDS[20mmol/l],EDS/CHXiCHX[100umol/l]

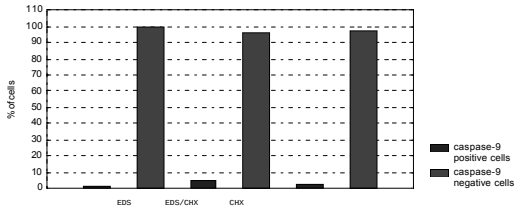

Fig.6.Theactiveformofcaspase-9incubated24h
whitEDS[20mmol/l],EDS/CHX,CHX[100umol/l]

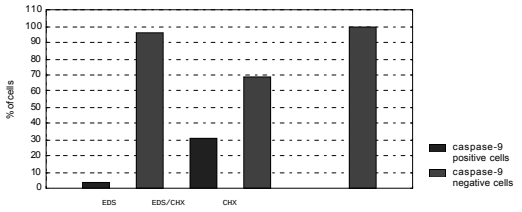

with EDS alone, EDS with CHX, and CHX alone, using an LSM 510 (Zeiss) confocal microscope.

Mitochondrial potential was assessed, using the fluorescent dye JC-1. Fluorescence was measured at 490nm (excitation) and 530nm (emission) for the JC-1 monomer (green colour) and 590nm for the JC-1 aggregate (orange colour) [6, 7].

Results and Discussion

It was established that EDS could induce apoptosis in CHO cells, however, the level of apoptotic cells was lower, when compared with the degree of apoptosis induced by EDS and CHX combined together. The number of apoptotic cells depended on the concentration of EDS and on the incubation time. The percentage of cells showed apoptotic features. When they were incubated with 10- and 20mmol/l, EDS was 10%, whereas the number of necrotic cells did not exceed 5% (Fig. 1 and 2). The highest level of apoptosis, about 50%, was observed for the cells, exposed to the action of both compounds: 10- and 20 mmol/l EDS and 100µmol/l CHX for 24h. The level of necrotic cells in that case was about 10%. At higher doses of EDS [50-, 100 mmol/l] apoptosis was inhibited, whereas necrosis increased to 15% (Fig. 3 and 4). Incubation with DMSO did not influence the cells, whereas incubation with CHX [100 µmol/l] alone for 24h caused apoptosis in about 5% of studied cells. After 24h incubation with EDS [10-, 20 mol/l], followed by addition of CHX (6h later than EDS), the percentage of apoptotic cells increased to 50%. The number of apoptotic cells was similar to that for the cells, incubated for 24h with EDS and CHX added together. The active form of caspase-9 was observed only after 12- and 24h incubation of cells with [20 mol/l] EDS and CHX. The highest percentage - 30% - of caspase-9 positive cells was observed after 24h incubation with EDS and CHX (Fig. 6). After 12h incubation, the level of cells with active form caspse-9 was low and did not exceed 5% (Fig. 5). During JC-1 assay, changes of cell mitochondria colours, from green to orange, were observed, corresponding to the changes of mitochondrial potential. The ultrastructure of cells, incubated with 20 mmol/l of EDS, showed typical apoptotic changes, like chromatin condensation and fragmentation of the nuclei or many vesicles, accumulating in the cytoplasm. In mitochondria, the cristae exhibited a loss of concavity and convexity and became more linear.

This study demonstrated that apoptosis of CHO cells, induced by EDS, required some expression of a new protein, synthesized already after the initiation of the process. CHX, which is capable to block protein synthesis, when combined with EDS, increased the number of apoptotic cells. Thus, the antiapoptotic proteins play an important role in apoptosis of CHO cells. The amount of apoptotic cells depended on the time of action of both EDS and CHX. When added together, those two compounds were able to induce apoptosis in more than 50% of the studied cells. It seems that a simultaneous addition of EDS and CHX causes a loss of pro- and antiapoptotic factors balance, leading to cell death. The results are consistent with the current view that apoptosis depends on the expression of specific genes [8, 9] and the amount of apoptot-

ic cells is related to the balance between anti- and proapoptotic proteins in the cell [10]. Further studies of the apoptotic pathway would be helpful in finding out the successful methods to regulate the process and to use it as an effective tool, interrupting the progressive course of many diseases.

References

1. Goswami J, Sinskey AJ, Steller H, Stephanopoulos GN, Wang DIC. Apoptosis in Batch Culture of Chinese Hamster Ovary Cells. Biotechnol Bioeng, 1999; 62: 632-40.

2. Morris ID. Leydig cell toxicology. In: Payne AH, Hardy MP, Russell LD (eds). The Leydig cell. Vienna: Cache River Press, 1996; 574-96.

3. Jong-Min K, Lindi L, Zirkin BR. Caspase-3 activation is required for Leydig cell apoptosis induced by ethane dimethanesulfonate. Endocrinol, 2000; 141:1846-53.

4. Rommerts FF, Kuhne L, van Cappellen GW, Stocco DM, King SR, Jankowska A.. Specific dose-dependent effects of ethane 1,2-dimethanesulfonate in rat and mouse Leydig cells and non-steroidogenic cells on programmed cell death. J Endocrinol, 2004; 181:169-78.

5. Wołuń-Cholewa M, Warchoł JB. Studies on the effect of photodynamic therapy on in vitro cultured neoplastic cells. Folia Histochem et Cytobiol, 2001; 39:213-14.

6. Reers M, Smiley, ST, Mottola-Hartshorn C, Chen A, Lin M, Chen LB. Mitochondrial membrane potential monitored by JC-1 dye. Methods Enzymol, 1995; 260: 406-17.

7. Desai BN, Mayers BR, Schreiber SL. FKBP 12-rapamycin-associated protein associates with mitochondria and senses osmotic stress via mitochondrial dysfunction. Cell Biology, 2002; 99: 4319-24.

8. Fulda S, Klaus-Michael D. Apoptosis pathways: turned on their heads? Drug Resistance, 2003; 6: 1-3.

9. Watanabe N, Iwamoto T, Dickinson DA, Iles KE, Forman HJ. Activation of the mitochondrial caspase cascade in the absence of protein synthesis does not require c-Jun N-terminal kinase. Archives of Biochem and Biophsics, 2002; 405: 231-40.

10. Lemaire C, Andréau K, Souvannavong V, Adam A. Specific dual effect of cycloheximide on B lymphocyte apoptosis: involvement of CPP32/caspase-3. Biochem Pharmacology, 1999; 58: 85-93.

The role of Bak expression in apoptosis of the oral squamous cell carcinoma (OSCC) and metastases to lymph nodes (LNMs)

Baltaziak M[1], Koda M[1], Barwijuk-Machała M[1], Musiatowicz B[2], Duraj E[3], Kańczuga-Koda L[2], Musiatowicz M[4], Reszeć J[2]

[1]Department of General Pathology, [2]Department of Clinical Pathology, [3]Department of Maxillofacialis Surgery, [4]Department of Paediatric Otorhinolaryngology, Medical University of Białystok, Poland

Abstract

The immunohistochemical method was applied to show Bak expression in oral squamous cell carcinoma and its metastases to lymph nodes (LNMs). Bak expression was evaluated by immunohistochemical methods in specimens with oral squamous cell carcinomas and their lymph node metastases. Immunohistochemical studies were performed, using goat polyclonal Bak antibodies (Santa Cruz Biotechnology, USA) at 1:200 dilution. Our studies revealed over expression (64%) of Bak in the cytoplasm of epithelial cells in primary tumours (PTs) and in (75%) LNMs. No statistically significant correlations were observed between Bak immunoreactivity and age, pT and G of the carcinoma in PTs and LNMs. We conclude that expression of Bak may be useful for better characterising and predicting the prognosis of OSCC but cooperative studies are needed to assess its applications in the clinical practice.

Key words: apoptosis, Bak, Squamous Cell Carcinoma, lymph nodes, metastases.

Introduction

At least 95% of cancers of the oral cavity (including tongue) are squamous cell carcinomas (SCC). Although most of them are readily accessible to discovery and biopsy, many are detected late and 50% of these lesions prove fatal. On histological examination, SCC range from well-differentiated keratinizing neoplasms to anaplastic, sometimes, sarcomatoid tumours. They infiltrate local tissues and subsequently metastasize to lymph node, the mediastinum, the lungs, the liver and bones [1]. The tumour growth is characterised by an imbalance between cell proliferation and programmed cell death (PCD)-apoptosis. The regulation of PCD is very important for neoplastic transformation. Bak is a pro-apoptotic member of the Bcl-2 genes family that are involved in the regulation of apoptosis [2]. In the present study, we examined the expression of Bak in SCC of the oral cavity and its metastases to lymph nodes.

Material and methods

Bak expression was evaluated in formalin-fixed, paraffin-embedded specimens from 47 males and 11 females, ranging in age from 30-76 years, with a median of 56,8 years with T1-T4 oral SCC and, out of whom, 25 presented with lymph node metastases. In our examination, we used TNM system and the 3rd degree grading system of histological malignancy. Immunohistochemical studies were performed, using goat polyclonal Bak antibodies (Santa Cruz Biotechnology, USA) at 1:200 dilution. The reaction was performed by the Labelled Streptavidin Biotin (LSAB) technique (DAKO). The slides were diagnosed, using a light microscope at 100-fold magnification. The immunostaining was evaluated by counting at least 500 cells in the tumour areas of each section. In negative controls, the primary antibodies were omitted. Bak expression was estimated semi-quantitatively as the percentage of positive cells as follows: 15-30% stained cancer cells - slight reaction (+), 31-50% stained cancer cells - moderate reaction (++), >50% stained cancer cells - strong reaction (+++) and <15% stained tumour cells were considered negative. Correlation of Bak and various clinicopathological features was done, using the Chi - square test. The significance level was set to p=0.05.

ADDRESS FOR CORRESPONDENCE:
Marek Baltaziak
Department of General Pathology
Medical University of Białystok
Waszyngtona 13, 15-228 Białystok, Poland
e-mail: drbal@poczta.onet.pl

Results

The expression of Bak in oral cancer and lymph node metastases is summarised in Tables 1 and 2. Our studies revealed over expression of bak in the cytoplasm of epithelial cells in 37/58 (64%) primary tumours (PTs) and 18/24 (75%) lymph node metastases (LNMs). Bak was detectable in higher percentage in pT4 groups (78%-of PTs and 80% of LNMs). According to the grading system of histological malignancy, we noticed a higher expression of Bak in G2 groups (68% in PT and 78.9 in LMNC). In G3 group, we found a difference between the primary tumours (33.3%- positive cells) and lymph node metastases (66.7% positive cells). In twelve cases, we observed a positive immunohistochemical reaction for Bak in PTs and LNMs between the primary tumours and their corresponding lymph node metastases. In five cases, it was a positive reaction for Bak in PTs and negative immunohistochemical staining in LNMs, then, in five cases, we noticed positive staining in LNMs and negative in PTs. There was no significantly statistical correlation in either age, pT or the grading system between primary tumour and lymph nodes metastases.

Table 1. The expression of Bak, according to staging (pT)

STAGING	PRIMARY TUMOURS		METASTASES	
	A	B	C	D
pT1	25	60%	9	67%
pT2	18	67%	8	75%
pT3	6	50%	3	67%
pT4	9	78%	5	80%

A- the number of primary tumours with expression of Bak in different pT groups
B- the percentage of primary tumours with expression of Bak in different pT groups
C- the number of tumours with LNMs and expression of Bak in different pT groups
D- the percentage of tumours with LNMs and expression of Bak in different pT groups

Table 2. The expression of Bak, according to grading (G).

GRADING	PRIMARY TUMOURS		METASTASES	
	A	B	C	D
GI	4	57%	2	50%
GII	31	69%	19	79%
GIII	2	33%	3	66%

A- the number of primary tumours with expression of Bak in different G groups
B- the percentage of primary tumours with expression of Bak in different G groups
C- the number of tumours with LNMs and expression of Bak in different G groups
D- the percentage of tumours with LNMs and expression of Bak in different G groups

Discussion

Lymph node metastases are crucial in the prognosis of cancer process. We have not found any scientific reports about Bak proteins in SCCs of the oral cavity and their lymph node metastases. The aim of our study was to assess the role of Bak, as a pro-apoptotic protein in primary SCCs of the oral cavity and lymph nodes metastases. Tumour progression is characterised by an imbalance between cell proliferation and apoptosis [3]. The process of apoptosis plays a very important role in elimination of abnormal cells from the tissues. The inhibition of this process can aid progress of cancer [4]. Proteins of the Bcl-2 family are central regulators of apoptosis and are thought to act primarily on the mitochondria [5]. Members of the Bcl-2 family are cellular homologous which are divided into three subfamilies: Bcl-2, Bax and BH3, which can perform either anti-apoptotic or pro-apoptotic functions. Proteins from the Bcl-2 family are known as inhibitors of apoptosis but Bax and BH3 as promotors of apoptosis. Bak belongs to the Bax subfamily [6]. Members of this family interact and form hetero- and homodimers, which control apoptosis. Some authors have noticed that Bak can form heterogeneous dimers with Bcl-2 or Bcl-xl to inhibit their anti-apoptotic functions [7]. In our experiment, we noticed that the expression of Bak is correlated with staging of the cancer (TNM system). The highest percent of Bak expression was observed in pT4 staging groups. Our observations are similar to those of Rosen at al., who indicated that Bak deficiency is correlated with the occurrence and development of tumours [8] and Kondo et al. who found that positive ratios of Bak expression negatively correlated with pathological and clinical stages of gastric cancer [9]. Although there are still many unanswered questions, regarding the exact mechanism by which Bak modulates apoptosis, we assume that Bak plays an important role in the process of apoptosis in SCCs of the oral cavity and their metastases to lymph nodes.

References

1. Rosai J. Oral cavity and oropharynx. In: Ackerman˘s Surgical Pathology.Vol,1.Mosby; 1996, p 223-55.
2. Petros AM, Olejniczak ET, Fesik SW. Structural biology of the Bcl-2 family of proteins. Biochim Biophys Acta, 2004; 1644: 83-94.
3. Sulkowska M, Famulski W, Sulkowski S, Reszeć J, Koda M, Baltaziak M, Kańczuga-Koda L. Correlation between Bcl-2 protein expression and some clinicopathological features of oral squamous cell carcinoma. Pol J Pathol, 2003; 54: 49-52.
4. Sulkowska M, Famulski W, Chyczewski L, Sulkowski S. Evaluation of p53 and Bcl-2 oncoprotein expression in precancerous lesions of the oral cavity. Neoplasma, 2001; 48: 94-8.
5. Burlacu A. Regulation of apoptosis by Bcl-2 family proteins. J Cell Mol Med, 2003; 7: 249-57.
6. Motyl T, Gajkowska B, Płoszaj T, Waręski P, Orzechowski A, Zimowska W, Wojewódzka U, Ryniewicz Z, Rekiel A. Role of Bax and Bcl-2 in regulation of mammary epithelial cells apoptosis. Post Biol Kom, 2000; 27: 31-51.
7. Degli Esposi M, Dive C. Mitochondrial membrane permeabilisation by Bax/Bak. Biochem Biophys Res Commun, 2003; 304: 455-61.
8. Rosen K, Rak J, Jin J, Kerbel RS, Newman MJ, Filmus J. Downregulation of the pro-apoptotic protein Bak is required for the ras-induced transformation of intestinal epithelial cells. Curr Biol, 1998; 8: 1331- 4.
9. Kondo S, Shinomura Y, Miyazaki ., Kiohara T, Tsutsui S, Kitamura S, Nagasavwa Y, Nakahara M, Kanayama S, Matsuzawa Y. Mutations of the Bak gene in human gastric and colorectal cancers. Cancer Res, 2000; 60: 4328 - 30.

Apoptosis phenomenon in the selected neoplasms of the glial origin

Szkudlarek M[1], Lebelt A[1], Klim B[1], Pawlak J[1], Lemancewicz D[1], Bogusłowicz W[1], Sulima D[1], Zimnoch L[2], Dzięcioł J[1]

[1]Department of Human Anatomy, [2]Department of Clinical Pathomorphology,
Medical University of Bialystok, Poland

Abstract

Gliomas cause a therapeutic problem because of their localization and asymptomatic growth in the initial phase. Neoplastic growth is connected with disturbance between proliferation and apoptosis. In the study, we assessed the Bcl-2 family proteins involved in apoptosis in gliomas. The study comprised 61 patients with gliomas and based on tissue material sent for the diagnosis. Apoptosis was assessed in various types of gliomas and was defined by the apoptotic index (IA) and shown immunohistochemically with using Bcl-2, Bax and Bcl-x antibodies. The data were statistically analyzed.. We found an increased percentage of the Bax (+) cells in less matured gliomas. A reverse dependence was revealed for Bcl-x. It was found that, probably in gliomas, the assessment of the Bcl-2 family proteins may serve only as an additional parameter for the evaluation of the disease course and the therapeutic success.

Key words: gliomas, apoptosis, Bcl-2, Bax, Bcl-x.

Introduction

The main principle of homeostasis in the multicellular organism is the maintaining of a quantitative balance between cell proliferation and death. Apoptosis, as a type of the physiological suicidal cell death, takes place during ontogenesis and cell replacement in constantly proliferating tissues. During apoptosis, morphological changes, observed within the cell, are the manifestation of intracellular biochemical reactions. Their key point is the cascade activation of the proteolytic enzymes known as caspases. Chain activation of caspases results in an origin of the active form of caspase 3, regarded as an enzyme responsible for proteolysis, observed during apoptosis [1]. The extrinsic mechanism, activating caspase 3, is connected with the stimulation of the outer cell membrane receptors of TNF family. In the intrinsic mechanism of apoptosis, the crucial role is played by mitochondria from which cytochrome c is released. In the cytoplasm, cytochrome c connects to Apaf-1 protein. Indirectly, this connection leads to an activation of caspase 3. The intrinsic apoptosis mechanism is controlled by the Bcl-2 family genes and proteins, comprising about twenty pro- and anti-apoptotic genes and proteins [1, 2]. Anti-apoptotic Bcl-2 protein co-operates in the regulation of apoptosis with pro-apoptotic Bax protein. Another homologue of the Bcl-2 family genes and proteins is the anti-apoptotic bcl-x gene. Its products are two antagonistic proteins: anti-apoptotic Bcl-X_L (consisting of 233 amino acids) and pro-apoptotic Bcl-Xs (consisting of 170 amino acids) [3]. In mitochondrial membranes, Bcl-2 and Bax proteins form ionic channels, regulating their permeability for cytochrome c and Apaf-1, either inhibiting (Bcl-2, Bcl-X_L) or facilitating (Bax, Bcl-Xs) their release. Thanks to the protein sections, called BH domains, Bcl-2 and Bax proteins form either Bcl-2/Bax heterodimers or homodimers. An overexpression of Bcl-2 leads to formation of anti-apoptotic Bcl-2/Bcl-2 homodimers. The overexpression of Bax results in forming pro-apoptotic Bax/Bax homodimers [4]. Disturbances of the balance between the pro- and anti-apoptotic factors of the Bcl-2 family proteins are observed in neoplasms. The overexpression of Bcl-2 and Bcl-X_L proteins prevents apoptosis and elimination of cells with abnormal genome. An insufficient expression of Bax protein influences the inhibition of apoptosis in cells of various neoplasms [5]. Disturbances between proliferative cell activity and apoptosis occur also in gliomas. The aim of the study was an assessment of the Bcl-2, Bax, Bcl-x proteins in gliomas of various histological types and malignancy grades.

ADDRESS FOR CORRESPONDENCE:
Magdalena Szkudlarek
Department of Human Anatomy
Medical University of Bialystok
Mickiewicza 2A; 15-230 Białystok, Poland
e-mail: anatomia@amb.edu.pl

Table 1. Apoptosis in various types of human gliomas.

Group	Number of cases	Bcl-2		Bax		Bcl-x	
		number of cases with positive reaction	percentage of cells with positive reaction (x ± SD)	number of cases with positive reaction	percentage of cells with positive reaction (x ± SD)	number of cases with positive reaction	percentage of cells with positive reaction (x ± SD)
Astrocytoma	14	11/14 (79%)	82.3±11.4	12/14 (86%)	39.5±8.3	9/14 (64%)	69.1±10.4
Anaplastic astrocytoma	18	12/18 (67%)	67.2±8.4	15/18 (83%)	47.8±10.2	10/18 (56%)	54.9±7.6
Glioblastoma multiforme	12	8/12 (67%)	70.3±8.7	10/12 (83%)	80.4±6.9	5/12 (42%)	65.4±9.8
Oligodendroglioma	10	9/10 (90%)	67.5±8.8	7/10 (70%)	38.9±5.3	8/10 (80%)	52.7±6.1
Anaplastic oligodendroglioma	7	5/7 (71%)	45.0±9.1	6/7 (86%)	56.0±9.8	4/7 (57%)	41.1±8.2

Figure 1. Oligodendroglioma. Different forms of neoplastic cells with positive immunohistochemical reaction for Bcl-2 antigen.

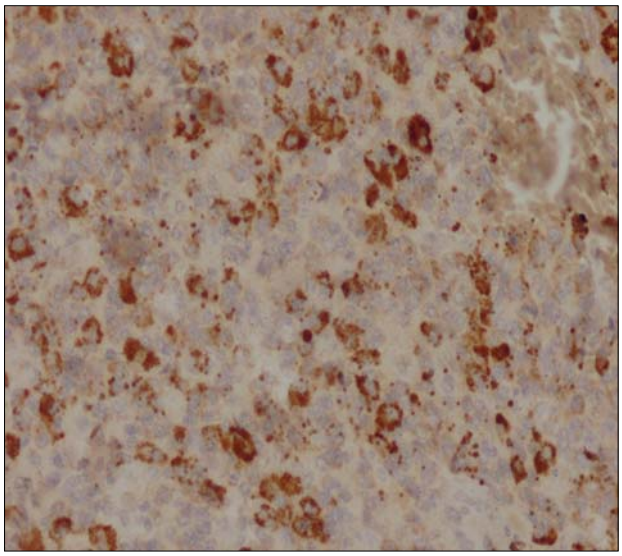

Figure 2. Glioblastoma multiforme. Different forms of neoplastic cells with positive immunohistochemical reaction for Bcl-x antigen.

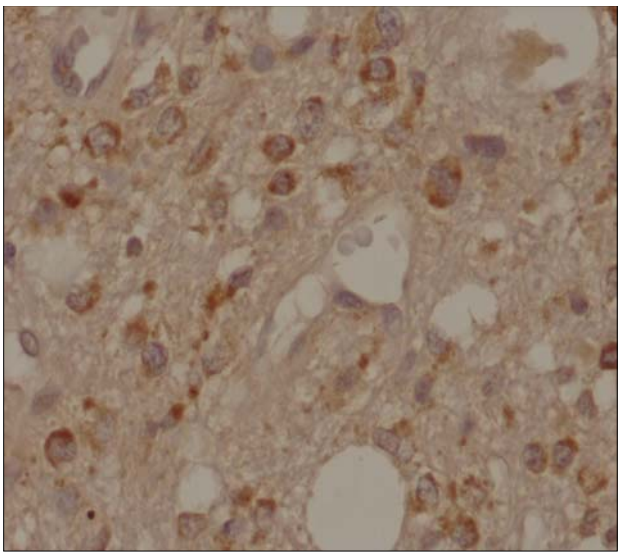

Material and Methods

The tissue material, used in the study, was obtained during operations of brain tumours, performed at the Neurosurgery Clinic of the Medical University of Białystok. Next, it was routinely sent for diagnostic evaluation to the Department of Clinical Patomorphology of the Medical University of Białystok. The tissue material was then used for scientific research after determining the histopathological diagnosis of brain tumour. The study comprised 61 patients, aged from 18 to 72 years, with brain tumours. An assessment of the incidence of apoptosis was performed in gliomas of various histological types and malignancy grades: astrocytomas (14), anaplastic astrocytomas (18), glioblastomas multiforme (12), oligodendrogliomas (10) and anaplastic oligodendrogliomas (7). Apoptosis was immunohistochemically demonstrated with the use of monoclonal Bcl-2 and Bax antibodies, and the policlonal Bcl-x antibodies (DAKO), employing an LSAB+Kit detective set and DAB as a chromogen. For the evaluation of the cells with indicating antigens, a computer software for image analysis - MicroImage

Olympus - was applied. Apoptosis was defined by the apoptotic index (IA), determined as the percentage of neoplastic cells with a positive reaction for the antigen. For particular IAs, means and standard deviations (SDs) were determined. Statistical evaluation of the data was performed, using the Statistica Pl software.

Results

Table 1 summarizes detailed results of the analysis of the Bcl-2, Bax and Bcl-x antibodies in 61 gliomas included in the study. Figures 1 and 2 illustrate immunohistochemical reactions with the Bcl-2 and Bcl-x antibodies

Discussion and Conclusions

The incidence of the positive reaction for the Bcl-2 protein was 70% in the study of Rieger et al. [6]. Stirk et al. [7] revealed - both in initial and recurrent glioblastomas - a high percentage of the Bcl-2 positive reaction (92% and 97%, respectively) and, in both cases, 100% positive reaction for Bcl-x. Whereas the percentage of the Bax positive reaction amounted to 84% and 73%, respectively. Krajewski et al. [8] revealed higher Bcl-2, Bcl-x and Bax expressions (92%, 98 and 98%, respectively) in gliomas. Similarly to our study, the Bcl-2 expression in astrocytomas was higher than that in glioblastomas multiforme. They also obtained an increased percentage of Bcl-x positive cells in tumours of higher differentiation grade but the Bax positive reaction was observed in less differentiated tumours. Krishna et al. [9] indicated the highest percentage of Bcl-2 positive cells in low- grade gliomas and a lack of significant dependence between IA and malignancy grade, while such a dependence was present in the case of proliferative activity. Wharton et al. [10] came to similar conclusions in the case of oligodendrogliomas. However, Deininger et al. [11] considered that overexpression of the anti-apoptotic Bcl-2 family proteins was connected with the progression of oligodendrogliomas and anaplastic oligodendrogliomas. Despite difficulties with the interpretation of the results, many authors consider that an evaluation of apoptosis by determining the expression of the Bcl-2 family proteins may be a prognostic factor, serving for the assessment of chances for successful radio- and (or) chemotherapy [12], of the recurrence risk after surgical treatment [7] and also, in the case of glioblastoma multiforme, for the assessment of the neoplastic growth rate and time of the patients' survival [13].

References

1. Reed JC. Mechanisms of apoptosis. Am J Pathol, 2000; 157: 1415- 30.

2. Scorrano L, Korsmeyer SJ. Mechanisms of cytochrome c release by proapoptotic BCL-2 family members. Biochem Biophys Res Commun, 2003; 304: 437- 44.

3. Borner C. The Bcl-2 family: sensors and checkpoints for life- or death decision. Mol Immunol, 2003; 39: 615- 47.

4. Kluck RM, Bossy-Wetzel E, Green DR, Newmeyer D. The release of cytochrome c from mitochondria: a primary site for bcl-2 regulation of apoptosis. Science, 1997; 275: 1132-6.

5. Soini Y, Pääkkö P, Lehto V-P. Histopathological evaluation of apoptosis in cancer. Am J Pathol, 1998; 153: 1041-53.

6. Rieger L, Weller M, Bornemann A, Schabet M, Dichgans J, Meyermann R. Bcl- 2 family protein expression in human malignant glioma: a clinical- pathological correlative study. Journal of Neurological Sciences, 1998; 155: 68-75.

7. Strik H, Deininger M, Streffer J, Grote E, Wickboldt J, Dichagans J, Weller M, Meyermann R. Bcl-2 family protein expression in initial and reccurent glioblastomas: modulation by radiochemotherapy. J Neurol Neurosurg Psychiatry, 1999; 67: 763-8.

8. Krajewski S, Krajewska M, Ehrmann J, Sikorska M, Lach B, Chatten J, Reed JC. Immunohistochemical analysis of Bcl-2, Bcl-x, Mcl-1, and Bax in tumors of central and peripheral nervous system origin. Am J Pathol, 1997; 150: 805-14.

9. Krishna M, Smith TW, Recht LD. Expression of bcl-2 in reactive and neoplastic astrocytes: lack of correlation with presence or degree of malignancy. J Neurosurg, 1995; 83: 1017-22.

10. Wharton SB, Hamilton FA, Chan WK, Chan KK, Anderson JR. Proliferation and cell death in oligodendrogliomas. Neuropathol Appl Neurobiol, 1998; 24: 21-8.

11. Deininger MH, Weller M, Streffer J, Meyermann R. Antiapoptotic Bcl-2 family protein expression increases with progression of oligodendroglioma. Cancer, 1999; 86: 1832-9.

12. Bredel M. Anticancer drug resistance in primary human brain tumors. Brain Research Reviews, 2001; 35: 161-204.

13. Cartron PF, Oliver L, Martin S, Moreau C, LeCabellec MT, Jezequel P, Meflach K, Vallette FM. The expression of a new variant of the pro-apoptotic molecule Bax, BaxΨ, is correlated with an increased survival of glioblastoma multiforme patients. Human Molecular Genetics, 2002; 11: 675- 87.

Bcl-xl and Bak protein expression in human optic nerve axons in eyeballs post- trauma and in the eyes with absolute glaucoma

Reszeć J[1], Zalewska R[2], Mariak Z[2], Sulkowski S[1]

[1]Department of Pathology Medical University of Bialystok, [2]Department of Ophthalmology
Medical University of Bialystok, Poland

Abstract

The aim of our study was an evaluation of Bcl-xl and Bak protein expressions in optic nerve axons in eyeballs after severe injury and absolute glaucoma. We examined a series of 41 eyeballs, which were enucleated, following extensive injury and a series of 19 eyeballs from patients with absolute glaucoma. The immunohistochemical reaction was performed, using antibodies against human Bcl-xl and Bak protein with LSAB and DAB. In the injured eyeballs in Group I, Bcl-xl protein expression was observed in 53.8%, Bak in 38.5%, in Group II, Bcl-xl in 40%, Bak 55%; in Group III, Bcl-xl in 62.5%, Bak in 62.5%. Nine (9), out of 19 (47.4%) cases showed Bcl-xl protein positivity, Bak 15, out of 19 (78.9%). The percentage of cases with Bak protein positivity was statistically higher than that for Bcl-xl (Bak/Bcl-xl p=0.0356). The results showed that there may be a dominance expression of proapoptotic proteins in optic nerve axons in glaucoma.

Introduction

Perforative or obtuse severe trauma of the eyeball frequently leads to complete and permanent loss of vision, which is usually caused by a direct mechanical damage to photoreceptors and nerve cells, as well as in result of necrosis and apoptosis. Retinal detachment can also be caused by trauma. In animal experimental models, apoptosis - the programmed death of cells - has been implicated as the major factor in the mechanism, leading to death of photoreceptors in this condition [1, 2]. It is known, that the death of retinal ganglion cells, the axons of which form the optic nerve, can be caused by experimental axotomy. It has been demonstrated that retinal ganglion cell degeneration, due to trauma of this kind, is caused by apoptosis [1, 2, 3, 4]. However, to date, there have been no reports concerning the mechanism of axon damage of ganglion cells, due to severe trauma of the eyeball. Glaucoma is an optic neuropathy, characterized by retinal ganglion cell death, axon loss, and an excavated appearance of the optic nerve head. Retinal ganglion cell mechanisms in experimental animal models of glaucoma and in human glaucoma have been shown to involve apoptosis [5, 6, 7, 8]. The apoptotic cascade invokes a series of cellular events which lead to cell death. Proteins from the Bcl-2 family play a major role in apoptosis regulation at its decisive stage [9, 10]. Bcl-2 protein family may inhibit apoptosis - anti-apoptotic: Bcl-2, Bcl-xl, Bcl-w and protein enhancing apoptosis -proapoptotic: Bcl-xs, Bak and Bax [9, 11, 12]. There are no reports on apoptotic protein expression in human retinal ganglion cells and their axons under physiological conditions. It is not known how protein expression in the Bcl-2 subgroup changes in posttraumatic conditions, the opportunity to assess the expression of these proteins in the unique material provided in the form of eyeballs enucleated as a result of severe trauma is interesting and useful in attempting to explain the process of apoptosis in retinal ganglion cells. The aim of our study was an evaluation of Bcl-xl and Bak expression in optic nerve axons in eyeballs after severe trauma and absolute glaucoma.

Material and Methods

We examined a series of 41 eyeballs, which were enucleated after an extensive injury at the Department of Ophthalmology of the Medical University of Bialystok over the period from 1991 to 2003, and a series of 19 eyeballs from patients with absolute glaucoma, suffering from severe ophthalmalgia and treated, of neces-

ADDRESS FOR CORRESPONDENCE:
Joanna Reszeć
Department of Pathology
Medical University of Bialystok
Waszyngtona 13; 15-269 Bialystok, Poland;
e-mail: joasia@zpk.amb.edu.pl

Table 1. Correlations between examined marker expressions and the type of injury

Protein expression	Type of injury				P value
	Closed injury		Perforating injury		
	%	N number	%	N number	
Bcl-xl -	47.8%	11	55.6%	10	p=0.74
Bcl-xl +	13%	3	16.7%	3	
Bcl-xl ++	39.1%	9	27.8%	5	
Bak -	43.5%	10	55.6%	10	p=0.22
Bak +	30.4%	7	38.9%	7	
Bak ++	26.1%	6	5.6%	1	

sity, by enucleation. After enucleation, the eyeballs were fixed in a 10% buffered formalin solution, embedded in paraffin at 56°C, then cut into 5 mm slices and stained with haematoxylin and eosin (H+E). The evaluation of Bcl-xl and Bak protein expressions was performed with the immunohistochemical reaction, using monoclonal antibodies from the Santa Cruz Biochemicals (Bak No N-20, sc-1035, Bcl-xl No A-20, sc- 7122). In order to visualize the antigen-antibody reaction, the LSAB technique was applied, using DAB (diaminobensidine). The IgG1 kappa (DAKO) antibody was used as a negative control, whereas samples of breast cancer tissue, which showed a strong positive Bcl-xl and Bak immunoreactions, were used as a positive control. Two independent pathologists performed the immunohistochemical evaluations of Bcl-xl and Bak proteins. The estimation of immunostaining was done under a light microscope in representative fields, using a lens with magnification of 20x in the optic nerve axons and sections were obtained from the retrolaminar region of the optic nerve head. The criteria for a positive reaction were as follows: (++) above 50% of axons of the field was showing positive immunostaining, (+) between 50%-10% and (-) below 10% of cells with positive immunostaining. Bcl-xl and Bak positive reaction in the optic nerve axons was observed as a granular, cytoplasmatic staining. We statistically analyzed Bcl-xl and Bak protein expression in relation to the time, elapsing from trauma to enucleation (all the cases were divided into 3 time-groups: on the day and one day post-trauma; 2-16 days post-trauma and 1 month till 4 years post-trauma enucleation was performed). Statistically analyzed were the relationships between the expression of examined proteins and the patients' sex and age, as well as the correlation between Bcl-xl and Bak protein expressions. Bcl-xl and Bak protein expressions were compared in both groups: in the absolute glaucoma and the post-trauma group. The obtained results were statistically analyzed, using the Fisher or Chi-square tests, as well as the Student's t-test for paired samples (the correlation between Bcl-xl and Bak protein expression), employing the SPSS software package v.8.0 for Windows (SPSS Inc., Chicago, IL). The values at $p< 0.05$ were considered statistically significant.

Results

The series of 41 examined eyeballs came from male patients, aged between 18 and 77 years (the average age: 45 years, SD +/-17,8). In 23 cases, we observed ruptured globes, secondary to severe blunt trauma. In 18 cases, the eye injury was caused by a sharp tool (severe corneal and scleral lacerations). In 13 patients, enucleation was performed on the day of trauma and 1 day post-injury (Group I), in 20 cases, 2-16 days post-injury (Group II) and in 8 patients, 1 month till 4 years after trauma (Group III). Bcl-xl and Bak protein expressions were observed in cellular cytoplasm. The analysis of expression of the examined proteins in both closed and perforating injury groups is shown in Table 1. Comparing the injury time groups and the expressions of proteins, the results are as followed: in Group I, Bcl-xl protein expression was observed in 53,8%, Bak in 38,5%, in Group II, Bcl-xl in 40%, Bak 55%; in Group III, Bcl-xl in 62,5%, Bak in 62,5%. There was no statistically significant correlation between the type of injury and either Bcl-xl or Bak protein expression. Closed injury was observed mainly in older patients. There was no correlation between Bcl-xl and Bak protein expressions. The series of 19 examined eyeballs came from male patients (11) and female patients (8), aged between 21 and 86 years (the mean age 59,7 +/-19,7). Nine (9), out of 19 (47,4%) cases showed Bcl-xl protein positivity, Bak - 15, out of 19 (78,9%). In the group with absolute glaucoma, there was no correlation between the patients' age, sex or Bcl-xl, Bak protein expression. The percentage of cases with Bak protein positivity was statistically higher than that for Bcl-xl (Bak/Bcl-xl p=0.0356). The results showed that there might be dominance expression of proapoptotic proteins in optic nerve axons in glaucoma, what may suggest axon cell death by apoptosis.

Discussion

Apoptosis, which is the reverse process to mitosis, is connected, amongst others, with tissue mass control, organ formation during morphogenesis and with removal of infected or genetically damaged cells, the survival of which would be harmful to the organism. In case of glaucomatous optic nerve atrophy, increased apoptosis is observed, causing an irreversible damage to optic nerve axons and, in consequence, resulting in vision loss. In our study, a significant Bak protein expression was noticed. Bcl-xl protein, which inhibits apoptosis, showed weak expression in optic nerve axons in glaucoma. In cases of post-traumatic retinal detachment and axotomy, a pathological intensification of apoptosis takes place, manifesting itself in photoreceptor and retinal nerve cell damage. Our study showed expres-

sions of Bcl-xl and of proapoptotic proteins similar both in closed and perforating injuries. Bak protein expression was high after 1 month from injury. The positive correlation between Bcl-xl and Bak protein expression may point out at an intensification of apoptosis process in optic nerve axons in injured eyeballs. On the day, 1 day and 1 month after trauma, programmed cell death seemed to achieve the highest activity, moreover, proapoptotic processes may have dominated the antiapoptotic ones in the matter of the time period from eyeball injury. Napankangas et al. observed increased Bax and Bak protein expressions on the 4th day after optic nerve transection [11]. The results of our study may suggest that there are significant differences between the expression of apoptotic proteins, such as Bcl-2, Bcl-xl, Bak and Bax in human optic nerve axons in the eyeballs after severe trauma. There may be a dominating expression of proapoptotic proteins in optic nerve axons in glaucoma, what may suggest axon cell death by apoptosis.

References

1. Bien A, Seidenbecher CI, Bockers TM, Sabel BA, Kreutz MR. Apoptotic versus necrotic characteristics of retinal ganglion cell death after partial optic nerve injury. J Neurotrauma, 1999; 16: 153-163.

2. Bonfati L, Chierzi S, Cenni MC, Liu XH, Martinou JC, Maffei L, Rabacchi SA. Protection of retinal ganglion cells from natural and axotomy - induced cell death in neonatal transgenic mice overexpressing bcl-2. J Neurosci, 1996; 16: 4186-94.

3. Cellerino A, Bahr M, Isenmann S. Apoptosis in the developing visual system. Cell Tissue Res, 2000; 301: 53-69.

4. Chang CJ, Lai WW, Edward DP, Tso MO. Apoptotic photoreceptor cell death after traumatic retinal detachment in humans. Arch Ophthalmol, 1995; 113: 880-6.

5. Brubaker RF. Deleyed functional loss in glaucoma. L II Edward Jackson memorial lecture. Am J Ophthalmol, 1996; 121: 473-83.

6. Napankangas U, Lindqvist N, Lindholm D, Hallbook F. Rat retinal ganglion cells upregulate the pro-apoptotic BH3-only protein Bim after optic nerve transection. Brain Res Mol Brain Res, 2003; 12: 30-7.

7. Nickells RW. Apoptosis of Retinal Ganglion Cells in Glaucoma: An Update of the Molecular Pathways Involved in Cell Death. Surv Ophthalmol, 1999; 43: 151-61.

8. Okisaka S, Murakami A, Mizukawa A. Ito J. Apoptosis in retinal ganglion cell decrease in human glaucomatous eyes. Jpn J Ophthalmol, 1997; 41: 84-8.

9. Allsopp TE, Wyatt S, Patersen HF, Davies AM. The proto-oncogene bcl-2 can selectively rescue neutrophic factor-dependet neurons from apoptosis. Cell, 1993; 73: 295-307.

10. Chittendent T, Harrington EA, O Connor R, Flemington C, Lutz RJ, Evans GJ, Guild BC. Induction of apoptosis by the BCL-2 homologue Bak. Nature, 1995; 374: 733-6.

11. Dietz GP, Kilic E, Bahr M, Isenmann S. Bcl-2 is not reguired in retinal ganglion cells surviving optic nerve axotomy. Neuroreport, 2001; 12: 3353-6.

12. Cook B, Levis GP, Fischer SK, Adler R. Apoptotic Photoreceptor degeneration in experimental retinal detachment. Invest Ophthalmol Vis Sci, 1999; 43: 151-61.

Bcl-2 and Bax protein expression in human optic nerve axons in the eyeballs after severe trauma and in the eyes with absolute glaucoma

Zalewska R[1], Reszeć J[2], Mariak Z[1], Sulkowski S[2], Proniewska-Skrętek E[1]

[1]Department of Ophthalmology, [2]Department of Pathology, Medical University of Bialystok, Poland

Abstract

The aim of our study was to evaluate the immunohistochemical expression of Bcl-2 and Bax protein in optic nerve axons after severe eyeball injury and in the eyes with absolute glaucoma. A series of 19 eyeballs, enucleated because of absolute glaucoma and 41 eyeballs, enucleated, following extensive injury, at the Department of Ophthalmology of the Medical University of Bialystok, were taken into our study. The immunohistochemical reaction was performed with Bcl-2 and Bax protein antibodies and by the LSAB technique. DAB was used in order to visualise the reaction. The optic nerve axons in glaucomatous eyeballs showed statistically significant higher Bax protein expressions than those of Bcl-2 proteins. In the optic nerve axons after severe eyeball injury, a non-significantly higher Bcl-2 protein expression was observed.

Key words: optic nerve axons, trauma, absolute glaucoma, apoptosis, Bcl-2, Bax.

Introduction

Almost all body cells have a capacity to undergo a programmed cell death process. They differ in the ease with which they are able to initiate apoptosis. The tendency to initiate apoptosis and the speed with which this program is triggered depend on the type of cells and their stage of development. Cells, which are difficult to replace, including neurons of the developed nervous system, undergo apoptosis with some difficulty. Nevertheless, under normal physiological conditions, the average person loses 10000 retinal ganglion cells annually, due to apoptosis [1, 2, 3]. Proteins from the Bcl-2 family play a major role in apoptosis regulation at its decisive stage [4, 5, 6]. There are few studies, concerning apoptotic protein expression in human retinal ganglion cells in pathological states [7, 8]. It is not known how Bcl-2 and Bax protein expressions change in posttraumatic conditions. Glaucomatous optic neuropathy is multifactorial in etiology. Both mechanical and vasogenic theories remain viable explanations for the observed nerve damage and the destructive effect of trophic withdrawal could be espoused by either theory. Each theory feeds into the final common pathway of cell death by apoptosis [9, 10]. The aim of our study was an immunohistochemical evaluation of Bcl-2 and Bax protein expression in the optic nerve axons in eyeballs after severe trauma and in the eyes with absolute glaucoma.

Material and methods

We examined a series of 41 eyeballs, which were enucleated, following extensive injury over the period between 1991 and 2003 and a series of 19 eyeballs from patients with absolute glaucoma, suffering from severe ophthalmalgia treated of necessity by enucleation during the same period at the Department of Ophthalmology of the Medical University of Bialystok. After enucleation, the eyeballs were fixed in a 10% buffered formalin solution, embedded in paraffin at 56°C, then cut into 5µm slices and stained with hematoxylin and eosin (H+E). The evaluation of Bcl-2 and Bax protein expression was performed by the immunohistochemical reaction, using monoclonal antibodies from The Santa Cruz Biochemicals and DAKO (Bax No P-19, sc-526, DAKO/Bcl-2 No MO887) and LSAB technique. The IgG1 kappa antibody was used as a negative control, whereas samples of breast cancer tissue, which showed a strong positive

ADDRESS FOR CORRESPONDENCE:
Renata Zalewska
Department of Ophthalmology
Medical University of Białystok
M. Skłodowskiej-Curie 24A, 15-276 Białystok, Poland
e-mail: renata-zalewska@wp.pl

Table 1. Correlations between examined marker expressions and the type of injury

Protein expression	Type of injury				p value
	Closed injury		Perforating injury		
	%	Number	%	Number	
Bcl-2 (-)	8,7	2	44,4	8	p= 0,012
Bcl-2 (+)	60,9	14	50	9	
Bcl-2 (++)	30,4	7	5,6	1	
Bax (-)	34,8	8	55,6	10	p= 0,36
Bax (+)	47,8	11	27,8	5	
Bax (++)	57,1	4	16,7	3	

Figure 1. Cytoplasmatic Bcl-2 protein immunostaining in the optic nerve axons after severe eyeball injury (mag.x200).

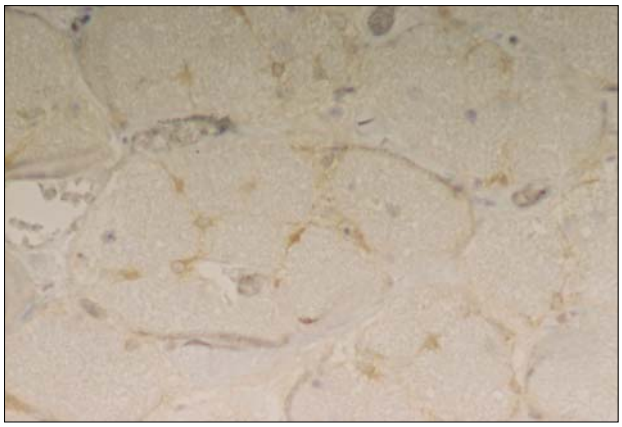

Figure 2. Cytoplasmatic Bax protein immunostaining in the optic nerve axons after severe eyeball injury (mag.x 400).

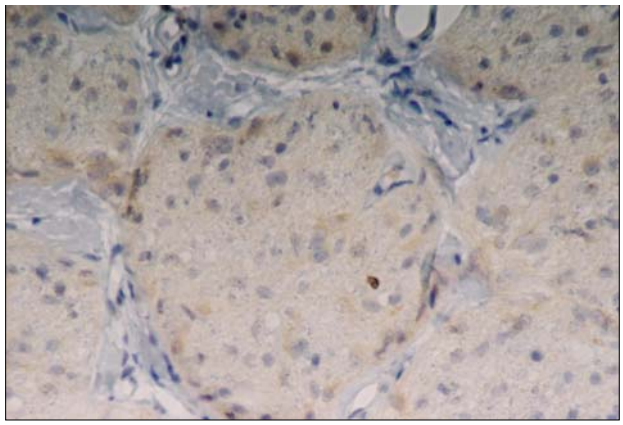

Bcl-2 and Bax immunoreaction, were used as a positive control. The estimation of immunostaining was done under a light microscope in representative fields, using a lens with a magnification of 20x in the optic nerve axons and sections were obtained from the retrolaminar region of the optic nerve head. The criteria for a positive reaction were as follows: (++) above 50% of axons of the field was showing positive immunostaining, (+) between 50%-10% and (-) below 10% of cells with positive immunostaining. We analyzed Bcl-2 and Bax protein expressions in relation to the patients age, sex and the relationships between the examined markers in both groups, as well as Bcl-2 and Bax protein expressions in relation to the time, elapsed from trauma to enucleation and to the type of injury. The obtained results were statistically analyzed, using Fisher and Chi-square tests. Differences at $p<0.05$ were considered statistically significant.

Results

The group of trauma patients: the series of 41 examined eyeballs came from male patients, aged between 18 and 77 years (the mean age: 45 years, SD±17,8). In 23 cases, we observed ruptured globes, secondary to severe blunt trauma. In 18 cases, the eye injury was caused by a sharp tool (severe corneal and scleral lacerations). All the injured and ruptured eyes were blind. In 13 patients, enucleation was performed on the day of trauma or 1 day post-injury (Group I), in 20 cases, 2-16 days post injury (Group II), and in 8 patients - 1 month till 4 years after trauma (Group III). Bcl-2 and Bax protein expressions were observed in cellular cytoplasm. The analysis of Bcl-2 and Bax protein expression in closed and perforating injury groups is shown in Table 1. In the entire trauma group, the mean age of patients without Bcl-2 protein expression in the optic nerve axons was 34.44±18.6 years and was lower than the mean age of patients with Bcl-2 overexpression: 49.04±19.78 years (p=0,065). Bcl-2 protein expression was stronger than Bax expression (statistically non-significant) in the group of trauma patients. In 92.3% patients with enucleation on the day of trauma, or 1 day post-trauma, Bcl-2 protein expression was observed, Bax in 61.5%. In the group with enucleation, 2-16 days post- injury, 60% cases showed Bcl-2 positive expression and Bax 50%. In the 1 month-4 years enucleation post-trauma group, Bcl-2 expression was observed in 87.5% cases, Bax in 62.5%. Bcl-2 and Bax expression did not correlate with the time period from severe trauma to eye enucleation. Bcl-2 protein expression did not correlate with Bax protein expression (Bcl-2/Bax p=0.445).

The group of glaucoma patients: the series of 19 examined eyeballs came from male patients (11) and female patients (8), aged between 21 and 86 years (the mean age: 59.7 years, SD±19.7). In the group of glaucoma patients without Bcl-2 expression, the mean age was 70.1±17 years and was statistically higher than the mean age of patients with Bcl-2 protein overexpression (53.7±18.8 years). Bax protein expression was statistically significantly stronger in the optic nerve axons than Bcl-2 one: Bax/Bcl-2 (p=0.0007) and correlated with Bcl-2 expression: p=0.0155. In the group of glaucoma patients, Bcl-2

and Bax expressions did not depend on sex. The trauma group consisted of male patients only. Bcl-2 and Bax expressions did not correlate with the age in either of the groups.

Discussion

Up until 1993, apoptosis had not been taken into consideration in the studies on the pathogenesis of nerve-related diseases. Disorders of apoptosis have widely been discussed in the literature with regards to neoplastic process [1, 11, 12]. A different situation is observed in cases of posttraumatic retinal detachment and glaucomatous optic neuropathy. A pathological intensification of apoptosis takes place, manifesting itself in retinal nerve cell damage and their axons, leading to sight loss [13, 14]. In our study, in the glaucomatous optic nerve axons, proapoptotic protein expression dominated, what might confirm the apoptotic nerve damage theory. The small percentage of statistically older glaucomatous patients with Bcl-2 protein positivity might be a proof for the proapoptotic tendency, even though, physiologically, a decreased apoptosis process is observed in the course of aging. The correlation Bcl-2 protein expression with Bax protein expression suggested a possibility of Bcl-2/Bax heterodimer creation and continuation of programmed cell death in the optic nerve axons, despite the absolute functional damage of the optic nerve.

Our study showed the expression of Bcl-2 protein to be more significant in the closed injury type group than in the perforating injury group. Bcl-2 protein expression was observed mainly in cases of older people. It is believed that older organisms lose their ability to induce apoptosis. In the whole group of trauma patients, a domination of Bcl-2 protein expression was observed. It was not statistically significant, however, it might be suggestive of some protection mechanism in the optic nerve axons after eye trauma. The results of our study might provoke thinking that, in the stage of absolute glaucoma in the optic nerve axons, proapoptotic Bax protein expression dominated, what is concordant with the apoptotic theory of glaucomatous optic neuropathy. Bcl-2 dominance in the optic nerve axons after severe eyeball trauma might suggest posttraumatic neuroprotection tendency in the optic nerve.

References

1. Allsop TE, Wyatt S, Petersen HF, Davies AM. The proto-oncogene bcl-2 can selectively rescue neurotrophic factor - dependent neurons from apoptosis. Cell, 1993; 73: 295-307.

2. Sulejczak D. Apoptoza i metody jej identyfikacji. Postępy Biologii Komórki, 2000; 4: 527-68.

3. Cellerino A, Bahr M, Isenmann S. Apoptosis in the developing visual system. Cell Tissue Res, 2000; 301: 53-69.

4. Chittendent T, Harrington EA, O'Connor R, Flemington C, Lutz RJ, Evans GJ, Guild BC. Induction of apoptosis by the Bcl-2 homologue Bak. Nature, 1995; 374: 733-6.

5. Levin LA, Schlamp CL, Spieldoch RL, Geszvain KM, Nickells RW. Identification of the bcl-2 family of genes in the rat retina. Invest Ophthalmol Vis Sci, 1997; 38: 2545-53.

6. Reszeć J, Sulkowska M, Guzińska-Ustymowicz K, Zalewska R, Sulkowski S. Wirus brodawczaka ludzkiego a proces apoptozy. Postępy Biologii Komórki, 2003; 2: 311-25.

7. Podesta F, Romeo G, Liu WH, Krajewski S, Reed JC, Gerhardinger C, Lorenzi M. Bax is increased in the retina of diabetic subject and is associated with pericyte apoptosis in vivo and in vitro. Am J Pathol, 2000; 156: 1025-32.

8. Zalewska R, Reszeć J, Mariak Z, Sulkowski S. Ekspresja białek Bcl-2, Bcl-xl, Bak i Bax w aksonach nerwu wzrokowego u chorych z jaskrą dokonaną. KL Oczna, 2004; 106: 155-7.

9. Okisaka S, Murakami A, Mizukawa A, Ito J. Apoptosis in retinal ganglion cell decrease in human glaucomatous eyes. Jpn J Ophthalmol, 1997; 41: 84-8.

10. Halpern DL, Grosskreutz CL. Glaucomatous optic neuropathy: mechanisms of disease. Ophthalmol Clin North Am, 2002; 15: 61-8.

11. Korsmeyer SJ. Bcl-2 initiates a new category of oncogenes: regulators of cell death. Blood, 1992; 80: 879-86.

12. Tatton WG. Apoptotic machanisms in neurodegeneration: possible relevance to glaucoma. Eu J Ophthalmol, 1999; 9: 22-9.

13. Chang CJ, Lai WW, Edward DP, Tso MO. Apoptotic photoreceptor cell death after traumatic retinal detachment in humans. Arch Ophthalmol,1995; 113: 880-6.

14. Nickells RW. Apoptosis of Retinal Ganglion Cells in Glaucoma: An Update of the Molecular Pathways Involved in Cell Death. Surv Ophthalmol, 1999; 43: 151-61.

Osteochondral defects of the talus treated by mesenchymal stem cell implantation - early results

Jancewicz P[1], Dzienis W[2], Pietruczuk M[3], Skowroński J[1], Bielecki M[1]

[1] Department of Orthopaedics and Traumatology, [2]Department of Radiology,
[3]Department of Diagnostic Haematology, Medical University of Bialystok, Bialystok, Poland

Abstract

The purpose of this study was to present early results of talus cartilage defects treatment with autologous mesenchymal stem cells CD34+ implantation technique. Nine (9) patients were treated, due to IV degree chondromalation (by ICRS). The applied standard procedure included: clinical examination, AP and lateral x - ray, MRI, preoperative, as well as during control examination. The surgical procedure consisted of the defect's debridement, harvesting and fixation of the periosteal flap and CD34+ implantation. Clinical results were assessed after 6 months to 3 years by clinical examination, Magee score and MRI. Good and very good clinical results were obtained and confirmed by MRI in 8 cases. In one case, cartilage hypertrophy was noted. There were no delamination and infection signs.

Key words: mesenchymal stem cells, cartilage repairs, osteochondral talus defects.

Introduction

Osteochondral defects with painful failure of the talocrural joint cause inconvenience for patients and decrease their vital activity. Joint cartilage defect is a cause of pain and swelling in lower limb, regardless whether loaded, or at rest. A limited potential for osteochondral defect healing may lead to ankle arthrosis. Usually, in talar chondral defects, the subchondral bone is involved, and either osteosclerotical or cystic lesions make natural healing processes impossible. Joint resurfacing by osteochondral autografts is limited to smaller defects of 2 - 4 cm^2 [1] and the potential donor site morbidity is discussed [2]. Allografts, although successful with some surgeons, impose limitations of donor availability and are associated with disease transmission. Autologous chondrocyte implantation (ACI) is currently indicated for focal, isolated defects [3, 4]. ACI-regenerated hyaline tissue is, sometimes, not properly integrated with the subchondral bone and with healthy chondral defect margins. In large, full thickness defects, delamination of regenerated tissue is frequent.

The new and promising direction of repairing cartilage defects by chondrogenic induction is the autologous mesenchymal stem cell implantation. Mesenchymal stem cells are a rare population of undifferentiated cells, isolated in adults from different tissue sources and differentiating into mesodermal lineages, like: bone, fat, muscles, cartilage, tendons and marrow stroma. Stem cells are multipotential with multidirectional lineage, stimulated by local intrinsic and extrinsic factors. Local environment interactions and tissue signalling molecules provide stimulation to the differentiation of a new line of cells and proper cartilage formation, rebuilding and integration [5, 6]. As for the physiology of healing processes in cartilage defects, the restitution of joint surfaces by hyaline cartilage, as well as subchondral bone reconstruction are of paramount importance, as they warrant normal biomechanical and biochemical properties and a good integration of regenerated tissues.

Materials and Methods

The authors assessed 9 patients, treated by the mesenchymal stem cell implantation technique. All the patients were treated, due to IV degree chondromalation (by ICRS). The standard procedure was: a clinical examination, AP and lateral x - ray and MRI, performed preoperatively, as well as during control assessment. The average defect was 0.5x0.7 cm with 0.5 - 1.0 cm

ADDRESS FOR CORRESPONDENCE:
Jancewicz Piotr
Department of Orthopaedics and Traumatology
Medical University of Białystok
M. C. Sklodowskiej 24A; 15-276 Bialystok, Poland
e-mail: ortopamb@o2.pl, tel: (48 85)7468282, fax: (48 85)7468623

Figure 1. Ankle MRI with osteochondral defect in talus medial site.

Figure 2. Intraoperative view - osteochondral defect.

Figure 3. Intraoperative view - implantation of cells

depth. In deep lesions (more than 0.5 cm), with subchondral bone involvement, autologous cancellous bone grafting (sandwich technique) was performed in all the cases. The defects as well as the operative solutions were photographically documented. The

Figure 4. MRI after 9 months from the operation.

patients were stimulated by growth factor G-CSF (0,3 mg subcutaneously per seven days). Cytometric assessment of patient blood and leukocytes and reticulocyte assessment were performed 3 times during the stimulation period. Mesenchymal stem cells were harvested from patient blood by cell separators on the day of the surgery. Cell suspension was measured in a flow haemocytometer and the quantity of cells with membrane CD34+ marker was counted (cell/cm^3 suspension).

The surgery procedure consisted of resection of damaged tissues, harvesting of the periosteal flap from anteromedial surface of the tibia, flap fixation by suturing and fibrin glue and, finally, an injection of CD34+ cell suspension. Surgical exposure to the talus was either anterior or by ankle osteotomy - medial and lateral. The site of osteotomy was fixed with screws. Clinical and radiological results were assessed after 3 months to 3 years after surgery. Ankle function was evaluated, both clinically and by the Magee 10-point score (patient subjective gait assessment [7].

Magee score:	
without limitation	10 points
pain after long distance	8
mild compliance	6
moderate compliance	4
walking with crutches	2

In MRI (T1, T2 and STIR sequences), major attention was paid to good defect reconstruction, rebuilding of subchondral bone, proper integration of regenerated cartilage with bone and intact defect margins.

Results

In all the cases, good wound healing was observed. No bacterial infections were observed in any of the patients. In 8 cases, gait assessment after operation (Magee score) improved and the patients, after three months, had not limitations in walking. We observed one case with longer bone healing at the site of ankle

osteotomy. In MRI (T1, T2 and STIR sequences), it was observed in all the patients that the defects were well refilled with tissue with signal the same as that from normal cartilage. In two cases, fibrotic changes in margin parts of regenerated tissue and the periosteal flap were found. In one patient, hypertrophic tissues of the reconstructed area were shown. Neither swelling, nor locking nor pain was observed after 3 months from the operation. Delamination of repaired cartilage was not observed in any of the cases. Furthermore, proper integration of regenerated cartilage with rebuilt subchondral bone and MRI confirmed intact defect margins. The examples of good results, confirmed by MRI, are shown in Fig. 1. - Fig. 4.

Discussion

The obtained early clinical results of talus resurfacing with mesenchymal stem cell CD34+ implantation provide promising operative prospects in talar chondromalatia. It is very important to confirm such early observations after 6-7 and more years from the surgery. An annual assessment and MRI control seems to be a valuable procedure for graft rebuilding, and biomechanics evaluation. In deep cystic osteochondral lesions, cancellous bone grafting was necessary for the restoration of normal bone stock to stem cell CD34+ implantation. This is also very important, due to the restoration of talus mechanical function in the ankle joint. The presented autologous stem cell implantation technique is, together with ACI, one of the valuable repair procedures, as it offers possibilities of defect refilling with hyaline or hyaline-like cartilage. Experimental studies [6] presented morphological, histological and histochemical rebuilding of stem cell grafts in animal models. Hyaline or hyaline-like cartilage were the final result of cell transplantation. Multidirectional potential of stem cell differentiation, stimulated by local environment factors, such as the transforming growth - factor - beta family or bone morphogenetic proteins [5, 8], gives possibilities of implant conversion to chondrocytes and revascularised subchondral bone. An important observation in this study was the proper refilling of large, full thickness defects with tissues, well integrated with the subchondral part. Delamination was not observed, due to possible rebuilding of subchondral bone with good revascularisation [6]. By contrast to the autologous chondrocyte implantation technique, bone bleeding predicts better subchondral healing and good integration of regenerated hyaline cartilage. Final MRI assessment in all the cases showed subchondral restoring and satisfactory integration of grafts, which may have good long-term results.

Conclusions

The stem cell CD34+ implantation technique is a valuable procedure in large, full thickness talus cartilage repair. Bone grafting must be performed in all cases of deep osteochondral defect to obtain bone stock restoration and proper chondral integration.

References

1. Bobic V. Osteochondral autologous graft transplantation in the treatment of focal articular lesions Seminars in Artroplasty, 1999; 10: 1-21.
2. Guettler J, Jurist K, Demetropoulos CK, Yang K. Dynamic evaluation of contact pressure and effect of graft harvest at osteochondral donor site in the knee. Program and abstracts of 27th Annual Meeting of American Orthopedic Society for Sports Medicine; June 28-July 1, 2001; Keystone, Colorado. Scientific Session.
3. Mandelbaum BR, Browne JE, Fu F, Micheli L, Mosely JB Jr, Erggelet C, Minas T, Peterson L. Articular cartilage lesions of the knee. Am J Sports Med, 1998; 26: 853-61.
4. Brittberg M, Lindahl A, Nilsson A, Ohlsson C, Isaksson O, Peterson L. Treatment of deep cartilage defects in the knee with autologous cultured chondrocytes transplantation. N Engl J Med, 1994; 331: 889-95.
5. Wakitani S, Goto T, Pineda SJ, Young RG, Mansour JM, Caplan AI, Goldberg VM. Mesenchymal cell-based repair of large, full-thickness defects of articular cartilage. J Bone Joint Surg Am, 1994; 76: 579-92.
6. Pittenger MF, Mackay AM, Beck SC, Jaiswal RK, Douglas R, Mosca JD, Moorman MA, Simonetti DW, Craig S, Marshak DR. Multilineage potential of adult human mesenchymal stem cells. Science, 1999; 284: 143-47.
7. Magee D J. Orthopedic physical assessment. W.B. Saunders Company Philadelphia 1992.
8. Urist MR, Nogami H. Morphogenic substratum for differentiation of cartilage tissues in culture. Nature, 1970; 225: 1051-2.

Comparison of cartilage self repairs and repairs with costal and articular chondrocyte transplantation in treatment of cartilage defects in rats

Szeparowicz P[1], Popko J[1], Sawicki B[2], Wołczyński S[3], Bierć M[1]

[1]Department of Paediatric Orthopaedics and Traumatology, [2]Department of Histology and Embryology,
[3]Department of Gynaecological Endocrinology, Medical University of Białystok, Poland.

Abstract

In our experiment, we tried to assess the potential of repair of full-thickness defects in articular cartilages of rabbit femurs. An artificially made, full-thickness defect in the rabbit's femoral patellar groove was created. The defects were divided into six groups. The reparative tissue was evaluated by macroscopic, histological, and immunohistochemical examinations. The reparative tissues in defects with transplanted chondrocytes, had mostly a hyaline-like cartilage appearance and were firmly attached to the surrounding normal cartilage. Only in the control group with periosteal flap and broken subchondral plate, there were signs of partial repair. Self repair of rabbit articular cartilage is very limited. Transplantation of chondrocytes, costal and articular, without differences between groups, is a very potential treatment, producing hyaline-like repair tissue with good histological results.

Key words: articular cartilage repair, costal and articular chondrocytes, transplantation.

Introduction

The intrinsic capacity of cartilage to self-repair chondral injuries is poor. Many different techniques to induce cartilage repair have been explored. Many, currently used, methods involve an introduction of chondrogenic cells into the defects [1, 2, 3]. Chondrogenic cell transplantation, held in place by a covering periosteal flap, produces a hyalin-like repair tissue [4, 5, 6]. In our experiment, we tried to answer the following questions: Is self-repair of articular cartilage possible? When does it occur? Is the self-repair comparable with chondrocyte transplantation?

ADDRESS FOR CORRESPONDENCE:
Janusz Popko
Department of Paediatric Orthopaedics and Traumatology,
Children's Hospital
Waszyngtona 17, 15-274 Białystok, Poland
Tel: +4885 7450896, Fax +4885 7450895; e-mail: jpopko@amb.edu.pl

Materials and methods

Nine (9) New Zealand White male rabbits were used in the experiment. Defects were created on the patellar grooves of the rabbit femur. A culture of chondrocytes and surgical procedures were performed as described before [7]. The defects were divided into 6 groups: A) filled with costal chondrocyte transplantation and covered with a periosteal flap. B) filled with articular chondrocyte transplantation and covered with a periosteal flap. Control groups without chondrocytes: C) covered with a periosteal flap without breaking the subchondral plate. D) without periosteal flap, without breaking the subchondral plate. E) without periosteal flap, with the broken subchondral plate. F) with a periosteal flap, with the broken subchondral plate. The surfaces of the grafts were inspected for colour, integrity, contour and smoothness.

The histological staining with Safranin O, haematoxylin-eosin and Azan methods (azocarmine + anilin blue) were performed. For immunohistochemical analysis, specific antibodies against rabbit collagen type II (Novocastra) were used.

Results

The reparative tissue, in the defects with the transplanted chondrocytes, showed an appearance, similar to that of normal cartilage in all the groups. The defects were filled with a white, glossy and smooth tissue and were firmly connected to the adjacent normal cartilage. (Fig. 1ABCD). The defects in the control groups were filled with a red semitransparent tissue with dis-

Figure 1. Gross photographs of patellar groove of rabbit femurs, a complete incorporation of the repair tissue into the surrounding cartilage with clearly recognizable margins of the defect (A, B - costal, C, D - articular chondrocytes transplantation).

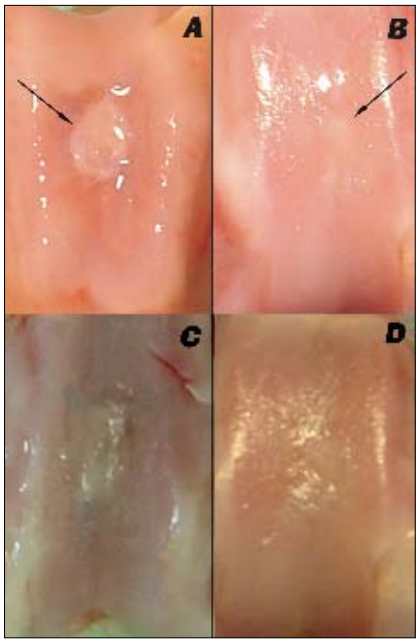

Figure 2. Gross photographs of patellar groove of rabbit femurs, partially filled by repair tissue (A- group E; B-group E; C-group C; D- group D).

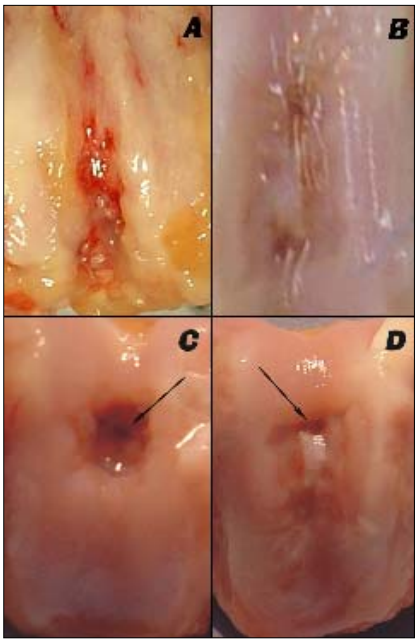

Figure 3. Photomicrograph of section of the reparative tissue with transplantation of costal chondrocytes, deep layers of scar tissue, at 4 weeks, showing numerous irregular groups of chondrocytes with abundance of the extracellular matrix. Safranin O staining, scale bar, 100 µm.

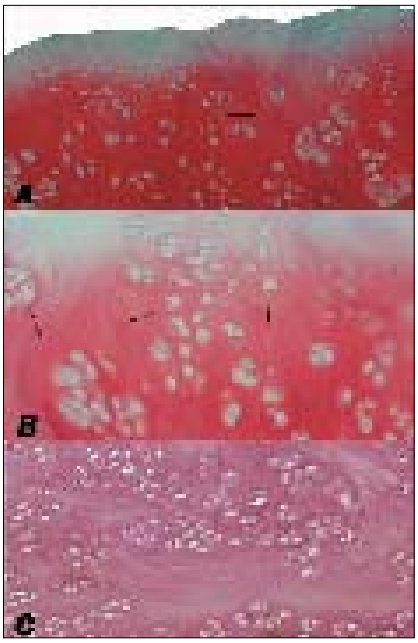

Figure 4. Photomicrograph of section of the reparative tissue with transplantation of articular chondrocytes (A, B), fibrocartilage (C). Safranin O staining, scale bar, 100 µm.

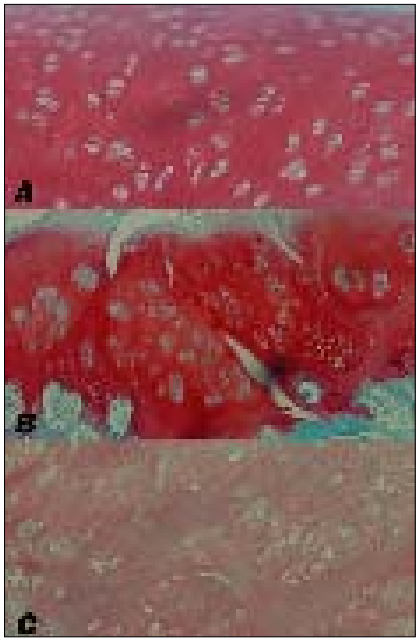

Figure 5. Photomicrograph of section of the reparative tissue with transplantation of costal chondrocytes, intense immunohistochemical positive staining for collagen II (B, C), healthy cartilage (A); scale bar 50 µm.

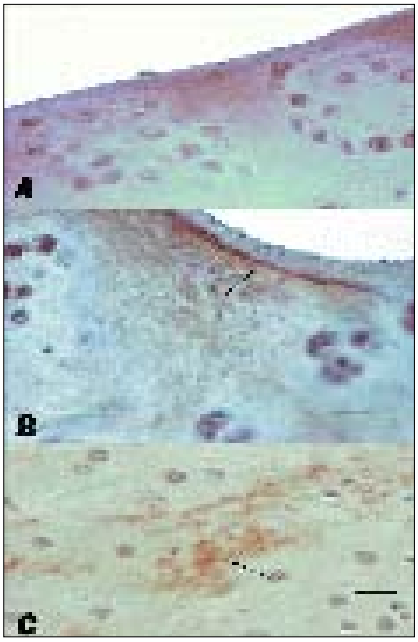

Figure 6. Photomicrograph of section of the reparative tissue, Group F- partial repair, scarce immunohistochemical positive staining for collagen II; scale bar 50 µm.

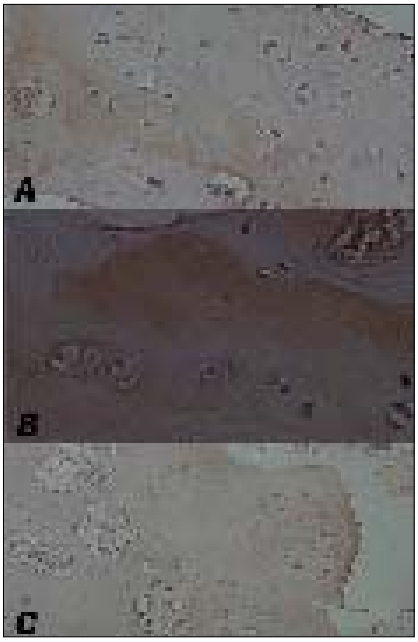

cernible edges and of very low compliance. Small fissures and fractures and loose attachments to the surrounding cartilage were present with no significant differences between groups (Fig. 2ABCD). The defects, transplanted with chondrocytes, were filled with newly formed tissues, firmly incorporated into the surrounding normal cartilage. Most of the defects were filled with a hyalin-like cartilage (Fig. 4, Fig. 5), resembling healthy cartilage. In some specimens, in varying localization, fibro-cartilage of lower hystological grade was present (Fig. 5C). The reparative tissue in the control groups, consisted mostly of numerous fibroblast-like cells, surrounded by many collagen fibres with a chaotic orientation. Its structure was characteristic of fibrous connective

tissue and did not show any significant changes between the groups. A positive immunohistochemical reaction with Collagen II antibody was observed in the repair tissue in each defect with chondrocyte transplantation. Staining distribution varied throughout the defects (Fig. 7BC). The immunopositive reaction in normal cartilage had a very similar appearance (Fig. 7C). Only in group F, the defects were covered with periosteum, with a broken subchondral plate and small islands of immunopositive tissue were present. Those places of incomplete repair were connected with a broken subchondral plate. No traces of immunopositive reaction were present in any of the other groups.

Discussion

Macroscopic observations of repair tissue in the defects with chondrocyte transplantation showed its good incorporation into the surrounding cartilage, which may be of higher importance than the quality of the tissue itself [8], protecting the surrounding normal cartilage from further deterioration [9]. Macroscopic observation in the control groups showed only a partial repair, with a slightly better outcome in Group F but still incomparable to that in the main groups. Those results are similar to findings of other authors [10, 11, 12]. Histological results in the two groups with chondrocyte transplantation, did not show any significant differences. Most of the defects were filled with hyalin-like tissue. In the control groups, only fibrous connective tissue was present. Positive staining with Safranin O, was present only in Groups A and B and showed an intensive production of proteoglicans in young cartilage [9]. Negative staining was present in all the control groups. Many authors have noticed that a partial regeneration of chondral defects can be induced by cells, either migrating from the surrounding tissue or from subchondral bone marrow. However, those cells were not able to induce healing, comparable with that, caused by transplated chondrocytes. That was confirmed by our control group. Repair tissues in empty defects, covered with a periosteal flap with a broken subchondral plate, were limited to small areas, adjacent to the subchondral defect and were of lower macroscopic and histological quality. Immunonegative reaction with Collagen II antibody was observed in every other control specimen. Our findings confirmed those by Kajitani et al [13]. According to this author, periosteal flap might act only as a mechanical barrier to prevent leakage of grafted chondrocytes without beneficial humoral or cellular effect on the formation of reparative tissue. Articular cartilage repair with chondrocyte transplantation gives good repair in terms of macroscopic and histological evaluations. Self-repair is very limited and can not give sufficient healing of the defect, even with the defect spreading under the subchondral plate.

References

1. Brittberg M, Nilsson A, Lindahl A, Ohlsson C, Peterson L. Rabbit articular cartilage defects treated with autologous cultured chondrocytes. Clin Orthop, 1996; 326: 270-83.

2. Chesterman P, Smith AU. Homotransplantation of articular cartilage and isolated chondrocytes. An experimental study in rabbits. J Bone and Joint Surg, 1968; 50B: 184-97.

3. Grande DA, Pitman MI, Peterson L, Menche D, Klein M. The repair of experimentally produced defects in rabbit articular cartilage by autologous chondrocyte transplantation. J Orthop Res, 1989; 7: 208-18.

4. Bentley G, Greer R. B. III. Homotransplantation of isolated epiphyseal and articular cartilage chondrocytes into joint surfaces of rabbits. Nature, 1971; 230: 385-88.

5. Brittberg M. Autologous Chondrocyte Transplantation. Clin Orthop Relat Res, 1999; 367S: 147-55.

6. Brittberg M, Faxen E, Peterson L. Carbon fiber scaffolds in the treatment of early knee osteoarthritis. A prospective 4-year follow-up of 37 patients. Clin Orthop, 1994; 307: 155-64.

7. Popko J, Szeparowicz P, Sawicki B, Wołczyński S, Wojnar J. Rabbit articular cartilage treated with cultured costal chondrocytes (preliminary report). Folia Morphol, 2003; 62: 107-12.

8. Buckwalter JA, Rosenberg LC, Coutts R, et al. Articular cartilage: Injury and repair. In Woo SL-Y, Buckwalter J (eds). Injury and repair of the muscosceletal soft tissues. Park Ridge, American Academy of Orthopedic Surgeons, 1987; 465-82.

9. Breinan HA, Minas T, Hsu HP, Nehrer S, Sledge CB, Spector M. Effect of cultured autologous chondrocytes on repair of chondral defects in a canine model. J Bone Joint Surg Am, 1997; 79: 1439-51.

10. Katsube K, Ochi M, Uchio Y, Maniwa S, Matsusaki M, Tobita M, Iwasa J. Repair of articular cartilage defects with cultured chondrocytes in Atelokollagen gel. Arch Orthop Trauma Surg, 2000; 120: 121-27.

11. Klompmaker J, Jansen HW, Veth RP, Nielsen HK, de Groot JH, Pennings AJ. Porous polymer implants for repair of full thickness defects of articular cartilage. An experimental study in rabbit and dog. Biomaterials, 1992; 13: 625-34.

12. Wakitani S, Goto T, Pineda SJ, Young RG, Mansour JM, Caplan AI, Goldberg VM. Mesenchymal cell-based repair of large, full-thickness defects of articular cartilage. J Bone Joint Surg [Am], 1994; 76: 579-92.

13. Kajitani K, Ochi M, Uchio Y, Adachi N, Kawasaki K, Katsube K, Maniva S, Furukawa S, Kataoka H. Role of the periosteal flap in chondrocyte transplantation: an experimental study in rabbits. Tissue Eng, 2004; 10: 331-42.

Intercellular junctions between odontoblasts as the transmitters of low charge electric current

Alwas-Danowska HM

Department of Pre-Clinical Dentistry and Dental Diagnosis, Medical University of Łódź, Poland

Abstract

The aim of the work was to demonstrate structures responsible for the conduction of pain impulses with regard to tight junctions after transmission of small charges of electric current. For the experiment, freshly extracted (for orthodontic reasons) teeth were used. Immediately after extraction, low charges of electric current were passed through the teeth and the teeth were fixed. Teeth pulps were prepared for TEM studies. The obtained results were compared to those in a control group. In electron microscopic pictures, intercellular junctions are visible irrespective of the value of the current applied on the approximal surfaces of the cells (between the odontoblasts or between the odontoblasts and the neural fibres) as short callosities of plasmolemma.

Key words: odontoblasts, belt desmosom, alternating current, TEM, active transport of water.

Introduction

Apart from many other functions, the odontoblasts are involved in the process of perception and conduction of pain stimuli from the tooth during stomatological procedures. A precise recognition of the structures. connecting the enamel through the dentine with the dental pulp, is a major aspect of dental science. The knowledge of these structures would give us a better understanding of many physiological processes.

In 1968, Frank, for the first time, described nerve endings that formed junctions with odontoblast processes in the first zone of dentin tubules [1]. The studies of dental pulp, predentin and dentin in electron microscope, carried out by this author and next by other researchers [2, 3], have resulted in a conclusion that there are numerous junctions between belt desmosome (zonula adherens), tight junctions (zonula occludens) and gap junctions (nexus) [4]. However, according to Sasaki, it is perhaps more accurate to use the terms fascia adherens and fascia occludens to describe the components of the modified distal junctional complex [5, 6, 7]. This does not change the fact that such junctions enable the, so-called, junctional transfer - a free flow of ions between cells, so they play a function of electric synapses [8, 9]. The presence of these junctions is also suggested by SEM images [10]. Structures, resembling synapses, which occur between the odontoblast processes and neurofibrils have also been reported; those were callosities of plasmolemma near which synaptic vesicles of 50-60 nm in diameter and agglomerations of mitochondria [1] could sometimes be observed [1]. Physiological and cytophysiological features of odontoblasts may suggest that they can be included to the class of the, so-called, paraneurons [11]. Three mechanisms of active transportation are known: 1) group translocation (in bacterial cells), 2) primary active transport and 3) secondary active transport. In the cells of dental pulp, primary and secondary active transports play the role. In the typical cell ion gradients, transversally to the cell membrane, high concentrations of Na^+ and Cl^- get into extracellular space and high concentration of K^+ ions get inside the cell. Ion concentrations balance the osmotic pressure and prevent an influx of water into the cell. The aim of this study was to present structures responsible for the transmission of sensory and pain reflexes, taking into account zonula adherens, after transmitting through them small electric charges.

ADDRESS FOR CORRESPONDENCE:
Alwas-Danowska HM
Department of Pre-Clinical Dentistry and Dental Diagnosis
Medical University of Łódź
Pomorska 251, 92-216 Łódź, Poland
e-mail: alwas@mnc.pl

Materials and methods

The studies were carried out on non-caries teeth, extracted for orthodontic reasons. The teeth were extracted with the use of local anaesthesia. Immediately after extraction, small charges

Figure 1. Dental pulp odontoblasts of the premolar tooth (-4), treated with electric current of 50 μA during 120 sec. Zonulae adherens - of desmosome type, surrounded with circles (white arrows). Black arrow shows the gap junction inside the circle of hemidesmosome (nexus) type. The first circle shows desmosome in the state of repose; the second and the third circles - an active stage. Magnification 30000 x.

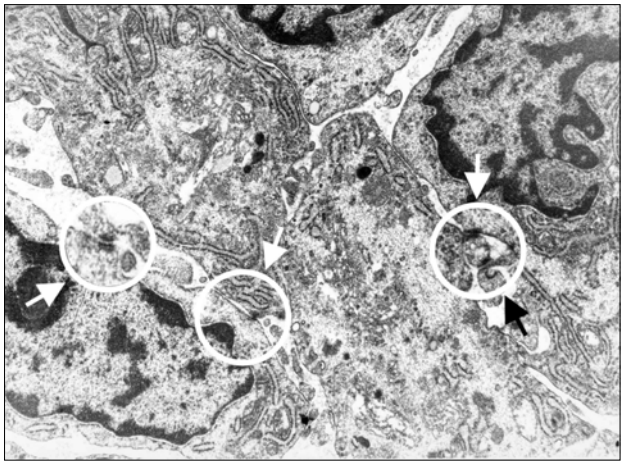

Figure 2. Zonulae adherens (circle) between the axon and odontoblast in active stage, near the vacuole (V). Dental pulp of the premolar tooth (+4), treated with the electric current of 80 μA during 120 sec. Magnification 25000 x.

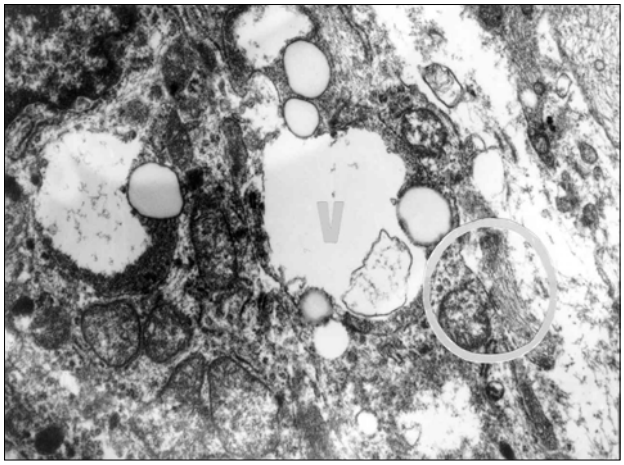

(15 μA, 50 μA, 60 μA, 80 μA for 120 s) of alternating current were transferred through the teeth and then, the teeth were fixed in 2% glutardialdehyde in cacodylate buffer. The teeth were cut and their pulps were fixed in 2% glutardialdehyde in cacodylate buffer and then, in 1% osmium tetroxide. After that, they were dehydrated and embedded in epoxy resin (EPON 812 with DDSA and MNA) for electron microscopic studies. Hemithin sections were prepared with the use of a Tesla BS 480 ultramicrotome and stained with buffered 1% toluidine blue. Ultra thin sections were cut in an MTI ultramicrotome and contrasted with uranyl acetate and lead citrate. They were investigated and photographed in a JEOL electron microscope. The results of the studies were compared with the image of dental pulp tissue through which no electric current had been transmitted and in which, no changes were revealed by the hard tissue. The pulp was also fixed immediately after the teeth extraction, using the method described above.

Results and discussion

In the specimens, through which current from 15 mA to 60 mA passed, belt desmosomes (zonula adherens) and gap junctions were not damaged. These juncturae adherentes are a space of 15-25 nm in width between the adjacent membranes, which contains electron dense material (Fig. 1). On the side of cytoplasm, there is a condensation of hyaloplasm and actin microfilaments. At higher magnifications, different activity stages (passive and active) are observed [12, 13]. The anatomical shape of belt desmosome reminds condensing lenses, what is of great importance in water and ions transportation; electric current (depending on the kind and value) intensifies these processes. As far as the alternating current is concerned, in most specimens, through which current of 80 μA was passed, a higher number of small vacuoles appeared at unchanged belt desmosome (zonula adherens) (Fig. 2). It is worth noting that, in analogical studies with the application of alternating current of similar parameters, fine vacuoles were not visible in a light microscope [14].

In the specimens, prepared for electron microscopy, on the side surfaces of cells (odontoblast-odontoblast, odontoblast - neuron, odontoblast - neutrophil) indirect junctions were observed in the form of callosities of plasmolemma. These junctions enable the, so-called, junctional transfer - a free flow of ions between the cells, thus playing the function of electric synapses. The results of the studies confirm the previously described junctions, observed in SEM.

It can be presumed that, depending on current intensity, a faster accumulation of vacuoles, that appear near the odontoblast nucleus, could induce detachment of a part of cell cytoplasm near zonula adherens (juncturae adherentaes), observed in SEM (that was probably related to the technical process of routine specimen preparation), described by H. Alwas-Danowska [10].

In the dental pulp cells of the experimental group, the cellular membranes and tight junctions were intact, but in the control group the picture of the junctions was indistinct, what could be connected with the water penetration. Because of their anatomical shapes, zonula adhaerens (resembling condensing lenses) in the odontoblasts have a possibility of water intensification and ion transportation processes and the passing electric current of low charges could change them.

Acknowledgement

This study was supported by grant No 502-12-859 from the Medical University in Łódź.

References

1. Frank RM. Ultrastructural relationships between the odontoblasts, its process and the nerve fibers in the dentine and pulp: their structure and functions. N.B.B. Symons ed., (1968), 115.

2. Callé A. Intercellular junctions between human odontoblasts. Acta anat, 1985; 122: 138-44.

3. Stockinger L, Pritz W. Morphologische Aspekte der Schmerzempfindung im Zahn. Dtsch Zahnarztl Z 1970; 25: 559.

4. Arana-Chavez VE, Katchburian E. Freeze fracture studies of the distal plasma membrane of rat odontoblasts during their differentiation and polarisation. Eur J Oral Sciences, 1998; 106; 132-6.

5. Igushi Y, Tamamura T, Hashimoto S, Horiuchi T, Shimono M. Intercellular junctions in odontoblasts of the rat incisor studied with freeze-fracture. Arch Oral Biol 1984; 24: 487-97.

6. Sasaki T, Garant PR. Structure and organization of odontoblasts. Anatomical Record, 1996; 245: 235-9.

7. Sasaki T, Tominaga H, Higashi S. Endocytic activity of kitten odontoblasts in early dentinogenesis. Thin section and freeze - fracture study. J Anat, 1984; 138: 485-92.

8. Bishop MA. Evidence for tight junctions between odontoblasts in the rat incisor. Cell Tissue Res, 1985b; 239: 137-40.

9. Bishop MA, Yoshida S. A permeability barrier to lanthanum and the presence of collagen between odontoblasts in pig molars. J Anat, 1922; 181: 29-38.

10. Alwas-Danowska HM. Scanning electron microscopic studies of the human odontoblasts. Folia Morphol, 1984; 153: 185-90.

11. Fujita M. The paraneurons concept. Neurobiol, 1979; 17: 21-6.

12. Sasaki T, Garant PR. Structure and organization of odontoblasts. Anatomical Record, 1996; 245: 235-49.

13. Sasaki T, Tominaga H, Higashi S. Endocytic activity of kitten odontoblasts in early dentinogenesis. Thin section and freeze - fracture study. J Anat, 1984; 138: 485-92.

14. Alwas-Danowska HM, Huysmans MC, Verdonschot EH. Effects of alternating and direct electrical current application on the odontoblastic layer in human teeth: an in vitro study. Intern End J, 1999; 32: 459-63.

Assessment expression of the adhesion molecules, CD134 and CD137, in patients with colorectal cancer by flow cytometry

Cepowicz D[1], Stasiak-Barmuta A[2], Zalewski B[1], Piotrowski Z[1]

[1]2nd Department of General and Gastroenterological Surgery, [2]Flow Cytometry Laboratory SPDSK
Medical University of Białystok, Poland

Abstract

The aim of the study was to assess the expression of adhesion molecules, CD134 and CD137, in the peripheral blood in correlation with clinical advancement, the histological grade, the size and type of tumour growth, tissue infiltration, and lymph node and metastases to lymph nodes and liver. The study involved 28 patients with primary colorectal cancer. The expression of both molecules was investigated on the day of the surgery, before the procedure and ten days after the operation by means of flow cytometry. The expression of CD134 was markedly higher, compared to CD137, both on the day of the surgery and ten days after the operation. A significant increase was observed in CD134 expression ten days after the surgery. CD137 expression increased with the higher stage of clinical advancement, but decreased with the enhancement of colon wall infiltration. CD134 showed a similar expression for all the stages of tumour clinical advancement.

Key words: colorectal cancer, adhesion molecules, CD134, CD137, metastases.

Introduction

A threat of metastases in colorectal cancer can be expressed as the percentage of risk in relation to the histological grade of the tumour, the extent of involvement at the primary site and lymph node metastases [1]. Immune defence mechanisms start to intervene at the moment of cancer cell formation, that is, at a later phase, when natural anticancerogenic mechanisms have failed. The aim of the study on neoplastic antigens is to evaluate their usefulness in detection, monitoring and treatment, e.g., with monoclonal antibodies, directed against these antigens or using a variety of vaccines that particularly stimulate cell-type response [2]. Studies on the locoregional expression and correlations in colorectal cancer metastasis formation have recently been directed towards immune mechanisms and forms of immunotherapy. Adhesion molecules (CD-clusters of differentiation) constitute a wide group of molecules that vary in structure and function and which are involved in immune responses in a number of pathologies The most commonly investigated ones include: CD49a, CD11a, CD54, CD44, CD102, CD62L [3]. Lately, the role of CD134 (OX-40) and CD137 (4-1BB)) in the course and therapy of colorectal cancer has been emphasized [2, 5, 6, 7, 8, 9]. CD134 (the OX-40 receptor) and OX-40L (ligand) belong to the TNFR superfamily and act as a pair of costimulatory molecules that facilitate the activation of Th2 lymphocytes and IL-4 (ligand) secretion by these cells. The activation of OX-40 leads to an enhanced secretion of antibodies by B cells. OX-40 is expressed on activated T and B cells, dendritic cells and endothelium [9]. CD137 (4-1BB) molecules are the receptors on the surface of T cells and NK (natural killer) cells, and their ligand 4-1BBL is produced by B cells, macrophages and dendritic cells. Due to costimulation of 4-1BB and 4-1BBL, T cells are induced to produce increased amounts of IL-2. The aim of the present study is to assess the expression of adhesion CD134 and CD137 molecules in the peripheral blood in correlation with clinical advancement, histological grade, the size and type of tumour growth, tissue infiltration and lymph node and liver involvement.

ADDRESS FOR CORRESPONDENCE:
Dariusz Cepowicz
2nd Department of General and Gastroenterological Surgery
Medical University of Białystok
M. C. Skłodowskiej 24 A; 15-276 Białystok, Poland
e-mail: darekce@wp.pl

Material and method

The study involved 28 patients with primary colorectal adenocarcinoma, aged 52-83 years, operated on at the 2nd Depart-

ment of General and Gastroenterological Surgery, Medical University of Białystok. Clinical advancement was evaluated, according to Dukes' scale: Dukes A- 2 (7.14%), Dukes B-13 (46.42%), Dukes C- 8 (28.57%) and Dukes D- 5 (17.86%) patients. The study material included fresh peripheral venous blood, collected on the day of the surgery before the procedure and 10 days after the operation. Lymphocytic cells were obtained by mechanical centrifugation. After a two-fold rinsing they were counted in a Burker's chamber. A 10^6 mononuclear cells/ ml RPU/1640 suspension was made and portioned out to obtain 100ul samples, each supplemented with 10 ul of monoclonal CD 134 and CD 137 antibodies, obtained from manufactured sets: CD134 (OX 40)-FITC-34464 X and CD137 (4-1BB)-PE-34465 X, Pharmingen. Then, the samples were quantitatively analysed in a flow cytometer EPICS XL (Coulter), 10^4 cells each time. The results were statistically analysed, using Fisher's test.

Results

The expression of CD134 was markedly higher, compared to CD137, both on the day of the surgery and ten days after the operation. The mean expression of CD134 in both examinations was 13.57% (SD - 9.95), being significantly higher than the mean expression of CD137-6.38% (SD - 10.86) ($p<0,001$). A significant increase was observed in the expression of CD134 ten days after the surgery. Although the mean activities were comparable, significant differences were noted between the medians: on the examination before surgery-10.45 and on the 10th day after surgery-14.35. Figure 1. CD137 expression before the operation (the mean value-5.14%) did not change significantly after the surgical procedure (the mean value-7.63%). CD134 showed a similar level, irrespectively of the tumour stage. The respective mean expression values were following: Dukes A-13.38%, Dukes B-13.41%, Dukes C-11.68%, Dukes D-17.38%, not differing much between the assays before and after the operation. Details, presented in Figure 2, showed that CD137 expression differed significantly between the respective stages of clinical advancement. The highest expression was noted in most advanced lesions ($p<0,001$). In Dukes D patients, high expression of CD137 was observed in both examinations. The activity of CD137 was significantly increased on day 10 after the surgery. In the remaining stages (Dukes A-C), the examinations revealed a similar, much lower activity. Depth of tumour infiltration did not cause any distinct differences in the expression of CD134 in pT1, pT3 and pT4 tumours. Reduced expression was observed in pT2. Tumour resection had no effect on the expression in the respective groups. A similar comparison of CD137 expression revealed its decrease, accompanied by enhanced colon wall infiltration. The mean CD137 expression was 7.38% for pT1, 8.78% for pT2, 6.59% for pT3, and 2.37% for pT4 ($p<0.01$). No differences were found between the examination before and after the operation. Figure 3.

Discussion

Studies on the locoregional tumour expression and correlations in metastasis formation in colorectal cancer have recently been directed towards immune mechanisms and forms of imunotherapy. In patients with cancer, immune reactions, especially of cell type, are attenuated. Moreover, certain immune processes, observed in the patients, may even promote tumour growth [1]. Our studies showed increased CD137 expression with a higher stage of tumour clinical advancement and decreased CD137 expression with enhanced infiltration of the colon wall. We also proved that tumour clinical stage advancement does not affect CD134 expression and its expression increases in the early postoperative period. No results have been found in the available world literature that could be compared with the present findings. Studies, conducted on animals in the USA on the OX-40 molecule and OX-40L ligand, indicate that the molecule is activated by CD4 on T cell surface. Observations on human and animal models revealed an improved therapy outcome in cases of colorectal cancer. In patients with high OX-40 expression, 20% lymphocytes were infiltrated, in approximately 40% of infiltrated cells along tumour margins, in 50% of tumour cells and in all the samples of mesenteric lymph nodes. The levels of OX-40 were not high in the healthy tissue margin. High expression of OX-40 in the primary tumour correlated with 2-55% longer survival time. It thus seems that CD134 molecules can be employed in colorectal cancer immunotherapy [5, 6]. Until now, studies on CD137 (4-1 BB) in colorectal cancer have been performed on animal models. The authors, who investigated mouse liver with metastatic tumours, due to colorectal cancer, reported an optimum outcome of the combined application of IL-12 and CD137 (4-1BB) [7, 8]. The results have indicated that

Figure 1. CD 134 expression before surgery and ten days after surgery.

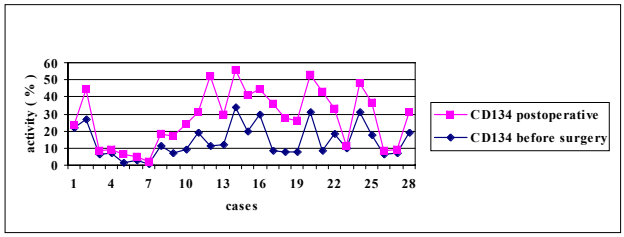

Figure 2. Mean values of CD 137 expression in relation to tumour clinical advancement.

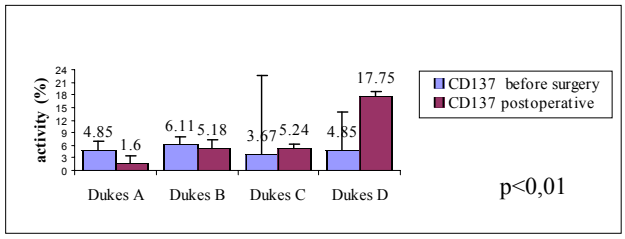

Figure 3. Mean values of CD 137 expression in relation to tumour infiltration depth.

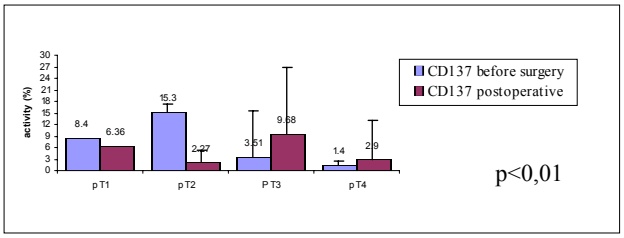

a synergistic action between congenital and acquired immunity can contribute to the treatment of metastatic colorectal cancer, mainly to the liver. However, no comparative studies of this adhesion molecule, conducted either on animal models or in humans, have been available so far [7, 8]. Very few trials have been described of its application in the immunotherapy of chosen neoplasms, including colorectal adenocarcinoma [2]. The two described above adhesion molecules (CD134 and CD137) may create a chance for a positive prognosis of colorectal cancer course and treatment. CD134 (OX-40) can affect the immunotherapy of the tumour itself and prevention of metastasis formation. CD137 seems to have a beneficial effect on the immunotherapy of metastases (mainly to the liver), the fact that inspired the present study. The determination of the level of chosen molecules in the tumour, border tissues, lesion-free margins of the colon and peripheral blood can help analyse the therapy outcome, as well as the risk of metastases and prognosis. It is necessary to perform further investigations of the CD134 and CD137 during 3-6 month postoperative control periods.

References

1. Tebbutt NC, Cattell E, Midgley R, Cunningham D, Kerr D. Systemic treatment of colorectal cancer. Eur J Cancer, 2002; 38: 1000-15.

2. Vonderheide RH, June CH. A translational bridge to cancer immunotherapy: exploiting costimulation and target antigens for active acrive and passve T cells immunotherapy. Immunol Res, 2003; 27: 341-56.

3. Melero I, Gabari I, Corbi AL. An anti-ICAM-2 (CD102) monoclonal antibody induces immuno-mediated regressions of transplantated ICAM-2 - negative colon carcinomas. Cancer Res, 2002; Jun 1, 62: 3167-74.

4. Araki T, Miki C, Kusunoki M. Biological implications of circulating soluble intercellular adhesion molecule-1 in colorectal cancer patients. Scand J Gastronterol, 2001; Apr, 36:299-404.

5. Weinberg AD, Rivera MM, Prell R. Engagement of the OX-40 receptor in vivo enhances antitumor immunity. J Immunol, 2002; Feb, 15: 2160-9.

6. Petty JK, He K, Corlen CL. Survival in human colorectal cancer correlates with expression of the T-cell costimulatory molecule OX-40 (CD134). Am J Surg, 2002; May, 183: 512-8.

7. Chen SH, Pham-Ngoyen KB, Martinet O. Rejection of disseminates metastases of colon carcinoma by synergism of IL-12 gene therapy and 4-1BB costimuloation. Mol Ther, 2000; Jul, 2: 39-46.

8. Martinet O, Ermekova V, Qiao JQ, Sauter B, Mandeli J, Chen SH. Immunomodulatory gene therapy with interleukin 12 and 4-1BB remission of lever metastases in a mouse model. J Natl Cancer Inst, 2000; Jun, 7, 92: 931-6.

9. Croft M. Costimulation of T cells by OX40, 4-1 BB, and CD27. Cytokine Growth Factor Rec, 2003; Jan-Aug; 14: 265-73.

Glycoprotein CD44 variant 4 expression in tumour epithelial cells of patients with colorectal cancer

Zalewski B[1], Stasiak-Barmuta A[2], Sulkowski S[3], Piotrowski Z[1], Myśliwiec P[1], Kukliński A[1]

[1]Department of General and Gastroenterological Surgery, [2]Laboratory of Flow Cytometry, Children Teaching Hospital,
[3]Department of General Pathomorphology, Medical University of Bialystok, Poland

Abstract

The aim of this study was to check if the expression of CD44v4 in epithelial cells of the colorectal cancer correlates with the pTN stage and the histopathological grade of malignancy - G. Samples of tumour tissue (TT), as well as those of healthy tissue (HT) and of tumour adjacent tissue (TAT) were obtained from 25 patients. An evaluation of the expression of CD44v4 was performed in a flow cytometer. The mean value of the percentage of epithelial cells with co-expression of CD44v4 was lower in pT2 stage than that in pT3 only in HT. The expression of CD44v4 in epithelial cells was higher in cases without lymph node metastases only in TAT. The expression of CD44v4 in epithelial cells was higher in G2 than in G3 degree only in TAT as well.. According to the obtained results, it is difficult to state if CD44v4 can influence the progress of colorectal cancer.

Key words: colorectal cancer, carcinogenesis, adhesion molecules, CD44.

Introduction

CD44 is a proteoglycan molecule, distributed on the surface of many types of epithelial cells [1]. It serves as a molecule, binding mononuclear and epithelial cells with extracellular ligands, as it acts as a receptor for hyaluronan, fibronectin and a lot of other substances [2]. Its role in inflammatory process and as adhesion molecule in intercellular communication during carcinogenesis and metastatic processes was described by many authors. However, its role in these processes is still unclear [2, 3, 4].

The aim of this study was to examine, whether the expression of CD44v4 isoform in epithelial cells of tumour, tumour adjacent tissues and healthy tissues of the large bowel in patients with colorectal cancer correlates with the pathomorphological stage of the tumour, acc. to WHO classification (pT), lymph nodes metastases (N) and the histopathological grade of malignancy (G).

Materials and methods

Twenty-five (25) patients were operated on sigmorectal adenocarcinomas in G2-G3 grade of malignancy and pT2- pT3 stage, acc. to WHO score, at our Department in 2002. There were 12 (48%) women and 13 (52%) men. The median age was 62.3 years (the age range: 46 - 84 years). Neoadjuvant radio- or chemotherapy had not been applied to any of the patients. The preoperative diagnosis was based on clinical symptoms and confirmed preoperatively by histopathological examination of biopsy specimens, obtained endoscopically. There were 13 (52%) tumours of the sigmoid colon and 12 (48%) rectal tumours. Other types of cancer and polyps, including inoperable tumours, were excluded from the investigation. There were 12 patients with tumours in G2 grade of malignancy and 13 with G3. Tumour tissue samples were obtained during operations. They were divided into two parts. One part of tissues was typically prepared and paraffin embedded sections were examined to estimate pTN stage and the grade of malignancy in G1-G3 score. There were 12 tumours with G2 and 13 with G3 grade of malignancy. pT2 stage was found in 8 tumours, whereas pT3 in 17. Metastases to lymph nodes were found in 11 patients. The second part of the specimens, consisting of three samples, obtained from healthy tissue (HT), tumour adjacent

ADDRESS FOR CORRESPONDENCE:
Bogdan Zalewski
Department of General and Gastroenterological Surgery
Medical University of Białystok
M. Sklodowskiej-Curie 24a, 15-276 Białystok, Poland
tel.:+48 85 7468287, fax: +48 85 7468624;
e-mail: bogdan-zalewski@wp.pl

Table 1. The mean value of the percentage of epithelial cells with co-expression of CD44v4 in different pT stages.

	CD44v4 (EMA) – medium values ± SD
pT2 / HT	5,2 ± 3,0
pT2 / TAT	12,2 ± 10,9
pT2 / TT	16,8 ± 15,4
pT3 / HT	22,2 ± 11,1
pT3 / TAT	13,7 ± 12,1
pT3 / TT	21,6 ± 13,3
Statistical analysis	pT2/HT v. pT3/HT p<0,009

Table 2. The mean value of the percentage of epithelial cells with co-expression of CD44v4 in different pN stages.

	CD44v4 (EMA) – medium values ± SD
pN0 / HT	20,1 ± 15,1
pN0 / TAT	24,0 ± 12,7
pN0 / TT	18,5 ± 12,2
pN1 / HT	20,0 ± 6,0
pN1 / TAT	8,5 ± 9,1
pN1 / TT	24,7 ± 15,4
Statistical analysis	pN0 / TAT v. pN1 / TAT p<0,006

Table 3. The mean value of the percentage of epithelial cells with co expression of CD44v4 in different grades of malignancy.

	CD44v4 (EMA) – medium values ± SD
G2 / HT	23,9 ± 14,6
G2 / TAT	23,3 ± 9,0
G2 / TT	19,4 ± 10,8
G3 / HT	16,3 ± 8,9
G3 /TAT	14,1 ± 2,5
G3 / TT	25,3 ± 18,8
Statistical analysis	G2 / TAT v. G3 / TAT p<0,05

tissue (TAT) and tumour tissue (TT) was placed in a sterile container with RPMI -1640. Immediately after collection (max. 2h), respective fragments of tissues were minced to receive a homogenous cells suspension. To each 100 µl of the cell suspension, 10 µl of monoclonal antibodies EMA-FITC (Epithelial Membrane Antigen - DAKO) and CD44v4-PE (Immunotech) were added. After 20 minutes of incubation at room temperature in the dark, an automatic lysis was performed (EPICS IMMUNOLOGY WORK STATION - Coulter). Analyses of cells were performed, using a Coulter EPICS XL flow cytometer. A minimum of 10^4 cells were counted. Conforming isotypic negative controls were used. The Mann-Whitney tests were used for a statistical comparison of flow cytometric results between the evaluated groups. The values of $p<0.05$ were accepted as statistically significant.

Results

The mean value of the percentage of epithelial cells with co-expression of CD44v4 was significantly lower in pT2 stage than in pT3 only in healthy tissues (Table 1). The expression of CD44v4 in epithelial cells was significantly higher in cases without lymph node metastases only in tumour adjacent tissues (Table 2). The expression of CD44v4 in epithelial cells was significantly higher in G2 than in G3 degree of malignancy only in tumour adjacent tissues too (Table 3).

Discussion

Colorectal cancer occupies the third position, regarding morbidity and mortality, just after the breast and lung and bronchus cancer in women and prostate and lung and bronchus cancer in men. The mortality is still high and depends on the progression of the disease and neoplasmatic metastases to lymph nodes and distal organs [5]. The relationships between the antigens of tumour cells and the possibility of the immunological system to recognize them play an important role in the progression of the disease. Isoforms of CD44 molecule reveal the co-expression in tumour cells, as well as in the leukocytes infiltrating the tumour [6].

CD44 molecule was described as a one of the leukocyte antigens in 1980 [7]. Different isoforms of CD44 and their role in neoplastic hyperplasia (breast, gastric, liver and others) were described in later years. [8, 9, 10]. However, there are only a few articles about role of CD44v4 in colorectal cancer [11]. Some authors have recently reported on a possible role of CD44 and its variants in the therapy [12, 13]. We have proved that the levels of CD44v5 and v6 variants in serum do not correlate either with pT stage or with the histopathological grade of malignancy [14].

This study evaluated the expression of CD44v4 isoform on the surface of epithelial cells in tumour tissues, tumour adjacent tissues and healthy tissues of the large bowel in patients with colorectal cancer. The statistically significant correlations, as demonstrated in the examinations, do not reveal anything about the influence of this variant on the process of carcinogenesis and the

progression of the disease. There have not been many studies about the expression of CD44v4 in colorectal cancer. Therefore, it is difficult to recognize if it either stimulates, or rather inhibits, the progression of the disease, while it is likely not to play any role in these processes.

References

1. Johnson P, Maiti A, Brown KL, Li R. A role for the cell adhesion molecule CD44 and sulfation in leukocyte-endothelial cell adhesion during an inflammatory response. Biochem Pharmacol, 2000; 59: 455-65.
2. Ponta H, Sherman L, Herrlich PA. CD44: from adhesion molecules to signalling regulators. Nat Rev Mol Cell Biol, 2003; 4: 33-45.
3. Tammi MI, Day AJ, Turley EA. Hyaluronan and homeostasis: a balancing act. J Biol Chem, 2002; 277: 4581-4.
4. Zalewski B, Famulski W, Sulkowska M, Sobaniec-Lotowska M, Piotrowski Z, Kisielewski W, Sulkowski S. CD44 expression in colorectal cancer. An immunohistochemical study including correlation with cathepsin D immunoreactivity and some tumour clinicopathological features. Folia Histochem Cytobiol, 2001; 39: 152-3.
5. Jemal A, Tiwari RC, Murray T, Ghafoor A, Samuels A, Ward E, Feuer EJ, Thurn MJ. Cancer Statistics, 2004. CA Cancer J Clin, 2004; 54: 8-29.
6. Webb DS, Shimizu Y, Van Seventer GA, Shaw S, Gerrard TL. LFA-3, CD44 and CD45: physiologic triggers of human monocyte TNF and IL-1 release. Science, 1999; 249: 1295-7.
7. Dalchau R, Kirkley J, Fahre JW. Monoclonal antibody to a human leukocyte-specific membrane glycoprotein probably homologous to the leukocyte-common (L-C) antigen of the rat. Eur J Immunol, 1980; 10: 737-44.
8. Wong K, Rubenthiran U, Jothy S. Motility of colon cancer cells: modulation by CD44 isoform expression. Exp Mol Pathol, 2003, 75: 124-30.
9. Wielenga VJ, Heider KH, Offerhaus GJ, Adolf GR, van der Berg FM, Ponta H, Herrlich P, Pals ST. Expression of CD44 variant proteins in human colorectal cancer related to tumour progression. Cancer Res, 1993; 53: 4754-6.
10. Heider KH, Dämmrich J, Skroch-Angel P, Müller-Hermelink HK, Vollmers HP, Herrlich P, Ponta H. Differential expression of CD44 splice variants in intestinal and diffuse-type human gastric carcinomas and normal mucosa. Cancer Res, 1993; 53: 4197-203.
11. Ni HM, Leong AF, Cheong D, Hool SC. Expression of CD44 variants in colorectal carcinoma quantified by real-time reverse transcriptase-polymerase chain reaction. J Lab Clin Med, 2002; 139: 59-65.
12. Heider KH, Kuthan H, Stehle G, Munzert G. CD44v6: a target for antibody-based cancer therapy. Cancer Immunol Immunother, 2004; 53: 567-79.
13. Nabel GJ. Genetic, cellular and immune approaches to disease therapy: past and future. Nat Med, 2004; 10: 135-41.
14. Zalewski B. Levels of v5 and v6 CD44 splice variants in serum of patients with colorectal cancer not correlating with pT stage, histopathological grade of malignancy and clinical features. World J Gastroenterol, 2004; 10: 583-5.

C-erb-B2 and Bcl-xl protein expression in Barrett´s oesophagus in correlation with morphological parameters

Barwijuk-Machała M, Reszeć J, Kemona A, Sobaniec-Łotowska M

Department of Pathology, Medical University of Bialystok, Poland

Abstract

The aim of the study was to evaluate the correlation of c-erb-b2 and Bcl-xl expression in biopsy specimens of Barrett´s oesophagus from 44 patients with morphological features. The examined group was subdivided into: negative for dysplasia, indefinite for dysplasia, positive for dysplasia - low grade, and adenocarcinoma with high grade dysplasia. Positive c-erb-B2 staining was found in 34.1% and Bcl-xl protein expression was observed in 96.9% of BE. The results showed increased c-erb-B2 and Bcl-xl protein expressions with progressive grades of dysplasia to adenocarcinoma. In conclusion, an evaluation of c-erb-B2 and Bcl-xl expression can be useful for the histopatologic diagnosis of BE and correct interpretation of dysplasia.

Key words: C-erb-B2, Bcl-xl, Barrett´s oesophagus.

Introduction

Barrett´s oesophagus (BE) is a complication of chronic gastroesophageal reflux disease and predisposes to dysplasia, which has been known as a precursor of adenocarcinoma [1, 2, 3]. Grading of dysplasia in BE is of great clinical importance and may serve to identify patients who are at high risk of developing cancer [4]. Attempts have been made to identify early markers of malignant transformation [5]. Bcl-xl is a protein, associated with cell survival, which prevents apoptosis [6]. The c-erb-B2 protooncogene encodes a transmembrane tyrosine kinase receptor that is homologous to EGF-R [7, 8]. The specimens of BE with severe dysplastic changes and adenocarcinoma showed an increased expression of c-erb-B2 protein on the cell membranes [8, 9]. The aim of our study was an evaluation of c-erb-b2 and Bcl-xl expressions in BE in correlation with morphological parameters.

ADDRESS FOR CORRESPONDENCE:
Małgorzata Barwijuk-Machała
Department of Pathology
Medical University of Bialystok
Waszyngtona 13; 15-269 Białystok, Poland

Material and methods

Paraffin sections from 44 BE-suffering patients with intestinal metaplasia, dysplasia and adenocarcinoma were retrospectively reviewed. The examined group was subdivided into negative for dysplasia - 19 cases - (I), indefinite for dysplasia, probably negative - 6 cases - (II), positive for dysplasia - low grade - 8 cases - (III) and adencarcinoma with high grade dysplasia - 11 cases - (IV). Immunostaining for c-erb-B2 and Bcl-xl was performed. using c-erb-B2 and Bcl-xl antibodies (Novocastra c-erb-B2 NCL - c-erb-B2 316, Santa Crus Biochemicals Bcl - xl No A 20, sc-7122). To visualize the antigen-antibody reaction, the LSAB technique was applied, using DAB (diaminobensidine) and ABC technique (working dilution 1:50). The stainability of c-erb-B2 was defined by the percentage of cells with a strongly stained cell membrane, often accompanied by cytoplasm staining as follows: 29% or bellow (-), between 30% and 59% (+) and 60% or over (++). The criteria for Bcl-xl reaction were as (++), when above 50% cells were immunopositive for the examined protein, (+) 50% -10% and as (-), when bellow 10% cells were immunopositive. Chi-squared test and Pearson correlation were used for statistical analysis. Values of $p< 0.05$ were considered as statistically significant.

Results and discussion

BE is defined as a replacement of the normal squamous epithelium of the lower oesophagus with metaplastic columnar

epithelium [2]. The diagnosis of BE should be made, based on the presence of goblet cells, which can easily be identified, using an Alcian blue PAS stain [10]. In our experience, this stain is very useful in the diagnostic procedure because of the necessity of discriminating goblet cells from reactive foveolar cells which may be very similar on H-E stain. Chronic oesophageal injury from gastroesophageal reflux may result in dysplasia, which is an intermediate step in the progression from metaplasia to adenocarcinoma [3]. Regular endoscopic surveillance, with histologic evaluation of biopsy specimens, has been recommended for patients with the diagnosis of BE [4]. The assessment of dysplasia in biopsy samples in BE may be difficult because of its multifocal distribution [3]. Bhargava et al. have stressed that only endoscopy with systematic mapping may provide better surveillance for an individual patient [5]. In our study, an initial microscopic examination revealed dysplasia in 57%. 8 patients with the diagnosis of BE had low grade dysplasia. High grade dysplasia was found adjacent to adenocarcinoma in the majority of examined cases. The coexistence of these abnormalites is very frequent in BE and is an evidence for a malignant transformation [3]. During microscopical examination, we had some difficulties with the diagnosis of dysplasia in 6 patients with BE. These cases were initially qualified to the indefinite for dysplasia, probably negative group. Staging of dysplasia is subjected to considerable inter and intra observer variations. Despite of the well defined pathological criteria for the diagnosis of BE, differentiating the degree of dysplasia, especially low-grade dysplasia from reactive changes may be difficult in the presence of inflammation [10]. Histological grading of dysplasia is important from the therapeutic point of view [4]. It may be helpful not only in the selection of therapy, but also in the monitoring of its effectiveness. Many investigators have tried to identify early markers of malignant transformation [5, 11]. The role for c-erb-B2 oncoprotein has not been clearly specified yet. In our study, positive c-erb-B2 staining was found in mucosa of BE patients with low grade dysplasia in 5 out of 8 cases (62.5%), in 8 out of 11 cases with high grade dysplasia (77.7%) and in 10 of 11 adenocarcinomas (90%), while it has not been found in any case of indefinite dysplasia. The reported prevalence of c-erb-B2 overexpression in esophageal adenocarcinomas varies from 10% to 64% [8, 9, 12]. Based on the large proportion of adenocarcinoma with c-erb-B2 expression and negative immunoreactivity in the dysplastic areas, it has been suggested that it is the late event in the dysplasia - carcinoma sequence [13]. The results of our study are in agreement with those obtained by other investigators, who have found positive c-erb-B2 staining in dysplastic epithelium but not in mucosa of BE without dysplasia [5]. In our study, the overexpression of c-erb-B2 increased significantly with the progressive grades of dysplasia to adenocarcinoma. Statistical analysis revealed significant ($p<0.05$) difference in c-erb-B2 expression between I - III, I-IV, II-III and III-IV groups. In Group I, 10.5% were (+) positive for c-erb-B2, in Group II, all the cases were negative for c-erb-B2, in Group III, 25% were (++) positive for c-erb-B2 and 81.8% tumours in Group IV were c-erb-B2 immunopositive ($p=0.00001$). Lesions, which overexpress c-erb-B2, may be associated with a higher degree of proliferation. Kim et al. found that the proliferation rate at the surface of BE gradually increased with progressive grades of dysplasia [12]. Those observations were also supported by Matsumoto et al., who noticed that enhanced cell proliferation correlated with morphological abnormalities in BE [3]. Chen et al. showed a shift of increased proliferation activity towards the upper crypt and the luminal surface with increasing severity of dysplasia [14]. The results, obtained by Whittles et al., revealed a significant increase in the glandular proliferation to apoptosis ratio in the progression of metaplasia through dysplasia to adenocarcinoma [15]. The authors observed the decrease in apoptosis in the upper crypt and luminal surface in dysplasia and adenocarcinoma, compared with metaplasia [15]. Those findings agreed with our results, concerning Bcl-xl protein that have shown an increase of expression with the progression of BE to adenocarcinoma. In our study, Bcl-xl protein expression was observed in 32, out of 44 cases with BE (96.9%), all the adenocarcinoma cases were Bcl-xl immunopositive. There were statistically significant differences of Bcl-xl protein expression between I and III, I and IV, as well as between II and IV groups. In Group I, 5.3% of al. cases were (++) positive for Bcl-xl, in Group II, 33.3%, in Group III, 62.5% and 90.9% tumours in Group IV were Bcl-xl immunopositive ($p=0.00063$). There is lack of data, concerning with apoptosis and BE, as well as adenocarcinoma development. Van der Woude et al. found an increased Bcl-xl expression through metaplasia to adenocarcinoma [6]. Soslow et al. observed a statistically significant linear association between Bcl-xl expression versus increasing histological severity in BE [16]. Our study support the hypothesis that neoplastic transformation through metaplasia, dysplasia to adenocarcinoma in BE may be associated with apoptosis proteins expression alterations and overexpression of some oncogenes, like c-erb-B2 protein, which can be useful for the correct interpretation of dysplasia in BE.

References

1. Shaheen N, Ransohoff DF. Gastroesophageal reflux, Barrett esophagus, and esophageal cancer: scientific review. JAMA. 2002; 287: 1972-81.

2. Kawakura Y, Tatsuzawa Y, Wakabayashi T, Ikeda N, Matsuda M, Nishihara S. Immunohistochemical study of p53, c-erbB-2, and PCNA in Barrett´s esophagus with dysplasia and adenocarcinoma arising from experimental acid or alkaline reflux model. J Gastroenterol. 2001; 36: 595-600.

3. Matsumoto Y, Arai N, Mieno H, Murakami K, Ishii K, Mitomi H. Adenocarcinoma comlicating Barrett´s esophagus: an analysis of cell proliferation. J Gastroenterol. 2001; 36: 410-14.

4. Cameron AJ. Management of Barrett´s esophagus. Mayo Clin Proc. 1998; 73: 457-461.

5. Bhargava P, Eisen GM, Holterman DA, Azumi N, Hartmann DP, Hanfelt JJ, Benjamin SB, Lippman ME, Montgomery EA. Endoscopic mapping and surrogate markers for better surveillance in Barrett esophagus. A study of 700 biopsy specimens. Am J Clin Pathol. 2000; 114: 552-63.

6. Van der Woude CJ, Jansen PL, Tiebosch AT, Beuving A, Homan M, Kleibeuker JH, Moshage H. Expression of apoptosis-related proteins in Barrett´s metaplasia-dysplasia-carcinoma sequence: a switch to a more resistant phenotype. Hum Pathol. 2002; 33: 686-92.

7. Al.-Kasspoles M, Moore JH, Orringer MB. Amplifi-

cation and overexpression of the EGFR and erbB-2 genes in human esophageal adenocarcinomas. Int J Cancer. 1993; 54: 213-9.

8. Friess H, Fukuda A, Tang WH, Eichenberger A, Furlan N, Zimmermann A, Korc M, Buchler MW. Concomitant analysis of the epidermal growth factor receptor family in esophagel cancer: overexpression of epidermal growth factor receptor mRNA but not of c-erbB-2 and c-erbB3. World J Surg. 1999; 23: 1010-8.

9. Illueca C, Llombart-Bosch A, Ferrando Cucarella J. Prognostic factors in Barrett´s esophagus: an immunohistochemical and morphometric study of 120 cases. Rev Esp Enferm Dig. 2000; 92: 726-37.

10. Haggitt RC. Barrett´s esophagus, dysplasia, and adenocarcinoma. Hum Pathol. 1994; 25: 982-93.

11. Kleeff J, Friess H, Liao Q, Buchler MW. Immunohistochemical presentation in non-malignant and malignant Barrett´s epithelium. Dis Esophagus. 2002; 15: 10-15.

12. Kim R, Clarke MR, Melhem MF, Young MA, Vanbibber MM, Safatle-Ribeiro AV, Ribeiro U Jr, Reynolds JC. Expression of p53, PCNA, and C-erbB-2 in Barrett´s metaplasia and adenocarcinoma. Dig Dis Sci. 1997; 42: 2453-62.

13. Hardwick RH, Shepherd NA, Newcomb PV, Alderson D. C-erb-B2 overexpression in the dysphagia/carcinoma sequence of Barrett´s oesophagus. 1995; 48: 129-32.

14. Chen L, Hu C, Gaboury L, Pera M, Ferraro P, Duranceau AC. Proliferative activity in Barrett´s esophagus before and after antireflux surgery. Ann Surg. 2001; 234: 172-80.

15. Whittles CE, Biddlestone LR, Burton A, Barr H, Jankowski JA, Warner PJ, Shepherd NA. Apoptotic and proliferative activity in the neoplastic progression of Barrett´s esophagus: a comparative study. J Pathol. 1999; 187: 535-40.

16. Soslow RA, Remotti H, Baergen RN, Altorki NK. Suppression of apoptosis does not foster neoplastic growth in Barrett´s esophagus. Mod Pathol. 1999; 12: 239-50.

Role of metallothionein expression in non-small cell lung carcinomas

Dzięgiel P[1], Jeleń M[2], Muszczyńska B[3], Maciejczyk A[4], Szulc A[4], Podhorska-Okołów M[1], Cegielski M[1], Zabel M[1, 5]

[1]Chair and Department of Histology and Embryology, University School of Medicine in Wrocław; [2]Chair and Department of Pathomorphology, University School of Medicine in Wrocław; [3]Lower Silesia Centre of Tuberculosis and Lung Diseases in Wrocław; [4]Lower Silesia Centre of Oncology in Wrocław; [5]Chair and Department of Histology and Embryology, University School of Medicine in Poznań

Abstract

Metallothionein (MT) is a low molecular weight protein, which participates in differentiation and proliferation of normal and tumour cells. In some malignant tumours (mammary, renal, ovarian cancers), its increased expression is thought to represent an unfavourable prognostic factor. Non-small-cellular lung cancers (mainly squamocellular cancer and adenocarcinoma) are characterised by ill-defined prognosis, which poses problems in the selection of effective post-surgical therapy. The present study aimed at demonstration of the prognostic significance of MT expression in cells of non-small cell lung cancers, attempting to correlate the intensity of MT expression with G grade and with the intensity of proliferation-associated antigen, Ki-67 expression. The studies were performed on archival paraffin blocks with samples of 25 cases of non-small cell lung cancers (5 squamous cell cancers, 20 adenocarcinomas). In paraffin sections of the studied tumours, immunocytochemical reactions were performed, using mouse monoclonal anti-MT and anti-Ki-67 antibodies. The expressions of MT and Ki-67 were demonstrated in all the studied tumours. An analysis of correlation between the expression of MT, Ki-67 antigen and G grade demonstrated a strong positive relation between the latter two parameters ($r=0.70$; $p<0.05$). Less pronounced positive correlations were disclosed between MT expression and G grade ($r=0.44$; $p<0.05$) and between MT expression and the expression of Ki-67 antigen ($r=0.41$; $p<0.05$). In addition, in 15 cases of examined tumours, survival analysis was performed, which disclosed a shorter survival in patients with high MT expression. The obtained results confirmed the relationship between MT expression and Ki-67 antigen expression, indicating an involvement of the proteins in processes of tumour cell proliferation. In turn, the shorter survival of patients with high expression of MT pointed to prognostic significance of the protein in non-small cell lung cancers.

Key words: metallothionein, nonsmall cell lung carcinoma.

ADDRESS FOR CORRESPONDENCE:
Piotr Dzięgiel
Chair and Department of Histology and Embryology
University School of Medicine in Wrocław,
Chałubińskiego 6A; 51-650 Wrocław, Poland
tel. +4871/784-00-81; fax. +4871/784-00-82;
e-mail: piotr@hist.am.wroc.pl

Introduction

Metallothioneins (MT) are low molecular weight (7 kDa) proteins. They consist of a polypeptide chain of 61 to 68 amino acids, of which around 30% are cystein residues. Due to their structure and function, four basic types of the protein are distinguished: MT-I, MT-II, MT-III and MT-IV, coded by genes, located in chromosome 16 [1]. MT are commonly present in normal tissues, as well as in cells of various tumours [2, 3, 4]. The earliest recognized function of MT involves their capacity to bind both toxic ions (Cd, Pb, Hg) and ions indispensable to the body (Zn, Cu). Sharing the potential to bind Zn ions, MT act as controllers of zinc-dependent enzymes, which participate in DNA replication, transcription, translation and in cell metabolism [1]. Augmented expression of MT in cells of some tumours is linked with worse prognosis, resistance to cytostatic drugs and to radiotherapy [2, 3]. The group of non-small cell lung carcinomas (NSCLC) includes squamous cell cancer, adenocarcinoma and large cell carcinoma. In such patients, the prognosis used to be difficult to define, among others, due to frequent non-uniform histological character of NSCLC. This creates problems in the selection of effective post-surgery treatment (chemo- and/or radiotherapy) [5]. The present study aimed at demonstrating the prognostic significance of MT expression in NSCLC cells and in the attempts to correlate the intensity of its expression with malignancy grade, G and with the intensity of expression of the proliferation-associated antigen, Ki-67 antigen.

Figure 1. Expression of metallothionein (MT) in cell nuclei and cytoplasm of cells in squamous cell lung cancer. x200; background staining with haematoxylin.

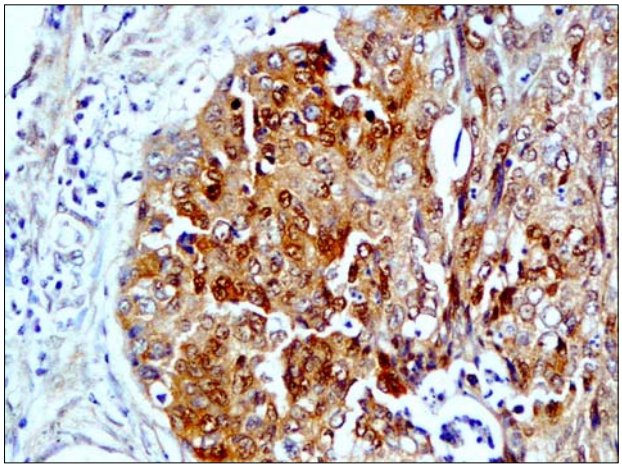

Figure 2. Duration of patients' survival in non-small cell lung cancers NSCLC) of a low (1-4 pts, n = 7) or a high (6-12 pts, n = 8) expression of metallothionein (MT).

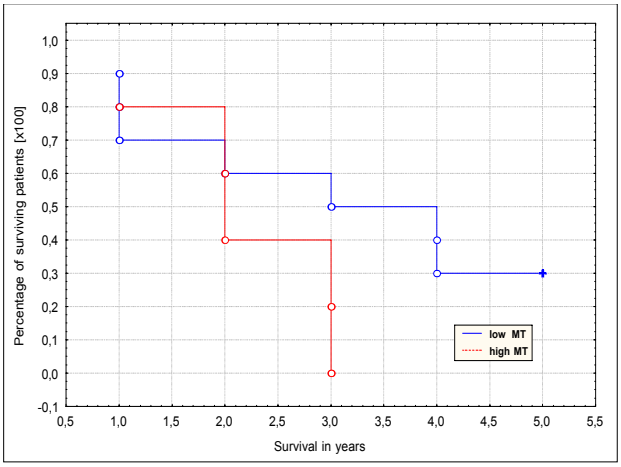

Material and Methods

The studies were performed on archival paraffin blocks, containing 25 histopathologically verified cases of NSCLC (T2N0 - 5 squamous cell carcinomas, 20 adenocarcinomas), subjected to surgery during the years 1998-99 at the Lower Silesia Centre of Tuberculosis and Lung Diseases in Wrocław. In paraffin sections of studied tumours, immunocytochemical reactions were performed, using mouse monoclonal antibodies, directed to MT-I and MT-II (clone E9) and to Ki-67 (clone MIB-1). The investigated antigens were visualised, using LSAB2 kit and diaminobenzidine (DAB). All the antibodies and reagents were purchased in DAKOCytomation (Denmark). MT expression was evaluated, using the semiquantitative IRS scale, according to Remmele [6] (0-12 points), which took into account the intensity of the colour reaction and the number of positive cells. The expression of Ki-67 antigen was appraised, considering the proportion of cells with nuclear colour reaction (0 pts - lack of reaction; 1 pt - 1-10%; 2 pts - 11-25%; 3 pts - 26-50%; 4 pts - over 50% positive cells). Grade of malignancy, G, was evaluated as recommended by WHO [7]. Clinical data (TNM classification, duration of survival) were recovered from the archives of the Lower Silesia Centre for Tuberculosis and Lung Diseases in Wrocław. The obtained results were subjected to statistical analysis, using the STATISTICA PL software (StatSoft, Poland) and employing Spearman's correlation tests and survival analysis of Kaplan-Meier.

Results

In all the examined tumours, variable expressions of MT and of Ki-67 antigen were observed. The most pronounced intensity of nuclear-cytoplasmic expression of MT (Fig. 1) and of Ki-67 antigen was noted in squamous cell cancers. The analysis of correlations between the expressions of MT, Ki-67 antigen and G grade of malignancy demonstrated a strong positive relationship between the two latter variables ($r = 0.7$; $p < 0.05$). Less pronounced positive correlations were disclosed between MT expression and G grade ($r = 0.44$; $p < 0.05$) and between MT expression and the expression of Ki-67 antigen ($r = 0.41$; $p < 0.05$). In addition, in 15 cases of NSCLC (7 squamous cell cancers, 8 adenocarcinomas), survival analysis was performed which demonstrated shorter survival times in patients with high expression of MT (Fig. 2).

Discussion

NSCLC represent a non-uniform group of tumours, regarding the histological structure, clinical course or the prognosis. This creates problems in the selection of appropriate therapeutic approach [8]. For several years, independent markers have been searched for, which could help in choosing an effective way of treatment after removal of the primary tumour. The expression of MT in normal cells and in some tumours is linked to cell proliferation and differentiation [9]. This has prompted us to examine the intensity of expression of the protein in NSCLC in attempts to use it in prognostic evaluation of the patients. However, the few papers, published on the subject till now, have presented contradictory results. Tcheocharis and collaborators [10] dealt with a group of 89 NSCLC, evaluating by immunocytochemistry, i.a., the expression of MT-I and MT-II. In part, they obtained results similar to those obtained by us, noting the highest intensity of MT expression in squamous cell cancers and a less pronounced expression in adenocarcinomas. However, in contrast to us, they found no correlation between MT expression and the other clinical and pathological variables. Volm et al. [11], as well as Mattern et al. [12], examined NSCLC in respect to their resistance to cytostatic drugs. Both in *in vitro* and *in vivo* experiments, they noted more extensive resistance to doxorubicin of MT (+) cells. Moreover, the intensity of MT expression was positively related to malignancy grade G and to the expression of another protein responsible for multi-drug resistance to cytostatic drugs, glutathion-s-transferase-Π. Similarly to tumours of other organs, the results obtained by us in NSCLC demonstrated a positive correlation between the expression of MT and Ki-67 antigen [2, 13]. This indicated participation of the protein in the processes of NSCLC cell proliferation. In turn, the shorter survival of patients with high MT expression may argue for prognostic significance of its expression in NSCLC.

References

1. Coyle P, Philox JC, Carem LC, Rofe AM. Metallothionein: The multipurpose protein. Cell Mol Life Sci, 2002; 59: 627-47.

2. Dzięgiel P. Expression of metallothioneins in tumor cells. Pol J Pathol, 2004; 55: 3-12.

3. Cherian MG, Jayasurya A, Boon-Huat B. Metallothioneins in human tumors and potential roles in carcinogenesis. Mutat Res, 2003; 533: 201-9.

4. Dzięgiel P, Suder E, Surowiak P, Kornafel J, Zabel M. Expression of metallothionein in synovial sarcoma cells. Appl Immunohistochem Mol Morphol, 2002; 10: 357-62.

5. Khan OA, Fitzgerald JJ, Field ML, Soomro I, Beggs FD, Morgan WE, Duffy JP. Histological determinants of survival in completely resected T1-2N1M0 nonsmall cell cancer of the lung. Ann Thorac Surg, 2004; 77: 1173-8.

6. Remmele W, Stegner HE. Recommendation for uniform definition of an immunoreactive score (IRS) for immunohistochemical estrogen receptor detection (ER-ICA) in breast cancer tissue. Pathologe, 1987; 8: 138-40.

7. Sayar A, Turna A, Solak O, Kiliçgün A, Ürer N, Gürses A. Nonanatomic prognostic factors in resected nonsmall cell lung carcinoma: the importance of perineural invasion as a new prognostic marker. Ann Thorac Surg, 2004; 77: 421-5.

8. Moran CA, Suster S. Tumors of the lung and pleura. In: Fletcher CDM, editor. Diagnostic histopathology of tumors. 2nd ed. London: Churchill Livingstone; 2000, p171-208.

9. Cherian MG, Apostolova MD. Nuclear localization of metallothionein during cell proliferation and differentiation. Cell Mol Biol, 2000; 46: 347-56.

10. Theocharis S, Karkantaris C, Philipides T, Agapitose A, Gika A, Margeli A, Kittas C, Koutselinis A. Expression of metallothionein in lung carcinoma: correlation with histological type and grade. Histopathology, 2002; 40: 143-51.

11. Volm M, Koomägi R, Mattern J, Efferth T. Protein expression profiles indicative for drug resistance of non-small cell lung cancer. Br J Cancer, 2002; 87: 251-7.

12. Mattern J, Koomägi R, Volm M. Expression of drug resistance gene products during progression of lung carcinomas. Oncol Rep, 2002; 9: 1181-4.

13. Dzięgiel P, Forgacz J, Suder E, Surowiak P, Kornafel J, Zabel M. Prognostic significance of metallothionein expression in correlation with Ki-67 expression in adenocarcinomas of large intestine. Histol Histopathol, 2003; 18: 401-7.

Association of collagen Type I α1 gene polymorphism with bone density in survivors of childhood cancer - preliminary report

Muszyńska-Rosłan K[1], Galicka A[2], Sawicka M[1], Krawczuk-Rybak M[1], Wołczyński S[3]

[1]Department of Paediatric Oncology, [2]Department of Medical Chemistry,
[3]Department of Gynaecological Endocrinology, Medical University of Białystok, Poland

Abstract

A candidate gene, involved in the regulation of bone mass is the COLIA1 gene encoding type I collagen, the major protein of bone matrix. The disease per se, the age of its onset and treatment options might exert an impact on bone mineralization in survivors of childhood malignancy. We examined possible allelic influences of COLIA1 gene polymorphism on BMI, BMD spine and total body in 41 survivors (15 girls) of childhood cancer (the mean age 8.9 years). Genotype distribution was 33 (80.5%) SS and 8 (19.5%) Ss. There were no differences in SDS BMD and SDS BMI between patients with SS and Ss genotype. A tendency towards lower SDS values of BMD spine and BMI was observed (not significant). In conclusion, our preliminary observations suggest that COLIA1 genotype may affect bone accrual in a population treated for childhood cancer. Further investigations in a greater population are needed.

Key words: childhood cancer, collagen type I, polymorphism, bone, osteoporosis.

Introduction

Osteoporosis is a common disease, characterized by reduced bone mineral density (BMD), damage of the architecture of bone tissue and an increased risk of non-traumatic fractures. Variation in the attainment of peak bone mass plays an important role in the development of osteoporosis. Based on family and twin studies, peak bone mass has been estimated to be up to 85%, as genetically determined. Several polymorphisms in "candidate" genes have been investigated as genetic factors that could influence bone mineral density [1]. In many studies, polymorphism Sp1 binding site, in the first intron of the collagen type Iα1 (COLIA1) gene, has been proved to be associated with low bone density [2, 3]. Treatment for malignancy in childhood can result in diminished peak bone mass and osteoporosis development in adults [4]. We hypothesize that COLIA1 genotype might affect anthropometric or densitometric characteristics of bone in children and young adults exposed to negative environmental factors, connected with malignant disease and its treatment. Therefore, we tried to investigate the incidence and association between COLIA1 polymorphism and bone characteristics in survivors of childhood cancer.

ADDRESS FOR CORRESPONDENCE:
Katarzyna Muszyńska-Rosłan
Department of Paediatric Oncology
Medical University of Bialystok
Waszyngtona 17 15-274 Białystok, Poland
e-mail: kmroslan@amb.edu.pl

Material and methods

We examined 41 patients (14 girls) diagnosed for leukaemia and lymphoma (n= 34) and solid tumour (n= 7) at the mean of age of 8.9 years (range 1.66 - 19.83). The mean age of diagnosis was 3.7 years. All the subjects had received chemotherapy (CHT), 24 additionally steroidotherapy (ST) and 7 - radiotherapy (RTX). All the patients underwent a physical examination; their height was assessed, using a fixed stadiometer, their weight on a standard clinical balance, the pubertal development, according to Tanner's scale. Body mass index was calculated, according to the formula: weight/height^2 (kg/m^2) and expressed as standard deviation score (SDS). Bone mineral density (BMD g/cm^2) was determined by dual energy x-ray absorptiometry (Lunar DPX-L Madison WI version 1.35) of the lumbar spine and total body in children over 5 years of age (n= 26) - the acquired results were compared with the results of 473 healthy references and expressed as SDS. The G to T polymorphism ratio in the Sp1 binding site in the COLIA1 gene was detected by the polymerase chain reaction-based method with primers

and reaction conditions, as described previously, using DNA extracted from whole blood. The reaction products were digested with the restriction enzyme MscI and analysed by agarose gel electrophoresis. The genotype was defined as "S" or "s", according to either the absence or presence of restriction site. Statistical analysis: to correct for the age differences between the genotype, anthropometric parameters and bone characteristics were expressed in age and sex-matched standard deviation scores (SDS). The data were analyzed by using t-test for unpaired samples. Linear regression was made to assess the dependence of bone mineral density on the independent variables, such as clinical characteristics and genotype. P-values of less than 0.05 were considered significant. The study was approved by the Medical Ethics Committee of the Medical Academy of Białystok

Results

The characteristics of the studied subjects are shown in Table 1. The genotype distribution was 33 (80.5%) SS - homozygous for absence of MscI site; 8 (19.5%) Ss heterozygous; we did not find ss - homozygous for presence of MscI site. There were no differences in SDS values of BMI and BMD total and spine between SS and Ss genotypes. We observed a tendency towards lower SDS values of BMI (0.654 ±2.11 vs -0.138 ±2.44) and BMD spine (0.43 ±1.33 vs -0.75 ±1.48) in children with Ss genotype; after an adjustment for BMS SDS, the COLIA1 genotype effect on BMD spine disappeared. There was no significant association between the age of diagnosis, the kind of neoplastic disease, body mass index and genotype.

Discussion

Type I collagen is the major protein of bone. Mutations in the coding regions of the COLIA1 genes are found in diseases associated with severe osteoporosis. Grant et al. detected polymorphism in the first intron of the COLIA1 gene, involving the binding site for the transcription factor Sp1, important for the regulation of gene expression and type I procollagen synthesis [5]. Most studies have shown a negative effect of COLIA1 "s" allele on BMD. However, they were performed in adults who had undergone substantial bone loss [2, 6]. Children had a shorter exposure to lifestyle and environmental factors which can influence the overall effect of genetic factors on bone development and mineralization. The studies in paediatric population have shown conflicting results because of different methods used to measure bone mass, the expression of data, the age and the gender. Berg et al. concluded that the polymorphism at the Sp1 binding site in the COLIA1 gene is not associated with BMD in healthy boys and girls [7]. No association was found between COLIA1 polymorphism and BMD or BMC (bone mineral content) in 428 prepubertal children examined by Willing et al. [8] On the other hand, Sainz et al. described lower bone density in prepubertal girls with the Ss and ss genotype, compared to girls with SS genotype, but no allele effect was found on bone size [9]. In childhood and especially during puberty, bone mineral density and body size change markedly. Van der Sluis et al.

Table 1. Clinical characteristics, anthropometric and densitometric parameters in relation to COLIA1 gene alleles.

Subjects	SS genotype	Ss genotype
N = 41	33	8
Age of study = 8,9 years	8.34 years	11.35 years
Sex: female N= 15 Male N= 16	F/ N=13 M/ N= 10	F/ N= 2 M/ N= 6

a) prepuberty N= 21
b) during puberty N= 10
c) post puberty N= 10
	a) N= 19;
	b) N= 8;
	c) N= 4
		a) N= 2;
		b) N= 2;
		c) N= 6

Treatment with CHT and RT N = 7	N= 5	N= 2
Treatment with CHT and ST N = 34	N= 28	N= 6
BMI (kg/m^2)	18.05 ±3.7	17.7 ±4.3
BMD total - (g/m^2)	0.883 ±0.15	0.947 ±0.22
BMD spine - (g/m^2)	0.719 ±0.22	0.820 ±0.35
BMD total SDS	-0.837 ±1.75	0.213 ±2.04
BMD spine SDS	0.436 ±1.33	-0.754 ±1.4
BMI SDS	0.655 ±2.12	-0.138 ±2.44

studied 148 healthy Caucasian children and showed that subjects with Ss and ss genotype had decreased SDS BMC and SDS BMD for both lumbar spine and total body and a shorter stature and smaller bones comparing to SS genotype. Similar associations were found at follow-up after 4 years [3]. The comparison various methods (DEXA, CT, and ultrasound) support the hypothesis that SP1 COLIA1 polymorphism is more strongly associated with bone morphology and quality than with mineralization [3, 7, 8, 9]. Children with malignant disease may be considered a subgroup at high-risk of developing osteoporosis. Unfavourable factors, e.g., cancer disease per se, the age of its onset, treatment options might influence bone mineralization in survivors of childhood malignancy [4]. In our preliminary study, we did not find any significant differences between genotype and SDS BMI and SDS BMD total and spine. The allele incidence rates of the COLIA1 variants were similar to those reported for other Caucasian population. We did not make any statistical analyses, dependending on Tanner's stage to compare children with SS and Ss genotype, due to a small population. We observed a tendency towards lower BMI SDS and BMD spine SDS in heterozygous patients, however, after a correction for BMI, the small differences between both groups decreased. The similar results, obtained in previous studies, indicate that the effect of the COLIA1 genotype on bone mineral density can partially be mediated by its genetic effect on body size. In summary, our preliminary observations suggest an influence of COLIA1 genotype on bone accrual in the population treated for childhood cancer. Further investigations on polymorphisms of other "candidate" genes in a greater cohort of children with neoplastic disease are needed.

References

1. McGuigan F, Murray L, Gallagher A, Davey-Smith G, Neville C, Boreham C, Ralston S. Genetic and environmental determinants of peak bone mass in young men and women. J Bone Miner Res, 2002; 17: 1273-9.

2. Mann V, Hobson E, Li B, Tewrat T, Grant S, Robins PR, Aspden R, Ralston S. A COLIA1 Sp1 binding site polymorphism predisposes to osteoporotic fracture by affecting bone density and quality. J Clin Invest, 2001; 107: 899-907.

3. Van der Sluis IM, de Muinck Keizer-Schrama SMPF, Pols HAP, Lequin MH, Krenning EP, Uitterlinden AG. Collagen Ia1 polymorphism is associated with bone characteristics in Caucasian children and young adults. Calcif Tissue Int, 2002; 71: 393-9.

4. Mandel K, Atkinson S, Barr RD, Pencharz P. Skeletal morbidity in childhood leukemia. J Clin Oncol, 2004; 22: 1215-21.

5. Grant SF, Reid DM, Blake G, Herd R, Fogelman I, Ralston SH. Reduced bone density and osteoporosis associated with a polymorphic Sp1 binding site in the collagen type I alfa 1 gene. Nature Genet, 1996; 14: 203-5.

6. Uitterlinden AG, Burger H, Huang Q, Fang Y, McGuigan F, Grant S, Hofman A, van Leeuwen J, Pols H, Ralston S. Relation of alleles of the collagen type Ia1 gene to bone density and risk of osteoporotic fractures in postmenopausal women. N Engl J Med, 1998; 338: 1016-21.

7. Berg JP, Lehmann EH, Stakkestad JA, Haug E, Halse J. The Sp1 binding site polymorphism in the collagen type Ia1 (COLIA1) gene is not associated with bone mineral density in healthy children, adolescents and young adults. Eur J Endocrinol, 2000; 143: 261-5.

8. Willing MC, Torner JC, Burns TL, Janz KF, Marshall T, Gilmore J, Deschenes SP, Warren JJ, Levy SM. Gene polymorphisms, bone mineral density and bone mineral content in young children: the Iowa bone development study. Osteoporosis Int, 2003; 14: 650-8

9. Sainz J, van Tornout JM, Sayre J, Kaufman S, Gilsanz V. Association of collagen type Ia1 gene polymorphism with bone density in early childhood. J Clin Endocrinol Metab, 1999; 84: 853-5.

Study on carcinogenesis in chronic cholecystitis

Zimnoch L[1], Szynaka B[1], Kupisz A[2]

[1]Department Medical Pathomorphology [2]District General Hospital, Medical University of Białystok

Abstract

Not only bile but also chronic cholecystitis may play a role in gallbladder carcinogenesis. Numerous studies have revealed a close correlation between chronic inflammation and neoplasia. The experiments were conducted on paraffin sections, obtained from 377 surgically resected gallbladders with chronic cholecystitis. Immunohistochemical reaction was conducted on deparaffinized sections, using a monoclonal antibody against 8-hydroxydeoxyguanosine (8-OHdG), a biomarker of oxidative DNA damage. An increase was found in the expression of 8-hydroxydeoxyguanosine in chronic cholecystitis. The level of 8-OhdG expression is associated with inflammation intensity and disease duration. DNA damage, observed in chronic cholecystitis. indicates a correlation between chronic inflammation and gallbladder carcinogenesis.

Key words: chronic cholecystitis, carcinogenesis, oxidative DNA damage, 8-hydroxydoxy-guanosine.

Introduction

Gallbladder carcinogenesis is related to bile mutagenic activity, although a number of studies ascribe an important role to chronic cholecystitis. There are well known examples of a close association between chronic inflammation and carcinogenesis in some organs, including ulcerative colitis and carcinoma of the colon, Helicobacter pylori-related gastritis and gastric cancer, viral hepatitis and hepatic cancer [1, 2, 3].

The likely mechanism of inflammation effects on carcinogenesis is associated with oxidative DNA damage [4]. Cytokines, released by inflammatory cells, destroy DNA and can inhibit its repair [5].

ADDRESS FOR CORRESPONDENCE:
Lech Zimnoch
Department Medical Pathomorphology
Medical Universtiy of Białystok
Waszyngtona 13, 15-269 Białystok, Poland
e-mail: lech@amb.edu.pl

Material and methods

The study was conducted on paraffin sections, obtained from 377 surgically resected gallbladders with chronic cholecystitis, at the District General Hospital in Białystok, within a five-year period (1999-2003). The control group consisted of normal gallbladder specimens, collected from carcinoma patients.

The analysed parameters included: the gender, the age (age groups: 1/0 - 30 years, 2/31-50 years, 3/ over 51 years), disease duration (1/ up to 2 years, 2/ 2-5 years, 3/ over 5 years), the size and number of gallstones (1/ no gallstones, 2/ single, large, 3/ varying in size, 4/ small, a large number), and the degree of inflammation, according to the following scale: I^0 - several lymphocytes (<20) in 10 large fields of vision in the lamina propria of the mucosa, II^0 - intensive inflammatory infiltration - 20-100 lymphocytes in 10 large fields of vision, III^0 - hyper-intensive inflammatory infiltration >100 lymphocytes in 10 large fields of vision without lymph nodules, IV^0 - hyper-intensive inflammatory infiltration with 2-3 lymph nodules in 10 large fields of vision.

The deparaffinized sections, obtained from the archival specimens, stored at the Department of Pathomorphology, were immunohistochemically investigated, using a monoclonal antibody against 8-hydroxydeoxyguanosine (8-OhdG), (Oxis) (dilution 1:200) with LSAB kit (Dako) and methods recommended by Seki et al. [6].

The expression of 8-OhdG (8-OhdG index) was determined by counting the number of positive-cells among 200 epithelial cells of gallbladder mucosa (the mean of two calculations at 200x magnification for each case).

Table 1. 8-0HdG index in relation to the gender, the age, disease duration, the number of gallstones and inflammation degree.

Statistical multiple regression	Dependent variable regression: 8-0HdG INDEX R= .30900511 R2= .09548416 Corrected. R^2= .08081633 F (6.370)=6.5098 p< .00000 Standard estimation error: 7.5326					
N=377	BETA	St. Error BETA	**B**	St. Error B	t (370)	Level p
Gender	.081484	.049724	1.736097	1.059412	1.638736	.102118
Age	.010475	.051901	.133829	.663088	.201827	.840163
Disease duration	.206034	.053915	1.769343	.463002	3.821460	.000156
No of gallstones	.008838	.063727	.080779	.582468	.138684	.889776
Inflammation intensity	.216200	.049948	2.192183	.506457	4.328467	.000019

Figure 1. Expresion 8-hydroxydeoxyguanosine in chronic cholecystitis. Immunohistochemical reaction. Mag. x 400.

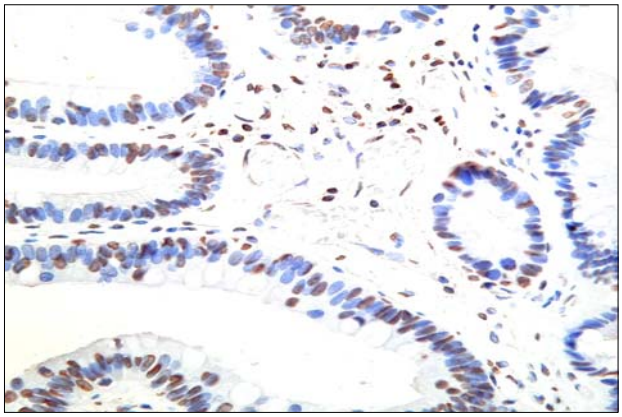

Multiple linear regression was used for statistical analysis, and p<0.005 was considered to be the level of significance.

Results The research material was obtained from 316 women and 61 men. The age group 1 (0-30 years) included 24 patients, the age group 2 (31 - 50 years) 13, and the age group 3 (over 51 years) - 217 patients. The disease duration: up to 2 years referred to 208 patients, from 2 to 5 years - 44 patients and over 5 years - 125 patients. No gallstones were found in 13 patients, 53 patients had single large gallstones, in 53 - gallstones varied in size and, in 192 - they were small and numerous. I^0 inflammation was noted in 90 patients, II^0 in 162, III^0 in 120 and IV^0 in 5 patients.

The performed immunohistochemical investigations revealed a varied expression of 8-hydroxydeoxyguanosine (8-OhdG) in the epithelial cells of gallbladder mucosa, ranging from very few coverage epithelial cells to a large number of cells. In some fields of vision, most cell nuclei of the surface epithelium and glandular tubes, lying underneath, showed a strong nuclear expression. In such cases, also lymphoidal cells in inflammatory infiltrations were positive for 8-OhdG (ryc.1). In the control group, the reaction was negative.

Statistical analysis showed a statistically significant difference between the level of 8-0HdG expression in gallbladder mucosal epithelium and the disease duration and inflammation degree (p< 0.0005). The remaining correlations, concerning the 8OhdG index and the gender and age, as well as the number and size of gallstones, showed no statistical significance (Table 1.).

Discussion

The immunohistochemical investigation, which employs antibody against 8-OhdG, serves to visualize oxidative DNA damage in human tissues and is considered a biomarker of considerable specificity [4]. Similarly as Seiko et al. [6], we found a correlation between the increase in the 8-0HdG index in gallbladder mucosal epithelium and inflammation degree. We also noted that the reaction intensity increased statistically significantly with the disease duration. The fields, where 80HdG expression in epithelial cells was markedly enhanced, also exhibited substantial lymphocytic infiltration. As similar observations have been reported by other authors, it can be assumed that inflammatory infiltration is the source of oxidative stress for gallbladder mucosal epithelial cells [7]. According to many authors, oxidative DNA damage plays a significant role in carcinogenesis [8]. Free oxygen radicals can be the major factors in promoting gene sequence instability, while inflammatory cytokines cause DNA damage and may inhibit the general mechanism of DNA repair. Although the precise role of 8-0HdG is unclear, in vitro studies have revealed that 8-0HdG accumulation in cellular DNA is mutagenic and carcinogenic; it is of great predictive significance for carcinogenesis in the breast [9].

Conclusions

In chronic cholecystitis, the expression of 8-hydroxydeoxyguanosine, a biomarker of oxidative DNA damage, is increased. The expression of 8-OHdG is associated with inflammation degree and disease duration. DNA damage, observed in chronic cholecystitis, indicates a correlation between cholecystitis and cancerogenesis.

References

1. Asaka M, Dragosics BA. Helicobacter pylori and gastric malignancies. Helicobacter, 2004; 9 Suppl 1: 35-41.

2. Seidelin JB. Colonic epithelial cell turnover: possible implications for ulcerative colitis and cancer initiation. Scand J Gastroenterol, 2004; 39: 201-11.

3. Poduri CD. Hepatitis C virus (HCV)--a review molecular biology of the virus, immunodiagnostics, genomic heterogeneity and the role of virus in hepatocellular carcinoma. Indian J Exp Biol, 2003; 4: 549-62.

4. Kasai H. Analysis of a form of oxidative DNA damage, 8-hydroksydeoksyguanosine, as a marker of cellular oxidative stress during carcinogenesis. Mutat Res, 1977; 387: 147-163.

5. Beckman KB, Ames BN. Oxidative decay of DNA. J Biol Chem, 1997; 272: 19633- 36.

6. Seki S, Kitada T, Yamada T, Sakaguchi H, Nakatani K, Onoda N, Satake K. Immunohistochemical detection of 8-hydroksydeokdyguanosine, a marker of oxidative damage, in human chronic cholecystitis. Histopathology, 2002; 40: 531- 8.

7. Feig DI, Reid TM, Loeb LA. Reactive oxygen species in tumorigenesis. Cancer Res, 1944; 54: 1890s - 94s.

8. Floyd RA. The role of 8- hydroksydoksyguanosine in carcinogenesis. Carcinogenesis, 1986; 7: 1849-51.

9. Musarrat J, Aresina-Wilson J, Wani AA. Prognostic and aetiological relevance of 8-hydroksydoksyguanosine in human brest carcinogenesis. Eur J Cancer, 1996; 32: 1209-14.

Clinical usefulness of K-RAS mutation detection in colorectal cancer and in surgical margins of the colon

Okulczyk B[1], Kovalchuk O[2], Piotrowski Z[1], Myśliwiec P[1], Chyczewski L[2]

[1]The 2nd Department of General and Gastroenterological Surgery, [2]Department of Molecular Biology,
Medical University of Białystok

Abstract

The incidence of K-RAS gene mutations in tumour and surgical margins was investigated in 63 patients with adenocarcinomas of varied clinical stage and histological grade. Point mutations of codon 12 K-RAS gene were detected, using the PCR-RFPL technique in cancer tissue in 23 patients (36.5%) and in colon margin mucosa in 1 patient (3.7%), out of 27 examined subjects. No significant correlations were found between the mutations and clinical features. Tumours, located in the left colon, and mucinous neoplasms displayed a higher incidence of mutations. No correlation was observed with either Dukes or TMN clinical advancement.

Key words: K-RAS mutations, colorectal cancer, surgical margins.

Introduction

Mutations of protooncogenes RAS are most commonly found in CRC, appearing early in the process of carcinogenesis, already in the phase of hyperproliferating epithelium, in anaplastic crypt foci (ACF), in adenocarcinomas and cancers [1, 2].

Determination of K-RAS mutations have recently been used to elucidate the prognostic role of surgical margin length during CRC resection, being more efficient than conventional histopathological examinations [3, 4, 5].

ADDRESS FOR CORRESPONDENCE:
Bogna Okulczyk
2nd Department of General and Gastroenterological Surgery
Medical University of Białystok
M.C. Skłodowskiej 24 A; 15-276 Białystok, Poland

The aim of the study was to clinically evaluate the usefulness of detection of K-RAS mutations in colorectal cancers and in surgical margins of the colon, with reference to their diagnostic and prognostic value in correlation with clinical features, histopathological picture, size, differentiation and metastases.

Material and Methods

The study involved 63 patients with CRC: 30 (47.6%) men, aged 51-80 years (the mean age: 68.0 years) and 33 women, aged 40-84 years (the mean age: 65.6 years) operated on during the period of 2001-2003. Tumours were located in the rectum in 30 patients, in the left colon in 19 and in the right colon in 14 subjects. In 25 cases, Dukes C tumours were found, 24 patients had Dukes B, 6 Dukes A and 8 Dukes D. Out of 61 patients with adenocarcinoma, 42 had G2 (68.8%), 14 G3 and 5 - G1 stage. In 7 patients, mucus-secreting tumours were isolated. Radical surgery was performed in 55 subjects (87.3%) from Groups A, B and C, palliative - in 8 D cases. Surgical margins of, at least, 5 cm in colon cancer and 2 cm in rectal cancer were preserved. The tumour and the margins were subjected to histopathological and molecular evaluation.

Genomic DNA was isolated from approximately 20 mg of tissue, using the GenElute Blood Genomic DNA Kit /Sigma/. The analysis of K-RAS mutation was performed by the RFLP-PCR technique with an additional enrichment of the genetic material with mutated alleles. The amplification proper (II PCR) and restrictive analysis with BstOI enzyme (sequences: KR1 5'-ACTGAATATAAACTTGTGGTAGTTGGACCT-3'KR2,5'-TCAAAGAAT-GGTCCTGCACC-3') followed the preliminary coping of the matrix. Digestion products were distributed, basing on differences in the molecular weight via electrophoresis in polyacrylamid gel. Electrophoregrams were subjected to computer analysis by UVI-KS400i/Image PC /Syngen Biotech. [6]. The chi2 test was used for statistical analysis: $p<0.05$ was the accepted level of significance.

Table 1. K-RAS mutations, according to age and sex of patients, tumour histological texture, histological and clinical advancement.

Feature	Number of patients	*K-RAS* mutation	p
Sex: Men	30	10 (33.3%)	
Women	33	13 (39.4%)	0.612
Age: under 60 years	17	6 (35.3%)	
over 60 years	46	17 (36.9%)	0.90
Tumour location: Rectum	30	10 (33.3%)	
Left colon	19	9 (47.3%)	
Right colon	14	4 (28.6%)	0.48
Dukes' scale: A	6	3 (50.0%)	
B	24	8 (33.3%)	
C	25	8 (32.0%)	
D	8	4 (50.0%)	0.98
Histological grade: G1	5	2 (40.0%)	
G2	42	15 (35.7%)	
G3	14	5 (35.7%)	0.98
Adenocarcinoma	56	19 (33.9%)	
Mucus-secreting tumours	7	4 (65.3%)	0.21
Feature T: pT1	6	3 (50.0%)	
pT2	6	2 (33.3%)	
pT3	37	13 (35.1%)	
pT4	14	5 (35.7%)	0.77

Results

K-RAS gene mutations in the study group of 63 patients were found in 23 cases (36.5%) in the tumour, in women 13/33 (39.4%) and in men - 10/30 (33.3%). Their incidence was similar in both age groups: under 60 in 6/17 patients (35.3%) and over 60 in 17/46 (36.9%). A higher percentage of mutations was observed in the tumours, located in the left colon: 47.3 and 28.6% (p=0.48) and in mucus-secreting tumours: 65.3% and 33.9% (p=0.2). No significant correlations were noted between Dukes scale and the tumour size (TNM) or histological differentiation (Table 1). K-RAS mutations were detected in 1 (3.7%), out of 27 surgical margins, with no neoplastic cells found in histopathological examination. In the group of 63 patients, a 6-24-month clinical follow-up revealed the disease recurrence in 5 (7.9%); two of them had K-RAS mutation in the primary tumour.

Discussion

Most clinical genetic researches tend to determine the prognostic significance of K-RAS mutations, but the reported data are not consistent [7, 8, 9]. The incidence of mutations in CRC ranges from 20% to 50% (the differences are due either to the selection of patients or to tissue fixation techniques), suggesting the existence of several different pathways of carcinogenesis which require thorough investigations [8, 9, 10]. In our material of 63 patients with colorectal cancer, mutations in codon 12 of K-RAS were found in 23 cases (36.5%). Similar results have been reported by other clinical centres [7, 9]. Like other authors, we found no correlation between the incidence of mutations and the clinical features, including clinical advancement [7, 8]. In our patients, a similar incidence of mutations was maintained from the earliest stages of tumour growth: 41.6% for T1 and T2 v. 35.2% for T3 and T4. No distinct correlations were seen between the presence of mutations in the tumour and its histological grade. Only in the mucus-secreting tumours, mutation incidence was close to significant 65.3% v. 33.9% (p=0.2). Similar correlations, resulting perhaps from a different genetic model of mucinous tumour growth, can be found in single reports of other authors [4, 9]. Neoplastic recurrence, following radical resection, was observed in 5 patients, out of 63 (7.9%), including 2 with gene K-RAS mutation. These observations, as well as the findings of other authors indicate that K-RAS mutations in CRC do not significantly correlate with either neoplastic recurrences or the survival time, although some contradictory data have been reported, e.g. the fact that either recurrences or remote metastases can be predicted, based on tests of tumour-drainage blood, bone marrow, lymph nodes, peripheral blood or stool [11, 12, 13]. Studies on K-RAS mutations are undertaken to detect micrometastases at the line of surgical incision of the colon margin. Their results (mutation range 6% - 53%) are difficult to compare because of the differences in the employed research models, in margin length and the methods of mutation detection [3, 4, 5]. In our own analysis of 27 margins >5 cm from the tumour border, mutation was detected in 1 (3.7%). The trials, which have been undertaken to determine K-RAS mutations in surgical margin mucosa, seem to confirm the possibility of their detection, when histopathological examination is negative. Determination of these mutations can be treated as one of the pathways, used to identify either high risk factors of micrometastases or recurrences in the postoperative period [5, 7, 10], what encourages research intensification.

Conclusions

No correlation was found of K-RAS gene mutations with clinical features of the tumour or with Dukes or TNM clinical advancement. A non-significant correlation was observed with the left-side location in the colon and with mucinous histotype.

In histologically unchanged mucosa of surgical margins, K-RAS point mutations were detected in 3.7% of CRC patients.

References

1. Fearon ER, Volgelstein B. A genetic model for colorectal tumorigenesis. Cell, 1990; 5: 759-67.

2. Strivastava S, Verma M, Henson DE. Biomarkers for early detection of colon cancer. Clin Cancer Res, 2001; 7:118-26.

3. Zhu D, Keohavong P, Finkelstein SD, Swalsky P, Bakker A, Weissfelf J, Srivatava S, Whiteside TL. K-ras Gene Mutation In Normal Colorectal Tissues from K-ras Mutation-positive Colorectal Cancer Patients. Cancer Res, 1997; 57: 2458-92.

4. Zhang H, Nordenskjold B, Dufmats M, Soderkvist P, Sun XF. K-ras Mutation in Colorectal Adenocarcinomas and

Neighbouring Transitional Mucosa. E Journal Cancer,1998; 34:2053-57.

5. Aivado M, Gynes M, Gorelov V, Schmidt WU, Roher HD, Goretzki PE. "Field cancerisation"-ein zusatzliches Phenomen in der Entwicklung von Colontumoren? Chirurg, 2000; 71:1230-35.

6. Puig P, Urgell E, Capella G. A highly sensitive method for K-RAS mutation detection is useful in diagnosis of gastrointestinal cancer. Int J Cancer, 2000; 85: 73-7.

7. Andreyev H, Norman AR. Kirsten ras mutation in patients with colorectal cancer; the multicenter " RASCAL" study. J Natl Cancer Inst, 1998; 90: 675-84.

8. Trzeciak L, Przybyszewska M, Nasierowska-Guttmejer A. Mutacje K-RAS oraz akumulacja białka p53 w rakach jelita grubego. Nowotwory, 2000; 50: 21-7.

9. Bazan V, Migliavacca M, Zanna I, Tubiolo C, Grassi N, Latteri A, La Farina M, Albanese I, Dardanoni G, Salerno S, Tomasino RM, Labianca R, Gebbia N, Russo A. Specific codon 13 K-ras mutation are predictive of clinical outcome in colorectal cancer patients, whereas codon 12 K-ras mutation are associated with mucinous histotype. Annals of Oncology, 2002; 13: 1438-46.

10. Pawłowska-Wakowicz B, Paluszkiewicz P, Karski J, Wojcierowski J. Białko p21-ras w rakach jelita grubego. Wiad Lek, 1997; 50, 76-81.

11. Etoh T, Ueo H, Inoue H, Ato K, Utsunomiya T, Barnard Gkitano S, Mori M. Clinical significance of K-Ras mutation in intraoperative tumor drainage blood from patients with colorectal carcinoma. Ann Surg Oncol, 2001; 8: 407-12.

12. Tortola S, Marcuello E, Gonzalez I. P53 and K-ras gene mutation correlate with tumor aggressiveness but are not of routine prognostic value in colorectal cancer. J Clin Oncol, 1999; 17: 1375-81.

13. Clarke GA, Ryan E, Crowe JP, O'Keane JC, Mac Mathuna P. Tumour-derived mutated K-ras codone 12 expression in regional lymph nodes of stage II colorectal cancer patients is not associated with increased risk of cancer-related death. Int J Colorectal Dis, 2001;16: 108-11.

Proliferating activity in the epithelial and stromal component of fibroadenomas and phyllodes tumours of the breast

Barwijuk-Machała M, Reszeć J, Baltaziak M, Musiatowicz B, Cylwik J

Department of Pathology Medical University of Białystok, Poland

Abstract

The aim of the study was an evaluation of PCNA and Ki-67 expression in the epithelial and stromal component of fibroepithelial tumours (FT) of the breast in correlation with morphological parameters. A series of 11 fibroadenomas (FA), including 8 cases of the cellular type (FAC), 19 benign phyllodes tumours (PTLGM), 8 bordeline (PTBM) and 6 malignant phyllodes tumours were assessed, using immunohistochemistry. The expressions of Ki-67 and PCNA in the epithelial component were significantly higher in PTLGM, when compared with FA and PTBM. A significant increase of Ki-67 and PCNA stromal expressions was associated with the progression from PTLGM to PTHGM. Our results show that Ki-67 and PCNA may be useful in the evaluation of stromal proliferation in phyllodes tumours (PT), which play an integral part in the progression from PTLGM through PTBM to PTHGM.

Key words: Ki-67, PCNA, fibroadenoma, phyllodes tumour

Introduction

Phyllodes tumour (PT) is a rare fibroepithelial neoplasm of the breast, composed of epithelial and stromal elements. Based on the stromal cellularity and overgrowth, nuclear pleomorphism, mitotic activity and the type of border PTs are classified as benign, borderline and malignant [1]. FA is the most common benign fibroepithelial neoplasm of the breast in young adult women. A rare variant of FA is that of the cellular type, what poses some problem in the diagnosis on FNA [2]. Attempts have been made to identify markers which may be useful in the differential diagnosis of FT and in predicting prognosis in patients with PT [1, 3, 4, 5]. Ki-67 and PCNA antigens have been shown to be useful in the analysis of cellular proliferation [1, 6, 7]. The aim of this study was to evaluate Ki-67 and PCNA expressions in epithelial and stromal elements of fibroepithelial tumours from 44 patients in correlation with morphological features.

Material and methods

The examined group included 11 cases of FA - Group I, 19 cases of PTLGM - Group II, 8 cases of PTBM - Group III and 6 cases of PTHGM - Group IV. In the series of FA, there were 8 cases of cellular type. All the PTs were histologically classified, taking into account stromal overgrowth, cellularity, mitotic activity and atypia, using the 1-3 scale. Immunostaining was performed with PCNA (PC - 10, Dako) and Ki-67 (Ki-67, Dako) monoclonal antibodies, using an LSAB KIT with DAB as a chromogen. Scores in the examined groups were based on the following scale: (-) below 10 % of the cells with positive reaction for PCNA and Ki-67 proteins, (+) between 10 % - 50 % and (++), when above 50 % cells were immunopositive. The obtained values were subjected to statistical analysis with the use of the chi-squared and Mann - Whitney tests. The correlation between the scores and pathological variables was evaluated, using Pearson and Spermans correlation analysis. Values of $p<0.05$ were considered as statistically significant.

Results and discussion

FA and mammary PT are biphasic lesions with epithelial and stromal elements. FA of a conventional type is a benign neoplasm. A cellular variant of FA shows a rapid growth and may

ADDRESS FOR CORRESPONDENCE:
Małgorzata Barwijuk-Machała
Department of Pathology Medical University of Bialystok,
Waszyngtona 13, 15-269 Białystok, Poland.
e-mail: joasia @zpkamb.edu.pl

Table 1. Ki-67 and PCNA expression in the epithelial component of fibroepithelial tumours

Groups	Ki-67				PCNA			
	(-)		(+)		(-)		(+)	
	No	%	No	%	No	%	No	%
I	4	*36.4*	7	*63.6*	2	*18.2*	9	*81,8*
II	0	*0*	19	*100*	0	*0*	19	*100*
III	8	*100*	0	*0*	8	*100*	0	*100*

Table 1. Ki-67 and PCNA expression in the stromal component of fibroepithelial tumours

Groups	Ki-67						PCNA					
	(-)		(+)		(++)		(-)		(+)		(++)	
	No	%	No	%	No	%	No	%	No	%	No	%
II	19	*100*	0	*0*	0	*0*	19	*100*	0	*0*	0	*0*
III	0	*0*	8	*100*	0	*0*	0	*0*	8	*100*	0	*0*
IV	0	*0*	0	*0*	6	*100*	0	*0*	0	*0*	6	*100*

attain large size in the breast [4]. The classification of PT as benign, borderline malignant and malignant tumour, reflects the probable clinical course, based on the histological appearance of the tumour [1]. The diagnosis of FTs in our series depended on the careful assessment of morphological features in numerous specimens. The group of FAs included 8 cases of those with stromal cellularity. The microscopic picture revealed enlarged ductules with hyperplastic epithelium and superimposed small papillations. The stroma was focally or diffusely hypercellular with considerable pleomorphism. Benign PT had bland, sometimes cellular spindle cells or myxoid stroma with low mitotic rate, minimal atypia and pushing borders. PTBM had an increased mitotic activity, cellularity, stromal overgrowth, nuclear pleomorphism and either pushing or infiltrative borders. Malignant tumours revealed a greatly increased cellularity, high mitotic rate, marked nuclear pleomorphism and an overgrowth of stromal elements. Most of them had also necrosis. The structural variability among PTs creates a substantial difficulty in the proper diagnosis of some lesions, sampled by FNA [2]. Many PTs exhibits epithelial hyperplasia, often represented by a variable increase in the thickness of the cuboidal or columnar epithelium, lining the glandular spaces. The epithelial component of PTs contains much higher concentrations of endothelin - 1 (ET - 1), when compared with FAs. Yomashita et al. suggest a possible paracrine role of endothelin 1 in stimulating the proliferation of stromal cells in PTs [8]. Sawhney et al. suggest that there is an interdependence of growth between the epithelial and stromal elements in PTs [9]. In our series, Ki-67 and PCNA protein expressions in the epithelial component were assessed as positive in 28, out of 44 cases (63,6%) and in 30, out of 44 (68,2%). There were statistically significant differences in Ki-67 and PCNA epithelial expression between Groups I - II and Groups II - III. In Group I, 63.6% and 81.8% were (+) positive for Ki-67 and PCNA respectively. In Group II, 100% of examined cases were (+) positive for Ki-67 and PCNA. In Group III, all the cases were immunonegative for Ki-67 and PCNA (Table 1). The epithelial elements of PTBM and PTHGM were not distinctive, when compared with PTLGM. Sawhney et al. suggest that stromal dependence on epithelium, which may become atrophic, is lost with increasing malignancy of PTs [9]. In our series, PCNA and Ki-67 positive reaction in the stromal component was observed in 14, out of 44 cases (31.7%). Statistical analysis revealed significant differences in Ki-67 and PCNA stromal expressions between Groups II -III and Groups III-IV. In Group II, all the cases were negative for Ki-67 and PCNA. In Group III, 100% were (+) positive for Ki-67 and PCNA. In Group IV, all the cases were (++) positive for Ki-67 and PCNA (Table 2). In the examined group, Ki-67 and PCNA protein expressions correlated significantly with stromal overgrowth, cellularity, mitotic count and atypia in PT. Our results support those from previous reports which showed that Ki-67 stromal expression correlated with the degree of malignancy in PT [6,

10]. In the examined group, we did not find any significant difference in Ki-67 and PCNA expressions between FAC and PTLGM. The findings are in agreement with those, obtained by Kaya et al, who observed proliferating activity almost at the same level in both of these entities [4]. Examinations, concerning the expression of the high molecular form of tenascin (HMT) in FA revealed 2 groups of lesions - the first and the second - which were above represented in 60% and in 20%, respectively. Tenascin is a glycoprotein, produced mainly by stromal cells, and its expressions correlates with cell proliferations. Borsi et al. revealed a significant presence of HMT in the stromal cells of benign PT and some FA with an evident proliferation of stromal elements [11]. Surgery is the treatment of choice in patients with FT of the breast. Accepted treatment of FA is surgical enucleation of the tumour mass. In women with a small PTLGM, PTBM and PTHGM, a local excision, with wide margins to prevent recurrence, or simple and radical mastectomy in case of larger tumour size has been recommended [3,5]. Based on the obtained results, the optimal therapy for patients with cellular FA should be a complete excision of the tumour, together with adequate margins of the breast tissue. In conclusion, Ki-67 and PCNA immunohistochemistry may be useful in the evaluation of the stromal proliferation in PTs, which plays an integral part in the progression from PTLGM to PTHGM.

References

1. Niezabitowski A, Lackowska B, Rys J, Kruczak A, Kowalska T, Mitus J, Reinfuss M, Markiewicz D. Prognostic evaluation of proliferative activity and DNA content in the phyllodes tumor of the breast: immunohistochemincal and flow cytometric study of 118 cases. Breast Cancer Res Treat, 2001; 65: 77-85.

2. Chhieng DC, Cangiarella JF, Waisman J, Fernandez G, Cohen JM. Cancer (Cancer Cytopathol), 1999; 87: 359-71.

3. Kleer CG, Giordano TJ, Braun T, Oberman HA. Pathologic, immunohistochemical, and molecular features of benign and malignant phyllodes tumors of the breast. Mod Pathol, 2001; 14: 185-90.

4. Kaya R, Pesterel HE, Erdogan G, Gülkesen KH, Karavel S. Proliferating activity in differential diagnosis of benign phyllodes tumor and cellular fibroadenomas: is it helpful? Pathology Oncology Research, 2001; 7: 213-16.

5. Erhan Y, Zekioglu O, Ersoy Ö, Tugan D, Aydede H, Sakarya A, Kapkaç M, Özdemir N, Özbal O, Erhan Y. P53 and Ki-67 expression as prognostic factors in cystosarcoma phyllodes. The Breast Journal, 2002; 8: 38.

6. Shpitz B, Bomstein Y, Sternberg A, Klein E, Tiomkin V, Kaufman A, Groisman G, Bernheim J. Immunoreactivity of p53, Ki-67, and c-erbB-2 in phyllodes tumors of the breast in correlation with clinical and morphologic features. J Surg Oncol, 2002; 79: 86-92.

7. Hasebe T, Imoto S, Sasaki S Tsubono Y, Mukai K. Proliferative activity and tumor angiogenesis is closely correlated to stromal cellularity of fibroadenoma: proposal fibroadenoma, cellular variant. Pathol Int, 1999; 49: 435-43.

8. Yamashita J, Ogawa M, Egami H, Matsuo S, Kiyohara H, Inada K, Yamashita S, Fujita S. Cancer Res, 1992; 52: 4046-9.

9. Sawhney N, Garrahan N, Douglas-Jones AG, Williams ED. Epithelial-stromal interactions in tumors. A morphologic study of fibroepithelial tumors of the breast. Cancer, 1992; 70: 2115-20.

10. Suo Z, Nesland JM. Phyllodes tumor of the breast: EGFR family expression and relation to clinicopathological features. Ultrastruct Pathol, 2000; 24: 371-81.

11. Borsi L, Carnemolla B, Nicolo G, Spina B, Tanara G, Zardi L. Expression of different tenasci isoforms in normal, hyperplastic and neoplastic human breast tissues. Int J Cancer, 1992; 52: 688-92.

Insulin-like growth factor-I receptor in human oral cancer

Reszeć J, Duraj E, Koda M, Musiatowicz B, Sulkowska M

Department of Pathology, Medical University of Bialystok

Abstract

The purpose of the study was to evaluate the expression of IGF-IR in primary tumours and lymph node metastases of oral cancers and the correlation between expression of IGF-IR and some clinicopathological features. Fifty-seven (57) oral cancers were examined by immunohistochemical studies, using the avidin-biotin-peroxidase method. Our study included only oral cancers, classified histopathologically as squamous cell carcinoma (7 cases in G1 grade, 44 (G2) and 6 (G3); 23/pT1 stage, 18/pT2, 7/pT3 and 9/pT4). Positive immunostaining for IGF-IR was noted in 32, out of 57 (56.1%) of oral tumours. We found a tendency (p=0.081) toward an association between IGF-IR expression in the primary tumours and their stage (pT3 and pT4). A comparison between the primary tumours and matching lymph node metastases revealed that 13, out of 20, (65%) cases showed a convergence between primary tumours and matching lymph node metastases with regard to either negative or positive staining.

Introduction

The IGF family of peptide ligands (IGF-1 and IGF-2) the IGF-1 and IGF-2 receptors are fundamentally involved in the regulation of somatic growth, cell proliferation, transformation and apoptosis. IGF-1 stimulates growth and metabolism by binding to the IGF-1R receptor, thereby activating, by protein tyrosine phosphorylation, a signal transduction cascade that is similar to the one, involved in insulin action. The IGF-IR, a tyrosine kinase receptor, is the major receptor for both IGF-I and IGF-II and consists of two α two ß subunits. The α subunits are entirely extracellular chains, containing a cysteine-rich domain responsible for ligand binding, and the ß subunits display a highly hydrophobic transmembrane domain, which divides the subunit into an extracellular and intracellular region, containing a tyrosine kinase domain [1]. Recently, lots of data suggested a role of IGF-1 and IGF-1R receptor in neoplastic transformation. A variety of tumour systems, including colon cancers, demonstrate an altered expression of IGF-I and IGF-II and their principle receptor IGF-IR [2]. However, the biological effect of IGF-I in malignant progression has not - so far - been fully elucidated. Some studies have shown that IGF-IR may prevent apoptosis in numerous tumour cell systems; in addition, it may play a role in induction of cell proliferation. Several studies have shown that IGF-IR is crucial for maintaining normal growth and development, as well as mitogenic activity, cell survival, and insulin-like actions are essential for embryogenesis, post-natal growth physiology, and breast development [3].

The purpose of the study was to evaluate the expression of IGF-IR in primary tumours and lymph node metastases of oral cancers. Moreover, we assessed the correlation between the expression of IGF-IR and some clinicopathological features.

Material and methods

We examined a series of 57 oral squamous cell cancers and 20 cases of lymph node metastases. The obtained biopsy specimens were fixed in a 10% buffered formalin solution, embedded in paraffin at 56°C, then cut into 5µm slices and stained with haematoxylin and eosin (H+E). The evaluation of IGF-IR expression was performed by immunohistochemical reaction, using monoclonal antibodies from Santa Cruz Biochemicals, USA. In order to visualize the antigen-antibody reaction, the LSAB technique was applied, using DAB (diaminobensidine)

ADDRESS FOR CORRESPONDENCE:
Joanna Reszeć
Department of Pathology
Medical University of Białystok
Waszyngtona 13; 15-269 Białystok, Poland

Table 1. Ki-67 and PCNA expression in the epithelial component of fibroepithelial tumours

Variable		IGF-IR (-)		IGF-IR (+)	
		No	%	No	%
Age	< 50	5	20,8	11	33,3
	> 50	19	79,2	22	66,7
PT	pT1	13	52,0	10	31,25
	pT2	8	32,0	10	31,25
	pT3	1	4,0	6	18,75
	pT4	3	12,0	6	18,75
G	G1	4	16,0	3	9,4
	G2	19	76,0	25	78,1
	G3	2	8,0	4	12,5

(DAKO Cytomation, Denmark). The IgG1 kappa (DAKO Cytomation, Denmark) antibody was used as a negative control, whereas samples of breast cancer tissue, which showed a strong positive IGF-IR immunoreactions, were used as a positive control. The estimation of immunostaining was done under a light microscope in representative fields, using a lens with a magnification of 20x. The criteria for a positive reaction were as follows: (+) above 10% cancer cells showing positive immunostaining, and (-) below 10% of cells with positive IGF-IR immunostaining. We analysed IGF-IR expression in relation to the patients' age, sex, grading and staging and lymph node metastases. The obtained results were statistically analyzed, using the Fisher and Chi-square tests, as well as the Students-test for paired samples, employing the SPSS software package v.8.0 for Windows (SPSS Inc., Chicago, IL). The values at $p<0.05$ were considered statistically significant.

Results

Our study included only oral cancers, classified histopathologically as squamous cell carcinoma: 7 cases in G1, 44 in G2 and 6 in G3. There were 23 tumours in pT1, 18 in pT2, 7 in pT3 and 9 in pT4. Twenty-three, out of fifty-seven (23/57) (40.4%) patients had lymph nodes involved at the time of diagnosis. The results are shown in Table 1. Thirty-two (32), out of 57 tumours (56,1%) showed IGF-IR positive immunoreaction; in 13, out of 20 (65%) lymph node metastases, IGF-IR positive expression was observed. Comparing the IGF-IR expressions in the primary tumours and metastases, the results are as shown: in 9, out of 13 pairs (69,2%) IGF-IR expression was positive; in 3, out of 13 pairs (23,1%) there was no positive expression of IGF-IR observed; in 4, out of 7 pairs (57,2%) IGF-IR was positively noted in lymph node metastases with no expression in the primary oral cancer; in 4, out of 7 pairs (57,2%) IGF-IR positive immunoreaction was observed in the oral squamous cell cancer, while no IGF-IR expression was found in lymph node metastases (Table 2). Above all, in our study, we observed a high tendency towards the association between tumour size and IGF-IR immunopositivity (p= 0,081), the higher percentage with IGF-IR expression was observed in pT3 and pT4 tumours. There were no statistically significant relationships between grading, the occurrence of lymph node metastases, the age and IGF-IR expression in primary oral squamous cell cancer, although IGF-IR positive lymph node metastases were observed in statistically older patients- after 50 years old (p= 0,017).

Table 1. Clinical characteristics, anthropometric and densitometric parameters in relation to COLIA1 gene alleles.

IGF-IR in primary tumours	Expression level	IGF-IR in metastases		
		(-)	(+)	Total number of cases
	(-)	3	4	7
	(+)	4	9	13
	Total number of cases	7	13	20

Discussion

There is no data in the literature, associated with IGF-IR expression in oral squamous cell cancer. Some studies have shown a strong correlation between IGF-IR receptor expression and colorectal, breast, prostate cancer development, but the evidence is unclear [4, 5, 6]. The studies found an association between raised plasma IGF-I levels and an increased prostate risk. Serum concentrations of IGF-II were higher in patients with colorectal adenomas, compared to those in normal controls [2]. Also other studies show IGF-I as a factor that determines a lifelong risk for breast cancer [7]. Freier at al [8] observed 40 times higher IGF-II expression in malignant colon tissue than in tissue, adjacent to the tumour. The expression of IGF-I receptor was 2.5 times higher in the malignant tissue than in tissue adjacent to the tumour. Weber et al [9] observed an overexpression of IGF-IR in colon carcinomas; colon carcinoma cells exhibited a positive staining for IGF-IR in 91% of all tumours (30, out of 33), whereas the adjacent normal colonic epithelial cells showed only either a very faint or no significant IGF-IR immunoreactivity. Reinmuth et al [10] showed IGF-I positive tumours with decreased tumour cell proliferation; furthermore, IGF-IR DN-transfected cells yielded significantly decreased tumorigenicity and growth in the liver.

In our study, 13, out of 20 (65%) tumour-metastases were IGF-IR-positive, what might suggest an association between IGF-IR expression in primary tumours and metastatic ability,

but the data must be investigated more carefully. IGF-IR expression in oral squamous cell cancer might be a predictive marker in tumour progression and metastases ability. We would like to emphasise the importance of studies, concerning the proteins involved in the proliferation in lymph node metastases because the knowledge about heterogeneity between primary tumours and lymph node metastases could shed some light on tumour biology and lead to a development of more effective anti-cancer therapies.

References

1. Grimberg A, Cohen P. Role of insulin-like growth factor and their binding proteins in growth control and carcinogenesis. Journal of Cellular Physiology, 2000; 183: 1-9.

2. Baciuchka M, Remacle-Bonnet M, Garrouste F, Favre R, Sastre B, Pommier G. Insulin-loke growth factor (IGF) - binding protein-3 (IGFBP-3) proteolysis in patients with colorectal cancer: possible association with the metastatic potential of the tumor. Int J Cancer, 1998; 79: 446-7.

3. Bustin SA, Dorudi S, Phillips SM, Feakins RM, Jenkins PJ. Local expression of insulin-like growth factor-I affects angiogenesis in colorectal cancer. Tumour Biol., 2002 ; 23: 130-8.

4. Zumkeller W. IGFs and IGFBPs: surrogate markers for diagnosis and surveillance of tumor growth? J Clin Pathol: Mol Pathol, 2001; 54: 285-8.

5. Holly JMP, Gunnell DJ, Davey Smith G. Growth hormone, IGF-I and cancers. Less intervention to avoid cancers? More intervention to prevent cancer? Journal of Endocrinology, 1999; 162: 321-30.

6. Rho O, Bol DK, You J, Beltran L, Rupp T, DiGiovanni J. Altered expression of insulin-like growth factor I and its receptor during multistage carcinogenesis in mouse skin. Mol Carcinog, 1996; 17: 62-9.

7. Stoll BA. Oestrogen/insulin-like growth factor-I receptor interaction in early breast cancer: clinical implications. Ann Oncol, 2002; 13: 191-6.

8. Freier S, Weiss O, Eran M, Flyvbjerg A, Dahan R, Nephesh I, Safara T, Shiloni E, Raz I. Expression of the insulin-like growth factors and their receptors in adenocarcinoma of the colon. Gut, 1999; 44: 704-8.

9. Weber MM, Fottner C, Liu SB, Jung MC, Engelhardt D, Baretton GB. Overexpression of the insulin-like growth factor I receptor in human colon carcinomas. Cancer, 2002; 95: 2086-95.

10. Reinmuth N, Liu W, Fan F, Jung YD, Ahmad SA, Stoeltzing O, Bucana CD, Radinsky R, Ellis LM. Blocade of insulin-like growth factor I receptor function inhibits growth and angiogenesis of colon cancer. Clin Cancer Res, 2002; 9: 3259-69.

Immunohistochemical evaluation of mast cells and mark activity tryptase and chymase in experimental fibrosarcoma

Kasacka I[1], Sawicki B[1], Roszkowska-Jakimiec W[2]

[1]Department of Histology and Embryology, [2]Department of Instrumental Analysis,
Medical University of Białystok, Poland

Abstract

The aim of the study was an evaluation of the activity of mast cells and mark activity tryptase and chymase and of protein levels in experimental fibrosarcoma, induced in rat skin. The experiments were carried out on 50 male Wistar rats. The cancer was induced in rats by one subcutaneous injection of 0.2 mg 3-methylcholanthrene in 0.25 ml of olive oil. Tissue material was fixed in Bouin's fluid. Immunohistochemical tryptase detecting reactions were performed - using specific antibodies and the ABC complex. The activities of tryptase and chymase and protein levels were determined in supernatant of 10% homogenate. We found a very significant growth of mast cell quantity in the connective tissue of tumours. We observed slight differences in the activity of examined enzymes in tumours of different mass.

Key words: mast cells, tryptase, chymase, protein, fibrosarcoma, rat.

Introduction

The synthesis of tryptase and chymase occurs in mast cells. These cells, while homing the connective tissue, are ubiquitous in the whole organism. Especially numerous are they in tissues which are on the borderline of the external and internal environment. That is why their increased numbers are observed in the skin, under the epidermis, in the gastric mucosa, as well as in the mucosa of the respiratory system and the uro-genital system. The mast cells occur in the neighbourhood of blood vessels and lymphatic ducts, however, their presence has not been confirmed in circulation [1, 2].

Since the first identification of the mast cells, research has been carried out at many scientific centres to explain their role in homeostasis and pathology of the system. Till now, it has not been possible to determine either the role or the function of mastocytes in the maintenance of health condition, however, growing is the number of diseases in which the mast cells affect their pathophysiology. Experimental studies, performed on models of mastocyte functioning in these processes, are very significant for the explanation of the specific role of mastocytes in the course of various pathological processes. Neither biological nor clinical consequences of mastocyte occurrence in neoplasmic tumours have yet been unveiled [3, 4]. Preliminary own studies have demonstrated a distinct increase of the mast cells in tissues of an experimentally induced tumours in rats [5].

The aim of this study was to evaluate the activity of mast cells and neutral proteases, such as tryptase and chymase, and protein levels in the homogenate of methylcholanthrene (3-MC) fibrosarcoma of different masses, induced in rats.

Materials and methods

The study involved 50 male Wistar rats (100-120g b. w.). The animals were given standard rat chow and water. All the animals were divided into three groups: 1. Fibrosarcoma was induced in 34 rats by one subcutaneous injection of 0.2mg 3-MC dissolved in 0.25ml of olive oil in the dorsal skin area; 2. Controls (a) - 8 animals received subcutaneous injection of 0.25ml pure olive oil; and 3. Controls (b) - 8 rats with no treatment. The animals from the experimental group were killed soon after tumour growth was observed. The tumours were extracted on the day of detection, and after 1, 2 and 3 days from their initial observation. Dissected tumours were weighed and measured. Next, two wedge-shaped sections of each tumour were taken. In the control animals, only subcutaneous tissue sections were collected. Some tissue sections

ADDRESS FOR CORRESPONDENCE:
Irena Kasacka
Department of Histology & Embryology
Medical University of Białystok
Kilińskiego 1; 15-089 Białystok, Poland
Tel. (48 85) 748 54 58; e-mail: kasacka@amb.edu.pl

Figure 1. Subcutaneous tissue from the control rat. Spindle-shaped mast cells are distributed close to small blood vessels. The nuclei of mastocytes are small and obscured by granules. Toluidine blue. x300.

Figure 2. A fragment of a large fibrosarcoma periphery. Mast cells are very numerous. Most of them contain large, light nuclei and very little number of granules (they are strongly degranulated). Toluidine blue. x 300.

Figure 3. A fragment of a large fibrosarcoma centre. Immunostaining for tryptase is visible in the main, large and mature mastocytes. x 300.

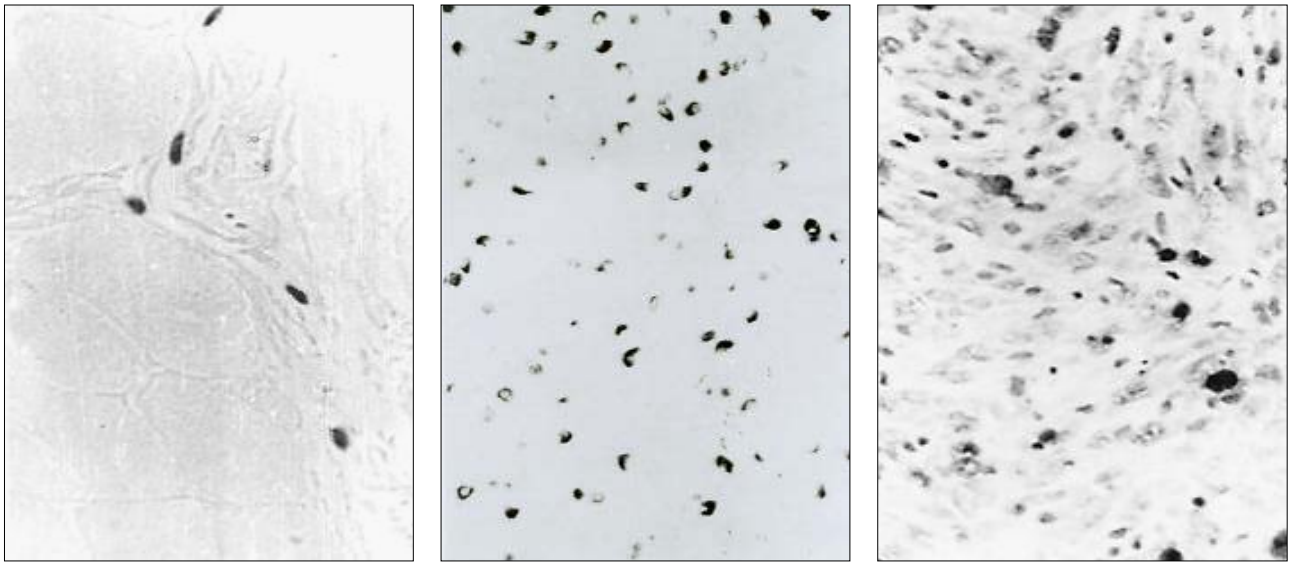

Table 1. Activity of tryptase and chymase and protein levels of methylocholanthrene fibrosarcoma.

Ingredient	Rats with tumour		
	small	intermediate	large
Tryptase	8.82 ± 1.0	9.58 ± 0.97	9.28 ± 0.82
Chymase	4.74 ± 0.43	5.06 ± 0.49	5.40 ± 0.5
Protein	30.39 ± 2.1	28.88 ± 1.9	28.24 ± 2.0

were fixed in Bouine's fluid and routinely embedded in paraffin. The obtained 5μm sections were stained with haematoxylin-eosin (H+E), as well as by the Azan method. Mast cells were stained with toluidine blue or alcjan blue+saphranine (Csaba methods) in pH 1.5. Immunohistochemical studies were performed by the ABC method (avidin-biotin peroxidase complex), using monoclonal specific mouse antisera against tryptase (DAKO Copenhagen). Control reactions always yielded negative results. Out of the second section, 10% homogenate was prepared in 0.15 M NaCl. The activity of tryptase was determined by means of Boc-Phe-Ser-Arg-AMC, and that of chymase by the use of Suc-Leu-Leu-Val-Tyr-AMC in pH of 7.5. The volume of released 7-amino-4-methylocoumarin was determined by measuring the absorbance at 560 nm, following the staining reaction with N-(1-naphthyl) in presence of sodium nitrite and ammonium sulphite. The results were read out of a calibration chart, made with the use of standard β-naphthylamine. The protein was determined by Bradford's method.

The obtained results were statistically evaluated by means of Student's 't' test.

Results

No significant differences were found between the control groups of rats, regarding the results of performed studies. For that reason, only the results of studies, performed on the animals injected with olive oil, were taken into account (Fig. 1.).

In the animals, in which the cancer was induced by 3-MC, tumours developed in the subcutaneous tissue after 3-4, 5-6 and 7-8 months and demonstrated the mass of 1-6, 20-55 and 80-176 g, respectively. All the tumours had a histological structure typical for fibrosarcoma, as mainly spindle-shaped cells constituted their structure. Many giant cells with numerous nuclei were found, as well as monstrous cells with giant nuclei, as well as other atypical cells. In the structure of the tumours, a tendency was observed towards an increase in the number of M cells during tumour growth (Fig. 2 and Fig. 3.).

However, significant individual differences were observed, as tumours of a similar size (especially the very large ones) sometimes differed in the concentration of M cell distribution.

Table 1 presents results of the measurements of tryptase and chymase activities and protein levels in the tumours with small, intermediate and large mass.

Discussion

So far, neither biological not clinical consequences of mast cell functioning in neoplastic tumours have unequivocally been determined.

In the performed own studies, a very distinct increase in the number of mastocytes was noted, mainly in the peripheral areas of fibrosarcoma. Other authors also observed an increased number of mast cells during carcinogenesis and their degranulation

related to tumour growth intensity [3, 6, 7]. However, in vitro experiments showed an anti-tumour activity of mast cells in culture conditions [2, 8]. The results of certain studies suggest that mastocytes may suppress the growth of neoplasms, e.g., via polysaccharide neutralisation [9] or by release of the tumour necrosis factor alpha (TNF-α), just as it has been reported from *in vitro* studies [4]. These views are contradicted by results of other studies, which demonstrate that TNF induces angiogenesis in normal tissues [10].

Fibrosarcomas of different mass, induced by 3-MC, showed slight differences in the activity of tryptase and chymase. No differences were found in the contents of protein in tumours of different mass, either. Immunopositive reaction for tryptase was seen only in some large M cells in the stroma of the fibrosarcoma. Toluidine blue staining always showed a few times higher number of mast cells in the same tumour fragments. It may probably have resulted from the occurrence of a large number of young and immature mast cells with scarce volumes of cytoplasm with a small number of secretory granulations [11]. Presumably, the parallelly growing number of mast cells in their stroma is of significant importance for quick tumour development. This problem, however, requires further investigations in order to explain the nature of mast cell influence on fibrosarcoma development.

References

1. Furgała A, Litwin JA. Distribution of mast cells along and across successive segments of the rat digestive tract: a quantitative study. Folia Histochem Cytobiol, 1998; 36: 19-27.

2. Metcalfe DD, Baram D, Mekori Y. Mast cells. Physiol Rev, 1997; 77: 1033-79.

3. Roche WR. Mast cells and tumors. The Specific enhancement of tumor proliferation in vitro. Am J Pathol, 1985; 119: 57-64.

4. Valent P. Mast cell differentation antigens: expresion in normal and malignat cells and use for diagnostic purposes. Europ J Clin Invest, 1995; 25: 715-20.

5. Sawicki B, Kasacka I, Chyczewski L, Sobolewski K. Preliminary evaluation of mast cells in rats with experimental fibrosarcoma induced by 3 methylcholanthrene. Folia Histochem Cytobiol, 2001; 39: 96-7.

6. Dvorak AM, Morgan ES, Lichtenstein LM, Weller PF, Schleimer RP. RNA is closely associated with human mast cell secretory granules, suggesting a role(s) for granules in synthetic processes. J Histochem Cytochem, 2000; 48: 1-12.

7. Riley JF. Mast cells and cancer in the skin of mice. Lancet, 1966; 2: 1457-9.

8. Dimitviadou V, Kotsilieris M. Mast cell-tumor cell interactions: for or against tumor growth and metastasis? Anticancer Res, 1997; 17: 1541-9.

9. Wolańska M, Sobolewska K, Bańkowski E, Chyczewski L. Alterations in glycosaminoglycan composition of methylcholanthrene-induced sarcoma of various stages of the tumor growth. Folia Histochem Cytobiol, 1996; 34: 21-6.

10. Kubes P, Granger DN. Leukocyte-endothelial cell interactions evoked by mast cells. Carrdiovascular Res, 1996; 32: 699-708.

11. Jamur MC, Grodzki ACG, Moreno AN, de Mello LFC, Pastor MVD, Berenstein EH, Siraganian RP, Oliver C. Identification and isolation of rat bone marrow-derived mast cells using the mast cell-specific monoclonal antibody AA4. J Histochem Cytochem, 2001; 49: 219-28.

Evaluation of proliferating markers Ki-67, PCNA in gastric cancers

Czyżewska J[1], Guzińska-Ustymowicz K[2], Lebelt A[3], Zalewski B[4], Kemona A[2]

[1]Department of Gastroenterology and Internal Dieseas, [2]Department of General Pathomorphology,
[3]Department of Human Anatomy, [4]2nd Department of General and Gastroenterological Surgery,
Medical University of Białystok, Poland

Abstract

Tumours from 45 patients with advanced gastric cancer were assessed by immunohistochemistry. Tissue sections were fixed in 10% buffered formaldehyde solution, embedded in paraffin and stained immunohistochemically with anti-human Ki-67 and PCNA antibodies. No correlation was found between Ki-67, PCNA protein expression, the age of patients and the localization of tumour. A significant, positive association was observed between the expression of Ki-67, PCNA and tumour differentiation and Lauren's classification. Also a strong correlation was found between lymph node involvement and the expression of Ki-67 protein. These data suggest that the expression of Ki-67, PCNA proteins were closely connected with the high grade of tumour malignancy.

Key words: Ki-67, PCNA, gastric cancer.

Introduction

Recent studies suggest that proliferating activity may provide important prognostic information in different types of tumours. Ki-67 and PCNA, the two most frequent used cell proliferation markers, recognized nuclear antigens as associated with all the phases of the cell-cycle expect G0 [1]. Antigen Ki-67, was originally discovered by Gerdes [1, 2]. The proliferating cell nuclear antigen (PCNA), the level of which increases in the nucleus, achieved the maximal level during the S phase (nearby before the beginning of DNA synthesis) [3].The aim of this study was to evaluate the expression of Ki-67, PCNA antigens in cases of gastric cancer in correlation with chosen clinico-pathological parameters.

ADDRESS FOR CORRESPONDENCE:
Katarzyna Guzińska-Ustymowicz
Department of General Pathomorphology
Medical University of Białystok
Waszyngtona 13, 15-889 Białystok, Poland
email: kguzinska@poczta.onet.pl

Material and methods

The 45 patients with gastric cancer, treated by surgery at the 2nd Department of Surgery, Medical University of Białystok, Poland, were selected for this study. Tissue specimens were collected immediately after tumour removal, fixed in 10% buffered formaldehyde solution and embedded in paraffin. Then, they were histopatologically examined, using standard haematoxylin-eosin staining, according to the TNM classification and Lauren's classification.

Immunohistochemistry: Slides of 4µm-thick serial sections of the primary tumour were prepared from each patient. The immunolocation of Ki-67 (M7240, DAKO) and PCNA (M0879, DAKO) was performed, using the labelled streptovidin biotin (LSAB) method protocol, described by DAKO (LSAB+HRP Kit, DAKO, Poland). In brief, the slides from each patient were dewaxed, using xylene and transferred to alcohol. Then, they were placed in citric buffer (pH=6.0) and heated in a microwave oven (700W) for 10 minutes to expose antigens. Endogenous peroxidase activity was blocked by incubating the section with 3% hydrogen peroxide in methanol for 10 minutes. After washing with PBS, the slides were incubated at 20°C for one hour with monoclonal antibodies. Anti-human Ki-67 protein monoclonal antibody (M7240, DAKO, dilution 1:100) was used for some slides and mouse anti-human PCNA monoclonal antibody (M0879, DAKO, dilution 1:200) was used for other slides. The reaction products were visualised with diaminobenzidine DAB (DAKO S3000, DAKO, Poland). Nuclear immunostaining was observed for both proteins (Fig. 1 and Fig. 2). Ki-67 and PCNA expression was semi quantitatively assessed in neoplastic cells of the primary tumour and defined as follows: Ki-67 and PCNA-negative (the lack of reaction or a reaction, present in less than 20% of cells) and Ki-67 and

Table 1. Expression of Ki-67, PCNA proteins and chosen parameters in gastric cancers.

Parameters		Expression of Ki-67		P value	Expression of PCNA		P value
		negative	positive		negative	positive	
Sex	Female	2(14%)	12(86%)	0.9	9(64%)	5(36%)	1
	Male	14(45%)	17(55%)		21(67.7%)	10(32,3%)	
Localization of tumour in the stomach	1/3 of up part	2(28.5%)	5(71.5%)	0.14	5(71.4%)	2(28.6%)	0.1
	1/3 of middle part	1(11%)	8(89%)		5(55.5%)	4(44.5%)	
	1/3 of down part	13(48%)	14(52%)		20(74%)	7(26%)	
	All stomach	0(0%)	2(100%)		0(0%)	2(100%)	
Lauren	Intestinal type	15(44%)	19(56%)	0.07	30(88.2%)	4(11.8%)	0.0001
	Diffuse type	1(9%)	10(91%)		0(0%)	11(100%)	
pN	absent	14(70%)	6(30%)	0.0001	16(80%)	4(20%)	0.1
	present	2(8%)	23(92%)		14(56%)	11(44%)	
Tumour differentiation	G2	14(66.7%)	7(33.3%)	0.0001	18(85.7%)	3(14.3%)	0.01
	G3	2(8.3%)	22(91.7%)		12(50%)	12(50%)	

Figure 1. Nuclear expression of Ki-67 in gastric cancer cells.

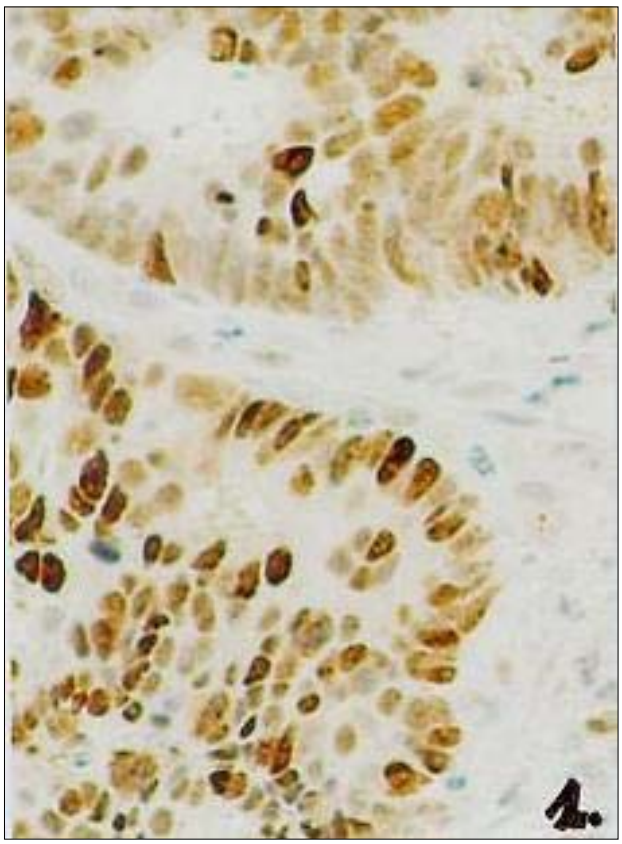

Figure 2. Nuclear expression of PCNA in gastric cancer cells.

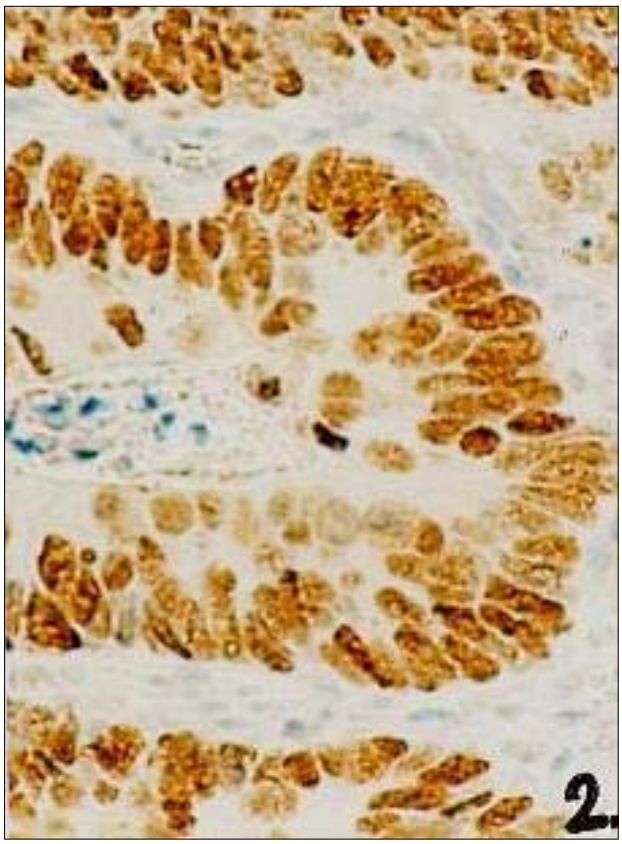

PCNA-positive (a reaction present in more than 20% of cells). The percentage of Ki-67 and PCNA positive cells was calculated in, at least, 500 neoplastic cells per sample, using a light microscope (x400). The χ^2 and Fisher's test were used for statistical analysis. P-values, smaller than 0.05, were considered statistically significant.

Results and discussion

Statistical analysis showed correlations between the expression of Ki-67, PCNA proteins and tumour differentiation and the tumour type (Lauren's classification). A strong expression was observed between the presence of lymph node metastasis and the expression of Ki-67 (p=0.0001). However, we did not find any of such correlation for PCNA (Table 1).

Maedera et al. [4] showed that, in patients with invasion, deeper than the muscle layer, the labelling index of PCNA was significantly higher than that in patients with only mucosal or submucosal invasion. The PCNA labelling index became higher as the histological stage increased. Similary, Elpek et al. [5] showed that the PCNA levels increased with histological stages and with lymph node involvement. Oya et al. [6] observed a sig-

nificantly higher value of Ki-67, PCNA in patients with lymph node metastasis. In our study, 23/25 patients with lymph node involvement showed Ki-67 expression higher than 20%. Műller et al.[7] showed a correlation between cell proliferation and Lauren's classification. The carcinomas of intestinal type showed a statistically significantly higher value for LI Ki-67 than signet-ring cell carcinomas. No correlation was found in the study between the proliferative activity and the depth of invasion (pT), lymph node involvement (pN) and the grade of differentiation [7]. Lee et al. [8] showed a positive correlation between the PCNA index and increasing age, male gender, larger tumour size, the type of tumour, according to Borman's classification (type I/II) and tumour differentiation. They also observed that, according to the Lauren classification, the intestinal type of gastric cancer had a more positive PCNA expression than the diffuse type of gastric cancer. We found the opposite: 30/34 cases of intestinal type were negative for PCNA expression. Xu et al. [9] showed an association between the Ki-67 expression in gastric cancer with peritoneal metastases to the liver, the ovary and the adrenals, but there was no correlation between the histological type, the grade of tumour growth, the depth of invasion and lymph node involvement. Yonemura et al. [10] described that large tumours, with diameter >6 cm, showed a higher Ki-67 expression than those with diameter <6 cm. However, there was no association between Ki-67 expression and peritoneal metastases, serosal invasion or macroscopic type. These results indicate that the high levels of expression of Ki-67 and PCNA were associated with tumour malignant parameters, such as lymph node involvement, or the grades of differentiation in gastric cancer.

References

1. Gerdes J, Schwab U, Lemke H, Stein H. Production of a mouse monoclonal antibody reactive with a human nuclear antigen associated with cell proliferation. Int J Cancer, 1983; 31: 13-20.

2. Gerdes J, Lemke H, Baisch H, Wacker H-H, Schwab U, Stien H. Cell cycle analysis of a cell proliferation-associated human nuclear antigen defined by the monoclonal antibody Ki-67. J Immunol, 1984; 133: 1710-15.

3. Holte H, Suo Z, Smeland EB, Kvaloy S, Langholm R, Stokka T. Prognostic value of lymphoma specific S- phase fraction compared with that of other cell proliferation markers. Acta Oncol, 1999; 38: 495-503.

4. Maedera K, Chung Y, Onoda N, Kato Y, Nitta A, Arimoto Y, Yamada N, Kondo Y, Sowa M. Proliferating cell nuclear antigen labeling index of preoperative biopsy specimens in gastric carcinoma with special reference to prognosis. Cancer, 1994; 73: 528-33.

5. Elpek GO, Gelen T, Aksoy NH, Karpuzaglu T, Keles N. Microvessel count, proliferating cell nuclear antigen and Ki-67 indices in gastric adenocarcinoma. Pathol Nocol Res, 2000; 6: 59-64.

6. Oya M, Yao T, Nagai T. Metestasing intramucosal gastric carcionomas. Well differentiated type and proliferative activity using proliferative cell nuclear antigen and Ki-67. Cancer, 1995; 75: 926-35.

7. Műller W, Schneiders A, Meier S, Hommel G, Gabbert HE. Immunohistochemical study on the value of MIB-1 in gastric carcinoma. B J Cancer, 1996; 74: 759-65.

8. Lee KE, Lee HJ, Kim YH, Yu HJ, Yang HK, Kim WH, Lee KU, Choe KJ, Kim JP. Prognostic significance of p53, nm23, PCNA and c-erbB-2 in gastric cancer. Jpn J Clin Oncol, 2003; 33: 173-9.

9. Xu L, Zhang S-M, Wang Y-P, Zhao F-K, Wu D-Y, Xin. Relationship between DNA ploidy, expression of Ki-67 antigen and gastric cancer metastasis. W J Gastroenterol, 1999; 5: 10-11.

10. Yonemura Y, Ohoyama S, Kimura H, Kamata T, Yamaguchi A, Miyzazki I. Asessment of tumour cell kinetics by monoclonal antibody Ki-67. Eur Surg Res, 1990; 22: 365-70.

Evaluation of protein products of cell cycle regulating genes in gastric cancer

Guzińska-Ustymowicz K[1], Gryko M[2], Czyżewska J[3], Kemona A[1]

[1]Departments of General Pathomorphology, [2]II Department of Surgery, [3]Gastroenterology and Internal Disease, Medical University of Białystok, Poland

Abstract

Formalin fixed, paraffin embedded tissue samples of 45 gastric carcinomas, resected curatively, were used for the study. An immunohistochemical analysis employed monoclonal antibodies: p53 (No N1581, DAKO) and $p27^{KIP1}$ (NCL-$p27^{KIP1}$, Novocastra). Positive nuclear protein expression was assessed at the 30% level. We found no correlations between the expression of either protein and Lauren's classification, the age of patients and tumour localization. Borderline significance of $p=0.07$ was noted in the association of p53 expression and histological differentiation. However, a decrease of p27 expression and an overexpression of p53 correlated with the presence of lymph node metastases ($p<0.01$). Simultaneously, the expression of p27 protein in main mass of tumour correlated with the lack of p53 expression in the main mass and lymph node metastases.

Key words: p53, p27, gastric cancer.

Introduction

Loss of cell-cycle regulation can play an important role in the process of tumour genesis and strongly correlates with the aggressiveness and progression of many neoplasms [1, 2]. Progression of the cell cycle depends on interactions between many cell-cycle regulators [3]. The cell cycle is controlled by cyclin-dependent kinasae (Cdks) [3]. Those cyclins regulate cell cycle and cell proliferation by checking G1-S and G2-M control points. Cdks are inhibited by many proteins, including p27KIP1, which is representative of the CIP/KIP CDK family of inhibitors [4]. In normal cells, the evaluation of p27 increases before the resting phase and quickly declines, when the cells are ready to enter a subsequent cell cycle [4]. The loss of p27 expression in cells is connected with susceptibility to carcinogenesis. p53 is also a regulator of the cell-cycle, which can stop cell cycle at G1/S and G2/M points. Inactivation of p53 protein by mutation has been found in many different types of neoplasia in humans [5,6]. Neoplastic cells with an overexpression of mutated p53 protein cannot regulate the progression of cell cycle in G0-G1 phase, and these tumours continue to grow. The aim of this study was to evaluate p53 and p27 expression in correlation with selected anatomo-clinical parameters.

ADDRESS FOR CORRESPONDENCE:
Katarzyna Guzińska-Ustymowicz
Department of General Pathomorphology
Medical University of Białystok
Waszyngtona 13, 15-889 Białystok, Poland
email: kguzinska@poczta.onet.pl

Materials and methods

Forty-five (45) patients with gastric cancer, treated by surgery at the 2nd Department of Surgery, Medical University of Białystok, Poland. were selected for the study. Tissue specimens were collected immediately after tumour removal, fixed in 10% buffered formaldehyde solution and embedded in paraffin. They were then histopathologically examined, using standard haematoxylin-eosin staining, according to the TNM classification and Lauren classification. Immunohistochemistry: Slides of 4μm thick serial sections of the primary tumour were prepared from each patient. Also, slides of metastatic lymph nodes were prepared from each patient. A Standard avidin-biotin immunoperoxidase (Novostain Super ABC Kit universal) method was used for the detection of p27KIP1 (NOVOCASTRA, No NCL-$p27^{KIP1}$, Biokom, Poland) expression. The immunolocalization of p53 protein was performed, using the labelled streptavidin biotin (LSAB) method protocol, described by DAKO (DAKO, LSAB Kit, Dako, Poland). In brief, the slides from each patient were de-waxed, using xylene and transferred to alcohol. They were then placed in citric acid buffer (pH=6.0) and heated in a

Table 1. Expression of p27, p53 proteins and selected parameters.

Parameters		Expression of p27		p	Expression of p53		p
		negative	positive		negative	positive	
Localization	1/3 of up part	3(43%)	4(57%)	0.1	4(57%)	3(43%)	0.3
	1/3 of middle part	8(90%)	1(10%)		2(22%)	7(78%)	
	1/3 of down part	19(70%)	8(30%)		16(60%)	11(40%)	
	All stomach	2(100%)	0(0%)		1(50%)	1(50%)	
Sex	female	12(86%)	2(14%)	0.2	8(57%)	6(43%)	1
	male	20(65%)	11(35%)		18(58%)	13(42%)	
Lymph node metastases	absent	9(45%)	11(55%)	0.001	18(90%)	2(10%)	0.0001
	present	23(92%)	2(8%)		5(20%)	20(80%)	
Lauren's classification	Intestinal type	24(70%)	10(30%)	1	20(59%)	14(41%)	0.1
	Diffuse type	8(73%)	3(27%)		3(27%)	8(73%)	
Histological type	G2	17(81%)	4(19%)	0.2	14(67%)	7(33%)	0.07
	G3	15(63%)	9(37%)		9(37%)	15(63%)	

Table 2. Expression of p53 and p27 proteins in the main mass of tumour and lymph node metastases.

Expression of		p27 in the main mass of tumour		P	p27 in lymph node metastases		p
		negative	positive		negative	positive	
p53 in main mass	negative	11(48%)	12(52%)	0.001	22(96%)	1(4%)	0.4
	positive	21(91%)	1(9%)		19(86%)	3(14%)	
p53 in lymph node	negative	14(54%)	12(46%)	0.003	24(92%)	2(8%)	1
	positive	18(95%)	1(5%)		17(89%)	2(11%)	

microwave oven (700W) for 15 minutes to expose antigens. Endogenous peroxidase activity was blocked by incubating the sections with 3% hydrogen peroxide in methanol for 10 minutes. After washing with PBS, the slides were incubated overnight at 4°C with monoclonal antibodies. Anti-human p27 protein monoclonal antibody (Novocastra, No NCL-p27, dilution 1:50, Biokom, Poland) was used for one slide, while for the other slides, mouse anti-human p53 monoclonal antibodies (clone DO-7; M7001; dilution 1:100; Dako, Poland) were applied. The reaction products were visualized with diaminobenzidine DAB (DAKO S3000, Dako, Poland). Nuclear immunostaining was observed for both proteins. p53 and $p27^{KIP1}$ expression was semi quantitatively assessed in neoplastic cells of the primary tumours and lymph node metastases and defined as follows: p53 and p27-negative (lack of reaction and the reaction present in less than 30% of cells) and p53 and p27-positive (the reaction present in more than 30% of cells). The percentage of p53 and p27 positive cells was calculated in, at least, 500 neoplastic cells per sample, using a light microscope (x400). The χ^2 and Fisher's exact test were used for statistical analysis. P values, smaller than 0.05, were considered statistically significant.

Results and discussion

Even though much attention has recently been paid to the evaluation of p53 and p27 expression in different carcinomas, the results and clinical implications remain conflicting [7,8]. Therefore, it was the aim of this study to evaluate the role of these factors after curative surgery solely for gastric cancer. In the present study, we found no associations between the expression of p53, p27 proteins and Lauren's classification, the patients' age and tumour localisation (Table 1). Furthermore, the expression of $p27^{KIP1}$ protein was observed in 13/45 cases, whereas the expression of p53 was detected in 22/45 cases of gastric cancers. It has been found in some studies that the nuclear accumulation of mutated p53 protein is associated with an unfavourable prognosis of gastric cancer [9]. However, other studies have not confirmed this association [8]. In most reports, the loss of $p27^{KIP1}$ expression and the overexpression of p53 were observed in cases with high aggressiveness. In this study, we found no association between the expression of $p27^{KIP1}$ and the histological grade of tumour. However, we observed a strong association between the overexpression of p53 protein in G3 gastric cancers. In our study, we observed that the overexpression of p53 strongly correlated

with the presence of lymph node metastases ($p<0.0001$), where there was a simultaneous loss of $p27^{KIP1}$ protein expression in the main mass of tumour. Our results strongly correspond with the results obtained by other authors [10], who observed an association between a decreased $p27^{KIP1}$ expression and the depth of invasion, lymph node involvement and vascular invasion. Moreover, the loss of $p27^{KIP1}$ expression was the parameter of short survival in patients with oesophageal, prostate, and gastric carcinomas [10, 11, 12]. Li J-Q et al. [13] showed that, in colorectal neoplasms, the loss of $p27^{KIP1}$ promotes lymph node metastasis. At the present study, we also analysed the association between the expression of $p27^{KIP1}$ in the main mass of tumour and lymph node metastases in correlation with p53 expression at the same localization (Table 2). We noted that the loss of $p27^{KIP1}$ expression in the primary tumour was strongly associated with the overexpression of p53 protein in the main mass of tumour and lymph node metastases. Our results suggest that the overexpression of p53 influenced the loss of p27 expression and the presence of lymph node metastases in the investigated gastric cancers.

References

1. Sherr CJ. GI phase progression: cycling on cue. Cell, 1994;79:515-55.
2. Hunter T, Pines J. Cyclins and cancer II: cyclin D and CDK inhibitors come of age. Cell, 1994; 79:573-82.
3. Grana X, Reddy EP. Cell cycle control in mammalian cells, Role of cyclins, cyclin-dependent kinases (CDKs), growth suppressor genes and cyclin-dependent kinase inhibitors (CKIs). Oncogene, 1995; 11:211-19.
4. Cheng M, Selx V, Sherr CJ, Roussel MF. Assembly of cyclin D-dependent kinase and titration of p27/Kipl regulated by mitogen-activated protein kinase (MEKI). Proc Natl Acad Sci USA, 1998; 95:1091-96.
5. Iggo R, Gatter K, Bartee J, Harris Al.: Increased expression of mutant form of p53 oncogene in primary lung cancer. Lancet, 1990; 335: 675-79.
6. Rodrigues NR, Rowan A, Smith MEF, Kerr IB ,Bodmer WF, Gannon JV, Lane DP: p53 mutation in colorectal cancer. Proc Natl Acad Sci USA, 1990; 87: 7555-59.
7. Tan P, Cady B, Wanner M, Worland P, Cukor B, Magi-Galluzi C, Lavin P, Draetta G, Pagano M, Loda M. The cell cycle inhibitor p27 is an independent prognostic marker in small (T1a,b) invasive breast carcinomas. Cancer Res, 1997; 57: 1259-63.
8. Mori M, Mimori K, Shiraishi T, Tanaka S, Ueno H, Sugimachi K, Akiyoshi T. P27 expresion and gastric carcinoma. Nat Med, 1997; 3: 593-5.
9. Ikeguchi M, Saito H, Katano K, Tsujitani S, Maeta M, Kaibara N. Expression of p53 and p21 are independent prognostic factors in patients with serosal invasion by gastric carcinoma. Dig Dis Sci, 1998; 43: 964-70
10. Yasui W, Kudo Y, Semba S, Yokozaki H, Tahara E. Reduced expression of cyclin-dependent kinase inhibitor p27Kip 1 is associated with advanced stage and invasivenes of gastric carcinomas. Jpn J Cancer Res, 1997; 88: 625-9.
11. Anayama T, Furihata M, Ishikawa T, Ohtuski Y, Ogoshi S. Positive correlation between p27Kip 1 expression and progression of human esophageal squamous cell carcinoma. Int J Cancer, 1998; 79: 439-43.
12. Cote RJ, Shi Y, Groshen S, Feng AC, Cordon -Cardo C, Skinner D. Association of p27 Kip1 levels with recurrence and survival in patients with stage C prostate carcinoma. J Natl Cancer Inst, 1998; 90: 916-20.
13. Li J-Q, Miki H, Wu F, Sao K, Nishioka M, Ohmori M, Imaida K. Cyclin A correlates with carcinogenesis and metastasis, and p27 Kip1 correlates with lymphatic invasion, in colorectal neoplasms. Human Path, 2002; 33: 1006-15.

Effects of changes at the site of E-cadherin expression as an indicator of colon cancer aggressiveness

Guzińska-Ustymowicz K[1], Chętnik A[2], Kemona A[1]

[1]Department of General Pathomorphology, Medical University of Białystok,
[2]Department of Gastroenterology and Internal Diseases, J. Śniadecki District Hospital, Białystok, Poland

Abstract

The aim of the work was to study the effects of changes in the location of E-cadherin from membrane to cytoplasm and the appearance of metastases and recurrence in patients with colon cancer of pT1 grade. The study group consisted of 34 patients with colon cancer. The material was fixed in 10% buffered, directly following surgery, fixed in formaldehyde and embedded in paraffin blocks by a standard method. Immunohistochemical reactions were performed, using monoclonal E-cadherin antibodies (Novocastra, NCL-E-Cad). Statistical analysis did not show any relation between the change in the location of E-cadherin expression, the patients' sex, and the location of changes. Simultaneously, we observed a strong relationship between the presence of exudate in the vessels from cancer cells, the histological grade and the loss of E-cadherin expression in the main tumour mass ($p<0.01$). We also noted a statistically significant correlation between the presence of lymph node invasion and distant metastases and the E-cadherin cytoplasmic reaction ($p=0.0001$, $p=0.000001$, respectively). A borderline significance of $p=0.06$ was noted in the association between the appearance of recurrence at the postoperative site and the change in location of E-cadherin expression in the main tumour mass from cytoplasm to membrane. On the basis of our results, we can conclude that a change in the location of E-cadherin expression (from membrane cytoplasm) is strongly associated with an increased aggressiveness of CRC, which is related to the appearance of proximal and distant metastases and to recurrence at the postoperative scar.

Key words: colorectal cancer, E-cadherin.

ADDRESS FOR CORRESPONDENCE:
Katarzyna Guzińska-Ustymowicz
Department of General Pathomorphology
Medical University of Białystok
Waszyngtona 13, 15-889 Białystok, Poland
email: kguzinska@poczta.onet.pl

Introduction

Intercellular associations are frequently analysed in various types of neoplasms. It has been confirmed, that a disturbance of the mechanism of cellular binding may be one of the parameters, indicating the behaviour of neoplastic cells. Adhesion molecules are surface receptors, involved in intercellular interactions and cellular-extracellular interactions [1]. According to their function and shape, they are divided into 4 main groups: cadherins, integrins, selectins, and adhesion molecules of the superfamily of immunoglobulins [2, 3]. E cadherins are membrane proteins. Their cytoplasmic domain interacts with a group of proteins, known as catenins, and join with either ß or γ catenin. The formed complex binds then with α catenin, which has a direct effect on the cytoskeleton [4]. Neoplasms often have a defect in E-cadherin function, due to an absent cytoplasmic domain. More detailed assessment of the role and function of adhesion molecules seems to be a very important area of research. It not only allows a deeper understanding of the biological formation of metastases, but it may also lead to new perspectives with regards to diagnostics and therapy.

Materials and methods

The study was performed retrospectively on postoperative material from 34 patients who underwent surgery at the Department of Surgery, The Śniadecki Hospital, Białystok, Poland, for cancer of the colon with pT1 grade. The observation period lasted 36 months. Postoperatively, the following other examinations were performed: abdominal US, colonoscopy and abdominal CT. On the basis of those examinations, it was decided whether distant metastases were present (all the cases indicated liver metastases). The site of operation was monitored in all the cases. All the cases of recurrence at the post-operative site were confirmed histopathologically. Immunohistochemistry: Slides of 4mm-thick serial sections of the primary tumour were prepared

Table 1. Expression of E-cadherin and chosen parameters.

parameters	n	Expression of E-cadherin		significance
		membranous	cytoplasmic	
Female	9	5(55.6%)	4(44.4%)	p=1
Male	25	12(48.0%)	13(52.0%)	
Colon	7	3(42.9%)	4(57.1%)	p=1
rectum	27	14(51.9%)	13(48.1%)	
G1	20	14(70.0%)	6(30.0%)	p=0.02
G2	12	3(25.0%)	9(75.0%)	
G3	2	0(0%)	2(100%)	
With lymph node metastasis	16	1(6.2%)	15(93.8%)	p=0.0001
Without lym. node metastasis	18	16(88.9%)	2(11.1%)	
With distant metastasis	14	0(0%)	14(100%)	p=0.000001
Without distant metastasis	20	17(85.0%)	3(15.0%)	
With vascular invasion	14	2(14.3%)	12(85.7%)	p=0.0005
Without vascular invasion	20	15(75.0%)	5(25.0%)	
With local recurrence	3	0(0%)	3(100%)	p=0.06
Without local recurrence	31	17(54.8%)	14(45.2%)	

from each patient. In brief, the slides from each patient were dewaxed, using xylene, and transferred to alcohol. They were then placed in citric acid buffer (10 mM) and heated in a microwave oven (700W) for 10 minutes to expose antigens. A Standard avidin-biotin immunoperoxidase (Novostain Super ABC Kit universal) method was used for the detection of E-cadherin protein expression (Novocastra, NCL-E-Cad, Biokom, Poland). Nonspecific mouse IgG was used as negative control. The reaction products were visualized with diaminobenzidine DAB (DAKO S3000, Dako, Poland). Appropriate positive and negative controls were used. The membranous and cytoplasmic immunostaining was observed for E-cadherin. Expression of E-cadherin was semi quantitatively assessed in neoplastic cells of primary tumour and defined as follows: E-cadherin -membranous (> 50% reaction was membranous in the main mass of tumour) and E-cadherin -cytoplasmic (>50% reaction was cytoplasmic in the main mass of tumour). The percentage of E-cadherin positive cells was calculated in, at least, 500 neoplastic cells per sample, using a light microscope (x400). Statistical analysis. The χ^2 and Fisher's exact test were used for statistical analysis. P-values smaller then 0.05 were considered statistically significant.

Results and discussion

Table 1 presents the obtained results. It is apparent that the presence of cancer cells in lymphatic vessels and veins, and also the appearance of lymph node invasion is a known risk factor for malignancy and for the formation of metastases. Moreover, the presence of these changes is strictly associated with the loss of association between cells, for which E-cadherin is responsible. Colon cancer cells, along with cancer cells from other tissues, show decreased adhesive properties. Some authors suggest that the presence of mutations of these molecules in colon cancer [2, 3, 5]. Many authors have analysed the expression of E-cadherin in colon cancer from normal colonic mucous membrane. Some authors have observed either a decrease in the expression or no correlation with the degree of histopathological invasiveness, metastases, or patient's life expectancy [6]. Others, however, have not observed such a correlation [7]. In the presented results, we performed an evaluation of E-cadherin expression in the main tumour mass, analysing the effect of changes in the location of its expression with: vascular invasion, lymph node metastasis, distant metastasis and local recurrence. The results of our study show a changing location of E-cadherin expression. Normal tissue shows a "clean" membrane immunohistochemical reaction, whereas in extra-membrane tumour mass tissue, E-cadherin is similarly observed in the cytoplasm, whilst the cytoplasmic reaction was strongest at the front of invasion. In the present study, statistical analysis did not reveal any association between the changes in E-cadherin expression location and the location of the tumour, or patient's sex. In the present study, we observed a cytoplasmic reaction for E-cadherin in 12/14 cases of vascular invasion. Similarly, out of 17 cases with cytoplasmic reaction, lymph node metastases were found in 15. Moreover, in all our subjects, a cytoplasmic reaction for E-cadherin was associated with the appearance of distant metastases and recurrence at the postoperative scar. Similar results have been observed by El-Bahrawy et al. [7]. When we compare our results to those of other authors, who have noted a decrease in the expression of E-cadherin, we see that the expres-

sion of E-cadherin does not show either any decrease or absence, only a shift from membrane to cytoplasm. This leads to a loss of function. Furthermore, E-cadherin, which is found in recurrent metastases, is found in membrane Mareel et al. [5]. It appears that for cell division ability,it is essential that they bind with one another. Moreover, in our study, the cytoplasmic reaction was observed mainly at the front of invasion, whereas the membrane reaction was found in the main mass of tumour. Similar results have been achieved by El-Bahrawy et al.[7]. The observations and the presented results may indicate a strong effect of a change in the location of E-cadherin expression and the aggressiveness of colon cancer.

References

1. Nigam A.K. Ahesion molecules in cancer. Eur J Surg Oncol, 1994;20: 82-4.

2. Birchmeier W, Weidner KM, Hulsken J. Molecular mechanism leading to cell junction (cadherin) deficiency in invasive carcinomas. Semin Cancer Biol, 1993; 4: 231-9.

3. Birchmeier W. Behrens J. Cadherin expression in carcinomas: role in the formation of cell junctions and the prevention of invasiveness. Biochim Biophys Acta, 1994; 1198: 11-26

4. Żak I. Receptory adhezyjne. Postępy Biol. Kom, 1996; 23(2): 221-42.

5. Mareel M. Bracke M, Roy F. Invasion promoter versus invasion supressor molecules: the paradigm of E-cadhenin. Mol Biol Rep, 1993;19: 45-67.

6. Van der Wurff AAM, Vermeulen SJT, Van der Linden EPM, Mareel MM, Bosman FT, Arends JW. Patterns of α and ß-catenin nd E-cadherin expression in colorectal adenomas and carcinomas.J Pathol, 1997; 182: 325-30.

7. El-Bahrawy MA, Poulsom R, Jeffery R, Talbot I, Alison MR. The expression of E-cadherin and catenins in sporadic colorectal carcinoma. Human Path, 2001; 32; 1216-24.

Macrophage/histiocytic antigen CD68 expression in neoplastic and reactive lymph nodes

Mazur G[1], Hałoń A[2], Wróbel T[1], Kuliczkowski K[1]

[1]Department of Haematology, Blood Neoplasms and Bone Marrow Transplantation,
[2]Department of Pathological Anatomy, Wrocław Medical University, Poland.

Abstract

There are some reports, suggesting that infiltrating macrophages may promote tumour progression in non-Hodgkin's lymphoma (nHL). The aim of the study was an evaluation of macrophages, marked by antibody against CD68 in indolent and aggressive nHL. The study was performed in 65 patients: 50 with nHL and 15 with lymph nodes affected by reactive hyperplasia. Immunohistochemical analyses were performed on paraffin-embedded specimens with monoclonal anti-CD68 antibody. Scoring on the basis of the percentage of positive cells indicated CD68 expression in 34/50 (68%) of the patients with nHL and in only 5/15 (33%) of the patients with reactive hyperplasia. The expression of CD68 was statistically significantly higher in the aggressive nHL than in indolent nHL. An increased number of CD68 positive macrophages in clinically aggressive nHL may confirm their role in tumour progression.

Key words: macrophages, CD68, lymphomas.

Introduction

Non-Hodgkin's lymphomas (nHL) are a heterogeneous group of lymphoid malignancies with a different pattern of clinical behaviour and response to treatment. In terms of clinical aggressiveness nHL may be divided into two groups: aggressive and indolent lymphomas. The infiltration of neoplastic tumour by leucocytes was described in 1863 by Virchow [1]. A large part of those leucocytes was macrophages. Macrophages constitute a primary line of defence mechanisms. They are found in many solid tumours, where they are known as tumour associated macrophages (TAM) [2]. There are some clinical observations, indicating that macrophages are important in the processes of cancer progression (growth, invasion and metastasis), making a connection between inflammation and cancer [3, 4, 5]. A close relationship has been found between the number of macrophages and the inhibition of tumour growth, as well as tumour progression. Some authors suggest that infiltrating macrophages may promote tumour progression in nHL. Vacca et al. reported a correlation between the number of macrophages and tumour microvessel density in nHL. An increased number of macrophages may be recruited and activated locally by more malignant B-cells [6]. The aim of the study was an evaluation of macrophages, marked by antibody against CD68 in indolent and aggressive nHL.

ADDRESS FOR CORRESPONDENCE:
Grzegorz Mazur
Department of Haematology, Blood Neoplasms
and Bone Marrow Transplantation
Medical University of Wrocław
Pasteura 4 , 50-367 Wrocław, Poland
Phone: +48 71 7842599, Fax: +48 71 784 0112,
e-mail: grzegmaz@hemat.am.wroc.pl

Material and methods

The study was performed on 50 patients with non-Hodgkin's lymphoma (NHL) and in 15 lymph nodes with reactive hyperplasia, diagnosed and histopathologically confirmed in at the Department of Haematology, Blood Neoplasms and Bone Marrow Transplantation and the Department of Pathological Anatomy, Medical University in Wroclaw by a pathologist with a profound experience in lymphomas. Clinical staging was done, according to the Ann Arbor classification system. The histological diagnosis of enrolled patients with lymphomas was made, according to the WHO/REAL classification. Out of the 50 patients with lymphomas, 43 (87%) B-cell and 7 (13%) T-cell lymphomas were diagnosed. The median age of the population was 57 years, clinical stage III and IV. Aggressive lymphomas constituted group of 28 cases (54%) and indolent - 22 (46%) cases. Histological classification of B-cell lymphomas revealed the following: peripheral leukaemia/lymphoma - 12 (27%), fol-

Table 1. The expression of CD68 in lymph nodes: reactive; indolent and aggressive non-Hodgkin's lymphomas.

Grade of CD68 expression	**nHL 50 patients**	**Reactive hyperplasia 15 patients**	**p**
I and II	24	10	NS
III and IV	26	5	
Grade of CD68 expression	**Indolent nHL 22 patients**	**Aggressive nHL 28 patients**	**p**
I and II	15	9	0.011
III and IV	7	19	
Grade of CD68 expression	**Reactive hyperplasia 15 patients**	**Aggressive nHL 28 patients**	**p**
I and II	10	9	0.03
III and IV	5	19	

Figure 1. A. Peripheral B-cell leukaemia/lymphoma; 210x. D68 expression: grade II (5-25%)

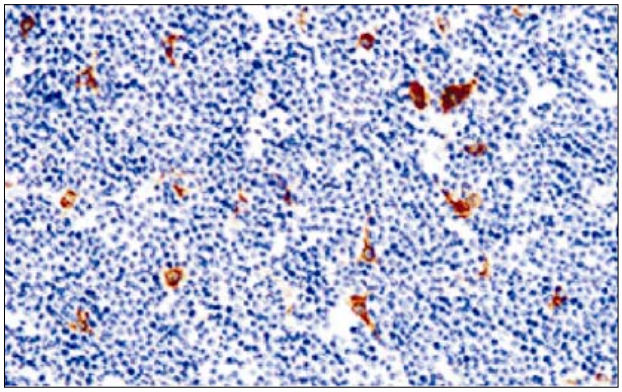

Figure 1. B. Immunoblastic B-cell lymphoma; 210x. CD68 expression: grade III (26-50%)

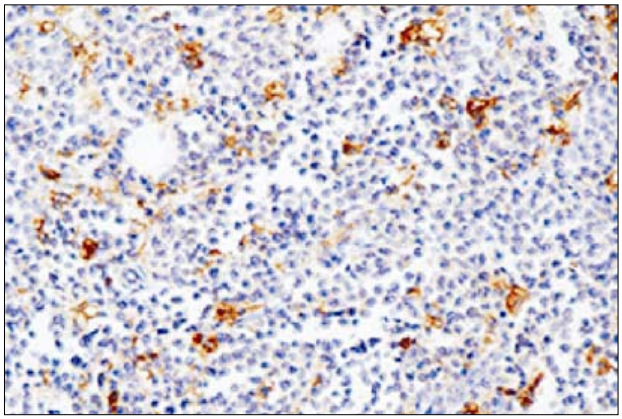

licular lymphoma - 7 (16%), mantle cell lymphoma - 7 (16%), immunoblastic/immunocytic - 4 (9%), other - 13 (32%). Immunohistochemical analyses were performed on paraffin-embedded specimens with monoclonal anti-human macrophage antigens - CD68 (cloneKP1) (DAKO, Denmark). The DAKO Fast Red Substrate System was used as a substrate and chromogen in immunocytochemical staining procedures, utilizing alkaline phosphatase. In each case, a control was included, in which, the specific antibody was omitted. CD68 expression was graded as the percentage of positive stained cells. Four grades of expression were established: grade I <5%; II - 5-25%; III - 26-50%; IV - >50% of positive cells. Statistical analysis was made using the Fisher test. Differences were considered statistically significant at $p<0.05$.

Results

CD68 expression in grade I (<5%) was only demonstrated in 18% (9, out of 50) of patients with lymphoma, examined by immunohistochemistry. In grade I, there were 16/50 nHL (31%) and no reactive lymph nodes. Grade II was found in 14/50 (28%) nHL patients and in 8/15 reactive lymph nodes (53%). Grade III was observed in 15/50 (30%) and 5/15 reactive (33%) observed. Grade IV was found in 13/50 (26%) nHL and 2/15 (13%) reactive lymph nodes noted. The results are presented in the (Fig. 1 a and b), Table 1 according to clinical aggressiveness. The expression of CD68 was statistically significantly higher in the aggressive nHL than that in indolent nHL and reactive lymph nodes.

Discussion

Lymph nodes, affected by lymphoma, are not only composed of malignant cells but also of many other cell types, including macrophages. TAMs have been considered to have an anti-tumour effect as a part of immune defence. Recently, it seems that they may have both protumour and antitumour activity. In tumours, macrophages are recruited and activated via several factors, secreted by tumour cells i.e. chemokines, VEGF. Their effect depends on tumour microenvironment and the tumour itself. TAMs can also produce various growth factors and cytokines, stimulating growth and angiogenesis, as well as facilitating the invasion by secreting cell membrane degrading enzymes [7, 8]. The results of various observations, using macrophage specific markers as a prognostic factor, are controversial. In papillary thyroid cancer, patients with tumours, containing TAMs exhibing neoplastic cell phagocytotic activities, had a better prognosis than patients without TAMs [9]. On the other hand, the presence of areas with high-density TAMs within "hot spots" was positively correlated with increased vascularity and metastasis and with reduced relapse-free and overall survival in breast cancer [10]. There is also a strong association between increased melanoma-specific mortality and the increasing number of CD68-positive macrophages [11]. The data, concerning the role of TAMs in nHL are very limited. Vacca et al. have demonstrated that macrophages promote angiogenesis and, in consequence, the progression of B-cell nHL [6]. In our study, we did not find any statistical differences in the CD68 expression between reactive lymph nodes and the whole nHL group. Nevertheless, the expression of CD68 was statistically significantly higher in the aggressive nHL than in

indolent nHL and reactive lymph nodes. This observation indicates a relationship between the number of TAMs in lymph nodes and the clinical aggressiveness of nHL.

Conclusions

An increased number of CD68 positive macrophages in clinically aggressive nHL may confirm their role in tumour progression.

Acknowledgements

Supported by Grant No 4 PO5B 009 18 from the State Committee for Scientific Research (KBN).

References

1. Virchow R. Die krankenhaften Geschwulste. Dreißig Vorlesungen, gehalten während des Wintersemesters 1862-1863 an der Universität zu Berlin. In: Vorlesungen über Pathologie. Verlag von August Hirschwald, Berlin, 1863.

2. Mantovani A, Bottazzi B, Colotta F, Sozzani S, Ruco L. The origin and function of tumour-associated macrophages. Immunol Today, 1992; 13: 265-70.

3. Lin EY, Pollard JW. Role of infiltrated leucocytes in tumour growth and spread. Br J Cancer, 2004; 90: 2053-8.

4. Mantovani A, Allavena P, Sica A. Tumour-associated macrophages as a prototypic type II polarised phagocyte population: role in tumour progression. Eur J Cancer, 2004; 40: 1660-7.

5. Balkwill F, Mantovani A. Inflammation and cancer: back to Virchow? Lancet, 2001; 357: 539-45.

6. Vacca A, Ribatti D, Ruco L, Giacchetta F, Nico B, Quondamatteo F, Ria R, Iurlaro M, Dammacco F. Angiogenesis extent and macrophage density increase simultaneously with pathological progression in B-cell non-Hodgkin's lymphomas. Br J Cancer, 1999; 79: 965-70.

7. Polverini PJ. How the extracellular matrix and macrophages contribute to angiogenesis-dependent diseases. Eur J Cancer, 1996; 32A: 2430-7.

8. Polverini PJ. Role of the macrophage in angiogenesis-dependent diseases. EXS, 1997; 79: 11-28.

9. Leek RD, Lewis CE, Whitehouse R, Greenall M, Clarke J, Harris AL. Association of macrophage infiltration with angiogenesis and prognosis in invasive breast carcinoma. Cancer Res, 1996; 56: 4625-9.

10. Fiumara A, Belfiore A, Russo G, Salomone E, Santonociro GM, Ippolito O, Vigneri R, Gangemi P. In situ evidence of neoplastic cell phagocytosis by macrophage in papillary thyroid cancer. J Clin Endocrinol Metab, 1997; 82: 1615-20.

11. Mäkitie T, Summanen P, Tarkkanen A, Kivelä T. Tumor-infiltrating macrophages (CD68+ cells) and prognosis in malignant uveal melanoma. Invest Ophthalmol Vis Sci, 2001; 42: 1414-21.

Survivin expression in lymph nodes, affected by lymphoma and reactive hyperplasia

Mazur G[1], Hałoń A[2], Wróbel T[1], Urbaniak J[3], Kuliczkowski K[1], Woźniak M[3]

[1]Department of Haematology, Blood Neoplasms and Bone Marrow Transplantation,
[2]Department of Pathological Anatomy, [3]Department of Clinical Chemistry;
Wrocław Medical University, Poland

Abstract

Survivin is a member of the inhibitors from the apoptosis family over-expressed in various human cancers. The aim of the study was to evaluate the expression of survivin in lymph nodes, invaded by non-Hodgkin's lymphomas (nHL) and in lymph nodes reactive hyperplasia. We analysed paraffin sections obtained from 50 patients with nHL and from 13 patients with reactive hyperplasia using, an anti-survivin antibody. There was abundant immunoreactivity cytoplasm in 34/50 (68%) patients with nHL and in only 5/13 (38%) with reactive hyperplasia. Out of the 27 patients with aggressive nHL, 19 (70%) revealed survivin expression in almost all tumour cells. Out of the 23 patients with indolent nHL, 16 (70%) revealed the expression but with lower immunoreactivity score. The study indicates that patients with nHL presented a high level of survivin expression, it was more pronounced in aggressive than in indolent nHL.

Key words: survivin, lymph nodes, reactive hyperplasia, lymphomas.

Introduction

Survivin (also termed *Birc5*) is a protein that regulates cell division and inhibits apoptosis through a pathway, different from that, involving the bcl-2 family [1]. Survivin contains a baclovirus inhibitor of apoptosis repeat (BIR) protein domain, classifying it as a member of the inhibitor of the apoptosis protein (IAP) gene family [1, 2, 3]. Unique among other IAP proteins, is survivin highly expressed during embryonic and foetal development and in rapidly dividing cells, whereas it is undetectable in terminally differentiated normal adult tissues [3, 4, 5]. Its expression is regulated in a strict cell cycle-depended manner with the maximum level, occurring during the G2/M phase, and it localizes to mitotic spindle microtubules in a reaction, required for apoptosis inhibition [2, 4, 5]. Over expression of survivin has an oncogenic potential because it may overcome the G2/M phase checkpoint to enforce the progression of cells through mitosis [3]. Survivin suppresses apoptosis, induced by Fas, Bax, caspase-3, caspase-7 and anticancer drugs [3].

Survivin is abundantly expressed in the majority of cancers, including haematological malignancies [3, 5, 6, 7]. Survivin has been shown to be expressed in 60 cancer cell lines, including breast, lung, prostate, colon, pancreas, stomach, brain, melanoma, ovarian, renal cancer, as well as leukaemia/lymphoma [3, 4, 5, 8, 9].

Although either retrospective predictive or prognostic studies on the impact of the survivin pathway in solid tumour have been reported, little is still known about the potential role of this molecule in haematopoietic malignancies. In this study, we investigated the potential expression and localization of survivin in patients with non-Hodgkin's lymphomas and in patients with reactive lymph node hyperplasia as the control. We analyzed the relationship between its expression and malignant potential and the potential prognostic impact for disease progression and the clinical outcome of lymphoma.

Material and methods

The analysis was performed in patients with lymph node enlargement, diagnosed at the Department of Haematology, Blood Neoplasms and Bone Marrow Transplantation, Medical

ADDRESS FOR CORRESPONDENCE:
Grzegorz Mazur
Department of Haematology, Blood Neoplasms
and Bone Marrow Transplantation
Medical University of Wrocław
Pasteura 4 , 50-367 Wrocław, Poland
Phone: +48 71 7842599, Fax: +48 71 784 0112,
e-mail: grzegmaz@hemat.am.wroc.pl

Figure 1. A. Peripheral B-cell leukaemia/lymphoma; 210x. Survivin expression: grade I (<25%).

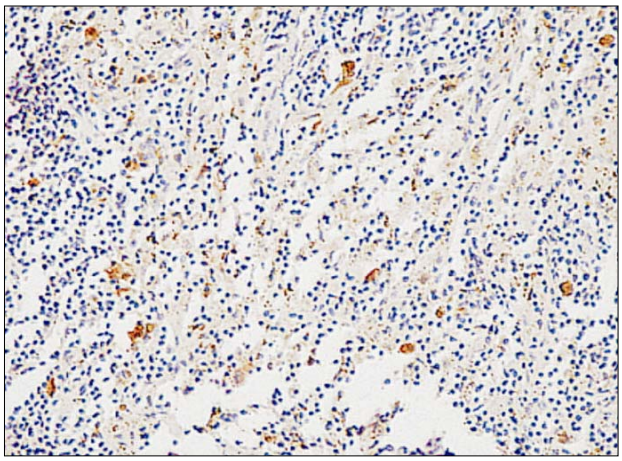

Figure 1. B. T-cell lymphoma; 210x. Survivin expression: grade IV (75-100%).

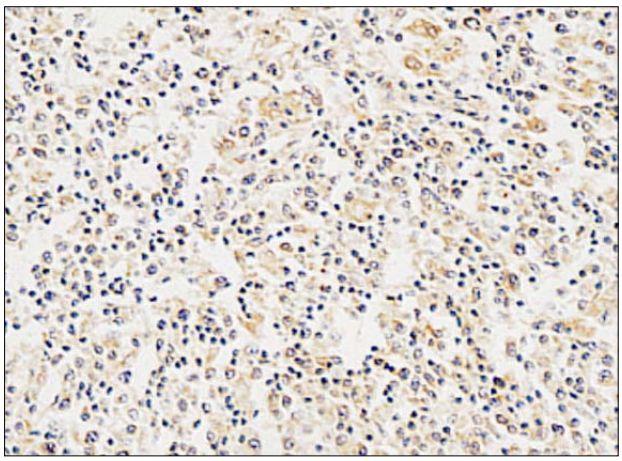

University in Wrocław. Samples were obtained from a total of 63 patients, including 50 patients with malignant non-Hodgkin's lymphoma (31 males, 19 females) and 13 patients with reactive lymph nodes hyperplasia (4 males, 9 females). The histological diagnosis of the enrolled patients with lymphomas was made, according to the REAL/WHO classification. Out of the 50 patients with lymphomas, 41 (82%) B-cell and 9 (18%) T-cell lymphomas were diagnosed. Aggressive lymphomas constituted a group of 27 cases (54%) and indolent ones - 23 (46%) cases. Histological classification of B-cell lymphomas revealed the following: peripheral leukaemia/lymphoma - 12 (29%), follicular lymphoma -7 (17%), mantle cell lymphoma - 6 (15%), immunoblastic/immunocytic - 5 (12%), other - 11 (27%). Immunohistochemical staining for survivin was performed, using an anti-survivin antibody (Chemicon International, USA) with formalin fixed, paraffin-embedded tissue samples. The investigated antigen was visualised, using the LSAB2 kit and diaminobenzidine (DAB). In each case, a control was included, in which the specific antibody was omitted. Evaluation of survivin expression based on immunoreactivity score of the percentage of positive cells was divided into four grades: I - <25% of positive cells; II - 26-50%; III - 51-75%; IV - 76-100%. Statistical analysis was performed, using the Fisher test. Differences were considered statistically significant at $p<0.05$.

Results

Survivin expression in the nucleus and/or cytoplasm was demonstrated in 62% of all the patients examined by immunohistochemistry (39 of 63). Scoring on the basis of the percentage of positive cells indicated survivin expression 34/50 (68%) patients with malignant lymphomas and in only 5/13 (38%) patients with lymph node reactive hyperplasia ($p<0.05$). Out of the 27 patients with aggressive lymphomas, 19 (70%) revealed survivin expression in virtually almost all tumour cells (grade III in 26% of cases, grade IV in 48% of cases). Out of the 23 patients with indolent lymphomas, 16 (70%) revealed survivin expression but with lower immunoreactivity score (grade I in 12, grade II in 4 cases).

Discussion

A considerable interest has recently focused around the critical role of apoptosis deregulation in the onset and progression of neoplasia and its ability to aberrantly prolong cell viability, facilitate the accumulation of mutations and promote drug resistance [6]. A candidate molecule to influence the cell death and cell viability balance in malignancies was identified in 1997: survivin, an apoptosis inhibitor of the IAP gene family [1, 2, 3, 4]. Present during foetal development, is survivin undetectable in terminally differentiated adult tissues [3, 5]. Its chromosomal location is 17q25, approximately 3% distance from the telomere and it comprises three introns and four exons, encoding 142 amino acids, including one copy of the baclovirus IAP repeat (BIR) essential for apoptosis inhibition [3, 5].

Survivin becomes prominently expressed in transformed cell lines and in all the most common human cancers of the colon, the stomach, the pancreas, the ovary, breast, the lung and prostate, in vivo [3, 5, 8, 9]. In most cancers, the expression of survivin correlated with reduced apoptotic index, poor prognosis and an increased risk of recurrence [2, 9]. Survivin over expression has been shown to be associated with aggressive forms of neuroblastoma and poor survival among patients with colorectal, stomach, breast, hepatocellular and non-small lung cancer [3, 4, 5, 8, 9]. Survivin expression was identified as an independent unfavourable prognostic factor in a randomized series of 69 acute myeloid leukaemia (AML) patients [6]. Although the expression of this protein did not seem to affect the complete remission (CR) rate, it significantly shortened the survival time of patients. Survivin is also found in approximately 50% of high-grade non-Hodgkin's lymphomas (centroblastic, immunoblastic), but not in low-grade lymphomas (lymphocytic) [2, 5]. Similarly, in our study, we demonstrated an increased expression of survivin not only in diffuse large B-cell lymphomas, but in other aggressive lymphomas, such as mantle cell lymphoma, follicular G3 lymphoma, lymphoblastic and Burkitt's lymphoma. Indolent lymphomas are characterized by a low proliferation index and impaired apoptosis. Interestingly enough, the expression of survivin in indolent lymphomas was much lower (predominantly grade I and II) than in aggressive lymphomas. This suggests that the inhibition of apoptosis in indolent lymphomas is related not only to survivin mechanisms. This observation requires further studies.

References

1. Chiou SK, Jones MK, Tarnawski AS. Survivin - an anti-apoptosis protein: its biological roles and implications for cancer and beyond. Med Sci Monit, 2003; 9: PI43-7.

2. Adida C, Haioun C, Gaulard P, Lapage E, Morel P, Briere J, Dombret H, Reyes F, Diebold J, Gisselbrecht C, Salles G, Altieri DC, Molina TJ. Prognostic significance of survivin in diffuse large B-cell lymphomas. Blood, 2000; 96: 1921-5.

3. Takai N, Miyazaki T, Nishida M, Nasu K, Miyakawa. Expression of survivin is associated with malignant potential in epithelial ovarian carcinoma. Int J Mol Med, 2002; 10: 211-6.

4. Verdecia MA, Huang H, Dutil E, Kaiser D, Hunter T, Noel JP. Structure of the human anti-apoptotic protein survivin reveals a dimeric arrangement. Nature, 2000; 7: 602-8.

5. Ambrosini G, Adida C, Altieri DC. A novel anti-apoptosis gene, survivin, expressed in cancer and lymphoma. Nat Med, 1997; 8: 917-21.

6. Adida C, Recher C, Raffoux, Daniel MT, Taksin AL, Rousselot P, Sigaux F, Degos L, Altieri DC, Dombert H. Expression and prognostic significance of survivin in *de novo* acute myeloid leukaemia. Br J Haematol, 2000; 111: 196-203.

7. Siegel S, Wagner A, Schmitz N, Zeis M. Induction of antitumour immunity using survivin peptide-pulsed dendritic cells in a murine lymphoma model. Br J Haematol, 2003; 122: 911-4.

8. Casati C, Dalerba P, Rivoltini L, Galliano G, Deho P, Rini F, Belli F, Mezzanzanica D, Costa A, Andreola S, Leo E, Parmiani G, Castelli C. The apoptosis inhibitor protein survivin induces tumor-specific CD8+ and CD4+ T cells in colorectal cancer patients. Cancer Res, 2003; 63: 4507-15.

9. Tu SP, Jiang XH, Lin MCM, Cui JT, Yang Y, Lum CT, Zou B, Zhu YB, Jiang SH, Wong WM, Chan AO, Yuen MF, Lam SK, Kung HF, Wong BC. Suppression of survivin expression inhibits *in vivo* tumorigenicity and angiogenesis in gastric cancer. Cancer Res, 2003; 63: 7724-32.

Expression of PCNA and Ki-67 in posterior uveal melanomas in adults

Proniewska-Skrętek E[1], Dzięcioł J[2], Zalewska R[1], Mariak Z[1]

[1]Department of Ophthalmology, [2]Department of Anatomy Medical University of Białystok, Poland

Abstract

The aim of the study was to evaluate the expression of cell proliferation markers (PCNA and Ki-67) in posterior uveal melanomas in adults. Thirty-six enucleated eyes (without prior treatment) were included in histopatological study. A series of 15 cases of spindle cell type melanomas, 12 epithelioid and 9 of a mixed type were assessed, using the immunohistochemical method with monoclonal PCNA and Ki-67 antibodies. PCNA expression was observed in 75% and Ki-67 in 13.8 % of all the examined tumours. The mean score of PCNA and Ki-67 index were the highest in tumours, which contained epithelioid cells and in large, more advanced (pT3, pT4) uveal melanomas. The results showed that the evaluation of expression of PCNA and Ki-67 may provide an additional information about the progression of tumor process.

Key words: PCNA, Ki-67, uveal melanoma.

Introduction

Different kinds of proteins play an important role in the control of the cell cycle. Some of them take place in cytological transformation and tumour progression. PCNA and Ki-67 are two of the nuclear markers, used to demonstrate the proliferative phase of the cell cycle. Proliferating cell nuclear antigen (PCNA) is a co-factor of DNA polymerase δ, which is necessary for DNA replication. The expression of PCNA is the highest in G1/S cell cycle phase. PCNA labelling was performed in several series of brain neoplasm [5, 7]. Ki-67 is an antigen, expressed in all the phases of the cell cycle, excluding the G0 phase

The aim of the study was to evaluate the expression of the proliferation markers (PCNA and Ki-67) in uveal melanoma in adults.

Material and method

Thirty-six patients: 20 females (the mean age 59.5 years, the age range 36-82 years) and 16 males (the mean age 68.4, the age range 58-78) were operated for posterior uveal melanoma (melanoma malignum choroideae) between 1994 and 2003 at the Department of Ophthalmology of the Medical University in Białystok. All the eyes were enucleated because of posterior uveal melanoma without prior treatment (they were disqualified for brachytherapy). They were included into histopatological study. The obtained material was fixed in formalin, routinely processed and paraffin embedded. The cytological material was stained with H-E. Those specimens were histopathologically (Callendar's classification) [2] and TNM (TNM Classification of Malignant Tumours) classified. The histological types of tumours, according to Callendar's classification, included 15 (41.7%) spindle cell type tumours, 12 (33.3%) that contained epithelioid cells and 9 (25%) mixed tumours. All the tumours were evaluated, using pathological tumour grading pT (range pT1 -pT4). In different histological types of melanomas, the proportions of tumours in the same stage were similar. Seventy-five (75) percent of uveal melanomas belonged to pT3 and pT4 grade. Table 1 shows the association between the histopatological type of the uveal melanomas and the grades (pT feature). Cell proliferation was determined by immunoreactivity for the proliferation marker with monoclonal antibodies Ki-67 (clone MIB-1; M 7240, DAKO) and PCNA (clone PC 10; M 0879, DAKO), using a LSAB KIT with (DAKO) DAB as a chromogen to visualize the antigen/antibody complex. The protein expression was defined as positive (+) if more than 10% of the cells showed

ADDRESS FOR CORRESPONDENCE:
Ewa Proniewska-Skrętek
Department of Ophthalmology
Medical University of Białystok
M. Skłodowskiej-Curie 24A; 15-269 Białystok, Poland
Tel. (+48 85) 746 86 28

Table 1. Association of histological cell type of melanomas to their grades.

Histological cell type	Number of tumours	pT1	pT2	pT3	pT4
spindle cell	15	0	4	8	3
epithelioid cell	12	1	2	2	7
mixed	9	1	1	2	5

Table 2. PCNA and Ki-67 expressions in histological cell type of uveal melanomas

Histological cell type of melanoma	Number of cases (n)	PCNA (+) (%)	Ki-67 (+) (%)
spindle cell	15	10 (66.7%)	2 (13.3%)
epithelioid cell	12	10 (83.3%)	2 (16.7%)
mixed	9	7 (77.8%)	1 (11.1%)

(+) - positive reaction for PCNA and Ki67 protein above 10% of the cells

Table 3. The proliferation index of PCNA (IP PCNA) and Ki-67 (IP Ki-67) according histological cell type of melanomas.

IP PCNA			
Histological cell type of melanoma	**Number of cases (n)**	**IP PCNA ±. SD**	**Range values**
spindle cell	15	13.2 ±7.4*	4.2-28.6
epithelioid cell	12	24.9 ±13.8*	6.8-50.1
mixed	9	16.1±9.0*	4.5-38.1
IP Ki-67			
Histological cell type of melanoma	**Number of cases (n)**	**IP Ki-67 ±. SD**	**Range value**
spindle cell	15	1.7±1.1*	0.5-14.3
epithelioid cell	12	3.1±1.9*	0.8 -27.6
mixed	9	1.9±2.1*	0.2-12.6

SD: standard deviation, *p<0.05

positive reaction for PCNA and Ki-67; and as negative (-) if less than 10% of cells had negative immmunostaining. The percentage of positive nuclei was expressed as a proliferating index (IP) (the number of positive-staining cells for antigen K-67 and PCNA was divided by the total cell count and expressed as a percentage) For the evaluation of IP, tumour areas with a high density of labelling were chosen. For each tumour, a total of five fields (total cell number > 2000) were counted. The MicroImage InCD UDF Packed Writing Software for Window Olympus was used for those calculations. The significance of differences in scores among all the groups was assessed, using Student's 't' test. Values at $p<0.05$ were considered significant.

Results

PCNA immunopositive nuclei (more than 10% cells, showing positive reaction for PCNA protein) were observed in 27, out of 36 cases. The highest percentage of those (83.3%) was found in the tumours that contained epithelioid cells. The expression in the spindle cell group was the lowest and was observed in 66.7% of cases. Positive immunostaining for Ki-67 was found in 5, out of 36 uveal melanomas: 2 cases in spindle cell and 2 epithelioid type tumours, and 1 in the mixed group (Table 2). PCNA and Ki-67 overexpression were found in a large number of big tumours (pT3, pT4).

The score of IP PCNA ranged from 4.2 to 50.1. The highest value of PCNA -24.9 was found in the epithelioid cell melanoma group. In the tumours, containing spindle cells, this index was more than 1.5 times lower (13.2) than that in the previous group. In the last group (mixed cells) the mean score of IP PCNA was insignificantly higher than that in the spindle cell type melanomas. The score of IP Ki-67 ranged from 0.2 to 27.6. The highest and the lowest values of IP Ki-67 were observed in similar proportions and in the same histological cell type tumours, like IP PCNA. In all the cases, the mean PCNA IP value was higher than the mean Ki-67 IP (Table 3). In more advanced tumours (pT3, pT4), IP PCNA and IP Ki-67 values were much higher than those in melanomas of grades pT1 and pT2.

Discussion

Different subjective methods, such as mitotic index and necrosis, which are used in determining the grade of tumour activity, are complemented by immunohistochemical analysis.. Karlsson et al. [6] have reported a high rate for Ki-67 and PCNA staining in 79 uveal melanomas. The activity of these nuclear markers was correlated with histopathological type and tumour size (large and epithelioid cell type tumours). Chowers et al. [3] have found a high incidence of Ki-67 positive cells in epithelioid cell melanomas too. The high levels of Ki-67 positivity were also

associated with shorter survival times. Liang et al. [8] have determined the score of Ki-67 index as 0.75 ±1.02. The IP Ki-67 was significantly higher in large tumours and in uveal melanomas that contained epithelioid cells. In our study, IP Ki-67 ranged from 0.6 to 27.6. The highest IP Ki-67 were found in epithelioid cell type. Our results of Ki-67 were higher than the ones reported in the literature because our five immunopositive melanomas were large (pT4). In the present study, PCNA immunostaining was more prominent than Ki-67 in all the cell types of uveal melanoma. According to Kayaseluck'a et al.[7], this feature may result from a long half-life of PCNA. Strong PCNA nuclear immunopositivity was observed in a large number of cells in 36 tumours. PCNA expression was the highest in epithelioid melanomas .This is consistent with other reports [4, 6]. In uveal melanomas, which contained epithelioid cells, local tumour recurrence (after local resection) was more often observed [1]. Some of the researchers concur with the opinion that Ki-67 is a more specific antibody to detect the proliferation index [7]. It is necessary to combine subjective methods, such as histology of tumours, with more objective methods, such as immunohistochemical analysis [4]. Evaluation of proliferating cell protein expressions (PCNA and Ki-67) in uveal melanoma cells may provide an additional information about the progression of tumour process.

References

1. Bachrakis NE, Sehu KW, Lee WR, Damato BE, Foester MH. Transformation of cell type in uveal melanomas: a quantitative histologic analysis. Arch Ophthalomol, 2000; 118): 1406-12.

2. Callender GR. Malignant melanotic tumors of the eye: a study of histologic type in 111 cases. Trans Am Acad Ophthalmol, 1931; 36: 131-42.

3. Chowers I, Folberg R, Livini N, Pe're J. p53 immunoreactivity Ki-67 expression and microcirculation patterns in melanoma of the iris, ciliary body, and choroides. Curr Eye Res, 2002; 24: 105-8.

4. Ghazvini S, Kroll S, Char DH, Frigillana H. Comparative analysis of proliferating cell nuclear antigen, bromodeoxyuridine, and mitotic index in uveal melanoma. Invest Ophthalmol Vis Sci, 1995; 36: 2762-7.

5. Enestorom S, Vavruch L, Franlund B, Nordenskjold B. Ki-67 antigen expression as a prognostic factor in primary and recurrent astrocytomas. Neurochirurgie, 1998; 44: 25-33.

6. Karlsson M, Boeryd B, Carstensen J, Franlund B, Gustafsson B, Sun XF, Wingren S. Correlations of Ki-67and PCNA to DNA ploidy, S-phase fraction and survival in uveal melanoma. Eur J Cancer, 1996; 32: 357-62.

7. Kayaselcuk F, Zorludmir S, Gumurdulu D, Zeren H, Erman T. PCNA and Ki-67 in central nervous system tumous: correlation with the histological type and grade. Journal of Neuro-Oncology, 2002; 5: 115-21.

8. Liang J, Yi C, Schilling H, Li X. Correlation of Ki-67 expression and histopathologic characteristic in uveal melanomas. Yan Ke Xue Bao, 2001; 17: 114-7.

Levels of lipid peroxidation in A549 cells after PDT *in vitro*

Saczko J, Kulbacka J, Chwiłkowska A, Ługowski M, Banaś T

Department of Medical Biochemistry, Medical University of Wrocław, Poland

Abstract

Photodynamic therapy (PDT) is an increasingly used treatment for various types of cancer. The principle of PDT involves the administration of a photosensitizer, followed by a distribution interval, and subsequent illumination of tumour area with light of an appropriate wavelength to excite the sensitizer to its triplet state. The aim of the study was to determine the level of lipid peroxidation and the level of thiol groups (-SH) in A549 cells after PDT. The final product of fatty acid peroxidation - malondialdehyde - was quantified

Spectrophotometrically, based on a set of MDA standards of known concentration. Protein damage was based on Ellman's method. The level of lipid peroxidation was significantly higher for cells after PDT, comparing to control cells. We observed much lower concentrations of -SH groups for cells after PDT treatment, in comparison with respective values in control cells. In conclusion, PDT with Ph II induces lipid peroxidation with accompanying protein damage in A549 cells, what can lead to distinct epidemiological, pathological and clinical features.

Key words: photodynamic therapy, photofrin II, lipid peroxidation, thiol groups (-SH).

Introduction

Since its introduction as a promising new method for cancer treatment about two decades ago, photodynamic therapy has become progressively well established as a mode of treatment of malignant as well as non-malignant diseases, characterised by the occurrence of unwanted or harmful cells. Photodynamic therapy (PDT) is an increasingly used treatment for various types of cancer [1, 2]. The principle of PDT involves an administration of a photosensitizer, followed by a distribution interval and subsequent illumination of tumour area with light of an appropriate wavelength to excite the sensitizer to its triplet state. There are several drugs that can be used as photosensitizing agents. The most common of these include ALA, Foscan and Photofrin. Photofrin II, derivative of haematoporphyrin was used in this study. This photosensitizer is taken up into intracellular membranes, mitochondrial membranes, as well as the endoplasmic reticulum and the Golgi system [1, 3].

Photoactivation of Photofrin II is known to generate singlet oxygen and superoxide anion radicals. The ensuing photochemical reaction is dependent on the presence of oxygen, it generates reactive oxygen species (ROS) and induces oxidative stress in the cells, what means tumour destruction [4]. ROS react with thiol groups of proteins and cause damage of cellular membranes. Oxidative stress causes damage to cellular macromolecules, such as nucleic acids, proteins and lipids. Among these targets, peroxidation of lipids is particularly more damaging because the formation of lipid peroxidation products leads to a facile propagation of free radicals. Among the products of lipid peroxidation is malondialdehyde (MDA) - an endogenous genotoxic compound [5, 6].

In this study, we examined the levels of lipid peroxidation and the level of thiol groups (-SH) in A549 cells after PDT.

Material and methods

Cells: human lung carcinoma cell line (A549). This line was initiated in 1972 by D.J. Giard, et al. through explant culture of lung carcinomatous tissue from a 58-year-old Caucasian male.

Cell culture: the cell line was grown in MEM medium with addition of 10% foetal bovine serum. For the experiments, the cells

ADDRESS FOR CORRESPONDENCE:
Jolanta Saczko
Department of Medical Biochemistry
Medical University of Wrocław
Chałubinskiego 10, 50-368 Wrocław, Poland
e-mail: michal@bioch.am.wroc.pl

were removed by trypsinizing, and washed with PBS. The cells were maintained in a humidified atmosphere at 37°C and 5% CO_2.

Photodynamic treatment: the cells were treated with 15 and 30 µg/ml Photofrin II in complete media 4 h in the dark. Then they were irradiated by the light dose of 6 J/cm^2 during 5 and 10 minutes, using a lamp (OPTEL) with polarized light and red filter (632,8 nm). After irradiation, the cells were incubated in a humidified atmosphere at 37°C and 5% CO_2 for 0, 3 and 6 h. Then the cells were fixed with formaldehyde for 10 min.

Lipid peroxidation: malondialdehyde (MDA), the final product of fatty acid peroxidation, reacts with TBA to form a coloured complex. The level of TBARS was measured on the basis of absorbance at the wavelength of 535 nm. The concentration of malondialdehyde was quantified spectrophotometrically, based on a set of MDA standards of known concentration [7].

Protein damage: protein damage was based on Ellman's method. This method uses reaction of 5,5'-dithiobis-2-nitrobenzoic acid (DTNB acid) with thiol groups (-SH) of proteins [7].

Results

The results of MDA concentration are presented in Fig. 1. The level of lipid peroxidation was significantly higher for cells after PDT, comparing to that in the control cells. After a 5-minute irradiation and 15µg/ml of Ph II, we obtained 0,49 µM/l MDA concentration, however, during the same time irradiation but with 30µg/ml of Ph II we got 0,35 µM/l MDA concentration. During a different time period of irradiation (10min) for 15µg/ml and 30µg/ml of Ph II the same MDA concentration (0,5 µM/l) was obtained.

The results of the thiol group (-SH) levels are shown in Fig. 2. We observed a much lower concentration of -SH groups for cells after PDT treatment, in comparison with respective values in the control cells. We obtained over 50nmol/l during 10min irradiation and 30µg/ml of Ph II.

Discussion

The primary objective of this study was to determine oxidative stress in A549 cells that induces PDT. The crucial factors, which determine the type of PDT-mediated cell death, include light dose, the sensitivity of cells and the subcellular distribution of the photosensitizer [4, 5, 6]. In our experimental setting, we studied the levels of the malonyldialdehyde - product of lipid peroxide oxidation in A549 cells, treated by photodynamic therapy, depending on the time and photosensitizer concentration. A high level of lipid peroxidation was found and that was an indication of an increasing, high activity of reactive oxygen species in the environment. Other results verify that lipid peroxidation is one of the photodynamic effects, exerted by hypericin in NPC cells. [8]. Peroxidation of membrane lipids is known to disrupt the membrane structure and induce loss of function, which could lead to cell death [9, 10]. Our investigation confirms earlier studies with PDT on different cell line, showing that, after PDT, the lipid peroxidation level was increased [3, 10]. It has been observed that it depends on different time of irradiation and different dose of photosensitizer. In our studies, we examined different times of irradiation and different concentrations of photosensitizer. We suggest that the best time for irradiation was 5 min for 15µg Ph II for A549 cell line. The higher concentration of Photofrin II requires longer expositions to light. Oxidative stress damage, that affects PDT, is also dependent on cell line and the incubation time with photosensitizing agent before and after exposure to light [4]. Our data represent the first investigation of A549 cellular damage after photodynamic treatment.

Figure 1. The levels of MDA in A549 cells, treated by PDT, comparing to control values.

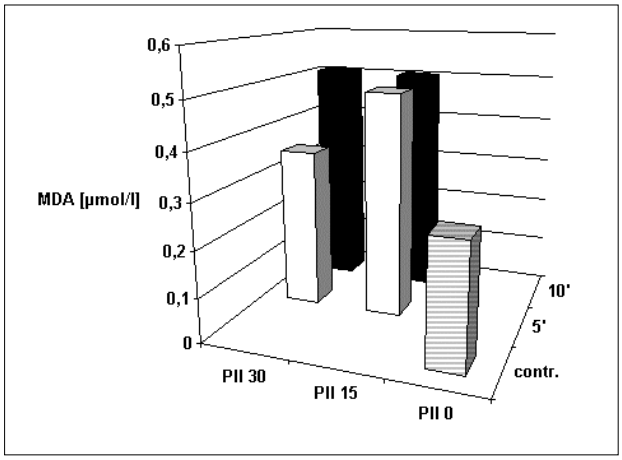

Figure 2. The levels of thiol groups in A549 cells, treated by PDT, in comparison to control values.

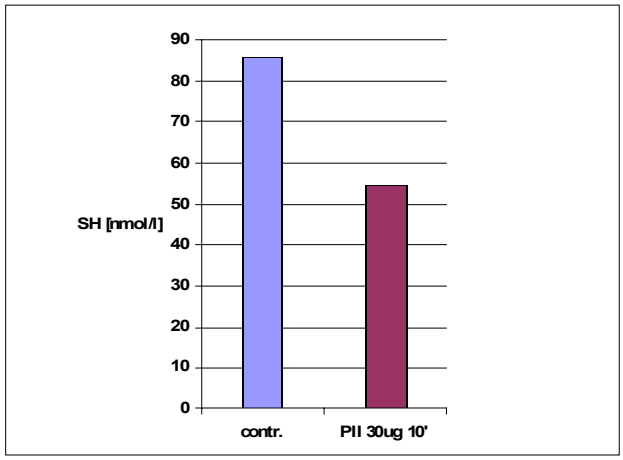

For confirmation of our results, also the oxidation of -SH groups was also determined. Our studies revealed that PDT treatment led to membrane damage through protein destruction. Examining single time irradiation and one concentration of Ph II, a distinct decrease of thiol groups concentration was observed [1, 10].

Conclusion

In conclusion, PDT with Ph II induces lipid peroxidation with accompanying protein damage in A549 cells, what can lead to distinct epidemiological, pathological and clinical features. Photofrin II-PDT appears to be an attractive alternative treatment modality for A549 cell line [12].

References

1. Girotti AW. Photosensitized oxidation of membrane lipids: reaction pathways, cytotoxic effects, and cytoprotective mechanisms. J Photochem Photobiol B, 2001; 63: 103-13.

2. Grönlund-Pakkanen S. The effect of photodynamic therapy on rat urinary bladder with orthotopic urothelial carcinoma. BJU Int, 2003; 92: 125-30.

3. Martins J. Photoactivation of phthalocyanine-loaded low density lipoproteins induces a local oxidative stress that propagates to human erythrocytes: protection by caffeic acid. Free Radic Res, 2002; 36: 319-28.

4. Dellinger M. Apoptosis or necrosis following Photofrin photosensitization: Influence of the incubation protocol. Photochem Photobio,l 1996; 64: 182-7.

5. Kessel D, Luo Y, Deng Y Chang CK. The role of subcellular localization in initiation of apoptosis by photodynamic therapy. Photochem Photobiol, 1997; 65: 422-6.

6. Hsieh YJ, Wu CC, Chang HC, Yu JS. Subcellular localization of photofrin determines the death phenotype of human epidermoid carcinoma A431 cells triggered by photodynamic therapy: when plasma membranes are the main targets. J Cell Physiol, 2003; 194: 363-75.

7. Rice-Evans CA, Diplock AT, Symons MCR. Techniques in Free Radical Research. Elsevier, 1991; Amsterdam, London, New York, Tokyo.

8. Hadjur C, Richard MJ, Parat MO, Jardon P Favier A. Photodynamic effects of hypericin on lipid peroxidation and antioxidant status in melanoma cells. Photochem Photobiol, 1996; 64: 375-81.

9. Wang HP, Que SY, Schafer FQ, Domann FE, Oberley LW Buettber GR. Phospholipid hydroperoxide glutatione peroxidase protects against singlet oxygen-induced cell damage of photodynamic therapy. Free Rad Biol Med, 2001; 30: 825-35.

10. Spiteller G. Are lipid peroxidation processes induced by changes in the cell wall structure and how are these processes connected with diseases? Med Hypotheses, 2003; 60: 69-83.

11. Chatterjee SR. Photodynamic effects induced by meso-tetrakis[4-(carboxymethyleneoxy) phenyl] porphyrin using rat hepatic microsomes as model membranes. Arch Biochem Biophys, 1997; 339: 242-9.

12. Du HY, Oliwo M, Kwong-Huat B, Bay BH. Hypericin-mediated photodynamic therapy induces lipid peroxidation and necrosis in nasopharyngeal cancer. Inter J Onc, 2003; 23: 1401-5.

Plasma VEGF-A and its soluble receptor R1 correlate with the clinical stage of colorectal cancer

Myśliwiec P[1], Piotrowski Z[1], Zalewski B[1], Kukliński A[1], Pawlak K[2]

[1]The 2nd Department of General and Gastroenterological Surgery; [2]Department of Nephrology and Transplantology;
Medical University of Białystok, Poland

Abstract

Our aim was to assess plasma VEGF-A and its soluble receptor R1 (sVEGF-R1) in patients with colorectal cancer, in comparison with apparently healthy subjects.

Methods. Samples of plasma were collected from 26 patients with colorectal cancer before surgery and on post-operative day 3 and 10, frozen and eventually assessed, using ELISA kits.

Results. We found an increase in VEGF-A in colorectal cancer patients and a strong positive correlation between metastatic spread and postoperative VEGF-A, which also correlated with CA19.9. Soluble VEGF-R1 showed a positive correlation with lymph node involvement. Conclusions. Our findings may suggest that the patients with high postoperative VEGF-A should be scanned for metastases. In view of our finding that sVEGFR-1 correlates with lymph node involvement, precautions must be taken in studies of sVEGFR-1 as a potential therapeutic agent.

Key words: colorectal cancer, VEGF-A, sVEGF-R1

Introduction

In most countries of the world, colorectal cancer is an increasing cause of morbidity and mortality. Although early surgical treatment can be curative, many patients already have metastases at the time of operation. Moreover, many patients present in late stages of the disease. In such cases, chemotherapy is warranted. Thus, it is of crucial importance to know, whether the malignancy is localised or disseminated. Modern imaging often permits localisation of macrometastases, however, in order to detect micrometastases, more sensitive methods are needed. Molecular markers of solid cancers are of high potential value in such circumstances [1].

Neo-angiogenesis is of crucial importance for colorectal cancer growth and nutrition, with vascular endothelial growth factor (VEGF) being the most important cytokine, involved in the process [2]. VEGF plays an important role in progression, invasion and spread of colorectal cancer by influencing the proliferation and migration of endothelial cells. Because of the positive correlation between plasma concentration of VEGF and the size of tumour in patients with colorectal cancer [3], there have been attempts to inhibit VEGF synthesis in patients with advanced colorectal cancer [1].

Total VEGF is not a sufficient diagnostic tool in patients with colorectal cancer because of small sensitivity (36%) [3]. VEGF comprises a number of cytokines: VEGF-A, VEGF-C, VEGF-D and VEGF-E. VEGF-A is most abundantly expressed in colorectal cancer tissues and, therefore, it seems to be of greater value then total VEGF [2].

The group of proteins, named together as VEGF, acts on two main specific receptors, marked with number 1 (VEGFR-1), 2 (VEGFR-2) and 3 (VEGFR-3). Out of the three, VEGFR-1 has been reported to be most important for solid malignancies [2]. Also the soluble form of VEGFR-1 (sVEGFR-1) has recently been demonstrated in blood. It acts in vitro as antagonist for VEGF-A and inhibits the biological activity of VEGF-A in vivo [4]. SVEGFR-1 is probably the only known and naturally occurring endogenous antagonist to VEGFR-1 receptor. As such, it was postulated to have an important role in the treatment aiming at angiogenesis inhibition [5].

The aim of the study was to investigate sVEGFR-1 and VEGF-A in plasma of patients with colorectal cancer, before and after surgical treatment in relation to chosen clinical and laboratory parameters, such as: sex, age, BMI, tumour localisa-

ADDRESS FOR CORRESPONDENCE:
Myśliwiec Piotr
2nd Department of General and Gastroenterological Surgery
Medical University of Białystok
M.C. Skłodowskiej 24 A, 15-276 Białystok, Poland
e-mail: mpiotr@amb.edu.pl

Table 1. Concentrations of VEGF-A and sVEGFR-1 in the control group ("Control") and in patients with colorectal cancer ("Pre-op" - preoperatively; "Post-op" - postoperatively). Data, given as the mean ± standard deviation; p values of comparison between the studied group and the control group are shown in brackets.

	Control [pg/ml]	Pre-op [pg/ml]	Post-op day 3 [pg/ml]	Post-op day 10 [pg/ml]
VEGF-A	38.3 ± 13.1	83.36 ± 151.61	79.53 ± 125.47	114.7 ± 198.13
p		**(p=0.0066**)**	**(p=0.0037**)**	**(p=0.0041**)**
sVEGFR-1	192 ± 245	83.4 ± 154.6	79.5 ± 125.5	114.2 ± 198.1
p		(p=0.546)	(p=0.336)	(p=0.485)

Table 2. Chosen correlations between pathological or laboratory parameters and the concentrations of VEGF-A and sVEGFR-1 in patients with colorectal cancer.

Correlation between	p
Preoperative VEGF-A and distant metastases	0.329
Postoperative VEGF-A (day 3) and distant metastases	**0.046***
Postoperative VEGF-A (day 10) and distant metastases	**0.031***
Postoperative VEGF-A (day 10) and postoperative CA19-9	**0.027***
Postoperative VEGF-A (day 3) and lymphocyte count	**0.045***
Preoperative sVEGFR1 and distant metastases	0.212
Preoperative sVEGFR1 and lymph node involvement	**0.015***
Postoperative sVEGFR1 (day 3) and distant metastases	0.798

tion within the bowel, Dukes' or clinical stage, the presence of distant metastases, lymph node involvement and albumins in serum.

Material and methods

The studies were performed on plasma samples, collected from 26 patients with colorectal cancer, treated at the 2nd Department of General and Gastroenterological Surgery, Medical University of Bialystok. The Control group consisted of 18 apparently healthy subjects: 8 men and 11 women, aged 32 to 78 (mean 65).

Among the patients with colorectal cancer, there were 11 men and 15 women. The mean age was 69.2 years (58 to 83 years). The cancer was localized in the rectum of 11 patients, in the sigmoid colon of 7, in the cecum of 3, in the ascending colon of 3, in the descending colon in 1 and in the transverse colon in 1 patient. Nineteen (19) patients underwent curative resection and 7 patients - palliative resection. In all the cases, pathological examination showed adenocarcinoma. According to Dukes' classification 11 patients were at stage B, 3 patients at C1, 5 at C2 and 7 at stage D. In all the patients with colorectal cancer, samples were collected before surgery and on the post-operative day 3 and 10. Patients and volunteers with either clinical or laboratory signs of infection were excluded from the study. All the subjects signed an informed consent.

Blood samples were collected after overnight fasting: 4.5 ml venous blood was poured into a tube, containing 0.5 ml 3.8% sodium citrate. Immediately after sampling, the specimens were centrifuged at 3.5 G for 10 minutes in 4°C. The supernatant-platelet poor plasma was transported to an Eppendorf's tube and frozen in -70°C until determination. The plasma samples were used for ELISA tests. VEGF-A was determined, according to George et al. [6] and sVEGFR-1 - as previously described [7], using a commercially available ELISA kits, purchased from the Research Diagnostics Inc., USA.

The following tests were used for statistical analysis: Shapiro-Wilk test for normality, Kruskal-Wallis test for variance analysis, Mann-Whitney test for inter-group comparison, Spearman's and Chi2 tests for correlations. A value of $p<0.05$ was regarded as significant for all the tests.

Results

We found a significant increase in VEGF-A concentrations in plasma of all the groups of patients with colorectal cancer (Tab.1), as compared to values in the control group ($p<0.01$). sVEGF-R1 (Tab.1) was detectable in 17 / 26 (65.4%) of cancer patients and in 15 / 18 (83.3%) of control subjects. The values of sVEGF-R1 tended to be lower in the studied group than those in the control group, however not significantly (p=0,336) (Tab.1). We found a positive correlation of the presence of distant metastases with VEGF-A concentration in plasma (Tab. 2), as assessed on the postoperative days 3 and 10 ($p<0.05$). There was also a negative correlation of VEGF-A in plasma on the postoperative day 10 with lymphocyte count ($p<0.05$) and a positive correlation of VEGF-A in plasma on the postoperative day 10 with CA 19.9 ($p<0.05$).

As far as preoperative sVEGF-R1 is concerned, we found its positive correlation with lymph node involvement, assessed on the basis of pathological examinations of surgical specimens (Tab.2). No correlations were observed for either the sex, the age, BMI tumour localisation within the bowel, Dukes' or clinical stage or for albumins in serum.

Discussion

VEGF-A expression has previously been studied in colorectal cancer tissues and showed an increased expression, as compared to its values in healthy subjects. An association of VEGF-A tissue expression was also reported with tumour grade and size [2]. It has been shown that VEGF-A mRNA expression in colorectal mucosa strongly correlates with liver metastases and that VEGF-A concentration is an independent predicting factor for the survival of patients with colorectal cancer [8].

Our results, concerning VEGF-A, confirm its significant correlation with the clinical stage of colorectal cancer. We demonstrated a significant increase of the cytokine level in plasma of the patients, as compared with that in healthy subjects. We found a strong positive correlation of VEGF-A plasma concentration, assessed postoperatively, with presence of distant metastases. That was in line with postoperative CA19.9 values. We also observed a moderate, though not significant, increase in VEGF-A level following a surgical procedure, performed in colorectal cancer patients. This might be attributable to the breakdown of thrombocytes and neutrophils, containing considerable amounts of VEGF, in result of surgical manipulations [9]. It was for the first time in 2002 that soluble VEGFR-1 was reported to be detectable in patients with colorectal cancer [5]. Chin et al. [8] reported initially that sVEGFR-1 in plasma could be detectable in 74% of patients with colorectal cancer. In their recent report, the detection was much lower [4]. The authors observed a suppression of sVEGFR-1 in patients with colorectal cancer. In our study, no statistical differences were observed in sVEGFR-1 plasma concentration in colorectal cancer patients, as compared to observed values in the normal controls. However, our observation of the highly significant positive correlation of sVEGFR-1 with lymph node involvement in colorectal cancer might be of importance.

In sum: the presented data may suggest that patients with high postoperative values of VEGF-A should be scanned for metastases. In view of our finding that sVEGFR-1 strongly correlates with lymph node involvement by colorectal cancer, precautions should be taken in studies of sVEGFR-1 as a potential therapeutic agent.

References

1. Tebbutt NC, Cattell E, Midgley R, Cunningham D, Kerr D. Systemic treatment of colorectal cancer. Eur J Cancer, 2002; 38: 1000-15.

2. Hanrahan V, Currie M, Gunningham S, Morrin H, Scott P, Robinson B, Fox S. The angiogenic switch for vascular endothelial growth factor (VEGF)-A, VEGF-B, VEGF-C, and VEGF-D in the adenoma-carcinoma sequence during colorectal cancer progression. J Pathol, 2003; 200: 183-94.

3. Broll R, Erdmann H, Duchrow M, Oevermann E, Schwandner O, Markert U, Bruch HP, Windhovel U. Vascular endothelial growth factor (VEGF)--a valuable serum tumour marker in patients with colorectal cancer? Eur J Surg Oncol, 2001; 27: 37-42.

4. Chin K, Greenman J, Reusch P, Gardiner E, Marme D, Monson J. Changes in serum soluble VEGFR-1 and Tie-2 receptors in colorectal cancer patients following surgical resections [In Process Citation]. Anticancer Res, 2004; 24: 2353-7 .

5. Kumar H, Heer K, Greenman J, Kerin M, Monson J. Soluble FLT-1 is detectable in the sera of colorectal and breast cancer patients. Anticancer Res, 2002; 22: 1877-80.

6. George ML, Tutton MG, Janssen F, Arnaout A, Abulafi AM, Eccles SA, Swift RI. VEGF-A, VEGF-C, and VEGF-D in colorectal cancer progression. Neoplasia, 2001; 3: 420-7.

7. Hornig C, Behn T, Bartsch W, Yayon A, Weich HA. Detection and quantification of complexed and free soluble human vascular endothelial growth factor receptor-1 (sVEGFR-1) by ELISA. J Immunol Methods, 1999; 226: 169-77.

8. Chin KF, Greenman J, Reusch P, Gardiner E, Marme D, Monson JR. Vascular endothelial growth factor and soluble Tie-2 receptor in colorectal cancer: associations with disease recurrence. Eur J Surg Oncol, 2003; 29: 497-505.

9. Werther K, Christensen IJ, Nielsen HJ, . Prognostic impact of matched preoperative plasma and serum VEGF in patients with primary colorectal carcinoma. Br J Cancer, 2002; 86: 417-23.

Serum levels of Osteoprotegerin (OPG) and Pro Gastrin Releasing Peptide (ProGRP) during chemotherapy of lung cancer

Naumnik W, Chyczewska E, Iżycki T, Ossolinska M

Department of Pneumonology; Medical University of Bialystok, Poland

Abstract

The aim of our study was to evaluate the usefulness of serum OPG and ProGRP during chemotherapy of lung cancer in relation to the histological type of the tumour, its clinical stage and the response to therapy. The levels of OPG and ProGRP were determined in 39 patients (20 NSCLC, 19 SCLC) and 10 healthy subjects. Blood samples were collected from each patient before and after chemotherapy. OPG and ProGRP levels in all the patients with lung cancer were higher than those in the controls. ProGRP were higher in SCLC group than in those NSCLC. In NSCLC group (after chemotherapy), OPG level in patients with Stage IV tumour was higher than in those with Stage IIIB (p=0,03). OPG in ED SCLC were higher than those in LD SCLC (p=0.04). In SCLC group, ProGRP were higher in LD patients than those with ED (p=0.04). Concluding, the measuring of OPG and ProGRP in lung cancer patients may be useful in clinical practice.

Key words: Osteoprotegerin (OPG), Pro Gastrin Releasing Peptide (ProGRP), lung cancer, non-small cell lung cancer-NSCLC, small cell lung cancer-SCLC.

Introduction

Lung cancer is one of the most prominent causes of mortality - because of neoplastic reasons - in industrialized countries, in particular, among the male population.

ADDRESS FOR CORRESPONDENCE:
Naumnik Wojciech
Department of Pneumonology
Medical University of Bialystok,
Zurawia 14; 15-540, Bialystok, Poland
Tel/fax +48 85 7324149, e-mail: naumw@mp.pl

OPG is a novel secreted member of the tumour necrosis factor superfamily [1]. OPG binds RANKL (receptor activator of NF-κB ligand), inhibiting its interaction with RANK and preventing osteoclast formation [2]. It has been reported that OPG expression is associated with bone metastasis of cancer [2]. High levels of OPG mRNA have been detected in the lung, the heart, the kidney, the liver, the stomach, the intestine and bones [1, 3]. It has been reported that the expression of OPG protein in gastric carcinoma tissues correlates with the clinical stage of the tumour [4]. The data about OPG in lung cancer patients are rather poor. Lipton et al. [5] have reported that there is no difference in serum OPG levels between healthy controls and lung cancer patients (16 pts). There were no observations, concerning the clinical stage and the histological type of the tumour.

ProGRP, a member of the bombesin family of peptides, has been shown to be produced by SCLC in an autocrine fashion [6]. It has been suggested that ProGRP is a potential tumour marker for SCLC [6]. In the SCLC chemotherapy group, ProGRP was higher in progressed patients than in the responders [6]. In order to determine the clinical significance of OPG and ProGRP in lung cancer patients, we analyzed levels of these proteins in relation to the histological type of the tumour, its clinical stage and response to therapy.

Materials and methods

The study included 39 patients (smokers; 20 NSCLC; 19 SCLC). The group consisted of 35 males and 4 females (the mean age of 64.0 years; the age range: 29-78 years). At the time of examination, the patients did not show any signs of clinically overt active inflammatory process. The control group comprised 10 healthy volunteers with the mean age of 61 years (non smokers, 8 males). The clinical stage of NSCLC was assigned, according to TNM classification. The classifications of SCLC were made, according to the VALCSG (LD-limited disease; ED-extensive disease). Standard criteria for the objective response to the applied therapy were used (WHO guidelines). Blood samples

Table 1. Serum OPG and ProGRP levels in lung cancer patients and controls.

Disease stage	before chemotherapy (P-VALUE VS CONTROLS)	after chemotherapy (P-VALUE VS CONTROLS)	Controls (n = 10)
patients (n=39) OPG Pro GRP	4,2 ± 1,2 p=0,003 30,8 (9 – 113)	4,2± 1,0 p=0,002 34,3 (13 – 305)	3,1 ± 0,6 21,8 (10 – 33)
NSCLC (n=20) OPG Pro GRP	4,2 ± 1,2 p=0,011 30,8 (9 – 113) p=0,011	4,5 ± 1,2 p=0,001 34,3 (13 – 305) p=0,001	
IIIB (n = 11) OPG Pro GRP	3,8 ± 1,2 25,7 (13 – 43)	3,9 ± 0,9 * 32,9 (17 – 41)	
IV (n = 9) OPG Pro GRP	4,6 ± 1,1 33,6 (9 – 113)	5,2 ± 1,3 ** 37,1 (13 – 305)	
SCLC (n = 19) OPG Pro GRP	4,3 ± 1,1 p=0,005 1152,2 (26–1802) p=0,00002	4,0 ± 0,6 p=0,0008 255,4 (18 – 1581) p=0,0001	
LD (n = 9) OPG Pro GRP	4,2 ± 1,0 1589,9 (39 – 1802)	3,7± 0,5 # 262,8 (63 – 1236) 1	
ED (n =10) OPG Pro GRP	4,5 ± 1,2 925,2 (26 – 1763)	4,3 ± 0,6 # # 67,6 (18 – 1581) 2	

Abbreviations: OPG- osteoprotegerin (pmol/l); Pro GRP - Pro Gastrin Releasing Peptide (pmol/l);
* vs ** p=0,03; # vs # # p=0,04; 1 vs 2 p=0,04

Table 2. Values of OPG and ProGRP before and after chemotherapy of lung cancer patients

	PR + NC (n = 11)		PD (n = 9)	
NSCLC (n = 20)	before chemotherapy	after chemotherapy	before chemotherapy	after chemotherapy
OPG Pro GRP	4,0 ± 1,2 30,8 (13 – 38)	4,2 ± 1,2 35,7 (19 – 74)	4,4 ± 1,3 23,5 (9 – 113)	4,7 ± 1,4 31,5 (13 – 305)
	PR + NC (n = 11)		PD (n = 8)	
SCLC (n = 19)	before chemotherapy	after chemotherapy	before chemotherapy	after chemotherapy
OPG Pro GRP	4,4 ± 1,0 1152,2 (39 – 1802)	4,0 ± 0,7 79,7 (18 – 1236)	4,3 ± 1,3 1375,0 (26 – 1763)	4,0 ± 0,6 1012,8 (48 – 1581)

PR- partial response; NC- no change; PD- progressive disease

were collected from each patient before and after chemotherapy. Serum OPG and ProGRP concentrations were measured by enzyme immunoassay (Biomedica-OPG; IBL Japan-ProGRP) Statistical differences were analyzed by Student's t test, the non-parametric Wilcoxon test and the Mann- Whitney's U- test. Any value of $p<0,05$ was considered statistically significant.

Results

As shown in Tab. 1, serum OPG and ProGRP levels in 39 patients with lung cancer were higher than those in the controls. No significant differences in serum OPG levels were observed with regard to the histological type of the tumour (Tab. 1). ProGRP were significantly higher in the SCLC group than in NSCLC (Tab. 1). In the NSCLC group (after chemotherapy) (Tab. 1), the mean OPG level in patients with Stage IV was higher than that in patients with Stage IIIB (p=0.03). OPG in ED SCLC were higher than those in LD SCLC (p=0.04). In the SCLC group, ProGRP were higher in LD patients than in those with ED (p=0.04) (Tab. 1). No significant differences in ProGRP levels were observed with regards to the tumour stage of NSCLC (Tab. 1). No differences in OPG and ProGRP levels were observed with regards to the response to applied therapy (Tab. 2).

Discussion

OPG is a key factor, inhibiting the differentiation and activation of osteoclasts, and is, therefore, essential for bone resorp-

tion. In healthy people, osteoclastic activity is regulated by the balance between OPG and its ligand (RANKL). In opinion of Lipton et al. [5], the elevations of circulating OPG in serum of patients with malignancy are not high enough to uniformly suppress osteoclast formation [5]. In our study, the levels of OPG were significantly higher in lung cancer patients than those in the controls. On the contrary, Lipton et al. [5] showed that the levels of OPG in lung cancer patients did not differ significantly from those in healthy volunteers. There were only 16 lung cancer patients in that study. Our study included 39 patients with lung cancer. To our knowledge, the current study is the second one to report serum OPG levels in lung cancer patients in relation to the clinical stage of tumour.

ProGRP has been demonstrated as a tumour marker for SCLC in the investigations of Oremek et al. [7]. In our studies, the mean serum values of ProGRP were higher in cancer patients than those in the controls. The SCLC patients had higher levels of ProGRP than the ones with NSCLC. We confirm the observations of Schneider et al. [6]. They reported that ProGRP was a good tool for discriminating NSCLC versus SCLC [6]. SCLC differs clinically and biologically from NSCLC types. The incidence of distant metastases of SCLC at the time of primary diagnosis is very high. In our studies, no significant differences of ProGRP were noted in relation to the NSCLC clinical stage. In accordance with the literature [6], ProGRP reached more elevated serum levels in patients with limited disease. Thus, serum levels of ProGRP could be used to discriminate between extensive disease SCLC versus limited one.

The expression of OPG protein in gastric carcinoma tissues correlates with the clinical stage of the tumour [4]. In our study, the mean OPG level in patients with Stage IV was significantly higher than that in patients with Stage IIIB. The same observations were made by Lipton et al. [5]. They noticed a trend towards higher levels of OPG in patients with metastatic disease, compared to those with localized malignancy [5]. Those observations confirm that different mechanisms are responsible for OPG increase in serum of lung cancer patients. OPG is a factor derived from tumour and bone [8]. In the studies by Eaton et al. [8], there has been a conclusion that OPG is a potential new marker, which is elevated in serum of patients with advanced prostate cancer. Our results, based on lung cancer patients, are in agreement with the studies by Eaton et al. [8].

In our studies, there were no significant differences in either OPG or ProGRP with respect to the response to applied therapy. To our knowledge, the current study is the first one to report serum OPG in relation to the response of lung cancer to applied therapy. Eaton et al. [8] showed that, in a prostate cancer group, OPG was an indicator of the disease progression. We did not confirm these observations in our patients with lung cancer.

ProGRP has been demonstrated as a promising tumour marker for SCLC monitoring [4]. Tumour markers may represent the total body tumour load. Rising tumour marker concentrations in lung cancer patients may indicate tumour progression, which may help avoiding the continuation of ineffective treatment. In our studies, the levels of ProGRP in progressed patients were the same as those in responder ones.

Concluding, the measurements of OPG and ProGRP can be useful in clinical practice. Their clinical significance in the monitoring of chemotherapy and for the prognosis of lung cancer needs further studies.

References

1. Simonet W, Lacey D, Dunstan C, Kelley M, Chang M. Osteoprotegerin: a novel secreted protein involved in the regulation of bone density. Cell, 1997; 89: 309-19.

2. Croucher PI, Shipman CM, Lippitt J, Perry M, Asosingh K, Hijzen A, Brabbs AC, van Beek EJ, Holen I, Skerry TM, Dunstan CR, Russell GR, Van Camp B, Vanderkerken K. Osteoprotegerin inhibits the development of osteolytic bone disease in multiple myeloma. Blood, 2001; 98: 3534-40.

3. Kwon BS, Wang S, Udagawa N, Haridas V, Lee ZH, Kim KK, Oh KO, Greene J, Li Y, Su J, Gentz R, Aggarwal BB, Ni J. TR1, a new member of the tumor necrosis factor receptor family, induces fibroblast proliferation and inhibits osteoclastogenesis and bone resorption. FASEB J, 1998; 12: 845-54.

4. Ito R, Nakayama H, Yoshida K, Kuraoka K, Motoshita J, Oda N, Oue N, Yasui W. Expression of osteoprotegerin correlates with aggressiveness and poor prognosis of gastric carcinoma. Virchows Arch, 2003; 443:146-51.

5. Lipton A, Ali SM, Leitzel K, Chinchilli V, Witters L, Engle L, Holloway D, Bekker P, Dunstan CR. Serum Osteoprotegerin levels in healthy controls and cancer patients. Clinical Cancer Res, 2002; 8: 2306-10.

6. Schneider J, Philipp M, Velcovsky H-G, Morr H, Katz N. Pro-Gastrin- Releasing Peptide (ProGRP), Neuron Specic Enolase (NSE), Carcinoembryonic Antigen (CEA) and Cytokeratin 19-Fragments (CYFRA 21-1) in Patients with Lung Cancer in Comparison to other Lung Diseases. Anticancer Research, 2003; 23: 885-94.

7. Oremek G, Sapoutzis N. Pro-gastrin-releasing peptide (Pro-GRP), a tumor marker for small cell lung cancer. Anticancer Res, 2003; 23: 895-8.

8. Eaton C, Wells J, Holen I, Croucher P, Hamdy F. Serum osteoprotegerin (OPG) levels are associated with disesase progression and response to androgen ablation in patients with prostate cancer. Prostate, 2004; 59: 304-10.

Molecule CD44 variant 10 expression in lymphocytes infiltrating tumour tissues and epithelial cells in patients with colorectal cancer

Zalewski B[1], Stasiak-Barmuta A[2], Guzińska-Ustymowicz K[3], Cepowicz D[1], Gryko M[1]

[1]Department of General and Gastroenterological Surgery, [2]Laboratory of Flow Cytometry, Children Teaching Hospital,
[3]Department of General Patomorphology, Medical University of Bialystok, Poland

Abstract

The aim of this study was to evaluate the expression of CD44v10 in colorectal tumour cells and in lymphocytes infiltrating the tumour (CD45+). Samples of tumour tissue (TT), as well as of healthy tissue (HT) and of tumour adjacent tissue (TAT), were obtained from 20 patients. An evaluation of CD44v10 expression was performed in a flow cytometer. The mean value of the percentage of CD45+ with co-expression of CD44v10 was significantly higher in the lower stage of the tumour (pT). The mean value of the percentage of epithelial cells with CD44v10 co-expression was significantly higher in pN2 than in pN1 stage. Only in TAT the mean value of the percentage of epithelial cells and CD45+ with tCD44v10 co-expression was significantly lower in the higher degree of histological malignancy. It is supposed that CD44v10 takes part in local cancer progression.

Key words: colorectal cancer, CD44v10, leucocytes, tumour tissue.

Introduction

Neoplasmal diseases are the second, or, according to some authors, the third cause of deaths all over the world. Colorectal cancers are, among other neoplasms, placed on the third position, regarding morbidity and mortality rates after the breast and lung and bronchus cancers in women and prostate and lung and bronchus cancers in men [1]. The recurrence of the disease depends on the progression of neoplasmal metastases to lymph nodules and distal organs and is the most common cause of death [2, 3].

The aim of this study was to evaluate, whether the expression of CD44v10 isoform on epithelial cells and leucocytes infiltrating tumour tissues, tumour adjacent tissues and healthy tissues of the large bowel in patients with colorectal cancer, correlates with the pathomorphological stage of the tumour, due to WHO classification (pT), lymph nodes metastases (N) and the histopathological grade of malignancy (G).

Material and methods

Twenty (20) patients were operated on sigmorectal adenocarcinomas in G2-G3 grade of malignancy and pT2- pT4 stage, acc. to WHO score, at our Department in 2003. There were 11 (55 %) women and 9 (45 %) men. The median age was 63.27 years (the age range: 32 - 78 years). Neoadjuvant radio- or chemotherapy had not been applied to any of the patients. Nobody of them had metastases to distal organs. The preoperative diagnosis was based on clinical symptoms and preoperatively confirmed by histopathological examination of a biopsy specimen, obtained endoscopically. Other types of cancer and polyps, including inoperable tumours, were excluded from the investigation. Tumour tissue samples were obtained during the operation. They were divided into two parts. One part of tissues was typically prepared and paraffin embedded sections were examined to estimate pTN stage and the grade of malignancy in G1-G3 score. The second specimen consisted of three samples, obtained from HT, TAT and TT and placed in a sterile container with RPMI - 1640. Immediately after collection (max. 2h), respective fragments of tissues were minced to receive the homogenous cells suspension. The cell suspension, obtained in this way, was twice washed with PBS with 0.5% bovine albumin and 2mM of EDTA. Two parts of 100 µl of cell suspension were conjugated - the first part with 10 µl of CD45-PerCP and the second one with 10 µl

ADDRESS FOR CORRESPONDENCE:
Bogdan Zalewski
Department of General and Gastroenterological Surgery
M. C. Skłodowskiej 24 A; 15-276 Białystok, Poland
Tel. (+48 85) 746 82 87 fax. (+48 85) 746 86 24;
e-mail: bogdan-zalewski@wp.pl

Table 1. The mean value of the percentage of CD45+ and epithelial cells with co-expression of CD44v10 in different pT stages.

TT /pT	CD45 / CD44 v10	EMA /CD44v10
2	76.6 ± 12.1	49.6 ± 9.6
3	48.7 ± 11.8	31.6 ± 17.1
4	43.8 ± 7.8	53.5 ± 10.1
Statistical analysis	2 v. 3; p<0.01 2 v. 4; p<0.04	Not significant
TAT /pT		
2	85.2 ± 13.2	36.9 ± 16.9
3	49.3 ± 10.2	29.2 ± 13.6
4	61.0 ± 12.1	46.3 ± 7.6
Statistical analysis	2 v. 3; p<0.001 2 v. 4; p<0.05	Not significant
HT /pT		
2	74.9 ± 19.5	32.4 ± 18.8
3	50.8 ± 14.1	19.2 ± 14.2
4	51.4 ± 10.4	31.5 ± 11.3
Statistical analysis	2 v. 3; p<0.05 2 v. 4; p<0.05	Not significant

Table 2. The mean value of the percentage of CD45+ and epithelial cells with co-expression of CD44v10 in different pN stages.

TT /pN	CD45 / CD44 v10	EMA / CD44 v10
0	52.0 ± 11.2	37.9 ± 15.6
1	53.1 ± 35.4	31.4 ± 16.1
2	53.8 ± 14.1	43.8 ± 13.7
Statistical analysis	Not significant	Not significant
TAT /pN		
0	57.7 ± 16.6	33.6 ± 14.4
1	61.0 ± 31.0	22.0 ± 4.2
2	57.6 ± 4.9	46.8 ± 9.8
Statistical analysis	Not significant	1 v. 2; p<0.05
HT /pN		
0	55.4 ± 16.0	26.5 ± 12.3
1	47.6 ± 19.1	31.4 ± 16.1
2	58.3 ± 9.7	40.9 ± 13.5
Statistical analysis	Not significant	Not significant

of Anti-EpCAM-PerCP-Cy 5.5 antibodies (Bencton Dickinson). After 20 minutes of incubation in room temperature, 10µl of CD44v10 antibodies (AB2082 Chemicon) were added. After 30 minutes of incubation in 4°C in the dark, the cells were washed three times in PBS solution. Next, IgG (Fab2 - Mouse antiRabbit IgG AP 1889 - Chemicon), conjugated with EMA-FITC (DAKO), was added and the suspension was again incubated during 30 minutes in 4°C. The cells were washed again three times. PBS and 1% solution of paraformaldehyde was added. Analyses of the cells were performed, using a Coulter EPICS XL flow cytometer. A minimum of 10^4 cells were counted. Conforming isotypic negative controls were used. The non-parametric ranking Mann-Whithney test was used for statistical analysis of flow cytometric results between the evaluated groups. Values of $p<0.05$ were accepted as statistically significant.

Table 3. The mean value of the percentage of CD45+ and epithelial cells with co-expression of CD44v10 in different grades of malignancy.

TT /G	CD45 / CD44 v10	EMA /CD44 v10
0	52.3 ± 10.4	35.1 ± 11.9
2	52.9 ± 16.7	41.2 ± 17.3
3	55.5 ± 9.2	20.0 ± 8.5
Statistical analysis	Not significant	Not significant
TAT /G		
0	59.7 ± 15.0	37.9 ± 14.4
2	63.0 ± 15.2	38.3 ± 12.5
3	40.7 ± 7.6	20.0 ± 9.7
Statistical analysis	0 v. 3; p<0.05 2 v. 3; p<0.03	0 v. 3; p<0.05 2 v. 3; p<0.03
HT /G		
0	49.9 ± 18.2	38.9 ± 13.6
2	60.5 ± 13.8	29.2 ± 20.4
3	41,3 ± 12,4	18,7 ± 12,6
Statistical analysis	Not significant	Not significant

Results

The mean value of the percentage of lymphocytes with co-expression of CD44v10, infiltrating all kinds of tissues, was significantly higher in the lower stage of the tumour, acc. to WHO classification (pT), whereas there were no correlations in this parameter, evaluated on the epithelial cells (Table 1). The mean value of the percentage of epithelial cells with co-expression of CD44v10 was significantly higher in pN2 than in pN1 stage. There were no significant correlations in this parameter, estimated on the leucocytes infiltrating tissues (Table 2). The mean values of the percentage of epithelial cells, as well as of leucocytes infiltrating tissues with co-expression of CD44v10, were significantly lower in the higher degree of histological malignancy (G) only inTAT (Table 3).

Discussion

CD44, described for the first time by Dalchau in 1980, is a molecule, which can take part in carcinogenesis and formation of metastases in lymph nodes and in distal organs [4]. It also plays an important role in intracellular communication and interactions between the cell and the extracellular matrix. It is responsible for lymphocyte T and natural killer activation, aggregation and cell B and T migration. It also induces the Tumour Necrosis Factor and interleukin 1 release. So, it is described as one of the main factors in the formation of metastases, however, the precise mechanism of its function is still unknown [5, 6]. Examinations of standard CD44 molecule in tumour tissues and in neoplasmatically changed lymph nodes show its higher expression [7, 8, 9, 10]. Examinations of some isoforms of CD44 in cancer and lymph node tissues show the same results but the number of examined patients is small [11, 12, 13]. We have recently reported that the levels of CD44v5 and v6 in serum of patients with colorectal cancer are not correlated with the progression of the disease [14].

This study evaluated the expression of CD44v10 isoform on the surface of epithelial cells and leucocytes infiltrating

tumour tissues, tumour adjacent tissues and healthy tissues of the large bowel in patients with colorectal cancer. The statistically significant correlations, found in results, inform that this variant of CD44 can play an important role in the local progression of the cancer and that it probably stimulates the growth of the tumour. However, it is rather of no importance in the development of neoplasmal metastases to lymph nodes. Due to a small number of examined patients, the role of CD44v10 demands further investigations.

References

1. Jemal A, Tiwari RC, Murray T, Ghafoor A, Samuels A, Ward E, Feuer EJ, Thurn MJ. Cancer Statistics, 2004. CA Cancer J Clin, 2004; 54: 8-29.

2. Al-Mehdi AB, Tozawa K, Fisher AB, Shientag L, Lee A, Muschel RJ. Intravascular origin of metastasis from the proliferation of endothelium - attached tumor cells: a new model for metastasis. Nature Med, 2000; 6: 100-2.

3. Wielenga VJM, van der Voort R, Taher TEI, Smit L, Beuling E, van Krimpen C, Spaargaren M, Pals ST. Expression of c-Met and Heparan-Sulfate proteoglycan forms of CD44 in colorectal cancer. Am J Path, 2000; 157: 1563-73.

4. Dalchau R, Kirkley J, Fahre JW. Monoclonal antibody to a human leukocyte-specific membrane glycoprotein probably homologous to the leukocyte-common (L-C) antigen of the rat. Eur J Immunol, 1980; 10: 737-44.

5. Isacke C, Yarwood H. The hyaluronan receptor, CD44. Int J Biochem Cell Biol, 2002; 34: 718-21.

6. Lindblom A, Liljegren A. Tumour markers in malignancies. BMJ, serial online, Feb 2000; 320: 424-7.

7. Liu PF, Wu MC, Cheng H, Qian GX, Fu JL. Clinical significance of expression of metastasisa2associated splice variants of CD44 mRNA in early primary liver cancer. China Natl J New Gastroenterol, 1996; 2: 112-4.

8. Fujisaki T, Tanaka Y, Fujii K, Mine S, Saito K, Yamada S, Yamashita U, Irimura T, Eto S. CD44 stimulation induces integrin-mediated adhesion of colon cancer cell lines to endothelial cells by up-regulation of integrins and c-Met and activation of integrins. Cancer Res, 1999; 59: 4427-34.

9. Llaneza A, Gonzales A, Andicoechea A, Fernandez JC, Allende MT, Garcia-Muniz JL, Vizoso F. CD44s, CD44v5 and CD44v6 protein contents in colorectal cancer and surrounding mucosa. Int J Biol Marker, 2000; 15: 192-4.

10. Zalewski B, Famulski W, Sulkowska M, Sobaniec-Lotowska M, Piotrowski Z, Kisielewski W, Sulkowski S. CD44 expression in colorectal cancer. An immunohistochemical study including correlation with cathepsin D immunoreactivity and some tumour clinicopathological features. Folia Histochem Cytobiol, 2001; 39: 152-3.

11. Harada N, Mizoi T, Kinouchi M, Hoshi K, Ishii S, Sasaki I, Matsuno S. Introduction of antisense CD44s CDNA down-regulates expression of overall CD44 isoforms and inhibits tumor growth and metastasis in highly metastatic colon carcinoma cells. Int J Cancer, 2001; 91: 67-75.

12. Wong LS, Cantrill JE, Morris AG, Fraser IA. Expression of CD44 splice variants in colorectal cancer. Br J Surg, 1997; 84: 363-7.

13. Chun SJ, Bae OS, Kim JB. The significance of CD44 variants expression in colorectal cancer and its regional lymph nodes. J Korean Med Sci, 2000; 15: 696-700.

14. Zalewski B. Levels of v5 and v6 CD44 splice variants in serum of patients with colorectal cancer are not correlated with pT stage, histopathological grade of malignancy and clinical features. World J Gastroenterol, 2004; 10: 583-5.

Antisense strategy in malignant brain tumours treatment

Trojan LA[1,2], Pan Y[1], Szpechcinski A[2], Ly A[3], Kopinski P [2,3,4], Chyczewski L[5], Kasprzak H[2], Donald A[1], Trojan J[2,3,5]

[1]School of Medicine, Case Western Reserve University, Cleveland, USA; [2]Medical University and University Hospital, Bydgoszcz, Poland; [3]INSERM, Robert Debre and Bichat Hospitals, Paris, France; [4]CMUJ and University Hospital, and Polish Academy of Sciences, Cracow, Poland; [5]Medical University and University Hospital, Bialystok, Poland

Antisense approach

Malignant glioma, the most common human brain cancer, is almost uniformly fatal. Median survival is less than one year. The principal strategies of gene therapy for treatment of gliomas, including antisense approach, have been proposed comming from 1990s [1, 2, 3, 4].

The antisense oligonucleotides become the important tool of anti - cancer approach [5, 6]. The "discovery" of antisense approach was done by the groupes of R.M. Harland and of F. Jacob [7, 8]; the untranscribed DNA strand, that has been regarded only as a stabilizer and a protector of genetic material, was shown to reveal transcription activity [9]. It has also been widely proven that a lot of genes present an open reading frame on its antisense strand. Open reading frame on the antisense strand has been found in all genomes studied, both in prokaryotes and eukaryotes [10].

Different molecular pathways altered in cancer were exploited as potential the antisense strand has been found in all genomes studied, both in prokaryotes and eukaryotes [10]. On the basis of mechanism of action, two classes of antisense oligonucleotide can be discerned: (a) the RNase H-dependent oligonucleotides, which induce the degradation of mRNA; and (b) the steric-blocker oligonucleotides, which physically prevent or inhibit the progression of splicing or the translational machinery. The majority of the antisense drugs investigated in the clinic functions via an RNase H-dependent mechanism [5].

In prokaryotes and eukaryotes genetic information is supported by double-stranded DNA in which only one strand (sense strand) is usually transcribed to messenger RNA. The second strand is called the antisense strand because its sequence of nucleotides is the complement of message sense. This observation gave the origin to many antisense (as well as non-sense) approaches based on antisense RNA or antisense oligonucleotides, both targeting genes involved in pathological cellular processes. The antisense RNA is delivered to the cells either by a plasmid vector (dsDNA) encoding an antisense RNA or by a single sequence of nucleotides is the complement of message sense). The antisense RNA sequence is then produced by intracellular transcription of plasmid vector and is able to hybridize to the mRNA with subsequent translation blockade. Once hybridization occurs, the duplex RNA-RNA (DNA) stimulates ribonuclease H, the enzyme involved in DNA replication [11].

The first antisense oligonucleotide used in clinical pharmacology was as anti-cytomegalovirus therapy (VitraveneTM) [12]. The antisense strategy was then largely used in order to analyze gene expression and intron splicing. The most widely studied oligonucleotides are phosphorothioates, because their nuclease stability are highly soluble and have excellent antisense activity. These data have led to the introduction of phosphorothioate oligonucleotides into clinical therapeutic tumour trials [13, 14].

The triple helix (TH) technology is the new approach, which belongs together with antisense approach to anti-gene strategies. The TH technology was "discovered" by groups of P.B. Dervan [15] and of C. Helene [16]. So called triple-helix forming oligonucleotides, TFOs, are delivered to cells both by cell transfection with chemical carriers and via vector plasmid that can drive the synthesis of TFO RNA. TFOs link to genomic double-strand DNA, form triple-helix structure with target gene and strongly inhibit its expression at transcriptional level [15]. The role of 22-23 mer RNA in triple helix RNA-DNA mechanism is strongly similar to that of recent "siRNA technonology" involving also 23 mer RNA [16] (21-23-mer double-stranded RNA molecules, known as siRNA, can effectively silence gene expression [17]).

Oncogenes and genes encoding growth factors constitute the principal target of antisense strategy in malignant tumours treat-

ADDRESS FOR CORRESPONDENCE:
Jerzy TROJAN
Lab. Developmental Neurology
INSERM E9935
Hospital Robert Debre
48, Bd Serurier, 75019 Paris, France
email: jerzytrojan@wanadoo.fr

ment. The classical examples of use of antisense oncogens are that of c myb [18], bcr/abl [11], bcl-2 [19, 20, 21] or K-ras family [22], the last also explored in triple helix approach [23]. Growth factors and their receptors (that usually act as cell membrane tyrosine kinases) consist the complex system considered at present as especially important in oncogenesis. TGF-beta [24], EGFR [22, 25], VEGF [26, 27, 28, 29] represent relevant targets for anti-tumor gene therapies. Insulin-like growth factor (IGF-I) and its receptor IGF-I-R are considered as the most important growth factors related to the normal and neoplastic differentiation [30]. Therefor IGF-I antisense and IGF-I-R antisense gene therapies were proposed to treat different malignant tumours [3, 31].

Brain tumours and antisense approach

Neuroblastoma is the most common neuroectoderma derived solid tumour of paediatric age. C-myb gene expression has been reported in neuroblastoma. The use of antisense oligonucleotides as therapeutic antineoplastic agents has been recently investigated. It was demonstrated that the inhibition of cell proliferation was dependent on the down-modulation of c-myb protein expression [32].

Dysregulation of hMYCN protein expression appears to be critically involved in the pathogenesis of childhood neuroblastoma. Human neuroblastoma IMR-32 cells, which have an amplified hMYCN gene was transfected, with hMYCN AS [33]. The authors have examined the effects of continuous treatment for 6 weeks with AS oligonucleotides via subcutaneously implanted microosmotic pumps on tumor growth in a transgenic mouse model of hMYCN-induced neuroblastoma. Transgenic mice treated with AS oligonucleotides had lower tumor incidence and statistically significantly lower tumor mass.

Liposomes are one of the most promising delivery systems for genes, proteins, and other biological molecules and they are expected to become a new therapeutic tool for the treatment of brain tumors, especially malignant gliomas [34]. Recently, the promising results were showed using the strategy based on IGF-I antisense or triple-helix technologies and liposomes as delivery system for treatment of glioblastoma patients [35, 36]. The triple helix of IGF-I consists with single RNA strand containing a 23-nucleotide (nt) oligopurine sequence capable to form triple-helix structure with an IGF-I gene oligopurine/oligopyrimidine promoter segment. The injected triple helix IGF-I "vaccine" has developed T CD8 mediated immune response [37]. The interesting approach was also proposed by the group of R. Baserga, using antisense of IGF-I receptor 1 in clinical treatment of brain tumours (2003, personal communication); however the supposed anti-cancer immune response was not demonstrated in that approach [3].

The impact of bcl-2, a key antiapoptotic protein, on malignant gliomas by suppressing its expression was also investigated: antisense human bcl-2 cDNA was transfected into human malignant glioma cells. Transplantation of antisense bcl-2 cells resulted in no tumor formation [38]. Antisense bcl-2 expression could effectively reduce glioma survival, including retarding in vitro growth, complete loss of tumorigenicity, and significantly enhanced cisplatin cytotoxicity.

Human Nr-CAM (Neuroglia related Cell Adhesion Molecule) is over expressed in glioblastoma. Subcutaneous injection of antisense hNr-CAM overexpressing glioblastoma cells into nude mice caused complete inhibition of tumor formation [39]. Intra-tumoral inoculation of antisense hNr-CAM expressing plasmid also caused slow tumor growth in nude mice in vivo. The authors concluded that hNr-CAM is a valid target for potential gene therapy of glioblastoma tumors.

Some experimental models of glioma treatment were recently developed targeting different factors as telomerase, urokinase-type plasminogen activator receptor or matrix metalloproteinases. Telomerase is a ribonucleoprotein enzyme that is detected in the vast majority of malignant gliomas but not in normal brain tissues. Thus, antisense against human telomerase RNA component (2-5A-anti-hTER) was investigated for its antitumor effect on an intracranial malignant glioma model in nude mice [40]. The authors demonstrated that 2-5A-anti-hTER reduced the viability of malignant glioma cell lines to 20-43%. The treatment of intracranial malignant gliomas in nude mice with 2-5A-anti-hTER was therapeutically effective.

The urokinase-type plasminogen activator receptor (uPAR) and the p16 tumor suppressor gene play a significant role in glioma invasion. It was demonstrated that downregulation of uPAR and overexpression of p16 using a bicistronic caused an additive and cooperative effect in the suppression of the tumor growth of glioblastoma cell lines in an ex vivo intracerebral tumor model [41].

Increased expression of matrix metalloproteinases (MMPs) has been associated with human glioblastoma tumor progression. For this reason down-regulate MMP-9 expression was done by stably transfecting a high-grade glioblastoma cell line with a plasmid vector capable of expressing an antisense transcript complementary to a 528-bp segment at the 5' end of human MMP-9 cDNA [42]. Intracerebral injection of antisense stable transfectants in nude mice produced no tumors. These results suggest that MMP-9 expression is essential for the invasiveness of glioblastoma cells.

Conclusions

Human gene therapy is defined as a medical intervention based on the administration of genetic material in order to modify or manipulate the expression of a gene product or to alter the biological properties of living cells. Cells may be modified ex vivo for subsequent administration or altered in vivo by gene therapy products given directly to the subject. Example that falls under this definition include use of antisense oligonucleotides to block gene transcription or use of sequence-specific oligonucleotides to correct a genetic mutation [43].

The gene therapies in comparison to surgery or chemotherapy are new, sophisticated and still experimental. A number of strategies for inhibiting gene expression have been developed: the triple helix approach, decoy transcription factor binding and oligodeoxynucleotides seek to disrupt gene expression at the level of transcription. The antisense oligonucleotides and short interfering RNA molecules attempt to disrupt expression at the level of mRNA translation [44, 45]. Antisense therapy has been widely used to specifically and selectively inhibit the expression

of selected genes at the messenger RNA level. Combinations of antisense oligonucleotides with chemotherapeutic agents may offer important advantages in cancer treatment [46]. Anti - gene therapies are the subject of many clinical trials. It is necessary to underline their high specifity, relative security and very promising results. For that reason we hope, that this modern type of treatment [47, 48, 49] will soon become alternative for more traditional methods used in cancer therapy including therapeutic strategies for brain tumors [50].

References

1. Culver K W, Rarn Z, Wallbridge S, Ram Z., Walltridge S, Ishii H, Oldfield EH, Blaese RM. In vivo gene transfer with retroviral vector- producer cells for treatment of experimental brain tumors. Science, 1992; 256: 1550-2.
2. Trojan J, Johnson TR, Rudin SD, Ilan Ju, Tykocinski ML, Ilan J. Loss of tumorigenicity of rat glioblastoma directed by episome-based antisense cDNA transcription of insulin-like growth factor 1. Science, 1993; 259: 94-7.
3. Resnicoff M, Sell C, Rubini M, Coppola D, Ambrose D, Baserga R, Rubin R. Rat glioblastoma cells expressing an antisense RNA to the insulin-like growth factor I (IGF-I) receptor are non tumorigenic and induce regression of wild-type tumors. Cancer Res, 1994 ; 54: 2218-22.
4. Komata T, Kanzawa T, Kondo Y, Kondo S. Telomerase as a therapeutic target for malignant gliomas. Oncogene, 2002; 21: 656-63.
5. Dias N, Stein CA. Basic concepts and antisense oligonucleotides mechanisms. Mol Cancer Therapeutics, 2002; 1: 347-55.
6. Marchini S, D'Incalci M, Broggini M. New molecules and strategies in the field of anticancer agents. Curr Med Chem Anti-Canc Agents, 2004; 1: 247-62.
7. Weintraub H, Izant JG, Harland RM. Antisense RNA as a molecular tool for genetic analysis. Trends Gen, 1985; 1: 23-5.
8. Rubinstein JL, Nicolas JF, Jacob F. L'ARN non sens (nsARN): un outil pour inactiver specifiquement l'expression d'un gene donne in vivo. C R Acad Sci Paris, 1984; 299(8): 271-4.
9. Ring BZ, Roberts JW. Function of a nontranscribed DNA strand site in transcription elongation. Cell, 1994; 78: 317-24.
10. Merino E, Balbas P, Puente JL, Bolivar F. Antisense overlapping open reading frames in genes from bacteria to humans. Nucleic Acids Res, 1994; 22: 19-38.
11. Galderisi U, Cascino A and Giordano A. Antisense oligonucleotides as therapeutic agents. J Cell Phys, 1999; 181: 251-7.
12. Vitravene Study Group. A randomized controlled clinical trial of intravitreous fomivirsen for treatment of newly diagnosed peripheral cytomegalovirus retinitis in patients with AIDS. Am J Ophthalmol, 2002; 133: 467-74.
13. Jansen B, Wacheck V, Heere-Ress E, Schlagbauer-Wadl H, Hoeller C, Lucas T, Hoermann M, Hollenstein U, Wolff K, Pehamberger, H. Chemosensitization of malignant melanoma by BCL2 antisense therapy. Lancet, 2000; 356: 1728 -33.
14. Geiger T, Muller M, Dean N M, Fabbro D. Antitumor activity of a PKC-antisense oligonucleotide in combination with standard chemotherapeutic agents against various human tumors transplanted into nude mice. Anticancer Drug Des, 1998; 13: 35-45.
15. Derwan P. Reagents for the site-specific cleavage of megabase DNA. Nature, 1992; 359: 87-8.
16. Helene C. Control of oncogene expression by antisense nucleic acids. Eur J Cancer, 1994; 30: 1721-6.
17. Sharp P A. RNA interference-2001. Genes Dev, 2001; 15: 485 -90.
18. Abaza MS, Al-Attiyah RJ, Al-Saffar AM, Al-Sawan SM, Moussa NM. Antisens oligodeoxynucleotide directed against c-myb has anticancer activity and potentiates the antiproliferative effect of conventional anticancer drugs acting by different mechanisms in human colorectal cancer cells. Tumour Biol, 2003; 24: 241-57.
19. Nahta R, Esteva FJ. Bcl-2 antisense oligonucleotides: a potential novel strategy for the treatment of breast cancer. Semin Oncol, 2003; 30: 143-9.
20. Van de Donk NW, de Weerdt O, Veth G, Eurelings M, van Stralen E, Frankel SR, Hagenbeek A, Bloem AC, Lokhorst HM. G3139, a Bcl-2 antisense oligodeoxynucleotide, induces clinical response in VAD refractory myeloma. Leukemia, 2004; 18: 1078-84.
21. Rudin CM, Kozloff M, Hoffman PC, Edelman MJ, Karnauskas R, Tomek R, Szeto L, Vokes EE. Phase I study of G3139, a bcl-2 antisense oligonucleotide, combined with carboplatin and etoposide in patients with small-cell lung cancer. J Clin Oncol, 2004; 22: 1110-7.
22. Morioka CY, Saito S, Machado MC, Ohzawa K, Kubrusly MS, Cunha JE, Watanabe H. Antisense therapy specific to mutated K-ras gene in hamster pancreatic cancer model. Can it inhibit the growth of 5-FU and MMC-resistant metastatic and remetastatic cell lines?. In Vivo 2004; 18: 113-7.
23. Alunni-Fabbroni M, Pirulli D, Manzini G, Xodo LE. (A,G)-oligonucleotides form extraordinary stable triple helices with a critical R.Y sequence of the murine c-Ki-ras promoter and inhibit transcription in transfected NIH 3T3 cells. Biochemistry, 1996; 35: 16361-9.
24. Weiss RH, Marshall D, Howard L, Corbacho AM, Cheung AT, Sawai ET. Suppression of breast cancer growth and angiogenesis by an antisense oligodeoxynucleotide to p21(Waf1/Cip1). Cancer Lett, 21; 189: 39-48.
25. Pu P, Liu X, Liu A, Cui J, Zhang Y. Inhibitory effect of antisense epidermal growth factor receptor RNA on the proliferation of rat C6 glioma cells in vitro and in vivo. J Neurosurg, 2000; 92: 132-9.
26. Niklinska W, Burzykowski T, Chyczewski L, Nikliski J. Expression of vascular endothelial growth factor (VEGF) in non small cell lung cancer (NSCLC): association with p53 gene mutation and prognosis. J Lung Cancer, 2001; 34: 59-64.
27. Riedel F, Gotte K, Li M, Hormann K, Grandis JR. Abrogation of VEGF expression in human head and neck squamous cell carcinoma decreases angiogenic activity in vitro and in vivo. Int J Oncol, 2003; 3: 577-83.
28. Wu HP, Feng GS, Liang HM, Zheng CS, Li X. Vascular endothelial growth factor antisense oligodeoxynucleotides with lipiodol in arterial embolization of liver cancer in rats. World J Gastroenterol, 2004; 10: 813-8.
29. Gu S, Liu CJ, Qiao T, Sun XM, Chen LL, Zhang L. Inhibitory effect of antisense vascular endothelial growth factor 165 eukaryotic expression vector on proliferation of hepatocellular carcinoma cells. World J Gastroenterol, 2004; 10: 535-9.

30. Le Roith D, Zumkeller W, Baxter RC. Insulin like-Growth Factor I. Ed. Landes Bioscience/ Eurekah & Kluwer Academic/Plenum Publishers, New York 2003, pp 1-484.

31. Upegui-Gonzalez LC, Ly A, Sierzega M, Jarocki P, Trojan L, Duc HT, Pan Y, Shevelev A, Henin D, Anthony D, Nowak W, Popiela T, Trojan J. IGF-I triple helix strategy in hepatoma treatment. Hepatogastroenterology, 2001; 48: 660-6.

32. Brignole C, Pagnan G, Marimpietri D, Cosimo E, Allen TM, Ponzoni M, Pastorino F. Targeted delivery system for antisense oligonucleotides: a novel experimental strategy for neuroblastoma treatment. Cancer Lett, 2003; 197: 231-5.

33. Burkhart CA, Cheng AJ, Madafiglio J, Kavallaris M, Mili M, Marshall GM, Weiss WA, Khachigian LM, Norris MD, Haber M. Effects of MYCN antisense oligonucleotide administration on tumorigenesis in a murine model of neuroblastoma. Natl Cancer Inst, 2003; 95: 1394-403.

34. Yoshida J, Mizuno M. Clinical gene therapy for brain tumors. Liposomal delivery of anticancer molecule to glioma. J Neurooncol, 2003; 65: 261-7.

35. Wongkajornslip A, Ouyprasertkul M, Sangruchi T, Huabprasert S, Pan Y, Anthony D. The analysis of peri-tumour necrosis following the subcutaneous implantation of autologous tumor cells transfected with an episome transcribing an antisense IGF-I RNA in a glioblastoma multiforme subject. J Med Assoc Thai, 2001; 4: 740-7.

36. Trojan LA, Kopinski P, Mazurek A, Chyczewski L, Ly A, Jarocki P, Niklinski J, Shevelev A, Trzos R, Pan Y, Gitis DJ, Bierwagen M, Czapiewska JL, Wei MX, Michalkiewicz J, Henin D, Popiela T, Evrard F, Kasprzak H, Anthony D, Trojan J. IGF-I triple helix gene therapy of rat and human gliomas. Ann Acad Med Bial (Rocz Akad Med Bial) 2003; 48: 18-27.

37. Ly A, Duc HT, Kalamarides M, Trojan LA, Pan Y, Shevelev A, François J-C, Noël T, Kane A, Henin D, Anthony D, Trojan J. Human glioma cells transformed by IGF-I triple-helix technology show immune and apoptotic characteristics determining cell selection for gene therapy of glioblastoma. Molec Pathol, 2001; 54: 230-9.

38. Zhu CJ, Li YB, Wong MC. Expression of antisense bcl-2 cDNA abolishes tumorigenicity and enhances chemosensitivity of human malignant glioma cells. J Neurosci Res, 2003; 74: 60-6.

39. Sehgal A, Ricks S, Warrick J, Boynton AL, Murphy GP. Antisense human neuroglia related cell adhesion molecule hNr-CAM, reduces the tumorigenic properties of human glioblastoma cells. Anticancer Res 1999; 19: 4947-53.

40. Mukai S, Kondo Y, Koga S, Komata T, Barna BP, Kondo S. 2-5a antisense telomerase RNA therapy for intracranial malignant gliomas. Cancer Res 2000; 60: 4461-7.

41. Adachi Y, Chandrasekar N, Kin Y, Lakka SS, Mohanam S, Yanamandra N, Mohan PM, Fuller GN, Fang B, Fueyo J, Dinh DH, Olivero WC, Tamiya T, Ohmoto T, Kyritsis AP, Rao JS. Suppression of glioma invasion and growth by adenovirus-mediated delivery of a bicistronic construct containing antisense uPAR and sense p16 gene sequences. Oncogene, 2002; 21: 87-95.

42. Kondraganti S, Mohanam S, Chintala S K, Kin Y, Jasti S L, Nirmala C, Lakka S S, Adachi Y, Kyritsis A P, Ali-Osman F, Sawaya R, Fuller G N, Rao J S. Selective suppression of matrix metalloproteinase-9 in human glioblastoma cells by antisense gene transfer impairs glioblastoma cell invasion. Cancer Research, 2000; 60: 6851-5.

43. Miller AE, Simek SL. Regulatory aspects of gene therapy. In: NS Templeton, DD Lasic" Gene therapy", Ed. Marcel Dekker, New York, 2000, pp 371-82.

44. Kalota A, Shetzline SE, Gewirtz AM. Progress in the development of nucleic acid therapeutics for cancer. Cancer Biol Ther,. 2004; 3: 4-12.

45. Biroccio A, Leonetti C, Zupi G. The future of antisense therapy: combination with anticancer treatments. Oncogene, 2003; 22: 6579-88.

46. Benimetskaya L, Stein CA. Antisense therapy: recent advances and relevance to prostate cancer. Clin Prostate Cancer, 2002; 1: 20-30.

47. Talmadge JE. Gene therapy of cancer - 12th International Conference. I Drugs 2004; 7: 100-4.

48. Zangemeister-Wittke U. Antisense to apoptosis inhibitors facilitates chemotherapy and TRAIL- induced death signaling. Ann N Y Acad Sci 2003; 1002: 90-4.

49. Bennett CF, Butler M, Cook PD, Geary RS, Levin AA, Mehta R, Teng CL, Desmukh H, Tillman L, Hardee G. Antisense oligonucleotides - based therapeutics. In: NS Templeton, DD Lasic " Gene therapy", Ed. Marcel Dekker, New York, 2000, pp 305-32.

50. Newton HB. Molecular neuro-oncology and development of targeted therapeutic strategies for brain tumors. Part 1: Growth factor and Ras signaling pathways. Expert Rev AnticanceTher, 2003; 3: 595-614.

Presence of MHC-I in rat glioma cells expressing antisense IGF-I-Receptor RNA

Szpechcinski A[1], Trzos R[2], Jarocki P[2], Trojan LA[1,3], Oficjalska K[1], Junkiert A[1], Wei MX[1], Mazurek M[4], Czapiewska JL[1], Niklinski J[4], Kopiński P[1,2,5], Chyczewski L[4], Kasacka I[6], Trojan J [1,2,5]

[1]Medical University and University Hospital, Bydgoszcz, Poland; [2]CMUJ and University Hospital, and Polish Academy of Sciences, Cracow, Poland; [3]School of Medicine, Case Western Reserve University, Cleveland, USA; [4] Medical University and University Hospital, Bialystok, Poland; [5]INSERM, Robert Debre and Bichat Hospitals, Paris, France; [6]Department of Histology and Embryology; Medical Universisty of Białystok, Poland.

Abstract

The supposed immunogenic character of glioma cells transfected with antisense IGF-I-Receptor (IGF-I-R) expression vector was tested for the presence of MHC-I currently present in cells of IGF-I antisense type. C6 rat glioma cell line was comparatively transfected in vitro with IGF I antisense (pMT-Anti-IGF I) or IGF I Receptor antisense (pMT-Anti-IGF I R) expression vectors. The wild and transfected cells were examined for the presence of IGF-I and MHC-I molecules. Using RT PCR technique, the transfected "antisens" cells showed total inhibition of IGF-I. The both transfected cultures of IGF-I and of IGF-I -R type were positively stained for MHC-I. Moreover "antisense IGF-I-R" cells as compared to "IGF-I antisense" cells showed slightly higher expression of MHC-I. The transfected cells showed also the feature of apoptosis in 60% of cells. The immunogenicity of IGF-I-R antisense glioma cells is related to MHC-I presence; therefore both approaches of antisense IGF-I and of antisense IGF-I-R could be use in paralel for cellular therapy of glioblastoma.

Key words: glioma, IGF I, IGF-I Receptor, antisense, MHC-I.

Introduction

Different strategies of gene therapy for treatment of gliomas have been proposed comming from 1990s [1, 2, 3]. Our strategy treatement is based on antisense [4, 5] anti - IGF-I (insulin-like growth factor I) technology [1]. IGF-I is a 70-amino acid polypeptide involved in tissue growth and differentiation [6, 7, 8, 9].

Deregulated expression of growth factors and/or their receptors, and especially of IGF-I, is associated as well with growth as with pathology of different diseases, including tumors [9, 10, 11, 12]. IGF-I acts via specific IGF-I receptor and subsequent activation of a protein tyrosine phosphorylic signal transduction cascade, similar to that of insulin action [13, 14]. IGF-I, mediated by IGF-I receptor has been reported to stop the apoptosis pathway in a variety of cell lines [9, 15]. The action of IGF-I on cellular metabolism depends on binding proteins (IGFBP), which prolong the half life of this factor and modify its interaction with receptor [16, 17]. The block of IGF-I synthesis, induces apoptotic and immunogenic phenomenons [18].

IGF-I is expressed at high levels in some nervous system-derived tumours, e.g. glioblastoma [19, 20] and tumour cell lines like C6 and CNS-1 rat gliomas [21, 22, 23].

Rat C-6 glioma cells become down-regulated in production of IGF-I when transfected with vector expressing IGF-I antisense RNA or IGF-I triple-helix forming oligonucleotides. The transfected cells lose tumorigenicity and elicit tumor specific immunity which leads to cure of established tumors. The immune response was shown to be mediated mainly by T lymphocytes as indicated by an abundant infiltration of the CD8 T cell subset in tumor tissues [12, 24]. Here we examine the possibility that the suppression of intracellular IGF-I in rat glioma cells, using antisense IGF-I-Receptor approach, alters the cell phenotype and the production of MHC-I as it was previously observed in IGF-I antisense approach [25, 26], and that this process is also associated with increase in programmed cell death - apoptosis.

Material and methods

Cell culture. C6 rat glioma cell line [21], was used. Cells were cultured in DMEM+F12 (v/v) (GIBCO-BRL) supplemen-

ADDRESS FOR CORRESPONDENCE:
Jerzy TROJAN
Lab. Developmental Neurology
INSERM E9935
Hospital Robert Debre
48, Bd Serurier, 75019 Paris, France
email: jerzytrojan@wanadoo.fr

ted with 10 % FCS, 2mM glutamine, 100 U/ml penicillin and 100 µg/ml streptomycin, at 37° C and 5 % CO_2. Hygromycin B (Boehringer Mannheim) at a concentration of 0,5 mg/ml was added 48 hours after transfection to select for transfected cell line. Then, the concentration of hygromycin B was changed to 2 mg/ml after one weak and maintained with each change of fresh medium during the next 3-4 month.

Plasmids

The episome based plasmids pMT-Anti IGF-I and pMT-Anti IGF-I-Receptor were constructed as previously described [1,3,27]. The vector pMT-EP, under the control of the metallothionein, MT-I, inducible promotor was used as its base. The casette contains the Epstein-Barr Virus origin of replication and the gene encoding nuclear antigen I which together drive extrachromosomal replication. Down stream of the insertion site is a poly A termination signal followed by the hygromycin B and ampilicin resistance genes. The vector pMT-EP with the lac-Z reporter gene, as insert was used in control experiments [28].

Transfection

Cultures of cells, 60-80 % confluent, were transfected in 6-well plates utilizing a ratio of 1 µg plasmid DNA per 400 000 cells. The FuGENE 6 Transfection Reagent (Boehringer Mannheim) was used according to the supplier's instructions. To determine the efficiency of transfection, the process was carried out using the pMT-EP construct containing lac-Z as a reporter gene. Cell cultures were washed in PBS and incubated at 37° C in the presence of the staining solution which contained 5mM $K_3Fe(CN)_6$, 2mM $MgCl_2$, 0,8 mg/ml X-gal made in PBS.

The cell lines, transfected and non transfected were comparativly analyzed for expression of IGF-I, IGFI-R and MHC-I in the presence and absence of ZnSO4 (stimulation of IGF-I metallothionin promoter).

RT PCR (Reverse transcriptase - polymerase chain reaction)

RNA from cells was isolated using High Pure RNA Isolation Kit (Roche Diagnostics GmbH nr 1828665), and the obtained mRNA was verified in 1,5% agarose gel stained with ethidium bromide. The applied components of RT PCR were used according Reverse Transcription System Promega Corporation (nr A3500). Samples composed as mentioned in Table 1. were amplified for 30 cycles.

Each cycle consisted of the following steps: denaturation at 94°C for 30 sec, then at 65°C for 30 sec.; annealing for 60 sec, primer extension at 72°C for 5 min in a DNA thermal cycler (GeneAmp PCR System 2700, Applied Biosystem).

The following primers were used for RT PCR study of:
IGF-I:
Primer "a"
Forward: TAG TCC CTG CCT CTT AAG AG
Reverse: AGG GGC GTT AAA ACT TGG GT
(sequence according "rgd" Rat Genome Database; primers synthetized in Institute of Biochemistry and Biophysics, Polish Academy of Sciences, Warsaw).

Table 1.

Components	Sample (µl)
cDNA	2
dNTPs, 10mM	1,8
$MgCl_2$, 25mM	7,5
RT 10x Bufor	9,8
rev IGF-I primer, 20µM	2
dir IGF-I primer, 20µM	2
DNA Pfu Polimerase (2,5)	0,5
Nuclease free water (100µl)	74.4

IGF-I:
Primer "b"
Forward: TCT GCT GAA GCC TAC AAA GT
Reverse: TTC CTC AAG CAG CAA AGG AT

IGF-I-Receptor:
Primer"c"
Forward: GAC AGT GAA TGA GGC TGC AA
Reverse: TCT CCA CCT CTG GCC TTA GA

MHC-I:
Primer "d"
Forward: ACA CTC GCT GCG GTA TTT CT
Reverse: CCT TGG CTT TCT GTG TCT CC

(primers synthetized in Institute of Pharmacology, Polish Academy of Sciences, Cracow)

Amplification products were analyzed in 1,5 % agarose gel; each well was loaded by 0,5 ug DNA stained by ethidium bromide. Standard markers were used (PCR markers, Promega Corporation, nr G316A).

Results

Morphological characterisation of tumoral cells.

C6 glioma cells demonstrated morphological characteristics similar to those previously described [1] (Fig. 1). The percent of IGF-I positive cells ranged from 70-90%. Each cell line was was subcloned to obtain IGF-I positive clones. IGF-I antisense transfected cells (pMT-Anti IGF-I) as well as IGF-I-R antisense transfected cells (pMT-Anti IGF-I-R) did not stain immunocytochemically for IGF-I [1, 27]. The frequency of transfection for the pMT-EP- LacZ vector, as determined by staining with X-gal at 24 hours after transfection, was in between 3-10 % for glioma lines (Fig. 2). In cultures of both IGF-I antisense and IGF-I-R transfected cells, approximately 40-50 % of the cells became rounded and detached. These cells were all apoptotic. In contrast, evidence of apoptosis was observed in less than 5-10 % of non-transfected cells. The apoptotic changes occurred within 5-6 hours after incubation of transfected cells in the presence of 60 microM of $ZnS0_4$. These results were confirmed in six separate experiments ($P < 0, 01$).

Figure 1. In vitro culture of C6 glioma cells. The cloned cells showing oftenly elongated shape, present a pseudo-fibroblastic character. The apoptosis phenomenon, oval cells with vacuolization is rare (less than 5%). X400

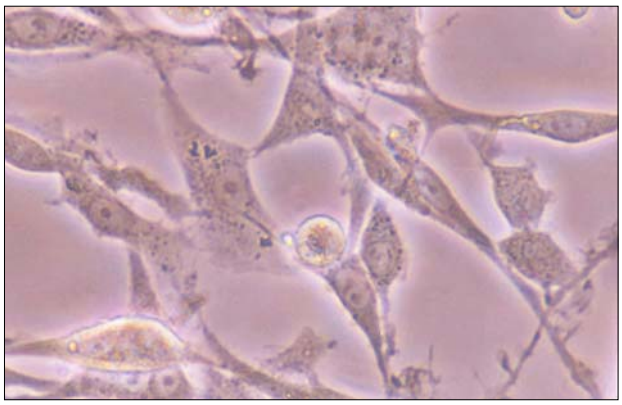

Figure 2. In vitro C6 glioma cells transfected with "antisense" pMT-Anti IGF-I-R vector and with pMT-EP construct containing lac-Z as a reporter gene. The transfected cells are morphologocally different from non transfected cells; they are all elongated. Note blue-green cells (X-gal staining) of cells transfected with beta-galactosidase expressing vector (lac-Z). X400

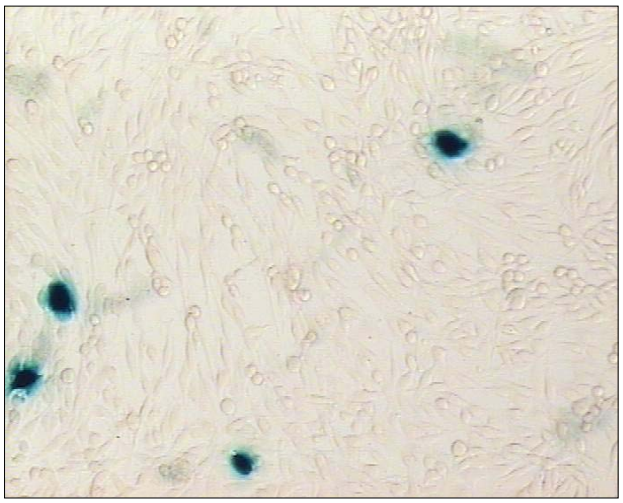

Molecular characterization of tumoral cells.

Analysis of C6 rat glioma, parental, non transfected cells is shown in the RT PCR gels (Figs. 3, 4a and b). Using primer for IGF-I and IGF-I-R, the presense of these two genes was demonstrated in non transfected cells. The DNA of non-transfected cells is distributed in 300-400 bp (Fig. 3) and 200 bp bands (Figs. 4a and b) corresponding to the different primers.

As far as transfected cells are considered, the presence of MHC-I was confirmed in "antisense IGF-I cells" [12] using RT PCR technique. These cells showing absence of IGF-I, demonstrated the expression of MHC-I after stimulation with Zn SO4 (Figs. 5a and b). The same striking phenomenon was observed in "antisense IGF-I-Receptor" cells, also stimulated with ZnSO4 (Figs. 6a and b), indicating the presense of MHC-I. Non stimulated cells show very weak bands of 200 bp or their absence using MHC-I primers.

Figure 3. The example of RNA isolation and of amplified DNA in C6 non transfected, parental cells. M - marker (PCR Markers, Promega Corporation, nr G316A. 1, 2, - isolated samples of RNA. 3, 4, 5, 6, 7 - amplified samples of DNA: note 300-400 bp bands confirm the expression of IGF-I using IGF-I primer "a" (see Material and methods).

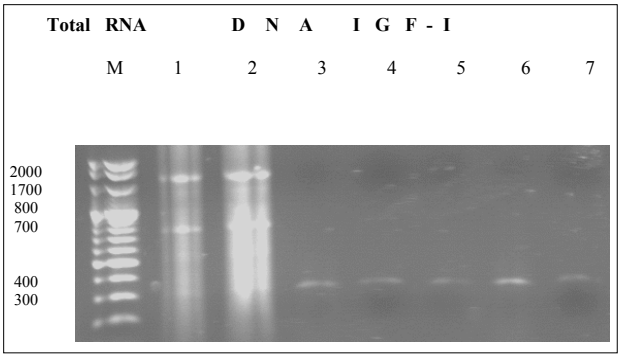

Figure 4a. C6 parental cells. The expression of IGF-I demonstrated by RT PCR. M- marker; 1,2,3 - 200 bp bands of amplified DNA using IGF-I primer "b" (see Material and methods).

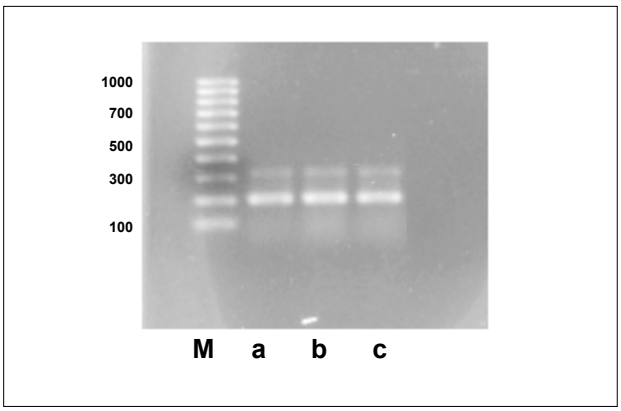

Figure 4b. C6 parental cells. The expression of IGF-I-Receptor demonstrated by RT PCR. M- marker; 1,2,3 - 200 bp bands of amplified DNA using IGF-I-R primer "c"; 300 bp is non specific (see Material and methods).

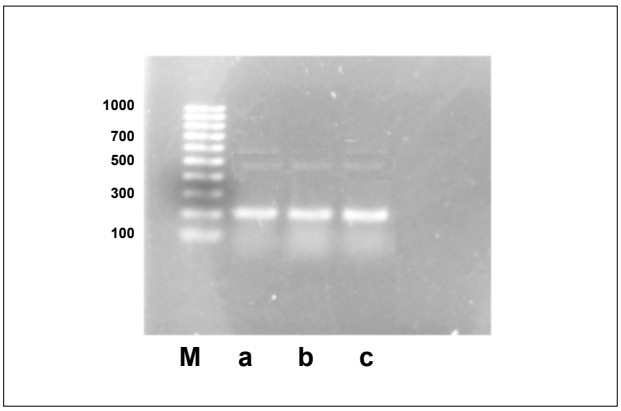

Discussion

Other studies have already shown, that the antisense strategy directed to the receptor of IGF induces a programmed cell death of tumor cells [9, 18, 22, 29]. As antitumor IGF-I strate-

Figure 5a. C6 glioma cells transfected with pMT-Anti IGF-I. Absence of expression of IGF-I demonstrated by RT PCR. M- marker; a, b, c, d, e, f - amplified DNA using IGF-I primer "b" (see Material and methods). The lines a, b, c correspond to non stimulated cells, and the lines d, e, f correspond to cells stimulated with Zn SO4.

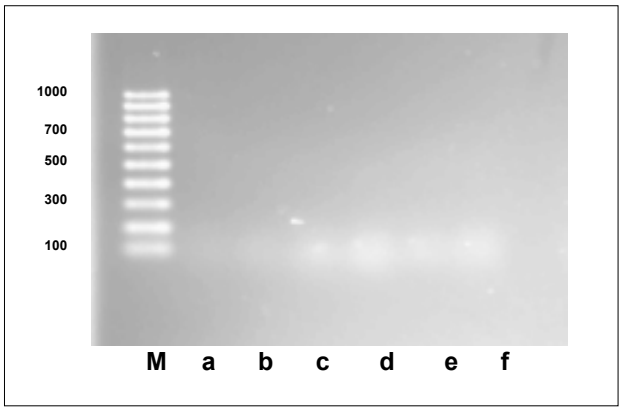

Figure 5b. C6 glioma cells transfected with pMT-Anti IGF-I. M- marker; a, b, c, d, e, f - amplified DNA using MHC-I primer "d" (see Material and methods). The lines a, b, c correspond to non stimulated cells, and the lines d, e, f correspond to cells stimulated with Zn SO4. Note the expression of MHC-I demonstrated by RT PCR in cells corresponding to lines d, e, and f.

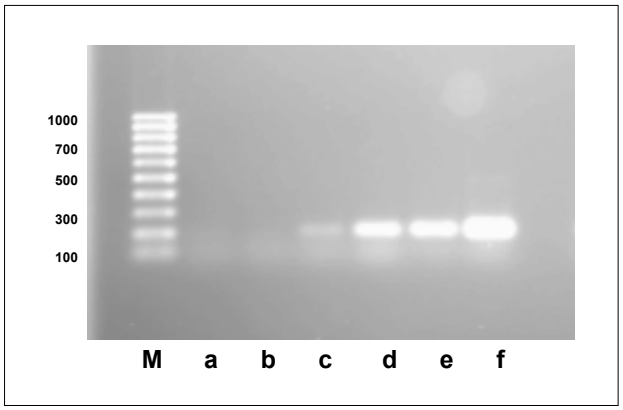

Figure 6a. C6 glioma cells transfected with pMT-Anti IGF-I-Receptor. Absence of expression of IGF-I demonstrated by RT PCR. M- marker; a, b, c, d, e, f - amplified DNA using IGF-I primer "b" (see Material and methods). The lines a, b, c correspond to non stimulated cells, and the lines d, e, f correspond to cells stimulated with Zn SO4.

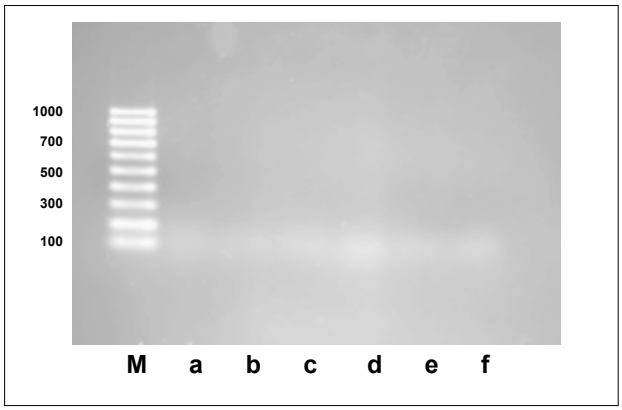

Figure 6b. C6 glioma cells transfected with pMT-Anti IGF-I-Receptor. M- marker; a, b, c, d, e, f - amplified DNA using MHC-I primer "d" (see Material and methods). The lines a, b, c correspond to non stimulated cells, and the lines d, e, f correspond to cells stimulated with Zn SO4. Note the expression of MHC-I demonstrated by RT PCR especially in cells corresponding to lines d, e, and f and weakly in non stimulated cells (c).

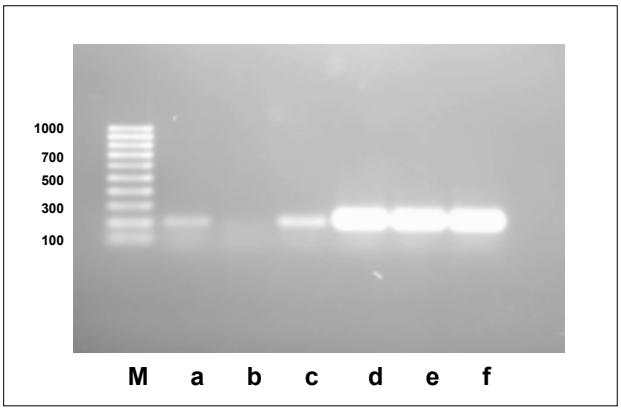

gy for the neuroectodermal neoplasia - glioblastoma multiforme - have evolved, we have showed that a relationship may exist between the anti-tumor immune response and apoptosis. We demonstrated that IGF-I antisense transfection induce MHC-I molecules, and that using vectors encoding MHC-I antisense cDNA: 1) MHC-I expression, related to IGF-I antisense and triple helix transfection, can be reversible; 2) suppression of MHC-I expression in immunogenic IGF-I antisense transfected cells is following by the strike decrease of apoptotic cells [30]. These data define the immune and apoptotic characteristics of tumoral cells selected for cellular therapy of glioma, and permited introduce the IGF-I antisense and triple-helix technology as a new gene therapy approach for treatement of human glioblastoma [23].

In here presented work down regulation of cellular IGF-I mRNA is accompanied by a decrease of cellular IGF-I. Transcription of the IGF-I gene is down regulated for 4 - 6 passages in rat glioma cells transfected with pMT-Anti IGF I-R vector. In control experiments using the same vector carrying the lacZ gene in place of IGF-I antisense DNA sequence, we have showed 24 hours after transfection a 3-10% transgene frequency (100 % after three weeks) and strong cytoplasmic staining for X-gal in rat C-6 cells. The induction of IGF-I antisense RNA in transfected cells was followed by change in cell morphology, increase in apoptosis and enhanced expression of MHC-I. Transfected cells were long and narrow in shape and frequently string-like in appearance. This change was associated with down regulation in IGF-I protein. The change might be the signal either a reversion of the malignant phenotype or the recovery of some antigenic potential of these cells. As to the MHC-I expression, down-regulation of MHC-I due to action of IGF-I has been reported for experiments with rat thyroid cells [31]. This would be in agreement with results reported here concerning the inverse correlation between IGF-I and MHC-I protein expression in glioma cells. In tumor cells, the absence of IGF-I, when induced by IGF-I antisense technology, is associated with

massive apoptosis as previously demonstrated in transfected hepatoma cells [32]. In here presented work, the occurrance of morphological features vacuolization of cytoplasm suggests that the intracellular growth factor may be a control point for modulating to apoptotic process of glioma cells. IGF-I has been reported to block the apoptosis pathway in a variety of cell lines [33]. In contrast rats given injections of C6 glioma cells expressing antisense IGF-I-R did not develop tumors and were protected from a subsequent challenge with wild-type C6 glioma cells for at least months [3]. However, total eradication of pre-existing wild type tumors was not described [3]. On the other side, a qualitative relationship between the level of IGF-I receptor and tumorigenesis in nude mice, which correlates to the extent of apoptosis has been shown [34]. When the function of IGF-I receptor is decreased, glioma cells undergo massive apoptosis. It was concluded for the IGF-I-R result, that this receptor activated by its ligand plays a protective role against programmed cell death. This protection was even more striking in vivo than in vitro [34]. Another possible interpretation could be that an immune response occurring in the animals inhibits tumorigenesis. This is probably because nude mice do have a residual immune system containing both natural killer cells and B lymphocytes [35]. Progress in defining the pathophysiological role of signalling and downstream of IGF-I-R in neoplasia might lead to the development of novel targeting strategies [36]. Recent research has shown that targeting IGF-I-R leads to impressive antineoplastic activity in many in vitro and in vivo models of common human cancers. Strategies that have been used include [36]: administration of molecules to interfere with ligand binding to IGF-I-R, such as IGFBPs, peptide or small-molecule competitive binding antagonists, or blocking anti-receptor antibodies [3, 37, 38], antisense or small interferring RNA strategies to reduce receptor expression [40]; introduction of a dominantnegative IGF-I-R to interfere with receptor action use of small-molecule IGF-I-R-specific tyrosine kinase inhibitors [41]; and targeting signalling pathways downstream of IGF-I-R with agents such as AKT or TOR inhibitors [42, 43]. The hypothesis that targeting the IGF-I-R will increase the efficacy of other antineoplastic treatments is based on evidence that survival signals originating at this receptor limit the efficacy of other treatments designed to induce apoptosis [36].

The results presented in this study show that inhibition of IGF-I-R up-regulates MHC-I expression in transfected " antisense " glioma cells. We need to add that increased expression of protease nexin I which may reduce the tumorigenic potential of the C-6 glioma cells was also observed when the IGF-I "triple-helix" cells or IGF-I receptor "triple-helix" cells were injected into nude mice [24, 27]. On the other hand, in our work concerning mouse hepatoma cells transfected by IGF-I triple-helix approach [28], we have observed the decrease of cytokines like Il-10, which is a strong immunosuppressor, and TNF-alpha, which can act as a factor stimulating a tumoral growth. Moreover we have found the increased level of TAP 1 and 2 in these cells. A further elucidation of the relationship between the immune process, related to MHC-I or HLA system [44], and the apoptotic process is under investigation. Our antisense IGF-I aproach together with that of antisense IGF-I-R and other actually studied antisense strategies of gene therapies targeting bcl-2 [45], telomerase [46], urokinase-type plasminogen activator receptor (uPAR) [47], neuroglia related Cell Adhesion Molecule [48] or matrix metalloproteinases [49] constitute the begining of successfull clinical trial to win "glioblastoma battle".

Acknowledgments

We are especially grateful to Profs. R. Baserga (Thomas Jefferson University, Philadelphia) and R. Przewlocki (Polish Academy of Science, Cracow), for useful discussion of experimental results. We are very thankful to Prof. J. Ilan (Case Western Reserve University, Cleveland) for generously facilitating the molecular biology technology. We are also indebted to A. Stefanska and K. Bartczak for technical assistance. This work was supported by grants of State Committee for Scientific Research, Poland, No 6 P05C 016 20 and 3 P05B 089 23, and NATO grant, Poland, No LST CLG 980517.

References

1. Trojan J, Blossey BK, Johnson T, Rudin S, Tykocinski M, Ilan Ju, Ilan J. Loss of tumorogenicity of rat glioblastoma directed by episome-based antisense cDNA transcription of insulin-like growth factor I. Proc Natl Acad Sci USA, 1992; 89: 4874-8.

2. Culver K W, Rarn Z, Wallbridge S, Ram Z., Walltridge S, Ishii H, Oldfield EH, Blaese RM. In vivo gene transfer with retroviral vector-producer cells for treatment of experimental brain tumors. Science, 1992; 256: 1550-2.

3. Resnicoff M, Sell C, Rubini M, Coppola D, Ambrose D, Baserga R. Rat glioblastoma cells expressing an anti-sense RNA to the insulin-like growth factor I (IGF-I) receptor are non tumorigenic and induce regression of wild-type tumors. Cancer Res, 1994; 54: 2218-22.

4. Izant JG, Weintraub H. Constitutive and conditional suppression of exogenous and endogenous genes by antisense RNA. Science, 1985 ; 229: 345-52.

5. Green P J, Pines O, Inouye M. The role of antisense RNA in gene regulation. Ann Rev Biochem, 1986; 55: 569-97.

6. Daughaday WH, Hall K, Raben MS, Salmon WD, Van den Brande JL, Wyk JI. Somatomedin: proposed designation for sulphation factor. Nature, 1972; 235: 107.

7. Froesch CS, Schwander J, Zapf J. Actions of insulin-like growth factors. Ann Rev Physiol 1985; 47: 443-67.

8. Han VKM, Hill DJ. In The Insulin-like growth factors : Structure and biological functions, Shofield PN (ed)., Oxford University Press, 1992; 178-219.

9. Baserga R. Oncogenes and strategy of growth factors. Cell 1994; 79: 927-30.

10. Rubin R, Baserga R. Biology of disease. Insulin-like growth factor I receptor. Its role in cell proliferation, apoptosis and tumorigenicity. Lab Invest, 1995; 73: 311-31.

11. Heldin CH, Westermark B. Growth factors as transforming proteins. Eur J Biochem, 1989: 184: 487-96.

12. Trojan J, Johnson TR, Rudin SD, Ilan Ju, Tykocinski ML, Ilan J. Treatment and prevention of rat glioblastoma by immunogenic C6 cells expressing antisense insulin?like growth factor I RNA. Science, 1993; 259: 94-7.

13. Werner H, Le Roith D. New concepts in regulation and function of of the insulin-like growth factors: implications

for understanding normal growth and neoplasia. Cell Mol Life Sci, 2000; 57: 932-42.

14. Adams TE, Epa VC, Garrett TP, Ward CV. Structure and function of the type I insulin-like growth factor receptor. Cell Mol Life Sci, 2000; 57: 1050-93.

15. Rodriguez-Tarduchy G, Collins MKL, Garcia I, Lopez-Rivas A. Insulin-like growth factor-I inhibits apoptosis in IL-3-dependent hemopoietic cells. Eur J Immunol, 1992; 149: 535-40.

16. Hva V, Oh Y, Rosenfeld RG. The insulin-like growth factor-binding protein superfamily. Endocr Rev, 1999; 20 : 761-87.

17. Zumkeller W, Westphal M. The IGF/IGFBP system in CNS malignancy. J Clin Pathol (Molec Pathol), 2001; 54: 227-9.

18. Upegui-Gonzalez LC, Duc HT, Buisson Y, Arborio M, Lafarge-Frayssinet C, Jasmin C, Guo Y, Trojan J. Use of the IGF-I antisense strategy in the treatment of the hepatocarcinoma. Adv Exp Med Biol, 1998; 451: 35-42.

19. Sandberg AC, Engberg C, Lake M, von Holst H, Sara VR. The expression of insulin-like growth factor I and insulin-like growth factor II genes in the human fetal and adult brain and in glioma. Neurosci Lett, 1988; 93: 114-9.

20. Antoniades HN, Galanopoulis T, Nevile-Golden J, Maxwell M. Expression of insulin like growth factor I and II and their receptor mRNAs in primary human astrocytomas and meningiomas : In vivo studies using in situ hybridization and immunocytochemistry. Int J Cancer, 1992; 50: 215-22.

21. Kiess W, Lee L, Graham DE, Greenstein L, Tseng L Y, Rechler M M, Nissley S P. Rat C6 glial cells synthesize insulin-like growth factor I (IGF-I) and express IGF-I receptors and IGF-ll / mannose 6-phosphate receptors. Endocrinology, 1989; 124: 1727-36.

22. Baserga R, Sell C, Porcu P, Rubini M. The role of IGF-I receptor in the growth and transformation of mammalian cells. Cell Prolif, 1994; 27: 63-78.

23. Trojan LA, Kopinski P, Mazurek A, Ly A, Jarocki P, Shevelev A, Trzos R, Pan Y, Gitis DJ, Niklinski J, Bierwagen M, Czapiewska LJ, Wei M, Chyczewski L, Michalkiewicz J, Henin D, Popiela T, Evrard P, Kasprzak H, Anthony D, Trojan J. IGF I triple helix gene therapy of rat and human gliomas. Roc Acad Med Bial (Ann Proc Med Sci), 2003; 48: 18-27.

24. Shevelev A, Burfeind P, Schulze E, Rininsland F, Johnson T, Trojan J, Chernicky C, Hélene C, Ilan J, Ilan J. Potential triple helix mediated inhibition of IGF-I gene expression significantly reduces tumorigenicity of glioblastoma in an animal model. Cancer Gene Therapy 1997; 4: 105-12.

25. Trojan J, Duc H, Upegui-Gonzalez L, Hor F, Guo Y, Anthony D, Ilan J. Presence of MHC-I and B-7 molecules in rat and human glioma cells expressing antisense lGF-1 mRNA. Neurosci Lett, 1996; 212: 9-12.

26. Anthony D, Pan Y, Wu S, Shen F, Guo Y. Ex vivo and in vivo IGF-I antisense RNA strategies for treatment of cancer in humans. Adv Exp Med Biol 1998; 451: 27-34.

27. Rininsland F, Johnson T, Chernicky C, Schulze E, Burfeind P, Ilan J. Suppression of insulin like growth factor type-I receptor by a triple-helix strategy inhibits IGF-I transcription and tumorigenic potential of rat C6 glioblastoma cells. Proc Natl Acad Sci USA 1997; 94: 5854-9.

28. Upegui-Gonzalez LC, Ly A, Sierzega M, Jarocki P, Trojan L A, Duc HT, Pan Y, Shevelev A, Henin D, Anthony D, Nowak W, Popiela T, Trojan J. IGF-I triple helix strategy in hepatoma treatement. Hepato/Gastroentero 2001; 48 : 660-6.

29. Baserga R. The insulin-like growth factor I receptor: a key to tumor growth? Cancer Res, 1995; 55: 249-52.

30. Ly A, Duc HT, Kalamarides M, Trojan LA, Pan Y, Shevelev A, François JC, Noël T, Kane A, Henin D, Anthony D, Trojan J. Human glioma cells transformed by IGF-I triple-helix technology show immune and apoptotic characteristics determining cell selection for gene therapy of glioblastoma. J Clin Pathol (Molec Pathol), 2001; 54: 230-9.

31. Saji M, Moriarty J, BanT, Singer D, Kohn L. Major Histocompatibility Complex class I gene expression in rat thyroid cells is regulated by hormones, methimazole and iodide as well as interferon. J Clin Endocrinol Metab, 1992; 75: 871-8.

32. Ellouk-Achard S, Djenabi S, De Oliveira GA, Dessay G, Duc HT, Zoar M, Trojan J, Claude JR Sarasin A, Lafarge-Frayssinet. Induction of apoptosis in rat hepatoma cells by expression of IGF-I antisense cDNA. J Hepatology, 1998; 29: 807-18.

33. Rodriguez-Tarduchy G, Collins MKL, Garcia I,. Lopez-Rivas A. Insulin-like growth factor-I inhibits apoptosis in IL-3-dependent hemopoietic cells. Eur J Immunol, 1992; 149: 535-40.

34. Resnicoff, M., Abraham, D., Yutanawiboonchai, W., Rotman, H.L., Kajustora, J. Rubin R. The insulin-like growth factor I receptor protects tumor cells from apoptosis in vitro. Cancer Res, 1995; 55: 2463-9.

35. Taghian A, Bucach W, Zietman A, Freeman J, Gioioso D, Smit HD. Quantitative comparison between the transplantability of human and murine tumors into the brain of NCr/Scd- nu/nu Nude and severe combined immunodeficient mice. Cancer Res, l993; 53: 5018-21.

36. Pollak MN, Shernhammer E,S, Hankinson SE. Insulin like growth factors and neoplasia. Nature Rev Cancer, 2004; 4: 505-18.

37. Maloney EK. Anti-insulin like growth factor-I receptor antibody that is a potent inhibitor of cancer cell proliferation. Cancer Res, 2003; 63; 5073-83.

38. Burtn D. A fully human monoclonal antibody to the insulin-like growth fades-I receptor blocks ligarid-dependent signaling and inhibits human tumor growth in vivo. Cancer Res, 2003; 63: 8912-21.

39. Jackson-Booth PG, Teny C, Lackey B, Lopaczynska M, Nissley P. Inhibition of the biological response to IGF-I in MCF 7 breast cancer cells by a new monoclonal antibody to the IGF-I-R. The importance of receptor down regulation. Hom Metab Res, 2003; 35: 850-6.

40. Bohula EA. The efficacy of small interfering RNA's targeted to the type I insulin-like growth factor receptor (IGF 11:3) is infIuenced by secondary structure in the IGF1 R transcript. J Biol Cheer, 2003; 278: 15991-7.

41. Garcia-Echeverria C. In vivo aiti-turrior activay of NVP-AEW541- A novel, potent and selective inhibitor of the IGF-IR kinase. Cancer Cell, 2004;5: 231-9.

42. Houghton P, Huang S. mTOR as target for cancer therapy. Curr Top Microbiol Immunol, 2004; 279: 339-59.

43. Bjornsti MA, Houghton PJ. The TOR pathway: a target for cancer therapy. Nature Rev Cancer, 2004; 4: 335-48.

44. Matthew L, Saiter B, Bhardwag N. Dendritic cells acquire antigen from apoptotic cells and induce class I restricted CTL. Nature, 1998; 392: 86-9.

45. Zhu CJ, Li YB, Wong MC. Expression of antisense bcl-2 cDNA abolishes tumorigenicity and enhances chemosensitivity of human malignant glioma cells. J Neurosci Res, 2003; 74: 60-6.

46. Mukai S, Kondo Y, Koga S, Komata T, Barna BP, Kondo S. 2-5a antisense telomerase RNA therapy for intracranial malignant gliomas. Cancer Res, 2000; 60: 4461-7.

47. Adachi Y, Chandrasekar N, Kin Y, Lakka SS, Mohanam S, Yanamandra N, Mohan PM, Fuller GN, Fang B, Fueyo J, Dinh DH, Olivero WC, Tamiya T, Ohmoto T, Kyritsis AP, Rao JS. Suppression of glioma invasion and growth by adenovirus-mediated delivery of a bicistronic construct containing antisense uPAR and sense p16 gene sequences. Oncogene, 2002; 21: 87-95.

48. Sehgal A, Ricks S, Warrick J, Boynton AL, Murphy GP. Antisense human neuroglia related cell adhesion molecule hNr-CAM, reduces the tumorigenic properties of human glioblastoma cells. Anticancer Res, 1999; 19: 4947-53.

49. Kondraganti S, Mohanam S, Chintala S K, Kin Y, Jasti SL, Nirmala C, Lakka SS, Adachi Y, Kyritsis AP, Ali-Osman F, Sawaya R, Fuller GN, Rao JS. Selective suppression of matrix metalloproteinase-9 in human glioblastoma cells by antisense gene transfer impairs glioblastoma cell invasion. Cancer Res, 2000; 60: 6851-5.

Presences of human papillomavirus DNA (HPV) and immunohistochemical p53 overexpression in papillomas of oral cavity

Barzał-Nowosielska M[1], Miąsko A[1,2], Chyczewski L[1]

[1]Department of Clinical Molecular Biology, [2]Department of Histology and Embryology;
Medical University of Bialystok, Poland

Abstract

HPV belongs to a family of tumorigenic viruses and induces cutaneous and mucosal proliferation of epithelial cells (papillomas, condylomas, warts). The abnormality accumulation of p53 protein appears to be a common step in the development of many human cancers and has been frequently reports in human cancers including head and neck. The aim of this study was to examine HPV infection incidens and p53 alteration in oral papillomas. HPV was detected by PCR, p53 accumulation by immunohistochemical detection. The overexpression of p53 was revealed in 20 cases (55%) out of 36 papillomas. We found p53 overexpression in 8 out of 13 HPV positive papillomas (61.5%) and in 12 out of 23 HPV negative papillomas (52%). Our findings indicate that HPV infection and/or changes in p53 protein coexist in oral cavity papillomas.

Key words: HPV, overexpression p53, papillomas of oral cavity.

Introduction

Many pathological lesions associated with HPV infection affect the oral cavity. Some of them, including pointed condyloma, common warts and papillomas, correspond to the changes found in the genital tract. Heck's disease is a HPV-related oral cavity lesion. Benign oral mucosa lesions are associated with HPV types 2, 4, 6, 11, 13 and 32, while malignant lesions with types 16 and 18 [1]. Papillomas belong to benign lesions, which in some circumstances may turn malignant [2]. Perhaps, it is the coexistence of HPV infection and p53 gene mutation that promotes this transformation.

Papillomaviruses belong to the group of oncoviruses that differ in oncogenic potential and are therefore classified as "low risk" and "high risk" types of neoplastic transformation. The role of HPV in neoplastic transformation of the cell is associated with the expression of E6 and E7 viral oncoproteins which have the ability to form complexes with the products of the p53 and pRB cell-supressor genes. The p53 protein is a major factor involved in cell-cycle regulation. The loss of p53 ability to regulate cell proliferation may lead to neoplastic transformation. This condition can be caused by protein inactivation by mutation of the p53 gene affecting the protein structure. An alternative mechanism for p53 inactivation is the E6 protein potential to form complexes with p53 protein and its earlier degradation in the presence of ubiquitine. The cell cycle becomes deprived of a very important regulator. The condition observed in the cell after viral infection promotes carcinogenic agents and may lead to cell transformation into the neoplastic ones.

Material and methods

Thirty-six oral papillomas were used as the research material. DNA was isolated and HPV was detected in earlier studies [3]. Immunohistochemical investigations were performed using monoclonal antibodies against human p53 protein (DAKOCytomation/p53 No M7001) and the biotin-streptavidin-peroxidase complex. DAB (DAKOCytomation No S3000) was used as chromogen to visualize the antigen-antibody complex. Lung cancer with p53-positive immunohistochemical expression and p53 gene mutation detected earlier was used as positive control. The primary antibody was not applied in negative control.

Results and Discussion The overexpression of p53 was revealed in 20 cases (55%) out of 36 papillomas, figure 1a,1b.

ADDRESS FOR CORRESPONDENCE:
Marta Barzał-Nowosielska
Department of Clinical Molecular Biology
Medical University of Bialystok
Waszyngtona 13, 15-269 Bialystok, Poland
e-mail: martabn@poczta.fm

Figure 1. Detection of p53 protein expression in papillomas of the oral cavity.

1a. - case of p53 positive

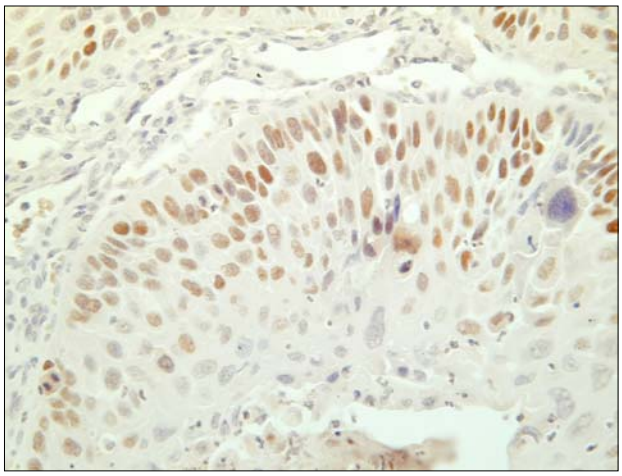

1b. - case of p53 negative

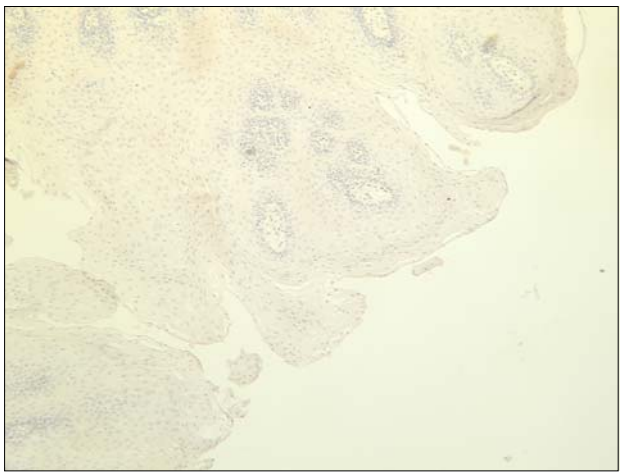

We found p53 overexpression in 8 out of 13 HPV-positive papillomas (61.5%) and in 12 out of 23 HPV-negative papillomas (52%). HPV expression was detected in 13 papillomas (36%), including 11 cases of high risk HPV and 2 cases of low risk HPV.

Human papillomavirus in the oral cavity lesions occurs with varied frequency. Zeuss et al. examined 30 papillomas of the oral cavity, finding HPV in 13.3% of cases [4]. Syrjanen et al. when examining benign neoplastic growth in oral mucosa found HPV in 33.8% of papillomas [5]. Previously we detected HPV expression in 14 out of 38 oral papilloma cases (36.8%) [3]. Recent years have brough an interest in the relationship between HPV infection and p53 expression and p53 gene mutations. This relationship has been analysed for oral cavity carcinomas. Worthy of mention are the studies conducted by Barten et al. [6], who examined 37 cases of oral and pharyngeal squamous epithelial cell carcinoma for HPV expression and assessed p53 protein expression using the immunohistochemical method. The p53 gene mutations were determined by TGGE method. The investigators revealed coexistence of HPV infection with protein p53 overexpression in 15 out of 26 HPV-positive cases (57.7%). Also investigations performed by Mao et al. [7] demonstrated that p53 protein overexpression can be accompanied by HPV infection. Patients with both p53 gene mutation and HPV expression exhibited high degree of the disease advancement. Shindoh et al. [8] examined 77 oral squamous cell carcinomas, revealing HPV expression in 31% of cases. Using the immunohistochemical method, they detected p53 expression in 26 carcinomas. Protein overexpression was detected in 6 cases, of which 4 were HPV-negative and 2 HPV-positive. Moreover, these authors analysed PCNA expression and showed a close correlation between PCNA expression and HPV infection. Shindoh et al. [8] assume that high risk HPV, by maintaining the proliferative state of epithelial cells, may contribute to the formation of malignant phenotypes. Chiba et al. [9] analysed 38 cases of oral squamous cell carcinomas, revealing high risk HPV expression in 8 cases (21%). The analysis of SSCP showed the presence of p53 gene mutations in 9 cases (24%). Two cases were both HPV- and p53 mutation-positive. Contrary to Mao et al. [7], Chiba et al. [9] believe that patients with mutation of p53 gene or with HPV infection have better prognosis. Aggelopoulou et al. [10] evaluated p53 protein expression in HPV-positive lesions of the oral cavity, reporting its detection in 50% (5/10) of hyperplastic lesions and in 59% (22/39) of carcinomas. Sisk et al. [11] detected HPV expression in 15 out of 32 squamous cell carcinomas (13%), and p53 gene mutations in 2/15 HPV-positive and in 6/17 HPV-negative cases. The analysis of patients' survival rate made them assume that HPV-positive lesions and those with normally functioning p53 protein have better prognosis [11]. Sulkowska et al. [12] evaluated the expression of p53 protein and PCNA in oral cavity papillomas, finding p53 overexpression in 70.9% of papillomas, PCNA expression in 80% of cases. The authors suggest that p53 protein overexpression together with PCNA expression can be used as the index of oral cavity papilloma transformation into malignancy. In the present study, because of research material shortage, we assessed p53 protein expression in 36 out of 38 previously examined papillomas. Our findings indicate that HPV infection and/or changes in p53 protein expression coexist in oral cavity papillomas.

References

1. Majewski S, Jabłońska S. Zakażenia wirusami brodawczaka i związane z nimi nowotwory jamy ustnej. Przeg Dermatol, 1998; 85: 185-90.

2. Popper HH, Wirnsberger G, Juttner-Smolle FM, Pongratz MG, Sommersgutter M. The predictive of human papilloma virus (HPV) typing in the prognostic of bronchial squamous cell papillomas. Histopathology, 1992; 21: 323-30.

3. Barzał-Nowosielska M, Miąsko A, Starosławska ER, Sulewska A, Chyczewski L. Detection of human papillomavirus in papillomas of oral cavity. Folia Histochem Cytobiol, 2001; 39: 189-90.

4. Zeuss MS, Miller CS, White DK. In situ hybrydization analysis of human papillomavirus DNA in oral mucosal lesions. Oral Surg Oral Med Oral Pathol, 1991; 71: 714-20.

5. Syrjanen SM, Syrjanen KJ, Happonen RP, Lamberg MA. In situ DNA hybridization analysis of human papillomavirus (HPV) sequences in bening oral mucosal lesions. Arch Dermato Res, 1987; 279: 543-9.

6. Barten M, Ostwald C, Milde-Langosch K, Muller P, Wukasch Y, Loning T. HPV DNA and p53 alterations in orpharyngeal carcinomas. Viechows Arch, 1995; 427: 153-7.

7. Mao EJ, Schwartz SM, Daling JR, Oda D, Tickman L, Beckmann AM. Human papilloma viruses and p53 mutation in normal pre-malignant and malignant oral epithelia. Int J Cancer, 1996; 69: 152-8.

8. Shindoh M, Chiba I, Yasuda M, Saito T, Funaoka K, Kohga T, Amemiya A, Sawada Y, Fujinaga K. Detection of human papillomavirus DNA sequences in oral squamous cell carcinomas and their relation to p53 and proliferating cell nuclear antigen expression. Cancer, 1995; 76: 1513-21.

9. Chiba I, Shindoh M, Yasuda M, Yamazaki Y, Amemiya A, Sato Y, Fujinaga K, Notani K, Fukuda H. Mutations in the p53 gene and human papillomavirus infection as significant prognostic factors in squamous cell carcinomas of the oral cavity. Oncogene, 1996; 18: 1663-8.

10. Aggelopoulou E, Troungos C, Goutas N, Skarlos D, Papadimitriou C, Kittas C. Immunohistochemical detection of p53 protein in HPV positive oral lesions. Anticancer Res, 1998; 18 :4511-5.

11. Sisk EA, Soltys SG, Zhu S, Fisher SG, Carey Te, Bradford CR. Human papillomavirus and p53 mutational status as prognostic factors in head and neck carcionoma. Head Neck, 2002; 24: 841-9.

12. Sulkowska M, Famulski W, Stasiak-Barmuta A, Kasacka I, Koda M, Chyczewski L, Sulkowski S. PCNA and p53 expression in relation to clinicopathological features of oral papilloma. Folia Histochem Cytobiol, 2001; 39: 193-4.

Diagnostic evaluation of oxidoreductive capability of sperm mitochondria

Piasecka M[1], Gączarzewicz D[2], Kurzawa R[4], Laszczyńska M[1], Kram A[3]

[1]Department of Histology and Embryology, [2]Department of Animal Reproduction University of Agriculture, [3]Department of Pathomorphology, [4]Clinic for Reproduction and Gynaecology, Pomeranian Medical University; Szczecin, Poland

Abstract

In the present paper, morphological and functional features of human sperm midpiece, contributing to the assessment of sperm fertility potential, have been described. The NADH-dependent NBT screening assay was used to identify and visualise: 1/ morphological defects of sperm midpiece, 2/ immature sperm forms with extensive cytoplasmic retention, reflecting developmental failure in spermatogenic remodelling process 3/ cytoplasmic sperm conglomerates, related to apoptotic bodies and 4/ sperm NADH-dependent oxidoreductase system at the mitochondrial level, related to the reaction intensity. The used assay is an adequate marker of sperm mitochondrial activity and sperm maturity. It can also help discover sperm defects that result in asthenozoospermia and can be used as an additional indicator in the evaluation of the sperm midpiece, as well as in routine morphological examination of spermatozoa, having a considerable predictive value for *in vivo* and *in vitro* fertilization.

Key words: spermatozoa, midpiece, mitochondria, cytochemistry, asthenozoospermia.

Introduction

Additional and complementary methods, enabling a precise and individual investigatation of spermatozoa, are needed to explain their pathophysiology, contributing to impaired fertility. Moreover, a precise diagnosis of spermatozoa is necessary, particularly to choose appropriate methods of assisted reproductive technique. The goal of our study was to determine morphological and functional features of sperm midpiece to discover defects leading to asthenozoospermia, very frequently associated with teratozoospermia.

ADDRESS FOR CORRESPONDENCE:
Małgorzata Piasecka
Department of Histology and Embryology
Pomeranian Medical University
Al. Powstańców Wielkopolskich 72; 70-131 Szczecin, Poland
tel/fax 0 91 4661677; e-mail: mpiasecka@ipartner.com.pl

Material and Methods

Studies were performed on ejaculated spermatozoa from patients of the Assisted Reproductive Technique Laboratory (n=80). Routine semen parameters were determined, using standard criteria, recommended by WHO [1] and morphological strict criteria, according Kruger et al. [2]. The sperm midpieces were assessed by means of a screening cytochemical test [3, 4, 5, 6] for mitochondrial NADH-dependent oxidoreductases (diaphorase, related to flavoprotein), using NADH and NBT (nitroblue tetrazolium) as electron donor and an artificial acceptor of electron, respectively (NADH dependent NBT assay). Morphological evaluation of sperm smears with cytochemical reaction was based on elaborated own criteria and, partly, on the criteria given by Hrudka [3]. The intensity of the reaction (visualized morphologically as abundant blue deposits of formazans within the midpieces of spermatozoa) was assessed by a computer image analysing system (Quantimet 600S, Cambridge, UK) measuring the mean optical density (MOD, in each pixel of midpiece) and the integrated optical density (IOD, for the whole midpiece) of the reaction product-formazans. The densitometric measurements were expressed as arithmetic means, stated for 100 spermatozoa for each case and were referred to the activity of sperm mitochondria. The densitometric values depended on the formazan precipitation, due to the NBT reduction, determined by the oxidoreductase system of these organelles. Therefore, the oxidoreductive capability of the mitochondria could be related to the intensity of the reaction [5, 6].

Results

Different patterns of the cytochemical reaction could appear in normozoospermia and in patients with low standard

Figures 1 A, B, C. Histograms of the mean optical density (MOD) distribution in the population of spermatozoa (stated for 100 cells) and sperm smears with NADH-dependent NBT assay of patient with normal standard sperm parameters (A), low sperm motility and morphology (B) and with low sperm concentration, motility and morphology (C). Intense cytochemical reaction in: morphologically normal (green arrow), deformed (blue arrow), deformed and coiled sperm midpieces (red arrow), immature sperm form (grey arrow), sperm conglomerates (red asterisk), containing active mitochondria, filled with abundant formazan deposits (compact pattern); absence of formazan deposits (black arrow) in different segments of morphologically normal midpieces (focal pattern); weak cytochemical reaction (yellow arrow) in morphologically normal midpieces, containing dysfunctional mitochondria (diffused pattern); x1200.

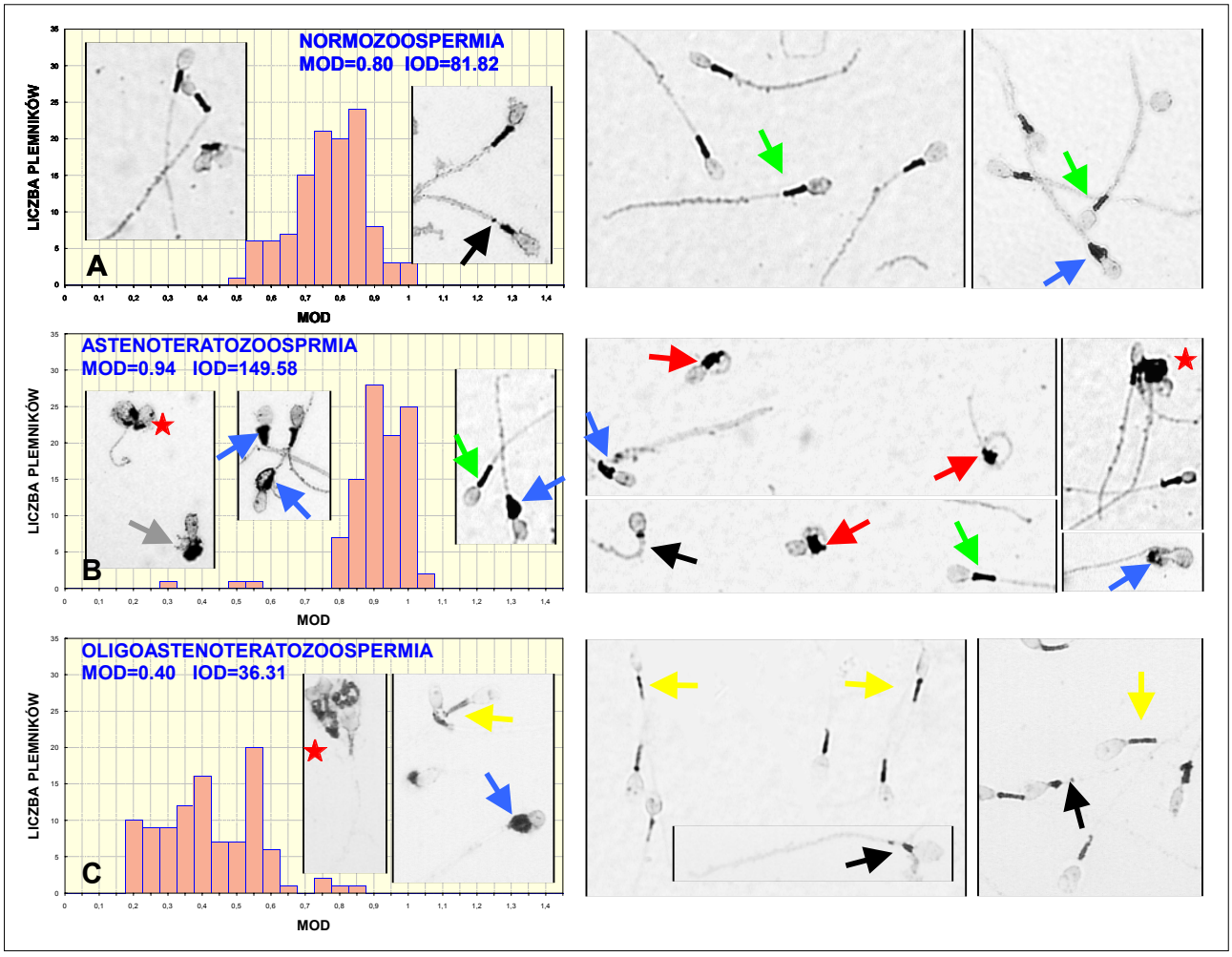

sperm parameters. A positive-intense reaction (high values of MOD and IOD) was found in: 1/ morphologically normal midpieces (>50% in patients with normal sperm motility) (Fig. 1A), 2/, coiled, displaced, to long and deformed midpieces, occasionally with different size and shape of persistent cytoplasmic droplet (Fig. 1B), 3/ immature sperm forms with cytoplasmic retention, either failed or with cytoplasmic "sacks" (Fig. 1B) and 4/ sperm cytoplasmic conglomerates (Fig. 1 B, C). The deformed midpieces, immature sperm forms and cytoplasmic conglomerates occurred more frequently in terato- and asthenoteratozoospermic subjects (Fig. 1 B, C).

A weak cytochemical reaction (a reduced amount of formazan deposits) or the absence of formazans in various parts of the sperm midpiece (low values of MOD and IOD) were observed mainly in the morphologically normal midpiece (Fig. 1C). It suggested a functionally impaired mitochondrial sheath which contained, besides active, also dysfunctional mitochondria. Our morphologically and densitometric findings indicated that the decreased values of MOD and IOD, stated for 100 spermatozoa (for each case), resulted from the increased percentage of morphologically normal spermatozoa with a weak cytochemical reaction (Fig. 1C).

Discussion

Our previous [7, 8] and present studies indicated that morphologically normal and defected midpieces contained functional mitochondria with complete oxidoreductive capability and a high mitochondrial membrane potential. The deformations of midpieces resulted from supernumerary, functional mitochondria, located under plasma membrane or in a cytoplasmic droplet, placed at the level midpiece, the neck and even the head of spermatozoa (Fig. 1). Previous electron microscopic investigations demonstrated sperm conglomerates, containing sperm head, midpieces, principal pieces, supernumerary active mitochondria and a large amount of membranes and granular materials [8]. The sperm cytoplasmic conglomerates can be related to apoptotic bodies and they may reflect apoptosis of spermatids at a different stage of their differentiation [8, 9].

The densitometric studies demonstrated that high values of optical density (MOD and IOD) occurred not only in patients with normal sperm motility but also in some cases of asthenozoospermic patients (Fig. 1B). It was evident that low sperm motility in those subjects was not associated with energetic disorders of sperm mitochondria because the high values of optical density reflected high oxidoreductive capability of sperm mitochodria, which could generate energy-ATP for sperm movement. Those densitometric results confirmed our previous cytofluorometric study of JC-1 stained spermatozoa [7, 8]. In some cases of asthenozoospermia, a high percentage of spermatozoa with high mitochondrial membrane potential (polarized, functional mitochondria) was detected. Morphological examination of sperm smears from those asthenozoospermic patients revealed that the semen contained a large number of immature sperm forms with functional mitochondria and/or a large number of spermatozoa with morphological deformations of mitochondrial sheath, containing redundant and supernumerary functional mitochondria and, occasionally, it contained sperm cytoplasmic conglomerates with active mitochondria. But, on the other hand, our study has also shown low densitometric values in some cases of asthenozoospermic patients (Fig. 1C). Those densitometric and morphological results of the patients suggested energetic disorders of mitochondria, mainly in large number of morphologically normal sperm midpieces (Fig. 1C). The findings were consistent with our previous results [7, 8].

Based on the date of the presented study, the asthenozoospermia could result from 1/ disturbances in spermatogenic remodelling process, particularly, in sperm midpiece morphogenesis, 2/ failed cytoplasmic extrusion, 3/ apoptosis of spermatids and 4/ energetic disorders of sperm mitochondria.

It should be emphasized that subtle and, occasionally, drastic defects of sperm midpieces, particularly with remnants of non discarded cytoplasmic droplet, were very frequently invisible in routine morphological examinations of sperm smears (staining, according to Papanicolaou) [1]. Therefore, the proposed cytochemical test can be applied as an assay not only to show normal midpieces but mainly to display their diverse defects. Moreover, this test can be considered as an adequate marker of cytoplasmic droplet and, simultaneously, of sperm immaturity [4], as a valuable and comprehensive test and can be applied as an additional indicator in the evaluation of sperm. The proposed test can be added to the routine clinical andrology workshop and can be of considerable predictive value for either *in vivo* or *in vitro* fertilization [4, 7, 8].

Acknowledgements

The authors wish to thank Prof. Wenancjusz Domagała for his kind permission to use the computer image analyzing system, and Jeremi Waroch and Dorota Waroch for the valuable and critical discussion of the manuscript.

References

1. WHO Word Heath Organization 3rd ed. Cambridge: Cambridge University Press.; 1992.
2. Kruger TF, Acosta AA, Simons KF, Swanson RJ, Matta JF, Oehninger S. Predictive value of abnormal sperm morphology in in vitro fertilization. Fertil Steril, 1988; 49: 112-7.
3. Hrudka F. Cytochemistry of oxidoreductases in spermatozoa: the technic revisited. Andrologia, 1979; 11: 337-52.
4. Gergely A, Kovanci E, Senturk L, Cosmi E, Vigue L, Huszar G. Morphometric assessment of mature and diminished-maturity human spermatozoa: sperm regions that reflect differences in maturity. 1999; 14: 2007-14.
5. Piasecka M, Wenda-Różewicka L, Kram A. Computerized analysis of cytochemical reaction of spermatozoa In rats chronically treated with lead acetate [Pb(II)]. Folia Histochem Cytobiol, 1997; 35: 129-31.
6. Piasecka M, Wenda-Różewicka L, Ogoński T. Computerized analysis of cytochemical reaction for dehydrogenases and oxygraphic studies as methods to evaluate the function of the mitochondrial sheath In rat spermatozoa. Andrologia, 2001; 33: 1-12.
7. Piasecka M, Kawiak J. Sperm mitochondria of patients with normal sperm motility and asthenozoospermia: morphological and functional study. Folia Histochem Cytobiol, 2003; 41: 125-39.
8. Piasecka M, Laszczyńska M, Gączarzewicz D. Morphological and functional evaluation of spermatozoa from patients with asthenoteratozoospermia. Folia Morphol, 2003; 479-81.
9. GandiniL, Lombardo F, Paoli D, Capobecchia L, Familiari G, Verlengia C, Dondero F, Lenzi A. Study of apoptotic DNA fragmentation in human spermatozoa. Hum Reprod, 2003; 62: 479-81.

Aging process of epithelial cells of the rat prostate lateral lobe in experimental hyperprolactinemia induced by haloperidol

Wylot M[1], Laszczyńska M[1], Słuczanowska-Głąbowska S[2], Piasecka M[1]

[1]Department of Histology and Embryology, [2]Department of Physiology,
Pomeranian Medical University of Szczecin, Poland

Abstract

The aim of the study was to examine the influence of hyperprolactinemia, induced by haloperidol (HAL) on age related morphology and function changes of epithelial cells in rat prostate lateral lobe. The study was performed on sexually mature male rats. Serum concentrations of prolactin (PRL) and testosterone (T) were measured. Tissue sections were evaluated with light and electron microscopy. Immunohistochemical reactions for Anti-Proliferating Cell Nuclear Antigen (PCNA) were performed. In rats of the experimental group, the mean concentration of: PRL was more than twice higher, whereas T concentration was almost twice lower than that in the control group. Light microscopy visualized the following: hypertrophy and epithelium hyperplasia of the glandular ducts, associated with increased PCNA expression. Electron microscopy revealed changes in columnar epithelial cells, concerning organelles, engaged in protein synthesis and secretion.

Key words: aging, lateral lobe, rat prostate, hyperprolactinemia.

Introduction

Due to the progress of aging of males in the industrialized civilization, disorders of the prostate gland. including inflammatory disorders, hyperplasia of the secretory epithelium, benign hypertrophy and malignancy become increasing problems in the population. The aetiology is, in general, searched for in paracrine endocrinological disorders. One of the reasons is hyperprolactinemia, revealing physiologically among men after the 60th year of life, or either as a symptom of various diseases or a side effect of various drug treatments. Influence of PRL on the prostate acts on dual level - as that of a pituitary hormone and that of cytokine, exerting either autocrine or paracrine effects. Prolactin membrane bound receptor (PRLR) is widely dispersed in the rat prostate - dorsal, lateral, ventral lobes [4], as well as in the human prostate [3]. An *in vivo* rodent grafted pituitary indicated a local direct proliferate, trophic effect of PRL on the prostate, independently of the circulating androgen levels, especially in the lateral lobe [1]. The metabolism of the prostate gland is also affected by PRL: in rats, the androgen independently stimulates citrate production, especially in the lateral lobe and changes cellular and mitochondrial zinc levels [2]. Androgens directly control most of the proteins, secreted by epithelial cells of the lateral lobe of the rat prostate. The aim of our study was to examine the influence of hyperprolactinemia on age-related changes in the morphology and function of epithelial cells of the rat prostate lateral lobe.

ADDRESS FOR CORRESPONDENCE:
Marcin Wylot
Department of Histology and Embryology
Pomeranian Medical University
Al. Powstańców Wielkopolskich 72; 70-111 Szczecin, Poland
tel. 91-4661678; tel. 505076626
e-mail: marlot@sci.pam.szczecin.pl

Material and Methods

The studies were performed on sexually mature 18 months old Wistar rats, divided into experimental and control groups, with 10 animals in each. Hyperprolactinemia was induced by intraperitoneal injections of a Haloperidol (Polfa Warszawa, Poland) 2.0 mg/kg body weight, administered for 14 days. Animals of the control group received saline in an equal volume. Serum levels of PRL were measured by ELISA (Spi-Bio, France), and T levels were measured by RIA (Orion Diagnostics, Finland). The prostate lateral lobe was fixed in 4% neutral buffered formalin or Bouin's fluid and embedded in paraffin. Histological analysis was performed on serial sections, obtained from prostatic samples stained with either H-E or P.a.s. For

Figure 1A. Cross section through the gland and stroma of prostate lateral lobe from an 18-mth control rat.

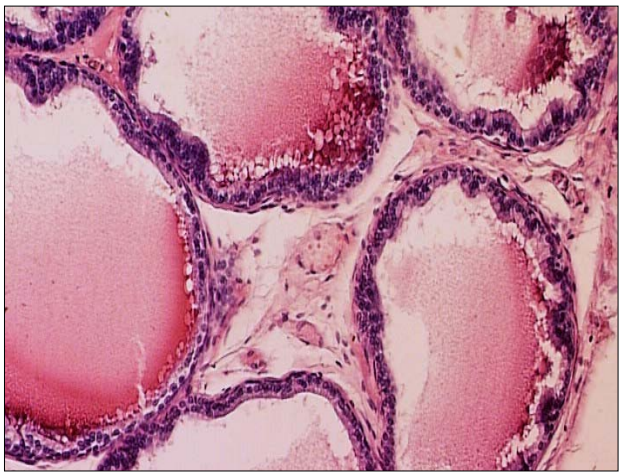

Figure 1B. Papillary infoldings and multistratified cell clusters in HAL rat (100x).

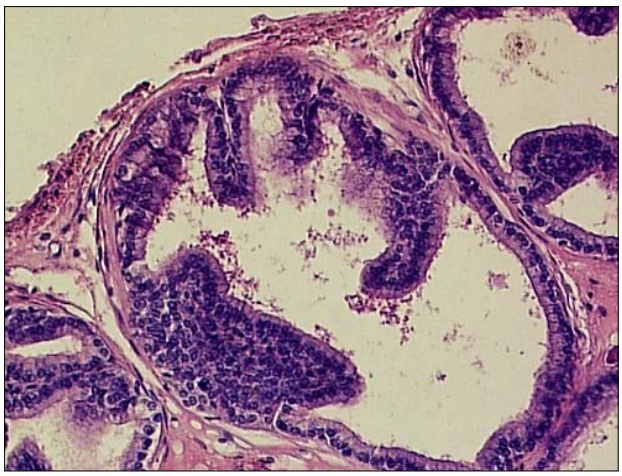

Figure 2A. The Golgi apparatus in the columnar epithelial cells of the lateral lobe of a control prostate.

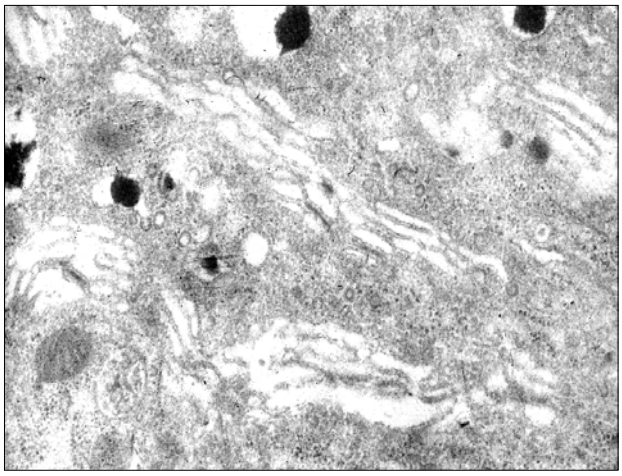

Figure 2B. Dilated cisterns GA and residual material in HAL rat, the lateral prostate (7000x).

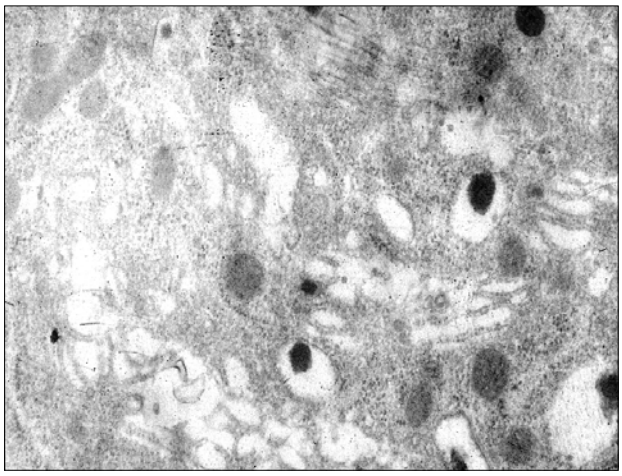

Figure 3A. Immunohistochemical expression of PCNA in the epithelial cells of the prostate lateral lobe in a control rat,

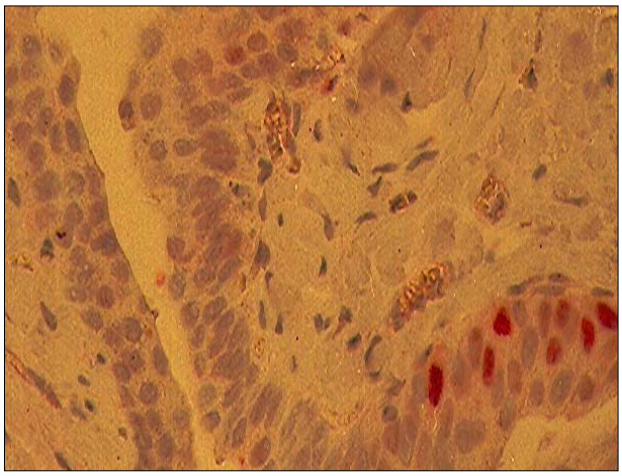

Figure 3B. and after HAL (400x).

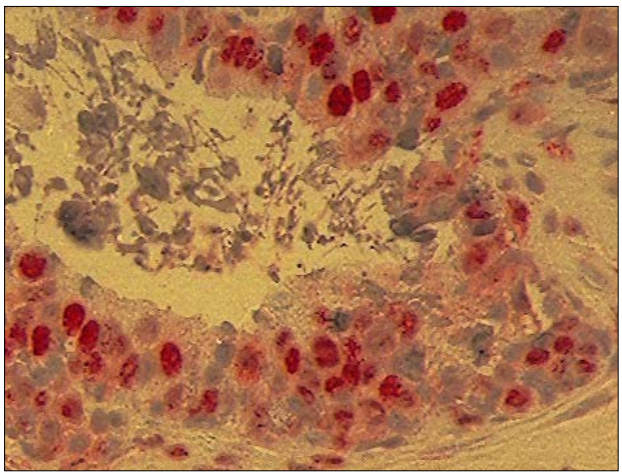

immunohistochemical detection of Proliferating Cell Nuclear Antigen (PCNA) in the prostate lateral lobe, DAKO EnVision System Alkaline Phosphatse (DAKO, Denmark). was used. Tissue sections were incubated with: primary antibody Monoclonal Mouse Anti-PCNA Clone PC10 and Fast Red (DAKO, Denmark) was used to visualize the reaction. Negative controls consisted of omissions of the primary antibody. For transmission electron microscopy (TEM), samples of the lateral lobe of the prostate were routinely prepared and finally examined under a JEM-1200 EX. Variations in plasma hormone levels were analyzed by the Cochran-Cox test. Statistical significance was established at levels of $p<0.05$.

Results

In rats of the experimental group, the mean concentration of PRL (79.7ng/ml) was almost twice higher, whereas the mean concentration of T (1.35ng/ml) was twice lower, compared to respective values in the control group (PRL 45.7ng/ml, T 3.42ng/ml). Also noticed were: hypertrophy of the glandular ducts, hyperplasia of epithelium, forming papillary infoldings and multistratified cell clusters. Within the hyperplastic areas in the connective tissue, we noticed inflammatory infiltrations, consisting of: lymphocytes, histiocytes and plasmocytes, surrounding the glands. The characteristic microscopic image, as described above, occurred focally, while other areas of the observed gland were unaffected.

Most of the changes, observed in electron microscopy, concerned intracellular organelles, engaged in protein synthesis and secretion - rough endoplasmatic reticulum, Golgi apparatus (GA) and the luminal secretory surface of epithelial cells. Immunohistochemical expression of PCNA antigen reveals a correlation to hyperplastic activity of the epithelium. An increased presence of PCNA was observed in papillary infoldings and clusters of epithelium in acini.

Discussion

Eighteen (18) months old rats are relative to 60 years old humans. Hyperprolactinemia brings into prominence the effect of PRL on pathology of the prostate gland [5]. Spontaneous prostate disease is described only in primates, whereas in rodent animal models, it is induced by chemical treatment or genetic modulations [1, 6, 10]. The prostate gland in rats consists of three lobes: ventral, lateral and dorsal, among which only the dorsal and the lateral lobe are homological to their human equivalents. Prolactin levels increase with age, whereas testosterone parallelly decreases, indicating the age-dependent role of PRL in the proliferation control of prostatic cells, causing a development of benign prostate hyperplasia, dysplasia and, possibly, prostate carcinogenesis in the human [7].

An essential role in the unbalance of apoptotic cell death and the proliferation rate in the ageing prostate, clinically observed in elderly men, is played by androgens. In the cross talk between PRL and T up-regulation of the androgen receptor (AR) [10], an influence on 5α-reductase occurs [9]. In 24 months old Brown Norway rats, despite a decline of T serum levels, prostatic hyperplasia reveals in dorsal and lateral lobes of the prostate, whereas it does not in the ventral lobe. As it has been revealed by results of immunohistochemical, and genetic studies, the epithelial cell proliferation rate correlates with AR expression: stronger in the dorsolateral prostate and weaker in the ventral lobe, when compared to respective values in the young rat [11]. As it was assessed in our previous studies, hyperprolactinemia is one of the causes, increasing AR expression in rat prostate epithelial cells [10]. Rats over 12 months reveal an inflammatory invasion, low acinar epithelium devoid secretory activities, acinies often have smaller diameters with a thick surrounding fibromuscular stroma and lumen, filled up with proliferating or exfoliated epithelium [8]. That was corresponding to the results, obtained in our study on 18 month old rats. We observed: large secretory vacuoles, containing dense bodies, large excessively dilated cisterns of rough endoplasmatic system and the Golgi apparatus in the supranuclear region, and only a few secreted granules. PRL plays an essential role in prostate pathology. The results, as obtained in animals, put aside the detailed knowledge of the mechanism ruling in biology of the prostate gland. The influence of PRL takes place directly, modulating the growth, proliferation and metabolism of prostate cells, as well as indirectly, via sex steroid hormones and their receptors.

References

1. Ahonen TJ, Harkonen PL, Laine J, Rui H, Martikainene PM, Nevalainen MT. Prolactin is a survival factor for androgen-deprived rat dorsal and dorsal and lateral prostate epithelium in organ culture. Endocrinology, 1999; 140: 5412-21.

2. Costello LC, Franklin RB. Effect of prolactin on the prostate. Prostate, 1994; 24: 162-6.

3. Leav I, Merk FB, Lee KF, Loda M, Mandoki M, McNeal JE, Ho SM. Prolactin receptor expression in the developing human prostate and in hyperplastic, dysplastic and neoplastic leasions. Am J Pathol, 1999; 154: 863-70.

4. Nevalainen MT, Valve EM, Ingelton PM, Harkonen PL. Expression and hormone regulation of prolactin receptor in rat dorsal and lateral prostate. Endocrinology, 1996; 137: 3078-88.

5. Laszczyńska M. Rola prolaktyny w męskim układzie płciowym. Post Biol Kom, 2002; 29: 45-59.

6. Van Coppenolle F, Slomianny C, Carpentier F, Le Bourhis X, Ahidouch A, Croix D, Legrand G, Dewailly E, Fournier S, Cousse H, Authie D, Raynaud JP, Beauviain JC, Dupouy JP, Prevarskaya N. Effects of hyperprolactinemia on rat prostate growth: evidence of androgeno-dependence. Am J Physiol Metab, 2001; 280: 120-29.

7. Untergasser G, Rumpold H, Hermann M, Dirnfoer S, Jilg G, Berger P. Proliferative disorders of the aging human prostate: involvement of protein hormones and their receptors. Experimental Gerontology, 1999; 34: 275-87.

8. Aumuller G, Endrle-Schmitt U, Seltz J, Muntzing J, Chandler JA. Ultrastructure and immunohistochemistry of lateral prostate in aged rats. The Prostate, 1987; 10: 245-56.

9. Steers WD. 5alpha-reductase activity in the prostate. Urology, 2001; 58: 17-24.

10. Słucznowska-Głąbowska S, Laszczyńska M, Wylot M, Piasecka M, Kram A. The expression of androgen receptors in the epithelial cells of the rat prostate lateral lobe in experimental hyperprolactinemia: a morphological and immunnohistochemical study. Folia Morphol, 2003; 62: 501-3.

11. Banerjee PP, Banerjee S, Brown Tr. Increased androgen receptor correlates with development of age-dependent, lobe specific spontaneous hyperplasia of the Brown Norway rat prostate. Endocrinology, 2001; 142: 4066-75.

Adrenergic innervation and steroidogenic activity of cystic porcine ovaries

Dzienis A[1], Majewski M[2], Wojtkiewicz J[2], Piskuła M[1], Jana B[1]

[1]Institute of Animal Reproduction and Food Research of the Polish Academy of Sciences, [2]Division of Clinical Physiology, Department of Functional Morphology, University of Warmia and Mazury, Olsztyn, Poland

Abstract

We studied both morphology and steroidogenic activity of porcine ovaries after dexamethasone (DMX)-induced polycystic status. In the polycystic-changed ovaries, an increase in the number of DßH-IR and/or NPY-IR nerve terminals was found in the wall of follicles, cysts and blood vessels. After DXM injections, we observed changes in the mean contents of progesterone, androstendione, estradiol-17ß, as well as noradrenaline, dopamine and adrenaline in the studied ovarian structures. The obtained data revealed that, in the polycystic ovaries of gilts, an increase in the number of adrenergic nerve terminals was associated with changes of the steroidogenic activity, what may suggest an important role of the adrenergic innervation in the ovarian cyst formation in the gilts.

Key words: ovarian cysts, catecholamines, steroidogenesis, gilts.

Introduction

The role of the nervous system in the control of normal ovarian function has already been documented in part. It is generally known that sympathetic nerves influence ovarian steroidogenesis and follicular development [1]. However, only little attention has, so far, been paid to the possibility that the derangement in neurogenic inputs may be an underlying component of some ovarian pathologies, such as cystic ovarian disease (COD). It has been suggested that an alternation in the activity of the sympathetic neurons, innervating the ovary, may contribute to etiopathogenesis of cysts in women [2] and rats [3]. COD is a common reproductive disorder in female domestic animals, leading to temporal or permanent infertility. According to our knowledge, there is still no available information on the role of sympathetic nerves in the etiopathogenesis of the ovarian cysts in pigs. Therefore, the purpose of our study was to determine the morphology and steroidogenesis of polycystic ovaries in pigs.

ADDRESS FOR CORRESPONDENCE:
Anna Dzienis
Institute of Animal Reproduction and Food Research
Polish Academy of Sciences
Tuwima 10, 10-747 Olsztyn, Poland
Tel (089) 5234686; e-mail: andzik@pan.olsztyn.pl

Material and Methods

We followed the principles of animal care (NIH publication No. 86-23, revised in 1985), as well as the specific national law on animal protection. The experiment was carried out on 12 crossbred gilts, aged 7-8 months, with controlled oestrous cycle. In the gilts of Group I (n=6), cysts were induced by i.m. injections of dexamethasone (DXM; Dexasone®, Norbrook Lab., Newry, UK, 3.3 µg/kg b.m., in a total volume of 6 ml), every 12 h, in the period from day 16th of the first studied oestrous cycle to day 9th of the second studied cycle. The control group (II, n=6), received similarly 6 ml of saline. The gilts were slaughtered on day 20th of the second cycle. The ovaries were dissected and the number of ovarian structures of interest (follicles, cysts) was counted. Cryostat ovarian sections were studied by means of a routine double-immunofluorescence technique, used to visualize the distribution of dopamine-ß-hydroxylase (DßH) and neuropeptide Y (NPY). The concentrations of progesterone (P4), androstendione (A4) and estradiol-17ß (E2) in follicular and cystic fluid, as well as in the wall was estimated by radioimmunoassay. The content of noradrenaline (NE), dopamine (DA) and adrenaline (A) was estimated in ovarian tissue and in the follicular or cystic fluid by high performance liquid chromatography. The expression of cytochrome $P450_{scc}$ and $P450_{arom}$ in follicular and cystic wall was determined by Western blot. Imm-

Figures 1 and 2. Single (a) DβH/NPY-IR nerve fibres (control animals) and numerous nerve terminals (b) in a DXM-treated pig, running in a close vicinity to follicles (Figure 1) and blood vessels (Figure 2). A - artery, F - follicle, (↑) - nerves, x 200.
Figure 3. Numerous DβH/NPY-IR nerve terminals in the vicinity of the cyst. C - cyst, (↑) - nerves, x 200.

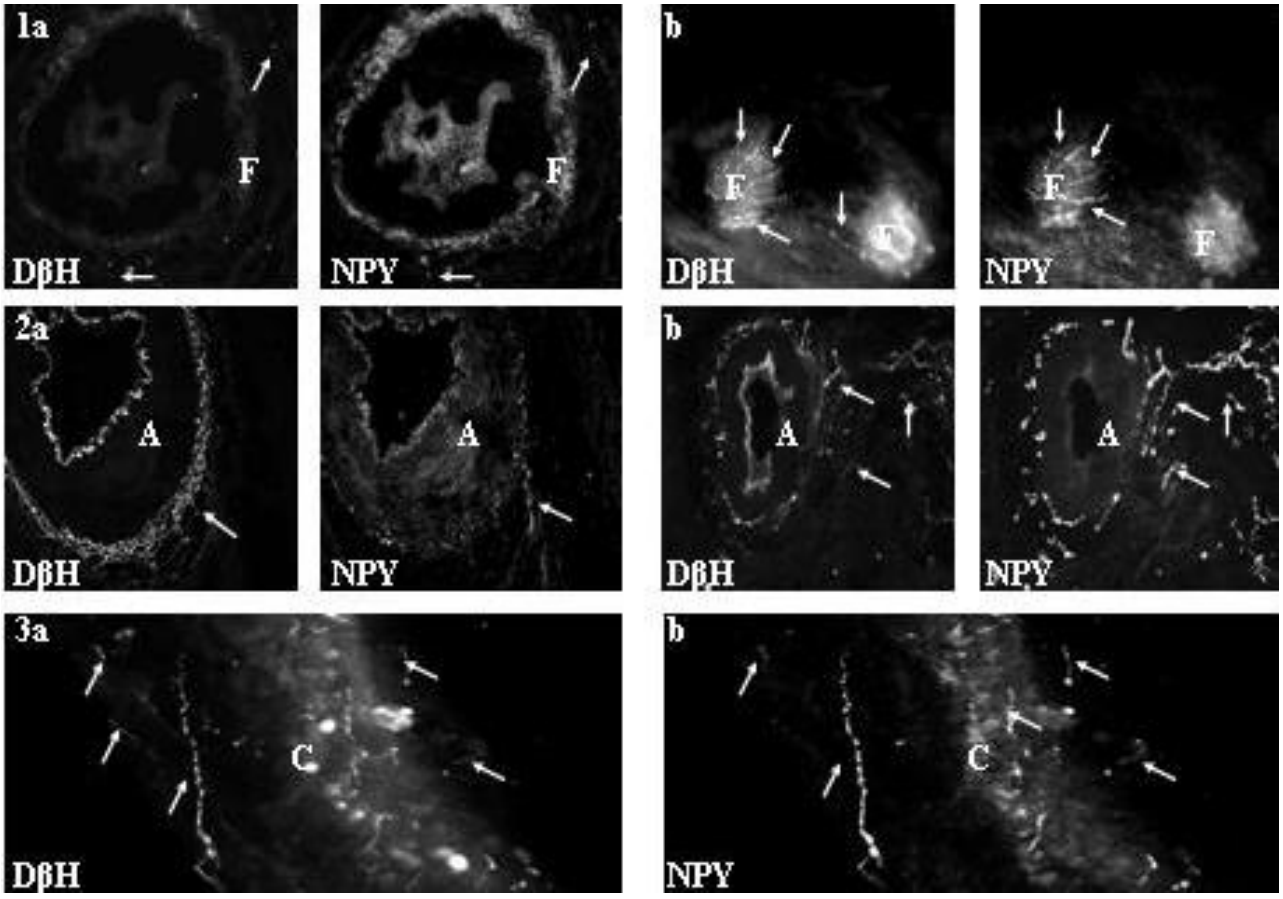

munoblots were quantified by scanning on the Kodak 1D Image Analysis Software (USA). The mean (±SEM) number of ovarian structures, as well as the content of hormones and catecholamines, were calculated for the control and DXM-treated groups. The data were compared by one-way analysis of variance (ANOVA).

Results

DXM injections resulted in an increase ($p<0.001$) in the number of follicles with the diameter of 3-6 mm (7.4±1.6 vs. 2.33±0.84; respectively) and in a formation of follicular cysts with the diameter of 1-3 cm (1.8±0.5). In both groups, the control and DXM-treated, the number of follicles with the diameter of 1-3 mm were not significantly different (6.7±0.9 vs. 7.4±1.2; respectively). Neither the follicles, measuring 6-10 mm in diameter, nor the corpora lutea were found after the administration of DXM.

In the gilts, receiving DXM, DβH-IR and/or NPY-IR nerves, located in the vicinity of the follicles (Fig. 1), and blood vessels (Fig. 2) were more numerous, compared to respective values in the control animals. The most numerous nerve terminals were found near the cysts (Fig. 3). DXM injections lead to a decrease ($p<0.05$-0.001) in the concentrations of P4 and A4 in the fluid from follicles (3-6 mm in diameter; 159.2±5.5 vs. 359.2±4.7 ng/ml, 3.8±0.5 vs. 34.5±2.6 ng/ml; respectively), as well as A4 and E2 in the cystic fluid (1.7±0.08 vs. 11.5±1.8 ng/ml, 0.8±0.1 vs. 4.8±0.4 ng/ml; respectively), compared to the follicles, measuring 6-10 mm in diameter, studied in the control animals. The content of P4 in the cystic wall was higher ($p<0.001$) than that found in follicles (6-10 mm in diameter) of the control gilts (4223±164.2 vs. 1651±287.2 ng/g of tissue; respectively). In the DXM-treated animals, an increase in the content of A in cystic wall and NA in cystic fluid was found, as compared to the follicles (6-10 mm in diameter) of animals of the control group (2.18±0.02 vs. 1.3±0.009 ng/g of tissue, 8.3±0.5 vs. 1.4±0.02 ng/ml; respectively). In gilts with the DXM-induced polycystic status, the content of NA was higher in the follicular wall (of the follicles, measuring 3-6 mm in diameter), when compared to that in the control animals (11.73±1.2 vs. 1.9±1.9 ng/g of tissue; respectively). After DXM treatment, the content of cytochrome $P450_{scc}$ and $P450_{arom}$ protein was lowered by 22.3% and 41.5%, respectively, in the follicular wall, whereas it was elevated by 77.4% and 6.3%, respectively, in the cystic wall, when compared to the values, found in the follicles of the control gilts.

Discussion

In polycystic-changed ovaries, we observed an increased number of follicles with diameter of 3-6 mm, paralleled by the lack of larger follicles (6-10 mm in diameter) and corpora lutea. This is in agreement with earlier studies, revealing higher numbers of follicles with diameter >6 mm, observed in sows, treated with DXM [4]. Furthermore, corpora lutea were not found in the ovaries of such treated pigs, either [5]. In addition, estradiol valerate-induced polycystic ovary syndrome in rats resulted also in a distinct reduction in the number of both the antral follicles and corpora lutea [6]. The present study showed an increase in the density of DßH- and NPY-immunoreactive nerve fibres, especially in the vicinity of the follicles, blood vessels and cysts after DXM injections. This is in line with the increased number of adrenergic nerves in the cyst wall in women [2] and rats [3], suffering from polycystic changed ovaries. Moreover, this was paralleled by an elevated content of NA in the cystic fluid. An increase in the levels of NA in the cystic fluid, as well as of A in the cystic wall, correlated with an increase in the concentration of P4 in the cystic wall. It can be explained by the stimulatory effect of NA on the production of P4, observed previously in the porcine granulosa [7] and bovine luteal cells [8]. Moreover, A elevated FSH-stimulated P4 synthesis in the human of granulosa layer [9]. Thus, it is possible that an increase in P4 production in the cysts may be associated with an increase in the content of $P450_{scc}$. In contrast to cysts, the content of P4 in the fluid from follicles of 3-6 mm in diameter was lower after DXM injections, than that, found in the control group. It can be attributed to an early atresia of follicular cells [4] and, in turn, to the drop in the expression of $P450_{scc}$, observed in our study. The decrease in the contents of A4 and E2 in the cystic fluid, as well as A4 in the follicular fluid from follicles of 3-6 mm in size, as observed in the present study after DXM administration, is in agreement with earlier observations in rats [2] and pigs [10] with cystic ovarian disease. The marked reduction of the $P450_{arom}$ content, observed by us in the follicular wall after DXM injections, was previously described in granulosa cells of pigs, treated with ACTH [11].

In conclusion, our data show that in the polycystic-changed porcine ovaries, the number of adrenergic fibres, as well as the content of catecholamines increased. Thus, as it was also accompanied by distinct changes in the steroidogenic activity, this may be indicative of an important role of adrenergic nerves in the ovarian cyst etiopathogenesis.

References

1. Lara HE, Ferruz JL, Luza S, Bustamante DA, Borges Y, Ojeda SR. Activation of ovarian sympathetic nerves in polycystic ovary syndrome. Endocrinology. 1993; 133: 2690-5.

2. Nakamura Y. Treatment of polycystic ovary syndrome: an overview. Horm Res, 1990; 33: 31.

3. Paredes A, Galvez A, Leyton V, Aravena G, Fiedler JL, Bustamante D, Lara HE. Stress promotes development of ovarian cysts in rats: the possible role of sympathetic nerve activation. Endocrine, 1998; 8: 309-15.

4. Gee CM, Geissinger HD, Liptrap RM. Morphometric and steroid hormone changes associated with experimental anovulatory follicles in the sow. Can J Vet Res, 1991; 55: 206-11.

5. Frautschy SA, Liptrap RM. Anovulation and plasma hormone concentrations after administration of dexamethasone during the middle of the luteal phase in sows undergoing oestrous cycles. Am J Vet Res, 1988; 8: 1270-75.

6. Lara HE, Dissen AG, Leyton V, Paredes A, Fuenzalida H, Fiedler JL, Ojeda SR. An increased intraovarian synthesis of nerve growth factor and its low affinity receptor is a principal component of steroid-induced polycystic ovary in the rat. Endocrinology, 2000; 141: 1059-72.

7. Wiesak T, Przała J, Muszynska A, Hunter MG. Effect of catecholamines and FSH on progesterone secretion by pig granulosa cells. Endocrinol Exp, 1990; 24: 449-56.

8. Kotwica J, Bogacki M, Rękawiecki R. Neural regulation of the bovine corpus luteum. Domest Anim Endocrinol, 2002; 23: 299-308.

9. Papenfuss F, Bodis J, Tinneberg HR, Schwarz H. The modulatory effect of catecholamines on gonadotropin-stimulated granulosa cell steroid secretion. Arch Gynecol Obstet, 1995; 253: 97-102.

10. Babalola GO, Shapiro BH. Sex steroid changes in porcine cystic ovarian disease. Steroids, 1990; 55: 319-24.

11. Ryan PL, Raeside JI. Steroidogenesis in granulosa cells after the induction of large cystic follicles with adrenocorticotrophin (ACTH) in the cyclic gilt. In: Proceedings of the Eleventh International Congress on Animal Reproduction and Artificial Insemination. Dublin, Ireland; 1988, p. 458.

Morphology of the testis and the epididymis in rats with dihydrotestosterone (DHT) deficiency

Kolasa A, Marchlewicz M, Wenda-Różewicka L, Wiszniewska B

Department of Histology and Embryology, Pomeranian Medical University Szczecin, Poland

Abstract

The aim of the study was to estimate morphology in the testis and epididymis of adult rats, treated with finasteride for 28 days (the time period of two seminiferous epithelium cycles) and 56 days (the time period of one spermatogenesis). A 28 days long DHT deficiency did not significantly influence the structure of seminiferous epithelium. After 56 days of treatment, finasteride induced sloughing of immature germinal cells (spermatids and rarely pachytene spermatocytes) into the lumen of the seminiferous tubules. A reduced content of spermatozoa was observed in the lumen of rat epididymis in rats with 56-day-long deficiency. The results indicated that 5α-reductase 2 activity is important for the maintenance of spermatogenesis. The decreased content of spermatozoa in the epididymal lumen of rats, treated with finasteride during one course of spermatogenesis, could reflect seminiferous epithelium condition.

Key words: testis, epididymis, DHT deficiency.

Introduction

Spermatogenesis, including meiosis, as well as germinal cell survival and the differentiation of round spermatids to elongated spermatids is known to be testosterone-dependent [1, 2]. Also epididymis function, in areas of maturation, transport and storage of spermatozoa is under testosterone control. In androgen target tissues, T can be intracellularly converted into DHT, the most potent androgen. Testicular and epididymal epithelial cells contain enzymes which control the ratio of testosterone to androgen metabolites and of androgens to other hormones, employed to regulate the male reproductive tract function (intracrine modulation). The irreversible conversion of T into DHT is catalyzed by steroid 5α-reductase (5α-red). Two isoforms of 5α-red were identified: type 1 (5α-red1) and type 2 (5α-red2), which are encoded by two different genes. 5α-red2 is more often expressed in male reproductive organs than 5α-red1 [3]. Finasteride is one of several steroid-based inhibitors, which has a higher affinity to 5α-red2, and is used in the treatment of aberrant prostate growth and prostate cancer. Therefore, one can create an experimental animal model to study the morphology of the testis and epididymis of rats with DHT deficiency, using finasteride as the inhibitor.

ADDRESS FOR CORRESPONDENCE:
Barbara Wiszniewska
Department of Histology and Embryology
Pomeranian Medical University
Al. Powstańców Wlkp. 72, 70-111 Szczecin, Poland
Tel/Fax 0-91 466-16-77,
e-mail: barbwisz@sci.pam.szczecin.pl

Material and methods

The study was performed in adult, male Wistar rats. The rats were randomly divided into 3 groups (with 5 animals in each): control and two experimental (I, II). The animals in the experimental groups received *per os* inhibitor of 5α-red2 (finasteride; Proscar®, MSD Sweden), during 28 days (Group I; the time period of two seminiferous epithelium cycles) and 56 days (Group II; the time period of one spermatogenesis) in 5mg/kg body weight doses. Sections of testis and epididymis, fixed in Bouin's solution and embedded in paraffin, were stained by the PAS method. The study was approved by the Local Ethics Committee and Animals Research.

Results

There were no changes in the morphology of testis of the rats, treated with finasteride during the time period of two seminiferous epithelium cycles (Fig. 2). Similarly as in testes from the control rats (Fig. 1), the seminiferous epithelium contained all the generations of germinal cells, corresponding to the stages of seminiferous epithelium cycle. In contrast, the inhibition of

Figures 1, 2, 3. Cross-section of seminiferous tubules of the testes from the control and the experimental rats. Seminiferous epithelium of the control rats contains all germinal cell generations, suitable for each cycle of seminiferous epithelium stage (1). Unchanged morphology of seminiferous epithelium of a rat with DHT deficiency through two seminiferous epithelium cycles (2). Sloughing of immature germinal cells into the lumens of the seminiferous tubules of rats with DHT deficiency during the time period of one spermatogenesis (3).
Figures 4, 5, 6, 7. Cross-section of seminiferous tubules of the testes from the rats with DHT deficiency during the time period of one spermatogenesis. The sloughing of spermatids in stages 3 and 16 (4); spermatid stages 4 (left tubule), and 17 and late pachyten spermatocytes (right tubule) (5); spermatids step 5 (6) and spermatids step 8 (7). Empty areas are seen in the seminiferous epithelium (5, 6).
Figures 8, 9, 10, 11, 12. 13. Cross-section of epididymis from the control rats (8, 9) and from the rats with 28-day (10, 11). The decrease content of spermatozoa in the lumen of caput (12) and cauda (13) epididymis of the rats with 56-day DHT deficiency.
PAS: 3 - x 160; 1, 2, 5 - x 320; 4, 6-13 - x 670.
Stages of seminiferous epithelium cycle in Figs. 4-7 are designated by Roman numbers.

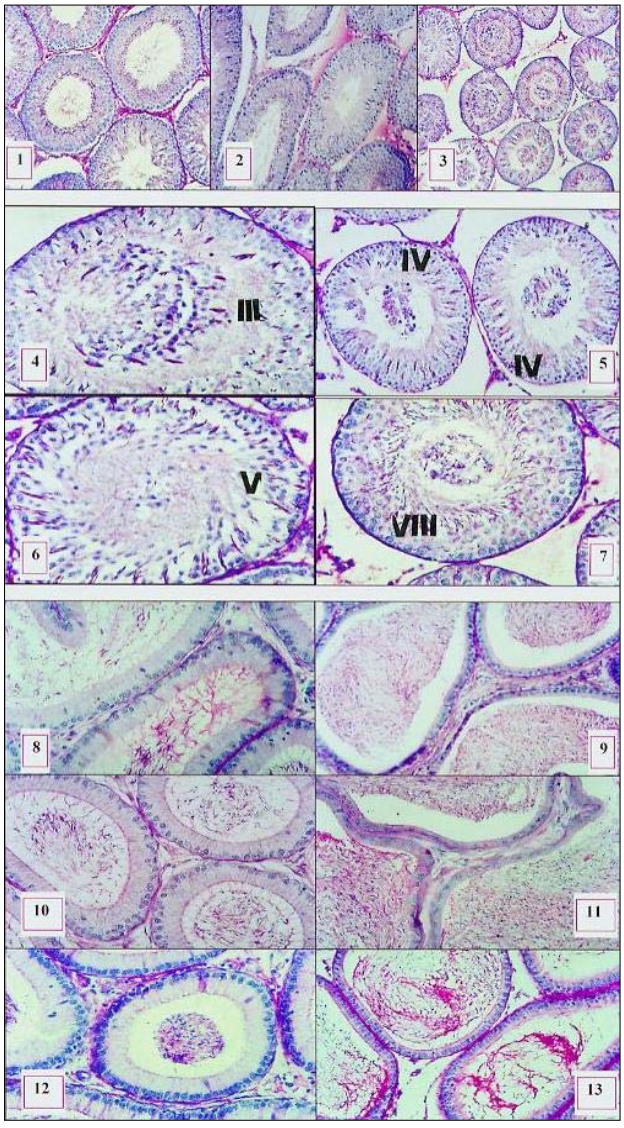

5α-red2 activity through the time period of one spermatogenesis duration altered the morphology of rat testis (Fig. 3). DHT deficiency resulted in sloughing of immature germinal cells. In the lumen of the tubules, there were mainly spermatids in different developmental stages (Figs. 4-7) and, rarely, late pachytene spermatocytes (Fig. 5). Moreover, empty areas within the seminiferous epithelium were observed as a result of cell sloughing (Fig. 6). The morphology of epithelial cells of the rat epididymides from Group I and Group II (the experimental groups) was not changed during finasteride treatment (Figs. 10-13), in comparison to the values in the control rats epididymides (Figs. 8, 9). A smaller amount of sperm was found in the lumen of epididymides of the rats with DHT deficiency throughout the time period of one spermatogenesis (56 days) (Figs. 12, 13).

Discussion

Changes in morphology were observed only in the testes of rats, receiving finasteride during the course of one spermatogenesis. An unchanged structure of testes of the rats, treated with finasteride through the time of two cycles of seminiferous epithelium, could be maintained by DHT, which was produced by 5α-red1 activity, the other type of enzyme presented in the testis [4], not inhibited by finasteride. It is possible that this pathway of T reduction is an alternative but short-term solution. On the other hand, the lack of morphological changes in the rats from the 28-day experiment could result from oxidative activity of 3α-hydroxysteroid dehydrogenase (3α-HSD), which catalyses the conversion of 3α-androstendiol into DHT [3]. Thus, the 28-day inhibition of 5α-red2 activity was too short to alter the morphology of the testis. Changes in morphology, observed in seminiferous epithelium of the rats with 56-day DHT deficiency, including the sloughing of immature germinal cells, are in agreement with other authors. O'Donnell et al. [5] have shown that 5α-reduction of testosterone is particularly important for the progression through midspermatogenesis (the transition of stage VII to stage VIII, in which the transition of round spermatids from step 7 to step 8 takes place). An alteration of testis morphology could result from the antyproliferative and apoptotic effects of finasteride [6, 7, 8]. A study of prostatic epithelial cells has shown finasteride-dependent changes of MAP kinase and Akt-1 factor expression, a decrease of Bcl-2 family peptide expression, Insulin-like Growth Factor I (IGF-I) and IGF-I receptor gene suppression [6, 7]. It is suggested that DHT initiates [9] and supports the process of spermatogenesis in rats [2, 5]. Normal morphology of rat epididymides, observed during finasteride treatment, could suggest that the organ develops an additional mechanism of protection. The reduced content of spermatozoa in the lumen, especially in cauda epididymis from the rats of Group II, could reflect seminiferous epithelium condition in those animals. It has been shown that men, receiving finasteride during 12 weeks, had semen quantity reduced by 25%. Moreover, the decrease of 5α-red activity causes oligoasthenozoospermia, oligozoospermia and even azoospermia.

Acknowlegments

The research was supported by the State Committee for Scientific Research as a Solicited Project PBZ-KBN-084/P06/2002 from the year 2003 to the year 2005.

References

1. McLachlan RI, O'Donnell L, Meachem SJ, Stanton PG, de Kretser DM, Pratis K, Robertson DM. Identification of specific sites of hormonal regulation in spermatogenesis in rats, monkeys, and man. Recent Prog Horm Res, 2002; 57: 149-79.

2. O'Donnell L, Stanton PG, Wreford NG, Robertson DM, McLachlan RI. Inhibition of 5 alpha-reductase activity impairs the testosterone-dependent restoration of spermiogenesis in adult rats. Endocrinology, 1996; 137: 2703-10.

3. Jin Y, Penning TM. Steroid 5α-reductase and 3α-hydroxysteroid dehydrogenases: key enzymes in androgen metabolism. Best Pract Res Clin Endocrinol Metab, 2001; 15: 79-94.

4. Pratis K, O'Donnell L, Ooi GT, McLachlan RI, Robertson DM. Enzyme assay for 5alpha-reductase type 2 activity in the presence of 5alpha-reductase type 1 activity in rat testis. J Steroid Biochem Mol Biol, 2000; 75: 75-82.

5. O'Donnell L, Pratis K, Stanton PG, Robertson DM, McLachlan RI. Testosterone-dependent restoration of spermatogenesis in adult rats is impaired by 5alpha-reductase inhibitor. J Androl, 1999; 20: 109-17.

6. Huynh H. Induction of apoptosis in rat ventral prostate by finasteride is associated with alteration in MAP kinase pathways and Bcl-2 related family of proteins. Int J Oncol, 2002; 20: 1297-303.

7. Huynh H, Seyam RM, Brock GB. Reduction of ventral prostate weight by finasteride is associated with suppression of insulin-like growth factor I (IGF-I) and IGF-I receptor genes and with an increase in IGF binding protein 3. Cancer Res, 1998; 58: 215-8.

8. Rittmaster RS, Norman RW, Thomas LN, Rowden G. Evidence for atrophy and apoptosis in the prostates of men given finasteride. J Clin Endocrinol Metab, 1996; 81: 814-9.

9. Killian J, Pratis K, Clifton RJ, Stanton PG, Robertson DM, O'Donnell L. 5alpha-reductase isoenzymes 1 and 2 in the rat testis during postnatal development. Biol Reprod, 2003; 68: 1711-8.

Influence of naringenin on the activity of enzymes participating in steroidogenesis in male rats

Papież M A

Department of Cytobiology and Histochemistry, Pharmaceutical Faculty, Medical College,
The Jagiellonian University, Kraków, Poland

Abstract

The aim of the experiment was to histochemically examine the activity of the following selected steroidogenic enzymes: $\Delta^5$3βHSD and 17βHSD and the housekeeping enzyme G6PDH, in experimental rats after subcutaneous injections of naringenin flavonoid, at a daily dose of 15 mg/kg of body mass. The enzyme activities were measured by the microdensitometric method. Additionally, radioimmunological assay for testosterone level was conducted in homogenates of testes. A significant decrease in the activity of 17βHSD and of G6PDH was found, while the activity of $\Delta^5$3βHSD was not significantly changed. The results permit a statement that naringenin causes minor changes in metabolic processes in the testes of rats but it does not significantly affect the synthesis of androgens.

Key words: $\Delta^5$3β-hydroxysteroid dehydrogenase, 17β-hydroxysteroid dehydrogenase, glucose-6-phosphate dehydrogenase, histochemistry, testis, rat, naringenin.

Introduction

Naringenin is a biphenolic compound, belonging to the group of flavonoids and to the class of flavanones. This flavonoid occurs in greatest quantities in citrus fruits, as well as in hop [1]. Because of its affinity to the estrogen receptor α and the ability to stimulate proliferation of cells in female reproductive tracts, this flavonoid is placed among the phytoestrogens, i.e., non-steroid compounds of plant origin, showing a structural similarity with 17β-estradiol [2, 3]. Like other phytoestrogens, naringenin inhibits the activities of 17βHSD and aromatase *in vitro* [4]. The objective of this study was to examine the *in vivo* effects of naringenin on the activity of selected steroidogenic enzymes: $\Delta^5$3βHSD and 17βHSD. as well as G6PDH, a housekeeping enzyme, providing the NADPH necessary for the synthesis of steroids. The studies were combined with an analysis of testosterone level.

ADDRESS FOR CORRESPONDENCE:
Papież Monika
Department of Cytobiology and Histochemistry
Pharmaceutical Faculty, Medical College,
Jagiellonian University
Medyczna 9, 30-688 Kraków, Poland
e-mail: mfpapiez@cyf-kr.edu.pl

Material and Methods

The experiments involved 20 sexually mature male rats of the inbred Wistar strain. The animals were kept in standard conditions: temperature 22°C, air humidity 50-60%, and the 12/12 hours L/D light regime. The animals were fed with standard fodder and had tap water available *ad libitum*. The rats were divided into two groups of 10 animals in each: control and experimental. The experimental rats received naringenin subcutaneously at a dose of 15 mg/kg b.m. in 0.2 ml dimethylsulphoxide (DMSO) each day for 14 consecutive days. The control rats were given subcutaneous injections of DMSO. After 14 days, the rats were decapitated and their testes removed and frozen in liquid nitrogen. The testes were then cut into 8 μm sections in a cryostat and subjected to histochemical reactions to detect $\Delta^5$3βHSD (EC 1.1.1.145) [5], 17βHSD (EC 1.1.1.51) [6,7], and G6PDH (EC 1.1.1.49) [8]. The enzyme activity in Leydig cells was assessed by the microdensytometric method. A computer-assisted image analyser, with the Multi Scan 6.08 software and an 8-bit grey scale, was used for the assessment. The intensity of the histoenzymatic reaction was estimated by measuring the integrated optical density (IOD) in the marked area. The intensity of histochemical reactions, shown on microphotographs, was assessed as either weak, moderate, or strong.

A portion of the material was placed aside to carry out a radioimmunological assay for testosterone level. This determi-

nation was completed with the use of a standard kit (from DSL) [9]. The significant differences between the groups were statistically tested, using ANOVA procedure.

Results

The greatest intensity of enzymatic reactions occurred in Leydig cells. The activity in the seminiferous epithelium was either weak or absent, depending on the examined enzyme.

The activity of $\Delta^5$3βHSD in Leydig cells of the control rats was strong (Fig. 1a), whereas in the rats, treated with naringenin, it was either high or moderate. The activity of 17βHSD in Leydig cells of the control rats was moderate, while the intensity of that reaction in the experimental rats was weak (Fig. 1 b,c). The activity of G6PDH in Leydig cells of the control rats was either moderate or high, whereas histochemical reaction in the experimental animals was moderate (Fig. 1d,e). Microdensitometric measurements showed a statistically significant decrease in 17βHSD and G6PDH activities in the experimental rats, compared with the respective values in the control animals (Fig. 2). The difference between the control and the experimental group in the $\Delta^5$3βHSD was not significant. In the homogenates of testes of the experimental rats, a statistically insignificant increase in testosterone content (120 ± 45 ng/g tissue) was found, compared with that in the control group (82 ± 26 ng/g tissue).

Discussion

This paper presents preliminary results of a study on the effects of naringenin *in vivo*, on the activity of selected enzymes, involved in the biosynthetic function of rat testes.

The observed drop of 17βHSD activity in the rats, receiving naringenin, may indicate a hormone-like effect of this flavonoid. It is known from literature that the administration of 17β-estradiol to male rats also leads to a drop in steroidogenic enzymes [10]. The obtained results match those of Le Bail et al. [4], who demonstrated that naringenin inhibited the activity of 17βHSD and aromatase in the microsomes, isolated from the human placenta. The application of naringenin to the rats did not result in any changes in the activity of 3βHSD, compared to respective values in the control. The results again agree with those, reported by Le Bail et al. [11], who demonstrated that naringenin in vitro had not affected the activity of 3βHSD, an enzyme, involved in steroidogenesis. Despite the drop in 17βHSD activity, in the rats receiving naringenin, a slight increase in testosterone level occurred in the testes of those individuals. One may thus presume that, in rats, naringenin inhibits the activity of the enzymes, participating in the metabolism of testosterone, such as aromatase and 5α-reductase. It should be added that the effect, exerted by phytoestrogens on the synthesis and release of androgens, has not yet been determined and the results of studies often contradict one another [12, 13]. In the rats, receiving naringenin, a decrease in the level of anabolic processes was noted, as indicated by a drop in the activity of G6PDH dehydrogenase. The decrease in

Figure 1. (a) Histochemical reaction for $\Delta^5$3βHSD (200x). Strong reaction in Leydig cells (arrow) of a control rat. (b,c) Histochemical reaction for 17βHSD (320x). The arrows show Leydig cells. (b) strong reaction in Leydig cells of a control rat. (c) Moderate and weak reaction in Leydig cells of an experimental rat. (d,e) Histochemical reaction for G6PDH (200x). (d) Moderate reaction in Leydig cells (arrow) of a control rat. (e) Weak reaction in Leydig cells (arrow) of an experimental rat.

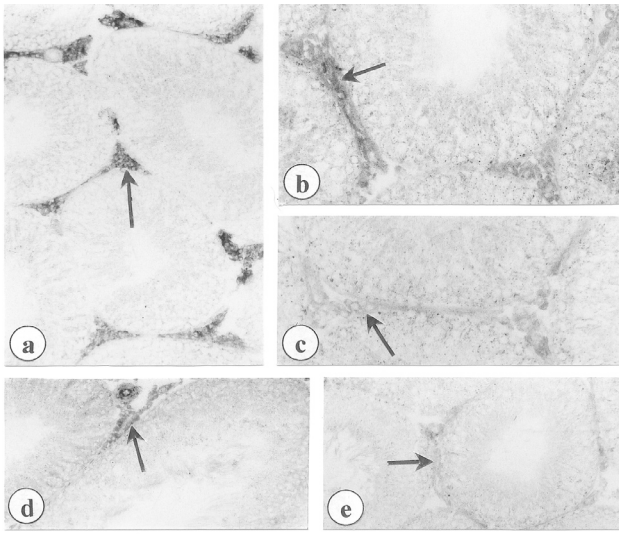

Figure 2. The activity of dehydrogenases in Leydig cells of the control and naringenin treated rats. Microdensytometrical analysis. Values are the means ± SD. Statistically significant differences as compared to the controls. *p<0.05, **p<0.01.

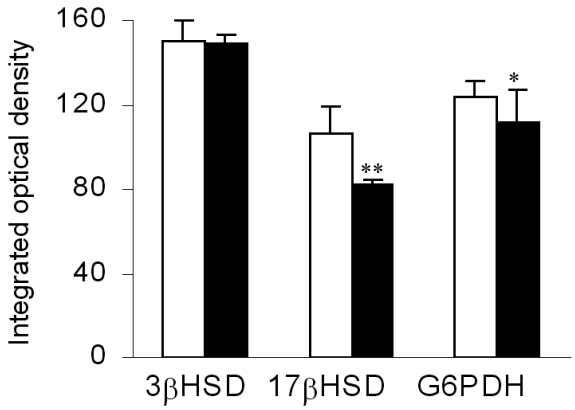

G6PDH was also observed after the administration of steroidogenesis-inhibiting chemicals [14]. The results of the present study allow for a statement that naringenin is an inhibitor of 17βHSD and G6PDH in the testes of rats and does not significantly affect the activity of $\Delta^5$3βHSD or the synthesis of testosterone.

Acknowledgements

The author is grateful to the staff of the Department of Clinical Biochemistry, Institute of Paediatrics, The Jagiellonian University, for the performed radioimmunological analysis. This study was supported by Grant No. BW/262/P/F/2004 from the State Committee for Scientific Research (KBN).

References

1. Tomas-Barberan FA, Clifford MN. Flavanones, chalcones and dihydrochalcones - nature, occurence and dietary burden. J Sci Food and Agric, 2000; 80: 1073-80.

2. Schaefer O, Humpel M, Fritzemeier KH, Bohlmann R, Schleuning WD. 8-Prenyl naringenin is a potent ERa selective phytoestrogen present in hops and beer. J Steroid Biochem, 2003; 84: 359-60.

3. Breinholt VM, Svendsen GW, Dragsted LO, Hossaini A. The citrus-derived flavonoid naringenin exerts uterotrophic effects in female mice at human relevant doses. Basic Clin Pharmacol Toxicol, 2004; 94: 30-6.

4. Le Bail JC, Laroche T, Founier F, Habrioux G. Aromatase and 17b-hydroxysteroid dehydrogenase inhibits by flavonoids. Cancer Lett, 1998; 133: 101-6.

5. Levy H, Wendler-Deane H, Rubin BL. Visualization of steroid-3b-ol-dehydrogenase activity in tissues of intact and hypophysectomized rats. Endocrinology, 1959; 65: 932-43.

6. Erpino MJ. Effects of substrate on histochemistry of 3b-HSD in testes. Gen Comp Endocr, 1971; 17: 563-6.

7. Schafers BA, Schlutius BG, Haider SG. Ontogenesis of oxidative reaction of 17b-hydroxysteroid dehydrogenase and 11b-hydroxysteroid dehydrogenase in rat Leydig cells, a histochemical study. Histochem J, 2001; 33: 585-95.

8. Pearse AGE. Histochemistry: Theoretical and Applied. Vol 2. 3th ed. London: Churchill-Livingstone: 1972.

9. Yalow R, Berson S. Introduction and general considerations. In: Odel WD, Daughday WH, editors. Principles of competitive protein binding assay. Philadelphia: JB Lippincott Co.; 1971.

10. Brinkmann AO, Leemberg FG, Roodnat EM, De Joung FH, Van der Molen Hj, A specific action of estradiol on enzymes involved in testicular steroidogenesis. Biol Reprod, 1980; 23: 801-9.

11. Le Bail J Ch, Champavier Y, Chulia A-J, Habrioux G. Effects of phytoestrogens on aromatase, 3b and 17b-hydroxysteroid dehydrogenase activities and human breast cancer cells. Life Sci, 2000; 66: 1281-91.

12. Roberts D, Veeramachaneni DN, Schlaff WD, Awoniyi CA. Effects of chronic dietary exposure to genistein, a phytoestrogen, during various stages of development on reproductive hormones and spermatogenesis in rats. Endocrine, 2000; 13: 281-6.

13. Papież M. The influence of hollyhock extract administration on testicular function in rats. J Mol Histol, 2004; 35: 1-8 (in press).

14. Vanitha-Kumari G. Effect of para-chlorophenylalanine on male rats: histopathological and biochemical changes in the testes. Indian J Physiol Pharmacol, 1986; 30: 223-31.

Effect of 5-aminolevulinic acid (ALA) doses and oestrogen/progesterone on protoporphyrin IX (PpIX) accumulation in human endometrial epithelial cells

Butowska W[1], Warchoł W[2], Nowak-Markwitz E[3], Wołuń-Cholewa M[1]

[1]Department of Radiobiology and Cell Biology, [2]Department of Biophysic,
[3]Clinic of Gynaecological Oncology and Department of Perinatology and Gynaecology
University of Medical Sciences, Poznan, Poland

Abstract

Endometriosis represents one of the most frequent causes of restricted fecundity. Despite the progress in medicine, appropriate diagnosis and treatment pose significant problems. The aim of this study was to evaluate ALA-induced PpIX fluorescence of normal endometrial epithelial cells for the diagnosis of endometriosis. PpIX-fluorescence was measured after stimulation with estradiol-17 beta (E2) or with estradiol-17 beta (E2) and progesterone (P) and after incubation with ALA under a confocal microscope. The epithelial cells showed a significantly higher fluorescence of PpIX in the course of 24 and 48h incubation with hormones, than the cells without stimulation. After 72h, a significant decrease in cellular PpIX concentration was noted. The results suggested that E2 and P were required to convert ALA to PpIX in epithelial cells and increased PpIX concentration in a time-dependent fashion.

Key words: endometriosis, *in vitro*, protoporphyrin IX, 17ß-estradiol, progesterone.

Introduction

Endometriosis is widely encountered in women during the period of sexual maturity. It is appraised to affect 3-10 % women in the generative age but, among infertile women and in women with pain in the pelvis, the incidence is supposed to reach 20-90% [1]. In clinical practice, the only reliable way to diagnose endometriosis is to visualize its typical alterations in the course of laparoscopy or laparotomy and to confirm the changes by histopathology [2]. In recent years, a photodynamic technique has been introduced to clinical practice, both for diagnostic and therapeutic purposes. It uses fluorescent drugs that concentrate preferentially in tumours and other hyperproliferative tissues. At present, among substances, applied in the photodynamic approach, a particular attention is focused on 5-aminolevulinic acid (ALA), which is a physiological requirement for heme production in cells. One of the compounds, which arises during heme biosynthesis, is protoporphyrin IX (PpIX), used in photodynamic therapy (PDT) as a photosensitizer. Till now, only few studies have been performed on PpIX accumulation in presence of ALA in endometrial cells [3, 4]. The studies have shown that, when exposed to ALA, the cells are more effective in the accumulation of PpIX. In animal models, endometrial grafts to peritoneum have been shown to accumulate PpIX in such a way that they could be detected, using PDD and could be subjected to photodynamic therapy [5, 6]. Nevertheless, in none of the above studies have female sex hormone effects on the obtained results been considered. This may explain the divergences in the extent of PpIX accumulation in myometrium and endometrium. Still, the results have demonstrated the capacity of the endometrium to accumulate more PpIX, as compared to other tissues, and allow to suggest that the phenomenon can be used for diagnosis and treatment of endometriosis, when the hormonal condition of female body is taken into account. Considering the above data, recognition of PpIX accumulation in isolated cells of endometrial uterine epithelium, as affected by estrogen and progesterone, may be of practical, not just theoretical, significance for the definition of requirements of photodynamic therapy.

ADDRESS FOR CORRESPONDENCE:
Maria Wołuń-Cholewa
Department of Radiobiology and Cell Biology
University of Medical Sciences of Poznań
Święcickiego 6, 60-781 Poznań, Poland
e-mail: doskon@amp.edu.pl

Figure 1. Epithelial cells, isolated from normal endometrium (A) and preincubated with E2 for 48h and, then, incubated with 2 mmol/l ALA for 2 h (B).

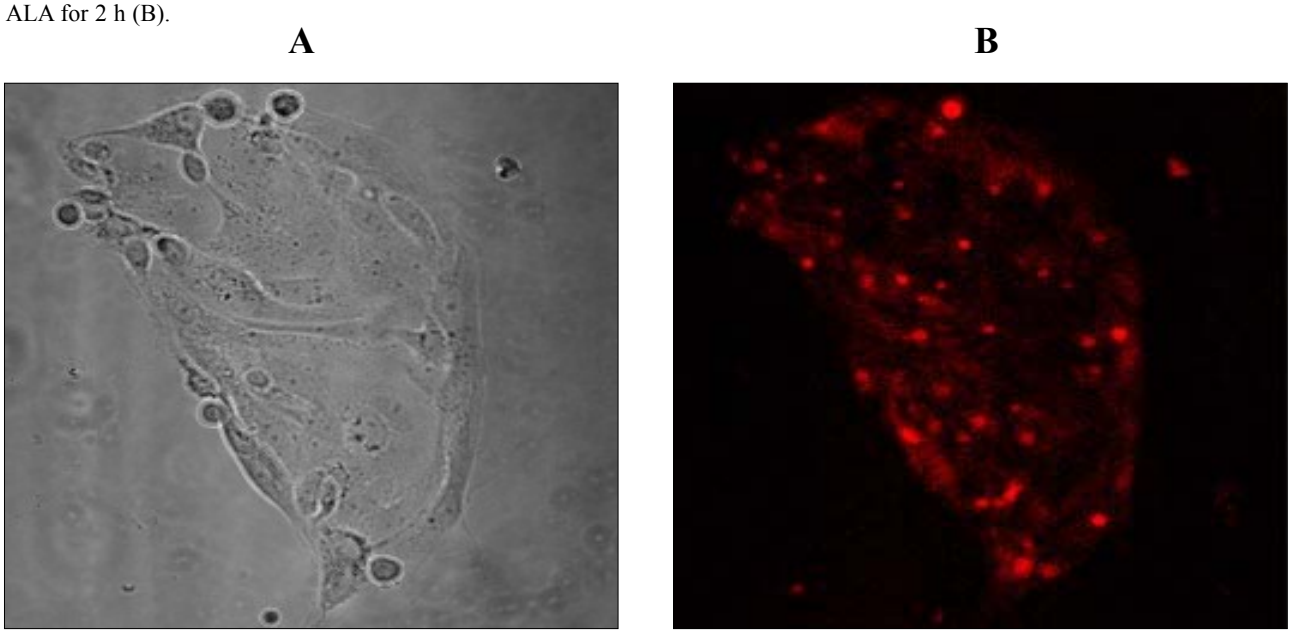

Figure 2. Alterations in the PpIX content in epithelial cells during incubation with E2 and ALA.

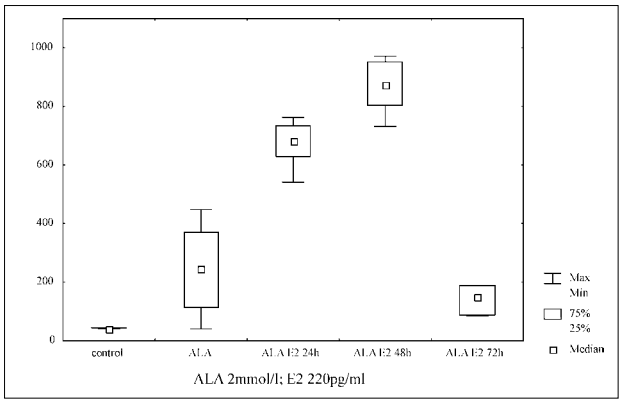

Figure 3. Alterations in the PpIX content in epithelial cells during incubation with E2/P and ALA.

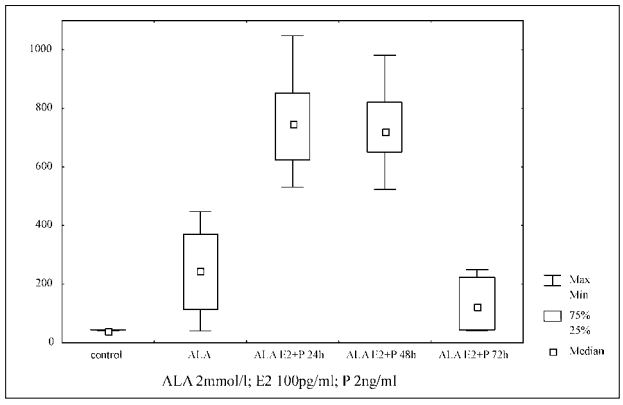

Methods

The studies were performed on human primary endometrial epithelial cells, originating from normal uterine cavity. The cells were isolated and cultured as described by Ryan et al. [7]. The cultures of epithelium cells were conducted in presence of estradiol-17 beta (E2) and progesterone (P) in concentrations typical for the follicular stage (E2 alone, 220 pg/ml) or the luteal stage (E2 100 pg/ml and P 2 ng/ml) for a period of 24, 48 or 72h (the hormone doses were selected to correspond to their blood levels during normal menstrual cycles in women) [8]. The effect of 5-aminolevulinic acid (ALA) concentration on the accumulation of protoporphyrin IX (PpIX) in cells was defined in the cells, following their incubation with 2.0 mmol/l ALA for a period of 2h (ALA concentration and the duration of incubation were selected on the basis of published data and our preliminary results) [4, 9]. Following that time, PpIX fluorescence in the cells was evaluated, using a confocal microscope (LSM 510, Zeiss). The estimations took advantage of PpIX-exciting laser beam of 458 nm wavelength, while the emitted light was analysed, using a 585 nm filter. PpIX content was evaluated, using the CytFlu 1.2 software and expressed as a product of an average intensity of fluorescence and percentage surface bearing area over the level of background (%AIF). In each experiment, cells of the control group, incubated in the same way, but in the culture medium devoid of ALA, were evaluated. Statistical evaluation of the obtained results involved the nonparametric U-Mann Whitney's test. P value <0.05 was considered to represent threshold of significance.

Results and Conclusion

Results of PpIX-specific fluorescence estimation in a confocal microscope, following the incubation with ALA and E2, are presented in Fig. 1. Protoporphyrin IX content, following 2h incubation with 2 mmol/l ALA without steroid treatment, was 244 %AIF. Following the 24h/E2 treatment of the epithelial cells, the intensity of the PpIX-specific fluorescence significantly increased ($p<0.001$) and, then, after subsequent 48h, again slightly increased to end up in a significant

decrease ($p<0.001$) after 72h (Fig. 2). The maximal peak of PpIX fluorescence (873 %AIF.) was noted on the 48th hour of the experiment (Fig. 2). PpIX-specific fluorescence in cells of the control group did not significantly change in the course of the entire experiment and never exceeded the value of 41 %AIF. A separate cycle of experiments was devoted to alterations in the PpIX content in epithelial cells, which were preincubated with E2 and P for the 24, 48 and 72h, then, transferred to the medium with ALA. The obtained results are illustrated in Fig. 3. An augmented and similar content of PpIX was observed after 24h and 48h. A significant decrease ($p<0.001$) in the cellular PpIX content was noted after 72h from the steroid treatment. The results demonstrated that incubation in a steroid-containing media (E2, P) and ALA induced an accumulation of PpIX in epithelial cells. Moreover, the application of E2 for 48h resulted in a significant, three-fold increase in PpIX-related fluorescence. An evident decrease in fluorescence intensity was noted, following the 72h incubation with oestrogen. The observed alterations should be interpreted as a result of an equilibrium between the synthesis of PpIX in the epithelial cells and the removal of PpIX, due to the binding of the compound to iron, its transformation to heme or its efflux out of the cells [10]. In the case of E2 and P treatment, the maximum value of PpIX-fluorescence should, for certain time (between 24 and 48h), exhibit a plateau. Probably, the synthesis of PpIX will balance off its elimination. The decrease in PpIX content after 72h in the studied cells might have reflected either an efflux of the compound or an increased activity of ferrochelatase, which catalyses the binding of PpIX with iron. The data on PpIX accumulation in endometrial cells, as related to the presence of 17ß-estradiol or progesterone in the incubation medium, may provide indications as to the menstrual cycle phase(s) in which PDD and/or PDT for endometriosis treatment should be performed. It is concluded that, for the diagnosis and treatment of endometriosis, the hormonal condition of female body must be taken into account.

References

1. Barbieri RL. Etiology and epidemiology of endometriosis. Am J Obstet Gynecol, 1990; 162: 565-7.

2. Walter AJ, Hentz JG, Magtibay PM, Cornella JL, Magrina JF. Endometriosis: correlation between histologic and visual findings at laparoscopy. Am J Obstet Gynecol, 2001; 184: 1407-11.

3. Fehr MK, Wyss P, Tromberg BJ, Krasieva T, DiSaia PJ, Lin F, Tadir Y. Selective photosensitizer localization in the human endometrium after intrauterine application of 5-aminolevulinic acid. Am J Obstet Gynecol, 1996; 175: 1253-9.

4. Roy BN, Van Vugt DA, Weagle GE, Pottier RH, Reid RL. Effect of 5-aminolevulinic acid dose and estrogen on protoporphyrin IX concentrations in the rat uterus. J Soc Gynecol Invest, 1997; 4: 40-6.

5. Wyss P, Caduff R, Tadir Y, Degen A, Wagnieres G, Schwarz V, Haller U, Fehr M. Photodynamic endometrial ablation: morphological study. Lasers Surg Med, 2003; 32: 305-9.

6. Krzemien A, Van Vugt DA, Fletcher WA, Reid R. Effectiveness of photodynamic ablation for destruction of endometrial explants in a rat endometriosis model. Fert Sterility, 2002; 78: 169-75.

7. Ryan IP, Schriock ED, Taylor RN. Isolation, Characterization, and Comparison of Human Endometrial and Endometriosis Cells in Vitro. J Clin Endocrinology Metab, 1994; 78: 125-30.

8. Midgley HR: Hafezy ESE, Evans TN (red): Human Reproduction, Harper and Row; 1973.

9. Wołuń-Cholewa M, Warchoł W. Effect of 5-aminolevulinic acid on kinetics of protoporphyrin IX production in CHO cells. Folia Histochem Cytobiol, 2004; 42: 131-5.

10. Bartosova J, Hrkal Z. Accumulation of protoporphyrin-IX (PpIX) in leukemic cell lines following induction by 5-aminolevulinic acid (ALA). Comp Biochem Physiol, 2000; 126: 245-52.

Male gonadal function before and after chemotherapy in prepubertal boys

Krawczuk-Rybak M[1], Solarz E[1], Wołczyński S[2]

[1]1Department of Paediatric Oncology, [2]Department of Gynaecological Endocrinology,
Medical University of Białystok, Poland

Abstract

We evaluated gonadal function in twenty prepubertal boys (6.87 ± 3.84 years old) at diagnosis and 2.5 ± 1.6 years after treatment for acute lymphoblastic leukaemia (ALL). We measured serum levels of inhibin B (RIA method), testosterone, FSH, LH (immunoenzymatic methods) and compared the results with controls (31 healthy boys in prepubertal stage). Results: Serum inhibin B levels were lower at diagnosis (55.81 ng/ml ± 33.74), comparing to respective values in the controls (105.89 ng/ml ± 46.64), $p<0.0002$. The values of inhibin B slightly augmented after 2.5 ± 1.6 years from chemotherapy (79.47ng/ml ± 47.39), $p<0.06$ but remained lower than those in the controls ($p<0.07$). We did not find any differences in FSH, LH or testosterone values, before and after chemotherapy, comparing to respective values in the controls. In conclusion, haematological malignancy and its treatment influence gonadal function before puberty with a possibility of recovery. During this period, inhibin B could be used as a sensitive indicator of testicular function.

Key words: acute lymphoblastic leukaemia, late effects, male infertility, children, inhibin B.

Introduction

Endocrine abnormalities are a common late effect of anticancer treatment, both in children and adults, including pituitary, thyroid and gonadal dysfunction [1]. Male gonads have two important functions: spermatogenesis and steroidogenesis. The production of testosterone and 17 b-estradiol by Leydig cells is under control of the hypothalamus and the pituitary gland (LH, luteinizing hormone). Follicle stimulating hormone (FSH) influences Sertoli cells to stimulate the release of a protein - inhibin B - which exerts a negative feedback of FSH secretion [2].

Gonadal damage, induced by neoplastic process per se or by chemotherapy and/or radiotherapy, affects both components of gonadal function, resulting in infertility and sexual dysfunction, which may compromise the quality of life of the survivors [1].

We do not have an unambiguous opinion if the testicular injury after anticancer treatment in boys is similar in prepubertal and pubertal stage. In this study, we evaluated the gonadal function in prepubertal boys, treated for acute lymphoblastic leukaemia (ALL).

Patients and methods

Twenty boys, at the mean age of 6.87 ± 3.84 years (at diagnosis), in Tanner stage I or II, were studied before and 2.5 ± 1.63 years after the treatment for ALL, according to BFM 90 protocol. Thirty-one healthy boys in a similar age (6.87 ± 2.41years old) were examined as controls.

We determined serum concentrations of inhibin B (radioimmunoassay method) and FSH, LH and testosterone (immunoenzymatic methods).

The study was approved by the local ethics committee.

Results

Serum inhibin B levels were lower at diagnosis (55.81 ng/ml ± 33.74), in comparison to the results, obtained in the control group (105.89 ng/ml ± 46.64), $p<0.0002$. After

ADDRESS FOR CORRESPONDENCE:
Maryna Krawczuk-Rybak
Department of Paediatric Oncology
Medical University of Białystok
Waszyngtona 17; 15-274 Białystok, Poland
e-mail: rybak@amb.edu.pl , fax. (085) 74 50 846

Table 1. Values of inhibin B, FSH, LH, testosterone, before and after antileukaemic treatment in prepubertal boys and in the control group.

	Before treatment	After treatment	Controls
Inhibin B (ng/l)	55.81 ± 33.74*	79.55 ± 47.39	105.89 ± 46.61
Testosterone (ng/dl)	13.58 ± 4.96	29.83 ± 36.5	25.9 ± 20.17
FSH (mIU/ml)	1.53 ± 1.19	2.31 ± 4.19	2.5 ± 1.8
LH (mIU/ml)	0.6 ± 0.7	1.43 ± 4.16	0.7 ± 0.9

*p<0.0002 between the values obtained before treatment and controls

Figure 1. Inhibin B values before and after treatment vs. controls

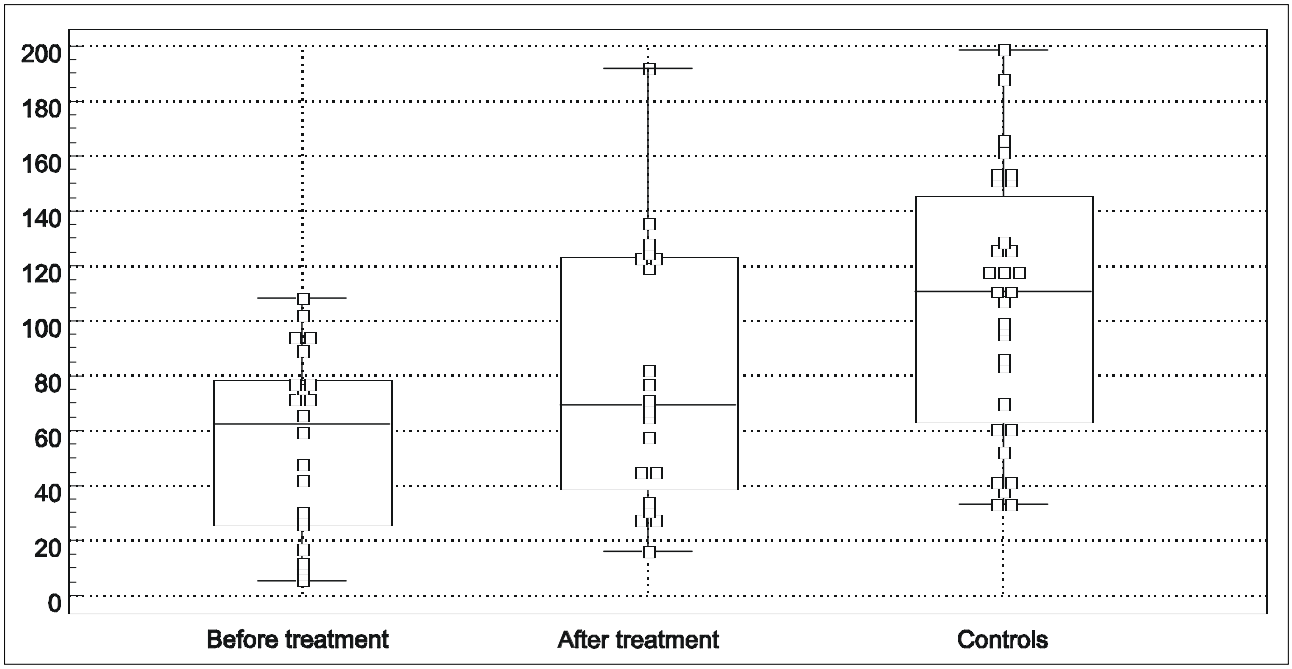

chemotherapy, the values of inhibin B augmented slightly (79.55 ng/ml ± 47.39), p<0.06 but remained lower than those in the controls (p<0.07). Tab 1. Fig.1.

We did not observe any differences in FSH, LH and testosterone values either before or after the treatment or in comparison to respective values in the controls. Tab.1.

We did not find any correlations between inhibin B and FSH values either before (r = -0.39 p = 0.21) or after the treatment (r = 0.31 p < 0.21).

Discussion

Examination of testicular function is easy in pubertal and post-pubertal boys, using routine hormone assays, whereas in prepubertal boys, it is difficult, due to a low activity of the hypothalamic-pituitary-gonadal axis. The measured level of serum inhibin B seems to be a good marker of testicular function, not only in adult men but also in young, prepubertal boys. During infancy, serum inhibin B is high and gradually decreases to the nadir at 6-10 years of age and, after an increase in early adolescence, it reaches a plateau in age 12 to 16 years. In younger age, inhibin values rest independent of FSH values, whereas an inverse relationship between inhibin B and FSH appears in puberty [2].

Cytostatics, especially alkylating agents, such as cyclophosphamide, cisplatin, procarbazine and/or abdominal irradiation, cause gonadal damage, inhibit DNA synthesis in differentiating spermatogonia, induce germinal aplasia and cause the absence of sperm in seminal fluid [1, 3]. Sperm production is more susceptible to damage at very low doses of irradiation (>1.2 Gy), whereas Leydig cell function is usually preserved up to 12 Gy [1]. Taking into consideration that Sertoli cells are more affected during anticancer treatment, it seems that inhibin B is a good marker to monitor the chemotherapy-induced testicular damage in adults, as well as in children [3].

The influence of age or pubertal stage at the time of treatment on a gonadal function in future has been discussed [4, 5]. Prepuberty, in predominant opinions, does not protect the male gonads from the late effects of chemotherapy, although some analysis suggest that prepubertal boys would be more resistant than adults to the effects of chemotherapy [1, 4]. Crofton et al. found normal values of inhibin B in prepubertal boys (before, during and after the treatment) [4]. In Kenney et al.'s opinion, infertility could be observed irrespectively of the pubertal status at the time of treatment in men, treated with high (>25g/m2) doses of cyclophosphamide [6].In our analysis, concerning prepubertal boys, we observed lower values of inhibin B at the time of diagnosis, comparing to respective values in the controls. The results, obtained some years after the end of the treatment, indicated a tendency towards higher values of inhibin B, in comparison to the results before the treatment (in the second part of analysis, more patients were in the 2nd stage of puberty). It suggests a possibility that a part of stem spermatogonia can survive

the cytotoxic treatment and spermatogenesis can restart after some years. Byrne et al. observed normal fertility in men, treated during childhood for ALL except for the men, receiving cranial irradiation (24Gy) before the age of 10 years [7]. In our group, cranial irradiation was not used.

We did not find any changes in either LH or testosterone production, which affirms the observation that Leydig cells are less susceptible to chemotherapy than Sertoli cells [1].

It is difficult to explain the low values of inhibin B in children at diagnosis. Semen abnormalities were found by Rueffer et al. in men with advanced stage of Hodgkin's disease prior to treatment. The authors suggested gonadal damage either by the disease itself or by cytokines, influencing spermatogenesis [8]. None of the patients in our group had, at diagnosis, any clinical symptoms of testicular infiltration by leukaemic process. This problem needs future observations in greater group.

In conclusion, haematological malignancy and its treatment influence gonadal function before puberty but with a possibility of recovery. During this period, inhibin B could be used as a sensitive indicator of testicular function.

References

1. Wallace H. Late endocrine effects of cancer treatment in childhood, Colwood House Medical Publications (UK) Ltd, 1994.

2. Crofton PM, Evans AEM, Groome NP, Taylor MRH, Holland CV, Kelnar CJH. Inhibin B in boys from birth to adulthood: relationship with age, pubertal stage, FSH and testosterone. Clin Endocrinol, 2002; 56: 215-21.

3. Cicognani A, Cacciari E, Pasini A, Burnelli R, De Iasio R, Pirazzoli P, Paolucci G. Low serum inhibin B levels as a marker of testicular damage after treatment for a childhood malignancy. Eur J Pediatr, 2000; 159: 103-7.

4. Crofton PM, Thomson AB, Evans AEM, Groome NP, Bath LE, Kelnar CJH, Wallace WHB. Is Inhibin B a potential marker of gonadotoxicity in prepubertal children treated for cancer? Clin Endocrinol, 2003; 58: 296.

5. Ciognoni A, Pasini A, Pession A, Pirazzoli P, Burnelli R, Barbieri E, Mazzanti L, Cacciari E. Gonadal function and pubertal development after treatment of childhood malignancy. J Pediatr Endocrinol Metab, 2003;16: 321-26.

6. Kenney LB, Laufer MR, Grant FD, Grier H, Diller L. High risk of infertility and long term gonadal damage in males treated with high dose Cyclophosphamide for sarcoma during childhood. Cancer, 2001;91:613-21.

7. Byrne J, Fears TR, Mills JL, Zeltzer LK, Sklar Ch, Meadows AT, Reaman GH, Robison LL. Fertility of long-term male survivors of acute lymphoblastic leukemia diagnosed during childhood. Ped Blood Cancer, 2004; 42: 364-72.

8. Rueffer U, Breuer K, Josting A, Lathan B, Sieber M, Manzke O, Grotenhermen F-J, Tesch H, Bredenfeld H, Koch P, Nisters-Backes H, Wolf J, Engert A & Diehl V. Male gonadal dysfunction in patients with Hodgkin's disease prior to treatment. Ann Oncol, 2001; 12:1307-11.

Experimental osteoporosis- different methods of ovariectomy in female white rats

Lasota A, Danowska-Klonowska D

Department of Cytophysiology, Histology and Embryology, Medical University of Lodz, Poland

Abstract

Rats are currently principal laboratory animals, used to investigate osteoporosis. The aim of the study was to present and compare two operative methods of inducing osteoporosis in rats. Materials and Methods: Ten 3 months old female Wistar rats were divided into two groups with five animals in each group. In the first group, ovariectomy was preceded by a midline dorsal skin incision, 3cm long. After removing the ovary, the previous incision of the muscle required suturing. In the second group, ovariectomy was performed by two dorso-lateral incisions, approximately 1 cm long above the ovaries. With the use of a sharp dissecting scissors, the skin was cut almost together with the dorsal muscles and the peritoneal cavity was accessed. There was no need of muscle suturing. Conclusion: The operation, performed in the second group, was technically easier, less time consuming and less harmful for the used female white rats.

Key words: model of osteoporosis, ovariectomy, female rats.

Introduction

Osteoporosis is a chronic, systemic, metabolic disease of the skeleton, characterised by reduced bone mass, architectural defects and lowered mechanical resistance to injuries, what eventually leads to higher risks of fractures. It is one of the most frequent diseases of the mankind that occurs in every tenth person in the whole world and in every third woman after the fifteenth year of life. In Poland, about 9 million persons are at risk of osteoporosis.

Experimental animal models play an important role in improving the knowledge of the aetiology, pathophysiology, and diagnosis, as well as on preventive and therapeutical techniques, regarding osteoporosis. Rats are currently principal laboratory animals, used to investigate this disease, since they are inexpensive to maintain, grow rapidly, have a relatively short lifespan and are widely available [1, 2]. There are also various methods of obtaining a standardised pattern of osteoporosis, such as, for example, low calcium diet, LHRH agonists or ovariectomy [2, 3]. The latter one is considered to be the procedure that gives reliable model of osteoporosis [4, 5]. Ovariectomy itself can be performed in some different ways. The choice of operative method is very important, particularly, when it is necessary to operate of a few dozen animals in a short time.

The aim of the study was to present and compare two operative methods, regarding the duration of procedure, the degree of difficulty of operative technique and access to gonads.

Materials and Methods

Ten 3- month old female Wistar rats weighing approximately 180 g were divided into two groups per five rats. In both groups operation was made after placing an animal on its ventral surface. In the first group, ovariectomy was preceded by a midline dorsal skin incision, 3 cm long, approximately half way between the middle of the back and the base of the tail (Fig. 1). Incisions of the muscles were made bilaterally. After peritoneal cavity was accessed, the ovary was found, surrounded by a variable amount of fat. Ligation of the blood vessels was necessary. The connection between the Fallopian tube and the uterine horn was cut and the ovary moved out. Because of muscle bleeding, its incision required suturing. Three single catgut stitches were

ADDRESS FOR CORRESPONDENCE:
Aneta Lasota
Department of Cytophysiology, Histology and Embryology
Medical University of Łódź
Narutowicza 60; 90-136 Łódź, Poland
e-mail: acharazka@op.pl

Table 1.

Investigated group of rats	The manner of incision	The mean time from the incision of the muscle to the ovary removal (minutes)	Muscle suturing
The first group n=5	Single midline dorsal 3cm long	4,7	Yes
The second group n=5	Two dorso-lateral 1cm long	1,6	No

Figure 1. Longitudinal, dorsal midline skin incision.

Figure 2. Three single catgut stitches on the skin wound.

Figure 3. Two dorso-lateral incisions of the skin and muscles.

Figure 4. One single catgut suture on the skin wound.

placed on the skin (Fig. 2). In the second group, ovariectomy was made by two dorso-lateral incisions, approximately 1 cm long above the ovaries (Fig. 3). With the use of a sharp dissecting scissors, the skin was cut almost together with the dorsal muscles and the peritoneal cavity was thus accessed. The further part of the operation was parallel to the one in the first group. The muscle incision required no suturing. Skin wounds were closed bilaterally with one single catgut suture (Fig. 4).

The obtained results are presented in Table 1. In the first group, the mean time from incision of the muscle to the ovary removal was 4.7 minutes, whereas in the second group, it was 1.7 minutes only. That fact signifies the importance of precise muscle incision, what results in a quick location of the ovary. Otherwise, wrongly configured and inordinately large muscle incision leads to bleeding and demands stitching.

Conclusion

Comparing the two presented methods of ovariectomy, we affirm that the operation, as conducted in the second group, was technically easier, less time consuming and less harmful for the female white rats.

References

1. Giardino R, Fini M, Giaversi G, Mongiorgi R, Gnudi S, Zati A. Experimental surgical model in osteoporosis study.Bollettino della Societa Italiana di Biologia Sperimentale. 1993; 69(7-8): 453-60

2. Turner RT, Maran A, LotinunS, Hefferan T, Evans GL, Zhang M, Sibonga JD. Animal models for osteoporosis. Reviews in Endocrine and Metabolic Disorders, 2001; 2: 117-27.

3. Geddes AD. Animal models of bone disease. In: Principals of Bone Biology. Bilezikians JP, Raisz LG, Rodan GA, editors. San Diego: Academic Press; 1996, p.1343-54.

4. Yamazaki I, Yamaguchi H. Characteristics of an ovariectomized osteopenic rat model. Journal of Bone Mineral Research, 1989; 13-22.

5. Gurkan L, Ekeland A, Gautvik KM, Langeland N, Ronningen H, Solheim LF.Bone changes after castration in rats. A model for osteoporosis. Acta Orthopedica Scandinavia, 1986; 57 (1): 67-70.

Activity of thyroid parafollicular (C) cells in rats with hyperthyroidism - preliminary ultrastructural investigations

Dadan J[1], Zbucki R[2], Andrzejewska A[3], Winnicka MM[2], Puchalski Z[1]

[1]1st Department of General and Endocrinological Surgery, [2] Department of General and Experimental Pathology,
[3] Department of Clinical Pathomorphology, Medical University, Białystok, Poland

Abstract

In the thyroid gland of mammals, except the basic follicular (F) cells, parafollicular (C) cells are detected. They belong to disperse neuroendocrine cells of the APUD system. Co-localisation of F and C cells in the thyroid gland is not accidental. It seems possible that there is an interaction between them, mediated by the peptidergic hormones. Calcitonin (CT) is proposed as an essential indicator of C cells. The role of C cells in the function of the thyroid gland has been not clarified till now, especially in hyperthyroid state. There are only a few data which document the ultrastructure of C cells in the physiological and pathological state. In the present study, the ultrastructure of thyroid C cells in an experimental model of hyperthyroidism was evaluated. Our preliminary study may confirm the functional interaction between follicular and parafollicular cells in the thyroid gland.

Key words: C cells, hyperthyroidism, calcitonin, ultrastructure.

Introduction

The ultrastructure of the parafollicular C cells is quite similar in all the experimental mammalian species and differs from the ultrastructure of the follicular C cells. Its important characters include: numerous, spherical and electron, densely delineated by cell membrane [1]. Normally, the grain size does not exceed 200nm and consists of homogeny and electron dense material. C cells are closely linked to the base of the F cell neighbouring follicle. Neither desmosoms nor any other type of epithelial connections exists between them. The basal membrane is common for the follicle and is linked to its C cells. An exact analysis of the further series of slices shows that, generally, the group of C cells, lying in the loose connective tissue between follicles has a common basal membrane with the neighbouring follicle [2].

Under an electron microscope, the structure of C cells is much more multilateral and irregular, as compared to the same structure, when observed under a light microscope [3]. Multilateral structure of C cells dominates frequently observed finger, like dendrites of its cytoplasm. Slightly longer dendrites are arranged along the basal membrane. These are linked directly to the base of F cells or run toward capillaries [4, 5]. Solitary lying C cells are usually bigger then F cells, having bigger oval or spherical nucleus. In many mammals, a frequent depression in the nuclear membrane can be observed. Chromatin is present as either a minute scattered structure or as a small dense material in the periphery of the nucleus. In the nuclear membrane, numerous nuclear pores are present. The nucleolus is big, electron dense, single and rarely double. Secreting granules, differing in size, accumulate in the region of cells, which are directly linked with capillaries [6, 7]. In spite of the very characteristic and different ultrastructure of the F cells and different hormonal function, there exists much evidence, showing a close structural and functional relationship between F and C cells. According to many authors, the co-operation between F and C cells is realized by the paracrine roots, by the synthesis of regulatory peptides RP, the number of which is constantly increasing. C cells are not only closely linked to the base of the F cells of its follicle but they also lie together with them in the space, surrounded by basal membrane. Some authors even differentiate a special functional group in the thyroid structure, in a form of group of follicles (epitheliomers), lying in appropriate bifurcated spaces, covered by the common basal membrane. Generated

ADDRESS FOR CORRESPONDENCE:
Jacek Dadan
1stDepartment of General and Endocrinological Surgery
Medical University of Białystok
M. Skłodowskiej-Curie 24A, 15-276 Białystok, Poland
e-mail: klchirog@amb.edu.pl

Figure 1. The thyroid gland of a control rat. Electron micrograph, showing parafollicular cell, which contains granules, filled with a homogenous substance of low and high density. x 7000

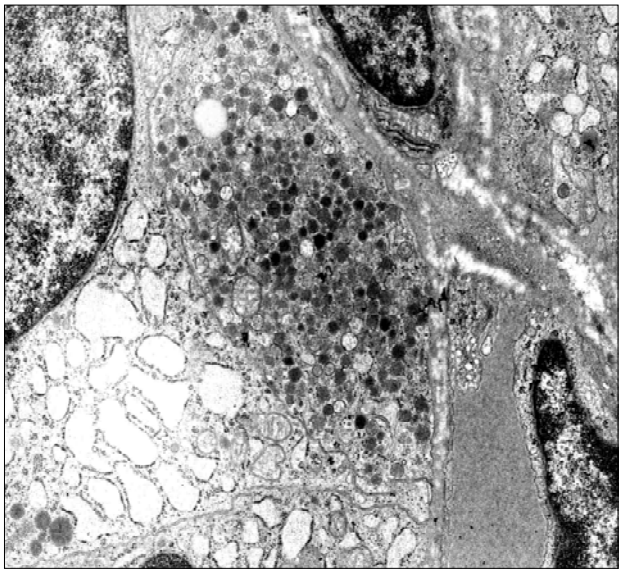

Figure 2. The thyroid gland of a rat with hyperthyroidism. Electron micrograph, showing parafollicular cell, fullfilled with dense granules. x 7000

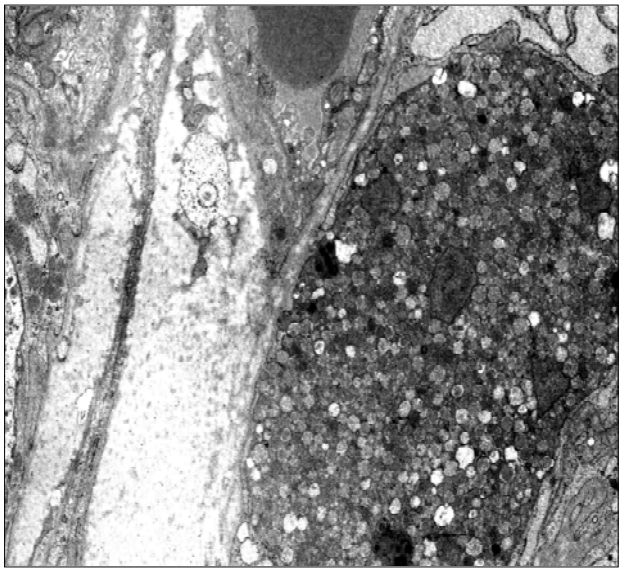

in this way, a new micro environment for the F and C cells is separated from the capillaries by the basal membrane, through which their endocrine function is realised. Due to such a structure, active biological factors, coming either from direct surrounding or from the distal tissue, can interact with the F and C cells. In this way, this complex structure, consisting of two different types of cells, is integrated with the functions of the whole organism. Simultaneously, the micro environment, formed in this way, enables an effective co-operation between cells by the paracrine root.

Material and methods

An experimental model of hyperthyroidism was induced by intraperitoneal injection of L-thyroxine (Sigma Chemical Co) at a dose of 40 μg/kg daily over 30 days. A group of ten control rats were treated with saline under the same experimental conditions. Male Wistar rats (n=18), weighing 90 - 100 g, were used in the experiment and given standard laboratory chow and water ad libitum. The animals were housed at 20° C and constant humidity, with the 12/12 light/dark cycle. All the procedures were performed in compliance with the European Community Council Directive of 24 November 1986 (86/609/EEC) and were approved by the Local Ethics Committee in Białystok.

At the end of the experiment, under pentobarbital sodium anaesthesia (50 mg/kg), blood was collected from the abdominal aorta of each rat to determine plasma TSH concentrations by radioimmunoassay (RIA). Subsequently, the rats were thyreoidectomized. The tissue, taken for examination, was cut into approximately 1 μm-thick sections and fixed for an hour at room temperature in 2.5% glutaraldehyde solution, prepared in 0.1M phosphate buffer (pH 7.4) and then, for the next 12 hours, in temperature of 4° C. During the subsequent stage, lasting from 17 to 20 hours, the tissue was rinsed in phosphate buffer and fixed for the following 2 hours in 1% OsO_4 solution, prepared in phosphate buffer (pH 7.4).

The material, prepared and fixed according to the routine procedure, was embedded in Epon 812 and sectioned by means of an ultramicrotome. Ultra thin sections of the thyroid glands were contrasted by uranyl acetate and amonium citrate and subsequently examined under TEM (Opton 900 PC type).

Results and discussion

Hyperthyroidism is a pathological syndrome in which tissue is exposed to excessive amounts of circulating thyroid hormone. The diagnosis of hyperthyroidism is generally straightforward, with raised serum thyroid hormones and suppressed serum thyrotropin. After 30 days of L-thyroxine treatment, plasma TSH concentration was significantly ($p<0.001$) reduced (mean 0.52 ng/ml), as compared to respective values in the control rats (mean 2.34 ng/ml). Calcitonin plasma level was also significantly ($p<0.05$) reduced (mean 13.34 pg/ml) in comparison to that in the control group (mean 16.69 g/ml). Clear changes in the construction of the ultrastructure existed among the experimental groups of rats. In rats with a low concentration of TSH, a tendency towards low activity of F and C cells was observed, particularly in comparison to respective values in the control group. Microvilli which penetrate within colloid were lower and less numerous. In the cytoplasm near microvilli less number of reabsorbing vacuoles and secreting granules were found. Apart from this, a decreased activity of the rough endoplasmic reticulum, its expansion, less regular shape and less dense ribosomes on the external cytoplasmic surface of its membrane were observed. Mitochondria had much spherical and less comb shape. C cells, situated in the direct neighbourhood of the F cells and surrounded by the common basal membrane, showed the presence of numerous, dark secreting granules, and an irregular cell nucleus, different from that in the control group of rats.

Ultrastructural diagnostic results, obtained from the control group, confirmed the characteristic feature of C cell structure and its colocation with F cell (Fig. 1). In order to examine the activity of the cells, certain points were taken into consideration, mainly the epithelial appearance, microcosmic, rough endoplasmic reticulum, cell nucleus, reabsorbing vacuoles and secreting granules. Ultrastructure of thyroid obtained from rats treated with L-thyroxine showed decreased of activity of endocrine cells, both F and C cells, mainly less numerous, low microvilli near which in the cytoplasm were found less number of reabsorbing vacuoles. Apart from this, a decreased activity of rough endoplasmic reticulum was observed. C cells, situated in the neighbourhood of F cells and together with them, surrounded by the common basal membrane, showed the presence of numerous, dark secretary granules and and irregular nucleus, different from that in the control group (Fig. 2).

Ultrastructural diagnostic results coincide with the previously proved immunoactivity of C cells, defined, using the immunohistochemical technique [8]. In the control group of rats, in C cell, dark and light secretary granules always existed, particularly in the perivascular area. In the cytoplasm of the rats, which received thyroxine, a higher number of secretary grains were observed, which may indirectly indicate an increased accumulation of the regulatory peptides. Cell nuclei in this group of rats were smaller and, some of them, were irregular, as compared to those in the control group.

Preliminary results of these experiments and ultrastructural diagnosis are very promising, forming an ideal supplement of the immunohistochemical diagnosis, proving the theory of close cooperation between C and F cells in the thyroid gland, both in physiological and pathological conditions. According to the authors, there is a justified need for the continuation of these experiments by taking molecular biology technique into account.

Acknowlegments

The study was supported by KBN grant No 1-40-065.

References

1. Ekholm R, Ericson LE. The ultrastructur of the parafollicular cells of the thyroid gland in the rat. J Ultrastruct Res, 1968; 23: 378-402.

2. Lupulescu A, Petrovici A. Ultrastructure of thyroid gland. Buchdruckerei Hutter AG, Reinach BL. 1968.

3. Teitelbaum SL, Moore KE, Shieber W. Parafollicular cells in the normal human thyroid. Nature, London, 1971; 230: 334-5.

4. Alumets J, Hakanson R, Lundqvist G, Sundler F, Thorell J. Ontogeny and ultrastructure of somatostatin and calcitonin cells in the thyroid gland of the rat. Cell Tissue Res, 1980; 206: 193-201.

5. Welsch U, Flitney E, Pearse AGE. Comparative studies on the ultrastructure of the thyroid parafollicular C cells. J Microsc, 1969; 89: 83-94.

6. Atack CV, Ericson LE, Melander A. Intracellular distribution of amines and calcitonin in the sheep thyroid gland. J Ultrastruct Res, 1972; 41: 484-98.

7. Fortney JA. Light and electron microscopic observations of thyroid parafollicular cells of opossum. Gen. Comp. Endocrinol, 1978; 36: 119-32.

8. Dadan J, Zbucki R, Sawicki B, Bialuk I, Zawadzka A, Winnicka MM, Puchalski Z. Preliminary immunohistochemical investigations of thyroid C cells in an experimental model of hyperthyroidism. Folia Morphol, 2003; 62: 319-21.

Activity of thyroid parafollicular (C) cells in rats with hyperthyroidism - immunohistochemical investigations

Dadan J[1], Zbucki RŁ[2], Sawicki B[3], Winnicka MM [2], Puchalski Z[1]

[1] 1st Department of General and Endocrinological Surgery, [2]Department of General and Experimental Pathology
[3]Department of Histology and Embryology, Medical University of Białystok, Poland

Abstract

The aim of this study was an evaluation of the activity of parafollicular (C) cells in a rat experimental model of hyperthyroidism, evoked by an intraperitoneal application of L-thyroxine (40 mg/kg daily) over 15 days. For that reason, immunohistochemical investigations and evaluation of calcitonin (CT) plasma concentrations were performed. Differences in the quantity and distribution, together with enhanced CT-immunoreactivity of C cells, were observed in hyperthyroid rats, in comparison to respective values in the control group, accompanied by a significant diminution of plasma TSH and CT levels. Our preliminary study may point to a functional interaction between follicular and parafollicular cells in the thyroid gland.

Key words: C cells, hyperthyroidism, calcitonin, immunohistochemical study.

Introduction

In the thyroid gland of mammals, except for the basic follicular cells, irregularly distributed cells have been described. The most common name for them is parafollicular cells, or C cells (calcitonin cells). According to Pearse [1], they belong to disperse neuroendocrine cells of the APUD system (amine precursor uptake and decarboxylation) [2]. The role of parafollicular cells in the function of the thyroid gland has not been clarified till now. Despite some controversial data, one could presume that co-localisation of the follicular and the parafollicular cells in the thyroid gland is not incidental. It seems possible that there is some interaction between them, mediated by the release of peptidergic hormones. The kind and amount of the released hormones depend on many factors, e.g., age, sex and health status [3, 4, 5]. Calcitonin (CT), a product of CT/CGRP gene expression, is proposed as an essential indicator of C cells activity [6]. The basic action of calcitonin is the diminution of Ca_{ion}, concentratiom by inhibition of the reabsorption activity of octeoclasts and by facilitation of calcium excretion in the kidneys [6]. The finding that, in homozygotic mice devoid of gene coding calcitonin osteopenia is developed, may indicate that this hormone plays a role in bone tissue homeostasis [7]. Thus, calcitonin is applied in hypercalcemia, Paget's disease and osteoporosis [3]. There are few publications, concerning the evaluation of the structure and function of parafollicular cells in the thyroid gland diseases. There are also only several data, dealing with the problem of the mutual relation between parafollicular and follicular cells in physiological and also in pathological conditions and only single observations, concerning the ectopic production of calcitonin in other tissues [3]. In our previous study, we reported a significant diminution of plasma TSH and CT levels, accompanied by enhanced CT-immunoreactivity in C cells of the thyroid glands in rats, chronically treated (over 30 days) with L-thyroxine [8].

In the present study, a distribution and CT-immunoreactivity of thyroid C cells in an experimental model of hyperthyroidism, evoked by the application of L-thyroxine over 15 days, was evaluated.

ADDRESS FOR CORRESPONDENCE:
Jacek Dadan
1stDepartment of General and Endocrinological Surgery
Medical University of Białystok
M. Skłodowskiej-Curie 24A, 15-276 Białystok, Poland
e-mail: klchirog@amb.edu.pl

Material and methods

Male Wistar rats (n=20), weighing 90 - 100 g each, were used in the experiment and provided with standard laboratory chow and water ad libitum. The animals were housed at 22^0 C and constant humidity, with a 12/12 light/dark cycle. All the pro-

Figure 1. Light micrograph of thyroid gland of control rat. Positive immunohistochemical reaction for calcitonin is observed in most of C cells. x 300.

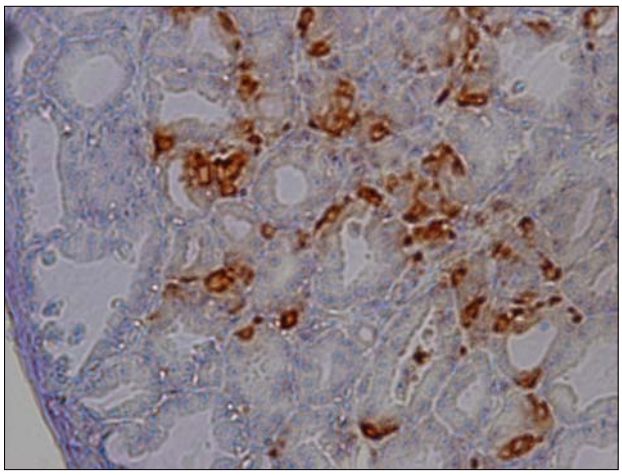

Figure 2. Light micrograph of thyroid gland of rat treated with L-thyroxine. The enhancement of immunohistochemical staining for calcitonin in C cells is observed. x 300.

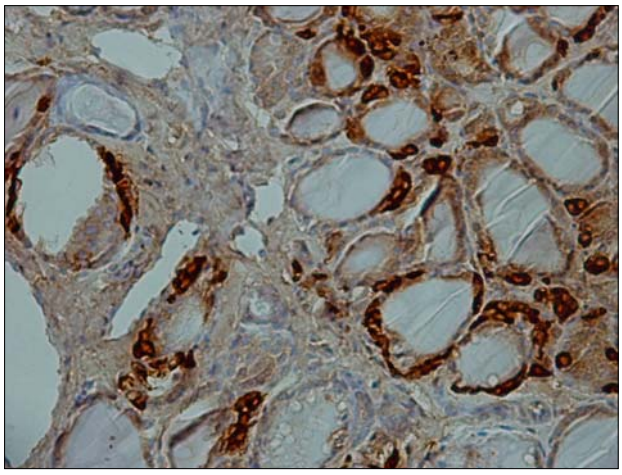

cedures were performed in compliance with the European Union Council Directive of 24th November 1986 (86/609/EEC) and were approved by the Local Ethics Committee in Białystok. The experimental model of hyperthyroidism was induced by an intraperitoneal injection of L-thyroxine (Sigma Chemical Co) at the dose of 40 µg/kg daily over 15 days. A group of ten control rats were treated with saline under the same experimental conditions. At the end of the experiment, under pentobarbital sodium anaesthesia (50 mg/kg), blood was taken from the abdominal aorta of each rat to determine plasma TSH and CT concentrations by radioimmunoassay (RIA). Subsequently, the rats were thyreoidectomized. Both thyroid lobes were placed in Bouin's fluid for 24 hours. An immunohistochemical reaction, used for detecting calcitonin in C cells, was conducted on 5 µm-thick paraffin sections, derived from the thyroid glands. In that procedure, specific rabbit antisera against calcitonin, which can be found only in C cells, were used. In the above immunohistochemical study, the ABC (avidin-biotin peroxidase complex) method was applied, according to Hsu et al. [9].

Results and discussion

After 15 days of L-thyroxine treatment, plasma TSH concentration was significantly ($p<0,0004$) reduced (mean 0.52 µIU/ml), as compared to the respective value in the control rats (mean 2.89 µIU/ml). Moreover, CT plasma level was also significantly ($p<0,0004$) attenuated (mean 13.54 pg/ml), in comparison to that in the control group (mean 16.43 pg/ml).

The reduction of plasma levels of both hormones was similar to those, observed in our previous study in rats, treated with L-thyroxine twice longer, i.e., over 30 days. Also the histological pictures of the thyroid glands, derived from the rats, treated with L-thyroxine for 15 days, was very similar to the pictures of the rats, injected with this hormone for 30 days. As we previously observed, the thyroid sections from the rats, treated with L-thyroxine, showed differences in the size of follicles with a predominance of macrofollicles, full of well-stained, homogenous colloid and enclosed by flattened cuboid epithelium (Fig. 2). Those follicles showed the presence of a few C cells, which were more CT-immunoreactive, in comparison to those in the control group (Fig. 1). On the contrary, the smaller follicles, with higher epithelium, were accompanied by a higher number of parafollicular cells, which were less immunoreactive.

There are only few publications, concerning the activity of parafollicular cells in thyroid gland diseases, as well as, the interaction between parafollicular and follicular cells in vivo. The enhancement of CT plasma concentration, observed in 19.2 % of patients with Graves' disease in our earlier study [4], performed on the thyroid glands, taken from patients with simple and hyperthyroid goitre, together with a weak immunoreactivity for CT within C cells, indicating an increase of their secretion potential, may point to an enhancement of the hormonal activity of C cells, evoked by the hyperactive parafollicular cells during Graves' disease. Also Vierhapper et al. [10], in spite of the high prevalence of thyroid C cell hyperplasia in patients with Graves' disease, observed an elevated CT plasma levels also in some patients with hyperthyroid nodular goitre. Till now, there have been no available data about the activity of C cells in the experimental model of hyperthyroidism. In our previous [8], and also in present investigations, the inhibition of parafollicular cells activity, evoked by an application of L-thyroxine, induced the inhibition of C cells activity, expressed by attenuation of CT plasma levels and by enhanced CT-immunoreactivity in C cells. On the contrary, the overactivation of parafaollicular cells observed in thyroid nodules in patients, operated because of Graves' disease [4], caused hyperactivity of neighbouring C cells. Also, Zabel et al. [11] have demonstrated an enhancement of CT mRNA expression by follicular cells in TT line cell cultures, pointing out to a possible interaction between follicular and TT cells, the latter derived from C cells. These data support the possibility that a direct mutual relation between parafollicular and follicular thyroid cells could play an important role in the regulation of the thyroid gland activity.

Acknowledgements

The study was supported by KBN (Committee of Scientific Research) grant No: 1-40-065.

References

1. Pearse AGE. Common cytochemical and ultrastructural characteristics of cells producing polypeptide hormones (APUD series) and their relevance to thyroid and ultimobranchial C cells and calcitonin. Proc. Roy. Soc. London B, 1968; 170: 71-80.

2. Clark MS, Lanigan TM, Page NM, Russo AF. Induction of a serotonergic and neuronal phenotype in thyroid C cells. J Neurosci, 1995; 15: 6167-78.

3. Dadan J, Zbucki R. Komórki C tarczycy i ich rola. Postępy biologii komórki, 2003; 30: 187-200.

4. Dadan J, Zbucki RŁ, Sawicki B, Winnicka MM, Puchalski Z. Activity of the thyroid parafollicular (C) cells in simple and hyperactive nodular goitre treated surgically - preliminary investigations. Folia Morphol, 2003; 62: 443-5.

5. Guyetant S, Rousselet MC, Durigon M, Chappard D, Franc B, Guerin O, Saint-Andre JP. Sex-related C cell hyperplasia in the normal human thyroid: a quantitative autopsy study. J Clin Endocrinol Metab, 1997; 82: 42-7.

6. Pondel M. Calcitonin and calcitonin receptors: bone and beyond. Int J Pathol, 2000; 81: 405-22.

7. Hoff A, Thomas P, Cote C. Generation of a calcitonin knockout mouse model. Bone, 1998; 23: 164.

8. Dadan J, Zbucki RŁ, Sawicki B, Bialuk I, Zawadzka A, Winnicka MM, Puchalski Z. Preliminary immunohistochemical investigations of thyroid C cells in an experimental model of hyperthyroidism. Folia Morphol, 2003; 62: 319-21.

9. Hsu SM, Raine L, Fanger H. Use of avidin-biotin-peroxidase complex (ABC) in immunoperoxidase techniques: a comparison between ABC and unlabeled antibody (PAP) procedures. J Histochem Cytochem, 1981; 29: 577-80.

10. Vierhapper H, Nowotny P, Bieglmayer C, Gessi A. Prevalence of hypergastrinemia in patients with hyper- and hypothyroidism: Impact for calcitonin? Horm Res, 2002; 57: 85-9.

11. Zabel M, Gębarowska E, Kasprzak A. Control of calcitonin gene expression in thyroid parafollicular cells co-cultured with thyroid follicular cells. Folia Histochem Cytobiol, 1999; 37: 61-2.

Expression of Ki-67, PCNA and MPM2 antigens in follicular cells of the thyroid gland after iodotherapy

Klim B[1], Dzięcioł J[1], Litwiejko-Pietryńczak E[1], Szkudlarek M[1], Pawlak J[1], Oniszczuk S[1], Tobiaszewska D[2]

[1]Department of Human Anatomy, Medical University of Bialystok, [2]Department of Endocrinology and Internal Diseases. Voivodship Hospital in Bialystok, Poland,

Abstract

Hyperfunctional nodular goitre is the most common thyroid non-neoplastic condition in endemic areas. Iodotherapy is the basic method in thyroid gland hyperfunction treatment. The aim of the study was to evaluate proliferation of thyroid follicular cells in nodular goitre after iodotherapy. The study was carried out on 32 women, 30-76 years old. Cytological and immunohistochemical evaluations were based on the material, obtained by Fine-Needle Aspiration Biopsy (FNAB). Proliferative activity was immunohistochemically assessed. The influence of radioiodine on thyroid follicular cells was evaluated as a difference between the proliferation of follicular cells before and after its application. It was concluded that the proliferative activity of thyroid follicular cells decreased considerably after radioiodine therapy.

Key words: hyperthyroidism, iodotherapy, proliferative activity, PCNA, Ki-67, MPM2.

Introduction

One of the most common thyroid gland conditions is the diseases that constitute the complex of symptoms, called hyperfunction. The most frequent illnesses with symptoms of hyperthyroidism include: Graves' disease, multinodular goitre, hyperfunctional autonomous thyroid nodule [1]. The north-east region of Poland is the area of iodine deficiency in which a predominant number of thyroid hyperfunction cases (over 60%) is connected with the presence of autonomous tissue [2, 3, 4]. The environmental iodine deficiency triggers the pathomechanism of thyroid hyperfunction with point mutations, related to TSH receptor, which stimulates thyroid gland growth and the excessive synthesis of its hormones [3, 5]. Iodine deficiency induces the activity of topical growth factors, which results in a decrease of antiproliferative TGF-ß value and an increase of IGF-1 and EGF concentrations [3]. It makes the thyroid tissue more sensitive to TSH activity, what also induces hyperplasia of thyreocytes.

The main lines of treatment of hyperthyroidism include pharmacotherapy (thyreostatics, inhibitors of ß-adrenergic receptors, tranquillisers), radioiodine treatment and surgical treatment [1, 6, 7, 8, 9]. Pharmacotherapy, especially in patients with nodular goitre, should be an introduction to a more radical treatment (thyroid gland surgery or radioiodine therapy) [1, 7, 9]. It has been found that therapeutic doses of iodine have no teratogenic effect and do not influence the human genome. It is considered to be a method of choice in the treatment of hyperthyroidism in all age groups [1, 6, 10].

The aim of the study was to evaluate proliferative activity of thyroid follicular cells in patients with nodular goitre after iodotherapy.

Materials and methods

The study was carried out on 32 women, aged 30 - 76 years. The cytological and immunohistochemical evaluation was performed on material, obtained by US-guided Fine-Needle Aspiration Biopsy (FNAB) and fixed by Cytofix. Proliferative activity was immunohistochemically assessed with the use of antibodies against Proliferating Cell Nuclear Antigen (PCNA), Ki-67 Antigen and Mitotic Proteins (MPM-2) (DAKO) by determination of the percentage of follicular cells, showing a positive reaction to the given antibody [11, 12]. The influence

ADDRESS FOR CORRESPONDENCE:
Beata Klim
Department of Human Anatomy
Medical University of Bialystok
Mickiewicza 2A; 15-089 Białystok , Poland
e-mail: anatomia@amb.edu.pl

Figure 1. Proliferative activity of thyroid cells before and after radioiodine therapy. PA is numerically equal to the mean percentage of cells positive for the respective antigens (PCNA, Ki-67 or MPM2)

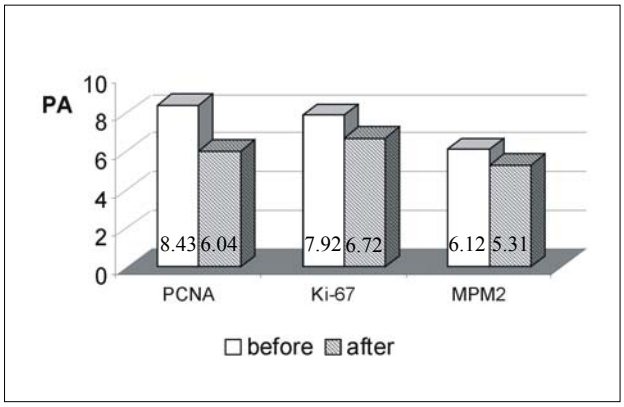

of radioiodine on thyroid follicular cells was evaluated as a difference between proliferative activity of follicular cells before and after iodotherapy. The results were statistically analysed with the Statistica Pl computer software. Student's t test was used for statistical analysis. The difference was considered as significant for $p < 0.05$.

Results

There were no essential morphological differences in the microscopical views of thyroid follicular cells before and after iodotherapy. The proliferative activity of follicular cells, referred to as PCNA before the radioiodine therapy, ranged from 6.1 to 15.4 - the mean value: 8.43, for Ki-67 from 6.39 to 15.61 - the mean value: 7.92 and for MPM-2 from 3.26 to 13.85 - the mean value: 6.12. The obtained values changed under the influence of I^{131} and amounted to: for PCNA: from 3.14 to 10.75 - the mean value: 6.04, for Ki-67 from 2.54 to 11.23 - the mean value: 6.72 and for MPM2 from 1.92 to 9.12 - the mean value: 5.31. Statistically significant differences between the means were found for PCNA, Ki-67 and MPM2, before and after the therapy. (Fig.1)

Discussion and conclusions

Therapeutic effect of I^{131}, mediated by beta radiation, emitted from I^{131} in the tissue. This radiation induced the formation of radioiodine free radicals which damage DNA structure. It results either in cell death or in loss of cell ability to grow and proliferate. Histological alterations include interstitial oedema, cell necrosis, lymphocyte infiltration and fibrosis [10]. Sporadically, drug-induced complications may appear after the treatment. In the early period after the isotope application, the complications appear in the form of an increased level of hormones, released from damaged follicular cells, hypermetabolic crisis or thyroid inflammation or ophtalmopathy; later on, they are manifested by thyroid hypofunction or, rarely, are observed as parathyroid hypofunction [1, 7, 9, 10, 13]. Nevertheless, this kind of treatment has certain advantages, including good therapeutic effects, scarce recurrences, comfort and comparatively high safety, low costs and the possibility of application to elderly patients [1, 8, 9, 13]. It is worth underlining that the application of radioiodine has been considered to be the best method of treatment of autonomous nodules and hyperfunction of multinodular goitre [6, 9, 13].

Basing on the obtained results, it has been concluded that the proliferative activity of thyroid follicular cells decreased considerably after radioiodine therapy, what indicates the necessity of constant monitoring of patients treated with iodotherapy.

References

1. Bonnema SJ, Bartalena L, Toft AD, Hegedüs L. Controversies in radioiodine therapy: relation to ophthalmopathy, the possible radioprotective effect of antithyroid drugs, and use in large goitres. Eur J Endocrinol, 2002; 147: 1-11.
2. Kristensen H L, Vadstrup S, Knudsen N, Sierback-Nielsen K. Development of hyperthyroidism in nodular goiter and thyroid malignancies in an area of relatively low iodine intake. J Endocrinol Invest, 1995; 18: 41-3.
3. Paschke R, Ludgate M. The Thyrotropin receptor in Thyroid Disease. N Eng J Med, 1997; 337: 1675-81.
4. Dremier S, Coppee F, Delange F, Vassart G, Dumont J E, Van Sande J. Thyroid autonomy: Mechanism and Clinical Effects. J Clin Endocrinol Metab, 1996; 81, 12: 4187-93.
5. Derwahl M, Broecker M, Kraiem Z. Thyrotropin may not be the dominant growth factor in benign and malignant thyroid tumors. 1999; J Clin Endocrinol Metab, 84: 829-34.
6. Allahabadia A, Daykin J, Sheppard MC, Gough SCL, Franklin JA. Radioiodine treatment of hyperthyroidism - prognostic factors for outcome. J Clin Endocrinol Metabol, 1986; 8: 3611-7.
7. Catargi B, Leprat F, Guyot M, Valli N, Ducassou D, Tabarin A. Optimized radioiodine therapy of Graves' disease: analysis of the delivered dose and of other possible factors affecting outcome. Eur J Endocrinol, 1999; 141: 117-21.
8. Franklin JA, Daykin J, Drole Z, Farmer M, Shepard MC. Long-term follow up of treatment of thyrotoxicosis by three different methods. Clin Endocrinol, 1991; 34:71-6.
9. Nygaard B, Hegedüs L, Ulriksen P, Nielsen KG, Hansen JE. Radioiodine therapy for mutinodular toxic goiter. Archiv Intern Med, 1999; 159: 1364-8.
10. Rivkees SA, Sklar C, Freemark M. The management of Graves' disease in children, with special emphasis on radioiodine treatment.. J Clin Endocrinol Metab 1998; 83: 3767-76.
11. Scholzen T, Gerdes J. The Ki-67 protein: from the known and the unknown. J Cell Physiol, 2000; 182: 311-22.
12. Bruno S, Crissman HA, Bauer KD, Darzynkiewicz Z. Changes in cell nuclei during S phrase: progeressive chromatin condensation and altered expression of the proliferation - associated nuclear proteins Ki-67, cyclin (PCNA), p 105, and p 34. Exp Cell Res, 1991; 196: 99-106.
13. Bonnema SJ, Nielsen VE, Hedegüs L. Long-term effects of radioiodine on thyroid function, size and patient satisfaction in non-toxic diffuse goitre. Eur J Endocrinol, 2004; 150: 439-45.

Morphometrical analysis of immunohistochemical reaction of inflammatory infiltrate in chronic thyroiditis

Nieruchalska E, Kaczmarek E, Jarmołowska-Jurczyszyn D, Majewski P

Laboratory of Morphometry and Medical Image Processing, Chair of Pathology
University of Medical Sciences, Poznań, Poland

Abstract

The aim of the study was to quantitatively evaluate B and T lymphocytes and macrophages, based on immunohistochemical investigations (CD43, CD20, CD8 and CD68) of chronic focal and Hashimoto thyroiditis. A new method of image analysis was applied, based on spatial visualization of the antigens reactivity. The obtained results indicated that the numbers of lymphocytes, in particular of cytotoxic T lymphocytes, and of macrophages increased with the progress of inflammatory process. Quantitative measurements of the markers made the results more objective and supported pathomorphological diagnosis.

Keywords: chronic thyroiditis, inflammatory infiltrate, spatial image analysis, measurements.

Introduction

Chronic thyroiditis is a heterogeneous group of diseases, regarding morphology and prognosis. Upon pathomorphological diagnosis of case with thyroiditis, immunohistochemical analysis is used to distinguish chronic focal thyroiditis from Hashimoto thyroiditis. The interpretation of results, obtained from routine visual evaluation in light microscopy and semi-quantitative assessment of immunohistochemical reaction strength, is highly subjective, in particular, in cases suspected to be progressing into Hashimoto thyroiditis. This may be a source of inconsistencies in the diagnosis, caused by diffusion of antigen, non-homogeneous expression of colour reaction in the measurement field and background staining. Therefore, the aim of our study was a quantitative assessment of the elements of inflammatory infiltrate: B and T lymphocytes and macrophages in chronic focal thyroiditis and Hashimoto cases by using a new method of digital image analysis, based on the spatial visualization technique.

ADDRESS FOR CORRESPONDENCE:
Elżbieta Kaczmarek
Laboratory of Morphometry and Medical Image Processing,
Chair of Pathology
University of Medical Sciences, Poznań
Przybyszewskiego 49; 60-355 Poznań, Poland
Tel (061) 869 18 16; e-mail: elka@amp.edu.pl

Material and Methods

Material for our study was obtained after thyroidectomy in patients with chronic focal thyroiditis and Hashimoto thyroiditis and used for immunohistochemical study. Sections were cut from a formalin-fixed and paraffin embedded archival tissue, stained with HE and then immunostained. The immunohistochemical stains were performed for the following antigens: CD20 (DAKO, dilution 1/100) present on B-lymphocytes, CD43 (Dako, dilution 1/100) expressed on the surface of T-lymphocytes, CD8 (Novocastra, dilution 1/40) found on the cytotoxic subset of human T-lymphocytes, CD68 (Dako, dilution 1/100) present on the surface of macrophages. Microscopy images, of 640x480 pixels each, were acquired by using a digital light microscope, running under Motic Images v. 1.2 software for Windows (Micro Optic Industrial Group Co) at 400x magnification. The obtained images were extended to their spatial representation by introducing image brightness as the third dimension. The colour immunohistochemical reaction was exposed on a three-dimensional view by reducing the scenery behind to the background. Then, filters of brightness and saturation were fixed for image series, acquired from each specimen, and colours, representing the immunohistochemical reaction, were extracted. The area and intensity of reaction in three-dimensional space were determined by using a computer program, programmed in C++ by Strzelczyk [1]. The results, obtained for chronic focal thyroiditis and Hashimoto thyroiditis, were compared by using the Mann-Whitney test.

Table 1. Area of positive reaction of the analyzed markers (per μm2).

Markers	Chronic Focal Thyroiditis	Hashimoto Thyroiditis	Significance level (p)
	Mean ± SD	Mean ± SD	
CD 20	0.206 ± 0.282	0.380 ± 0.154	P<0.001
CD 43	0.204 ± 0.236	0.369 ±0.301	P<0.005
CD 8	0.014 ± 0.028	0.836 ± 0.098	P<0.001

Table 2. Intensity of immunohistochemical stains.

Markers	Chronic Focal Thyroiditis	Hashimoto Thyroiditis	Significance level (p)
	Mean ± SD	Mean ± SD	
CD 20	122 ± 29	97 ± 12	P<0.001
CD 43	125 ± 18	101 ± 14	P<0.001
CD 8	144 ± 18	120 ± 12	P<0.001

Figure 1. CD43 in chronic focal thyroiditis (left) and in Hashimoto thyroiditis (right). The lower row shows the spatial representation of original images from the upper row.

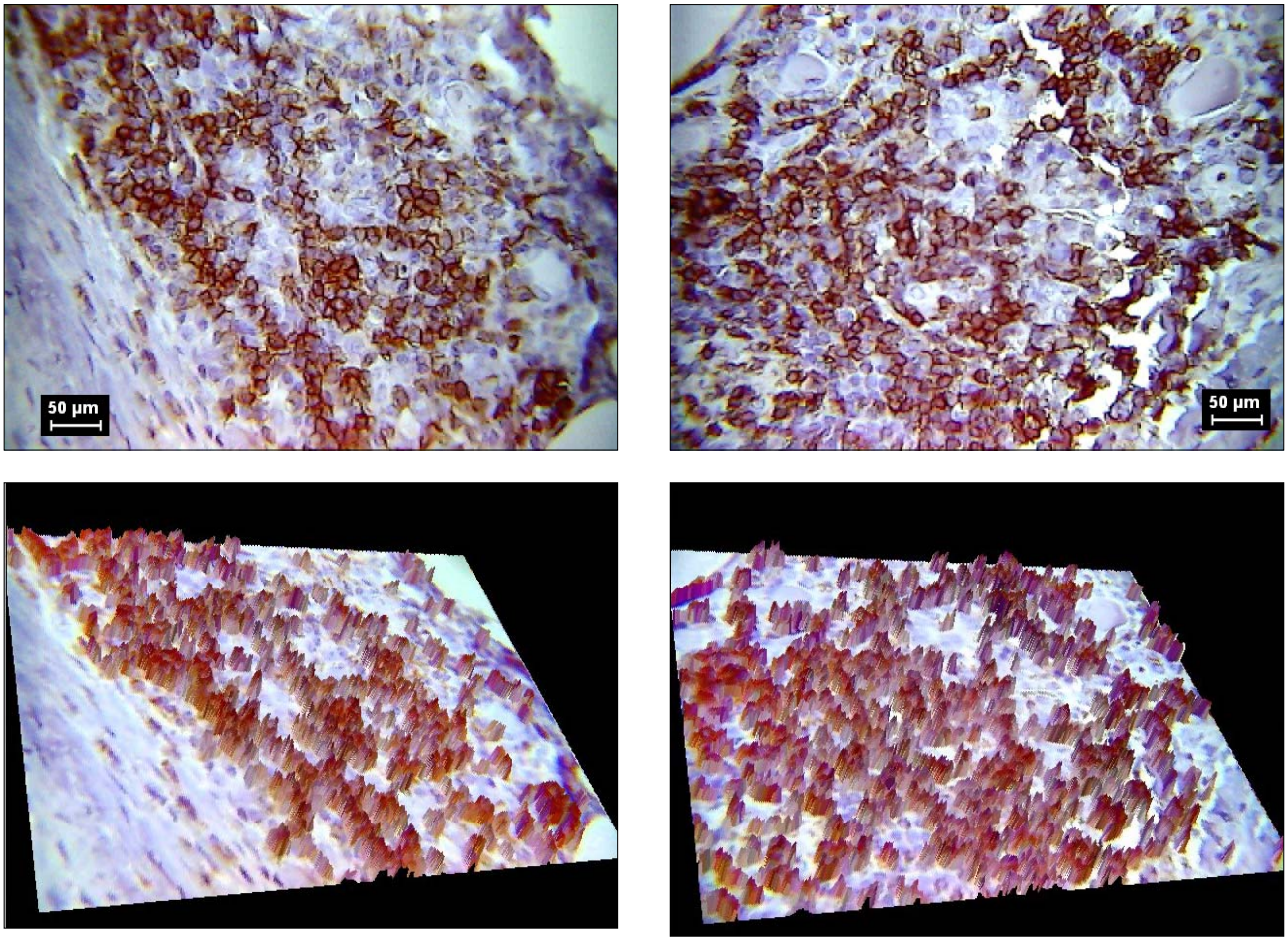

Results

The reactivity of CD43, CD20 and CD8 was significantly lower in chronic focal thyroiditis than in Hashimoto disease (Tab. 1). In particular, numerous cytotoxic T lymphocytes occurred in Hashimoto cases, while in focal thyroiditis, they were less frequent. The average colour intensity of CD43+, CD20+ and CD8+ markers was significantly higher in chronic focal thyroiditis than in Hashimoto disease (Tab. 2). Inflammatory foci areas became larger and larger in the course of disease progress and were occupied by dense clusters of lymphocytes (Figs. 1-2).

The number of macrophages, visualized with CD68 marker, significantly increased in Hashimoto cases (25 ± 11 per image), comparing to respective values in chronic focal thyroiditis (10 ± 8 per image).

Figure 2. CD20 in chronic focal thyroiditis (left) and in Hashimoto thyroiditis (right). The lower row shows the extracted reaction from the original images (upper row).

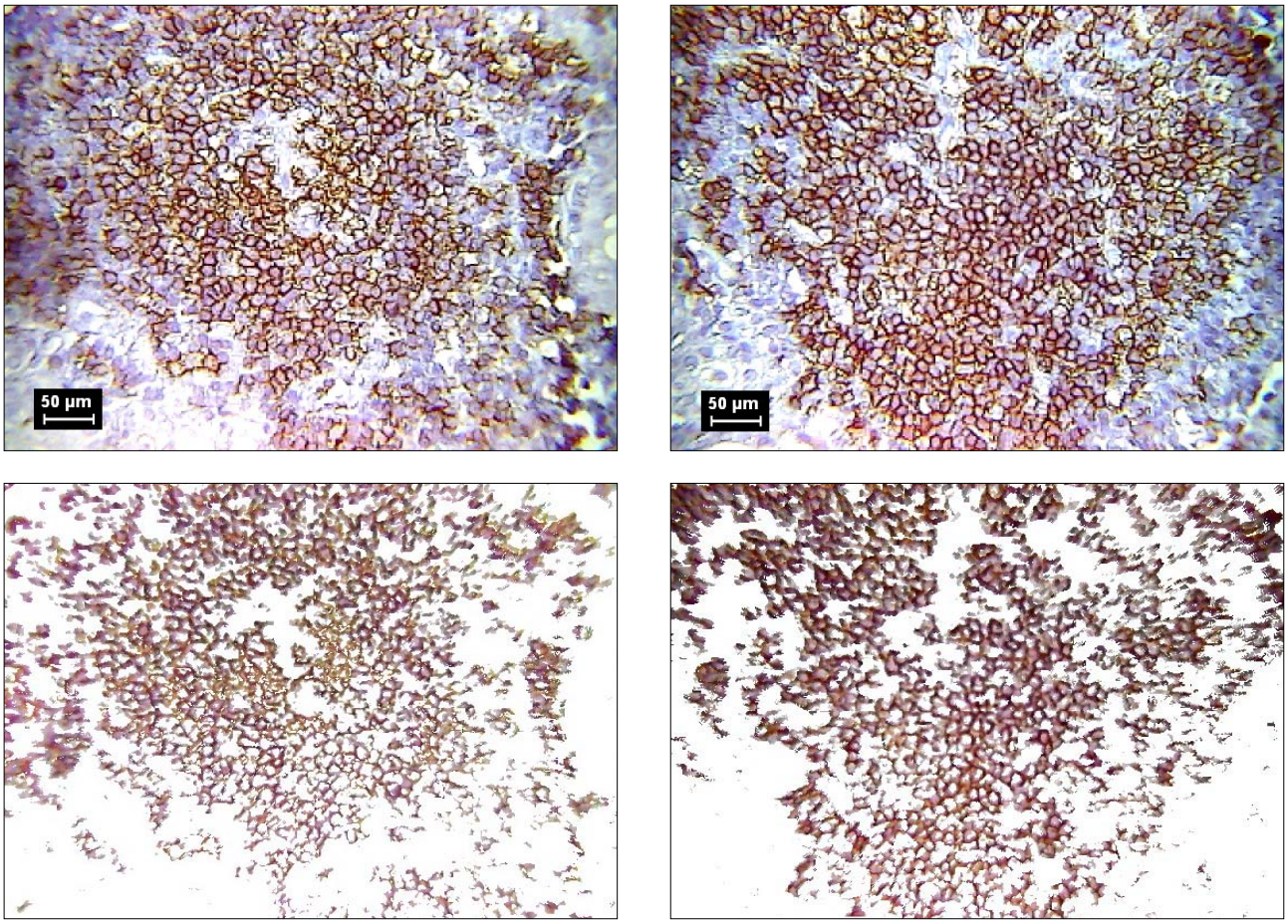

Final remarks

At present, measurements of immunohistochemical reactions in raw colour images make a potential benefit in quantitative studies [2, 3]. The method, based on three-dimensional visualization of the immunohistochemical markers and used in this study, permitted to obtain objective results and indicate extremely significant differences between morphological features of inflammatory foci in chronic thyroiditis and large inflammatory areas in Hashimoto cases. The results indicated that lymphocytes, in particular cytotoxic T lymphocytes, and macrophages increased with the progress of inflammatory process. Lymphocytes were visualized with the markers in light brown colours with dark brown contours (Figs. 1-2). Lower average colour intensity of CD43+, CD20+ and CD8+, observed in chronic focal thyroiditis than that, found in Hashimoto disease (Tab. 2), can be explained by the increasing number of large inflammatory foci in the course of progressing disease. Therefore, the average results of colour intensities were lower. Concluding, quantitative measurements of inflammatory process markers made the results more objective and supported the pathomorphological diagnosis.

References

1. Nieruchalska E, Strzelczyk R, Woźniak A, Żurawski J, Kaczmarek E, Salwa-Żurawska W. A quantitative analysis of the expression of a-smooth muscle action in mesangioproliferative (GnMes) glomerulonephritis. Folia Morph, 2003; 62: 451-3.

2. Matkowskyj K, Schonfeld D, Benya R. Quantitative immunohistochemistry by measuring cumulative signal strength using commercially available software Photoshop and Matlab J Histochem Cytochem, 2000; 48: 163-74.

3. Matkowskyj KA, Cox R, Jensen RT, Benya R. Quantitative immunohistochemistry by measuring cumulative signal strength accurately measures receptor number. J Histochem Cytochem, 2003; 51: 205-14.

Influence of cannabinoids on immunoreactivity of regulatory peptides, produced in rat thyroid C cells; preliminary investigations

Sawicki B[1], Zbucki RŁ[2], Hryniewicz A[2], Kosiorek P[2], Bialuk I[2], Winnicka MM[2], Dadan J[3]

[1]Department of Histology and Embryology, [2]Department of General and Experimental Pathology
[3]1st Department of General and Endocrinological Surgery, Medical University of Białystok, Poland

Abstract

Mammalian tissues contain two types of cannabinoid receptors CB1 and CB2. The aim of our study was an evaluation of the influence of a single ip injection of a stable analogue of an endogenous cannabinoid anandamide - R-(+)-methanandamide (2.5 mg/kg) and CP 55,940 (0.25 mg/kg), which is an exogenous agonist of CB1 receptors, on the immunoreactivity of regulatory peptides, produced in rat thyroid C cells: calcitonin, CGRP, somatostatin and synaptophysin. This study indicates that a single injection of cannabinoids: R-(+)-methanandamide and CP 55,940 alters the immunoreactivity of regulatory peptides in thyroid parafollicular cells.

Key words: thyroid C cells, regulatory peptides, cannabinoids, rat.

Introduction

The psychoactive properties of the marijuana plant, *Cannabis sativa*, have been known for thousands of years. The pharmacological actions of its main active compound,

Δ^9-tetrahydrocannabinol (Δ^9-THC) have recently been documented, following the discovery of two distinct cannabinoid receptors: CB1 (expressed mainly in CNS) and CB2 (that occur mainly in the immune cells) [1]. The identification of naturally occuring ligands for these receptors, anandamide and 2-arachidonylglycerol (2-AG), has prompted a large research effort, aimed at investigating the physiological role of the endogenous cannabinoid system, as well as its potential use as a target for novel therapeutic interventions [1]. Recent studies suggest that endocannabinoids, among others, also play a role in the regulation of the activity of endocrine cells. It has been reported that Δ^9-THC and endocannabinoids exert an inhibitory influence on the regulation of reproduction. An administration of Δ^9-THC and anandamide decreased serum levels of luteinizing hormone and prolactin, while increased the levels of ACTH and corticosterone [1]. Further studies, performed with Δ^9-THC [2], and WIN 55,212-2 [3], a selective CB1 receptors agonist, while showing diminution of T_3 and T_4 plasma levels after a single injection of these compounds, confirmed their influence on the endocrine system. High levels of CB1 mRNA, observed during the late embryological stages of rat thyroid, and the presence of CB1 mRNA and protein in the adult rat thyroid, both in follicular and parafollicular (C) cells, may point to an involvement of cannabinoid receptors in the mediation of the thyroid gland activity [4].

The aim of this study was an evaluation of the influence of a single ip injection of a stable analogue of endogenous cannabinoid anandamide - R-(+)-methanandamide and CP 55,940, an exogenous agonist of CB1 receptors on the immunoreactivity of the regulatory peptides, produced in rat thyroid C cells: calcitonin (CT), CGRP, somatostatin (SS) and synaptophysin (SY).

The study was conducted on 30 male Wistar rats, weighing 180-185 g each, which were divided into 3 groups. All the animals were housed in plastic cages, four animals per cage, in temperature of 22^0 C and constant humidity, with a 12/12 light/dark cycle. Food and water were freely accessible. All the procedures were performed in compliance with the European Communities Council Directive of the 24th November 1986 (86/609/EEC) and were approved by the Local Ethics Committee in Białystok. R-(+)-Methanandamide and CP 55,940 (Tocris), dissolved in 19% solution of 2-hydroxypropyl-B-cyclodextrin (RBI) were injected once, at the intraperitoneal dose of 2.5 mg/kg or 0.25 mg/kg, respectively. The control rats

ADDRESS FOR CORRESPONDENCE:
Bogusław Sawicki
Department of Histology and Embryology
Medical University of Białystok
Kilińskiego 1; 15-089 Białystok, Poland
Tel. +48 85 748 54 54; e-mail: sawboghe@amb.edu.pl

Figure 1. CGRP-immunoreactivity: A) Thyroid gland of control rats (x 200); B) Thyroid gland of rats treated with R-(+)-methanandamide (x 200); C) Thyroid gland of rats treated with CP 55,940 (x 400).

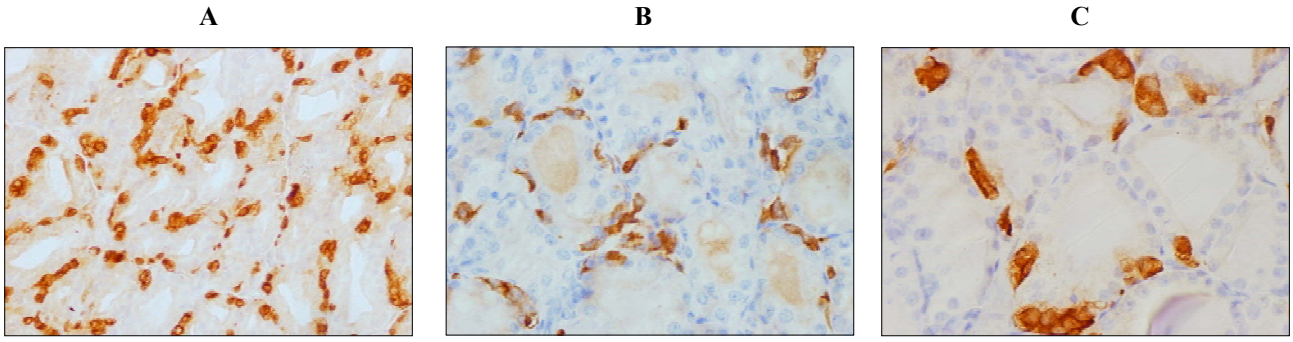

Figure 2. Somatostatin-immunoreactivity: A) Thyroid gland of control rats (x 400); B) Thyroid gland of rats treated with R-(+)-methanandamide (x 400); C) Thyroid gland of rats treated with CP 55,940 (x 400).

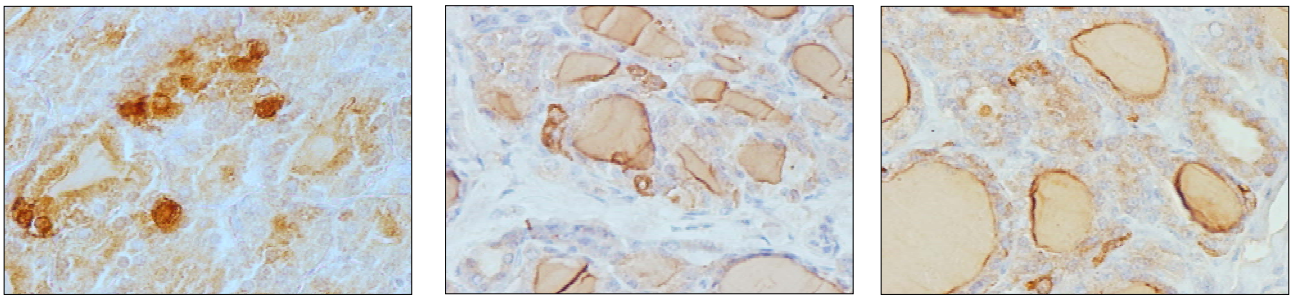

Figure 3. Synaptophisin-immunoreactivity: A) Thyroid gland of control rats (x 200); B) Thyroid gland of rats treated with R-(+)-methanandamide (x 200); C) Thyroid gland of rats treated with CP 55,940 (x 400).

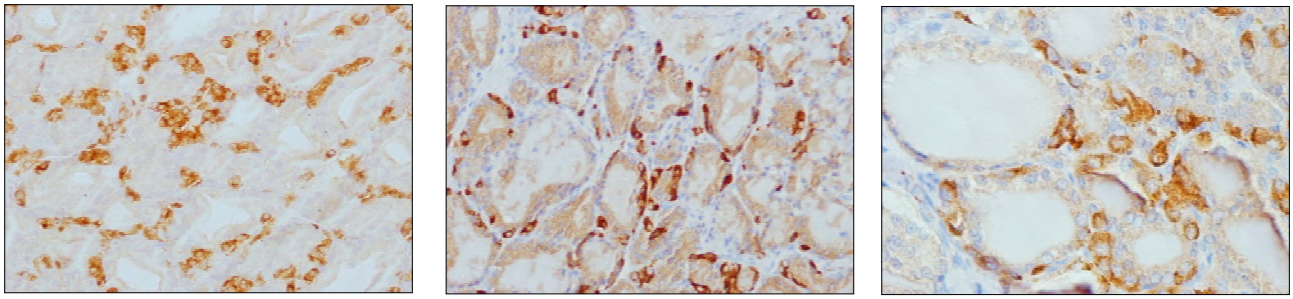

were injected only with the vehicle solution. Four hours after the injections, under pentobarbital sodium anaesthesia (50 mg/kg), both thyroid lobes were extracted and fixed in Bouin's fluid. Paraffin 5-µm sections were made. Immunocytochemical reactions were performed, using the ABC technique. Specific antibodies were used against: calcitonin, synaptophysin (SY), somatostatin (DAKO) and CGRP (Sigma, Aldrich). Control reactions yielded negative results.

Four hours after a single injection of both cannabinoids, the majority of thyroid follicles, particularly those, peripherally located, were of large size with a low epithelium, and blood-vessels were dilated. In addition, the application of CP 55,940 and, in a lesser degree, of R-(+)-methanandamide, caused an enhancement of the immunoreactivity of CGRP (Fig. 1 A, B, C) and synaptophysin (Fig. 3 A, B, C), while both cannabinoids attenuated the immunoreactivity of somatostatin (Fig. 2 A, B, C), as compared to respective values in the control group. Moreover, the enhancement of CT-immunoreactivity was similar to those, observed in our previous study [6].

Porcella et al. [5] have demonstrated the presence of CB1 receptors in the thyroid gland, which are, probably, tonically activated by endogenous cannabinoids, similarly as those in the central nervous system. Since cannabinoids exert an inhibitory action on the peptides release, the attenuation of SS-immunoreactivity is probably connected with their influence on SS synthesis. In our previous study, the enhancement of CT-immunoreactivity in parafollicular cells, accompanied by a significant diminution of CT plasma concentration, was observed after a single injection of both cannabinoids [6]. That observation points to an inhibiting role of cannabinoids on the secretion activity of C cells. Therefore, the activation of CB1 receptors, located on parafollicular cells [7], by R-(+)-Methanandamide and CP 55,940 probably leads to decreased CT plasma concentration, owing to the inhibition of calcium-dependent CT release. Since CT and CGRP are produced by the same gene and cannabinoids enhanced their immunoreactivity in C cells, the same mechanism of this action may be considered. Recently, we have demonstrated a mutual relation between parafollicular and

follicular cells *in vivo* [7]. The hypoactivity of follicular cells, evoked by an i.p. application of L-thyroxine, brought about an inhibition of C cells activity, expressed by attenuation of CT plasma levels and an enhancement of CT-immunoreactivity in C cells. Also Hillard et al. [3] observed a significant reduction of TSH, T_3 and T_4 serum levels after a single injection of Δ^9THC, with the maximal TSH decrease occurring one hour after the administration, followed by a significant diminution of T_3 and T_4 serum concentrations, observed 3 and 6 hours later, respectively. Also Nazar et al. [8] have demonstrated a meaningful attenuation of thyroxine plasma concentration 6 hours after Δ^9THC administration, either single or repeated for 3 days. These observations provide a presumption that cannabinoids may regulate the activity of C cells directly, via CB1 receptor, and also indirectly, by an influence on the activity of follicular cells. Another possibility of cannabinoid action may be the inhibition of noradrenaline release from sympathetic nerve terminals. The autonomic nervous system takes place in the regulation of the follicular and parafollicular cell activity. Current data indicate increased basal calcitonin plasma concentrations after an application of the ß-adrenergic receptor agonist, reversed by an administration of this receptor antagonist [9].

Synaptophysin, as evaluated in our study, is an integral membrane glycoprotein of the vesicles of synapses and neuroendocrine cells, which play some role in the neurotransmitter and hormone release from synaptic vesicles and neuroendocrine cells by making an exocytolitic fusion pore [10]. The increase of SY-immunoreactivity of C cells, caused by CP 55,940, and, in a lesser degree, by R-(+)-Methanandamide administration, may indicate an important role of synaptophysin in the regulation of peptide secretion from C cells, e.g., CT and CGRP.

This study indicates that a single injection of cannabinoids: R-(+)-methanandamide and CP 55,940, alters the immunoreactivity of regulatory peptides in the thyroid parafollicular cells. Therefore, the significant impact of cannabinoids on the secretory activity of C cells should be taken into consideration.

References

1. Wenger T, Moldrich G. The role of endocannabinoids in the hypothalamic regulation of visceral function. Prostagl Leukotr Ess, 2002; 66: 301-7.

2. Lomax P. The effects of marijuana on pituitary-thyroid activity in the rat. Agents Actions, 1970; 1: 252-7.

3. Hillard JC, Farber NE, Hagen TC, Bloom AS. The effects of ?-9-tetrahydrocannabinol on serum thyrotropin levels in the rat. Pharmacol Biochem Behav, 1984; 20: 547-50.

4. Buckley NE, Hansson S, Harta G, Mezey E. Expression of the CB1 and CB2 receptor messenger RNAs during embryonic development in the rat. Neuroscience, 1998; 82: 1131-49.

5. Porcella A, Marchese G, Casu MA, Rocchitta A, Lai ML, Gessa GL, Pani L. Evidence for functional CB1 cannabinoid receptor expresses in the rat thyroid. Eur J Endocrinol, 2002; 147: 255-61.

6. Winnicka MM, Zbucki RŁ, Dadan J, Sawicki B, Hryniewicz A, Kosiorek P, Bialuk I, Puchalski Z. An immunocytochemical study of the thyroid parafollicular (C) cells in rats treated with cannabinoids - preliminary investigations. Folia Morphol (Warsz), 2003; 62: 419-21.

7. Dadan J, Zbucki RŁ, Sawicki B, Bialuk I, Zawadzka A, Winnicka MM, Puchalski Z. Preliminary immunohisochemical investigations of thyroid C cells in an experimental model of hypothyroidism. Folia Morphol (Warsz), 2003; 62: 319-21.

8. Nazar B, Kairys DJ, Fowler R. Effects of Δ-9-tetrahydrocannabinol on serum thyroxine concentrations in the rat. J Pharm Pharmacol, 1977; 29: 778-9.

9. Zbucki RŁ, Dadan J, Sawicki B, Bialuk I, Kosiorek P, Winnicka MM, Puchalski Z. Propranolol alters the activity of thyroid C cells in the experimental model of hypothyroidism in rats. Pol J Pharmacol, 2004; 56: 223.

10. Llona I. Synaptic like microvesicles: do they participate in regulated exocytosis? Neurochem Int, 1995; 27: 219-26.

Estimation of influence of high doses of cholecalciferol on thyroid parafollicular and respiratory tract neuroendocrine cells; preliminary investigations

Sawicki B[1], Zbucki RŁ[2], Winnicka MM[2], Kasacka I[1], Nowosielski C[1], Hukałowicz K[3]

[1]Department of Histology and Embryology, [2]General and Experimental Pathology,
[3]Department of Bromatology Medical University of Bialystok

Abstract

The aim of this study was to compare what changes are caused by high doses of cholecalciferol (100000 UI vD_3) and $CaCl_2$ on thyroid parafollicular (C) cells and airways neuroendocrine (NE) cells in rat. Overdosage of vD_3 and $CaCl_2$ causes hypocalcaemia and strong hypercalcitoninemia in blood; C cells showed mainly signs of hypertrophy; simultaneously, the number of strong calcitoninpositive cells decreased significantly (statistically significant changes). Immunohistochemical reactions, detecting CGRP, somatostatin, synaptophysin and neuronspecific enolase did not fall under statistic analysis. Airways NE cells re-acted to hypercalcemia differently than C cells – they probably respond to different regulatory mechanisms.

Key words: Vitamin D_3, immunohistochemistry, calcitonin concentration, thyroid, lung.

Introduction

The basic hormone, synthesized in thyroid parafollicular (C) cells, is calcitonin (CT). Some airways NE cells also release CT [1, 2]. Response of thyroid C cells to chronic hypocalcaemia – after high doses of vitamin D_3 (vD_3) - has been described in detail in several publications [3, 4]; the studies did not pertain, however, to the problem of calcitonin positive airways neuroendocrine (NE) cells. The aim of this study was to compare what changes were caused by high doses of cholecalciferol [intraperitoneal (ip.) injection of 100000 UI v. D_3 (Vigantol)], and 0,5% $CaCl_2$ in drinking aqueous solution – on thyroid C cells and airways NE cells in rats.

ADDRESS FOR CORRESPONDENCE:
Bogusław Sawicki
Department of Histology & Embryology
Medical University of Białystok
Kilińskiego 1, 15-089 Białystok, Poland
tel. +48 85 748 54 54 ; e-mail: sawboghe@amb.edu.pl

Material and methods

The study was performed on 40 male Wistar rats weighting c. 200g. The animals were housed under controlled, standard conditions. All the animals had a free access to drinking (0,5% aqueous solution of $CaCl_2$) and standard food. The rats were divided into 4 groups, 10 rats in each group. Three (3) experimental groups were given ip. injections of Vigantol, Merck (100000 UI v. D_3); the animals were killed under pentobarbital (Vetbutal) anaesthesia during the following intervals: Group 1D after 24h, Gr. 7D after 7 days and Group 14D after 14 days. Group 4C consisted of control rats which were given ip. injections of physiological solutions. Blood was collected for analysis: to determine blood plasma calcitonin concentration by RIA (radioimmunoassay) and the concentration levels of total and ionized calcium (Ca^{2+}). In all the applied procedures, the control reactions yielded negative results. Thyroid lobes and two specimens from the airways (the trachea, and the right lung) were fixed in Bouin's fluid. Paraffin 5-µm sections were made. Immunocytochemical reac-tions were performed, using the ABC technique. Polyclonal and monoclonal specific antibod-ies were used against: calcitonin (CT), somatostatin (SS), synaptophysin (SF), neuronspecific enolase (NSE) (everything from DakoCytomation), and CGRP (SigmaAldrich). Control reactions were also performed – in all the cases, they yielded negative results. The immunohistological preparations were subjected to a quantitative analysis, using: an Olympus Bx50 microscope, a PC computer, a morphological program for quantitative picture analysis (Lucia G, Nikon). In that way, the number of strong CT immunopositive endocrine cells of the thyroid and lung was evaluated in all the experimental groups. In statistic analyses, the results of all the calculations were compared, using an unpaired Student's t-test and non-parametric Mann-Whitney U-test. Significance was considered to be at $P < 0.05$.

Figure 1. Average concentrations of ionised Ca in blood serum in examined groups.

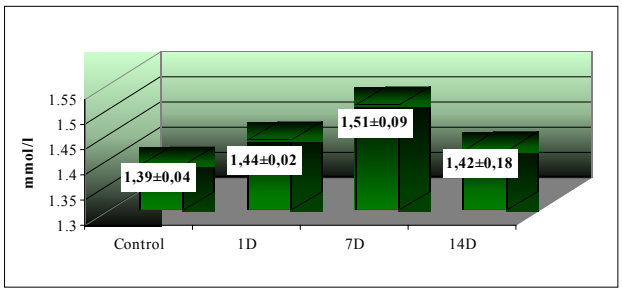

Figure 2. Average concentrations of total calcium in blood in examined groups.

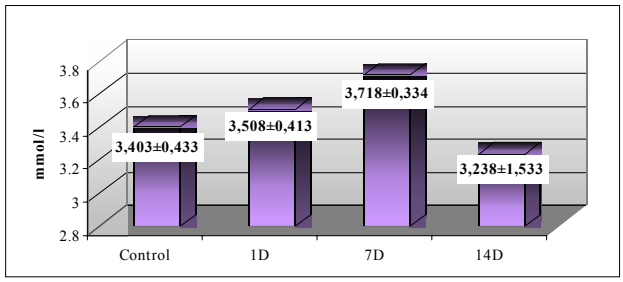

Figure 3. Average calcitonin (CT) concentrations in blood serum in examined groups.

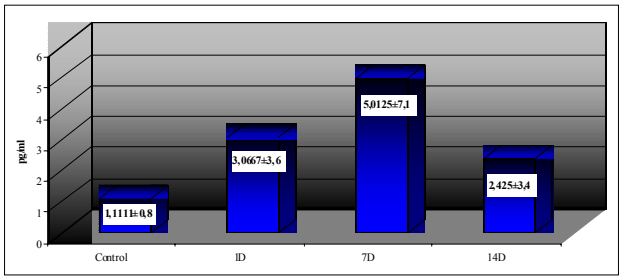

Figure 4. Comparition strong CT immunopositive NE cells in the thyroid and the lung.

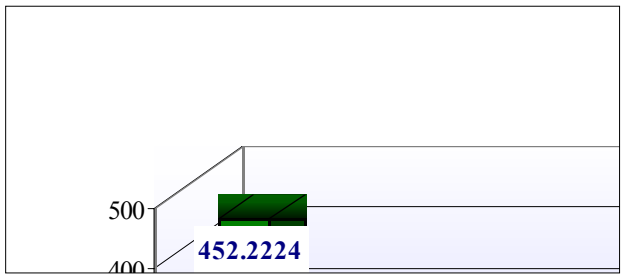

Figure 5. Control. Strong CT immunopositive reaction in the cytoplasm of thyroid C cells, x 400.

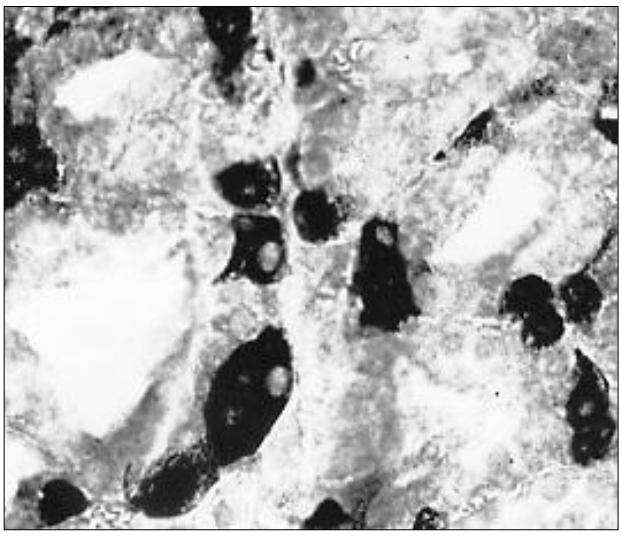

Figure 6. Group 14D. Many C cells show strong CT immunoreactivity similar to that in the control group. CT positive colouring of the environment is still visible, x 400.

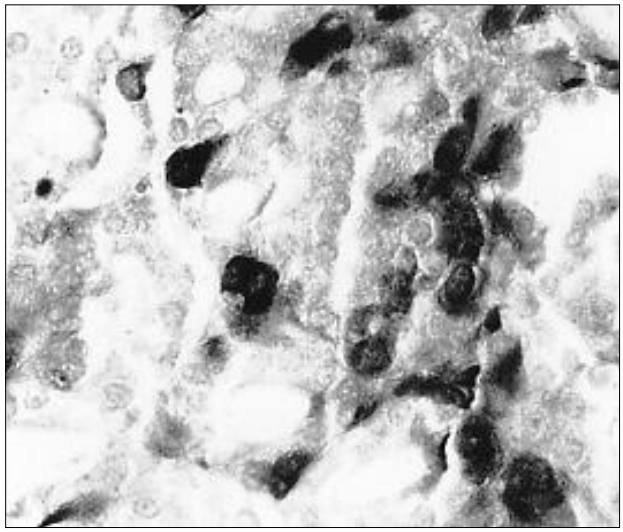

Results and discussion

After intraperitoneal injection of 100000 UI vD_3 and constant loading of $CaCl_2$, a statistically significant increase of the concentration of ionised calcium (Ca^{2+}) occurred in serum in the following groups: 1D (after one day) and even more significant in Group 7D (Fig. 1). In Group 14D, the increase was statistically insignificant; there were big individual differences. Changes in total Ca concentration in blood were less obvious in the experimental groups, in comparison to Ca^{2+} (Fig. 2). The most obvious, statistically significant changes of the experiment were observed in CT concentrations in serum (Fig. 3). The biggest increase of CT concentration in serum was in Group 2D. In the control group, the majority of thyroid C cells displayed a strong CT immunopositive reaction in cytoplasm (Fig. 5). In Group 1D, a statistically significant and very strong decrease in the number of strong CT immunopositive C cells was found; in their surroundings, strong diffusive CT immunopositive colouring to the background was observed. Weakly CT immunopositive C cells were difficult to distinguish from the environment (Fig. 6). Weaker, but also statistically significant decrease in the number of strong CT immunopositive thyroid C cells was observed in Group 7D. The comparison of specimens from CT immunopositive reactions with other immunohistochemically stained specimens (SF, NSE and CGRP) indicated that probably not real decrease of thyroid C cells occurred in the experimental animals. The morphological changes indicated hypertrophy of thyroid C cells and a more intense secretion of

Figure 7. 14D group. Weakly CT immunopositive reaction in single and in group airways NE cells at bronchiolar bifurcation epithelium, x 400.

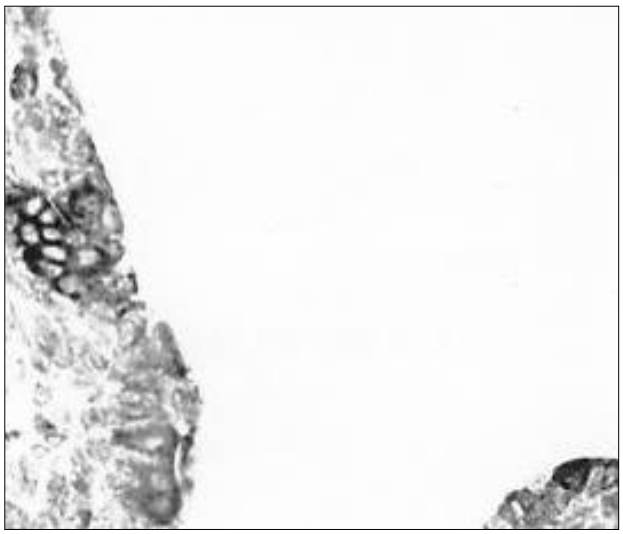

Figure 8. 14D group. Strong synaptophysin positive reaction in NE cells in the lung , x 400.

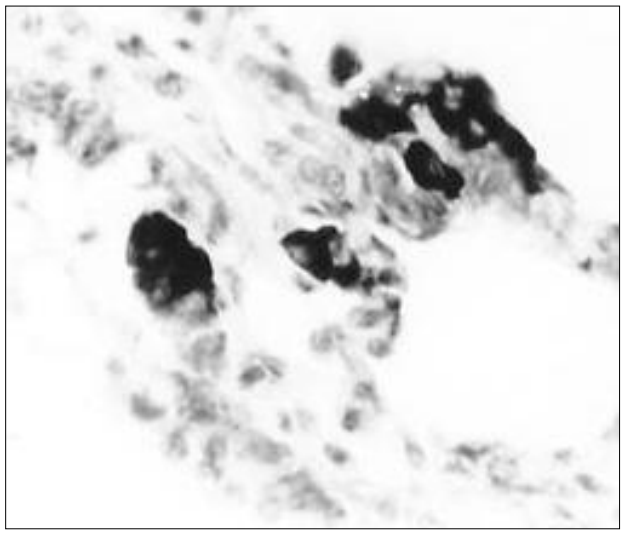

calcitonin. Moreover, the majority of researchers observed a significant decrease of CT immunoreactivity in C cells [3], some also found a relatively not high proliferative activity of thyroid C cells in rats with hypocalcaemia [4]. A few C cells demonstrated the presence of somatostatin in and all the experimental groups – here SS positive reaction was stronger than that in the control. A distinctly positive correlation was found between serum concentrations of calcitonin and Ca^{2+}. A negative correlation was observed between the number of strong CT immunopositive C cells and serum concentrations of CT, as well as Ca^{2+} (Fig. 1, 2, 3, 4). However, no correlation was found between those concentrations and the number of strongly CT immunopositive airways NE cells (Fig. 6, 7). Airways NE cells reacted to hypocalcaemia differently than C cells (Fig. 7, 8) - they probably respond to different regulatory mechanisms.

References

1. Kasacka I, Azzadin A, Sawicki B, Malla H. Immunoreactivity of neuroendocrine cells in the respiratory tract in rats with experimental uremia after thyroparathyroidectomy. Folia Histochem Cytobiol, 2001; 39: 64-5.

2. Sawicki B, Nowosielski C, Arciszewska E, Borowska H. Preliminary evaluation of thyroid and respiratory tract neuroendocrine cells in the rat after experimental hypercalce-mia. Folia Morphol (Warsz), 2004; 63: 111-3.

3. Zabel M, Schafer H. Effect of hypercalcemia on parafollicular cells in the rat thyroid gland. Histochemistry, 1988; 88: 623-8.

4. Pavlov AV. The mitotic activity of the follicular and parafollicular (C) cells in the thyroid of rats with hypercalcemia. Morfologiia, 1992; 102: 99-105.

Pulmonary neuroendocrine cells in chronic renal failure

Kasacka I[1], Sawicki B[1], Ostrowska H[2]

[1]Department of Histology and Embryology, [2]Department of Biology, Medical University, Białystok, Poland

Abstract

In patients with chronic renal failure, mechanical and haemodynamic changes could occur in the lungs without obvious pulmonary symptoms and findings, and their effects could pave the way to pulmonary functional disorders. Numerous studies have demonstrated that the respiratory system is a site of synthesis of many compounds, which play biological roles ascribed to hormones.

The present article is an attempt to make a synthesis of current opinions and views, based on the world literature survey and on our own studies, concerning the effect of homeostatic dysfunction of the kidneys on the morphology and action of DNES cells in the lung.

Key words: chronic renal failure, lung, DNES cells.

Introduction

A considerable progress has recently been observed in the knowledge on hormones, produced by dispersed neuroendocrine system cells (DNES). Using immunological methods, a number of APUD cells have been discovered and their hormonal activity linked to respective peptides [1, 2]. The epithelium, lining the airways and the peripheral air spaces of the lung contains, a population of amine and peptide-secreting pulmonary neuroendocrine cells (PNEC), which act as regulatory elements [3].

Pulmonary complications, such as pulmonary oedema, pleural effusions, pulmonary fibrosis, pulmonary calcification, pulmonary hypertension, haemosiderosis and pleural fibrosis are seen in patients with chronic renal failure [4, 5]. Partly, these symptoms may result from abnormal functioning of hormone-producing endocrine cells, which act in concert with higher neural and endocrine control systems to maintain the pulmonary structure and function [6].

Their precise roles remain unclear, but mediation of pulmonary response to uraemia appears to be an important function [7].

Basic characteristics of the Diffuse Neuroendocrine System (DNES). Apart from endocrine cells, which accumulate to form either distinct endocrine glands or isolated groups of cells in other specialized organs, there is an extensive system of neuroendocrine cells, found singly, among other epithelial cells, especially in the airways [3] and in the gastrointestinal tract [8]. The DNES family was proposed to include over 60 types of cells. As some relevant cells were shown to lack the APUD property and to be unable to produce bioactive peptides, the significance of the APUD concept became unclear, and the term APUD has been replaced by the term "diffuse neuroendocrine system" on the basis of the common characteristics of the endocrine-like cells and neurons [9].

Functionally, the neuroendocrine cell is a receptor-secretory cell, with surface receptors on the cellular membrane and reacting via secretion to a respective stimulus. The receptors of APUD cells have the ability to receive chemical stimuli from the blood or tissues [10].

The primary site of hormone action (paracrine effect) is situated in a direct vicinity of DNES cells, i.e., vascular endothelium and muscular coat, nerve fibres and the connective tissue. Distant target organs, according to the classic endocrine theory, are the further aim, following hormone absorption to the blood vessels [3].

Pulmonary neuroendocrine cells (PNEC). The pulmonary neuroendocrine system is represented in the bronchopulmonary tract by solitary neuroendocrine cells (NES) and the intra-epithelial innervated corpuscles to name them "neuroepithelial bodies" (NEB) (Fig.1). The precise function of interplay between these

ADDRESS FOR CORRESPONDENCE:
Irena Kasacka
Department of Histology & Embryology
Medical University of Białystok
Kilińskiego 1; 15-089 Białystok, Poland
Tel. (48 85) 748 54 58;
e-mail: kasacka@amb.edu.pl

Figure 1. Bronchial section from the rat; a cluster and a solitary (arrows) of neuroendocrine cells. ABC method for somatostatin; mag. 200x.

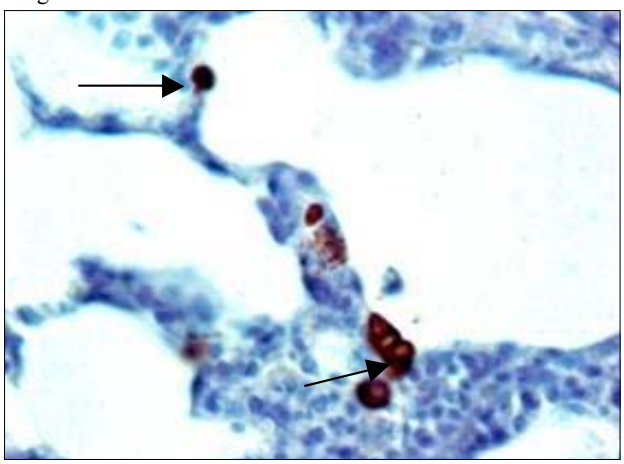

Figure 2. Photomicrograph of the lung of the rat. Haematoxylin and eosin; mag. 200x.

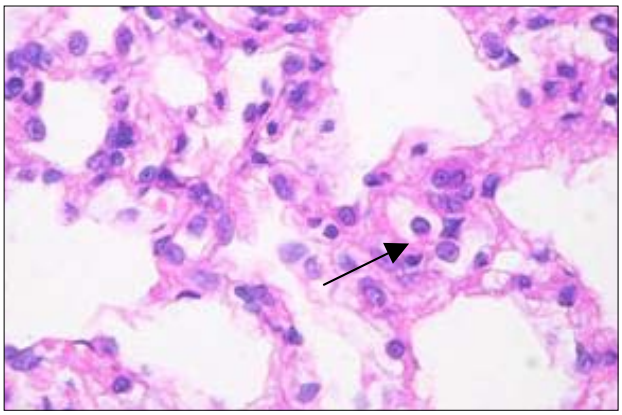

Figure 3. A fragment of the lung in the rat. Endocrine cell, impregnated with silver, according to Grimelius's method; mag. 400x.

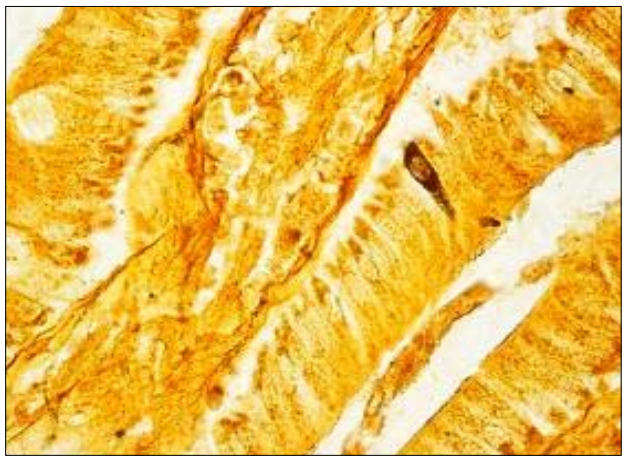

Figure 4. Electron micrograph of an enteroendocrine cell with secretory granules (arrows) from the rat lung; mag. 3000x.

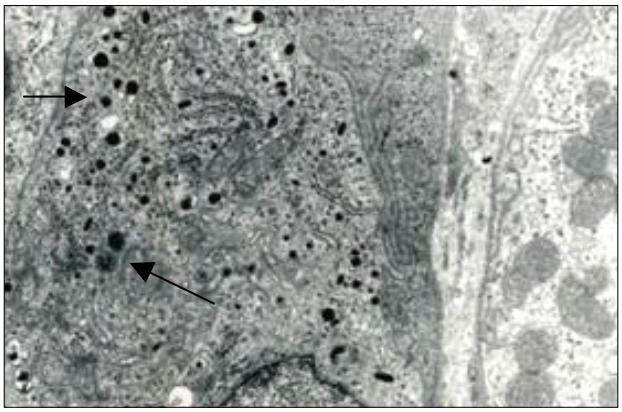

two components under physiologic and pathologic conditions is not entirely clear. Current indications are such that NEB act as intrapulmonary chemoreceptors, sensitive to hypoxia and hypercapnia, whereas solitary NES cells may have a paracrine, regulatory function [11].

Morphological and histochemical properties of PNEC. In sections, stained with H+E, PNEC can be recognized by their clear cytoplasm (Fig. 2). However, with only H+E staining to prove the neuroendocrine character of the cells, PNEC determination is rather difficult. Before the advent of immunohistochemical techniques, argyrophilic stains had been used as a relatively reliable method to detect PNEC (Fig. 3).

Ultrastructure of PNEC. The apical surface of PNEC has small microvilli. In the cytoplasm of PNEC, cored dense granules are seen as a hallmark of members of the diffuse neuroendocrine system [12]. The size and electron density of the secretory granules vary, according to the animal species and their contents. (Fig. 4).

Chronic renal failure (CRF) is a pathological syndrome, developing, due to the progressive destruction of renal structures by chronic nephropathies, characterized by a gradually increasing function impairment. Direct causes of clinical symptoms of CRF and its final stage - uraemia - have not yet been recognized. Beyond argument is the assumption that most symptoms are due to metabolic disorders, caused by the accumulation of toxic substances in body fluids, which interfere with cellular processes.

Symptoms from the pulmonary tract. Lung changes in the course of uraemia attracted attention at the beginning of the 20th century. The radiological picture of pulmonary oedema was then described in patients with chronic renal failure as parahilar thickening with the shape of butterfly wings which occupy two thirds of the central pulmonary region and disappear towards the periphery, giving a zone of clearing up chest X-rays [5].

Clinical or subclinical pulmonary oedema and pleural effusions are the most common pulmonary complications. Other complications include pulmonary fibrosis, pulmonary calcification, pulmonary hypertension, haemosiderosis and pleural fibrosis in patients with chronic renal failure.

An analysis of our results [7, 13], together with literature data, indicates that PNEC cells actively participate in the pathogenesis of early dysfunctions of the bronchopulmonary tract in CRF and initiate the mechanism of subsequent adaptive response of DNES.

Conclusion

The above considerations, based on literature survey and our own results, allow the statement that CRF leads to severe

disorders in the system of endocrine cells of the lung. These disorders may involve quantitative changes and function impairment, that is, disturbances in the mechanisms of the release of polypeptide hormones (dysfunction, excessive accumulation of polypeptide in secretory granules).

Taking into consideration homeostatic disturbances of the organism, induced by the impairment of renal parenchyma and the key role of neuroendocrine cells in many organs, which regulate the functioning of the organism, it should be assumed that PNEC are greatly involved in the chain of physiological events, taking place in the lungs during uraemia. However, as long as the mechanisms of mutual relations and interactions are not elucidated, it is difficult to determine whether the clinical symptoms from the respiratory system result from the impairment of structure and function of single DNES cells, or if their occurrence is due to the reaction of enteroendocrine cells to homeostatic disorders. This can be explained by the fact that the products, synthesized in DNES cells, particularly biogenic amines (serotonin, catecholamines), act as tissue hormones which indirectly control and regulate homeostasis. A more detailed knowledge of the structure and function of neuroendocrine cells in the airways will undoubtedly contribute to better understanding of the pathological processes with PNEC involvement and may have a great practical significance in diagnostics; however, the issue still requires a number of investigations.

References

1. Palisano JR, Kleinerman J. APUD cells and neuroepithelial bodies in hamster lung: methods, quantitation, and response to injury. Thorax, 1980; 35: 363-70.

2. Tzaneva M, Julianov IA. Chromogranin A-, somatostatin- and serotonin-containing endocrine cells in the corporal gastric mucosa of patients with helicobacter pylori associated chronic gastritis. Endocr Regul, 1999; 33: 79-82.

3. Ito T. Differentiation and proliferation of pulmonary neuroendocrine cells. Prog Histochem Cytochem, 1999; 34: 247-322.

4. Kalender B, Erk M, Pekpak M, Apaydin S, Ataman R, Serdengecti K, Sariyar M, Erek E. The effect of renal transplantation on pulmonary fuction. Nephron, 2002; 90: 72-7.

5. Słomian M, Mosiewicz J, Myśliński W. Lung function in chronic uremia. Ann Univ Mariae Curie Sklodowska Lublin-Polonia Sectio D. LV, 2000; 23: 147-53.

6. Gosney JR. Neuroendocrine cell populations in postnatal human lungs: minimal variation from childhood to old age. Anat Rec, 1993; 236: 177-80.

7. Kasacka I, Azzadin A, Sawicki B, Malla H. Immunoreactivity of neuroendocrine cells in the respiratory tract in rats with experimental uremia after thyroparathyroidectomy. Folia Histochem Cytobiol, 2001; 39: 64-5.

8. Norlén P, Curry WJ, Björkqvist M, Maule A, Cunningham RT, Hogg RB, Harriott P, Johnston CF, Hutton JC, Hakanson R. Cell-specific processing of chromogranin A in endocrine cells of the rat stomach. J Histochem Cytochem, 2001; 49: 9-18.

9. Kvetnoi IM, Iakovlova ND. Peptidergic innervation and the APUD system in normal conditions and in various pathological states. Arkh Patol, 1987; 49: 85-92.

10. Marchevsky AM, Kleinerman J. Immunocytochemical studies of APUD cells in airways: effects of nitrosodiethylamine and nitrogen dioxide. Arch Pathol Lab Med, 1982; 106: 400-3.

11. Lauweryns JM, Van Ranst L. Immunocytochemical localization of aromatic L-amino acid decarboxylase in human, rat and mouse bronchopulmonary and gastrointestinal endocrine cells. J Histochem Cytochem, 1988; 36: 1181-6.

12. Herrera GA, Turbat-Herrera EA, Lockard VG. Ultrastructural immunolabeling in the evaluation, diagnosis, and characterization of neuroendocrine neoplasms. Ultrastruct Pathol, 1993; 17: 93-113.

13. Azzadin A, Kasacka I, Sawicki B, Malla H, Dadan J, Buczko W. Preliminary evaluation of neuroendocrine cells in the respiratory tract in rats with experimental uremia. Folia Histochem Cytobiol, 2001; 39: 205-6.

Histological evaluation of the thyroid structure after co-exposure to cadmium and ethanol

Piłat-Marcinkiewicz B[1], Brzóska MM[2], Kasacka I[1], Sawicki B[1]

[1]Department of Histology and Embryology,
[2]Department of Toxicology, Medical University of Białystok, Poland

Abstract

The aim of this study was to evaluate the influence of co-exposure to cadmium (Cd) and ethanol on the structure and function of the thyroid. Male Wistar rats were exposed to 50 mg of Cd/dm^3 in drinking water and ethanol in a dose of 5 g/kg body wt/24 h (administered intragastrically in two equal doses for 5 days a week) for 12 weeks. The structure of the thyroid was assessed in a light microscope. Immunohistochemical methods were used to determine calcitonin (CT), the calcitonin-gene related peptide (CGRP), somatostatin (ST) and synaptophysin (SPh) in the thyroid parafollicular cells (C cells). Weakening of the reactions for CT, CGRP, ST, SPh was observed in C cells. The animals, exposed to a combined action of Cd and ethanol, showed signs of enhanced activity (elevated light follicular epithelium and rarefied colloid), as well as features of intensified remodelling (partial or total follicular atrophy and the appearance of new follicles) of the thyroid gland. In some fragments of the connective tissue stroma mononuclear cell infiltration was observed. The nature of the changes, observed in the rats, simultaneously exposed to Cd and ethanol, may suggest an enhancement in the function of C cells.

Key words: cadmium, ethanol, thyroid, morphology, immunohistochemistry, rat.

ADDRESS FOR CORRESPONDENCE:
Barbara Piłat-Marcinkiewicz
Department of Histology and Embryology
Medical University of Białystok
Kilińskiego 1; 15-089 Białystok, Poland
Tel. (48 85) 748 54 55; e-mail: bmarcink@amb.edu.pl

Introduction

Cadmium (Cd), one of the most toxic heavy metals, is a major chemical environmental pollutant. Cigarette smoking can be an essential source of exposure to this metal. Prolonged exposure to Cd poses a serious threat to humans and animals [1, 2], as Cd can damage various organs and tissues, especially the kidneys, the lungs, the testes and bones [1, 2]. Literature data and our own findings have provided some evidence that Cd can also affect the thyroid which an important regulatory gland [3, 4]. Also alcoholism is a serious problem in almost all countries [5]; however, not many data are available, regarding the effect of ethanol on the thyroid. Ethanol abusers can simultaneously be exposed to substantial amounts of Cd, due to its presence in the human environment, in tobacco smoke and, frequently, at work [1, 2]. No evidence has been found in the available literature on the structure and function of the thyroid at co-exposure to both substances. Since Cd and ethanol can damage the structure and function of the thyroid, and the functional state of this gland is known to affect ethanol metabolism, changes that can be induced by these substances, administered jointly, are difficult to predict. Therefore, we decided to examine the structure and function of the thyroid at co-exposure to Cd and ethanol.

Material and methods

Fourteen 8-weeks old male Wistar rats of 170g initial body weight were used in the study. The animals were housed under controlled conditions (temperature: 22 ± 2^{0}C, relative humidity: 50 ± 10%, natural light-dark cycle) and had a free access to standard rodent laboratory LSM chow (Argopol, Motycz, Poland) and drinking water. The animals were randomly divided into two groups of seven rats in each. One group was exposed to 50 mg Cd/dm^3 (as cadmium chloride) in drinking water and ethanol in a dose of 5 g/kg body wt/24 h (administered intragastrically in two equal doses for 5 days a week) for 12 weeks.

Table 1. Changes, observed in the thyroid structure of animals exposed to cadmium and ethanol

Change	Intensity degree of changes and the frequency of their occurrence		
	+	++	+++
Remodelling of glandular structure of the thyroid	0	5*	2
Mononuclear cell infiltration in connective tissue	0	7	0
Rarefied colloid	0	5	2
Elevated epithelium, light cytoplasm of follicular cells	0	5	2

The following changes were observed: + - only in some follicles of the thyroid, ++ - in some fragments of the thyroid, +++ - almost in all the fragments of the thyroid, *the number of animals in which a change was observed.

Table 2. Intensity of immunohistochemical reactions in C cells of the thyroid

Group	n	ST	SPh	CT	CGRP
Control	7	+++	+++	+++	+++
Cd+ethanol	7	+	+++ or ++*	++	++

Reactions were performed in 7 animals of each group. +++ -strong reaction in most of C cells, ++ -weakening of the reaction in most C cells, + - general weakening of the reaction in C cells, * ++ - weakened reaction was observed in some animals only.in all the fragments of the thyroid, *the number of animals in which a change was observed.

Figure 1. Anti-CGRP antibodies induce strongly immunopositive reaction in most C cells of control rats. (mag. x150).

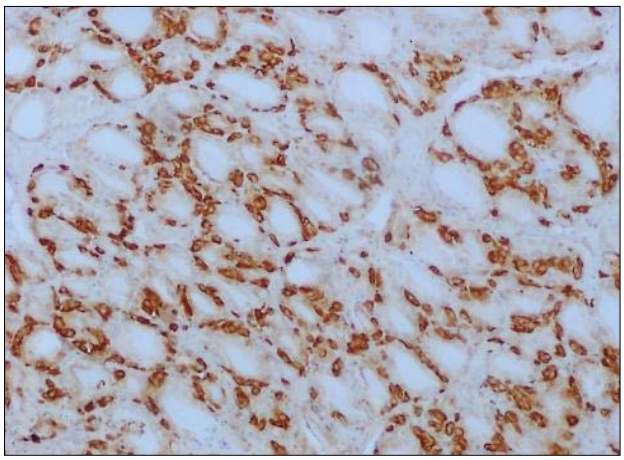

Figure 2. Most of C cells of the control thyroids show strongly immunopositive reactions for CT (mag. x300).

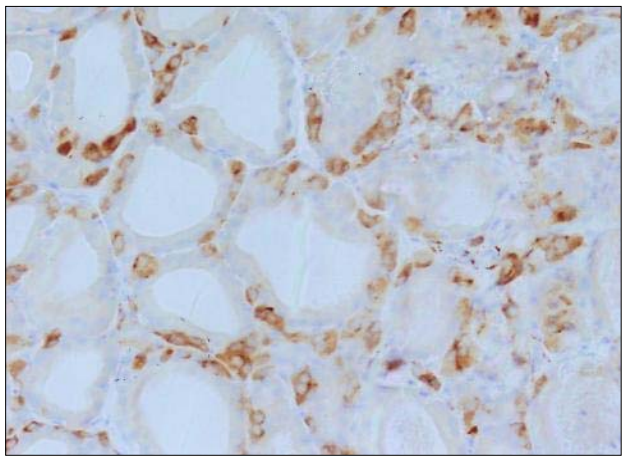

Figure 3. Weak reaction for CGRP in C cells of the rats exposed to Cd + ethanol (mag. x300).

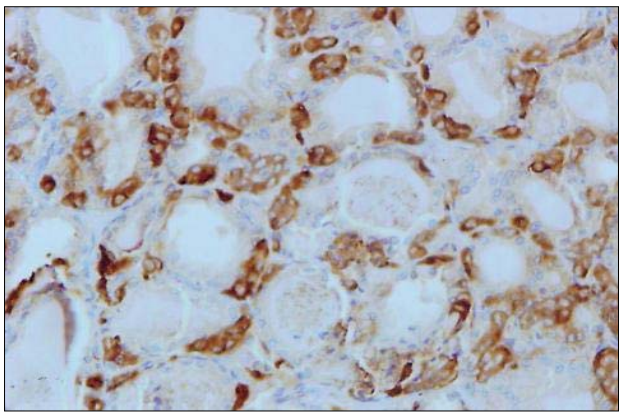

Figure 4. Most of C cells of the Cd + ethanol-exposed rats show a weak reaction for CT (mag. x300).

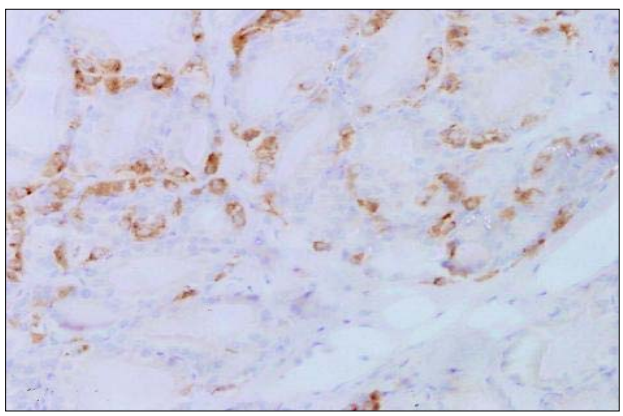

The second group, which drank water free of Cd, served as control. At the end of that study, both thyroid lobes (together with parathyroids) were collected under anaesthesia and immediately fixed in Bouin's fluid for 24 hours. Next, the thyroid lobes were embedded in paraffin, cut into 5-6 mm sections, routinely stained with hematoxylin and eosin (H+E) and examined in a light microscope (NIKON ECLIPSE E 400, USA). Moreover, silver impregnation was performed for the identification of C cells [6]. The assessment of changes in thyroid structure included a determination of their intensity, according to the following criteria: + - a change occurs in some thyroid follicles only, ++ - in some thyroid fragments or +++ - in almost all thyroid fragments. Moreover, immunohistochemical reactions (the avidin-biotin technique) [7] for the hormones produced by C cells, such as calcitonin (CT), the calcitonin-gene related peptide (CGRP) and somatostatin (ST), as well as functionally important protein - synaptophysin (SPh) were performed on thyroid paraffin sections, using specific rabbit antibodies (DAKO).

The study was approved by the Local Ethics Committee for Animal Experiments in Bialystok (Poland).

Results and discussion

Microscopic analysis of the thyroid revealed some histological changes in the animals subjected to co-exposure to Cd and ethanol. Some fragments showed remodelling of the glandular structure of the thyroid, an inflow of mononuclear cells and alterations in the structure of the epithelial lining of follicles. Only in two rats, those changes occurred in almost all the fragments of the thyroid (Table 1). In the control animals, as revealed by immunohistochemical examinations, the antibodies, used against CGRP (Fig. 1), CT (Fig .2), SPh and ST, reacted with respective antigens, inducing a strongly positive reaction in the majority of C cells. In the Cd + ethanol exposed animals, all the reactions were weakened (Table 2), especially those for CGRP (Fig. 3) and CT (Fig. 4), in comparison to respective values in the control. The immunohistochemical reaction for ST was found in a considerably smaller number of cells, compared to that in the control. The reaction for SPh was weakened in some animals only. The intensity of reactions with silver salts in C cells was similar in control and experimental animals. The above data demonstrate effects of Cd and ethanol on the structure and the functional state of the thyroid. Previously, we found that Cd induced changes within the structure of follicular cells and follicles, what can suggest thyroid function disorders already at the level, corresponding to the human environmental exposure (5 mg Cd/dm^3). Most of the data, which are available on toxic effects of ethanol on the thyroid structure, have been obtained from experiments, in which ethanol was injected directly to this gland [8, 9]. We have found some histological changes and disturbances in the secretory function of the thyroid in rats after oral ethanol administration [10]. The changes, observed in the animals exposed to Cd + ethanol in the present study, resemble those described previously after the exposures to Cd or ethanol alone, although, in intensity, they are similar to those induced by Cd alone. The nature of histological changes in the animals exposed to a combined effect of Cd and ethanol suggests an enhanced activity of the thyroid gland. The weakened immunohistochemical reaction for CT, CGRP and ST might result from their increased secretion. The issue needs further studies.

References

1. WHO. Environmental Criteria, 134 Cadmium. IPCS, Geneva, 1992.
2. Järup L. Cadmium overload and toxicity. Nephrol Dial Transplant, 2002; 17: 35-9.
3. Hiratsuka H, Katsuta O, Toyota N, Tsuchitani M, Akiba T, Marumo F, Umemura T. Iron deposition at mineralization fronts and osteoid formation following chronic cadmium exposure in ovariectomized rats. Toxicol Appl Pharmacol, 1997;143: 348-56.
4. Piłat-Marcinkiewicz B, Brzóska M M, Sawicki B, Moniuszko-Jakoniuk J. Structure and function of thyroid follicular cells in female rats chronically exposed to cadmium. Bull Vet Puławy Inst, 2003; 47: 157-63.
5. Meyer C, Rumpf H J, Hapke U, Dilling H, John U. Prevalence of alcohol consumption, findings from the German tacos study. Transitions in alcohol consumption and smoking. Soc Psych Psychiatr Epidemiol, 2000; 35: 539-47.
6. Sawicki B. Evaluation of the role of mammalian thyroid parafollicular cells. Acta Histochem, 1995; 97: 389-99.
7. Sawicki B, Zabel M. Immunocytochemical study of parafollicular cells of the thyroid and ultimobronchial remnants of the European Bison. Acta Histochem, 1997; 99: 223-30.
8. Bartos M, Pomorski L. The influence of a single ethanol injection on normal thyroid tissue of the rat. Cytobios, 2000; 101: 123-30.
9. Nakada K, Katoh C, Kanegae K, Tsukamoto E, Itoh K, Tamaki N. Peracutaneous ethanol functioning thyroid nodule. Ann Nucl Med, 1996; 10: 171-9.
10. Piłat-Marcinkiewicz B, Brzóska M M, Sawicki B, Moniuszko-Jakoniuk J. Morphological and immunohistochemical evaluation of the thyroid of rats exposed to ethanol. Pol J Environ Stud, 2003; 12: 217- 9.

Techniques of image analysis for quantitative immunohistochemistry

Kaczmarek E, Górna A, Majewski P

Laboratory of Morphometry and Medical Image Processing, Chair of Pathology,
University of Medical Sciences, Poznań, Poland

Abstract

The aim of this paper was to evaluate the usefulness of digital image analysis techniques to measure the amount and strength of immunohistochemical markers. The new method, based on the spatial visualization technique, was confronted with methods of colour sampling and grey scale thresholding. Examples of applications of the techniques for apoptosis and proliferation markers are also presented.

Key words: immunohistochemistry, image analysis, measuring expression of reaction.

Introduction

The use of immunohistochemistry in routine pathomorphological diagnosis brought a substantial methodological problem, related with an evaluation of the amount and strength of specific reaction. Often, specimens are evaluated qualitatively by assigning scores, based on appropriate criteria. The interpretation of such results is subjective and causes certain inconsistencies upon the evaluation process. In order to make immunohistochemical studies more objective, quantitative techniques, based on computer-assisted microscopy, have been developed. Our earlier attempts involved transforming colour images to grey scale. The area of reaction was then determined by thresholding segmentation as the number of pixels from the range of grey levels corresponding with the specific reaction [1]. Subsequent attempts employed colour thresholding by using commercial software, followed by either counting the total number of pixels of positive reaction [2] or calculating the cumulative signal strength of the evaluated image [3]. Typically, measurements in quantitative immunohistochemistry include the area fraction of colour pixels present in specific reaction in the evaluated material. However, processing and analysis of raw colour images is still difficult.

In this paper, we present the use of digital image analysis techniques to measure the amount and strength of immunohistochemical markers: bcl-2, caspase-3, Ki-67 and PCNA, in human thyroid and parathyroid glands.

ADDRESS FOR CORRESPONDENCE:
Elżbieta Kaczmarek
Laboratory of Morphometry and Medical Image Processing, Chair of Pathology,
University of Medical Sciences, Poznań
Przybyszewskiego 49; 60-355 Poznań, Poland
Tel (061) 869 18 16; e-mail: elka@amp.edu.pl

Material and methods

Our study was performed on specimens, obtained from goitres resected from patients with either focal chronic thyroiditis or hyperparathyroidism. Proliferating cells were detected by immunostaining for mouse monoclonal anti-Ki-67 antibodies (M7240, Dako) with dilution of 1/150 and mouse monoclonal anti-PCNA antibodies (M0879, Dako) with dilution of 1/400. Moreover, immunohistochemical stains were performed for primary mouse monoclonal antibodies against bcl-2 (M0887, Dako) with 1/40 dilution and polyclonal mouse anti-human caspase-3 (AF835; R&D Systems) with 1/1000 dilution. From each specimen, twenty colour images of 640x480 pixel resolution (at 400x magn.) were acquired with a light digital microscope (Motic Instruments) running under Motic Images v. 1.2 for Windows (Micro Optic Industrial Group Co).

Methods of segmentation of immunohistochemical reaction

Greyscale thresholding

Colour images were first converted to greyscale images and enhanced with the median filter. Then, the interval of grey shades, corresponding to the reaction, was defined and the area, occupied by the reaction, was extracted. The thresholding oper-

Table 1. Area fraction of the markers, calculated by using colour sampling and the spatial method.

Marker	Colour sampling method	Spatial visualization Technique	
	Area fraction	Area fraction	Colour intensity
caspase-3	0.04	0.05	134
bcl-2	0.27	0.26	83
Ki-67	0.02	0.02	134
PCNA	0.11	0.12	135

Figure 1. Micrographs of caspase-3 (left) and bcl-2 (right) in chronic thyroiditis.

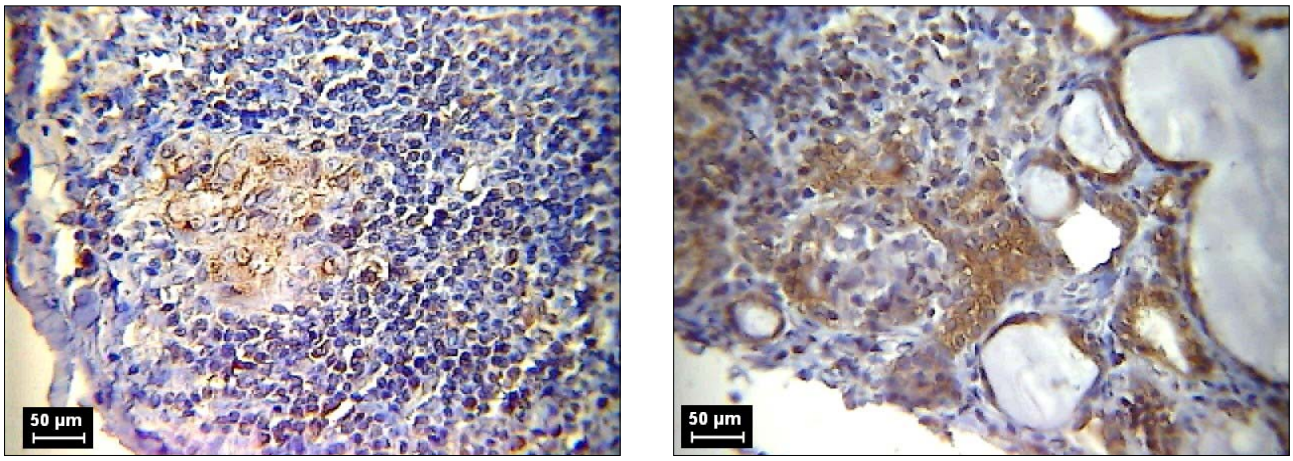

Figure 2. Pixels extracted from images in *Fig. 1* by using an "eye dropper" tool.

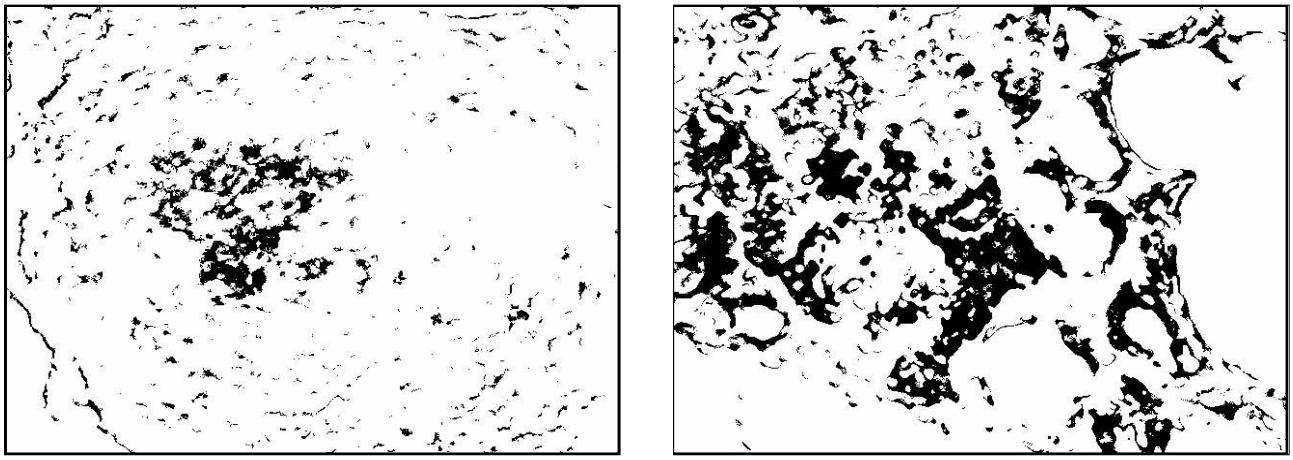

ation converted foreground pixels into black colour, while background pixels into white colour. Thus, the binary image represented the analyzed reaction. The area of positive reaction was estimated by the number of black pixels. The area fraction of positive reaction was determined as the percentage of black pixels in the binary image.

Method based on colour sampling

The area, occupied by the immunohistochemical reaction, was selected by colour sampling, using an "eye dropper tool" in commercial software (Figs 1-2). The number of selected pixels was read from the histogram of colours and their percentage per section was then determined.

Method based on spatial visualization of colour reaction

Colour images were processed in HSB (hue, saturation, brightness) colour space and extended to three-dimensional images by introducing the intensity of colour reaction as the third dimension (Fig. 3). For quantitative measurements of colour reaction, spatial images were linearly converted to 256 colours. Pixels in red and yellow colours corresponded to brown shades of the reactions analyzed in this study and

Figure 3. Spatial visualization of the images presented in *Fig. 1.*

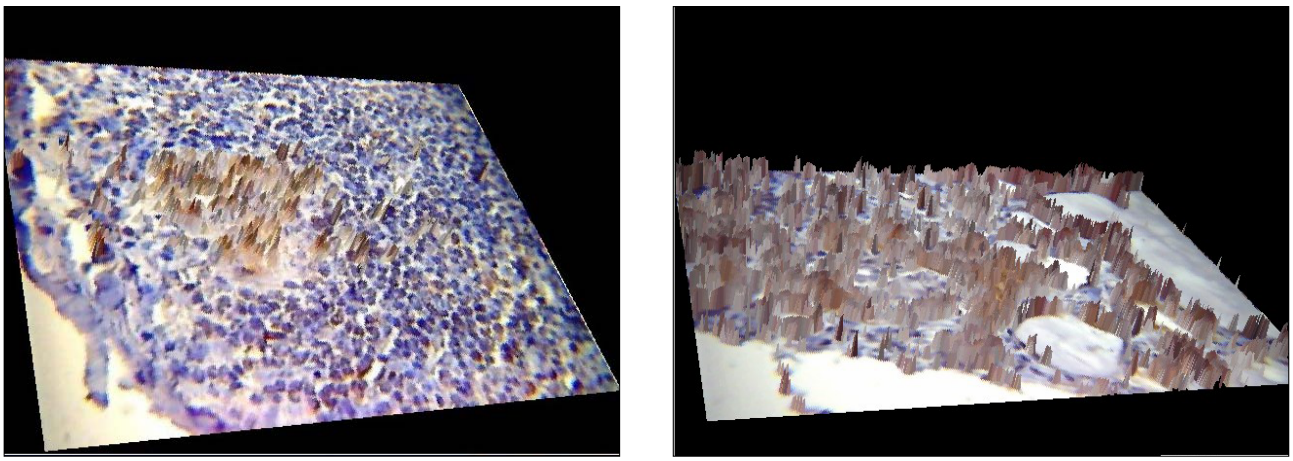

Figure 4. Segmented markers: caspase-3 (left) and bcl-2 (right).

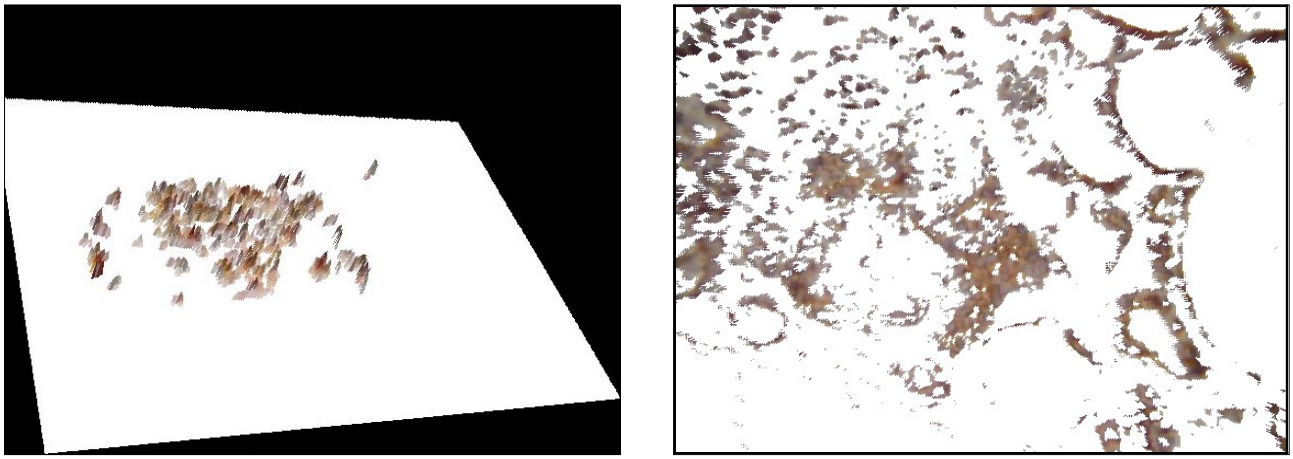

Figure 5. Micrographs of Ki-67 (left) and PCNA (right) in chronic parathyroiditis.

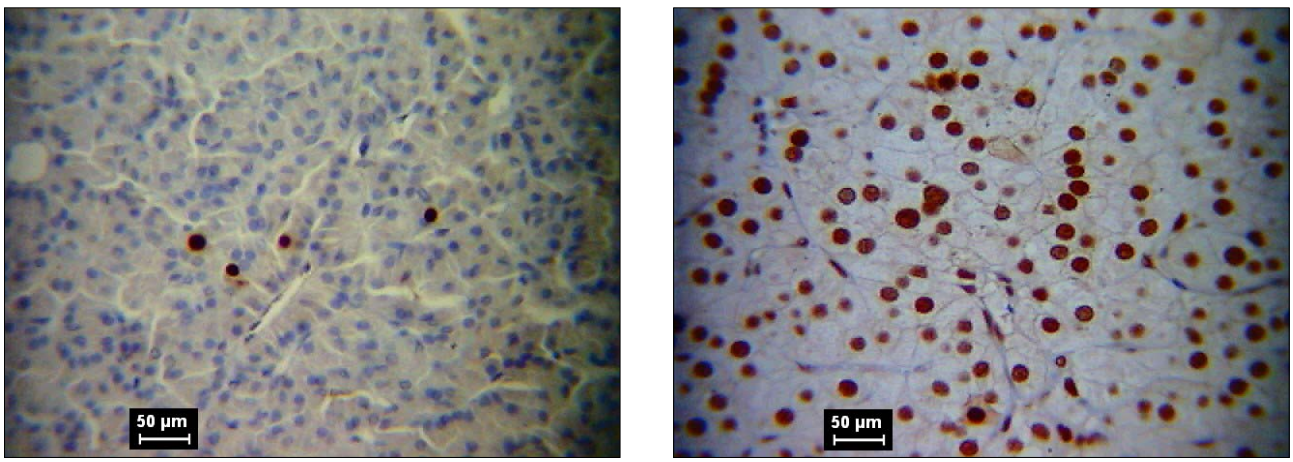

were used to assess the area, volume and the intensity of colour reaction. The spatial representation of the reaction was considered as a set of connected prisms and pyramids to determine the reaction total volume. The reaction total area was derived from the orthogonal projection of the prisms and pyramids onto the plane. The reaction intensity was derived from the volume/area ratio. Spatial image processing was performed by using a computer program, designed and programmed in C++ by Strzelczyk [4].

Results

Results of the segmentation, based on the spatial visualization technique, were consistent with the results obtained by colour sampling (Tab. 1).

However, the time required for the measurement with our new technique was repeatedly shorter. Greyscale thresholding was not performed for caspase-3 and bcl-2 stained specimens because discarding colour information caused weak-

Figure 5. Spatial representation of Ki-67 and PCNA images (see Fig. 5).

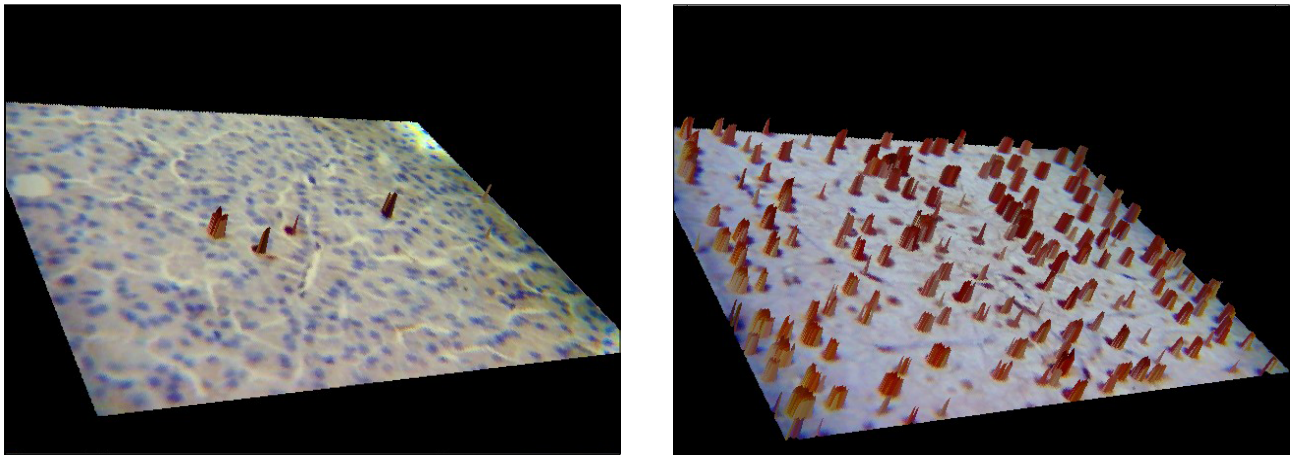

ness of the reaction recognition. Results of greyscale thresholding for Ki-67 and PCNA were also consisted with colour based methods, shown in Table 1.

Discussion

The advantages of our technique, based on spatial visualization, include a shorter time of processing and analysis, approx. 50 images per hour, including visual control of each image by an analyst [4]. Moreover, the use of the same filters of colours, brightness and saturation for the sequence of images, showing a similar brightness and saturation, makes the analysis more objective [3].

References

1. Kaczmarek E. Fuzzy logic for image processing and analysis of renal glomeruli observed in light, confocal and electron microscopes. In: Imaging Processing III: Mathematical methods, algorithms and applications. Chichester (England); 2001, p. 102-12.

2. Brelińska R, Kaczmarek E, Ostalska D. Kinetics of thymic stroma development in the foetal period. Folia Histochem. Cytobiol. 2001; 39: 195-6.

3. Matkowskyj K, Schonfeld D, Benya R. Quantitative immunohistochemistry by measuring cumulative signal strength using commercially available software Photoshop and Matlab. J Histochem Cytochem, 2000; 48: 163-74.

4. Nieruchalska E, Strzelczyk R, Woźniak A, Żurawski J, Kaczmarek E, Salwa-Żurawska W. A quantitative analysis of the expression of a-smooth muscle action in mesangioproliferative (GnMes) glomerulonephritis. Folia Morphol, 2003; 62: 451-3.

Histomorphometry of marrow megakaryocytes in experimental uraemia in rats

Bogusłowicz W[1], Lemancewicz D[1], Pawlak D[2], Dzięcioł J[1]

[1]Department of Human Anatomy, [2]Department of Pharmacodynamics,
Medical University of Bialystok, Poland

Abstract

Uraemic patients frequently demonstrate tendencies towards life-threatening bleeding. Reduced platelet counts and their functional immaturity seem to be caused, among other things, by disorders in the system of marrow megakaryocytes. The aim of the study was a histomorphometric evaluation of marrow megakaryocytes in the course of experimental uraemia in rats. Uraemia was induced by means of right nephrectomy and a partial removal of the left kidney cortex in rats. Morphometric analysis was conducted, using the Microlmage program set. The number of MK, MK area, N/C, CDMK, CDNMK and MK cluster formation were analysed. Uraemic rats showed a reduction in the MK count and their area and an increase in the N/C ratio, CDMK, CDNMK and in the incidence of MK clusters. The results indicate that platelet disorders, observed in uraemia, can also be conditioned by disturbed maturation of MK.

Key words: megakaryocyte, histomorphometry, uraemia.

Introduction

Patients with uraemia frequently demonstrate haemostatic disorders and platelet dysfunction. Different types of haematological alterations, such as bleeding tendency or thrombotic events, are observed. They lead to rapid progression of atherosclerosis, thrombosis and cardiovascular complications [1, 2]. Platelet count in uraemic patients is usually normal but the function of platelets is impaired and they tend to aggregate. Platelet dysfunction likely results from failure of bone marrow thrombopoiesis and peripheral platelet destruction-sequestration. There are no conclusive studies that would explain the thrombopoietic status in uraemic patients. The main factor, responsible for these disturbances is probably the circulating TPO - the major regulator of megakaryocyte production. Bleeding tendency in uraemic patients is associated with an excessive formation of nitric oxide (NO) [3, 4]. Kienast and Schmitz [5] suggest that an RNA-rich reticulated platelet count may be an exponent of thrombopoiesis in the marrow. Ando et al. [3] showed a reduction in MK production in the marrow, indirectly by evaluating the number of RNA-rich reticulated platelet counts. The majority of studies on thrombopoiesis have been based on morphological and functional analyses of platelets. Histological investigations of bone marrow MK in uraemia are still missing.

The aim of the study was a histomorphometric assessment of bone marrow MK in experimental uraemia in rats.

Material and methods

The study was carried out on 60 male Wistar rats (200-220 g b.w.). Experimental uraemia was produced by surgical resection of the right kidney and removal of approximately 50% of the left kidney cortex [6]. Control Group I (20 rats) consisted of animals without surgical manipulation and Control Group II (20 rats) contained animals with decapsulation and removal of fat adherent to the kidney. After decapitation, a fragment of bone marrow (0.1 x 1 cm) was fixed in the so-called "Oxford solution" and put into paraffin bars. Paraffin sections (5μm) were cut with a microtome. Routine haematoxylin and eosin, and immunohistochemistry stainings were used to identify immature MK (antibodies CD61 and VIII factor - DAKO). Morphometric analysis was conducted, using the standard Microlmage program set (Olympus) with DP 12 Analysis. The number of

ADDRESS FOR CORRESPONDENCE:
Wanda Bogusłowicz
Department of Human Anatomy
Medical University of Bialystok
Mickiewicza 2A, 15-230 Bialystok, Poland
+48 85 748 56 61, fax +48 85 748 56 64,
e-mail: anatomia@amb.edu.pl

Table 1. Histomorphometric features (means ± standard deviations) of megakaryocytes in bone marrow in the study group.

	MK number	MK area	N/C ratio	CD MK	CD NMK	Cluster Forms (%)
Group I No surgical manipulation	38.9±6.2	189.9±46.2	32.7±6.7	0.84±0.08	0.57±0.07	0.0
Group II Sham operation	39.6±5,9	186.2±53.7	33.2±7.1	0.85±0.06	0.58±0.09	0.0
Group III Uraemic rats	35.2±6.9	164.5±41.7	36.9±5.4	0.89±0.09	0.61±0.08	15.0

MK/mm^2, MK area in μm^2, N/C ratio, circular deviation factor of MK (CD MK) and their nuclei (CD NMK), and the incidence of MK clusters were determined. The obtained results were analysed, using the Statistica Pl. computer program.

Results and discussion

We found statistically significant differences in the mean MK area ($p<0.05$) and in the number of cluster forms of MK between rats with uraemia and the animals in Control Groups I and II. Statistically insignificant differences in the total number of MK were observed between those groups. The highest, but not statistically significant was the N/C ratio, CD MK and CD NMK in uraemic rats Table 1.

Until now, the studies on thrombopoietic disorders in uraemic patients have concerned blood platelets [7]. Uraemic patients show platelet dysfunction, associated with multifunctional platelet defects. It has been demonstrated that blood platelets are characterized by, e.g., disorders in membrane glycoprotein expression, reduction in platelet phospholipids and Ib glycoproteins. A functional defect may cause a decrease in the expression of IIb - IIIa glycoproteins. Interesting is also the reduced mean platelet volume in uraemic patients. Neither cause of platelet fragmentation nor its functional dysfunction has been elucidated. The mechanism may be complex and related to lipid metabolic disorders [8, 9]. The most common platelet disorders include a low content of granule nucleotides [7, 10], an impairment of thromboxane formation and an increase in cholesterol-rich platelets [11]. The results of the present study may help explain these disturbances. Our experiments indicate changes in marrow MK. Experimental uraemia, induced in rats, causes a reduction in the total MK count and in the MK area, thus suggesting an accelerated production of platelets, which may develop abnormalities, as reported by other authors. Marrow MK are immature, and this is indicated by changes, observed in CD MK and their nuclei - they have a characteristic immature shape and form clusters. The mechanism of their formation is unknown. Immaturity of marrow MK in uraemia has also been confirmed by the analysis of their ploidy. Winkelmann et al. [12] have shown that high creatinine levels and low haemoglobin or creatinine clearance correlate with a low average ploidy of MK. Our results indicate that platelet disorders, observed in uraemia, can also be conditioned by MK maturation disturbances.

References

1. Casserly LF, Dember LM. Thrombosis in end-stage renal disease. Kindey Blood Press Res, 2003; 26: 50-4.

2. Małyszko J, Małyszko JS, Hryszko T, Myśliwiec M. Effects of long-term treatment with simvastatin on some hemostatic parameters in continuous ambulatory peritoneal dialysis patients. Am J Nephrol, 2001; 21: 373-8.

3. Ando M, Iwamoto Y, Suda A, Tsuchiya K, Nihei H. New insights into the thrombopoietic status of patients on dialysis through the evaluation of megakariocytopoiesis in bone marrow and of endogenous thrombopoietin levels. Blood, 2001; 97: 915-21.

4. Salvati F, Liani M. Role of platelet surface receptor abnormalities in the bleeding and thrombotic diathesis of uremic patients on hemodialysis and peritoneal dialysis. Int J Artif Organs, 2001; 24: 131-5.

5. Kienast J, Schmitz G. Flow cytometric analysis of thiazole orange uptake by platelets: a diagnostic aid in the evaluation of thrombocytopenic patients. Blood, 1990; 75: 116-21.

6. Ormrod D, Miller T. Experimental uremia. Nephron, 1980; 26: 249-54.

7. Mezzano D, Tagle R, Panes O, Perez M, Downey P, Munoz B, Aranda E, Barja P, Thambo S, Gonzalez F, Mezzano S, Pereira J. Hemostatic disorder of uremia. The platelet defect, main determinated of prolonged bleeding time, is correlated with indices of activation of coagulation and fibrinolysis. Thromb Haemost, 1996; 76: 312-21.

8. Gawad MP, Dobos G, Spath M, Schollmeyer P, Gurland HJ, Mujais SK. Impaired function of platelet membrane glycoprotein IIb-IIIa in and-stage renal disease. J Am Soc Nephrol, 1994; 5: 336-46.

9. Sloand EM, Prodouz K, Klein HG, Yu MW, Harwath L, Fricke W. Reduction of platelet glycoprotein Ib in uremia. Br J Haematol, 1991; 77: 375-81.

10. Zwaginga JJ, Ijsseldijk MJW, De Groot PG, Vos J, De Bos Kuil RLJ, Sixma JJ. Defects in platelet adhesion and aggregate formation in uremic bleeding disorder can be attributed to factors in plasma. Arterioscler Thromb, 1991; 11: 733-44.

11. Vecino A, Navarro-Antolin J, Teruel J, Navarro J, Cesar J. Lipid composition of platelets in patients with uremia. Nephron, 1998; 78: 271-3.

12. Winkelmann M, Dorr U, Pfitzer P, Schneider W. Is lower ploidy of megakariocytes another reasonfor uremic thrombocytopathy? Klin Wochenschr, 1986; 64: 540-4.

Assessment of potassium and sodium ion concentrations in the vitreous humour of swine isolated eyeballs after organism death

Brzeziński P M, Godlewski A

Department of Cell Physiology, Histology and Embryology, Medical University, Łódź, Poland

Abstract

Potassium and sodium ion concentrations were estimated by the flame photometry and potentiometry in the vitreous fluid of isolated porcine eyeballs at time of death and of eyeballs, stored at temperature of 6-8^{0}C during post-mortem intervals: 4, 28, 52, 75, 100, 124 and 148 hours. The increase of K^+ concentration and decrease of Na^+ concentration were proportional to the increasing post-mortem time intervals. The results of the potentiometric measurements of K^+ and sodium ion concentrations were significantly lover, as compared to those after flame photometry. In all the vitreous fluid smears after 124 and 148 hours, Gram (-) bacteria were found. Our results suggest that bacterial infection participates in the variability of K^+ levels. The influence of bacterial infection on the margin of error for the K^+ post-mortem test remains unanswered and needs further studies.

Key words: post mortem interval, vitreous fluid, swine, potassium and sodium ions, bacteria.

Introduction

Precise determination of the post-mortem interval (PMI) remains unsolved up to now. From the year 1959, in legal medicine, popular has been the estimation of PMI effects on the results of vitreous fluid K^+ concentrations. Different, mainly linear, equations that describe the relationship between the vitreous fluid K^+ concentrations and PMI have been developed. Normal vitreous K^+ concentration (3.14-8 mmol/L) and the PMI hour increase coefficient (0.14-0.55 mmol/L) were different in manner, depending on the paper's authors. The human vitreous K^+ level is dependent on different factors, e.g., temperature, agony, and ion determination methods [1, 2, 3]. In the veterinary research, a promising diagnostic method of assessing the cause of animal death is the estimation of the chemical composition of the vitreous fluid [4]. These studies also include an estimation of K^+ and Na^+ ion concentrations. The aim of the study, reported here, was an assessment of K^+ and Na^+ ions by two different analytical methods (flame photometry and potentiometry) in the liquid portion of the vitreous fluid (LPVF) of isolated porcine eyeballs at time of death and stored at temperature of 6-8^{0}C during selected post-mortem intervals.

ADDRESS FOR CORRESPONDENCE:
Piotr Brzeziński
Department of Cell Physiology, Histology and Embryology
Medical University of Łódź
Narutowicza 60, 90-136 Łódź, Poland
tel. (+48 42) 6319807.

Materials and Methods

The eyeballs were collected from pigs, each 100-120 kg of body weight, delivered to butchery during up to 60 min. before death. All the animals were inspected by veterinary control. The animals were struck by electric shock and exsanguinated. The eyeballs, collected immediately after animal death (up to 10 min.), were included into the control group. Each eyeball was covered by a parafilm and aluminium foil, packed in a small plastic container (the cornea on top) and stored at temperature of 6-8^{0}C. Those eyeballs were divided into groups, according to the following post-mortem intervals: 4, 28, 52, 76, 100, 124, 148 hours. The vitreous fluid was collected, acc.to Coe's method [5]. For separation of LPVF, nylon (0.42 μm) filters were employed. Separation control of the gelatinous portion from the LPVF (for ion concentration study) was performed on stained fluid smears, prepared before and after the separation (H&E -for cells, nuclei and other cellular structures or Gram method- for bacteria, microscopy- 100x immersion). The volume of 1.5 -2.0 LPVF was divided into two portions of equal volumes. In each liquid portion volume, Na^+ and K^+ ion concentrations were

Table 1. Average concentration of K^+ and Na^+ (mmol/L) ions in the control group and PIM (in hours) in the liquid portion of the swine vitreous fluid, estimated by flame photometry and potentiometry methods.

	C	4	28	52	76	100	124	148
Potassium Flame Photometry	x = 6.7 SD = 0.85 n = 20 v =12.68%	x = 8.45 SD = 1.12 n = 108 v = 13.25%	X =15.85 SD =1.05 n =36 v = 6.62%	x =22.48 SD =1.48 n = 36 v = 6.58%	x =23.35 SD =1.48 n =36 v = 6.33%	x =26.75 SD =1.96 n = 36 v = 7.32%	x =23.12 SD =4.46 n = 36 v = 19.29%	x = 24.5 SD =3.33 n = 36 v = 13.59%
Potassium Indirect Potentiometry	x = 5.94 SD= 0.64 n= 10 v =10.77%	x = 7.02 SD= 0.53 n= 14 v = 7.54%	x = 12.85 SD= 1.25 n= 6 v = 9.72%	x = 20.08 SD= 2.35 n= 6 v = 11.7 %	x = 22.65 SD= 2.01 n= 6 v = 8.87%	X = 27.06 SD= 1.72 n= 6 v = 6.35 %	x = 24.06 SD= 3.20 n= 6 v = 13.3 %	x = 25.13 SD= 4.42 n= 6 v = 17.58 %
Sodium Flame Photometry	x = 143.6 SD= 2.5 n=20 v = 1.74%	x = 141.24 SD= 1.94 n= 108 v = 1.37%	x = 136.5 SD= 2.96 n= 36 v = 2.16%	x = 126.55 SD= 3.19 n= 36 v = 2.52%	x = 129.58 SD= 4.37 n= 36 v = 3.37%	x = 123.0 SD= 5.64 n= 36 v = 4.58%	x = 120.36 SD= 6.44 n= 36 v = 5.35%	x = 117.22 SD= 4.54 n= 36 v = 3.87%
Sodium Indirect Potentiometry	x = 140.3 SD= 1.76 n= 10 v = 1.25%	x = 134.57 SD= 1.65 n= 14 v = 1.22%	x = 133.66 SD= 3.44 n= 6 v = 2.57%	x = 126.66 SD= 2.06 n= 6 v = 1.62%	x = 132.50 SD= 5.24 n=6 v = 3.95%	x = 127.16 SD= 4.79 n= 6 v = 3.76%	x = 118.33 SD= 4.41 n= 6 v = 3.72%	x = 113.33 SD= 5.16 n= 6 v = 4.55%

estimated by flame photometry and potentiometry. The Corning 4800 flame photometer was used for the estimation of K^+ ions (the range: 0-150 mmol/L, variability 1.1%) and for Na^+ ions (the range 0-200 mmol/L, variability 0.4%). The biochemical automatic Vitros device was employed for the potentiometric estimation of K^+ (the range 2.5-175 mmol/L, variability 3.6%) and Na^+ ions (the range 5-250 mmol/L, variability 2.7%). The controls and the standards for the Corning 4800 flame photometer and for the biochemical automatic Vitros device were obtained from manufactures. The obtained results were statistically analyzed for the distribution of the results, variance, and differences between particular groups. A normal distribution of data was noted very rarely, and non-parametric tests were employed.

Results

In the smears of vitreous fluid before filtration, stained by H&E, the cells and their fragments were observed at different frequencies in all the studied groups. Moreover, during post-mortem intervals, up to 76 hours, no bacteria were visible in Gram-stained smears. From the 100 hour post-mortem interval, in some Gram stained smears, with different frequency (per microscope field), Gram+ and Gram- bacteria (1-3 per filed) were noted. In all the smears after 124 and 148 hours, bacteria cells were visible, mainly Gram negative. After filtration the smears from LPVF were free from bacterias, cells and their fragments.

A lack of normal distribution of flame photometry results and of potentiometry of both ion concentrations were noted in the studied groups. The results of Mann-Whitney and Kolmogorov-Smirnoff tests showed that significant differences existed between median and data distribution in Na^+ and K^+ levels, derived from the measurement by flame photometry and potentiometry methods in the control and in other studied groups (after 28, 52, 76, 100 post-mortem time intervals), except for the 4 hour and the 128 - 140 hour time intervals. The results of Na^+ and K^+ concentration in the latter post-mortem time intervals revealed a higher variability, as compared to the results in the groups from 28-100 hour PMI. The increase of K^+ concentration in LPVF was proportional to the increase of post-mortem time interval. The decrease of Na^+ concentration in that LPVF was proportional in a similar manner. Such relationships were not dependent on the employed methods. However, the results of the potentiometric measurement of K^+ and Na^+ ion concentrations were significantly lover, as compared to those after flame photometry (Table 1). The increase of K^+ (y) concentration in relation to PMI (x) was not dependent on used method. It was described by two models of regression: y= a + b*sqrt(t) and y= a+b*t, (where "a" is a control level of K^+ concentration, "b" slope per hour (1.98 mmol/L - flame photometry; 2.08 mmol/L - potentyometry). The differences in correlation coefficients and the percentage of explained data were not significant. The concentration of Na^+ ions in LPVF decrease was described by a similar type of equations but: y= a - b*sqrt(t) and y= a - b*t . The first equation was optimal for flame photometry method and the second one - for potentiometry. All the correlation coefficients for all the equations were within the range of 0.86-0.96 with probability p> 0.01

Discussion

The studies on the chemical composition of the vitreous fluid are mainly performed on the eyeballs without removing the organs from the body [4, 6, 7]. Separated eyeballs have been used very rarely and mainly on laboratory animals, e.g., rabbits. The PMI, employed in experimental studies (e.g. pigs, dogs and small laboratory rodents), is limited, in general, to 48 hours post mortem. The presence of Gram minus bacteria in the eyeball and in the aspirated vitreous liquor, established in our studies after 100 post-mortem hours, was not surprising because eyeball sampling was performed in non sterile conditions. Such a bacterial invasion may be a substantial limitation in PMI studies on changes in the eye structure and on the

chemical composition of vitreous body and vitreous fluid. The major advantages of experiments on separated swine eyeballs include: similar weight and age of the animals, veterinary control, identical death, well known time of death and of the collection of organs, very good access to the control of the experimental conditions (e.g. humidity, temperature) [2]. The temperature, at range 6-8^{0}C, is commonly used for the human cadaver storage. In such conditions, as we described earlier, a slower progress of post-mortem changes may better be observed in morphological and immunohistochemical studies [8, 9]. This lowering effect was also visible in our studies on ion concentrations. The changes in K^+ and Na^+ levels in the vitreous fluid, as estimated by us by two different methods, demonstrated a closely related direction. Those changes were in a good agreement with the results of other authors [4, 6, 7]. The differences in the results between flame photometry and potentiometry were described earlier in studies on human vitreous fluid [2]. In the changes of post-mortem K^+ and Na^+ levels in LPVF, two different periods were distinct with a high variability of results. The first period was visible during the first 10 hours post-mortem, the second one - during the last 48 hours of the study. The results during the first period may be dependent on the animal stress [4], an unknown ability of ion binding by gelatinous portion of the vitreous fluid and/or rapid death of ten neural cells, including the autonomic ganglia (interlethal period). The second period may depend mainly on the breaking of the ocular barrier (in situ blood-ocular barrier) by bacterial invasion and storage of the ions by growing bacterial cells. In many publications on the vitreous K^+, determined at post-mortem intervals, the problem of bacterial invasion was not discussed. Our results suggest that bacterial infection participates in the variability of K^+ levels. The influence of bacterial infection on the margin of error for the K^+ post-mortem test remains unanswered and needs further studies. This is very important because such errors can sometimes make this test worthless [2].

Acknowledgments

This study was supported by Grant No 502-11-774 from the Medical University of Łódź.

References

1. Gamero Lucas JJ, Romero JL, Ramos HM, Arufe MI, Vizcaya MA. Precision of estimating time of death by vitreous potassium - comparison of various equations. Forensic Sci Int, 1992; 56: 137-45.

2. Coe J I. Vitreous potassium as a measure of the postmortem interval: an historical review and critical evaluation. Forensic Sci Int, 1989; 42: 201-13.

3. Munoz JI, Suarez-Penaranda JM, Otero XL, Rodriguez-Calvo MS, Costas E, Miguens X, Concheiro L. A new perspective in the estimation of postmortem interval (PMI) based on vitreous [K^+]. J Forenic Sci, 2001; 46: 209-14.

4. Henke SE, Demarais S. Changes in vitreous humor associated with postmortem interval in rabbits. Am J Vet Res, 1992; 53: 73-7.

5. Coe J I. Postmortem chemistry updata: emphisis on forensic aplication. Am J Forensic Med Pathol, 1993; 14: 91-117.

6. McLaughlin PS, McLaughlin BG. Chemical analysis of bovine and porcine vitreous humours: correlation of normal values with serum chemical values and changes with time and temperature. Am J Vet Res, 1987; 48: 467-73.

7. Schoning P, Strafuss AC. Postmortem Biochemical Changes in Canine Vitreous Humor. J Forensic Sci, 1980; 25: 53-9.

8. Brzeziński PM, Godlewski A. The assessement of post mortem PCNA+ cell frequency in the rat epidermis. Folia Histochem Cytobiol, 2001; 39: 225-7.

9. Brzeziński PM, Godlewski A. Topographical and quntitative post mortem assessement of the rat skin mast cells. Folia Histochem Cytobiol, 2001; 39: 227-8.

Histological structure of bovine coronary arteries at varying distance from their origins from the aorta (a preliminary study)

Bylina D, Węgrzyn M, Rowiński J

Department of Anatomy, Department of Physical Education in Biała Podlaska,
The Jozef Pilsudski Academy of Physical Education in Warsaw, Biała Podlaska, Poland

Abstract

Coronary arteries of three bovine hearts, obtained from animals, aged about 2 years, were studied. Both right and left coronary arteries were dissected out, divided into 10 mm long segments, fixed in formalin and embedded in paraffin. Histological sections were cut in a plane perpendicular to the axis of the vessel and stained, using van Gieson's method; additional staining with resorcin-fuchsin.

We observed a distinct thickening of the tunica media, formed by circular layers of smooth muscle cells and by a small amount of elastic fibres, in the ramus interventricularis subsinuosus and paraconalis. The tunica media thickenings were situated in the middle segments of the coronary arteries at a distance of about 2-3 cm from its origin in the aorta.

Key words: heart, coronary vessels, tunica media, histology.

Introduction

The mechanisms, which regulate blood flow through the inner organs of animals, and the morphological structures of arteries, which are involved in this regulation, remain unsatisfactorily known in spite of numerous physiological and histological descriptions [1-6]. Thickenings of the tunica media in the arteries of muscular type were described in recent years [7-11] in limbs of several mammal species. We undertook a microscopic study of the walls of bovine coronary arteries in search for similar morphological specializations, presumably participating in blood flow regulation.

ADDRESS FOR CORRESPONDENCE:
Dorota Bylina
Department of Anatomy, Department of Physical Education in Biała Podlaska,
The Jozef Pilsudski Academy of Physical Education in Warsaw
Akademicka 2; 21-500 Biała Podlaska, Poland
tel. +(83) 342 8 736;
e-mail: dorota.bylina@awf-bp.edu.pl or dorb@vp.pl

Material and methods

Three bovine hearts were obtained immediately post mortem at the slaughterhouse from cows of the black and white breed, about 2 years of age. Both right and left coronary arteries were dissected. The vessels were divided into successive 10 mm long segments, starting from the origin from the aorta, and fixed in 5% formalin. Next the segments were embedded in paraffin; 8 μm thick histological sections were cut in a plane perpendicular to the axis of the vessel and mounted onto microscopic glasses. They were stained, using van Gieson's trichrome method (for the differentiation between muscle cells and connective tissue fibres). Additional staining with resorcin-fuchsin, according to Weigert (for visualization of elastic fibres), was performed on the same sections. It enabled us to differentiate separate components of the arterial walls (smooth muscle cells, collagen fibres, elastic fibres). We also measured the thickness of the three layers of arterial wall: tunica intima, tunica media and tunica adventia. The measurements were made, using the Microscan V 1×30 computer program with accuracy of 0.001 mm.

Results

The qualitative morphological characteristics of the coronary arteries, resulting from the specimens, prepared as described above, are given below.

The left coronary artery (arteria coronaria sinistra) has a relatively short trunk which divides into 2 big branches: (a) ramus interventricularis paraconalis, which runs to the heart's tip, and

Figures 1, 2 and 3. Microphotographs of the histological preparations of the coronary arteries (ramus interventricularis paraconalis of arteria coronaria sinistra), stained by van Gieson's trichrome method and with resorcin?fuchsin. Proximal segment (Fig. 1), middle segment (Fig. 2 and 3). Labels: a-tunica intima, b- tunica media, c- tunica adventitia; 1- elastic tunica intima, 2- circular layers of smooth muscle cells, 3- elastic fibres.

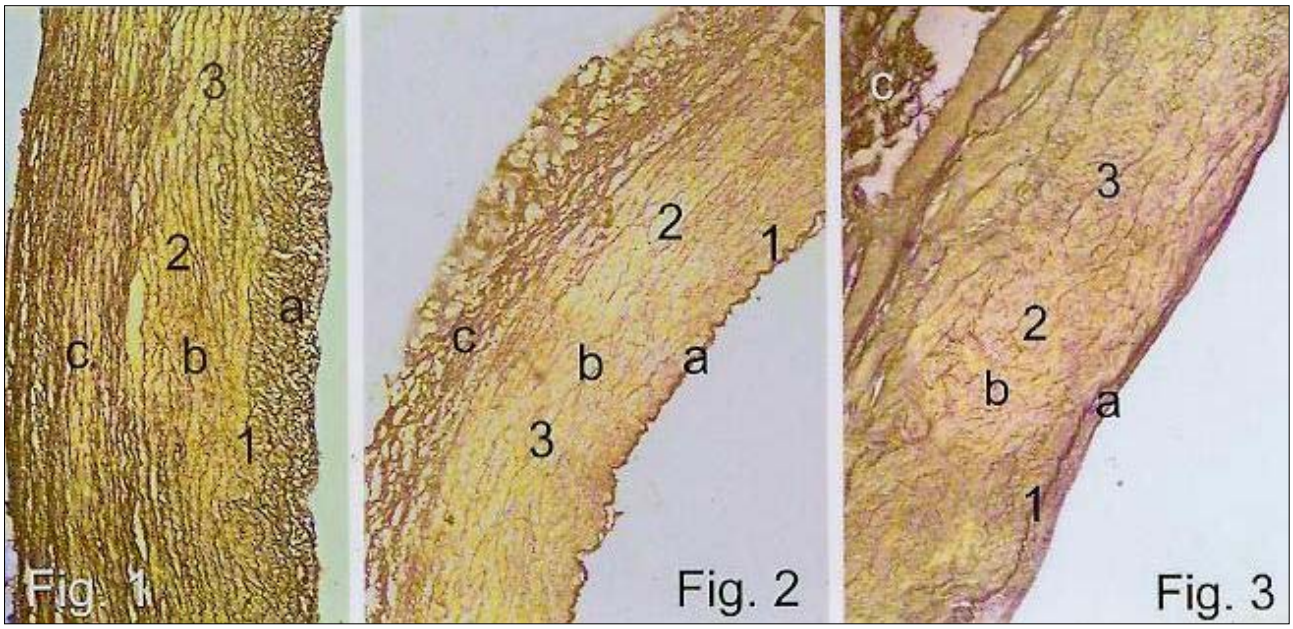

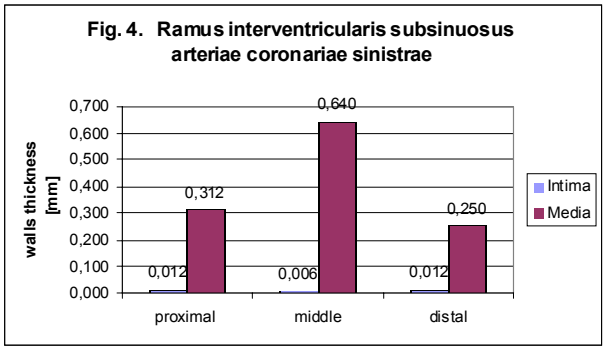

(b) ramus circumflexus, running along the coronary groove; this vessel in cattle passes into ramus interventricularis subsinuosus.

The ramus interventricularis paraconalis varies in its structure in different segments. The proximal segment is short and has a thin tunica media, composed of smooth muscle (Fig. 1-b) and of elastic fibres (Fig. 1-3). The middle segment (Fig. 2, 3-b) is situated 2 cm away from the aorta, it is 2-3 cm long and its tunica media gradually increases in thickness (to 0.437 mm); it contains considerably smaller amount of elastic fibres, as compared to the proximal segment. The distal segment of the vessel begins 5 cm away from the beginning of the artery; it is characterized by a gradually decreasing thickness of tunica media (0.375 mm), which is composed of smooth muscle cells and of a subtle network of elastic fibres. Tunica intima is comparatively thick in the proximal segment of the artery, farther on, it undergoes a definite thinning (Fig. 1; 3-a). Tunica adventitia (an external coat) becomes thinner along with the farther run of the artery. The ramus circumflexus has a similar structure of tunica media and its distinct thickening can be observed in the middle segment, between the 2nd and the 5th cm away from the origin of the vessel. The ramus interventricularis subsinuosu (a distal branch) in cattle is a continuation of the ramus circumflexus of the arteria coronaria sinistra. This distal branch has a thin tunica media (0.312 mm) but, at the point of transition into the ramus interventricularis subsinuosus, it grows definitely thicker (0.640 mm) and, along its farther course, it gradually becomes again distinctly thinner (0.25 mm) (Fig. 4).

In the right coronary artery (arteria coronaria dextra), the tunica media of the proximal segment is comparatively thin (0.344 mm). in the middle segment, it becomes thicker (0.562 mm) and, in the distal segment, it again becomes thinner.

Discussion The walls of the coronary arteries, as described here, are characterized by thickening of the tunica media in the middle segments. These thickenings are formed by several layers of circular smooth muscle cells and by a network system of elastic fibres. A similar thickening has been described in the arteries of limbs in a number of mammalian species [7-11]. In conditions of psychical stress, a complete closure of these arteries has been observed, what proves the view that "muscle rings" may stop the blood supply to body parts [11]. Our results, reported here, are preliminary ones. It is necessary to study larger material before any final conclusions may be drawn. The preliminary results indicate that "muscle rings" [7-11] are also present in the coronary arteries of cattle. They presumably participate in the regulation of blood supply to myocardium.

Acknowlegments

The project was supported financially from academic grant Nr VII/153.

References

1. Baum H. Der Zirkulationsapparat. in: Handbuch der vergleichenden mikroskopischen Anatomie der Haustiere-Ellenberger. Berlin: P Parey, Berlin, 1911; 1-66.

2. Bijak A. W poszukiwaniu przyczyn kurczu tętnic wieńcowych. Kard. Pol, 1986; 29: 484-93.

3. Cliff W. Blood vessels. Cambridge University Press, 1976; 144-5.

4. Drenckhahn D, Zenker W. Benninghoff Anatomie. Urban-Schwarzenberg, 1994; 1: 652-85.

5. Jasiński K. Choroba niedokrwienna serca. Warszawa: PZWL, 1987.

6. Schummer A. Morphologische und funktionelle Betrachtungen zum peripheren Blutkreislauf. Tierarzt. Umschau, 1954; 21: 374-8.

7. Węgrzyn M. The thickening of the arterial walls in the extremities of European bison (Linnaeus 1758). Ann Wars Agric Univ Vet Med, 1988; 14: 29-40.

8. Węgrzyn M. The thickening of the arterial walls in the extremities of domestic dog, Canis familiaris (L.), Ann Wars Agric Univ Vet Med, 1990; 16: 19-29.

9. Węgrzyn M, Janiuk I, Huk E. Arterial muscle rings in the limbs of horse - Equus caballus L. Ann Wars Agric Univ Vet Med, 1996; 20: 25-33.

10. Węgrzyn M, Tokarska E, Huk?Wieliczuk E. Denervation of arterial muscle rings in the limbs of the experimental animals. Bull Pol Ac: Biol, 1999; 47: 27-33.

11. Węgrzyn M, Tokarska E, Enbergs H, Huk-Wieliczuk E. Muscle arterial rings function during stress in mammals. Bull Pol Ac: Biol, 2001; 49: 19-23.

Modulatory effect of quercetin on DNA damage, induced by etoposide in bone marrow cells and on changes in the activity of antioxidant enzymes in rats

Cierniak A[1], Papież M[2], Kapiszewska M[1]

[1]Department of General Biochemistry, Faculty of Biotechnology, Jagiellonian University, [2]Department of Cytobiology and Histochemistry, Faculty of Pharmacy, Collegium Medicum, Jagiellonian University, Poland

Abstract

The aim of the studies was to evaluate the influence of quercetin on etoposide-induced DNA damage in rat bone marrow cells and on changes in the activities of superoxide dismutase (SOD), catalase and antioxidant power in lung tissue (AOP). Quercetin was administrated by gavage at a dose of 135 mg/kg b.w. for three consecutive days, and one hour after the last dose, etoposide was intraperitoneally injected, at dose of 80 mg/kg b.w. Bone marrow cells were harvested from the femurs 24 hours later and DNA damage was evaluated by the comet assay, under alkaline condition. The study provided evidence that quercetin, administered to rats, provides major protection against etoposide-induced DNA damage in bone marrow cells and does not influence either the SOD activity, lowered by etoposide, or AOP, enhanced by etoposide.

Introduction

One of the most important questions in chemotherapy regards the possibility of DNA damage prevention in healthy bone marrow cells during treatment with etoposide, without lowering the antitumour potency of the drug. We approached this issue by checking the effect of etoposide treatment, followed by quercetin administration, on DNA in bone marrow cells of healthy rats. The rationale behind that attempt was such that quercetin may prevent oxidation of etoposide phenoxyl radicals, generated by myeloperoxidase, a constitutively expressed enzyme, the activity of which is particularly high in myeloid progenitor cells [1-3]. Such an antioxidant recycling may enhance the antioxidative potential [2]. However, quercetin can react with etoposide only if it is still in circulation. Because the maximum quercetin concentration occurs within up to 1 h after its intake, at least, in human studies [4], the etoposide was administered after 1 h from the last quercetin exposure. A significant decrease in DNA damage in bone marrow cells was observed 24 h later. Those results confirmed our previous observation with stimulated human lymphocytes, which also showed that quercetin, given together with etoposide, lowered the extent of DNA damage [5].

ADDRESS FOR CORRESPONDENCE:
Maria Kapiszewska
Department of General Biochemistry, Faculty of Biotechnology
Jagiellonian University
Gronostajowa 7, 30-387 Kraków
Tel. (012) 6646139; e-mail: mkapisze@if.uj.edu.pl

Material and Methods

Quercetine was administered by gavage at final concentration of 135 mg/kg b.w. to two groups of rats (three-month-old male Wistar rats -WAG/Krf), every 24 hours for three consecutive days. On the third day, 1 h after the last dose of quercetin, the first group (designated in all figures and tables as "quercetin") was sacrificed. At the same time, the etoposide, at a dose of 80 mg/kg b.m., was intraperitoneally given to the second group of rats, pretreated with quercetin (designated in all figures and tables as "quercetin +etoposide". The third group of rats received only etoposide (designate in all figures and tables as"etoposide"). After 24 h from the exposure to etoposide, each individual was sacrificed. The lungs were removed from all the rats in each group and stored at - 20^0 C. Bone marrow cells were flushed from femurs into PBS (Ca^{2+}, Mg^{2+} free) and gently resuspended in a mixture, containing dimethylsulphoxide (DMSO) and fetal bovine serum (FBS), to obtain final concentrations of DMSO at 10% v/v and FBS at 50% v/v. The cellular mixture was cooled at approximately 10C per min. and stored at -80^0C until analysis was performed (within less than two weeks). The control rats were also sacrificed at that time. The activity of SOD was measured by the Misry and Fridovich

Table 1. The activity of SOD, catalyse and a ferric-reduction antioxidant power (FRAP) was measured in the homogenate of lung tissue isolated from the control group of rats (1) and 24 hours after: (2) last dose (135 mg/kg b.w.) of quercetin; (3) etoposide (80 mg/kg b.w.); (4) etoposide treatment 1 h after last quercetin administration. Post-hoc test (one-way ANOVA) was performed and differences (P - values) between groups (means) are presented.

treatment SOD activity	[1]	[2]	[3]	[4]
control [1]		0.576	0.066	0.163
quercetin [2]	0.576		0.014	0.061
etoposide [3]	0.066	0.014		0.925
quercetin+etoposide [4]	0.164	0.0614	0.925	
treatment catalase activity	[1]	[2]	[3]	[4]
control [1]		0.853	0.918	0.448
quercetin [2]	0.853		0.916	0.522
etoposide [3]	0.918	0.916		0.448
quercetin+etoposide [4]	0.448	0.522	0.448	
treatment antioxidant power	[1]	[2]	[3]	[4]
control [1]		0.812	0.009	0.012
quercetin [2]	0.812		0.009	0.013
etoposide [3]	0.009	0.009		0.537
quercetin+etoposide [4]	0.012	0.013	0.537	

Figure 1. The mean values of DNA damage (TDC) measured by comet assay in bone marrow cells isolated from control rats and isolated 24 hours after: a) the last dose (135mg/kg b.w.) of quercetin administrated for three consecutive days; b) etoposide (80mg/kg b.w.); c) etoposide treatment given 1 h after the last dose of quercetin (135mg/kg b.w.) administration.

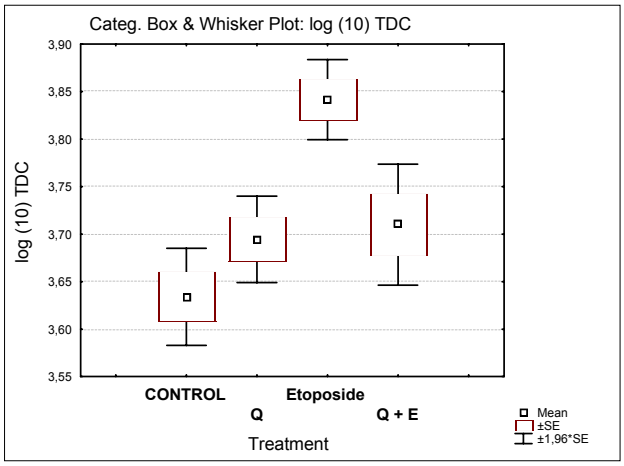

method [6] and catalase activity was evaluated by the Aebi assay [7]. The ferric-reducing antioxidant power (FRAP) was determined in homogenate of lung tissue by the Bezni and Strain method [8].

The comet assay was performed, according to the original laboratory protocol for the application of the pH>13 alkaline single cell gel assay, to detect DNA damage in the cells [9]. Electrophoresis was conducted at 0.74 1V/cm for 30 min. The current was adjusted to 300 mA. An image analysis system (CometPlus from ThetaSystem GmbH, Germany) was used for the quantification of DNA damage. The percentage of DNA in the tail (TDC) was automatically generated. At least two slides per one rat, with 50 randomly selected cells per slide, were analyzed. The one-way ANOVA and post-hoc test comparison of the means was performed to detect differences between the groups (means) of data from the FRAP, SOD and catalase activity tests. The data, obtained from the comet test (TDC), were analyzed by the same test, following log transformation. The experiments were performed in accordance with Polish legal requirements and under a license, granted by the Commission of Bioethics of the Jagiellonian University.

Results and Discussion

The amount of endogenous alkali-labile DNA damages, analyzed by the comet assay in bone marrow cells, was not changed by quercetin administration (P= 0.09), whereas etoposide treatment induced highly significant DNA damage (P = 0.000000). Ouercetin, administered before etoposide treatment, drastically lowered the amount of DNA strand breaks, as compared to the values, when etoposide was given alone (P=0.0008). That amount was non-significantly different from the damages, observed in bone marrow cells after quercetin administration alone (P=0.7) (Fig. 1).

It is evident from Table 1, that quercetin, administered alone, slightly increased the activities of both antioxidant enzyme, as SOD, and catalase. The same trend was observed with regard to the AOP, measured by the FRAP assay. However, the statistical analyses revealed that that enhancement was not significantly different from the control values.

The effects of etoposide administration were evaluated after 24 h. As shown in Table 1, etoposide treatment did not influence catalase activity but decreased the SOD activity only at the borderline of statistical significance (P = 0.066). In spite of that, AOP was significantly higher (P = 0.009), as compared to the respective value in the control rats. When etoposide injection was given 1 h after the last quercetin dose and lung tissue was

removed 24 h later, the catalyze activity remained unchanged, as compared to: the control (P=0.918), etoposide (P= 0.448) and quercetin given alone (P=0.522). SOD activity continued to be the same, as compared with that, when etoposide was given alone (P=0.925), being at the borderline of statistical significance (P= 0.0614), when compared with respective values, when quercetin was given alone. The AOP after treatment with both compounds was still significantly higher than that in the control (P=0.012) and after quercetin alone (P=0.013), but it did not significantly differ (P=0.537) from the values, observed in etoposide treatment.

The presented data provide evidence that a prolonged exposure to quercetin does not affect either SOD or catalase activities. That what was also shown by Breinholt et all [10]. Similarly, Hilbert et al showed [11] that no significant down regulation of SOD or CAT was observed in the lung lavage cells, despite an increased concentration of vitamin E and beta carotene. The lowered SOD activity in etoposide-treated rats is opposed to expected results if SOD was to be important for DNA damage protection. An analogous result was obtained after bleomycin treatment. Two days after bleomycin administration, total lung SOD, CAT, and GSHP activities were significantly depressed - between 15 and 25%. [12].

Effects of prolonged administration of quercetin, causing the decrease in genotoxicity of etoposide treatment, may indicate that nutritional strategies for preventing or ameliorating the DNA damage in normal cells is possible.

Acknowledgements

This research was supported by the State Committee for Scientific Research, project No. 3 P05E 016 25.

References

1. Andoh T. Mechanism of occurrence of secondary tumours by antitumor drugs. Gan To Kagaku Ryoho, 1999; 26: 1988-98.

2. Kagan VE, Yalowich JC, Borisenko GG, Tyurina YY, Tyurin VA, Thampathy P, Fabisiak JP. Mechanism-based chemopreventive strategies against etoposide-induced acute myeloid leukemia: free radical/antioxidant approach. Mol Pharmacol, 1999; 56: 494-506.

3. Joseph CD, Praveenkumar V, Kuttan G, Kuttan R. Myeloprotective effect of a non-toxic indigenous preparation Rasayana in cancer patients receiving chemotherapy and radiation therapy. A pilot study. J Exp Clin Cancer Res, 1999; 18: 325- 29.

4. Hollman PC, Katan MB. Absorption, metabolism and health effects of dietary flavonoids in man. Biomed Pharmacother, 1997; 51: 305-10.

5. Cierniak A, Kapiszewska M. The effect of quercetin on DNA damage induced by etoposide. Polish J Environm Studies, 2002; 11: 111-5

6. Misra HP, Fridovich I. The role of superoxide anion in the autooxidation of epinephrine and a simple assay for superoxide dismutase. J Biol Chem, 1972; 247: 3170-5.

7. Ross D, Weening RS, Wyss SR, Aebi HE. Protection of human neutrophils by endogenous catalase:studies with calls from catalase-defiecient individuals. J Clin Invest, 1980; 65: 1515-22

8. Bezni I, Strain J. The ferric reducing ability of plasma (FRA) as a measure of "Antioxidant power": the FRAP assay. Annal Biochemistry, 1996; 239: 70-6.

9. Tice RR, Andrews PW, Hirai O, Singh NP. The single cell gel (SCG) assay: an electrophoretic technique for the detection of DNA damage in individual cells. Adv Exp Med Biol, 1991; 283: 157-164.

10. Breinholt VM, Nielsen SE, Knuthsen P, Lauridsen ST, Daneshvar B, Sorensen A. Effects of commonly consumed fruit juices and carbohydrates on redox status and anticancer biomarkers in female rats. Nutr Cancer, 2003; 45: 46-52.

11. Hilbert J, Mohsenin V. Adaptation of lung antioxidants to cigarette smoking in humans. Chest, 1996; 110: 916-20.

12. Fantone JC, Phan SH. Oxygen metabolite detoxifying enzyme levels in bleomycin-induced fibrotic lungs. Free Radic Biol Med, 1988; 4: 399-402.

Influence of doxycycline on the epiphyseal plate cartilage of the rats in experimental osteoarthrosis, induced by iodoacetate

Cylwik J[1], Kita K[2], Barwijuk-Machała M[1], Reszeć J[1], Klimiuk P[2], Sierakowski S[2], Sulkowski S[1], Cylwik M

[1]Department of Pathology, Medical University, Białystok, [2]Department of Rheumatology and Internal Diseases,

Medical University, Białystok, Poland

Abstract

In 36 Wistar rats with the iodoacetate-induced experimental osteoarthrosis (OA), effects of doxycycline, given orally, were determined on histochemical reactions of glycosaminoglycans (GAG) in the epiphyseal plate cartilage.

The epiphyseal plate of rats with OA was reduced in height (especially the proliferative zone), cell columns were disorganized, many chondrocytes were irregular and polygonal, their nuclei were pycnotic, the intensity of GAG staining was irregular and predominantly reduced, which can be interpreted as signs of degeneration. A concomitant administration of doxycycline in the second group of rats prevented, to some extent, the negative effects of iodoacetate on chondrocytes and led to a more pronounced intensity of GAG reactions in the matrix of the epiphyseal plate.

Key words: osteoarthrosis, mono- iodoacetate, doxycycline.

Introduction

In the previous work, we studied histochemical reactions of GAG in the articular cartilage of rats, treated with iodoacetate, suggesting that a concomitant administration of doxycycline had some protective potential on the content of GAGs in chondrocytes and the articular matrix [1].

The aim of the present study was to determine, whether or not doxycycline might play any role of the GAGs histochemical reactions in the epiphyseal plate cartilage of the rats in experimental osteoarthrosis, inducted by iodoacetate.

ADDRESS FOR CORRESPONDENCE:
Jacek Cylwik
Department of Pathology
Medical University of Bialystok
Waszyngtona 13; 15-274 Białystok, Poland
e-mail: jacylwik@poczta.onet.pl

Material and methods

The procedure of the experiment was previously described [1]. Shortly, on the first day, iodoacetate was given to the left posterior knee joint (I group).

The second group of the rats additionally received doxycycline through the gastric tube in doses, comparable with those, used in men. The rats were sacrificed after 7, 14, 21 days (6 rats in each group). Tissue sections were stained with H+E and Safranin O.

Results

In the epiphyseal cartilages from the control right posterior knee joints, four well defined zones: the resting, proliferative, hypertrophic and mineralized, can be determined. The epiphyseal plates in the first group of rats were predominantly strongly reduced in height and, in most areas, the organization of cell columns was severely disturbed. Many of the chondrocytes were of irregular shape and with pycnotic nuclei.

The intensity of GAG staining was predominantly reduced. Focal loss of chondrocytes, negative staining of GAG with fibrillations perpendicular splits, clefts and irregular lacunae were often observed. A great intensity of changes, which can be interpreted as signs of degeneration or necrosis, was observed in almost all the rats Table 1.

Similar histological and histochemical changes were observed in the second group of rats but in 8/18 animals, they were somewhat less pronounced Table 1. The epiphyseal plates were higher, the organization of cell columns was partly preserved, the number of chondrocytes was focally increased with positive GAG histochemical reactions in their vicinity.

Table 1. Approximate evaluation of histological and histochemical changes in the rats with iodoacetate osteoarthrosis, treated with doxycycline.

Group	**I**			**II**		
Days	7	14	21	7	14	21
Intensity of lesions						
• Less pronounced	-	-	-	-	-	-
• More pronounced	2/6	-	-	3/6	2/6	3/6
• Severe	4/6	6/6	6/6	3/6	4/6	3/6

Legend
Counter- the number of rats with lesions
Denominator- the number of rats in subgroup.

Discussion

Intraarticular injections of iodoacetate in experimental animals induce degenerative changes of the articular cartilage, which are similar to osteoarthrosis in men [2]. This model is used to study the effects of some non-steroidal and steroidal drugs in the course of osteoarthrosis treatment [3, 4].

The results of this study indicate that iodoacetate, injected to the joint, damages not only the superficial articular cartilage but it deeply penetrates the joint structures with similar lesions in the epiphyseal plate cartilage.

Some investigations have shown that matrix metalloproteinase inhibitors, among them doxycycline, are partially protective against cartilage and subchondral bone damage, induced by iodoacetate [3, 4].

As in the previous study [1], in some rats, treated with doxycycline, we observed signs of focal chondrocyte proliferation and of matrix GAG production, what may have indicated a normalizing effect of this drug. Nevertheless, the results of this study need verification by other methods of investigation. They must also be evaluated with an appropriate caution in the extrapolation of results to human osteoarthrosis.

References

1. Cylwik J, Kita K, Barwijuk-Machała M, Reszeć J, Klimiuk P, Sierakowski S, Sulkowski S. The influence of doxycycline on articular cartilage in experimental osteoarthrosis induced by iodoacetate. Folia Morphol, 2004; 63: 237-9.

2. Kalbhen DA, Blum V. Theoretisches Konzept and experimentelle Bestätigung für ein neues Arthrose Modell am Versuchstier. Arzneimittelforschung, 1977; 27: 527-31.

3. Janusz MJ, Hookfin EB, Heitmeyer SA, Woessner JF, Freemont AJ, Hoyland JA, Brown KK, Hsieh LC, Almstead NG, De B, Natchus MG, Pikul S, Taiwo YO. Moderation of iodoacetate- inducted experimental osteoarthritis in rats by matrix metalloproteinase inhibitors. Osteoarthr Cartilage, 2001; 9: 751-60.

4. Yu LP Jr, Smith GN Jr, Brandt KD, Myers SL, O'Connor BL, Brandt DA. Reduction of the severity of canine osteoarthritis by prophylactic treatment with oral doxycycline. Arthritis Rheum, 1992; 35: 1150-9.

Expression of PCNA and Ki-67 in the rat submandibular gland after one year cadmium intoxication - a preliminary study

Czykier E[1], Dzięcioł J[2]

[1]Department of Histology and Embryology, [2]Department of Anatomy, Medical University of Białystok, Poland

Abstract

The aim of our study was to determine to what degree one-year exposure of female rats to cadmium at a dose of 5, 50 and 100 mg Cd/l affects cell proliferation in the submandibular gland, shown by PCNA and Ki-67 expression. In the present study, we found a positive nuclear reaction for PCNA in single cells in microscopic preparations of control rats. In Group I, an increase was observed in the number of PCNA-positive cells, compared to that in the control. In Group II, the number of PCNA-positive cells was markedly higher than that in Group I and in the control. In the submandibular glands of rats in Group III, the number of PCNA-positive cells was similar to that, found in Group II. However, Ki-67 expression was sporadically observed in control submandibular glands, but not in Groups I, II and III.

Key words: submandibular gland, rat, expression of PCNA and Ki-67.

Introduction

Cadmium (Cd) is a trace metal which accumulates in the body organs with age [1, 2, 3]. Until now, it has been demonstrated that a 24-week exposure to cadmium at a dose of 5 and 50 mg Cd/l not only leads to its accumulation in the submandibular gland, but it also increases the percentage of cells, showing a positive reaction for the proliferating cell nuclear antigen (PCNA) in both experimental groups, compared to the control, with lack of human Ki-67 antigen (Ki-67) expression [4]. PCNA is treated as a co-factor for DNA polymerase in both the S phase of the cell cycle and in DNA synthesis, associated with DNA repair [5]. The Ki-67 antigen occurs in proliferating cells in the G_1, G_2, S and M phases of the cell cycle, but is absent during DNA repair [6]. The aim of the present study was to determine to what a degree one year exposure of female rats to cadmium at a dose of 5, 50 and 100 mg Cd/l affects cell proliferation in the submandibular gland, manifested in PCNA and Ki-67 expression.

ADDRESS FOR CORRESPONDENCE:
Elżbieta Czykier
Department of Histology and Embryology
Medical University of Białystok
Kilińskiego 1; 15-089 Białystok, Poland
e-mail: czykier@amb.edu.pl

Material and methods

The study involved twenty-two young female Wistar rats, allocated to 4 groups. Six control rats received only redistilled water to drink. Eighteen experimental rats were given an aqueous solution of cadmium chloride (CdCl2): six rats in Group I received a dose of 5mg CD/l, six animals in Group II received a dose of 50 mg Cd/l and the remaining four in Group III - 100 mg Cd/l. The animals were sacrificed in pentobarbital narcosis. Immunocytochemical reaction was performed, using specific monoclonal mouse antibodies against PCNA 1:50 Clone PC10, Code No. M0879 (Dako) and monoclonal human antibodies against Ki-67 1:50 Clone MIB-1, Code No. M 7240 (Dako). The sections were counterstained with Mayer's haematoxylin.

Results

After one-year of the experiment, we observed a positive nuclear reaction for PCNA in single cells in microscopic preparations of the control rats (Fig. 1). In the submandibular glands of Group I rats, we found an increased number of PCNA-positive cells, compared to that in the control (Figs. 1, 2). In Group II, the number of PCNA-positive cells was markedly higher than that in Group I and in the control (Figs. 1-3). In the submandibular glands of Group III rats, the number of PCNA-po-

Figure 1. The control. Strong immunoreactivity for PCNA in single serous cell nuclei. (X 400).

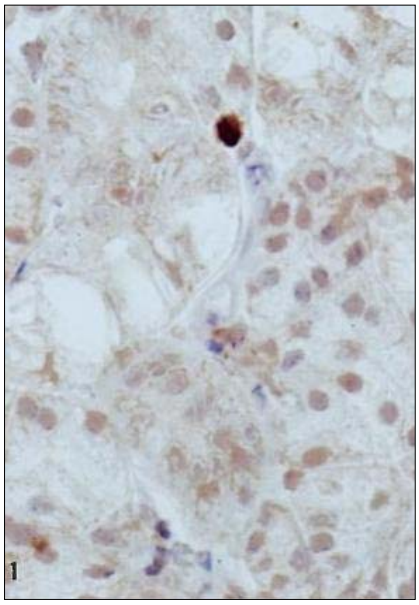

Figure 2. Group I. 5 mg Cd/l. Strong immunostaining of PCNA is present in a few serous cell nuclei. (X 400).

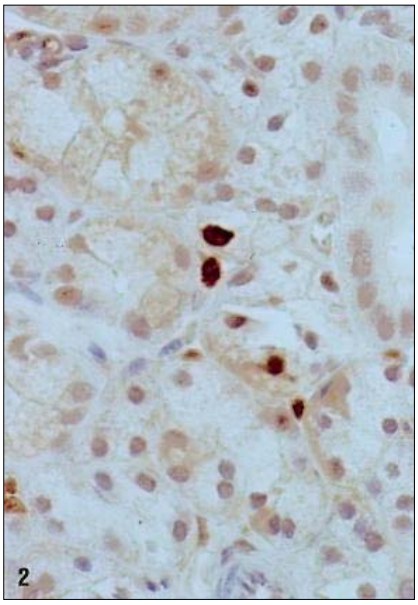

Figure 3. Group II. 50 mg Cd/l. Strong reaction for PCNA in many serous cell nuclei. (X 400).

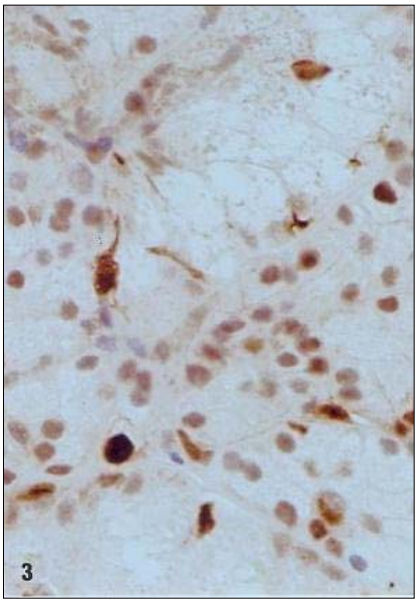

Figure 4. Group III. 100 mg Cd/l. Strong immunoreactivity for PCNA in many serous cell nuclei. (X 400).

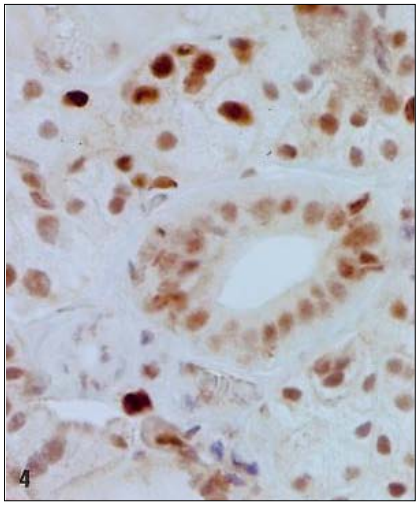

Figure 5. Control. Weaker immunostaining of Ki-67 is present in single serous cell nuclei. (X 400).

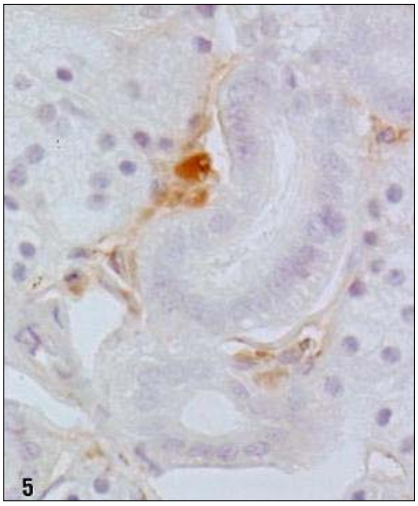

Figure 6. Group III. 100 mg Cd/l. Negative reaction for Ki-67 in the cell nucleus. (X 400).

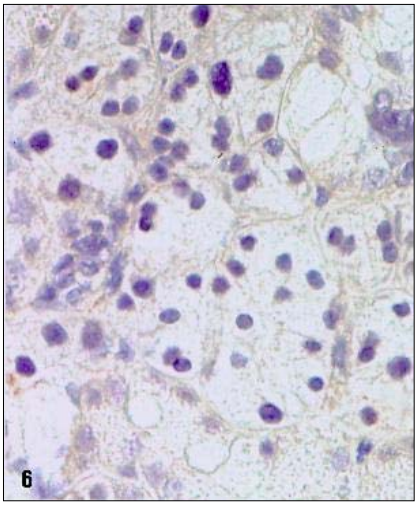

sitive cells was similar to that, found in Group II (Figs. 3, 4). Ki-67-reaction was sporadically found to be positive in the submandibular glands of the control rats, and was negative in Groups I, II and III (Figs. 5, 6).

Discussion

In the present study, after one-year exposure of female rats to cadmium at a dose of 5, 50 and 100 mg Cd/l, an increase was found in the number of PCNA-positive cells in the submandibular glands in all the three experimental groups, compared to that in the control. Considerably more PCNA-positive cells were observed in the submandibular glands of the rats in Group II and Group III, receiving 50 and 100 mg Cd/l, respectively. We obtained similar results in our previous experimental model, during a 24-week exposure of rats to cadmium at a dose of 5 and 50 mg/Cd/l, when the increase in the number of PCNA-positive cells in the rat submandibular glands was dose-dependent [4]. In the present study, the reaction for Ki-67 was negative in all the three experimental groups, compared to respective values in the control. That was similar to our previous model of a 24-week exposure to cadmium, when the reaction for Ki-67 was negative in both experimental groups, compared to that in the control [4]. The increased number of PCNA-positive cells in the submandibular glands of the rats in Groups I, II and III could be associated either with an enhanced proliferation of those cells or with DNA repair processes. In our experiment, the increased number of PCNA-positive cells seems to indicate a predominance of DNA repair processes, rather than cell proliferation, hence the lack of Ki-67 expression, which is a proliferation exponent [6]. Cadmium destroys DNA both in cell culture with

cadmium and in acute or subacute exposure of rat to this metal [7]. We believe that also in the case of one-year exposure of female rats to cadmium, cell DNA is damaged, which is evident in disturbed cell proliferation.

The present experiment indicates that one-year administration of cadmium to rats at a dose of 5, 50 and 100 mg Cd/l, leads to disorders in cell proliferation in the submandibular glands, which is manifested by an increased PCNA expression in cell nuclei and by the lack of Ki-67 expression.

References

1. Gonzalez M, Banderas JA, Baez A, Belmont R. Salivary lead and cadmium in a young population residing in Mexico city. Toxicol Lett, 1997; 93: 55-64.

2. Menegario AA, Packer AP, Gine MF. Determination of Ba, Cd, Cu, Pb and Zn in saliva by isotope dilution direct injection inductively coupled plasma mass spectrometry. Analyst, 2001; 126: 1363-66.

3. White MA, O'Hagan SA, Wright AL, Wilson HK. The measurement of salivary cadmium by electrothermal atomic absorption spectrophotometry and its use as a biological indicator of occupational exposure. J Expo Anal Environ Epidemiol, 1992; 2: 195-206.

4. Czykier E, Dzięcioł J, Zalewska A, Zwierz K. A preliminary study of the submandibular gland of the rat after long-term cadmium intoxication. Folia Morphol, 2003; 62: 305-7.

5. Shivji KK, Kenny MK, Wood RD. Proliferating cell nuclear antigen is required for DNA excision repair. Cell, 1992; 69: 367-74.

6. Scholzen T, Gerdes J. The Ki-67 protein: from the known and the unknown. J Cell Physiol, 2000; 182: 311-22.

7. Stohs SJ, Bagchi D, Hassoun E, Bagchi M. Oxidative mechanisms in the toxicity of chromium and cadmium ions. J Environ Pathol Toxicol Oncol, 2000; 19: 201-13.

A preliminary study of the submandibular gland of the rat after one-year cadmium intoxication. Part II. Pathomorphology and ultrastructure

Czykier E[1], Szynaka B[2], Dzięcioł J[3]

[1]Department of Histology and Embryology, [2]Department of Pathomorphology, [3]Department of Anatomy, Medical University of Białystok, Poland

Abstract

The aim of the present study was to establish to what degree a one-year exposure of rat females to 5, 50 and 100 mg of Cd/l affects cell morphology of the submandibular glands. After one-year cadmium exposure of female rats, at doses of 5, 50 and 100 mg Cd/l, a pathomorphological examination revealed periductal fibrosis in the submandibular glands of rats in all the three experimental groups, which increased with cadmium dose. We also found foamish cytoplasm in the cells of the submandibular glands in all the experimental groups, the intensity of that phenomenon also increasing with Cd dose. The ultrastructural examination revealed no abnormalities in Group I. However, in Groups II and III, we observed numerous granules with a secretion, varying in shape and size that filled up the cytoplasm both in the mucous and serous cells.

Key words: submandibular gland, rat, cadmium, pathomorphology, ultrastructure.

Introduction

Cadmium (Cd) is a trace metal found in high concentrations in the polluted air of large urban agglomerations and highly industrialized areas. It penetrates all body organs, including the submandibular glands [1, 2]. The presence of cadmium was detected in the saliva of workers who were professionally exposed to cadmium and in young subjects, inhabiting large urban agglomerations [1, 3]. An increase in salivary cadmium level in humans was also observed after cadmium isotope administration [2]. The aim of the present study was to establish to what degree a one-year exposure of rat females to 5, 50 and 100 mg Cd/l affects cell morphology of the submandibular glands.

ADDRESS FOR CORRESPONDENCE:
Elżbieta Czykier
Department of Histology and Embryology
Medical University of Białystok
Kilińskiego 1, 15-089 Białystok, Poland
e-mail: czykier@amb.edu.pl

Material and methods

For the study, twenty-two young female Wistar rats were used, allocated to 4 groups. Six control rats received only redistilled water to drink. Eighteen experimental rats were given aqueous solution of cadmium chloride ($CdCl_2$) to drink: six rats from Group I received a dose of 5mg Cd/l, six animals from Group II received a dose of 50 mgCd/l and the remaining four from Group III - 100 mg Cd/l. After one-year of the experiment, the animals were sacrificed in pentobarbital narcosis. A fragment of one submandibular gland was fixed in Bouin's fluid. 5 µm sections were stained with H+E and, according to Azan's method. Sections for ultrastructural examinations were fixed in 3.6% glutaraldehyde at temp. of 4^0C for 2 hours, postfixed in 2% osmium tetroxide, dehydrated in alcoholic series, propylene oxide and embedded in Epon 812. Semithin preparations were stained with toluidine blue, while ultra thin sections were contrasted with uranyl acetate and lead citrate, and evaluated in an OPTON 900 PC transmission electron microscope.

Results

After one-year of the experiment, a histopathological examination of the submandibular glands in Group I revealed slight periductal fibrosis and, in some cells, an increased translucence of the cytoplasm. In Group II, periductal fibrosis was enhanced, compared to that in Group I and in the control, and single cells with foamish cytoplasm and single atypical cells could still be observed. In Group III, the submandibular glands showed increased periductal fibrosis, in comparison to that in Groups II, I and in the control; some cells exhibited more pronounced nuclear atypia and more foamish cytoplasm. In some fields of vision, cellular membranes and basement membranes of the

Figure 1. Group II. 50 mg Cd/l. Numerous secretory granules, irregular in shape and binding together, with disrupted limiting membranes. (*) N-cell nucleus with irregular contours. (original magnification X 4400).

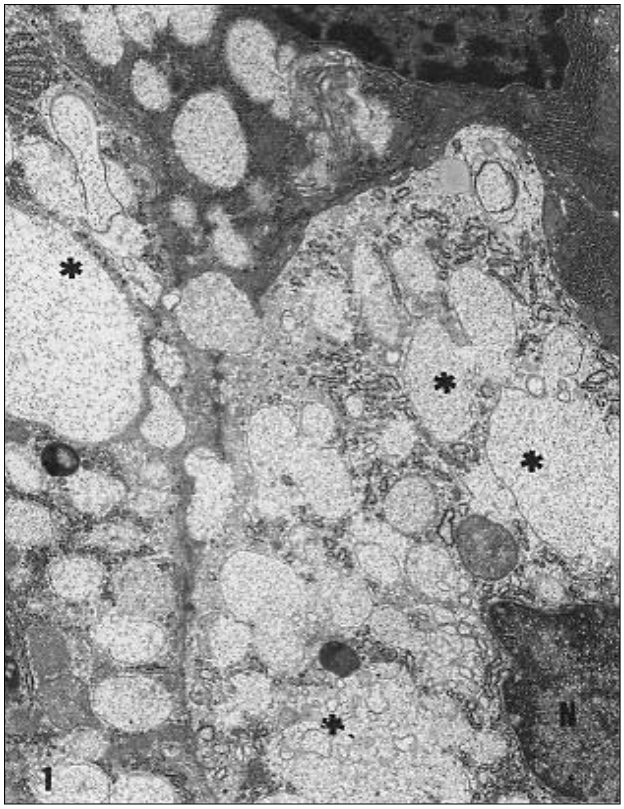

gland tube were blurred. No abnormalities were observed in the ultrastructural examination of the submandibular glands in either Group I or the control. Changes, which could be seen in Groups II and III, were similar, being more pronounced in the latter. We found: 1) irregular contours of cell nuclei with clumping of nuclear chromatin on the periphery (Fig. 1); 2) activation of Golgi apparatus in the form of a higher number and dilation of cisterns (Fig. 1); 3) blurring of the internal structure in some of the mitochondria with segmental destruction of the limiting membranes. In mucous cells, secretory granules combined to form large vacuoles which, sometimes, filled up the cytoplasm and pressed the cell nucleus (Figs. 1, 2). The limiting membranes of the secretory vacuoles were frequently disrupted and their contents were flowing out to the cytoplasm (Fig. 1). Serous cells contained numerous secretory granules, which varied in shape and size (Fig. 3), among which single large granules were frequently encountered. The lumina of serous vesicles and mucous tubes had a smoothed surface and were, sometimes, completely devoid of microvilli (Fig. 3). In the stroma, around the vesicles, rare collagen fibres were observed.

Discussion

The present study has revealed that a one-year exposure of female rats to cadmium at doses of 5, 50 and 100 mg Cd/l leads to irreversible changes in the submandibular glands, being manifested in periductal fibrosis, observed in histopathological examination. In the ultrastructural examination, collagen fibres were visible in the stroma. Fibrosis was found to increase with

Figure 2. Group III. 100 mg Cd/l. Secretory granules in the cytoplasm, blending to form the, so-called, "pools" (*) (original magnification X 3000).

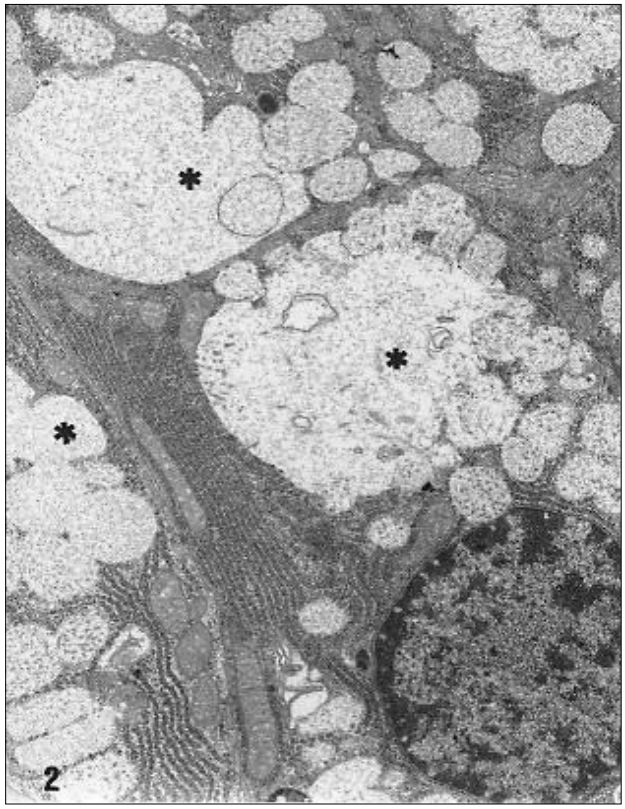

Figure 3. Group III. 100 mg Cd/l. Numerous serous granules, varying in size and shape, accumulated around the vesicular lumen (Lu) with smoothed surface (original magnification X 3000).

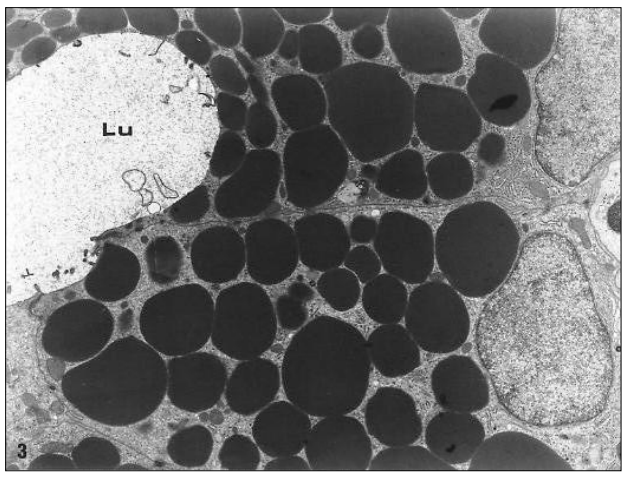

the increase in cadmium dose, administered to the rats. The remaining changes, detected in the submandibular glands of female rats, both in histopathological and ultrastructural examination, were reversible. Nevertheless, they caused secretion disorders in mucous and serous cells of the submandibular glands, expressed by the presence of foamish cytoplasm in histopathological examination and seen as secretory granules, filling up the cytoplasm in the ultrastructural examination. Other authors have observed similar changes in the form of either single or multiple vacuoles in serous cells of the rat parotid glands [4]. According

to Maier [5], cadmium is not only accumulated in the rat parotid gland but it is also "excreted via the parotid gland" to the saliva. We think that the same phenomenon may occur in the rat submandibular gland. It is likely that an active excretion of cadmium to the rat saliva inhibits massive secretion of the secrete, accumulated in cytoplasm of the submandibular gland. The pathomorphological changes, observed in the present study in the submandibular glands of female rats after one-year exposure to cadmium, were not only cadmium-specific, but they may also occur, following intoxication with other toxic compounds, such as herbicides [6]. According to other authors, pathomorphological changes, observed in the salivary glands of rats, exposed to cadmium, may occur, both due to its accumulation in the gland and be caused by general intoxication with this metal [4].

Conclusions

The present experiment indicates that one-year exposure to cadmium at doses of 5, 50 and 100 mg Cd/l induces dose-dependent pathomorphological and ultrastructural changes both of reversible and irreversible nature.

References

1. Gonzalez M, Banderas JA, Baez A, Belmont R. Salivary lead and cadmium in a young population residing in Mexico city. Toxicol Lett, 1997; 93: 55-64.

2. Menegario AA, Packer AP, Gine MF. Determination of Ba, Cd, Cu, Pb and Zn in saliva by isotope dilution direct injection inductively coupled plasma mass spectrometry. Analyst, 2001; 126: 1363-6.

3. Gervais L, Lacasse Y, Broduer J, P,an A. Presence of cadmium in the saliva of adult male workers. Toxicol Lett, 1981; 8: 63-6.

4. Jarzynka W, Miętkiewska B, Mikulski T. Wpływ kadmu na tkanki zębowe i ślinianki przyuszne szczurów. Czas Stomatol, 1985; 38: 673-80. [In Polish].

5. Maier H, Merk S, Zieliński D. Excretion of cadmium in rat parotid saliva. J Clin Chem Clin Biochem, 1989; 27: 241-3.

6. Jarzynka W, Put A. Wpyw niektórych środków chwastobójczych na ślinianki przyuszne i błonę śluzową jamy ustnej u szczurów. Czas Stomatol, 1985; 38: 198-204. [In Polish].

A preliminary study of the submandibular gland of the rat after one-year cadmium intoxication. Part I. Cadmium concentration

Czykier E[1], Dzięcioł J[2], Gałażyn-Sidorczuk M[3], Moniuszko-Jakoniuk J[3]

[1]Department of Histology and Embryology, [2]Department of Anatomy, [3]Department of Toxicology,
Medical University of Białystok, Poland

Abstract

The aim of the present study was to establish to what degree a one-year exposure of rat females to 5, 50 and 100 mg Cd/l affects the weight of the submandibular glands and their cadmium levels. We observed a decrease in the weight of the submandibular glands in the rat females from Groups I, II and III, compared to the control rats. We also found an increase in cadmium levels in the submandibular glands in Groups I, II and III, in comparison to the control. The highest cadmium concentration was noted in the submandibular glands in Group III, which was accompanied by the greatest weight reduction, the correlation being negative. The present experiment indicates that one-year administration of cadmium to rat females at a dose of 5, 50 and 100 mg Cd/l leads to a cadmium dose-dependent decrease in the weight of the submandibular glands.

Key words: submandibular gland, rat, cadmium concentration.

Introduction

Cadmium (Cd) is a trace metal, found in the polluted environment of towns, in water and food. During a prolonged exposure, this metal accumulates mainly in the kidneys and in the liver [1, 2]. Cadmium levels in the submandibular gland, although considerably lower, lead to function disorders in this organ, including a decrease in protein content and amylase activity in the saliva, and a rise in salivary Ca level [1, 2, 3]. The aim of the present study was to establish to what degree a one-year exposure of rat females to 5, 50 and 100 mg Cd/l affects the weight of the submandibular glands and their cadmium levels.

ADDRESS FOR CORRESPONDENCE:
Elżbieta Czykier
Department of Histology and Embryology
Medical University of Białystok
Kilińskiego 1; 15-089 Białystok, Poland
e-mail: czykier@amb.edu.pl

Material and methods

The study involved twenty-two young female Wistar rats, allocated to 4 Groups. Six control rats received only redistilled water to drink. Eighteen experimental rats were given aqueous solution of cadmium chloride ($CdCl_2$): six rats in Group I received a dose of 5mg Cd/l, six animals in Group II received a dose of 50 mg Cd/l and the remaining four in Group III - 100 mg Cd/l. The animals were sacrificed in pentobarbital narcosis. Both submandibular glands were collected from each rat. One of them was weighed and the cadmium concentration was measured by the atomic absorption spectrometry method. Experimental groups were compared, using a one-way analysis of variance (ANOVA) by the Kruskal-Wallis ranks test and the Mann-Whitney test. A linear Pearson's correlation analysis was performed to evaluate the relationship between submandibular gland weight and Cd concentrations in the gland. P-values < 0.05 were considered significant. Statistical tests were performed, using Statistica 6.0. The experiment received acceptance No 2001/6 from the Local Ethical Committee for Animal Testing in Białystok.

Results

After one year, the weight of the submandibular glands in rats was 0.25±0.02 g (0.23-0.29) in the control, 0.24±0.02 g (0.22-0.27) in Group I, 0.23±0.03 g (0.19-0.26) in Group II and 0.18±002 g (0.17-0.21) in Group III. Statistically significant differences were noted in the weights between Group III

Figure 1. Submandibular gland weights (g) of rats exposed to Cd (0, 5, 50 or 100 mg/l water) after one year. * p<0.05 in comparison to those in the control, ** p<0.05 in comparison with 5mg Cd/l, *** p<0.05 in comparison with 50 mg Cd/l.

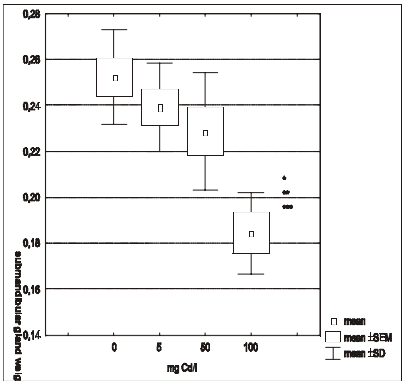

Figure 2. Cd concentrations in the submandibular glands (µg/g wet weight) of rats exposed to Cd (0, 5, 50 or 100 mg/l water) after one year. * p<0.05 in comparison to those in the control, ** p<0.05 in comparison with 5 mg Cd/l, *** p<0.05 in comparison with 50 mg Cd/l.

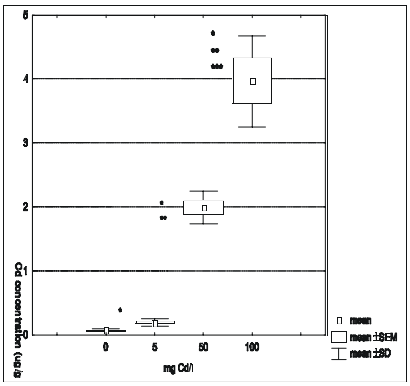

Figure 3. Correlation between submandibular gland weight and Cd concentrations in the submandibular glands of rats, exposed to Cd (0, 5, 50 or 100 mgCd/l water) after one year.

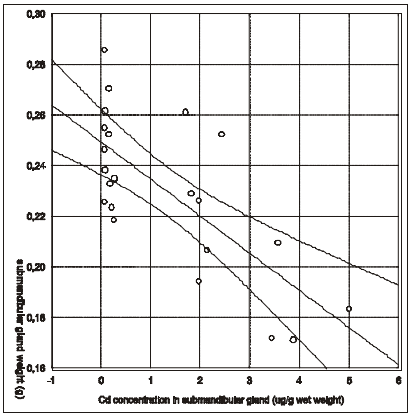

and the other three groups (Fig. 1). Cadmium concentration in the submandibular glands was found to be 0.07±0.01 µg Cd/g (0.05-0.09) in the control rats, 0.19±0.5 µg Cd/g (0.13-0.27) in rats exposed to 5 mg Cd/l, 1.99±0.26 µg Cd/g (1.70-2.43) in rats exposed to 50 mg Cd/l and 3.96±0.71 µg Cd/g (3.43-4.99) in rats receiving 100 mg Cd/l. Statistically significant differences were noted between the control group and the three experimental groups, as well as between Groups I, II and III, and Groups II and III (Fig. 2). The increase in cadmium concentrations in the rat submandibular glands was found to be accompanied by a decrease in the gland weights, the correlation being negative (Fig. 3).

Discussion

After one year of the experiment, a cadmium dose-dependent decrease was observed in the weights of the rat submandibular glands in Groups I, II and III, compared to the respective values in the control. The results, as reported by other authors for doses of 5 and 50 mg Cd/l after 24-week exposure, did not reveal any decrease in the weight of the rat submandibular glands [4]. These discrepancies may be due to the fact that, in our experimental model, the exposure to cadmium was twice as long [4].

We also found cadmium accumulation in the rat submandibular glands, which was dose-dependent. Our results, concerning cadmium concentrations in the submandibular glands, are consistent with our previous observations of rats which were administered 5 and 50 mg Cd/l for 24 weeks [5]. After one year, in comparison to the 24-week exposure, the increase in cadmium concentration in the rat submandibular gland was 58% with the dose of 5 mg Cd/l, and 70% at a dose of 50 mg Cd/l [5]. The relatively high accumulation of cadmium, noted in the female rat submandibulary glands after one-year exposure, compared to the 24-week exposure of male rats (at the same Cd doses) can, according to some authors, be influenced by age and sex [6]. According to Taguchi [6], the half-life of 109 Cd of the older mice is twice as long as that of the younger mice and that of the female mice is longer, compared to the males. The effects of age and sex on Cd elimination may also occur in rats.

The present experiment indicates that the one-year exposure of cadmium to rat females, at doses of 5, 50 and 100 mg Cd/l, leads to a decrease in the weight of the submandibular glands, which is cadmium-dose dependent.

References

1. Maier H, Merk S, Zieliński D. Excretion of cadmium in rat parotid saliva. J Clin Chem Clin Biochem, 1989; 27: 241-3.

2. Norberg GF, Nishiyama K. Whole-body and hair retention of cadmium in mice. Arch Environ Health, 1972; 24: 209-14.

3. Abdollahi M, Dehpour A, Kazemian P. Alteration by cadmium of rat submandibular gland secretory function and the role of the 1-arginine/nitric oxide pathway. Pharmacol Res, 2000; 42: 591-7.

4. Zalewska A. Aktywność egzoglikozydaz ślinianek podżuchwowych w doświadczalnym zatruciu chlorkiem kadmu [Ph D thesis]. Akademia Medyczna w Białymstoku, 2002; 1-102. [In Polish].

5. Czykier E, Dzięcioł J, Zalewska A, Zwierz K. A preliminary study of the submandibular gland of the rat after long-term cadmium intoxication. Folia Morphol, 2003; 62: 305-7.

6. Taguchi T, Suzuki S. Influence of sex and age on the biological half-life of cadmium in mice. J Toxicol Environ Health, 1981; 7: 239-49.

Ultrastructural study of the mitochondria in the submandibular gland, the pancreas and the liver of young rats, exposed to NaF in drinking water

Dąbrowska E[1], Balunowska M[1], Letko R[1], Szynaka B[2]

[1]Department of Social and Preventive Dentistry, [2]Department of Medical Pathomorphology, Medical University of Białystok, Poland

Abstract

The aim of the experiment was to determine the effect of fluoride on ultrastructural changes in the submandibular gland, the pancreas and the liver. The experimental rats received fluoride in aqueous solutions of sodium fluoride at concentrations of 10.6 NaF/dm^3 and 32.0 NaF/dm^3. In the ultrastructural examination, mitochondria were most damaged.

Key words: Ultrastructural study, rats, submandibular gland, pancreas, liver, natrium fluoride

Introduction

Fluorine, most frequently found in the form of fluorides, shows a high biological activity. Due to its affinity to magnesium and calcium ions, it can affect the activity of many enzymes, mainly oxydoreductases, transferases, hydrolases, enzymes of Krebs cycle, ATP production, protein synthesis, thus disturbing metabolism in the internal organs [1, 2, 3]. In dentistry, it is used in endogenous caries prophylaxis [4]. The aim of the experiment was to examine the effect of fluoride on the mitochondria in the submandibular gland, the pancreas and the liver of young rats, depending on the dose and the administration period. NaF is well soluble in water and easily absorbable in the alimentary tract.

Material and Method

The material for analysis included submandibular glands, pancreases and livers of 90 rats, aged 14, 30 and 90 days, whose mothers, from conception and later with the offspring, received drinking water, containing NaF at the following concentrations: 10.6mg NaF/dm^3 (group I - optimum dose) and 32.0 mg NaF/dm^3 (group II - superoptimum dose). The animals were exposed to fluoride up to 90 days of life. The experiment was terminated on day 120. The tissue material was collected and prepared for ultrastructural analysis, following the generally accepted rules [5].

Results and Discussion

Ultrastructural examinations revealed most pronounced changes in the cell mitochondria. The action of fluoride ions caused alterations in the size and shape of the mitochondria - mitochondrial crests were blurred and the membranes showed features of damage. In experimental Group I, the ultrastructural picture was similar to that, observed in the control group, what may suggest a slight effect of fluoride ions at concentration accepted as optimal. In hepatocytes of 14 and 30 days old rats, only few mitochondria were changed in shape and revealed a condensed mitochondrial matrix. Pronounced alterations in the cells were observed in experimental Group II, in which NaF was administered at a concentration three times higher than that in Group I. The most intensified ultrastructural changes were noted in the submandibular glands, the pancreases and the livers of 30 days old rats in Group II. In 30 days old animals in Group II, the changes were markedly enhanced (Fig. 1, Fig. 2). The mitochondria were polymorphic, with condensed matrix and blurred internal structure. After termination of NaF administration, in the hepatocytes of 120 days old rats the mitochondria were still polymorphic. In the acinar cells of the submandibular gland, evident changes appeared in Group II, growing in intensity with the age and the time of exposure to NaF. In the cells of the submandibular glands of 30 days old rats, swollen mito-

ADDRESS FOR CORRESPONDENCE:
Ewa Dąbrowska
Department of Social and Preventive Dentistry
Medical University of Białystok
Kilińskiego 1, 15-276 Białystok, Poland
e-mail: helpdentamb@o2.pl

Figure 1. Rat hepatocyte. Round cell nucleus (N), round mitochondria (M), rough endoplasmic reticulum (RER), glycogen granules (GLY), control group, 30 days, x 4400.

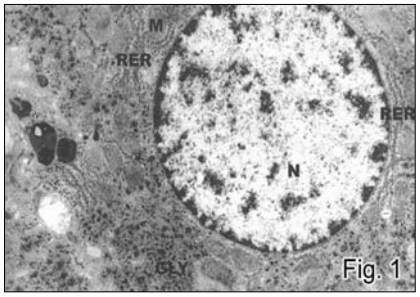

Figure 2. Cell nucleus of hepatocyte (N), with plicated membrane, polymorphic mitochondria (M), shortened and irregular RER channels, activated Golgi apparatus (GA), Group II, 30 days, x 4400

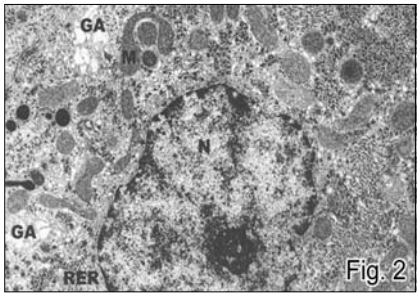

Figure 3. Fragment of acinar cell of the submandibular gland with damaged mitochondria (M), well-developed Golgi apparatus (G), blending secretory granules (*),Group II, 30 days, x 12000.

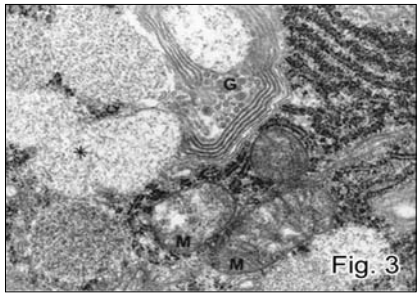

Figure 4. Pancreatic acinar cell, polymorphic mitochondria with condensed matrix (M), large focus of RER degranulation, Group II, 30 days, x 7000.

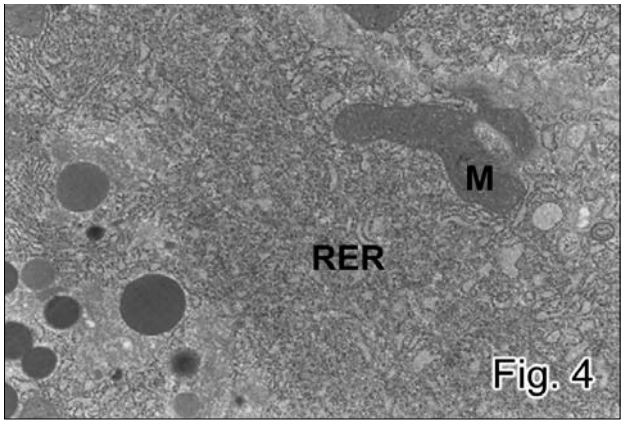

chondria and destruction of mitochondrial crests of varied degree were observed. (Fig. 3).

In the ultrastructural examination of the pancreas, which structurally resembles the submandibular gland, intensification of changes also increased with the administration time and NaF concentration. Like in the other examined organs, the damage to cell organelles was most pronounced in 30 days old rats in Group II and involved mitochondria, which displayed substantial polymorphism and had condensed matrix (Fig. 4). The most significant morphological changes, observed in the tissues of exposed to NaF animals, included damage to mitochondria of varied degree. Those changes could have disturbed the energetic processes in the cell. Ogoński et al. [6], in in vitro studies, have demonstrated that fluoride ions penetrate mitochondria via simple diffusion. Mitochondrial swelling, observed in the experiment, may be a manifestation of ATP deficiency-related energetic demand and not resulting from degenerative lesions.

Cittanowa et al. [7] consider mitochondria to be the major target of the toxic action of fluoride ions in the kidneys; other researchers have described this effect in the muscles [8]. Lavrushenko has demonstrated fragmentation and disintegration of mitochondrial crests [9].

The enhanced functioning of the secretory apparatus of the cells in the examined organs may be associated with the excretion of exogenous toxins, which have been introduced to the organism. The outcome of the present study, compared to the data reported by other authors, indicate a harmful effect of natrium fluoride on the examined organs of experimental animals, convergent in its biological effects with other toxic agents.

Conclusions

1. Chronic application of a superoptimum NaF dose induces ultrastructural changes in the cells of the submandibular gland, the pancreas and the liver of young rats.
2. The mitochondria are the most damaged organelles in the cells of examined organs.

References

1. Bardsen A, Bjorvatn K. Risk periods in the development of dental fluorosis. Clin Oral Invest, 1998; 2: 155-60.
2. Dąbrowska E, Balunowska M, Letko R. Zagrożenia wynikające z nadmiernej podaży fluoru. Nowa Stomatologia, 2001; 4: 22-7.
3. Grucka-Mamczar E, Machoy Z, Tarnawski R, Briknerer E, Polaniak R, Mamczar A. Wpływ jonu fluorkowego podawanego z wodą pitną na zawartość fluorków, magnezu i wapnia w zębach szczurów. Czas Stomat, 1998; 51: 427-32.
4. Shellis RP, Duckworth RM. Studies on cariostatic mechanisms of fluoride. Int Dent J, 1994; 44: 263-73.
5. Sjonstrand FS. Electron Microscopy of Cells and Tissues. Vol I. Instrumentation and Techniques. Academie Press New York and London; 1967.
6. Ogoński T, Wieczorek P, Paszkiewicz E, Machoy Z. Transport jonów fluorkowych przez wewnętrzną błonę mitochondrialną. Metabolizm Fluoru, 1992; 5: 92-3.
7. Cittanova ML, Lelongt B, Verpont MC, Geniteau-Legendre M, Wahbe F, Prie D, Coriat P, Ronco PM. Fluoride ion toxicity in human kidney collecting duct cells. Anesthesiology, 1996; 84: 428-35.
8. Jing-xi L, Jun-dong W. Effects of NaF on soft tissue structure of rabbits. Fluoride, 1991; 24: 123.
9. Lavrushenko LF, Trunov VI, Okunev VN. Morphofunctional characteristics of some rat hepatocytes ultrastructures under long-period influence of sodium fluoride. Citologia i Genetica, 1980; 14: 10-12.

From immunohistochemistry to pathophysiology of rheumatoid arthritis: Cross reactivity of self anti-immunoglobulin antibodies with collagen(s) may contribute to mechanisms of connective tissue damage (a hypothesis)

Rowiński Jan

Department of Anatomy, Faculty of Physical Education in Biała Podlaska,
The Jozef Pilsudski Academy of Physical Education in Warsaw

Abstract

The mechanism of initiation and development of rheumatoid arthritis was a subject of several hypotheses. None of those hypotheses has, however, convincingly explained all important facts, related to clinical, immunological and pathological aspects of the disease. A hypothesis is presented here, suggesting that, in the course of rheumatoid arthritis, an immune system produces anti-immunoglobulin antibodies, cross-reacting with self collagen(s). This cross-reactivity may be a significant part of the complex set of pathological phenomena, characteristic for rheumatoid arthritis. The hypothesis originated from the author's own observations of binding of the anti-immunoglobulin antibodies to the fibrous connective tissue (presumably to collagens contained in it) in histological sections, subjected to immunohistochemical procedures.

Key words: rheumatoid arthritis, immunoglobulins, collagen, connective tissue, histology.

Introduction

Rheumatoid arthritis (RA) is a chronic inflammatory disease of joints with an involvement of the heart, the lungs, the brain, the eyes, nerves and bone marrow [1, 2]. A large body of knowledge about RA has been acquired during the last century as a result of clinical, pathologic, immunologic and genetic studies of RA patients [1, 2, 3]. It has been complemented with studies of experimentally-induced arthritis in mice [4, 5, 6]. Today we know that the susceptibility to RA depends on the allelic variability of genes, coding for MHC class II molecules [3], on genes, coding for a number of cytokines [2, 5], and on other factors, like age and gender [1, 2]. The aetiology of RA is not yet, however, known. Among the unsolved problems is a question what the primary "arthritogenic molecule" is which initiates a cascade of events, resulting ultimately in destruction of joints [1, 2, 3, 4, 6]. The candidate molecules include: collagen(s), certain epitopes of MHC class II molecules (QKRAA motif or "the shared epitope" [3]), the component(s) of staphylococcal cell wall, the Epstein-Barr virus protein, and other [1, 2]. A comprehensive pathophysiological theory of RA has to be built upon these facts and hypotheses; they may be imagined as elements of a jigsaw puzzle, with some pieces of bizarre shape, and some other missing. That is why new observations, experiments and theoretical concepts are desired.

Hypothesis: The hypothesis, as presented here, has originated from a reflection on the peculiar immunohistochemical artefact, observed by the author and his associates [7, 8], namely, the binding of the anti-immunoglobulin antibodies (anti-Ig Abs) to a fibrous connective tissue, presumably to collagen(s) of this tissue (Figs 1, 2, 3). One may ask if a similar phenomenon occurs in vivo and, if so, whether it plays some role in the pathophysiological mechanisms of RA.

Hypothesis: In the course of rheumatoid arthritis (RA), the immune system produces anti-immunoglobulin antibodies (anti-Ig Abs) which cross-react with self collagen(s); this cross reactivity contributes to a complex set of pathologic phenomena, constituting RA, and thus, it may be a factor involved in causing damage of the connective tissues in joints.

The hypothesis is provisional but I believe it has an operational utility - it may help raise a number of questions both for theoretical consideration and practical testing. (1) Can a collagen-binding antibody be induced not only by a foreign collagen but by another, non-collagen foreign antigen? (2) May a collagen be auto-immunogenic and capable of inducing anti-collagen

ADDRESS FOR CORRESPONDENCE:
Jan Rowiński
Zakład Anatomii AWF, Zamiejscowy Wydział Wychowania Fizycznego w Białej Podlaskiej
Akademicka 2, 21-500 Biała Podlaska, Poland
e-mail: jan.rowinski@awf-bp.edu.pl

Figure 1. Binding of an anti-immunoglobulin antibody to endomysium. The unfixed cryostat section of a quadriceps muscle of the mdx mouse [9] was incubated with the HRP-conjugated goat antibody against mouse immunoglobulins (DACO, code No. P 447) [7]. The brown precipitate (a product of reaction catalyzed by HRP) surrounds individual muscle fibers, so its localization corresponds to endomysium (see Fig. 2 for comparison). Magnification 600x. Comments: The reaction is interpreted as due to the cross-reactivity of anti-Ig antibodies with collagen(s) [7, 8].

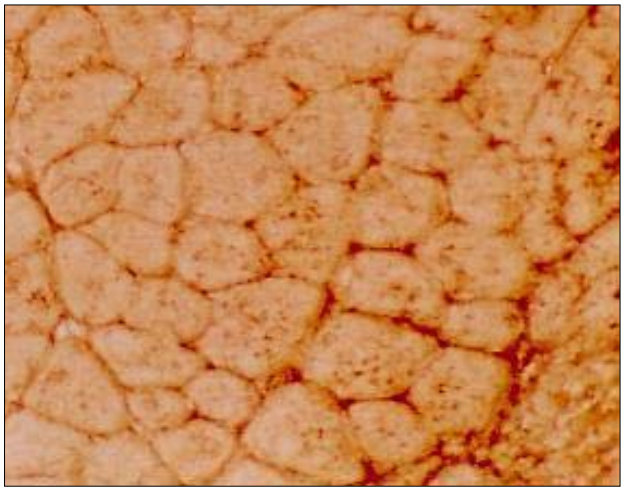

Figure 2. Localization of collagen in skeletal muscle. The quadriceps muscle of the mdx mouse [9] was fixed in Bouin's fluid, embedded in paraffin, cut into sections, deparaffinized and stained with Sirius red [7, 10]. Magnification 600x. Comments: The staining is specific for collagen [10], so, red color indicates localization of collagen(s) (in endomysium), similarly to the localization of sites, binding the anti-Ig antibodies, as seen in Fig. 1.

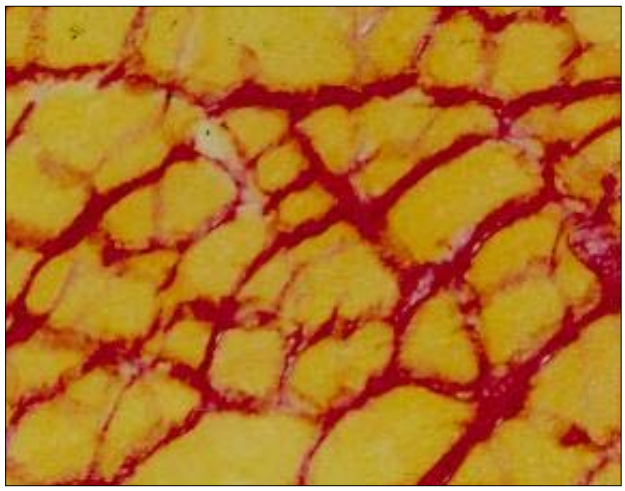

Figure 3. Immunohistochemical artifact in the test for IgG deposits in human kidney. Histological section of a formalin-fixed, paraffin-embedded sample of kidney (kindly provided by dr. Anna Sulikowska-Rowińska, University Medical School, Warsaw). Magnification 450x. Steps of immunostaining [11]: (a) incubation with the primary, unlabelled, rabbit/mouse antibodies specific for human IgG; (b) incubation with the secondary, biotinylated, goat antibody against rabbit/mouse Ig; (c) incubation with Streptavidine, conjugated with alkaline phosphatase; (d) visualization of alkaline phosphatase activity with Fast Red system (all reagents from DAKO). Cell nuclei and cytoplasm stained blue with haematoxylin. The reddish-brown reaction product, deposited over connective tissue, surrounding renal tubules, and over walls of capillary vessels (presumably over basement membranes) in a glomerulus. Comments: In the light of other tests performed on the same biopsy, the reaction seen in Fig. 3 is an artifact. Localization of IgG in the stroma of kidney and in the walls of glomerular capillaries was not confirmed by other tests. Instead, a presence of immune complexes in mesangium has been revealed Dr Sulikowska-Rowińska, personal communication. The explanation of the artifact: the primary or the secondary antibody or both cross-reacted with collagens of the stromal connective tissue and of the capillary basement membrane.

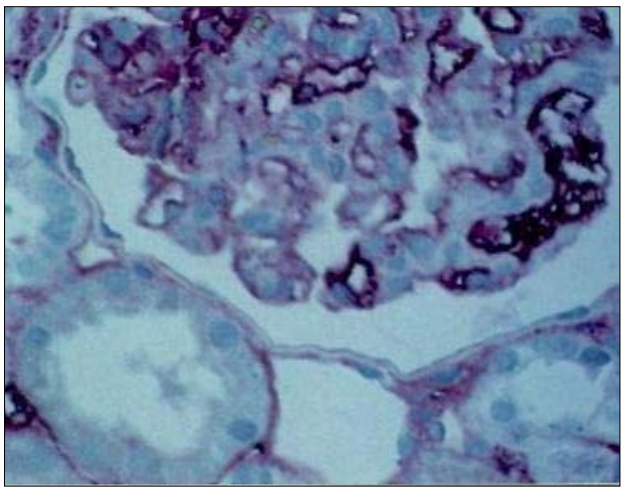

antibodies, which cross-react with immunoglobulins? (3) Do susceptibility to RA depend, in addition to the genes, already known as the ones, controlling this susceptibility, also on genes, coding for collagens and/or for factors, controlling post-translational modifications of potentially immunogenic motifs on collagen molecules? (4) Can the anti-Ig Abs, while cross-reacting with collagen, interfere with a normal structure of the network of extracellular fibers in connective tissues? (5) Do the anti-idiotypic antibodies against the anti-collagen antibodies play any role in RA induction or development? (Note that antibodies of this type should bind, theoretically, certain collagen ligands, since the secondary anti-idiotypic antibodies may mimic epitopes of the original immunogene).

The above questions were intended to inspire scientists with new concepts, relevant to pathophysiology of RA, a disease, upsetting the life of many patients and disturbing the minds of all rheumatologists.

References

1. Mackiewicz S. Osiągnięcia i porażki reumatologii XX wieku (Choroby reumatyczne a proces zapalny). The successes and misfortunes of rheumatology in XX century (Rheumatic diseases and inflammation). Nowa Medycyna - Reumatologia IV, 1999, 12; < http://www.borgis.pl/czytelnia/nm-reumatologia/01.php > (30 July 2004).

2. Bathon JM. Rheumatoid arthritis pathophysiology. Johns Hopkins Arthritis, 2004; The Johns Hopkins Arthritis Center website; <http://www.hopkins arthritis.org/rheumatoid/rheum_clin_path.html> (17 July 2004).

3. Gregersen PK, Silver J, Winchester RJ. The shared epitope hypothesis: An approach to understanding the molecular genetics of susceptibility to rheumatoid arthritis. Arthritis Rheum, 1987; 30: 1205-13.

4. Bäcklund J, Nandakumar KS, Bockermann R, Mori L,

Holmdahl R. Genetic control of tolerance to type II collagen and development of arthritis in an autologous collagen-induced arthritis model. J Immunol, 2003, 171: 3493?9.

5. Finnegan A, Kaplan CD, Cao Y, Eibel H, Glant TT, Zhang J. Collagen induced arthritis is exacerbated in IL 10 deficient mice. Arthritis Res Ther, 2003; 5: 18-24.

6. Wipke BT, Wang Z, Nagengast W, Reichert DE, Allen PM. Staging the initiation of autoantibody-induced arthritis: a critical role for immune complexes. J Immunol, 2004, 172: 7694-702.

7. Kozłowska H, Rowiński J, Koter Z, Górecki D. Binding of anti-immunoglobulin antibodies to the fibrous connective tissue of skeletal muscle. Folia Histochem Cytobiol, 1996; 34: 95-6.

8. Kozłowska H, Rowiński J, Bem W, Kwarecki K. Fibrous connective tissue of rat binds anti-immunoglobulin antibodies. Folia Histochem Cytobiol, 1997; 35: 123-4.

9. Bulfield G, Siller WG, Wight PA, Moore KJ. X chromosome?linked muscular dystrophy (mdx) in the mouse. Proc Natl Acad Sci USA, 1984, 81: 1189-92.

10. Junqueira LCU, Bignolas G, Brentani RR. Picrosirius staining plus polarization microscopy, a specific method for collagen detection in tissue sections. Histochem J, 1979, 11: 447-55.

11. Sulikowska-Rowińska A, Małdyk J, Fiejka E. Comparison of various methods for detecting immune complexes in renal glomeruli in bioptic material. Abstracts, XV Congress of Polish Society of Pathologists. Polish Journal of Pathology, 2001; 52: 94.

Chemical compound content and enzyme activity in supernatant and sediment of liver homogenate

Gacko M, Kowalewski R, Guzowski A, Worowska A, Łapiński R

Department of Vascular Surgery and Transplantology, Medical University of Bialystok, Poland

Abstract

Evaluation was performed of chemical compound contents and enzyme activities in the whole homogenate, its supernatant and sediment. Six rabbit livers were pulverized in liquid nitrogen and homogenized. After centrifugation, the contents of protein, haemoglobin, vitamin A, vitamin E, vitamin C, as well as the activities of cathepsin B, cathepsin D, superoxide dismutase, catalase, glutathione peroxidase and reductase were assessed in the whole homogenate, its supernatant and sediment. Protein, vitamin A, superoxide dismutase, catalase, cathepsin D, glutathione peroxidase and reductase reveal uniform localisation. Vitamin C and cathepsin B are localized in supernatant, whereas haemoglobin is localized mainly in sediment. Evaluation of chemical compounds and enzyme activities should be performed in the whole homogenate, supernatant and sediment to obtain a real interpretation of biochemical disturbances in the investigated material.

Key words: whole homogenate, homogenate supernatant, homogenate sediment, chemical compounds, enzymes.

Introduction

Chemical compound contents and enzyme activity are evaluated in homogenate soluble fraction [1, 2]. Its composition depends on medium type, used for homogenisation, the type of homogeniser and the method of homogenisation. Evaluation of insoluble fraction composition is omitted. However, it can also contain soluble components, which are bound in non-covalent way with cell and organelle membranes [3]. The aim of the study was to compare the contents (activities) of some components in the whole liver homogenate, as well as in its soluble (supernatant) and insoluble (sediment) fractions.

Material and methods

Six rabbit livers were used. Directly after harvesting, they were perfused with cold 0.15 mol/l NaCl until the reaction for haemoglobin with Beau reagent disappeared. The tissue samples were pulverized in liquid nitrogen in a stainless pulveriser [4]. Cold 0.15 mol/l NaCl containing 167 µmol/l BHT (1:9 w/v ratio) was added to pulverised material, which was then extracted for 30 minutes with continuous stirring at 2^0C and filtrated through gauze to remove connective tissue fibres. One part of the obtained homogenate was centrifuged (2700 x g, 30 minutes, 2^0C). The sediment was washed with cold 0.15 mol/l NaCl three times and suspended in the initial volume of this solution after the third wash.

The contents of protein [5], haemoglobin [6], vitamin A [7], vitamin E [8], vitamin C [9], as well as the activities of cathepsin B [10], cathepsin D [11], superoxide dismutase [12], catalase [13], glutathione peroxidase [14] and reductase [15] were assessed in the whole homogenate, as well as in its supernatant and sediment. The obtained results were calculated per gram of fresh tissue.

Results

The highest content of assessed compounds is present in the whole homogenate (Table 1). Protein, vitamin A and vitamin E are by half localized in supernatant and in sediment. More than

ADDRESS FOR CORRESPONDENCE:
Gacko Marek
Department of Vascular Surgery and Transplantology
Medical University of Bialystok
M. Curie-Sklodowskiej 24A, 15-276 Bialystok, Poland
Tel. +48 85 7468276; fax. +48 85 7468896;
e-mail: mgacko@poczta.onet.pl

Table 1. The content of some compounds in liver homogenate and in supernatant and sediment of liver homogenate

Compound	Homogenate	Supernatant	Sediment
Protein (mg/g of tissue)	172.8 ± 16.7	73.8 ± 6.8	93.5 ± 10.8
Haemoglobin (mg/g of tissue)	3,6 ± 0.4	0.2 ± 0.001	3.5 ± 0.1
Vitamin A (nmol/g of tissue)	56.2 ± 5.3	28.9 ± 2.3	28.8 ± 2.4
Vitamin E (nmol/g of tissue)	536.3 ± 50.4	254.6 ± 26.0	278.7 ± 29.6
Vitamin C (ng/g of tissue)	82.1 ± 3.7	80.6 ± 3.6	trace

Table 2. The activity of some enzymes in liver homogenate and in supernatant and sediment of liver homogenate

Activity	Homogenate	Supernatant	Sediment
Superoxide dismutase (IU/g of tissue)	14.8 ± 1.5	6.8 ± 0.7	6.9 ± 0.6
Catalase (IU/g of tissue)	242.6 ± 20.6	117.0 ± 16.2	115.6 ± 12.4
Cathepsin B (pNA nmol/g of tissue)	23.4 ± 1.8	21.6 ± 1.2	trace
Cathepsin D (Tyr nmol/g of tissue)	7.9 ± 0.8	3.6 ± 0.2	3.9 ± 0.2
Glutathione peroxidase (IU/g of tissue)	9.4 ± 1.1	3.1 ± 0.4	5.2 ± 0.5
Glutathione reductase (IU/g of tissue)	5.8 ± 0.5	2.2 ± 0.2	3.1 ± 0.3

70% of haemoglobin is found in sediment, whereas vitamin C is mainly present in supernatant. The highest activity of evaluated enzymes is also found in the whole homogenate (Table 2). The activities of superoxide dismutase, catalase, cathepsin D, as well as of glutathione peroxidase and reductase are localized by half in supernatant and in sediment. Cathepsin B activity is mainly present in supernatant.

Discussion

In the previously performed studies, the contents of chemical compounds and enzyme activities were assessed in the supernatants of homogenates, which were prepared in isotonic 0.25 mol/l saccharose or 0.15 mol/l NaCl solutions with or without detergent. The sage of different types of homogenisers, different homogenisation times and different centrifugation conditions lead to marked differences in the content (activity) of components in prepared supernatants. The obtained results have a limited diagnostic meaning and a limited value in the attempts to interpret biochemical disturbances.

Evaluation of the contents of chemical compounds and of enzyme activities in the whole homogenate, supernatant and sediment eliminates the above-mentioned inconveniences. Pulverisation in liquid nitrogen provides a complete disintegration of cells and cell organelles with a release of soluble components and formation of membrane structure fragments. The extract, prepared in 0.15 mol/l, is centrifuged, providing supernatant and sediment. Many cellular soluble components are bound in non-covalent way with fragments of cell membranes [3, 16]. It is then necessary to evaluate the content (activity) in the whole homogenate and in its supernatant and sediment as well. The measured content (activity) is calculated per gram of fresh or dry tissue, as well as per number of cells or mg of deoxyribonucleic acids [2, 17, 18].

References

1. Gohda E, Nagahama J, Makumara O, Tsubouchi H, Yasushi D, Pitot H. Increased activities of liver cathepsins B and D in carbon tetrachloride-treated rats. Biochim Biophys Acta, 1984; 802: 362-71.

2. Frei J. The meaning of enzyme activity measurements in human tissue. Enzymol Biol Clin, 1970; 11: 3-7.

3. Zubrzycka E. Solubilization and reconstruction of biological membranes. Post Biol Kom, 1975; 2: 233-45.

4. Ladynsky H, Consolo S, Sanvito A. Simple apparatus for pulverization and rapid quantitative transfer of frozen tissue. Anal Biochem, 1972; 49: 294-7.

5. Bradford MM. A rapid and sensitive method for quantitation of microgram quantities of protein utilizing the principle of protein-dye binding. Anal Biochem, 1976; 72: 248-54.

6. Beau A. Method for hemoglobin determination on serum and urine. Am J Clin Pathol, 1962; 38: 111-2.

7. Arnaudi J, Fortis I, Blachier S. Simulations determination of retinol, α-tocopherol and ß-carotene by isocratic high-performance liquid chromatography. J Chromatogr, 1991; 572: 103-16.

8. Ostrowski J, Hertel Z. Spectrofluorimetric determination of serum tocopherol. Diagn Lab, 1977; 13: 215-22.

9. Kyaw A. A simple colorimetric method for ascorbic acid determination in blood plasma. Clin Chim Acta, 1978; 86: 153-7.

10. Tawari T, Kawabata Y, Katunuma N. Crystalization and properties of cathepsin B from rat liver. Eur J Biochem, 1979; 102: 279-89.

11. Greczaniuk A, Roszkowska-Jakimiec W, Gacko M, Worowska A. Determination of cathepsin D activity in blood plasma using hydrochloric acid denaturate haemoglobin. Diagn Lab, 2000; 36: 97-101.

12. Sykes JA, McCormac FX, O'Brien TJ. Preliminary study of the superoxide dismutase content of some human tumours. Canc Res, 1978; 38: 2759-62.

13. Aebi H. Catalase in vitro. Meth Enzymol, 1984; 105: 121- 6.

14. Paglia DE, Valentine WN. Studies on the quantitative and qualitative characterization of erythrocyte glutatione peroxidase. J Lab Clin Med, 1967; 70: 158-169.

15. Mize CE, Langdon RG. Hepatic glutatione reductase. I. Purification and general kinetic properties. J Biol Chem, 1962; 237: 1589-95.

16. Krawczyński J. Basis of enzymologic diagnostics. Diagn Lab, 1971; 7: 321-37.

17. Alaniz MJT, Gomez T, Dumm IN, Brenner RR. Comparative studies regarding different ways of expression of enzymatic activity. Enzymologia, 1970; 38: 85-8.

18. Fiszer-Szafarz D. DNA and protein content as cellular biochemical parameters. A discussion with two examples: acid phosphatase and cathepsin D in rat liver and hepatoma and acid phosphatase in human breast normal tissue and adenocarcinoma. Anal Biochem, 1984; 138: 255-8.

Assessment of connective tissue fibres in walls of allogenic arterial grafts preserved by the method of cold ischemia - a preliminary report

Gacko M[1], Łapinski R[1], Płoński A[1], Kowalewski R[1], Guzowski A[1], Andrzejewska A[2], Ostapowicz R[1]

[1]Department of Vascular Surgery and Transplantology, [2]Department of Medical Pathomorphology,
Medical University of Bialystok, Poland

Abstract

The aim of the study was to evaluate microscopic changes in the wall structures of allogenic arterial grafts, preserved by the method of cold ischemia in relation to the storage period and to test the possibility of the storage period prolongation by allograft freezing at -70°C. The middle layer ultrastructure is well preserved till 30 days from allograft harvesting, however, allograft freezing results in total destruction of elastic and collagen fibres in the arterial wall. An application of allogenic arterial grafts, preserved by the method of cold ischemia till 30 days from their harvesting, seems an efficient therapeutic method in the treatment of patients with synthetic vascular graft infection. Further prolongation of the storage period at -70°C made the allograft useless for implantation.

Key words: arterial allograft, vascular graft infection, cold ischemia preservation, elastic and collagen fibres.

Introduction

Infection of synthetic vascular grafts is one of essential therapeutical problems in vascular surgery. Pharmacological treatment has, in these cases, an unfavourable prognosis, so, the standard procedure is to replace the infected graft [1, 2]. For this purpose, allogenic arterial grafts or silver-coated synthetic prostheses can be used [3, 4]. Both methods have been applied at the Department of Vascular Surgery and Transplantology of the Medical University of Bialystok since 2002. Due to better therapeutical effect, we prefer to use allogenic arterial grafts, preserved by the cold ischemia method, which, in comparison to commonly applied liquid nitrogen allograft freezing, does not require any special equipment and is characteristic of low costs [5]. The aim of the study was to evaluate microscopic changes in wall structures of allogenic arterial grafts, preserved by the method of cold ischemia, in relation to the storage period and to test the possibility of the storage period prolongation by allograft freezing at -70°C.

Material and methods

The allografts were prepared as follows. Sections of abdominal aorta with iliac and femoral arteries were harvested from organ donors, put in a solution, composed of cephasoline (10 mg/100ml), metronidasol (7 mg/100ml) and heparin (5000u/100ml) and stored at 4°C. The allograft wall ultrastructure was assessed at 8 days and then between 20 and 30 days from allograft procurement. In order to test the possibility of the storage period prolongation, the allograft was frozen at -70°C after 30 days of cold ischemia. It was thawed in 0.9% NaCl ice solution after 14 days of storage at -70°C and its wall was once again examined. The evaluation of the allograft wall ultrastructure was performed by electron microscopy. At all the assessed storage periods, five specimens (about 1 mm^3) of the allograft wall were taken from its different parts, fixed in 3.6% glutaraldehyde with 0.1mol/l cacodylate buffer (pH 7.4) for 3 hours, washed with the buffer and postfixed in 2% osmium tetroxide for 1 hour. The samples were then dehydrated in alcohol and propylene oxide and embedded in Epon 812. Ultra thin sections were cut from each specimen on a Reichert ultramicrotome, stained with lead citrate and uranyl acetate and studied under an Opton 900 PC transmission electron microscope.

ADDRESS FOR CORRESPONDENCE:
Gacko Marek
Department of Vascular Surgery and Transplantology
Medical University of Bialystok
M. Curie-Sklodowskiej 24A, 15-276 Bialystok, Poland
Tel. +48 85 7468276; fax. +48 85 7468896;
e-mail: mgacko@poczta.onet.pl

Figure 1. Considerable damage of the vessel internal layer with a total destruction of endothelial cells (arrow). Disintegrated smooth muscle cells (*) and well preserved elastic and collagen fibres in the allograft middle layer (Original magnification 4400 x).

Figure 2. Well preserved collagen (C) and elastic fibres and fragments of disintegrated cells (*) in the allograft wall middle layer (Original magnification 4400 x).

Figure 3. Total destruction of elastic and collagen fibres and disintegration of smooth muscle cells (*) in the allograft wall middle layer. (Original magnification 4400 x).

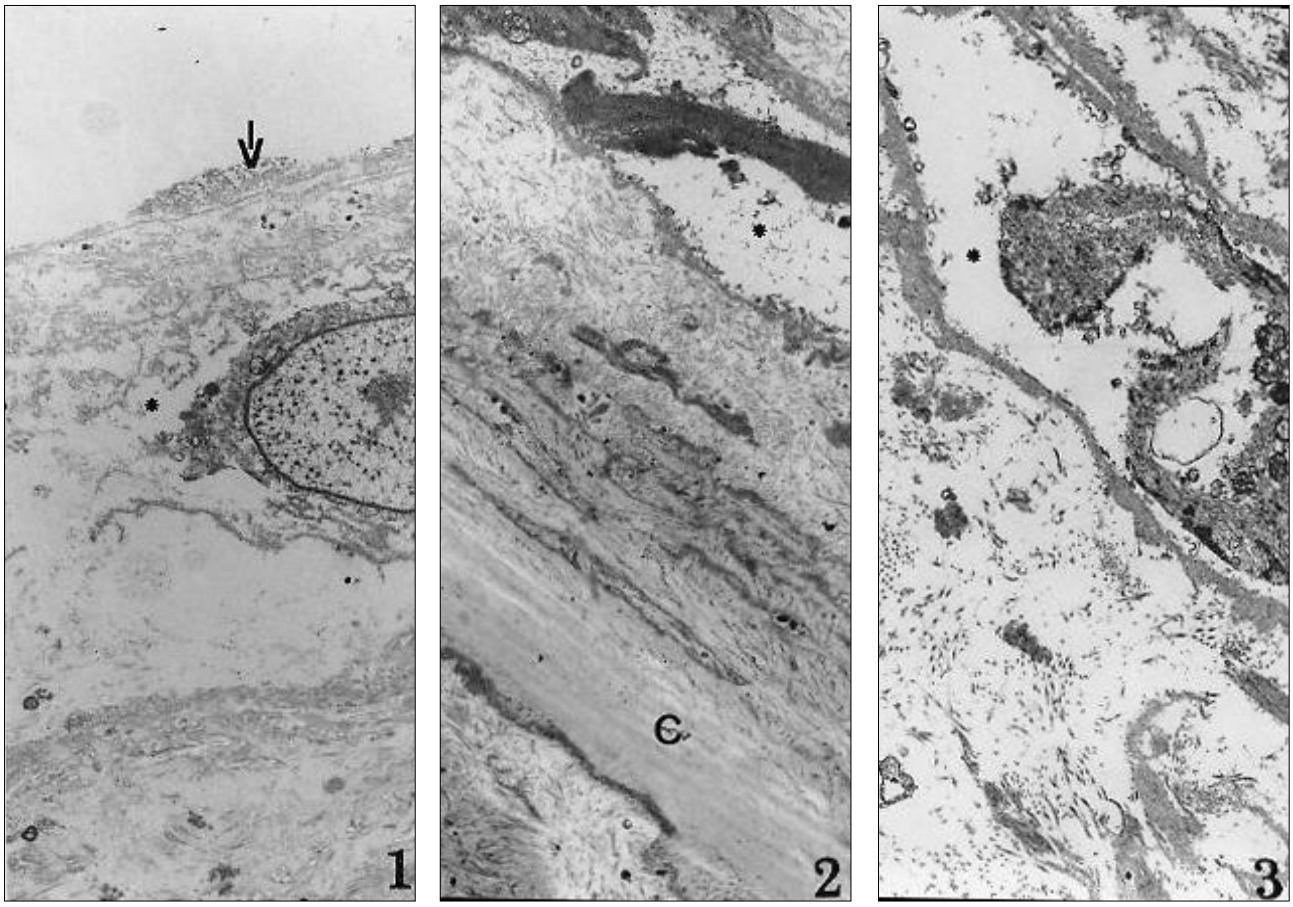

Results

After 8 days, a destruction of cells in all the layers of the allograft wall was observed, whereas the structures of elastic and collagen fibres in the middle layer were well preserved (Fig. 1). Their structure was quite well preserved till 30 days after allograft harvesting (Fig. 2), whereas prolongation of the allograft storage at -70^{0}C caused a total destruction of elastic and collagen fibres in the allograft wall (Fig. 3).

Discussion

The method of cold ischemia provides elimination of viable cells with simultaneous good preservation of elastic and collagen fibres. Destruction of cells in the allograft wall and their content release into the preserving solution takes place during the first days of preservation. The lack of viable cells prevents the immunological response after allograft implantation, because native elastin and collagen of the same species do not show antigenic properties. It reduces the inflammatory reaction, protease activation and protects the structural proteins of implanted allograft against destruction [6]. Due to the lack of viable cells, all the problems, associated with blood compatibility, as well as with histocompatibility, can be omitted. However, the short period, available for allograft application after its procurement is an essential limitation of the method of cold ischemia preservation. Prolongation of the storage period above 30 days at 4^{0}C is not possible because of the damage of elastic and collagen fibres. Therefore, we tested the possibility of the storage period prolongation by freezing the allograft at -70^{0}C. However the method of prolonged allograft preservation at -70^{0}C occurred unsuccessful, due to the total destruction of connective tissue fibres, which are responsible for the mechanical resistance of the arterial wall. It could be supposed that water ice crystals, forming in the absence of dehydrating agents during the allograft freezing process, were the cause the of ultrastructure damage. It seems that adding DMSO to preservation solution could avoid that. Nevertheless, a longer storage period of an allograft can be achieved by secondary liquid nitrogen freezing or lyophilization [7, 8].

Conclusion

Application of allogenic arterial grafts, preserved by the

method of cold ischemia till 30 days from their harvesting, is an easily accessible and simple method of treatment of patients with synthetic vascular graft infection. Prolongation of the allograft storage period by freezing at -70^{0}C made the allograft useless for implantation because of damage and fragmentation of elastic and collagen fibres

References

1. Pukacki F, Gabriel M, Chęciński P, Oszkinis G, Dzieciuchowicz Ł, Zapalski S. Six-year experience in frozen arterial allografts used in the treatment of infected aortic prosthesis grafts. Pol Przegl Chir, 2003; 75: 579-95.

2. Ziaja K, Urbanek T, Bursig H, Zaniewski M, Tochowicz M, Żabski M, Majewski E, Markiel Z. Homografts in therapeutic management of vascular prosthesis infection. Pol Przegl Chir, 1998; 70: 920-9.

3. Pupka A, Skóra J, Janczak D, Ruciński A, Korta K, Barć P, Stępiński P, Szyber P. The treatment of massive prosthetic grafts infections with the use of silver/collagen coated dacron vascular prosthesis. Polim Med, 2003; 33: 41-5

4. Vogt PR, Brunner-LaRocca HP, Lachat M, Ruef Ch, Turina MI. Technical details with the use of cryopreserved arterial allografts for aortic infection: Influence on early and midterm mortality. J Vasc Surg, 2002; 35: 80-6.

5. Geremek M, Trochimczuk M, Krasowski G, Kruk M, Borkowski M. Allogenic venous grafts in the reconstruction of peripheral blood vessels. Pol Przegl Chir, 1998; 70: 484-7.

6. Allaire E, Guettier C, Bruneval P, Plissonier D, Michel JB. Cell-free arterial grafts: Morphologic characteristics of aortic isografts, allografts, and xenografts in rats. J Vasc Surg, 1994; 19: 446-56.

7. Gacko M, Płoński A, Ostapowicz R, Andrzejewska A, Guzowski A, Łapiński R. Allogenic arterial grafts in the treatment of patients with infected vascular grafts- the suggestion of the new way of allografts preservation. Acta Angiologica, 2004; 10: 39-45.

8. Kaliszan A. Lyophilization of tissue grafts for therapeutic purposes. Probl Tech Med, 1974; 5: 333-6.

Some components of oxidative-antioxidative system in human blood plasma and serum

Gacko M[1], Radziwon P[2], Kowalewski R[1], Worowska A[1], Guzowski A[1]

[1]Department of Vascular Surgery and Transplantology, Medical University of Białystok;
[2]Regional Centre for Transfusion Medicine in Bialystok, Poland.

Abstract

Comparison of the concentrations and activities of components in the oxidative-antioxidative system between blood plasma and serum. Blood plasma and serum samples were obtained from 38 healthy adults to evaluate malondialdehyde concentration, the total antioxidative capacity, superoxide dismutase activity, protein and non-protein sulphydryl groups, ascorbate, haemoglobin, methaemoglobin and protein. Blood plasma shows higher activity of superoxide dismutase, as well as higher concentrations of low-molecular sulphydryl groups and ascorbate, when compared to those in blood serum. The total plasma antioxidative capacity is also higher than that assessed in blood serum. Processes of blood coagulation and blood clot retraction lead to antioxidant consumption. The evaluation of oxidative-antioxidative system for diagnostic purposes should be performed in blood plasma.

Key words: plasma, serum, oxidative - antioxidative system.

Introduction

Plasma is a natural environment for blood morphological components. Serum is formed *in vitro* as a result of generation and retraction of either arterial or venous blood clot, creating its environment. Serum differs from plasma by the lack of I, II, V, VIII and XIII coagulation factors, as well as in higher concentrations of components, released from blood platelets, such as ß-thrombomodulin and platelet factor 4 [1, 2]. Blood platelets and erythrocytes in particular, contain numerous chemical compounds and enzymes, which are involved in oxidative - antioxidative processes [3, 4].

The aim of the study was to compare the concentration and activity of some components of the oxidative - antioxidative system in plasma and serum, obtained in vitro from blood of healthy volunteers.

Material and methods

Blood samples for the studies were collected from ulnar veins in 38 healthy adults, including 34 men and 4 women, aged from 25 to 30 years. The blood was collected into 0,1 mol/l natrium citrate (9:1 v/v) to polypropylene tubes and to glass ones without anticoagulant. Blood, collected into natrium citrate, was centrifuged (2700 x g; 30 minutes; 20C) to obtain plasma. Blood, collected without anticoagulant, was incubated for 1 hour at 37^{0}C and then centrifuged in the same conditions as described above, to obtain serum. The following were evaluated in blood plasma and serum: malondialdehyde concentration [5], the total antioxidative capacity [6], superoxide dismutase activity [7], protein and non-protein sulphydryl groups [8], ascorbate [9], haemoglobin [10], methaemoglobin [11] and protein [12]. The results obtained in plasma were multiplied by 1.25, due to dilution of the collected blood in citrate [13]. The obtained results were submitted to statistical analysis with Student's 't' test, accepting $p<0.05$ as significant.

Results

Malondialdehyde concentration is higher in plasma than in blood serum (Table 1). The total plasma antioxidative capacity, superoxide dismutase activity, as well as concentrations of most antioxidative system components are also higher in plasma, than those in blood serum. Only the concentration of protein sul-

ADDRESS FOR CORRESPONDENCE:
Gacko Marek
Department of Vascular Surgery and Transplantology
Medical University of Bialystok
M. Curie-Sklodowskiej 24A, 15-276 Bialystok, Poland
Tel. +48 85 7468276; fax. +48 85 7468896;
e-mail: mgacko@poczta.onet.pl

Table 1. Some components of the oxidative - antioxidative system in blood plasma and serum.

Component	Plasma (1)	Serum (2)	p 1 vs. 2
Malondialdehyde, µmol/dl	59.8 ±18.2	47.6 ± 13.6	0.0014
Total antioxidative capacity, µmol/dl	175.3 ± 34.3	128.2 ± 33.4	0.0001
Superoxide dismutase, j/dl	378.1 ± 118.0	276.3 ±113.2	0,0003
Protein SH-groups, µmol/dl	225.6 ± 21.2	219.6 ± 14.5	0.1541
Non-protein SH-groups, µmol/dl	34.2 ± 3.9	28.4 ± 2.8	0.0001
Ascorbate, µmol/dl	2.04 ± 0.71	1.6 ± 0.57	0.0039

Table 2. Haemoglobin, methaemoglobin and protein concentrations in blood plasma and serum.

Component	Plasma (1)	Serum (2)	p 1 vs. 2
Haemoglobin, mg/dl	2.8 ± 0.3	27.1 ± 3.6	0.0001
Methaemoglobin, µg/dl	42.3 ± 5.8	384.6 ± 52.8	0.0001
Protein, g/dl	7.5 ± 0.6	7.1 ± 0.5	0.0023

phydryl groups in plasma is comparable to that, assessed in blood serum. Concentrations of haemoglobin and methaemoglobin are markedly lower, whereas protein concentrations is higher in plasma than those in blood serum (Table 2)

Discussion

The total antioxidative capacity, and some of its components, such as superoxide dismutase activity, as well as the concentrations of non-protein sulphydryl groups and ascorbate, is higher in plasma, when compared to respective values in blood serum. It indicates their consumption in the processes, accompanying clot formation. Lower serum concentration of malondialdehyde can probably be the result of its non-covalent binding to low-molecular sulphydryl compounds. Plasma haemoglobin concentration, lower than its concentration in serum, gives evidence of increased permeability of erythrocyte cell membranes after blood extravasation. Bivalent iron in haemoglobin takes part in reductive processes that leads to haemoglobin conversion to methaemoglobin. Hypoxia and acidosis are developed with the time, following thrombus formation in arteries or veins, which results in increased permeability of cell membranes in entrapped erythrocytes and other morphological elements. Enzymes, which are present in erythrocytes in big quantities, such as acidic phosphatase, cathepsin D, aminotransferase, some enzymes of glycolytic cycle and many antioxidative enzymes, as well as reduced glutathione, are released into serum [14, 15, 16, 17, 18]. Due to extensive differences between blood plasma and serum, the evaluation of oxidative - antioxidative system for diagnostic purposes should be performed in blood plasma.

References

1. Triplett D.A.: Haemostasis. Igaku-Shoin Ltd., New York, Tokyo, 1985, 6-9.
2. Zieliński T, Wachowicz B. Secretory process in blood platelets. Post Bioch, 2003; 49: 175-93.
3. Brüne B, Von Appen F, Ullrich V. Oxidative stress in platelets. In: Sies H, editor. Oxidative stress. Oxidants and antioxidants. San Diego: Acad Press, 1991; 421-43.
4. Stocker R, Frei B. Endogenous antioxidant defence in human blood plasma. In: Sies H, editor. Oxidative stress. Oxidants and antioxidants. San Diego: Acad Press, 1991; 213-43.
5. Esterbauer H, Lang J, Zadravec S, Slater TF. Detection of malonaldehyde by high-performace liquid chromatography. Meth Enzymol, 1984; 105: 319-28.
6. Miller NJ, Rice-Evans C, Davies MJ, Gopinathan V, Milner A. A novel method for measuring antioxidant capacity and its application to monitoring the antioxidant status in premature neonates. Clin Sci, 1993; 34: 407-12.
7. Sykes JA, McCormac FX, O'Brien TJ. Preliminary study of the superoxide dismutase content of some human tumours. Canc Res, 1978; 38: 2759-62.
8. Ellman GL. Tissue sulfhydryl groups. Arch Biochem Biophys, 1959; 82: 70-7.
9. Kyaw A. A simple colorimetric method for ascorbic acid determination in blood plasma. Clin Chim Acta, 1978; 86: 153-7.
10. Beau A. Method for hemoglobin determination in serum and urine. J Clin Pathol, 1962; 32: 111-2.
11. Elvelyn KA, Malloy HT. Microdetermination of oxyhemoglobin, methemoglobin, and sulfhemoglobin in a single sample of blood. J Biol Chem, 1938; 126: 655-62.
12. Gornall AC, Bardawill CJ, David HM. Determination of plasma proteins by means of the biuret reaction. J Biol Chem, 1949; 177: 751-66.
13. Shinowara GY. Spectrophotometric studies on blood serum and plasma. The physical determination of hemoglobin and bilirubin. Am J Clin Pathol, 1954; 24: 696-707.
14. Caraway WT. Chemical and diagnostic specificity of laboratory tests. Am J Clin Pathol, 1962; 37: 445-64.
15. Greczaniuk A, Roszkowska-Jakimiec W, Gacko M, Worowska A. Determination of cathepsin D activity in blood plasma using hydrochloric acid denatured haemoglobin. Diagn Lab, 2000; 36: 97-101.
16. Loegering DJ, Carr FK, Saba TM. Cathepsin clerance from the circulation and reticuloendothelial function. Exp Molec Pathol, 1977; 27: 277-83.
17. Richterich R, Colombo JP, Weber H. Ultrametoden in klein klinische laboratorium. VII. Bestimung der sauren prostataphosphatase. Schweiz Med Wschr, 1962; 92: 1496-1500.
18. Solbach HG, Englhardt A, Merten R. Unterschiede der enzymativitäten in serum und plasma und ihre bedeutung für die klinische enzymdiagnostik. Klin Wschr, 1962; 40: 1136-39.

Usefulness of some primary anti-human antibodies in immunohistochemistry in guinea pig

Gendek-Kubiak H[1], Gendek EG[2]

[1]Department of Cytophysiology, Histology and Embryology, [2]Department of Chemistry and Clinical Biochemistry
Medical University of Łódź, Poland

Abstract

The commercially available antibodies for immunohistochemical purposes, though numerous and diversified, are mostly designed to detect human antigens. This study was undertaken to evaluate the usefulness of anti-human antigen antibodies in guinea pig tissues. The subjects of our interest were mostly skin and striated muscles and it was important for us to stain vascular and neural elements and to visualize separate cell kinds, including also skin Langerhans cells and the cells, contributing to inflammatory infiltrations.

Key words: guinea pig, immunohistochemistry, skin, skeletal muscles.

Introduction

Though human tissues are difficult to be obtained for research from diseased and, even more, from healthy people, animal derived biopsy/section material is relatively easily available, allowing for a proper selection of controls and for experiment planning. On the other hand, the commercially available antibodies for immunohistochemical purposes, though numerous and diversified, are mostly designed to detect human antigens. Additional difficulties arise when the antibodies are to be applied to paraffin sections. Thus, a researcher, performing animal experimental studies, apparently has a limited access to some research areas, potentially relevant for the elucidation of human disease mechanisms. This report summarizes several years of our studies on guinea pig tissues and it presents the adversities, overcome in the process. The reports, published by us to date, contain illustrations of immunohistochemical reactions to neuropeptides: β-endorphin [1], neuropeptide Y (NPY), calcitonin gene related peptide (CGRP), protein gene product 9.5 (PGP-9.5) [2], protein S-100, T lymphocytes and macrophages in guinea pig tissues [3, 4]. The panel of all primary antibodies and their used dilutions has been listed in Table 1. Out of the antibodies, used by us, only the one against pan-T-cell antigen (Serotec, Oxford, UK) was specially designed for studies in guinea pigs. The subjects of our interest were mainly the guinea pig skin and striated muscles and we considered staining of all possible cell kinds in those tissues, including epidermal Langerhans cells (LC), as well as the infiltrating elements, vascular and neural components. Neuropeptides are phylogenetically old protein compounds, occurring in humans and in animals with a high degree of identity among vertebrate species [5]. PGP 9.5 has been reported to be a marker for neurons and neuroendocrine cells [6]. Langerin (CD207), an antigen of human epidermal LC, is known to distinguish LC from other dendritic cell subsets and is characteristic for immature LC [7]. Fascin - an actin-binding protein is characteristic for different cell types, for example, for mature dendritic cells and endothelial cells [8]. CD56, neural cell adhesion molecule (NCAM) is a marker of myoblasts and regenerating muscle fibres [9]. CD59 (protectin) protects cells from lysis by complement compounds and is present on the surface of many cell types [10]. The proliferating cell nuclear antigen (PCNA) is a marker of proliferation.

ADDRESS FOR CORRESPONDENCE:
Hanna Gendek-Kubiak
Department of Cytophysiology, Histology and Embryology
Medical University of Łódź
G. Narutowicza 60, 90-136 Łódź, Poland
e-mail: h_kubiak@hotmail.com

Material and methods

The tests were performed by means of a few immunohistochemical methods in specimens from different tissues and organs of control guinea pigs and from inflamed skeletal mus-

Table 1. A list of used antibodies. Abbreviations: Rb (rabbit), Mo (mouse), Sh (sheep), TBS (The Binding Site).

Antibody anti-	Type	Clone	Dilution	Source
beta-endorphin	Rb		1 : 400	Eurodiagnostica
neuropeptideY	Rb		1 : 400	Eurodiagnostica
CGRP	Rb		1 : 800	Eurodiagnostica
protein S-100	Sh		1 : 50	TBS
PGP 9.5	Sh		1 : 50	TBS
T cells	Mo	CT5	1 : 120	Serotec
macrophages	Mo	MAC387	1 : 100	Serotec
hsp90	Mo	JPB24	1 : 40	Novocastra
PCNA	Mo	PC10	1 : 80	DakoCytomation
CD59 (protectin)	Mo	MEM-43	1 : 10	Serotec
(CD56) NCAM	Mo	1B6	1 : 40	Novocastra
von Willebrand factor	Sh		1 : 40	TBS
desmin	Mo	DE-R-11	1 : 40	TBS
myoglobin	Sh		1 : 120	TBS
fascin	Mo	IM20	1 : 40	Novocastra

Figure 1. A - myoglobin immunostaining (red) in guinea pig skeletal muscle. Three types of myofibres are visible. Magnification 240x. B. Desmin immunostaining (red) in guinea pig skeletal muscle. Sharp striations and, probably, muscle satellite cells are strongly positive. Magnification 600x. C. Positive immunostaining for hsp90 is present in endothelial cells of capillaries and in some connective tissue cells of endomysium in guinea pig skeletal muscle, showing slight inflammatory changes. Magnification 600x. D. Positive immuno-staining for PCNA in guinea pig germinal centre of lymph follicle. Magnification 240x.

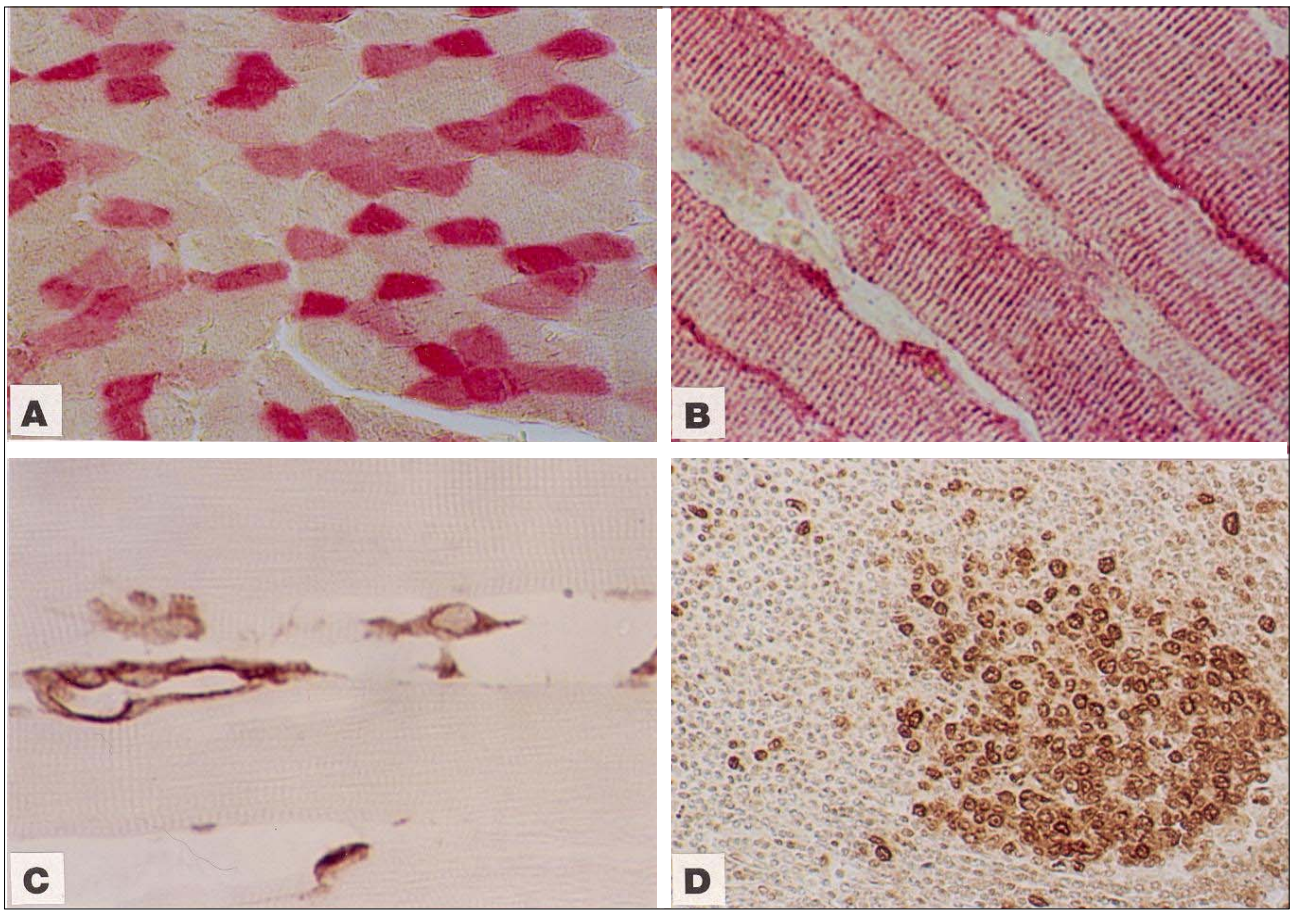

cles and skin. Normal, male guinea pigs of Dunkin-Hartley line, weighing 350-400 g each, were used throughout the study. Guinea pig tissue specimens, derived from the control animals and from the ones with experimentally induced skin and/or striated muscle inflammations, were collected by us during the years 1996-2003. Guinea pigs underwent pentobarbital intraperitoneal anaesthesia and decapitation. All the experiments had been approved by the Local Ethics Committee. The

material was fixed in Bouin's solution, in Carnoy's solution or in 10% formalin. The samples were paraffin embedded. Five µm sections were used throughout the study. Stainings were performed, using a number of techniques: a two-step indirect immunohistochemical method with peroxidase-labelled rabbit $F(ab')_2$ anti-mouse IgG (Serotec, Oxford, UK), labelled streptavidin biotin procedure, using LSAB2 System-HRP kit (DakoCytomation) and enhanced polymer procedure, using DAKO EnVision System with alkaline phosphatase (DakoCytomation); different antibody dilutions and unmasking antigen methods were applied. Primary antibodies were incubated for 1 h with tissue sections after blocking endogenous peroxidase with 2% hydrogen peroxide in peroxidase employing procedures. Slides were washed with PBS and incubated with the proper secondary antibody, depending on the used system, according to prescriptions. A negative control was obtained by omitting the primary antibody or by using a properly diluted respective non-immune serum instead of the antibody. After thorough washing in PBS, the antibody, bound to the antigen, was revealed by staining, done with 3,3'-diaminobenzidine substrate solution (Sigma) or Fast Red TR/Naphthol AS-MX (Sigma) for alkaline phosphatase-labelled antibody.

Results and Discussion

Positive immunohistochemical staining on guinea pig tissues was obtained with anti-neuropeptide antibodies, anti-myoglobin (Fig. 1A), anti-desmin (Fig. 1B), anti-protein S-100, anti-PGP 9.5, anti-macrophages, anti-heat shock protein 90 (hsp90) (Fig. 1C), anti-PCNA (Fig. 1D), anti-von Willebrand factor and, of course, with anti guinea pig T-cells antigen. Out of the anti-human antigens antibodies, used by us, negative results were visible with anti-langerin, anti-fascin, anti-CD59 and anti-NCAM (CD56) antibodies; that fact reflecting substantial differences in those molecule structures between the man and the guinea pig. Differences in epitope structures in components, characteristic for dendritic cells, between the man and the guinea pig makes impossible the application of described here anti-langerin and anti-fascin antibodies on guinea pig tissues for detection of LC. Additionally, S-100 protein is known to be widely distributed, among others in LC and in melanocytes, so, this fact hinders the unquestionable identification of epidermal LC by anti-S-100 antibody application [11]. Additionally, neither Bouin's solution nor 10% formalin for fixation was useful for desmin detection; Carnoy's fixative was not suitable for hsp90 and PGP 9.5 detection (completely negative stainings).

Acknowledgements.

The study was supported by a grant from the Medical University of Łódź (No. 502-11-168).

References

1. Gendek-Kubiak H. Immunohistochemical demonstration of beta-endorphin in guinea pig sebaceous glands of normal skin and during immune inflammation. Folia Histochem Cytobiol, 1998; 36: 15-8.

2. Gendek-Kubiak H, Kmieć BL. Immunolocalization of CGRP, NPY and PGP 9.5 in guinea pig skin. Folia Morphol, 2004; 63: 115-7.

3. Gendek-Kubiak H. Effect of intramuscular application of selected neuropeptides on morphology of muscle. Cell Mol Biol Lett, 2002; 7: 1059-64.

4. Gendek-Kubiak H, Gendek EG. Histological pictures of muscles and an evaluation of cellular infiltrations in human polymyositis/dermatomyositis, as compared to the findings in experimental guinea pig myositis. Cell Mol Biol Lett, 2003; 8: 297-303.

5. Karanth SS, Springall DR, Kuhn DM, Levene MM, Polak JM. An immunocyto-chemical study of cutaneous innervation and the distribution of neuropeptides in man and commonly employed laboratory animals. Am J Anat, 1991; 2191: 369-83.

6. Thompson RJ, Doran JF, Jackson P, Dhillon AP, Rode J. PGP 9.5 - a new marker for vertebrate neurons and neuroendocrine cells. Brain Res, 1983; 278: 224-8.

7. Mizumoto N, Takashima A. CD1a and langerin: acting as more than Langerhans cells markers. J Clin Invest, 2004; 113: 658-60.

8. Al-Alwan MM, Rowden G, Lee TD, West KA. Fascin is involved in the antigen presentation activity of mature dendritic cells. J Immunol, 2001; 166: 338-45.

9. Cashman NR, Covault J, Wollman RL, Sanes JR. Neural cell adhesion molecule in normal, denervated, and myopathic human muscle. Ann Neurol, 1987; 21: 481-9.

10. Navenot JM, Villanova M, Lucas-Heron B, Malandrini A, Blanchard D, Louboutin JP. Expression of CD59, a regulator of the membrane attack complex of complement, on human skeletal muscle fibers. Muscle Nerve, 1997; 20: 92-6.

11. Atoji Y, Nakaoka T, Yamamoto Y, Suzuki Y. Antigen stimulation alters the expression of S-100 protein in the giant macrophages and follicular dendritic cells of the guinea pig lymph nodes. Acta Anat, 1994; 149: 203-8.

Expression of tissue transglutaminase in blood and lymphatic vessel endothelia and in mesothelium

Gendek-Kubiak H[1], Gendek EG[2]

[1]1Department of Cytophysiology, Histology and Embryology, [2]Department of Chemistry and Clinical Biochemistry
Medical University of Łódź, Poland

Abstract

This study was undertaken to evaluate tissue transglutaminase (TG2) expression in guinea pig tissues, using an antibody against the guinea pig liver TG2. The tests were performed by means of a few immunohistochemical methods in specimens from: gut, skin, the lungs, lymph nodes, the heart, the thymus, the spleen, skeletal muscles of control guinea pigs and from inflamed skeletal muscles and skin. TG2 expression was found in artery, vein and lymphatic vessel endothelia, in mesothelia of pleura, pericardium and peritoneum, and in smooth muscle cells. Spleen deserves a special attention, since this organ, especially rich in TG2, may be much more involved in celiac disease and in liver diseases than it has been accepted so far. The subject calls for further elucidation.

Key words: tissue transglutaminase, guinea pig, immunohistochemistry.

Introduction

Type II transglutaminase (TG2) is an enzyme, the activity of which requires Ca^{2+} ions presence. It catalyzes reactions, producing cross-linking amide bonds between proteins, but also between proteins and polyamines. Tissue transglutaminase, or transglutaminase 2 (TG2, EC 2.3.2.13), belongs to the superfamily of Ca^{2+}-dependent enzymes. It catalyzes a variety of post-translational modifications of proteins. The most common among them is the formation of isopeptide bonds, producing crosslinks between proteins [1, 2]. During skeletal muscle development, there is a transient expression of this protein [3]. The TG2 is the main, if not the sole, target of the endomysium celiac disease-specific autoantibodies; assigned to this enzyme is the role of master regulator of celiac disease [4]. In experimental mice, TG2 plays a protective role in hepatic injury [5]. Thus, TG2 is physiologically constantly expressed in some regions, while in others, it may be induced. This study was undertaken to perform immunohistochemical detection of TG2 in guinea pig different organs to evaluate its expression in normal guinea pig tissues and in inflamed skeletal muscles and skin, using an antibody against the guinea pig liver TG2.

ADDRESS FOR CORRESPONDENCE:
Hanna Gendek-Kubiak
Department of Cytophysiology, Histology and Embryology
Medical University of Łódź
G. Narutowicza 60, 90-136 Łódź, Poland
e-mail: h_kubiak@hotmail.com

Material and methods

Normal 6 male guinea pigs of Dunkin-Hartley line, weighing 350-400 g each, were used throughout the study. Additionally, we used a material, derived from our experiments on the induction of skin and muscle inflammation by intradermal/intramuscular injections of dermatomyositis patient sera, as described earlier [6]. Experimental animal tissue specimens were taken at different time points after the sera injections (3 to 72 hrs). Tissue specimens were taken after pentobarbital intraperitoneal anaesthesia. The experiment was approved by the Local Ethics Committee.

One half of each sample was fixed in Bouin's solution, while the other one in Carnoy's solution; they were paraffin embedded and used for immunohistochemistry. The tests were performed by means of a few immunohistochemical methods in specimens from: gut, skin, the lungs, lymph nodes, the heart, the spleen, the thymus, skeletal muscles of control guinea pigs and from inflamed skeletal muscles and skin. Five (5) μm sections were used throughout the study. The mouse anti-guinea pig liver TG2 monoclonal IgG1 antibody, clone CUB 7402 (DakoCytomation), in dilution of 1:50 - 1:150, was used as a primary antibody. Stainings were performed, using a number of techniques: the two-step indirect immunohisto-

Figure 1. Immunolocalization of transglutaminase 2 in guinea pig organs. A. Fragment of normal intestine. Positive immunostaining is visible in mesothelial cells of peritoneum, in myocytes, forming longitudinal and circular layers of intestinal wall, in endothelia of blood and lymphatic vessels and in single cells of intestinal glands; intestinal nervous ganglia are completely negative. Immunoperoxidase method, DAB, used as a chromogen (brown). Magnification 240x. B. Spleen of normal guinea pig. Endothelia of capillaries and lymphatic vessels show very strong immunostaining; peripheral zone of lymph follicle shows intensive staining, too. Immunoperoxidase method, DAB, used as a chromogen (brown). Haematoxylin counterstain. Magnification 240x. C. In the lymph node, interdigitating cells of the subcapsular region form a zone, showing positive immunostaining. Immunoperoxidase method, Vector SG, used as a chromogen (dark blue). Nuclear fast red counterstain. Magnification 240x. D. Fragment of "C" micrograph . Magnification 600x.

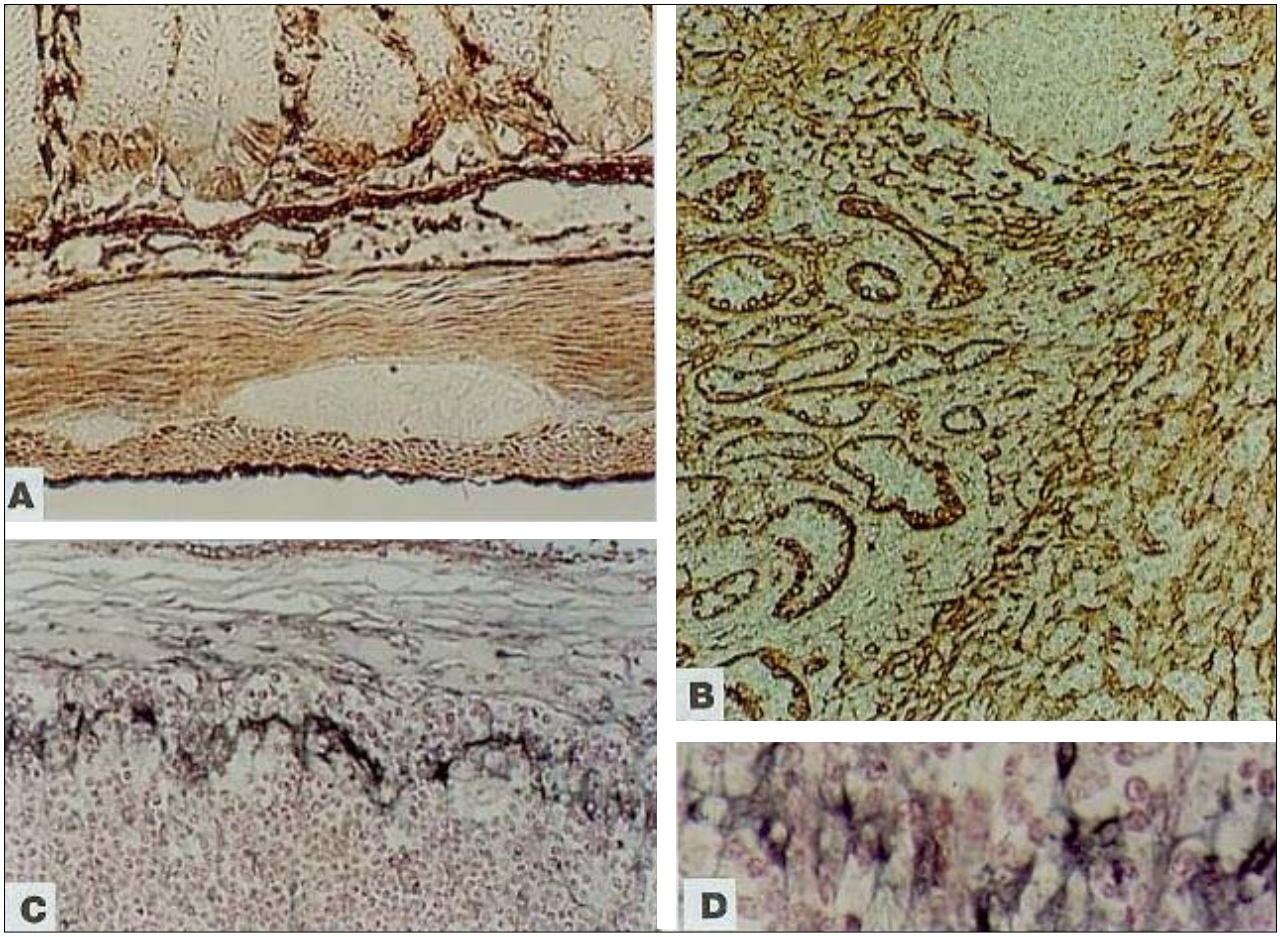

chemical method with peroxidase-labelled rabbit F(ab')2 anti-mouse IgG (Serotec, Oxford, UK), the labelled streptavidin biotin procedure, using an LSAB2 System-HRP kit (DakoCytomation) and the enhanced polymer procedure, using the DAKO EnVision System with alkaline phosphatase (DakoCytomation). Primary antibodies were incubated for 1 h with tissue sections after blocking endogenous peroxidase with 2% hydrogen peroxide in peroxidase employing procedures. Slides were washed with PBS and incubated with the proper secondary antibody, depending on the used system, according to prescriptions. A negative control was obtained by omitting the primary antibody. After thorough washing in PBS, the antibody, bound to the antigen, was revealed by staining with 3.3'-diaminobenzidine substrate solution (Sigma) or Vector SG (Vector) for peroxidase and Fast Red TR/Naphthol AS-MX (Sigma) for alkaline phosphatase-labelled antibody.

Results

TG2 expression was found in artery, vein and lymphatic vessel endothelia, in mesothelia of pleura, pericardium and peritoneum, and in smooth muscle cells. In the gut, besides the intestine reaction in mesothelium and in smooth myocytes, an intensive staining was present in endothelial cells of blood and lymphatic vessels of villi (Fig. 1A). Sporadically, epithelial cells of the gut were positive, mainly in the intestinal glands (Fig. 1A). In the spleen, both lymphatic and blood vessel endothelia were intensively stained, but also in lymph follicles, especially at their periphery, the reaction was pronounced (Fig. 1B). In the thymus, the strongly positive cells were large, scattered mainly in cortical parts of this organ and vascular endothelia were positive. A positive reaction to the antigen was also observed in sinuses of lymph nodes; positive interdigitating cells formed a zone in the subcapsular region of lymph nodes (Fig. 1C, Fig. 1D). In normal capillaries of the skin and skeletal muscles, the reaction was negative. In tissue specimens from experimental myositic muscles, significantly dilated lymphatic vessels with strongly immunoreactive endothelium were found and some of them seemed to surround (squeeze) blood vessels. The endothelia of capillaries in endomysium were positive, too.

Discussion

In the literature, different functions of TG2 are pointed out (including: protein crosslinking, GTP-ase activity, acting as G protein, kinase activity), implying an opinion that still the knowledge on this protein is far from being complete, but a progress in it seems very promising.

In the present study, a strong TG2 expression was shown in endothelia and in mesothelia, what can be considered as an indication of some role of this protein in creating barriers, regulating molecular flow (infiltration). The used by us antibody seems to be especially useful and valuable for lymphatic vessel detection, which are often overlooked in histologically examined tissues. The spleen deserves a special attention, since this organ, especially rich in TG2 (Fig. 1B), may be much more involved in celiac disease [4] and in liver diseases [5] than it has been thought so far. The subject calls for further elucidation.

Acknowledgements

The study was supported by grant from the Medical University of Łódź (No. 502-11-168). The dermatomyositis patients' sera were kindly provided by Prof. A. Sysa and Prof. A. Kaszuba from the Medical University of Łódź.

References

1. Lorand L, Conrad SM. Transglutaminases. Mol Cell Biochem, 1984; 58: 9-35.
2. Mishra S, Murphy LJ. Tissue transglutaminase has intrinsic kinase activity: identification of transglutaminase 2 as an insulin-like growth factor-binding protein-3 kinase. J Biol Chem, 2004; 279: 23863-8.
3. Lee SK, Chi JG, Park SC, Chung SI. Transient expression of transglutaminase C during prenatal development of human muscles. J Histochem Cytochem, 2000; 48: 1565-74.
4. Caputo I, D'Amato A, Troncone R, Auricchio S, Esposito C. Transglutaminase 2 in celiac disease: Minireview article. Amino Acids, 2004; 26: 381-6.
5. Nardacci R, Falciatori I, Moreno S, Stefanini S. Immunohistochemical localization of peroxisomal enzymes during rat embryonic development. J Histochem Cytochem, 2004; 52: 423-36.
6. Gendek-Kubiak H, Gendek EG. Histological pictures of muscles and an evaluation of cellular infiltrations in human polymyositis/dermatomyositis, as compared to the findings in experimental guinea pig myositis. Cell Mol Biol Lett, 2003; 8: 297-303.

Quantitative evaluation of immuno- and histochemical reaction intensity by spatial visualization techniques

Górna A, Kaczmarek E, Nieruchalska E, Jarmołowska-Jurczyszyn D, Majewski P

Laboratory of Morphometry and Medical Image Processing, Chair of Pathology University of Medical Sciences, Poznań, Poland

Abstract

The aim of this study was an application of spatial visualization techniques for quantitative measurements of immuno- and histochemical reactions. For a quantitative histochemical study, specimens, collected from patients with chronic gastritis, were stained with paS/AB, while for immunohistochemical evaluation, specimens were used, collected from patients with chronic parathyroiditis and were analyzed with Ki-67 proliferation marker and apoptosis bcl-2 protein. The new technique permitted to obtain quantitative objective results. Statistical cluster analysis of those results indicated small groups of cases for reevaluation and supported the final diagnosis.

Key words: quantitative histochemistry, measure of marker expression, spatial image analysis.

Introduction

Quantitative measurement of the intensity of immuno- and histochemical staining is a significant problem in pathomorphological diagnosis. Routinely, visual evaluation is performed in light microscopy and semi-quantitative assessment of reaction strength is expressed in scores, usually from 0 to +++. In order to improve the objectivity of assessment, a computer technique was developed for raw colour images, extended to three-dimensional space by introducing image intensity as the third dimension [1]. In our study, this method was used for cases of intestinal metaplasia, illustrating the evaluation of histochemical reaction, and for cases with hyperparathyroidism, presenting the application for immunohistochemical investigation.

ADDRESS FOR CORRESPONDENCE:
Elżbieta Kaczmarek
Laboratory of Morphometry and Medical Image Processing
Chair of Pathology
University of Medical Sciences, Poznań
Przybyszewskiego 49; 60-355 Poznań, Poland
Tel (061) 869 18 16; e-mail: elka@amp.edu.pl

Material

For quantitative histochemical study, twenty needle biopsy specimens, obtained from patients with chronic gastritis, were stained with paS/AB pH 2,5 (Fig. 1). For quantitative immunohistochemical evaluation, our study was conducted on resected goitres from patients with chronic parathyroiditis. Immunohistochemical staining was performed for apoptosis bcl-2 protein (Dako). Proliferating cells were detected by immunostaining for Ki-67 (Dako). Images of 640x480 pixels each (at 400x magn.), were acquired by the use of a digital light microscope, running under the Motic Images v. 1.2 software (Micro Optic Industrial Group Co) for Windows.

Methods

The acquired images were visualized in three-dimensional space by introducing image brightness as the third dimension. The colours of immuno- or histochemical reactions were then exposed by reducing the remaining elements to the background with the use of three filters. A filter of brightness extracted the pixels with brightness, exceeding the defined threshold value and corresponding to the colour of the reaction. The remaining elements were reduced. The second, colour filtering, gave pixels with colours compatible with the reaction, present in histological specimen. Third, a filter of saturation was used, removing reaction free elements. The filters were fixed for each series of images acquired from a specimen. The surface of extracted positive reaction was computed as the total number of pixels in colours of the reaction. In order to compute the reaction volume, its spatial representation was divided into small prisms and

Table 1. Quantitative assessment of paS/AB in cases of intestinal metaplasia

Intestinal metaplasia	Group I (n=13)	Group II (n=6)	p-level
Measurements	Mean ± SD	Mean ± SD	
Area of paS/AB [per 1 μm^2]	0.021 ± 0.014	0.079 ± 0.032	p<0.001
Expression of paS/AB	86 ± 10	93 ± 17	ns

Table 2. Area and expression of Ki-67 and bcl-2 in cases of parathyroiditis

Hyperparathyroidism	Hyperplasia		Adenoma		p-level
Measurements	Mean ± SD	Min-Max	Mean ± SD	Min-Max	
Area of bcl-2+ [per 1 μm^2]	0.077±0.041	0.010-0.122	0.087±0.006	0.039-0.125	ns
Expression of bcl-2+	125 ± 12	100 - 137	130 ± 3	125 - 134	ns
Area of Ki-67+ [per 1 μm^2]	0.004±0.002	0.001-0.007	0.006±0.002	0.002-0.009	p<0.05
Expression of Ki-67+	152 ± 22	113 - 180	144 ± 23	101 - 169	ns

Table 3. Clustering of hyperplasia and adenoma cases in parathyroiditis.

	Area of Ki-67+ [per 1 μm^2]	Expression of Ki-67+	Area of bcl-2+ [per 1 μm^2]	Expression of bcl-2+
	Mean ± SD	Mean ± SD	Mean ± SD	Mean ± SD
Hyperplasia (cluster I)	0.003 ± 0.002	117 ± 14	0.143 ± 0.052	130 ± 17
Hyperplasia (cluster II)	0.004 ± 0.003	165 ± 13	0.038 ± 0.029	123 ± 13
Adenoma (cluster I)	0.006 ± 0.005	161 ± 13	0.157 ± 0.038	134 ± 6
Adenoma (cluster II)	0.005 ± 0.004	113 ± 20	0.069 ± 0.029	128 ± 5

pyramids. The volume of each solid shape was computed. The reaction volume was derived as the sum of all prism and pyramid volumes. The expression of the reaction was assessed as the ratio of its volume divided by its surface. Image processing was performed by the use of a computer program, designed and programmed in C++ language by Strzelczyk [1]. The obtained results were compared between groups by the Mann-Whitney test. A consistency between semi-qualitative evaluation of specimens (Sydney scale) and the computed spatial technique was assessed by Spearman's correlation coefficient. Cluster analysis (the K-means method) was also performed to assess homogeneity of the results, based on the following two features: the area and colour intensity of investigated reactions. The statistical analyses were carried out with the Statistica PL v.6 (StatSoft Inc.) computer program.

Results

The area of paS/AB in intestinal metaplasia was, on the average, 0.039 ± 0.034 per 1mm^2 and ranged from 0.002 to 0.138 per 1mm^2. The intensity of reaction colour measured in 256 colours' scale was on average 88 ± 12 and ranged from 75 to 112. K-means clustering showed a non homogeneity of results and revealed two groups among them. (Table 1). The area of paS/AB per 1 μm^2 was significantly different in those groups, while the intensity of reaction was similar.The area of paS/AB reaction correlated well with the Sydney scale assessment (r=0.759, p<0.05) in Group I, while it was not correlated in Group II (r=0.086, p<0.05). In immunohistochemical studies of hyperparathyroidism cases, a significant difference was found between parathyroid hyperplasia and adenoma for Ki-67+ (Table 2). The analysis of area and of the expression of Ki-67 and bcl-2 by the use of K-means clustering showed heterogeneity of cases with parathyroiditis. Adenoma cases were divided into two clusters. Similarly, the cases with hyperplasia were also divided into two subgroups (Table 3).

Final remarks

The technique of spatial visualization allowed us to obtain quantitative and more objective results. Cluster analysis indicated a small group of cases with intestinal metaplasia, showing advanced changes, associated with additional disease symptoms. Quantitative immunohistochemical analysis, performed in our study in chronic hyperthyroiditis, permitted to find groups of cases with hyperplasia and adenoma, showing a minor intensity and area of the markers. That was helpful in the final diagnosis. The evaluation by the the use of spatial techniques, as presented in this paper, is more objective than semi quantitative evaluation [2].

Figure 1. Reaction paS/AB in intestinal metaplasia

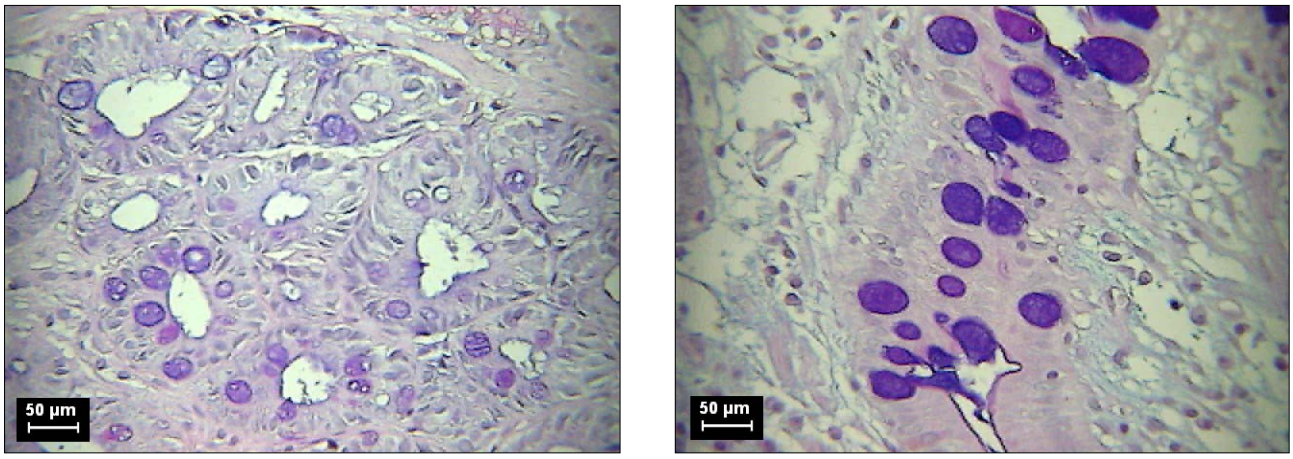

Figure 2 Spatial representation of paS/AB in Figure 1.

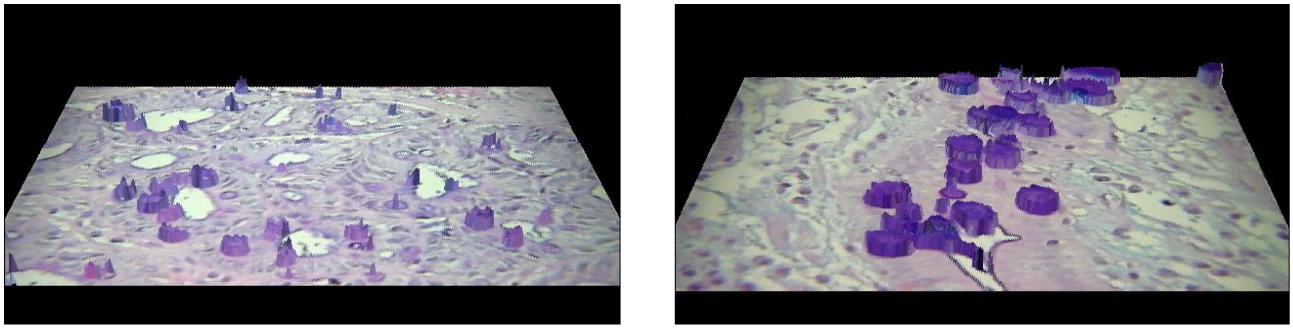

Figure 3. Orthogonal projection of paS/AB (Fig. 2) onto the plane

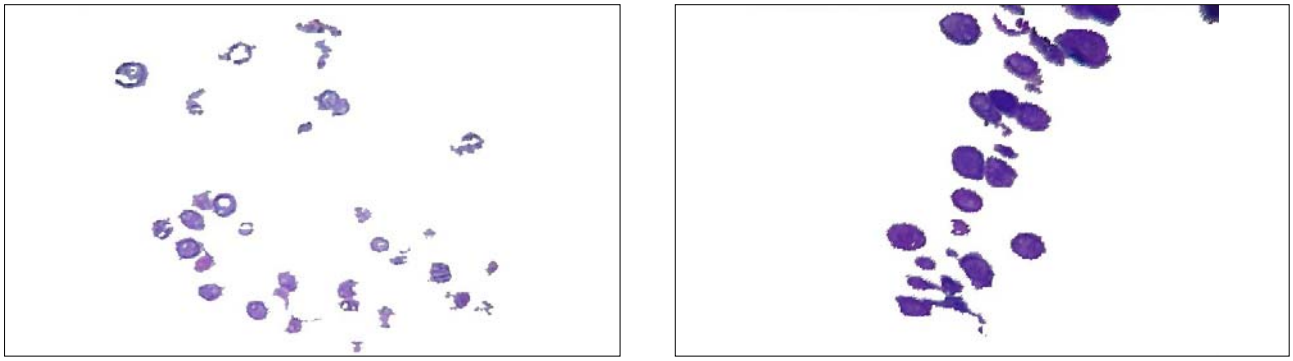

Figure 4. Expression of bcl2 in adenoma case (left) and the segmented reaction (right).

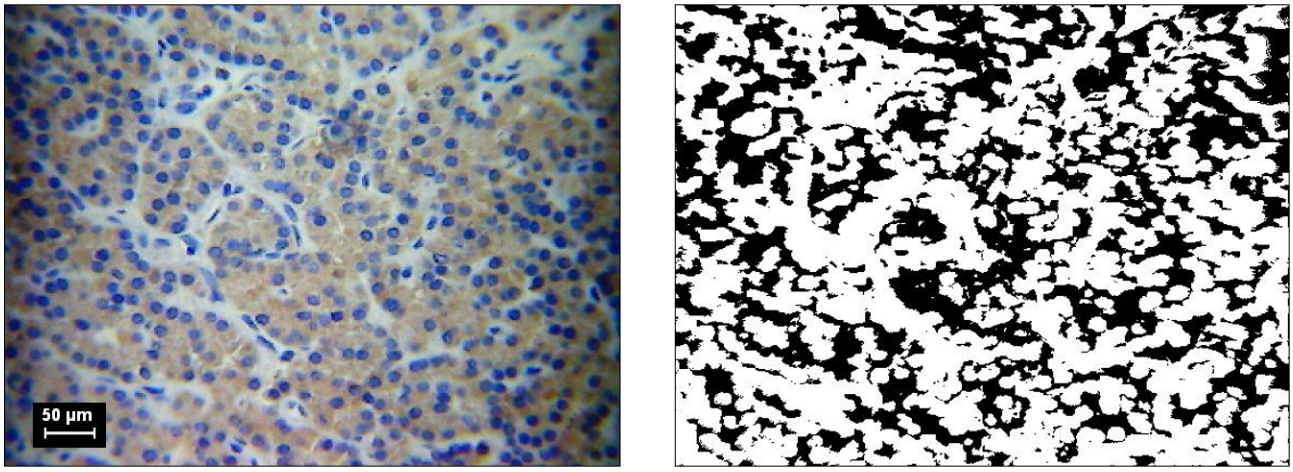

Figure 5. Spatial visualization of Ki-67 (left) and bcl-2 (right) in chronic parathyroiditis.

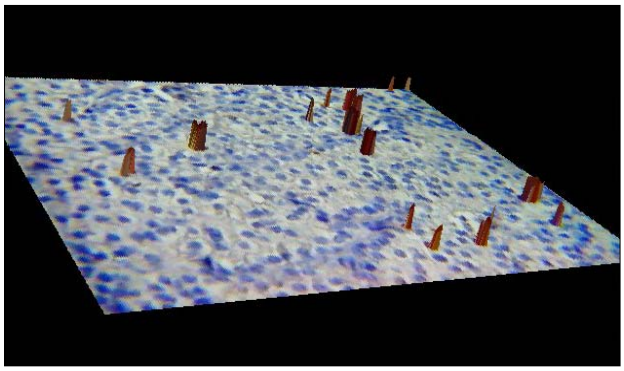

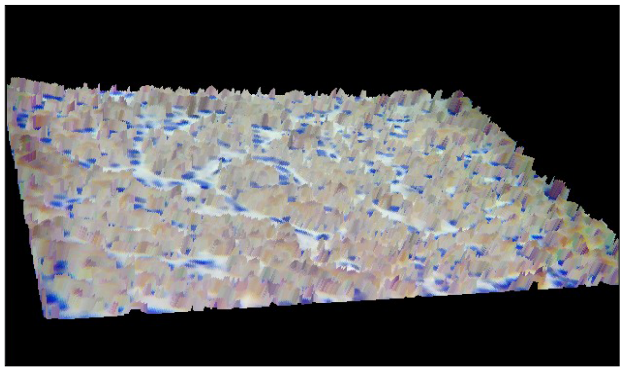

References

1. Nieruchalska E, Strzelczyk R, Woźniak A, Żurawski J, Kaczmarek E, Salwa- Żurawska W. A quantitative analysis of the expression of a-smooth muscle action in mesangioproliferative (GnMes) glomerulonephritis. Folia Morph, 2003; 62: 451-3.

2. Matkowskyj K, Glover S, Benya R, Quantitative Immunohistochemistry: A New Algorithm Measuring Cumulative Signal Strength and Receptor Number. Microscopy and Analysis, 2004; 18: 31-3.

Haemoglobin of varicose vein, varicose vein with thrombophlebitis and in parietal thrombus of varicose vein

Guzowski A, Gacko M, Worowska A, Kowalewski R, Łapiński R, Ostapowicz R, Płoński A

Department of Vascular Surgery and Transplantology, Medical University of Bialystok, Poland

Abstract

Saphenous veins were taken for examination: unchanged, varicose with thrombophlebitis and varicose thrombus. The contents of haemoglobin and protein were determined in the homogenate of that material. Only small quantities of haemoglobin were found in walls of unchanged veins. Greater amounts of haemoglobin were observed in walls of varicose veins, especially in walls of varicose veins with thrombophlebitis. The varicose vein thrombus also contained marked quantities of haemoglobin.

Key words: varicose vein, varicose thrombus, haemoglobin.

Introduction

Chemical and enzymatic composition of the vein wall depends on the cellular composition, which changes in pathological conditions, such as varices and inflammatory processes [1, 2]. These changes are often accompanied by parietal thrombus [3, 4]. Erythrocytes dominate in vein thrombus. Haemoglobin, released during haemolysis of erythrocytes, may infiltrate into the vein wall. The aim of this report was to evaluate the contents of haemoglobin in unchanged veins, varicose veins and varicose veins with thrombophlebitis and in varicose vein thrombus.

ADDRESS FOR CORRESPONDENCE:
Marek Gacko
Department of Vascular Surgery and Transplantology
Medical University of Bialystok,
M. Skłodowskiej-Curie 24A, 15-276 Białystok, Poland.
tel. (85) 746 82 77; fax. (85) 746 88 96;
e-mail: mgacko@poczta.onet.pl

Material and methods

The following saphenous veins were taken for the study: unchanged macroscopically veins, varicose veins, varicose veins with thrombophlebitis and parietal thrombus, obtained during surgery from 8 patients. Retracted blood clots, obtained in vitro from blood samples, collected from the patients before the surgery, served as control material. Samples of unchanged and varicose vein walls, thrombus and blood clots were stored at the temperature of -75^{0}C. The samples were pulverized in nitrogen in a stainless steel pulverizer directly before determinations. Cooled 0.15 mol/l NaCI (1:9 v/v) was added to the pulverized material and extracted at the temperature of 2^{0}C for 30 minutes. Supernatant, obtained by centrifugation (2700 x g, 30 min, 2^{0}C), was used for the examinations. The contents of haemoglobin [5] and protein [6] were determined in the homogenates, and were converted to 1 g of wet tissue. Gell filtration of the homogenate proteins was carried out in a Sephadex G-75 column of 1 x 40 cm in size. Five (5) mg of the homogenate protein was placed in the column. A 0.15 mol/l NaCl solution was used for elution. One (1) ml fractions were collected in 10 minute intervals, using an automatic fraction collector. Haemoglobin was determined by the measure of absorbance at 625 nm [5]. Haemoglobin was identified by means of the calibration curve, expressing the dependence of elution volume on the logarithm of molecular weight. The results of the determination were analyzed by Student's 't' test. The values of $p<0.05$ were accepted as statistically significant.

Results

The content of haemoglobin in the homogenates of unchanged saphenous veins amounted to 4.0 mg/g of tissue, varicose vein - 6.8 mg/g of tissue and varicose vein with thrombophlebitis - 17.2 mg/g of tissue (Table 1). The content of protein in the vein homogenate amounted to: unchanged vein: 27.5 mg/g of tissue, varicose vein: 29.0 mg/g of tissue, varicose vein with thrombophlebitis: 34.5 mg/g

Figure 1. Gel filtration in Sephadex G-75 of saphanous vein homogenate haemoglobin:
o - unchanged vein, trangle - varicose vein, rectangle - varicose vein with thrombophlebitis

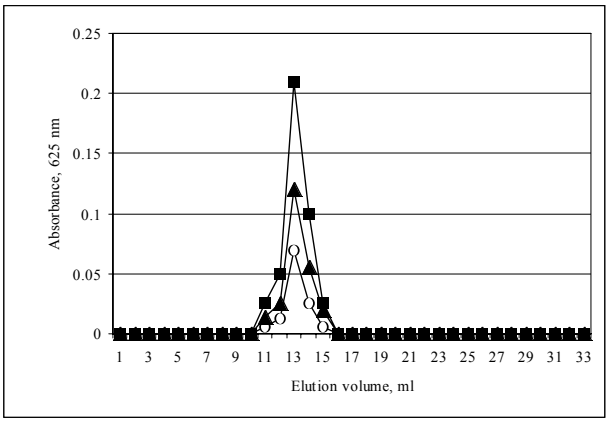

Figure 2. Gel filtration in Sephadex G-75 of homogenate haemoglobin: o - blood clot, rectangle - vein thrombus

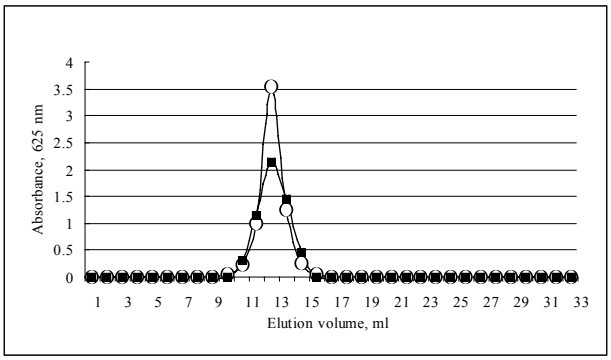

of tissue. The content of haemoglobin in the vein thrombus homogenate amounted to 152.6 mg/g of tissue and in the blood clot homogenate amounts to 298.4 mg/g of tissue (Table 2). The content of protein in the vein thrombus homogenate amounted to 166.8 mg/g of tissue and in the blood clot homogenate, it amounted to 335.5 mg/g of tissue. Gel filtration in the Sephadex G-75 column showed that homogenates of the vein, varicose vein and varicose vein with thrombophlebitis contained haemoglobin (Fig.1). The homogenates of the vein thrombus and blood clot also contained haemoglobin (Fig. 2).

Discussion

In the physiological state, haemoglobin is found in erythrocytes of the circulating blood and it constitutes 90% of their dry mass. In pathological state, erythrocytes haemoglobin and free haemoglobin are also present in vein thrombus, in the wall of veins, changed in inflammatory processes, and in the blood extravasated into tissues and body cavities. Disturbances of oxidative-antioxidative processes are observed in walls of lower extremity varices [7, 8]. Haemoproteins, especially haemoglobin and its derivatives, may participate in these processes [9, 10]. The presence of haemoglobin, containing Fe2+ in a wall of varicose vein and, especially, in walls of veins, changed, due to thrombophlebitis, and in varicose thrombus should be taken into consideration, when estimating the systems, generating reactive forms of oxygen and, when estimating the concentrations of

Table 1. The contents of haemoglobin and protein in the saphenous vein wall: unchanged, varicose and varicose with thrombophlebitis.

Saphenous vein	Haemoglobin, mg/g of tissue	Protein, mg/g of tissue
Unchanged	4.0 ±0.2	27.5 ±2.2
Varicose	6.8 ±0.4*	29.0 ±3.0
Varicose with thrombophlebitis	17.2 ±1.2*	34.5 ±2.4*

* - statistically significant difference, p< 0.0001

Table 2. The contents of haemoproteins and protein in varicose thrombus and blood clot.

Examined material	Haemoglobin, mg/g of tissue	Protein, mg/g of tissue
Varicose thrombus	152.6 ±12,4	166.8 ±13.7
Bloot clot	298.4 ±23.8*	335.5 ±30.2*

* - statistically significant difference, p< 0.0001

antioxidants. Lower contents of haemoglobin in vein thrombus than those in blood clot, obtained in vitro, result in haemolysis of erythrocytes and in their release from the thrombus. The degree of haemoglobin loss may be a measure of thrombus duration. This time can also be determined by the content of von Willenbrand's factor, as well as by the contents of DNA and hydroxyproline.

References

1. Leu HJ. Morphology of chronic venous insufficiency - light and electron microscopic examination. Vasa, 1991; 20: 330-4.
2. Yamada T, Tomita S, Mori M, Sasatoni E, Suenaga E, Itoh T. Increase mast cell infiltration in varicose veins of the lower limbs: a possible role in the development of varices. Surgery, 1996; 119: 494-7.
3. Campbell B. Thrombosis, phlebitis and varicose veins. Br Med J, 1996; 312: 198-9.
4. Golledge J, Quigley FG. Pathogenesis of varicose veins. Eur J Vasc Endovasc Surg, 2003; 25: 319-24.
5. Beau A. Method for hemoglobin determination in serum and urine. J Clin Pathol 1962; 32: 111-2.
6. Bradford MM. A rapid and sensitive method for the quantitation of microgram quantities of protein utilizing the principle of protein-dye binding. Anal Biochem, 1976; 72: 248-54.
7. Stępień A, Michalak J, Ledwożyw A. Activities of free radicals metabolizing enzymes in varicous veins in women patients. Acta Physiol Pol, 1988; 39: 75.
8. Deby C, Hariton C, Pincemail J, Coget J. Decreased tocopherol concentration of varicose veins is associated with a decrease in antilipoperoxidant activity without similar changes in plasma. Phlebology, 1989; 4: 113-21.
9. Winterboum CC (1985) Reactions of superoxide with hemoglobin, in: Handbook of methods for oxigen radical reaserch, ed. RA Greenwald. Boca Raton, Fl, CPC, 1985; 137-41.
10. Halliwell B, Gutteridge JMC. Iron and free radical reactions: two aspects of antioxidant protection. Trends Biochem Sci, 1986; 11: 372-5.

Morphological evaluation of the lungs in rats with experimentally induced renal failure

Kasacka I[1], Piłat-Marcinkiewicz B[1], Pankiewicz W[2], Sulewska A[2]

[1]Department of Histology and Embryology, [2]Department of Clinical Molecular Biology
Medical University of Białystok, Poland

Abstract

The study aimed at morphological evaluation of changes in the lungs of rats during experimentally induced uremia. The studies were performed in three (3) groups of rats: C - a control group (15 animals), SO - 15 rats, submitted to sham operation, U - an uremic group - 21 rats with experimental renal failure. After 1, 2 and 4 weeks from the surgery, the collected lungs were fixed in Bouin's fluid and in 2.5% purified glutaraldehyde for electron microscopy. Paraffin specimens were cut into 5 μm slices and stained by H+E, by Azan's method and with silver, according to Grimelius. Ultra thin sections contrasted with uranyl acetate and lead citrate. Blood serum urea and creatinine levels were determined. In the uremic rats, increased concentrations of serum creatinine and urea were observed.

Chronic renal failure affected the progress and the degree of development of the changes in the lungs, the final effect of which was fibrosis. In microscopic pictures of the lungs from the uremic rats, numerous changes were observed, characteristic for chronic oedematous conditions of different intensification.

Key words: chronic renal failure, lung, morphology.

Introduction

The final stage of chronic renal failure (CRF) is chronic uremia, characterised by severe metabolic disorders, inducing clinical symptoms in the majority of organs [1, 2].

ADDRESS FOR CORRESPONDENCE:
Irena Kasacka
Department of Histology & Embryology
Medical University of Białystok
Kilińskiego 1; 15-089 Białystok, Poland
Tel. (48 85) 748 54 58; e-mail: kasacka@amb.edu.pl

Oedema with pleural exudate is the most frequently observed pulmonary complication, fairly often asymptomatic in its course. Pulmonary oedema results from an increased hydrostatic blood pressure in capillary vessels, the pressure rise being in proportion to fluid overload, as well as to an increased permeability of pulmonary capillaries [3, 4]. Mechanic and haemodynamic changes in the lungs may occur without any basic clinical syndromes, leading to serious pulmonary function disturbances, which may further result in injuries of the walls of the perialveolar capillaries, reducing the efficiency of gas exchange [4].

In order to increase the knowledge on the pathogenesis of respiratory disorders in (CRF), as well as with regards to the lack of an unequivocal evaluation of causes of the changes, observed in the respiratory tract, it seemed fairly interesting to attempt a thorough study of the dynamics of morphology in changes of the lung in experimentally induced renal failure.

The goal of the performed studies was morphological evaluation of changes in the lungs in the course of experimentally induced uremia.

Materials and Methods

The study was carried out on 51 young male Wistar rats, 200-250 g body weight (mean 220±10g) at the beginning of the experiment. The animals had a free access to drinking water and standard granulated diet. The experimental uremia was produced in 21 rats. The control animals underwent a sham operation, i.e. decapsulation and removal of the adherent fat (15 rats). The other control group did not undergo any surgical procedure (15 animals). Experimental uremia was induced, using the method, described by Ormrod and Miller [6], and Azzadin [5]. The rats were anesthetized with pentobarbital, administered intraperitoneally in a dose of 50 mg/kg. Nephrectomy of the right kidney was performed and 70% of the left kidney cortex was removed, leaving the renal medulla intact.

Figure 1. Lung of a control animal. H+E stain, mag. 200x.

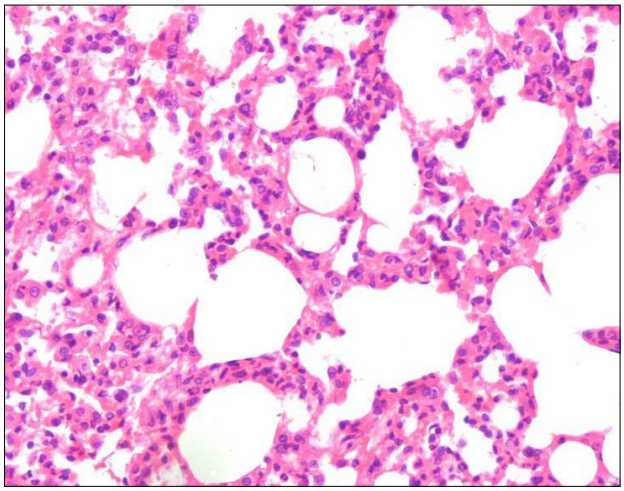

Figure 2. A lung fragment of a rat with uremia after 1 week of the experiment. Advanced atelectasis and oedema. Azan stain, mag. 250x.

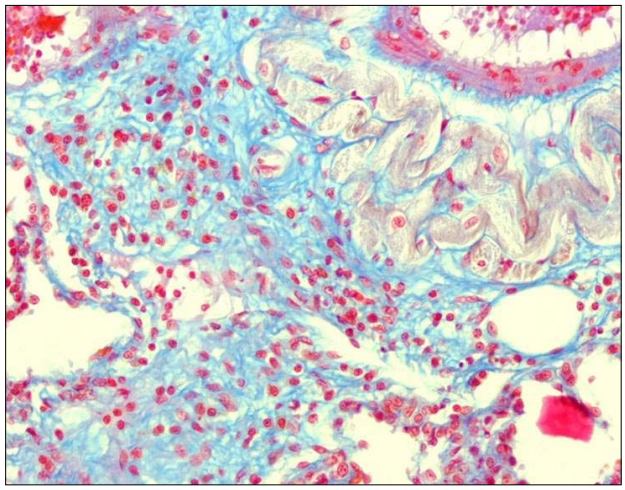

Figure 3. Lung specimens of rats with uremia after 2 and 4 weeks of the experiment. Lung fibrosis, obliterative bronchiolitis - connective tissue cells within the bronchial fibrosis, metaplasia of bronchial epithelium. H+E stain, mag. 250x.

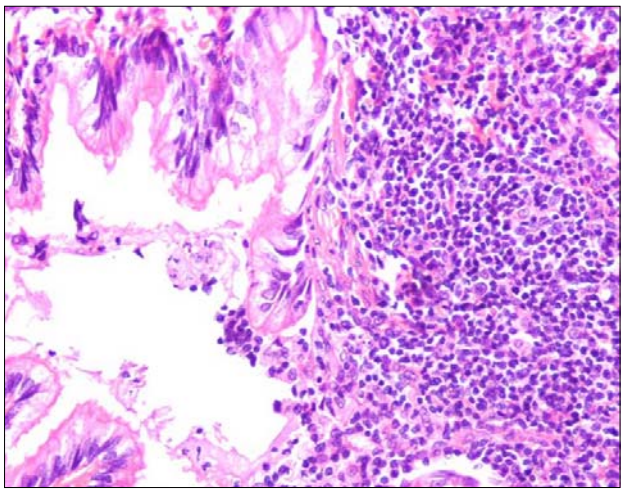

Figure 4. Degenerative changes of epithelial and endothelial cells. Micropinocytosis (representative of the group rats with uremia after 4 weeks of the experiment), mag. 7 000x.

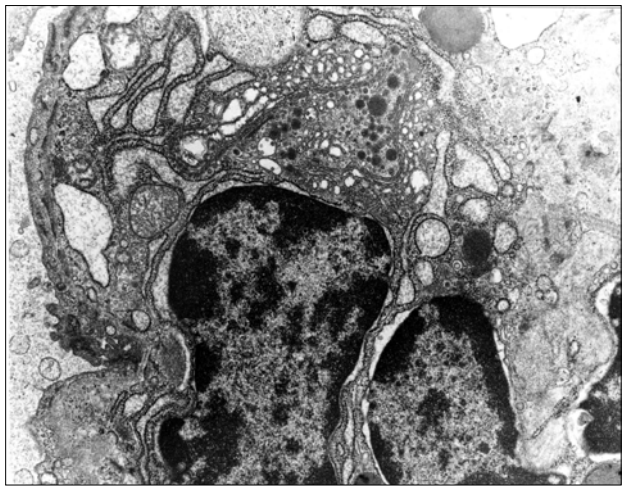

Table 1. Serum concentrations of creatinine and urea in control and uremic rats (mg/dl).

	control	1 week	2 weeks	4 weeks	* p-value
Creatinine	0.52 ± 0.052	0.63 ± 0.092	0.94 ± 0.058	0.72 ± 0.12	<0.05
Urea	35.33 ± 5.98	52.91 ± 16.39	95.10 ± 11.90	85.58 ± 9.766	<0.05

After 1, 2 and 4 weeks from the surgery, the rats were anaesthetised with pentobarbital and blood was collected from their hearts. Then, the animals were sacrificed by decapitation and the lung was fixed in Bouin's fluid for 24 h in temperature of +4^{0}C and embedded in paraffin in a routine way. For electron microscopy, the specimens were embedded in 2.5% purified glutaraldehyde. The specimens were cut in 5µm slices and stained by hematoxylin-eosin, by Azan's method and with silver, according to Grimelius.

Ultra thin sections, contrasted with uranyl acetate and lead citrate and were examined in an OPTON 900 PC electron microscope.

Blood serum urea and creatinine levels were determined.

Statistical analysis was performed by the Shapiro-Wilk's test. The analysis was performed, using the SAS ATAT software package. A probability level $p<0.05$ was considered significant.

Results

No significant differences were found between the control groups of rats and, therefore, only the results referring to the animals subjected to a sham operation are discussed.

Increased concentrations of urea and creatinine are one of the indicators of renal insufficiency.

Table 1. Serum concentrations of creatinine and urea in the control and the uremic rats (mg/dl).

A statistical increase of serum creatinine and urea concentrations was demonstrated in all the groups of animals with experimental renal insufficiency, when compared with respective values in the control groups (Table 1).

Morphological pictures of the lungs from the control animals were normal. In turn, in the group of uremic rats, changes, atelectatic in character, and erythrorrhagia were found in their lungs, evaluated after 1, 2 and 4 weeks from the surgery. Collapses of capillary lumen and obliterations of interalveolear septa were observed (Fig. 1). In the preparations from the 14th and the 28th day, the fluid, which normally occurs in the pulmonary alveoli, was also observed in lumen of the upper airways, where it accumulated on the epithelial surface. Also, young connective tissue cells occurred in the pictures, distorting the lung structures - the pictures corresponding to pulmonary fibrosis (Fig. 2). In that mass of fibrotic pulmonary tissue, various sections of the respiratory tract with obliterative bronchiolitis were found (Fig. 3).

Using an electron microscope, moderate atrophy of type II pneumocytes and sectional smoothing of microvilli on the free surface of those cells were seen. Necrotic changes of cells were also observed. In the endothelial, as well as in the epithelial cells of the respiratory tract, translucent sites were found in cytoplasm (Fig. 4).

Discussion

Effects of uremia on the respiratory tract are still little known. It has been found that, in the course of renal failure, changes of different character may occur in the lungs. Disturbed pulmonary function and weaker respiration control are among the uremic consequences in the respiratory tract [2, 3, 4].

In the performed studies, the morphological pictures of the lungs from the uremic rats corresponded to changes characteristic for massive atelactasis, chronic oedematous conditions and bronchiolitis, as well as to pulmonary fibrosis. In the course of renal failure, a progression of pulmonary changes was noted, regarding their degree and dynamics.

Pathomorphological changes, observed in uremia, may - via different mechanisms - lead to surfactant function disturbances or to injury of the alveolo-capillary barrier, reducing the carbon monoxide diffusion capacity, what may result in pulmonary oedema [4]. In the course of renal insufficiency, chronic pulmonary interstitial oedema is often observed [3, 7, 8]. In uremia, atrophy of both bronchial and alveolar epithelium (especially of type II pneumocytes) is found. This process may, however, be accompanied by regeneration attempts of the epithelium.

The advanced progression of pulmonary changes, as observed during experimental chronic uremia, indicates the existence and a continuous effect of factors, damaging the pulmonary tissue. So far, no particular factor has been found, which could be responsible for the pulmonary changes, observed in uremia.

Summing up, it can be stated that experimental CRF causes changes in the lungs, which are characteristic for the syndrome of uremic lung. The degree of progression of the pulmonary changes may be related to the time period of renal insufficiency.

References

1. Adachi Y, Sasagawa I, Tateno T, Tomaru T, Kubota Y, Nakada T. Testicular histology in experimental uremic rats. Arch Androl, 1998; 41: 51-55.

2. Levillain O, Marescau B, Possemiers I, Al Banchaabouchi M, De Deyn PP. Influence of 72% injury in one kidney on several organs involved in quanidino compound metabolism: a time course study. Pflügers Arch, 2001; 442: 558-69.

3. Słomian M, Mosiewicz J, Myśliński W. Lung function in chronic uremia. Ann Univ Mariae Curie Sklodowska, 2000; 55: 148-53.

4. Kalender B, Erk M, Pekpak M, Apaydin S, Ataman R, Serdengecti K, Sariyar M, Erek E. The effect of renal transplantation on pulmonary function. Nephron, 2002; 90: 72-77.

5. Azzadin A, Wollny T, Pawlak R, Małyszko J, Małyszko JS, Myśliwiec M, Buczko W. L-carnitine effects on anemia in uremic rats treated with erythropoetin. Nephron, 1999; 83: 370-71.

6. Ormord D, Miller T. Experimental uremia. Nephron, 1980; 26: 249-254.

7. Lee HY, Stretton TB, Barnes AM. The lung in renal failure. Thorax, 1975; 30: 46-53.

8. Bush A, Gabriel R. Pulmonary function in chronic renal failure: Effects of dialysis and transplantation. Thorax, 1991; 46: 424-28.

Intracellular expression of pro-inflammatory cytokines (IL-1α, TNF-α, and IL-6) in chronic hepatitis C

Kasprzak A[1], Seidel J[1], Spachacz R[1], Biczysko W[2], Małkowska A[1], Kaczmarek E[2], Zabel M[1,3]

[1]Department of Histology and Embryology, [2]Department of Clinical Pathomorphology, University of Medical Sciences, Poznań, Poland,
[3]Department of Histology, University of Medical Sciences, Wrocław, Poland

Abstract

The study aimed at localizing TNF-α, IL-1α, IL-6 at light and electron microscope levels in patients with chronic hepatitis C, using the immunocytochemical techniques in biopsy material from patients with chronic hepatitis C and at comparing the expression of the cytokines with histopathological changes. Our studies demonstrated an augmented expression of all cytokines in liver biopsies in chronic hepatitis C, in comparison with respective values, obtained in control biopsy material. The highest expression of the cytokines was observed in hepatocytes. That was confirmed by electron microscopy, which demonstrated the cytokines mainly in altered ER cisterns and in the cytoplasm. In children, the expression of IL-1α was negatively correlated with staging, while in adult patients; the staging was positively correlated with the expression of TNF-α. The new element involves demonstration of cellular and subcellular expression of TNF-α, IL-1α and IL-6 in hepatocytes in in vivo infection.

Key words: chronic hepatitis C; pro-inflammatory cytokines; immunocytochemistry.

Introduction

The role of pro-inflammatory cytokines has been documented in acute phase reactions in the liver, in normal proliferation of hepatocytes, in autoactivation of Kupffer cells and proliferation of Ito cells, in cirrhotic processes in the liver and in regeneration of the organ in chronic hepatitis C [1-3]. In chronic hepatitis C, augmented serum levels of TNF-α, IL-1 and IL-6 have been detected [4-6]. Controversies prevail as to the amounts of the cytokines, detected in tissues in chronic hepatitis C and as to the correlations between the expression of the cytokines on one hand, and grading and/or staging of intrahepatic viral load on the other [2, 4, 7, 8]. Cellular expression of pro-inflammatory cytokines in the liver has been observed mainly in Kupffer cells, activated stellate cells and in the endothelium of liver sinusoids [3, 6, 8]. Individual studies have shown that also hepatocytes are capable to produce cytokines in response to the infection with hepatitis C virus (HCV) [6, 7, 8].

The aim of the study was to investigate the intrahepatic localization of TNF-α, IL-1α and IL-6 in liver specimens from patients, chronically infected with HCV, to determine the cellular and subcellular localization of these cytokines. Attempts were also made to correlate the number of cells with cytokine expression with inflammation activity (grading) and the advancement of fibrosis (staging) and to compare cytokine expression in groups of children and adults with chronic hepatitis C.

Material and Methods

Thirty-one patients were studied (19 children, and 12 adults) with chronic hepatitis C confirmed serologically (anti-HCV and HCV RNA positive), in whom liver biopsies were performed before anti-viral therapy. The control group consisted of six liver biopsies of serologically HCV, HBV, HCMV, EBV and HIV negative patients with non-specific changes in the liver. Tissue specimens were fixed in 10% formalin and embedded in paraffin for purposes of light microscopy. For electron microscopy, the material was fixed in paraformaldehyde/glutaraldehyde, embedded in epon, and ultrathin sections became subject of ultraimmunocytochemistry. Histopathological lesions were evaluated, following the classical H+E staining, as well as

ADDRESS FOR CORRESPONDENCE:
Aldona Kasprzak
Chair and Department of Histology and Embryology
University School of Medicine in Wrocław
Chałubińskiego 6A; 51-650 Wrocław, Poland
tel. (+ 48 61) 869 91 81 w. 555; e-mail: akasprza@amp.edu.pl

Figure 1. Localization of IL-6 in hepatocyte from patient with chronic hepatitis C. Original magn.x400

Figure 2. Localization of IL-6 in hepatocyte from patient with chronic hepatitis C. Gold particles overlay mainly dilated endoplasmic reticulum (ER) and cytoplasm. Streptavidin-colloidal gold. TEM x30.000

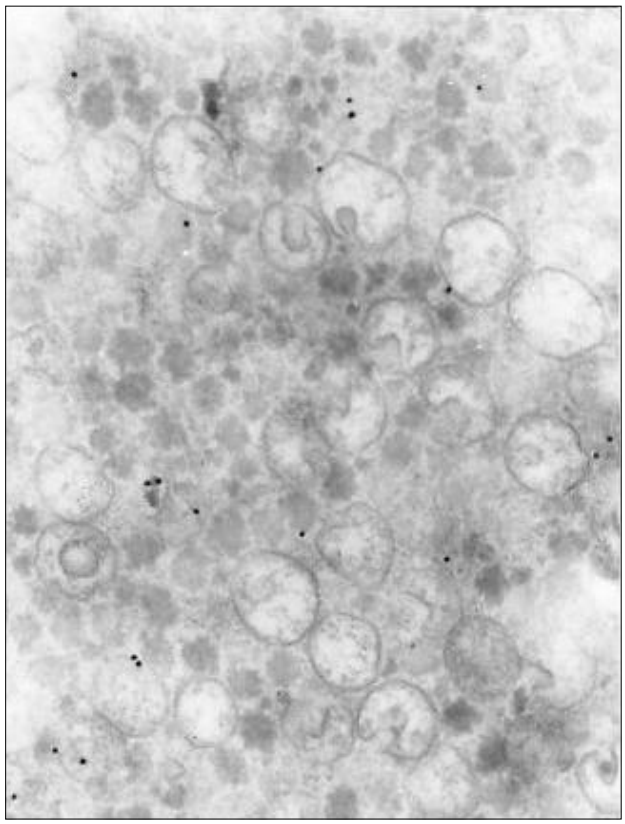

the tri-chromate technique, according to Masson, and periodic acid-Schiff with diastase pre-treatment. Each biopsy specimen was evaluated, using a simple numerical scoring system for the grade of portal/periportal necroinflammation (G1) (0-4), the grade of lobular necroinflammation (G2) (0-4), and for the stage of fibrosis (S) (0-4). Biopsies from chronic HCV patients were compared first between the two groups of patients (children and adults) and, then, in the entire group of patients (n=31), the expression of each cytokine was compared between lobules and portal spaces, as well as the total expression of a cytokine in the patients was compared with the total expression of the cytokine in control biopsies. The following specific MAbs were used: (a) mouse anti-human TNF-α antibody, (b) goat anti-human IL-1α antibody (c) mouse anti-IL-6 antibody (all from R&D Systems), (d) mouse anti-human macrophage antibody, CD68 (DAKO) and (e) anti-human Von Willebrand Factor antibody (DAKO EPOS A/S, Denmark). The studies followed the classical ABC technique alone or associated with the ImmunoMax amplification. Ultrathin sections were subjected to a labelling with 15 nm colloidal gold-coated streptavidin. The contents of three cytokines in liver biopsies, demonstrated by the ImmunoMax technique, were calculated by the semiquantitative technique, relating the score of 0 to 4 points to the fraction of stained cells (score 0 - 0% cells, 1 - less than 5% cells, 2 - 5-20% cells, 3 - 20-40% and 4 - more than 40% positive cells). The preparations were examined under a light microscope, at 400x magnification. In each section of the liver biopsy, five fields in hepatic lobules and periportal area and, at least, five different portal spaces in each specimen were examined. Statistical analysis took advantage of the Mann-Whitney U test for nonparametric independent data and the Wilcoxon test for nonparametric dependent data. Correlations between data rows were determined, employing Spearman's rank correlation index.

Results and Discussion

Both the grade of inflammation and the stage of fibrosis were significantly lower in children than those in adults (G1+G2, 1.8±0.2 vs. 3.7±0.4, respectively, $p<0.004$ and S, 1.1±0.2 vs. 2.5±0.3, respectively, $p<0.008$). Our studies demonstrated an augmented expression of all pro-inflammatory cytokines and of IL-1α and IL-6, particularly in the livers of chronic hepatitis C patients of either age group, as compared to their expressions in the control ($p<0.05$). This has corroborated our earlier observations and results of other investigators [6, 7, 8]. The augmented expression of the three cytokines was noted in hepatic lobules, as compared to portal spaces ($p<0.0001$). No difference was detected in the total expression of studied cytokines between the affected children and adult patients. In children, significantly higher numbers of cells with IL-6 expression were noted, as compared to cells with TNF-α ($p<0.05$) and IL-1α ($p<0.02$) expression. In adult patients cells with IL-1α expression and those with IL-6 expression were more numerous than those with TNF-α expression ($p<0.05$). In the lobules, expression of the studied cytokines pertained mainly the cytoplasm of hepatocytes (Fig. 1), which corroborated by ultrastructural studies. Apart from the cytoplasm, ultrastructural studies

documented presence of the cytokines also in altered cisterns of endoplasmic reticulum (Fig. 2). This confirmed the observations of other investigators related to IL-6 [6]. The novel element in the present results involved ultrastructural demonstration of the TNF-α and IL-1α and their demonstration, first of all, in hepatocytes. The other cells with the expression of cytokines included individual cells of liver sinusoids (macrophages and endothelial cells) and individual lymphocytes in inflammatory infiltrates. In the control material, a scanty expression of the cytokines was noted in individual hepatocytes and cells of liver sinusoids. In children, a negative correlation was disclosed between the expression of IL-1α protein and staging (Spearman's correlation coefficient of -0.557; $p<0.05$), in adults, a positive correlation was detected between the expression of TNF-α protein and staging (Spearman's correlation coefficient of 0.689; $p<0.05$). The results confirmed the literature data, related to the correlation between serum cytokine levels and histopathological evaluation of the biopsies [5, 6]. Our results have pertained the expression of TNF-a, IL-1a and IL-6 in HCV infection in vivo and may point to a direct involvement of the cytokines, both in the development of inflammation and fibrosis of the organ, as well as the ineffective anti-viral defence.

References

1. Cressman DE, Greenbaum LE, DeAngelis RA, Ciliberto G, Furth EE, Poli V, Taub R. Liver failure and defective hepatocytes regeneration in interleukin-6-deficient mice. Science, 1996; 274: 1379-83.

2. Kinnman N, Andersson U, Hultcrantz R. In situ expression of transforming growth factor-beta 1-3, latent transforming growth factor-beta binding protein and tumor necrosis factor-alpha in liver tissue from patients with chronic hepatitis C. Scand J Gastroenterol, 2000; 35:1294-1300.

3. Tsukamoto H. Cytokine regulation of hepatic stellate cells in liver fibrosis. Alcoholism: Clin Exp Res, 1999; 23: 911-6.

4. Larrea E, Garcia N, Qian C, Civeira MP, Prieto J. Tumor necrosis factor alpha gene expression and the response to interferon in chronic hepatitis C. Hepatology, 1996; 23: 210-7.

5. Malaguarnera M, Di Fazio I, Romeo MA, Restuccia S, Laurino A, Trovato BA. Elevation of interleukin 6 levels in patients with chronic hepatitis due to hepatitis C virus. J Gastroenterol, 1997; 32: 211-5.

6. Oyanagi Y, Takahashi T, Matsui S, Takahashi S, Boku S, Takahashi K, Furukawa K, Arai F, Asakura H. Enhanced expression of interleukin-6 in chronic hepatitis C. Liver, 1999; 19: 464-72.

7. Gonzalez-Amaro R, Garcia-Monzon G, Garcia-Buey L, Moreno-Otero R, Alonso JL, Yague E, Pivel JP, Lopez-Cabrera M, Fernandez-Ruiz E, Sanchez-Madrid F. Induction of tumor necrosis factor alpha production by human hepatocytes in chronic viral hepatitis. J Exp Med, 1994; 179: 841-8.

8. Kasprzak A, Zabel M, Biczysko W, Wysocki J, Adamek A, Spachacz R, Surdyk-Zasada J. Expression of cytokines (TNF-α, IL-1α, and IL-2) in chronic hepatitis C: comparative hybridocytochemical and immunocytochemical study in children and adult patients. J Histochem Cytochem, 2004; 52: 29-38.

Bone marrow megakaryocytes in human ontogenesis

Litwiejko-Pietryńczak E, Szkudlarek M, Klim B, Pietrewicz TM

Department of Human Anatomy, Medical University of Bialystok, Poland

Abstract

The aim of the study was a histomorphometric evaluation of bone marrow megakaryocytes (MK). The study was based on bone marrow histological evaluation. Morphometric evaluation was carried out with the aid of the MicroImage Olympus computer image analysis software. We evaluated the amount of megakaryocytes (MK) per 1 mm^2, MK area, the nuclear-cytoplasmatic (N/C) ratio and circular deviation (CD). Bone marrow was examined in premature newborns, full-term newborns and adults. The obtained data were statistically analysed with the aid of the Statistica PL computer software. Statistically significant differences were found in MK quantity, their distribution in relation to non-haematopoietic elements of haematopoietic microenvironment of sinusoid vessels system. To a smaller extent, did the differences refer to MK area, the N/C ratio or shape.

Key words: bone marrow, megakaryocytes, histomorphometric features, human ontogenesis.

Introduction

Human haematopoesis begins at about 2-6 week of intrauterine life in the wall of the yolk sac of the foetus. The blood islets belong to the, so-called, mesoblastic period of haematopoiesis. From the 6th to the 16th week of prenatal development, the main site of haematopoesis is the liver and, to a smaller extent, the spleen. Liver-spleen haematopoesis in physiological conditions does not occur in postnatal development [1, 2, 3]. Since the 20th week of prenatal life, the bone marrow starts its haematopoietic functions and remains the only site of haematopoesis in further developmental periods. Bone marrow can be found in marrow cavities of spongy bones, in the stroma, consisting of reticular tissue. It is full of sinusoid blood vessels of up to 30 μm in diameter. Till the 5th year of postnatal life, this red bone marrow presents main haematopoietic properties. In further stages of ontogenesis, there is more and more yellow bone marrow which, till the 18th year of life, replaces 50% of the red bone marrow. In adults, the red bone marrow is mostly located in sternum, ribs, and vertebrae, pelvic and cranial bones and in the epiphyses of humeral and femoral bones. The amount of the red bone marrow undergoes further reduction with age.

Proper haematopoietic activity, together with the efficient blood / bone marrow barrier, condition certain cell properties of individual developmental lines in peripheral blood and maintain the organism homeostasis. Developmental disorders in megakaryocytic line belong to the most common causes of the clotting system dysfunctions and may result in death. They are usually manifested by haemorrhagic diathesis or thrombosis, which often result from the syndrome of disseminated intravascular clotting (DIC). This syndrome occurs in various stages of human ontogenetic development and is characterised by high mortality. The disorders, observed in the course of DIC, may result, among others, from immaturity of the megakaryocytic bone marrow system [4, 5].

The aim of the study was a histomorphometric evaluation of bone marrow megakaryocytes (MK) in selected stages of human ontogenesis.

Material and Methods

The study was based on bone marrow histological evaluations. Biopsy examination was performed within 12 hours after

ADDRESS FOR CORRESPONDENCE:
Elżbieta Litwiejko-Pietryńczak
Department of Human Anatomy
Medical University of Bialystok
Mickiewicza 2A, 15-230 Bialystok
Tel. +48 85 748 56 61, fax +48 85 748 56 64,
e-mail: anatomia@amb.edu.pl

Table 1. Histomorphometric features (mean± standard deviation) of age groups

Age Groups	N	Number of MK		Area of MK		N/C		CD	
		X	SD	x	SD	x	SD	x	SD
NN	6	20.0	3.6	287.7	40.6	0.29	0.04	0.78	0.06
ND	6	23.2	4.0	298.8	25.1	0.26	0.02	0.79	0.04
< 10	6	21.2	5.9	224.7	65.1	0.33	0.13	0.73	0.04
11-20	6	18.7	5.1	255.2	51.0	0.39	0.23	0.80	0.08
21-40	6	17.2	3.9	216.3	64.1	0.37	0.16	0.82	0.06
41-60	6	17.2	3.1	197.5	42.5	0.32	0.12	0.82	0.07
> 60	6	16.7	3.3	180.0	52.2	0.40	0.13	0.84	0.03

N/C-nuclear-cytoplasmatic ratio
CD-circular deviation

death. Bone marrow was collected from sternum at II intercostal space. The material was fixed in the 'Oxford' fixing agent for 48 hours. After fixing, it underwent standard histological processing. Morphometric evaluation was carried out with the aid of the MicroImage Olympus computer image analysis software. We evaluated the amount of megakaryocytes (MK) per 1 mm^2, MK area, nuclear-cytoplasmatic (N/C) ratio, cellular shape, disorder-circular deviation (CD). Bone marrow was examined in premature newborns, (N=6), full-term newborns (N=6) and adults (N=30), divided into age groups (1mth - 10 yrs, 11-20, 21-40, 41-60, and over 60 yrs).

Results

It was found that the highest number of megakaryocytes per 1 mm^2 occurred in full-term newborns and amounted to the mean value of 23,2 (±4.0), while the lowest number was found in the group of adults over 60 and amounted to the mean value of 16.7 (±3.3). Similar relations were observed, regarding the MK area. In the group of full-term newborns, the value was the highest and amounted to the mean value of 298.8 mm2 (±25.1) and, in the oldest age group, it was the lowest and amounted to the mean value of 180.0 mm^2 (±52.2). The nuclear-cytoplasmatic (N/C) ratio was the lowest in the group of full-term newborns and the highest in the group over 60. CD coefficient was the lowest in the groups of newborns and children up to the 10^{th} year of life and then, it gradually grew in the consecutive groups. Detailed data are presented in Table 1. The obtained data were statistically analysed with the aid of the Statistica Pl computer software. The mean values of the examined parameters were compared in individual groups. Statistically significant differences were found in MK quantity in the compared groups. It was observed that in preterm newborns the percentage of MK, occurring in the direct vicinity of sinusoid vessels, was the highest and amounted to 6-10%, the mean value- 8.4%, in full-term newborns - 4-7%, the mean value - 5.5% and, in the other groups - 3-5%, the mean value- 4.5%. The differences were less significant, regarding the MK area, N/C relation or CD.

Discussion

The obtained results indicate considerable morphological differentiation of the bone marrow MK system in the examined groups. The to-date's studies and developmental standards refer mainly to the percentage composition of individual bone marrow developmental lines [6, 7, 8]. The aim of the study, beside the morphometric evaluation of MC, was also an analysis of the topographic localisation of megakaryocytes. It was observed that, in neonatal period, MK were located closer to sinusoid vessels and were composed into bunches, their surface being more irregular. In the course of development, the examined cells were dispersed in the marrow stroma. A presence of cell nuclei of other developmental lines, mostly leukocytes, was observed in megakaryocytes cytoplasm. With progression of age this phenomenon (so-called, emperipolesis) in the marrow of adults and elderly people was scarce. It is difficult to make a clear-cut definition of the above phenomenon, but it may result from the functional immaturity of MK, which may clinically result in worse quality platelets and clotting system disorders, as mentioned above. Further studies of the observed topographic changes in bone marrow are essential.

Acknowledgements

Authors want to thank Ms. Irena Mańkowska, M.Sc. for the statistical analysis and Ms. Elżbieta Urban, M.Sc. and Ms. Joanna Jaworska M.Sc. for technical assistance.

References

1. Traver D, Miyamato T, Christensen J, Iwasaki-Arai J, Akashi K, Weissman I L. Fetal liver myelopoiesis occurs through distinct, prospectively isolatable progenitor subsets. Blood, 2001; 98: 627-35.

2. Kashiwakura I, Kuwabara M. Radiation sensitivity of

megakaryocyte colony-forming cells in human placental and umbilical cord blood. Radiat Res, 2000; 153: 144-52.

3. Ryu K H, Chun S, Carbonierre S, Im S-A. Apoptosis and megakaryocytic differentiation during ex vivo expansion of human cord blood CD 34 cells using thrombopoietin. Br J Haematol, 2001;113: 470-8.

4. Watts T L, Murray NA, Roberts IAG. Thrombopoietin has a primary role in the regulation of platelet production in preterm babies. Pediatr Res, 1999; 46: 28-32.

5. Murray NA, Watts TL, Roberts IAG. Endodenous thrombopoietin levels and effect of recombinant human thrombopoietin on megakaryocyte precursors in term and preterm babies. Pediatr Res, 1998; 43: 148-51.

6. Murray NA, Roberts IA. Circulating megakaryocytes and their progenitors in early thrombocytopenia in preterm neonates. Pediatr Res, 1966; 40: 112-29.

7. Nishihira H, Toyoda Y, Miyazaki H, Kigasawa H, Ohsaki E. Growth of macroscopic human megakaryocyte colonies from cord blood in culture with recombinant human thrombopoietin (c-mpl ligand) and the effects of gestational age on frequency of colonies. Br J Haematol, 1996; 92: 23-8.

8. De-Alarcon PA, Graeve JL. Analysis of megakaryocyte ploidy in fetal bone marrow biopsies using a new adaptation of the feulgen technique to measure DNA content and estimate megakaryocyte ploidy from biopsy specimens. Pediatr Res, 1996; 39: 166-70.

mRNA for chosen pro- and anti-inflammatory cytokines in T-lymphocytes in paediatric leukemias and lymphomas - a preliminary report

Łuczyński W[1], Kovalchuk O[2], Krawczuk-Rybak M[1], Malinowska I[3], Mitura-Lesiuk M[4], Matysiak M[3], Kowalczyk J[4], Chyczewski L[2]

[1]Department of Paediatric Oncology, [2]Department of Clinical Molecular Biology, Medical University of Białystok;
[3]Department of Paediatrics, Haematology and Oncology, Medical University of Warsaw,
[4]Department of Paediatric Haematology and Oncology, Medical University of Lublin

Abstract

We assessed mRNA for chosen pro- and anti-inflammatory cytokines in T-lymphocytes of peripheral blood in paediatric patients with leukemias and lymphomas. Levels of four different cytokine mRNAs (IFN-γ, IL-10, IL-4, TGF-β) were determined by the real-time PCR technique. In the whole examined group, at the time of diagnosis, we noted lower amounts of mRNA for TGF-β_1, comparing to respective values in the control patients. In the ALL group, we observed the following: 1) at the time of diagnosis: lower amounts of mRNA for IL-4 and for TGF-β_1, comparing to respective values in the control group; 2) lower amounts of mRNA for IL-10 after remission induction, comparing to the time of diagnosis. In our opinion, "immunedysregulation" in lymphoproliferative diseases in children is not caused by IFN-γ deficiency. The deficit of anti-inflammatory cytokines, i.e., IL-4, TGF-β, with higher amounts of IL-10, suggests their role in cancer development.

Key words: leukaemia, lymphoma, children, mRNA, cytokines, T-lymphocytes

Introduction

Haematological malignancies represent a unique group of proliferative diseases, in which neoplastic cells arise from the immune system and thus, they exert a potential immunomodulatory effect. Leukaemic blasts, like normal lymphocytes, are produced in bone marrow and these two types of cells may interact. It is likely that neoplastic cells produce substances, which impair the immune response, thus promoting cancer expansion. The main role in antitumour immunity is played by T-lymphocytes. According to produced cytokines, T-cells can be differentiated into Th_1/Tc_1 subsets (producing IL-2 and IFN-γ), Th_2/Tc_2 (IL-4, IL-5, IL-10) and Th_3/Tr_1 (TGF-β, IL-10). Most of the authors report a Th2 polarization profile in haematological malignancies and normalization of the Th_1/Th_2 balance in remission [1]. A type 1-to-type 2 cytokine shift may be responsible for reduced antitumor immunity and is correlated with disease progression. We previously found Th_2 (the percentage of $CD4^+IL\text{-}4^+$ cells - flow cytometry) predominance at the time of diagnosis of acute lymphoblastic leukaemia (ALL) [2]. In the present, study we assessed mRNA for chosen pro- and anti-inflammatory cytokines at the time of diagnosis of most common lymphoproliferative diseases in children.

ADDRESS FOR CORRESPONDENCE:
Włodzimierz Łuczyński
Department of Paediatric Oncology
Medical University of Białystok
Waszyngtona 17, 15-274 Białystok, Poland
e-mail: vlodek@amb.edu.pl

Material and methods

Twenty (20) patients with ALL (n=13), Hodgkin lymphoma (n=4) and non-Hodgkin lymphoma (n=3) were prospectively enrolled into this study. Peripheral blood (1 ml) was taken at the time of diagnosis and in ALL - after prednisone prophase (day 8^{th}), during (day 15^{th}) and after remission induction (day 33^{rd}). The control group included 30 children from the Department of Paediatric Surgery, subjected to minor surgical operations.

$CD4^+$ and $CD8^+$ cells were isolated from whole peripheral blood by immunomagnetic bead separation (Dynabeads, Dynal Biotech, Oslo, Norway). mRNA was isolated from sorted lymphocyte subpopulations, using Dynabeads mRNA DIRECT Micro Kit (DYNAL) according to the producer's instructions. First strand cDNA was synthesized, using random hexamers as primer and a High Capacity cDNA Archive Kit by AppliedBiosystems. Levels of four different cytokines mRNAs (IFN-γ, IL-10, IL-4, TGF-β) were determined by the real-time PCR technique with the TaqMan chemistry, using ready-to-use

Figure 1. Amplification plot (log view) of TGF-b mRNA

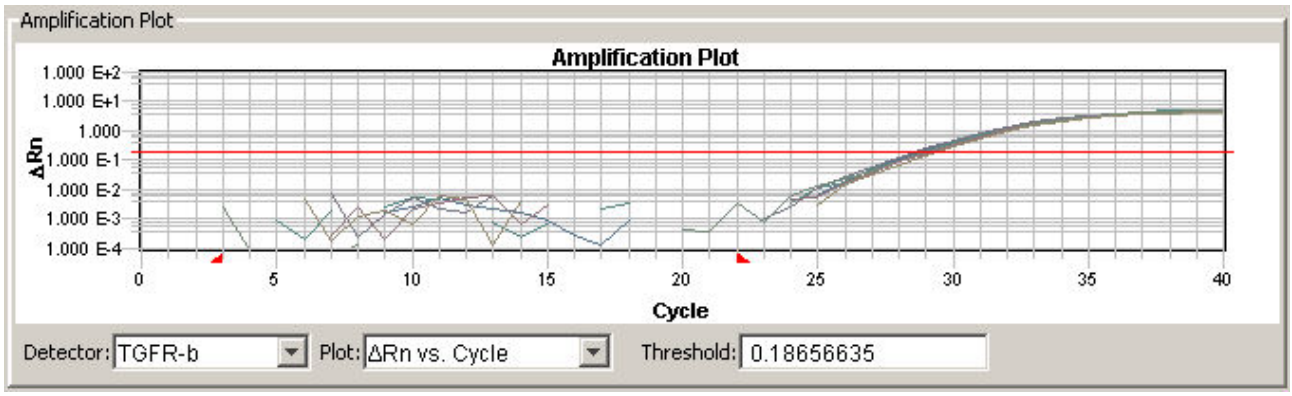

Assays-on-Demand Gene Expression Products by AppliedBiosystems, which contain target-specific primers and probe, and a TaqMan Universal Master Mix, containing AmpErase uracil-N-glycosylase (UNG) to prevent re-amplification of carryover PCR products. PCR amplification and fluorescence data collection were performed with the ABI PRISM 7900HT Sequence Detection System (AppliedBiosystems). In order to normalize the amount of expressed cytokine mRNAs, the internal housekeeping gene GAPDH was used and each complementary DNA (cDNA) product was tested in triplex for each of the four cytokines mRNA and GAPDH mRNA. For the calculation of our data we used the Comparative Ct method for relative quantification (ΔΔCt method), which describes the change in expression of the target gene in a test sample relative to a calibrator sample and provides an accurate comparison between the initial levels of template in each sample. We used Total Raji RNA by AppliedBiosystems, as a calibrator sample, which was processed in the same way as the test samples. The obtained data were analysed with the Sequence Detector System (SDS) software, version 2.1 (AppliedBiosystems).

Results

In the examined groups and in the control group, we found the following: a) in $CD4^+$ cells: positive correlations between mRNA for IFN-γ and: IL-4 ($r=0.83$, $p<0.0001$), TGF-β_1 (0.91, $p<0.0001$); and between IL-4 and TGF-β_1 ($r=0.86$,$p<0.0001$); b) in $CD8^+$ cells: a negative correlation between mRNA for IFN-γ and IL-10 ($r=-0.44$, $p=0.0007$); a positive correlation between IFN-γ and IL-4 ($r=0.43$, $p=0.01$), IFN-γ and TGF-β_1 ($r=0.81$, $p<0.0001$); also a positive correlation between IL-4 and TGF-β_1 ($r=0.7$, $p<0.0001$). In the whole examined group, at the time of diagnosis, we noted lower amounts of mRNA for TGF-β_1 in $CD4^+$ cells (the difference not statistically significant) and in $CD8^+$ cells ($p=0.01$) comparing to the control patients; the amounts of other cytokines (IFN-γ, IL-4, IL-10) did not differ between those in the whole examined group and those in the control patients. In the ALL group, we observed: a) at the time of diagnosis: lower amounts of mRNA for IL-4 (both in $CD4^+$ and $CD8^+$ cells, $p=0.02$ and $p=0.04$) and for TGF-β_1 (also in both subpopulations $p=0.03$ and $p=0.01$), comparing to respective values in the control group; b) lower amounts of mRNA for IL-10 after remission induction, comparing to the time of diagnosis ($p=0.05$). An example of amplification plot for TGF-β is presented on Figure 1.

Discussion

The only report, concerning Th_1/Th_2 balance in children with ALL, was performed by Zhang et al. [3]. The authors found lower Th_1/Th_2 and Tc_1/Tc_2 ratios at the time of diagnosis and recovery after achieving complete remission. Regarding IFN-γ, we did not find any difference between the examined group and the control. This confirms our previous results, obtained with flow cytometry, and the results obtained by Kiani et al. in CML patients [2, 4]. Podhorecka et al. found a higher Th_1 percentage in patients with B-cell chronic lymphocytic leukaemia (B-CLL) than in controls and the Th_2/Tc_2 shift during disease progression [5]. The amounts of mRNA for IL-4 were lower in ALL patients at the time of diagnosis. Similar results, concerning IL-4, were obtained by Kiełbiński et al. in acute leukaemias in adults [6]. In contrast to our results, Kamińska et al. observed, comparable with the control levels of IL-4 in supernatants from the whole blood cell cultures of adult patients with ALL [7]. Mori et al. reported polarization to Th_2 in untreated B-cell diffuse large cell lymphoma patients and to Th_1 in complete remission [1]. We noted a tendency (not significant) to higher amounts of mRNA for IL-10 at the time of diagnosis of leukemias and lymphomas. IL-10 production in patients with cancer was higher than that in healthy controls, so it is possible that tumour cells secrete cytokines, shifting T-cells to produce more IL-10 [8]. Kebelmann-Betzing et al. suggest that the secretion of IL-10 (from leukaemic blasts) and the lack of down-regulation of adhesion and costimulatory molecules determine the mechanism of escape from immune surveillance in relapsed ALL [9]. In the whole examined group and, especially in ALL patients, we observed lower amounts of mRNA for TGF-β, comparing to the values in the control patients. Tatsumi et al. found Th_2, but not Th_3, type response against renal cell carcinoma or melanoma [10]. In our opinion "immunedysregulation" in lymphoproliferative diseases in children is not caused by IFN-γ deficiency. The deficit of anti-inflammatory cytokines, i.e., IL-4, TGF-β and the higher amounts of IL-10, revealed in that group of children, suggests their role in cancer development, but it should be confirmed in a greater cohort of patients. The very strong correlations, observed among all the assessed substances, suggest their

interdependence in cytokine network in the human organism. Determination of the factors, that affect Th and Tc profiles, may lead to a better understanding of the immunological status and development of immunotherapy.

The study supported by The State Committee for Scientific Research (project number P05E08025)

References

1. Mori T, Takada R, Watanabe R, Okamoto S, Ikeda Y. T-helper (Th_1)/Th_2 imbalance in patients with previously untreated B-cell diffuse large cell lymphoma. Cancer Immunol Immunother, 2001; 50: 566-8.

2. Łuczyński W, Stasiak-Barmuta A, Krawczuk-Rybak M, Malinowska I, Matysiak M, Mitura-Lesiuk M, Kowalczyk J, Jeromin A. Równowaga limfocytów Th_1/Th_2 w ostrej białaczce limfoblastycznej u dzieci. Przeg Lek, 2004; in press.

3. Zhang X-L, Komada Y, Chipeta J, Li Q-S, Inaba H, Azuma E, Yamamoto H, Sakurai M. Intracellular cytokine profile of T cells from children with acute lymphoblastic leukemia. Cancer Immunol Immunother, 2000; 49: 165-72.

4. Kiani A, Habermann I, Schake K, Neubauer A, Rogge L, Ehninger G. Normal intrinsic Th_1/Th_2 balance in patients with chronic phase chronic myeloid leukemia not treated with interferon-alpha or imatinib. Haematologica, 2003; 88: 754-61.

5. Podhorecka M, Dmoszyńska A, Roliński J, Wasik E. T type 1/type 2 subsets balance in B-cell chronic lymphocytic leukemia - the three-color flow cytometry analysis. Leuk Res, 2002; 26: 657-60.

6. Kiełbiński M, Podolak-Dawidziak M, Prajs I, Haus O, Jaźwiec B, Kuliczkowski K. Limfocyty Th_1 i Th_2 w nadzorze odporności w ostrych białaczkach. Acta Hematol Pol, 2003; 34: 360.

7. Kamińska T, Hus I, Dmoszyńska A, Kandefer-Szerszeń M. Cytokine production in whole blood cell cultures of patients with B-lineage acute lymphoblastic leukemia. The influence of granulocyte-macrophage colony-stimulating factor. Arch Imm Ther Exp, 2001; 49:71-7.

8. Kallio R, Surcel H-M, Syrjala H. Peripheral mononuclear cell IL-10 and IL-12 production is not impaired in patients with advanced cancer and severe infection. Cytokine, 2002; 20: 210-4.

9. Kebelmann-Betzing C, Korner G, Badiali L, Buchwald D, Moricke A, Korte A, Kochling J. Characterization of cytokine, growth factor receptor, costimulatory and adhesion molecule expression patterns of bone marrow blasts in relapsed childhood B cell precursor ALL. Cytokine, 2001; 13: 39-50.

10. Tatsumi T, Kierstaed LS, Ranieri E, Gesualdo L, Schena FP, Finke JH, Bukowski RM, Mueller-Brghaus J, Kirkwood JM, Kwok WW. Disease-associated bias in T helper type 1 (Th_1)/Th_2 $CD4^+$ T cell responses against MAGE-6 in HLA-DRB1*0401^+ patients with renal cell carcinoma or melanoma. J Exp Med, 2002; 195: 619-29.

Cytotoxic lymphocytes (CD8$^+$) in the antrum mucosa in children with chronic Helicobacter pylori - related inflammation before and after bacteria eradication

Maciorkowska E[1], Kasacka I[2], Kondej-Muszyńska K[3], Kaczmarski M[3], Kemona A[4]

[1]Department of Paediatric Nursing, [2]Department of Histology and Embryology,
[3]The 3rd Department of Children's Diseases, [4]Department of General Pathomorphology
Medical University of Białystok, Poland

Abstract

The authors assessed the expression of cytotoxic CD8$^+$ lymphocytes in the antrum mucosa of children with chronic Helicobacter pylori - related inflammation, before and after bacteria eradication. Biopsy specimens of gastric mucosa were evaluated in specimens, collected from 59 H. pylori-positive patients (Group I), 29 patients after H. pylori infection (Group II) and 18 H. pylori-negative children (Group III). The obtained specimens were assessed for infection and inflammation and the expression of CD8$^+$ lymphocytes was estimated, using monoclonal antibodies. The number of CD8$^+$ lymphocytes in the mucosa was counted.

The results of the study showed an increase in the expression of CD8$^+$ lymphocytes in children with H. pylori infection, in comparison to the values in children after bacteria eradication. The increased expression of CD8$^+$ lymphocytes correlated with the severity degree of antrum gastritis.

Key words: Helicobacter pylori, antrum mucosa, cytotoxic lymphocytes (CD8$^+$).

Introduction

CD8$^+$ phenotype cells compose most intraepithelial (IEL) lymphocytes of the digestive system, scattered among the epithelial cells. They are usually localized below the nuclei and their specific migration to the surface of the intestinal lumen may depend on the reaction of $\alpha E\beta 7$ integrin (CD103) with E cadherin of the epithelial cells. Approximately 15% of IEL have TCR γ/δ receptors, very rarely present in the peripheral blood cells [1]. Some IEL present with features, characteristic for the natural cytotoxic cells but the role of these lymphocytes has not been explained completely, so far. It has been suggested that they may function as suppressors, preventing from a systemic immune response to food antigens. Moreover, they eliminate some pathogenic microorganisms and stimulate intestinal epithelium regeneration. CD8$^+$ lymphocytes of Th1 profile, producing IFNγ, were described in the course of H. pylori infection [2, 3].

The aim of the study was to assess the expression of CD8$^+$ lymphocytes in the antrum mucosa in children with chronic inflammation of H. pylori aetiology, before and after bacteria eradication.

Material and methods

Gastric mucosal biopsy specimens from the following three groups of individuals were studied by light microscopy: (I) 59 children (29 girls and 30 boys; the age range, 2-19 years) with chronic active inflammation of the gastric mucosa with H. pylori infection with positive IgG antibody anti- H. pylori; (II) 29 children (14 girls and 15 boys; the age range, 3-19 years) after H. pylori infection without either timely colonization or active inflammation of the gastric mucosa with maintaining positive IgG antibody anti- H. pylori. (III) 18 children (12 girls and 6 boys; the age range, 5-17 years) with gastrointestinal disease, without H. pylori infection, with correct level IgG antibody anti- H. pylori. In all the examined children, endoscopic examinations and histopathological studies of the stomach were performed. The sample sections were diagnosed, according to the Sydney System [4]. Urease test was performed in the course of endoscopy in all the children. Specimens were fixed in 10% buffered formalin. They were processed, oriented on edge, embedded in paraffin, cut in sequential 5-μm sections,

ADDRESS FOR CORRESPONDENCE:
Elżbieta Maciorkowska
Department of Paediatric Nursing
Medical University of Białystok
Kilińskiego 1; 15-089 Białystok, Poland

Photo 1. Antrum gastric mucosa. Immunohistochemical reaction with CD8⁺. Mag. 200x.

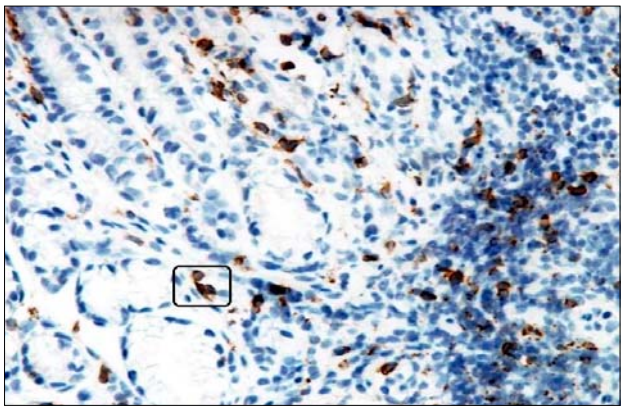

Figure 1. Correlation between the level of CD8+ lymhocytes and the severity of antral gastritis in the children with Helicobacter pylori infection (group I)

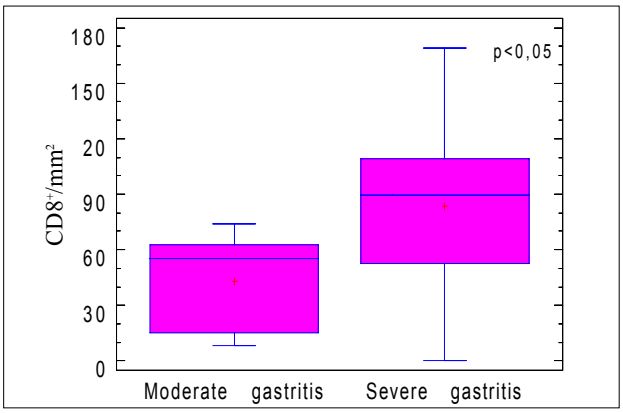

Table 1. CD8⁺ lymphocytes in antrum mucosa of children.

Experimental groups	CD8⁺ lymphocytes in the antrum mucosa /mm²								
	Number of patients (N)	Result (min)	Result (max)	Arithmetic mean (x)	Median value (ME)	Moda	Standard deviation (SD)	Low quartile	High quartile
Group I	23	0	169	64.1	57	57	42.2	40.0	90.0
Group II	17	3	66	26.9	20	-	21.4	9.0	41.0
Group III	9	0	98	35.8	27	-	32.7	16.0	42.0

and stained by H+E for the evaluation of inflammation and Giemsa method was used to identify H. pylori bacteria (according to Gray) [5]. All the biopsy specimens from each of the study groups were stained by the immunohistochemical method for the evaluation of CD8⁺ lymphocytes in the mucosa. The ABC method was used, according to commercial protocol. The number of CD8⁺ lymphocytes in the mucosa was counted in discrete areas, measuring 0.785 mm², each by using a light microscope. All the counts were performed, using a magnification of 200x. The numbers of positively stained cells were presented as mean values per 1 mm² of the analysed gastric section area. All the CD8⁺ lymphocyte counts were performed by a single observer (I. K.), who was unaware of either the H. pylori status or the subject's clinical group.

An analysis of the preparations and their photographic documentation were performed with an Olympus Bx50 light microscope, with video circuit and a Pentium 120 PC computer with Lucia G (Nikon) software for microscope image analysis.

CD8⁺ lymphocyte density was compared between the groups of studied subjects, using Student's 't' test. Statistical calculations included the arithmetic mean, standard deviation (SD), the median value (ME), the minimal result (min) and the maximal result (max). The levels of studied parameters were compared by means of Ch^2 test, either for independent or paired tests. All the differences were regarded significant at $p<0.05$. The obtained results have graphically been presented. Both the clinical examinations and all laboratory tests were performed in the children, following previous unrestrained consents of either their parents or legal protectors and after an approval of the Ethical Commission at the Medical University of Białystok.

Results

According to Sydney's Classification, severe gastric mucosa inflammation was diagnosed in only 45.8% of the children in Group I, moderate - in 52.5% of the children with H. pylori infection and in 6.9% of the children after H. pylori infection eradication, mild - in 1.7% of the children in Group I, in 13.8% of the patients in Group II and in 15.4% of the children in the control group. Normal gastric mucosa of the antrum was found in 79.3% of the children from Group II and in 84.6% of the children in the control group.

A quantitative assessment of CD8⁺ lymphocytes in the antrum mucosa (the mean number of cells per 1 mm² of specimen area), performed by immunohistochemical staining, revealed an increase in their expression in children with H. pylori infection (64.1 cells/mm²), in comparison with the results in children after eradication (26.9 cells/mm²) and those in the controls (35.8 cells/mm²) Table 1. and Photo 1.

Statistically significant differences were proved between the expressions of $CD8^+$ in the antrum mucosa in relation to the severity degrees of antrum gastritis ($p<0.05$) Fig. 1.

The expression of $CD8^+$ lymphocytes increases with intensification of the inflammatory process. In the H. pylori infected children with moderate antrum gastritis, the mean level of $CD8^+$ lymphocytes was 42.91cells/mm^2. In the case of severe antrum gastritis, the mean level was 83.58 cells/mm^2. In the H. pylori infected children with moderate degree gastritis, the mean level of $CD8^+$ lymphocytes was 38.25 cells/mm^2. In the case of severe degree inflammation, the mean expression of those lymphocytes was 69.58 cell/mm^2.

Discussion

The expression of $CD8^+$ lymphocytes in the antrum mucosa of children with gastritis in the course of H. pylori infection was the highest and differed significantly, in comparison with the expression in the group with past infection ($p<0.001$). It was proved that the expression of infiltrating $CD8^+$ cells increased with the severity of antrum gastritis.

Bamford et al. [3] reported an increase in both $CD4^+$ and $CD8^+$ expressions and an increased production of IFN-γ and IL-12. They showed that Th_1 type response was predominant in T lymphocytes. Similarly, Sommer et al. [6] found $CD4^+$ cells of the Th_1 phenotype infiltrating the antrum and corpus mucosa in the course of H. pylori, which, according to the authors, may determine the incapability of the immune system of H. pylori eradication. Stromberg et al. [7] presented similar results, showing an increase in the levels of $CD8^+$ lymphocytes in the antrum mucosa in the course of H. pylori.

Terres et al. [8] demonstrated an increase in the expression of $CD8^+$ lymphocytes in the lamina propria in gastritis in the course of H. pylori infection. The expression of intraepithelial $CD8^+$ lymphocytes correlated with the severity of the inflammation, but it was independent of the degree of H. pylori colonization.

Summing up, it should be noted that an increased expression of $CD8^+$ cells in an inflammatory infiltrate in the antrum mucosa correlates with the severity of gastritis in children with H. pylori infection, in comparison respective values, observed in children after the bacteria eradication.

References

1. Graham DY. Pathogenic mechanisms leading to Helicobacter pylori-induced inflammation. Eur J Gastroenterol Hepatol, 1992; 4: 9-16.

2. Lindholm C, Quiding-Jarbrink M, Lonroth H, Hamlet A, Svennerholm AM. Local cytokine response in Helicobacter pylori infected subjects. Infect Immun, 1998; 66: 5964-71.

3. Bamford KB, Fan X, Crowe SE, Leary JF, Gourley WK, Luthra GK, Brooks EG, Graham DY, Reyes VE, Ernst PB. Lymphocytes in the human gastric mucosa during Helicobacter pylori have a T helper cell 1 phenotype. Gastroenterology, 1998; 114: 482-92.

4. Misiewicz JJ. The Sydney System: a new classification of gastritis. Introduction. J Gatroenterol Hepatol, 1991; 6: 207-8.

5. Gray SF, Wyatt JI, Rathbone BJ. Simplified techniques for identifying. Campylobacter pyloridis. J Clin Pathol, 1986; 39: 1279.

6. Sommer F, Faller G, Konturek P, Kirchner T, Hahn EG, Zeus J, Rollinnghoff M, Lohaff M. Antrum-and corpus mucosa- infiltrating CD4(+) lymphocytes in Helicobacter pylori gastritis display a Th1 phenotype. Infect Immun, 1998; 66: 5543-46.

7. Stromberg E, Lundgren A, Edebo A, Lundin S, Svennerholm AM, Lindholm C. Increased frequency of activated T-cells in the Helicobacter pylori-infected antrum and duodenum. FEMS Immunol Med Microbiol, 2003; 36: 159-68.

8. Terres A M, Pajares JM. An increased number of follicles containing activated CD69+ helper T cells and proliferating CD71+ B cells are found in H. pylori-infected gastric mucosa. Am J Gastroenterol, 1998; 93: 579-83.

Helicobacter pylori infection and mast cells of the antrum mucosa

Maciorkowska E[1], Kasacka I[2], Kondej-Muszyńska K[3], Kaczmarski M[3], Kemona A[4]

[1]Department of Paediatric Nursing, [2]Department of Histology and Embryology, [3]3rd Clinic of Children's Teaching Hospital, [4]Department of General Pathomorphology, Medical University of Białystok

Abstract

The studies aimed at evaluating mast cells in inflammatory infiltration of gastric mucosa in children with H. pylori infection, as well as in those after the infection eradication.

Biopsy specimens of gastric mucosa were evaluated, the specimens collected from 59 H. pylori-positive patients (Group I), 29 patients after H. pylori infection (Group II) and 18 H. pylori-negative children (Group III). The specimens were assessed for infection and inflammation and stained with anti-human mast cell tryptase to count mucosal mast cells. The evaluations of histopathological changes in the antrum mucosa of the children were performed, according to Sydney's Classification. In morphometric evaluation, slight differences were found in the numbers of mast cells among Groups: I, II and III of the examined children (the number of mastocytes being: 86.4, 81.4 and 70.2 cells/mm^2 of specimen, respectively).

Key words: Helicobacter pylori, antrum mucosa, mast cell.

Introduction

Helicobacter pylori (H. pylori) infection elicits conspicuous infiltration with neutrophils, eosinophils, lymphocytes and plasma cells. The pathogenesis of the basic lesion, i.e., chronic active inflammation of the gastric mucosa, remains incompletely understood. Following the results of to-date's studies, it has been proven that cytokines, produced by mast cells, affect all the effector cells of inflammation, as well as the majority of reactions, which occur at the site of action of an inflammation inducing stimulus [1, 2]. H. pylori or H. pylori extracts (potentiate histamine release from serosal rat mast cells in vitro and can induce mast cell degranulation around rat mesenteric venules) lead to mast cell degranulation and to a release of active chemical compounds in in vitro conditions [3]. Using a monoclonal antibody for human mast cell tryptase for mucosal mast cell identification in formalin-fixed human tissue, a study was designed, attempting to determine whether mast cells participate in inflammatory responses of the gastric mucosa, in order to evaluate their possible role in the inflammatory infiltrations of H. pylori-infected children, as well as in children after H. pylori infection eradication.

ADDRESS FOR CORRESPONDENCE:
Irena Kasacka
Department of Histology & Embryology
Medical University of Białystok
Kilińskiego 1; 15-089 Białystok, Poland
Tel. (48 85) 748 54 58; e-mail: kasacka@amb.edu.pl

Material and methods

Gastric mucosal biopsy specimens from the following three groups of individuals were studied by light microscopy: (I) 59 children (29 girls and 30 boys; the age range: 2-19 years) with chronic active inflammation of the gastric mucosa with H. pylori infection with positive IgG antibody anti- H. pylori; (II) 29 children (14 girls and 15 boys; the age range: 3-19 years) after H. pylori infection without timely colonization and without active inflammation of the gastric mucosa with maintaining positive IgG antibody anti- H. pylori. (III) 18 children (12 girls and 6 boys; the age range: 5-17 years) with gastrointestinal disease, without H. pylori infection, with correct levels of IgG antibody anti- H. pylori. In all the examined children, endoscopic examinations and histopathological studies of the stomach were performed, classifing the obtained results in accordance to Sydney's Classification [4].

The urease test was performed in the course of endoscopy in all the children.

The specimens were fixed in 10% buffered formalin. They were processed, oriented on edge, embedded in paraffin, cut in sequential 5-µm sections, and stained by haematoxylin and eosin (H+E) for the evaluation of inflammation and by the Giemsa method. All the biop-

Table 1. Mast cells in the antrum mucosa of the examined children.

Experimental Groups	Mast cells in the antrum mucosa /mm²								
	Number of patients (N)	Result (min)	Result (max)	Arithmetic mean (x)	Median value (ME)	Mode	Standard deviation (SD)	Low quartile	High quartile
Group I	25	0	187	86,4	99,0	0	46,5	53,0	107,0
Group II	15	52	113	81,4	78,0	52	21,1	65,0	101,0
Group III	6	32	101	70,2	82,5	-	30,0	44,8	88,8

Figure 1. The degree of inflammation of the antrum mucosa in the examined children

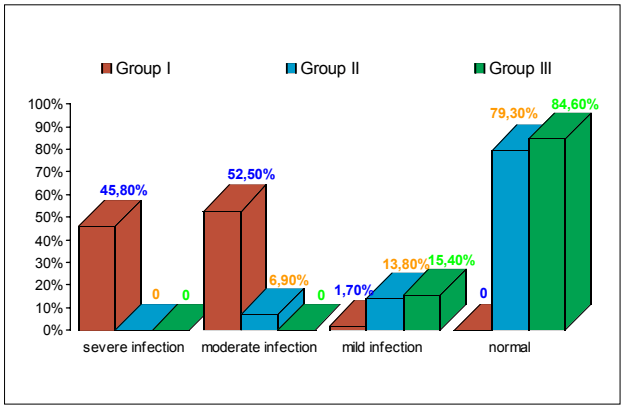

Photo 1. Antrum mucosa. Immunohistochemical reaction with mast cells (tryptase-positive). Magnification 400x.

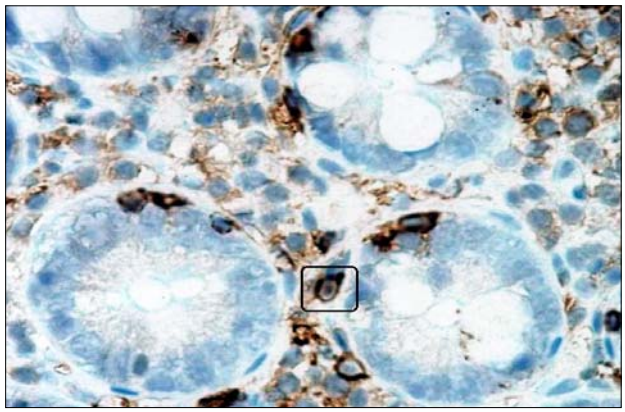

sy specimens from each of study group were stained by an immunohistochemical method for the evaluation of mast cells in the mucosa. The ABC method was used, according to commercial protocol. The number of mast cells in the mucosa was counted in discrete areas, measuring 0.785 mm² each, by using a light microscope. All the counts were performed, using a magnification of 200x.

The numbers of positively stained cells were presented as the mean values per 1 mm² of analysed gastric section area. All the mast cell counts were performed by a single observer (I. K.), who was unaware either of the H. pylori status or of the subject's clinical group.

The analysis of the preparations and their photographic documentation were performed with an Olympus Bx50 light microscope, with a video circuit and a Pentium 120 PC computer with the Lucia G (Nikon) software for microscope image analysis.

Mast cell density was compared between the groups of studied subjects, using the Student's't' test. Statistical calculations included the arithmetic mean, standard deviation (SD), the median value (ME), the minimal result (min) and the maximal result (max). The levels of the studied parameters were compared by means of Student's t test, either for independent or paired tests. All the differences were regarded significant at $p<0.05$. The obtained results have graphically been presented. Both the clinical examinations and all the laboratory tests were performed in the children, following previous unrestrained consents of their parents or legal protectors and an approval of the Ethical Commission at the Medical University of Białystok.

Results

According to Sydney's Classification, severe gastric mucosa inflammation was diagnosed in only 45.8% of the children in Group I, moderate - in 52.5% of the children with H. pylori infection and in 6.9% of the children after H. pylori infection eradication, mild - in 1.7% of the children in Group I, in 13.8% of the patients in Group II and in 15.4% of the children in the control group. Normal gastric mucosa of the antrum was found in 79.3% of the children from Group II and in 84.6% of the children in the control group (Fig. 1).

A quantitative assessment of mast cells in the antrum mucosa (the mean number of cells per 1 mm² of specimen area), performed by immunohistochemical staining, revealed comparable numbers of mast cells in the group of H. pylori-affected children (86.4 ± 46.5 cells/mm²), in the group after H. pylori infection eradication (81.4 ± 21.1 cells/mm²) and in the control group (70.2 ± 30 cells/mm²) (Table 1, Photo 1).

Discussion

Mast cells are an important element in the cellular infiltration in the course of gastric mucosa inflammation with H. pylori infection [2, 5]. In result of secreted mediators, mast cells actively participate in the induction and enhancement of the inflammatory process by their influence on: vascular dilation and an increased

blood flow capacity, migration of inflammatory cells and inflammatory infiltration development [3, 6].

There is but little data in the available literature, concerning the number of mast cells in chronic inflammation of the gastric mucosa of H. pylori aetiology in children. In own studies of children with gastric mucosa inflammation in the course of H. pylori infection, the number of mastocytes in the antrum mucosa was not statistically significantly higher from the number of cells in the group of children with gastric mucosa inflammation, in whom the bacteria had been eradicated. The number of mast cells did not change with inflammatory process enhancement in the antrum mucosa. Similar results were obtained by Sulik, who had employed the same diagnostic approach [3]. In studies, concerning adult population, Nakajiama et al. [6] demonstrated an increased number of mast cells in gastric mucosa inflammation with H. pylori infection. The obtained results correlated with the degree of inflammation, while the number of mast cells decreased after treatment. In contrast to the population of children, the absolute numbers of mast cells were higher in adults, what may be explained by their number, increasing with the body growth and the achievement of target values in the adult age. Similar observations were also made by Whitneyet et al. [7]. Kurose [8] was the first, who demonstrated that H. pylori extracts could induce mast cells to degranulation. That was found already after 10 minutes from the mesentery exposition to an aqueous extract of H. pylori. Activated mast cells release also pro-inflammatory factors, which may increase vascular flow capacity. Attention should be drawn to the increased numbers of mast cells, found in gastric biopsy specimens from not only H. pylori-infected children but also from those infected by Giardia Lamblia intestinalis but without any clinical or biochemical features of alimentary allergy [5].

The results of the studies suggest that mast cells play an important role in disturbing the functioning of the gastric mucosa in infected children but without allergy features.

References

1. Crabtree JE. Immune and inflammatory responses to Helicobacter pylori infection. Scand J Gastroenterology, 1996; 31: 3-10.

2. Supajatura V, Ushio H, Wada A, Yahiro K, Okumura K, Ogawa H, Hirayama T, Ra C. Cutting edge: VacA, a vacuolating cytotoxin of Helicobacter pylori, directly activates mast cells for migration and production of proinflammatory cytokines. J Immunol, 2002; 168: 2603-7.

3. Sulik A, Kemona A, Sulik M, Ołdak E. Mast cells in chronic gastritis of children. Pol Merk Lek, 2001; 57: 156-60.

4. Crabtree JE. Immune and inflammatory responses to Helicobacter pylori infection. Scand J Gastroenterology, 1996; 31: 3-10.

5. Dixon MF, Genta RM, Yardley JH, Correa P. Classification and grading of gastritis. The updated Sydney System. International Workshop on the Histopathology of Gastritis. Am J Surg Pathol, 1996; 20: 1161-81.

6. Maciorkowska E. Zmiany morfologiczne błony śluzowej żołądka i dwunastnicy a stężenie wybranych cytokin u dzieci z nadwrażliwością pokarmową, infekcją Helicobacter pylori i giardiazą. Rozprawa habilitacyjna. Wydawnictwo Uczelniane Akademii Medycznej w Białymstoku 2000.

7. Nakajima S, Krishnan B, Ota H, Segura AM, Hattori T, Graham DY, Genta RM. Mast cell involvement in gastritis with or without Helicobacter pylori infection. Gastroenterology, 1997; 113: 746-54.

8. Whitney AE, Guarner J, Hutwagner L, Gold BD. Helicobacter pylori gastritis in children and adults: comparative histopathologic study. Ann Diagn Pathol, 2000; 4: 279-85.

9. Kurose I, Granger DN, Evans DJ Jr, Evans DG, Graham DY, Miyasaka M, Anderson DC, Wolf RE, Cepinskas G, Kvietys PR. Helicobacter pylori- induced microvascular protein leakage in rats: role of neutrophils, mast cells and platelets. Gastroenterology, 1994; 107: 70-9.

B (CD20$^+$) lymphocytes in the antrum mucosa of children with Helicobacter pylori infection

Maciorkowska E[1], Kasacka I[2], Kondej-Muszyńska K[3], Kaczmarski M[3], Kemona A[4]

[1]Department of Paediatric Nursing, [2]Department of Histology and Embryology,
[3]III Department of Children's Diseases, [4]Department of General Pathomorphology,
Medical University of Białystok, Poland

Abstract

The aim of the study was to estimate the expression of CD20$^+$ lymphocytes in the antrum mucosa in children, infected with Helicobacter pylori and after bacteria eradication.

Biopsy specimens of gastric mucosa were the specimens, collected from 59 H. pylori-positive patients (Group I), 29 patients after H. pylori infection (Group II) and 18 H. pylori-negative children (Group III). The collected specimens were assessed for infection and inflammation and the expression of CD20$^+$ lymphocytes was estimated, using mice monoclonal antibodies. The expression of CD20+lymphocytes in the inflammatory infiltrate of the antrum mucosa correlated with the severity of gastritis, found in children with Helicobacter pylori infection and was the highest in comparison with the group of children after H. pylori eradication.

Key words: B lymphocytes, gastric mucosa, Helicobacter pylori, children.

Introduction

A chronic inflammatory response is characterized by damage to the epithelium and the infiltrate of mononuclear cells, including T and B-lymphocytes, plasmatic cells, macrophages or eosinophils [1]. The lymphocytes, accumulated in the pyloric mucosa, form lymphatic follicles in a significant percentage of children infected with H. pylori (50-100%). Lymphoidal texture in the gastric mucosa, found mainly in patients at the developmental age, is responsible for the granulation in the gastric mucosa, described in the endoscopic examination [2, 3].

ADDRESS FOR CORRESPONDENCE:
Elżbieta Maciorkowska
Department of Pediatric Nursing
Medical University of Białystok
Kilińskiego 1; 15-089 Białystok, Poland

The aim of the study was to evaluate the expression of CD20$^+$ lymphocytes in the antrum mucosa of children, infected with H. pylori and after its eradication, and to find a correlation between the expression of CD20$^+$ and the inflammation of the gastric mucosa. Material and methods Gastric mucosal biopsy specimens, collected from the following three groups of individuals, were studied by light microscopy: (I) 59 children (29 girls and 30 boys; the age range: 2-19) with chronic active inflammation of the gastric mucosa with H. pylori infection with positive IgG antibody anti- H. pylori; (II) 29 children (14 girls and 15 boys; the age range: 3-19) after H. pylori infection without timely colonization and without active inflammation of the gastric mucosa with maintained positive IgG antibody anti- H. pylori. (III) 18 children (12 girls and 6 boys; the age range: 5-17) with gastrointestinal disease, without H. pylori infection, with correct level IgG antibody anti- H. pylori. In all the examined children, endoscopic examinations and histopathological studies of the stomach were performed. Obtained sample sections were diagnosed, according to the Sydney System [4]. Urease test was performed in the course of endoscopy in all the children. The specimens were fixed in 10% buffered formalin. They were processed, oriented on edge, embedded in paraffin, cut in sequential 5-µm sections, and stained by H+E for the evaluation of inflammation and by Giemsa to identify H. pylori bacteria (according to Gary's) [5]. All the biopsy specimens from each of the study groups were stained by an immunohistochemical method for the evaluation of CD20$^+$ lymphocytes in the mucosa. ABC method was used, according to commercial protocol. The number of CD20$^+$ lymphocytes in the mucosa was counted in discrete areas, measuring 0.785 mm^2, each by using a light microscope. All the counts were performed at magnification of 200x. The numbers of positively stained cells were presented as the mean values per 1 mm^2 of the analysed gastric section area. All the CD20$^+$ lymphocyte counts were performed by a single observer (I. K.), who was unaware of either the Helicobacter pylori status or of the subject's clinical group.

The analysis of the preparations and their photographic documentation were performed with an Olympus Bx50 light micro-

Table 1. CD20⁺ lymphocytes in the antrum mucosa in children.

Experimental Groups	CD20⁺ lymphocytes in the antrum mucosa /mm²								
	Number of patients (N)	Result (min)	Result (max)	Arthmetic mean (x)	Median volue (ME)	Moda	Standard deviation (SD)	Low quartile	High quartile
Group I	23	2	194	109,9	96	72	51,4	76	146
Group II	14	0	79	20,6	13	0	25,8	2	25
Group III	5	0	43	17,4	18	-	17,6	2	24

Figure 1. Correlation between the expression of CD20⁺ lymphocytes and the activity degree of antrum mucosa inflammation in children with Helicobacter pylori infection (Group I)

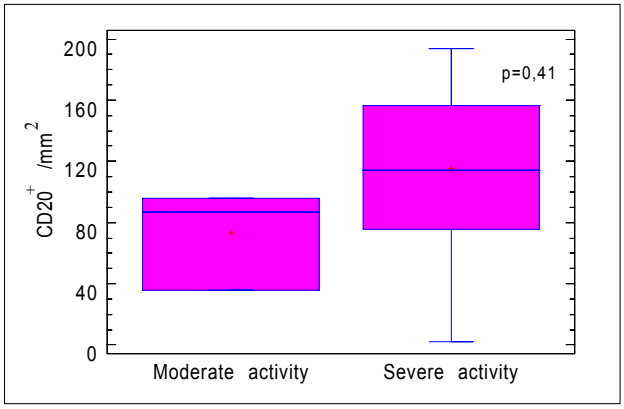

Photo 1. Antrum mucosa. Immunohistochemical reaction with CD20⁺. Magnification 200x.

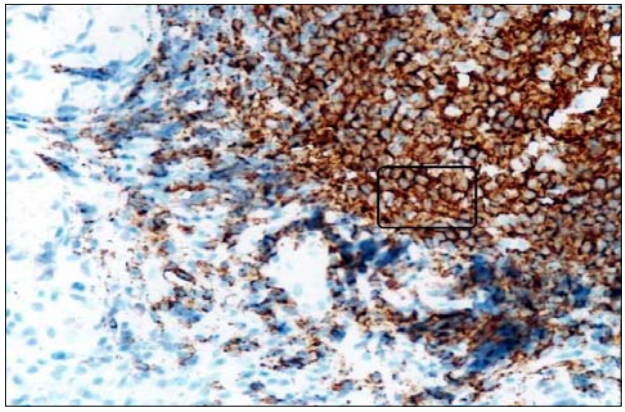

scope, with a video circuit and a Pentium 120 PC computer with Lucia G (Nikon) software for microscope image analysis. CD20⁺ lymphocytes density was compared between the groups of studied subjects, using Student's "t" test and Chi². Statistical calculations included the arithmetic mean, standard deviation (SD), the median value (ME), the minimal result (min) and the maximal result (max).

Both clinical examinations and all the laboratory tests were performed in the children, following previous unrestrained consents of either their parents or of legal protectors and an approval of the Ethical Commission at the Medical University of Białystok.

Results

When evaluating antrum gastritis, according to the Sydney System in Group I with H. pylori infection, severe inflammation was reported in 45.8% of the examined children; moderate inflammation in 52% and mild inflammation in 1.7% of the patients. In Group II after H. pylori eradication, moderate inflammation was observed in 6.9% of the examined children; mild inflammation in 13.8% and 79.3% of children had normal gastric mucosa. In controls, mild inflammation was reported in 15.4% of children and 79.3% had normal gastric mucosa.

The performed histopathological assessment of the antrum gastric mucosa showed that 28.8% of the children with active H. pylori infection had lymphatic follicles. In children after H. pylori eradication, lymphatic follicles were present in 20.7% of them.

A quantitative assessment of CD20⁺ lymphocytes in the antrum mucosa (the mean number of cells per 1 mm² of specimen area), performed by immunohistochemical staining, revealed a significant increase in their expression in children with H. pylori infection (109.9 cells/mm²), in comparison with children after eradication (20.6 cells/mm²) and in the controls (17.4 cells/mm²) Table 1 and Photo 1.

The expression of CD20⁺ increased with the severity of inflammation in the gastric antrum. The expression of CD20⁺ lymphocytes in moderate inflammation of the antrum mucosa equalled 86.7 cells/mm² in the children with H. pylori infection. In case of severe inflammation of the antrum mucosa, the expression of CD20⁺ lymphocytes was 127.77 cells/mm² (Fig. 1).

Discussion

The quantitative analysis of CD20⁺ lymphocytes in the antrum mucosa showed their five -fold higher expression in children with ongoing H. pylori infection than in those after past infection, which may prove a significant role of the humoral response in the elimination of H. pylori infection in the examined group. The expression of CD20⁺ lymphocytes correlated with the severity of inflammatory process in the antrum.

Elitsur et al. [6] compared the composition of immunocompetent cells in the lymphatic nodules in children and in the MALT type lymphoma in adults, using the immunohistochemical techniques. T lymphocytes were observed only in the lymphatic follicles of children. No such lymphocytes were found in the MALT - type lymphoma in adults. Apart from $CD20^+$ markers, no significant differences were observed between B lymphocytes in the lymphatic follicles of children and B - cell lymphomas of the MALT - type in adults. Krenska - Wiącek et al. [7] evaluated B-lymphocytes with $CD19^+$ marker in blood serum from children with Helicobacter pylori - related gastritis. The authors found a higher percentage of B $CD19^+$ lymphocytes in children with infection than in healthy children and a significant decrease in the percentage of these lymphocytes after eradication.

Our study proved a higher expression of $CD20^+$ lymphocytes in the inflammatory infiltrate of the antrum mucosa and a correlation between their expression and the severity of the inflammation in children with H. pylori infection, in comparison with children after bacteria eradication. This confirms a role of B-lymphocytes in the complex pathogenic mechanisms of inflamed gastric mucosa in children H. pylori infected.

Conclusion

The expression of $CD20^+$ lymphocytes, assessed in the antrum mucosa of children with H. pylori infection, increased with the severity of inflammatory process and differed statistically significantly with regards to the inflammation grade.

References

1. Mattsson A, Quiding-Jarbrink M, Lonroth H, Hamlet A, Ahlstedt I, Svennerholm A. Antibody-secreting cells in the stomachs of symptomatic and asymptomatic Helicobacter pylori infected subjects. Infect Immun, 1998; 66: 2705-12.

2. Aceti A, Celestino D, Caferro M, Casale V, Citarda F, Conti EM, Grassi A, Grilli A, Pennica A, Sciarretta F. Basophil-bound and serum immunoglobulin E directed against Helicobacter pylori in patients with chronic gastritis. Gastroenterol, 1991; 101: 131-7.

3. Bąk-Romaniszyn L, Pokoca L, Zeman K, Płaneta-Małecka I. Interleukin 1-b and 8 concentration in the gastric juice and the serum of children with Helicobacter pylori infection. Pediatria Współcz, 2000; 2: 273-7.

4. Price AB. The Sydney System: histological division. J Gastroenterol Hepatol, 1991; 6: 209-22.

5. Gray SF, Wyatt JI, Rathbone BJ. Simplified techniques for identifying. Campylobacter pyloridis. J Clin Pathol, 1986; 39: 1279.

6. Elitsur Y, Jackman S, Keerthy S, Lawrence Z, Maynard VL, Triest WE. T and B cell repertoire in gastric lymph follicles in children with Helicobacter pylori infection. Pediatr Pathol Mol Med, 2002; 21: 31-9.

7. Krenska-Wiącek A, Szaflarska-Szczepanik A, Wysocki M. Cytofluometric evaluation of the percentages of lymphocyte - subpopulation in the peripheral blood of children with chronic gastritis and duodenal inflammation with and without Helicobacter pylori infection. Pol Merk Lek, 2002; 13: 107-10.

Memory cells in the antral mucosa of children with Helicobacter pylori infection

Maciorkowska E[1], Kondej-Muszyńska K[2], Kasacka I[3], Kaczmarski M[2], Kemona A[4]

[1]Department of Paediatric Nursing, [2]3rd Department of Children's Diseases, [3]Department of Histology and Embryology, [4]Department of Pathomorphology, Medical University of Białystok, Poland

Abstract

A total of 106 patients, included in the study, were divided into three groups with regard to Helicobacter pylori infection. Endoscopy and histopathological examination of the stomach, based on the Sydney's System, were performed in all the children. CD45RA and CD45RO cells were identified by means of specific antibodies in the inflammatory infiltrate of the antral mucosa. An increased expression of CD45RO and CD45RA lymphocytes was reported, basing on the results of the study.

Key words: antral mucosa, memory cells, Helicobacter pylori, children.

Introduction

T lymphocytes are activated in response to H. pylori infection. Large amounts of cells with markers: $CD4^+$, CD45RO and $CD69^+$, are usually found in the antral mucosa [2]. The response from $CD4^+$ lymphocytes predominates, whereas $CD8^+$ lymphocytes are not so numerous and an increase in the relation $CD4^+/CD8^+$ takes place [1, 3]. $CD4^+$ lymphocytes, inducing an immune response in combination with the molecules of major histocompatibility complex (MHC) of class II, recognize specific peptides coming from extracellular phagocytized antigens. These cells express an isoform of CD45RO antigen (described as "virgin" or "naive") and CD45RO (described as "memory" and associated with the state of activation). Approximately 85% of $CD4^+$ lymphocytes have CD45RO molecule [3]. CD45RO are more helpful in the production of immunoglobulins by B lymphocytes than the "naive" cells. They produce IL-4, IL-5, IL-10, IFN-gamma. Basing on L-selectin expression on their surface, CD45RO cells are divided into two groups: the group expressing L-selectin and producing mainly IL-4 and IL-5 and the group without expressing L-selectin and producing mainly IFN-gamma. Such a profile of cytokines coincides with the profile of Th1and Th2 lymphocytes [4].

ADDRESS FOR CORRESPONDENCE:
Elżbieta Maciorkowska
Department of Pediatric Nursing
Medical University of Białystok
Kilińskiego 1; 15-089 Białystok, Poland

Material and methods

Group I - 59 children (29 girls and 30 boys; the age range: 2-19 years) with chronic gastritis in the course of H. pylori infection with positive IgG antibody anti- H. pylori. Group II - 29 children (14 girls and 15 boys; the age range: 3-19 years) after past H. pylori infection, without bacterium colonization and gastritis, but with a maintained positive titre of antibodies in IgG class against H. pylori. Group III - 18 children (12 girls and 6 boys; the age range: 5-17 years) with functional disorders of the gastrointestinal tract, without H. pylori infection, with normal IgG concentration against H. pylori (the control group). The samples from the antrum pyloric section were diagnosed, according to the Sydney's System.

All the biopsy specimens from each study group were stained by an immunohistochemical method for the evaluation of CD45RA and CD45RO lymphocytes in the antrum mucosa, performed, using mice monoclonal antibodies against human T lymphocytes (CD45RA and CD45RO) of the DAKO firm. The ABC method was used, according to commercial protocol. The number of CD45RA and CD45RO lymphocytes in the mucosa was counted in discrete areas, measuring 0.785 mm^2 each, by using a light microscope. All the counts were performed, using a magnification of 200x. The numbers of positively stained cells were presented as the mean values per 1 mm^2 of analysed gastric section area. All

Table 1. CD45RA lymphocytes in the antrum mucosa in children

Examined groups	CD45RA lymphocytes in the antrum mucosa /mm								
	Number of patients (N)	Minimum (min)	Maximum. (max)	Arithmetic mean. (x)	Median (M)	Mode	Standard Deviation (SD)	Lower Quartile	Upper Quartile
Group I	17	0	197	46.8	26	3	59.2	4	40.0
Group II	7	0	22	8.0	7	-	7.2	4	10.0
Group III	3	0	5	1.7	0	0	2.9	0	2.5

Table 2. CD45RO lymphocytes in the antrum mucosa in children

Examined groups	CD45RO lymphocytes in the antrum mucosa/mm^2								
	Number of patients (N)	Minimum (min)	Maximum (max)	Arithmetic mean. (x)	Median (M)	Mode	Standard Deviation (SD)	Lower Quartile	Upper Quartile
Group I	20	0	817	262.1	236	0	230.9	132	284
Group II	15	0	270	142.3	147	117	89.5	90	210
Group III	6	67	278	153.5	130	-	85.7	90	212

Figure 1. Correlation between the expression of CD45RA lymphocytes and the severity grade of antral gastritis in children with Helicobacter pylori infection (Group I)

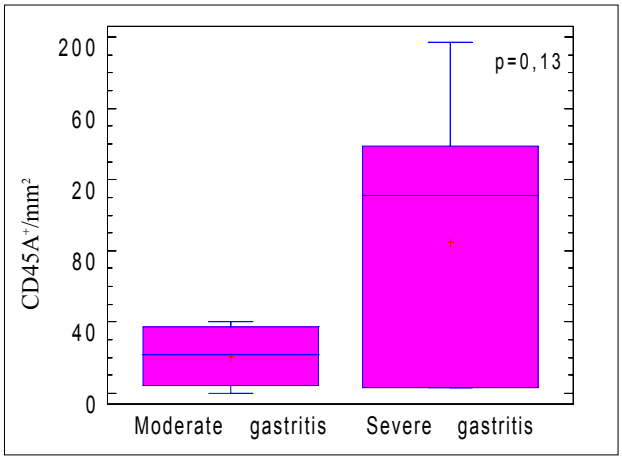

Figure 2. Correlation between the expression of CD45RO lymhocytes and the severity grade of gastritis in children with Helicobacter pylori infection (Group I)

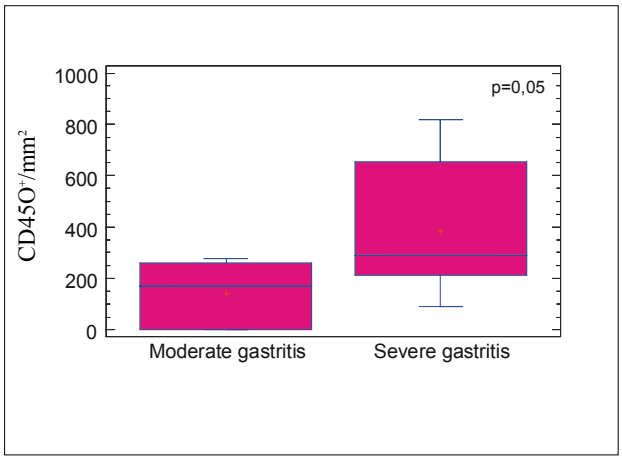

the lymphocyte counts were performed by a single observer (I. K.), who was unaware of either the H. pylori status or the subject's clinical group. Descriptive statistics included the arithmetic mean (x), the median (Me), standard deviation (SD), and the minimum (min) and maximum (max) result. The level of the parameters was compared by means of the U Mann-Whitney test for either independent or paired trials. The differences were regarded statistically significant at $p<0.05$. The correlation between the features, measured in the nominal scale, was evaluated by means of an independence test Chi^2 and the results were presented as frequency tables. All the clinical and laboratory tests were performed in the children after a prior consent from their parents and guardians, and of the approval by the Bioethical Board of the Medical University of Białystok.

Results

The quantitative assessment of CD45RA in the antral mucosa by means of an immunohistochemical method showed an increase in their expression in the children with H. pylori infection (46.8 cells/mm^2), in comparison with the children after H. pylori infection (8.0 cells/mm^2) and the controls (1.7 cells/mm^2). Table 1. However, the expression of CD45RA lymphocytes was higher in more severe inflammation. The expression of CD45RA lymphocytes in moderate antral gastritis equalled on the average 20.2 cells/mm^2 in the children with H. pylori infection. In severe antral gastritis, the mean expression of CD45RA lymphocytes was 84.71 cells/mm^2. In mild grade activity gastritis, the mean expression of CD45RA was 11.67 cells/mm^2 in children with Helicobacter pylori (Fig.1).

Moderate activity antral gastritis was characterized by the mean expression of 54.29 cells/mm^2. The quantitative analysis of CD45RO "memory" lymphocytes in the antral mucosa by immunohistochemical method showed a significant increase in the expression of those lymphocytes in children with Helicobacter pylori infection (262.1 cells/mm^2). In children after H. pylori infection, with positive antibodies against H. pylori (142.3 cells/mm^2), the expression of CD45RO lymphocytes was comparable with their expression in the controls (153.5 cells/mm^2) Table 2. When assessing the expression of CD45RO lymphocytes in the antral mucosa in Group I in relation to the severity grade of antral gastritis, the reported differences were on the border of statistical significance (p=0.05). However, the expression of CD45RO lymphocytes was higher in more severe inflammation. In children with H. pylori infection, the mean expression of CD45RO was 139.3 cells/mm^2 in moderate gastritis. Severe gastritis was characterized by the mean expression of CD45RO lymphocytes, which equalled 384.9 cells/mm^2. In case of moderate gastritis, the mean expression of CD45RO lymphocytes was 142.67 cells/mm^2 in Group I (Fig. 2).

Discussion

The quantitative assessment of CD45RA cells in the antral mucosa, using monoclonal antibodies, proved their highest expression in children with H. pylori and a significantly lower expression in children after bacteria eradication, and the lowest one in the controls. The expression of CD45RA correlated positively with the severity and activity grade of antral gastritis in children with H. pylori and was higher in the severe grade inflammation. However, no statistically significant differences were found between the groups. When assessing CD45RO cells in the antral mucosa, their highest expression was established in children with H. pylori infection and approximately, twice lower expression in children after bacteria eradication. The expression of CD45RO was higher in more severe antral gastritis of children with H. pylori infection, and there were statistically significant differences with regard to the severity grade of gastritis ($p<0.05$). The increased expression of CD8$^+$, CD45RA and CD45RO lymphocytes in the antral mucosa may suggest that Th1 and Th2 lymphocytes took part in response to H. pylori infection in the examined children. Hatz et al. [4] obtained results, which were similar to ours, showing an increased expression of CD4$^+$ and CD8$^+$ lymphocytes with predominance of CD4$^+$ in both the lamina propria and the intraepithelium, and an increased relation of CD4$^+$/CD8$^+$. Additionally, they found a doubled expression of CD45RO cells and an activation of TCR α/β^+ receptor on the lymphocytes in the lamina propria of the gastric mucosa. The changes in the expression of cells correlated positively with the severity grade of the inflammatory process. Kikuchi et al. [5] demonstrated an increased secretion of RANTES, a major basic protein (MBP) and an increased expression of CD45RO lymphocytes in an inflammatory infiltrate in the gastric mucosa, in comparison with the respective values in patients after eradication and in healthy people. However, the secretion of RANTES was enhanced up to 2 years after eradication, as well as chronic infiltration with CD45RO cells and eosinophils [5]. Lungren et al. [6], explaining a suppressed immune response to H. pylori infection, showed a suppressed response of T CD4$^+$ memory lymphocytes.

Conclusions

1. An increased expression of memory lymphocytes (CD45RO) was found in the antral mucosa in children infected with Helicobacter pylori, being correlated with the severity grade of inflammation. 2. The quantitative analysis proved the increased expression of CD45RA lymphocytes in children with Helicobacter pylori infection but no correlation was found between their expression and the severity grade of the inflammation.

References

1. Sommer F, Faller G, Konturek P, Kirchner T, Hahn EG, Zeus J, Rollinghaff M,

Lohoff M. Antrum - and corpus mucosa-infiltrating CD4(+) lymphocytes in Helicobacter pylori gastritis display a Th1 phenotype. Infect Immun, CD45RA and CD45RO 1998; 66: 5543-6.

2. Stromberg E, Lundgren A, Edebo A, Lundin S, Svennerholm AM, Lindholm C.

Increased frequency of activated T-cells in the Helicobacter pylori - infected antrum and duodenum. FEMS Immunol Med Microbiol, 2003; 36: 159-68.

3. Hatz RA, Meimarakis G, Bayerdorffer E, Stolte M, Kirchner T, Enders G.

Characterization of lymphocytic infiltrates in Helicobacter pylori-associated gastritis. Scand J Gastroenterol, 1996; 31: 222-8.

4. Kanegane H, Kasahara Y, Niida Y, Yachie A, Sughii S, Takatsu K, Taniguchi N,

Miyawaki T. Expression of L-selectin (CD62L) discriminates Th1- and Th2 - like cytokine-producing memory CD4+ T cells. Immunology, 1996; 87:186-90.

5. Kikuchi T, Kato K, Ohara S, Sekine H, Arikawa T, Suzuki T, Noggguchi K, Saito M,

Saito Y, Nagura H, Toyota T, Shimosegawa T. The relationship between persistent secretion of RANTES and residual infiltration of eosinophils and memory T lymphocytes after Helicobacter pylori eradication. J Pathol, 2000; 192: 243-50.

6. Lundgren A, Suri-Payer E, Enarsson K, Svennerrholm AM, Lundin BS.

Helicobacter pylori-specific CD4+CD25 high regulatory T-cells suppress memory T cell responses to H. pylori in infected individuals. Infect Immun, 2003; 71: 1755-62.

Macrophages of the antral mucosa in children with Helicobacter pylori infection and after eradication

Maciorkowska E[1], Kondej-Muszyńska K[2], Kasacka I[3], Kaczmarski M[2], Kemona A[4]

[1]Department of Pediatric Nursing, [2] III Department of Children's Diseases, [3]Department of Histology and Embryology, [4]Department of General Pathomorphology, Medical University of Białystok, Poland

Abstract

Our study included 59 children, aged 12.2 ± 4.6 years, with Helicobacter pylori infection and 29 children, aged 11.0 ± 4.2 years, with past H. pylori infection after spontaneous eradication with positive IgG antibodies against H. pylori and with functional disorders of the gastrointestinal tract, without H. pylori infection, with normal IgG concentration against H. pylori. All biopsy specimens from each of the study groups were stained by an immunohistochemical method for the evaluation of $CD68^+$ macrophages in the antral mucosa.

Histopathological changes in the antral mucosa of children with Helicobacter pylori are characterized by an increased infiltrate of macrophages, dependent on the severity grade of inflammation.

Key words: macrophages, antral mucosa, Helicobacter pylori, children.

Introduction

Infiltrating cells synthesize and produce mediating molecules which influence the recruitment and activation of further inflammatory cells and potentiate the triggering activity of cytokines and chemokines, for example: neutrophils express IL-1, IL-8, TNF-α [3], and macrophages, which are the source of MIP1-α [1,2,4]. Integrins: CD11a/CD18, CD11c/CD18, α4b1 and α4 β7, play an essential role in the inflammatory process. These are adhesive molecules present in numerous cells and built up of two polypeptides (α and β), fixed in the cell wall. The macrophage-activating complex-CD11b/CD18 (Mac-1), located on monocytes and neutrophils, belongs to one of them. Being a receptor for iC3b, it takes part in a complement-dependent bacteria phagocytosis and lysis [5]. It is the expression of macrophages, which initiates a local inflammatory state in the course of Helicobacter pylori infection [2, 6].

The aim of the study was to assess the expression of macrophages in the inflammatory infiltrate of the antral mucosa in children with H. pylori infection and after eradication.

Material and methods

A total of 106 patients, divided into three groups with regard to the presence of H. pylori infection, were included in the study. Group I - 59 children (29 girls and 30 boys; the age range: 2-19 years) with chronic gastric mucosa inflammation in the course of H. pylori infection with a positive titre of antibodies in IgG class against H. pylori. Group II - 29 children (14 girls and 15 boys; the age range 3-19) with past H. pylori infection, but with a maintaining positive titre of antibodies in IgG class against H. pylori. Group III - 18 children (12 girls and 6 boys; the age range 5-17) with functional disorders of the gastrointestinal tract, without H. pylori infection, with normal IgG concentration against H. pylori (the control group). Endoscopy and histopathological examinations of the stomach, basing on the Sydney System [7] were performed in all the children. The urease test was performed in the course of endoscopy in all the children. The specimens were fixed in 10% buffered formalin. They were processed, oriented on the edge, embedded in paraffin, cut in sequential 5-μm sections and stained by H+E for the evaluation of inflammation and by the Giemsa method, used to identify H. pylori bacteria. All the biopsy specimens from each study group were stained by an immunohistochemical method for the evaluation of $CD68^+$ macrophages in the antral mucosa. The ABC method was used, according to commercial protocol. The

ADDRESS FOR CORRESPONDENCE:
Elżbieta Maciorkowska
Department of Pediatric Nursing
Medical University of Białystok
Kilińskiego 1; 15-089 Białystok, Poland

Table 1. CD68+ cells in the antral mucosa in children.

Examined groups	CD68+ cells in the antral mucosa/mm²							
	Number of patients (N)	Minimum (min)	Maximum (max)	Arithmetic mean (x)	Median (M)	Standard Deviation (SD)	Low Quartile	High Quartile
Group I	23	19	95	54.1	60	19.4	76.0	146.0
Group II	17	0	54	11.3	8	15.3	3.0	10.0
Group III	7	0	45	9.4	4	15.9	1.5	7.0

Figure 1. Correlation between the expression of CD68+ cells and the severity grade of antral gastritis in children with Helicobacter pylori infection (Group I)

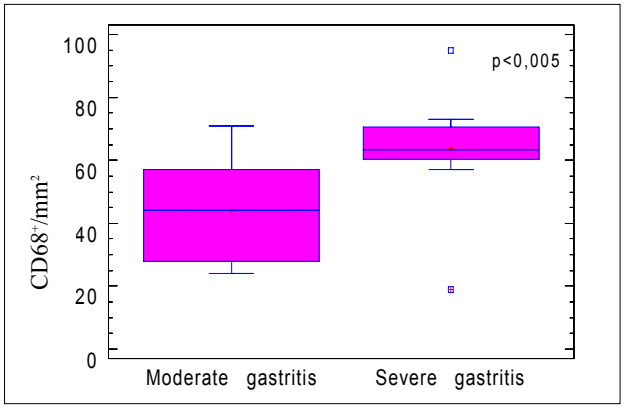

Photo 1. Antral mucosa. Immunohistochemical reaction with CD68+. Mag. x 400.

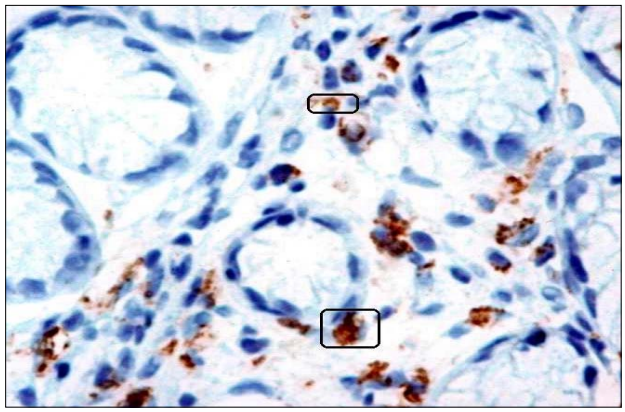

number of CD68+ macrophocytes was counted in discrete areas, measuring 0.785 mm² each, by using a light microscope. All the counts were performed, using a magnification of 200x. The numbers of positively stained cells were presented as the mean values per 1 mm² of analysed gastric section area. All the CD68+ macrophages counts were performed by a single observer (I. K.), who was unaware of either the H. pylori status or of the subject's clinical group.

An analysis of the preparations and their photographic documentation were performed with on Olympus Bx50 light microscope, with a video circuit and a Pentium 120 PC computer with the Lucia G (Nikon) software for microscope image analysis.

Descriptive statistics included the measures of central tendency: the arithmetic mean (x), median (Me) the measures of dispersion: standard deviation (SD), and the minimum (min) and maximum (max) result. The levels of the parameters were compared by means of the U Mann-Whitney test for independent or paired trials. The differences were regarded as statistically significant at $p<0.05$.

All the clinical and laboratory tests were performed in children with a prior consent of their parents and guardians, and of the Bioethical Board of the Medical University of Białystok.

Results

According to Sydney's Classification, the severe grade activity was found in 69.5% of the infected children and the moderate grade activity in 30.5% of these children. Neither severe nor moderate grade activity was found in children with past infection and after eradication, whereas mild grade activity was revealed only in 20.7% of the group. The analysis of antral gastritis by means of Chi² proved statistic significance ($p<0.001$) in the examined groups. The quantitative analysis of CD68+ macrophages in the antral mucosa showed a significant increase in their expression in children with H. pylori infection (54.1 cells/mm²). In children with past H.pylori infection, the expression of macrophages (11.3 cells/mm²) could be compared to their expression in the controls (9.4 cells/mm²). Photo 1.

When evaluating CD68+ cells in the inflammatory infiltrate, statistically significant differences were revealed between Group I and Group II ($p<0.001$) and between Group I and Group III ($p<0.01$). Table 1.

The quantitative analysis of CD68+ cells showed statistically significant differences in relation to the severity of antral gastritis ($p<0.005$). The expression of macrophages (CD68+) increased in the inflammatory infiltrate, together with the severity of the inflammation. In the children, infected with H. pylori (Group I) (Fig. 1), the expression of CD68+ cells equalled on the average 43.82 cells/mm² in a moderate inflammation of the antral mucosa. In case of severe inflammation of the antral mucosa, the mean expression of CD68+ cells was 63.58 cells/mm² ($p<0,005$). The expression of CD68+ cells in children with H. pylori infection was 45.75 cells/mm² in the antral mucosa with a moderate activity inflammation. In case of severe activity inflammation, the mean expression of CD68+ cells amounted to 55.89 cells/mm².

Discussion

When assessing $CD68^+$ cells in the antral mucosa, their predominating expression was revealed in children with H. pylori infection. Statistically significant differences were also reported between Group I and II ($p<0.001$) and between Group I and III ($p<0.01$). A positive correlation was found between the expression of $CD68^+$ cells and the severity grade of antral gastritis ($p<0.005$). The expression of macrophages increased directly proportionally to the severity grade of antral gastritis. In children, who spontaneously eradicated Helicobacter pylori, the expression of macrophages was lower in the inflammatory infiltrate, what may prove suppression of inflammatory process, due to an effective immune response in the examined patients. An increased expression of $CD68^+$ macrophages in the inflammatory infiltrate in the lamina propria, associated with Helicobacter pylori infection, was observed by Kusugami et al. [2]. They described a chemokine-macrophage inflammatory protein-1α, for which $CD68^+$ macrophages are target cells. The authors found an increased synthesis and secretion of MIP-1α in more than 50% of patients with Helicobacter pylori, located in the antrum [2].

Phagocytosis is ineffective in Helicobacter pylori infection, in spite of the increased expression of macrophages. Numerous mechanisms were developed by Helicobacter pylori, such as: mechanisms inhibiting oxygenic killing, interactions with lysosomal proteins, a protective activity of surface bacterial proteins: fetuin, heparin sulphate, hyaluronic acid, vitronectina in the presence of complement elements [8, 9].

Conclusion

Histopathological changes in the antral mucosa of children with Helicobacter pylori are characterized by an increased infiltrate of macrophages, dependent on the severity grade of inflammation.

References

1. Maciorkowska E. Morphological changes in the gastric and duodenal mucosa and the concentration of chosen cytokines in children with food allergy, Helicobacter pylori infection and giardiasis. Habilitation thesis. Białystok. Medical Unversity, 2000.

2. Kusugami K, Ando T, Imada A, Ina K, Ohsuga M, Shimizn T, Sakai T, Konagaya T, Koneko H. Mucosal macrophage inflammatory protein-1 alpha activity in Helicobacter pylori infection. J Gastroenterol Hepatol, 1999; 14: 20-26.

3. Kim J, Jung HC, Kim JM, Song IS, Kim CY. Interleukin-8 expression by human neutrophils activated by Helicobacter pylori soluble proteins. Scand J Gastroenterol, 1998; 33: 1249-55.

4. Kusugami K, Ando T, Ohsuga M, Imada A, Shinoda M, Konagaya T, Ina K, Kasuga N, Fukatsu A, Ichiyama S, Nada T, Ohta M. Mucosal chemokine activity in Helicobacter pylori infection. J Clin Gastroenterol, 1997: 25: 203-10.

5. Ross GD, Vetvicka V. CR3 (CD11b, CD18): a phagocyte and NK cell membrane receptor with multiple ligand specificities and functions. Clin Exp Immunol, 1993; 92: 181-4.

6. Hansen PS, Petersen SB, Varming K, Nielsen H. Additive effects of Helicobacter pylori lipopolysacharide and proteins monocyte inflammatory responses. Scand J Gastroenterol, 2002; 37: 765-71.

7. Misiewicz JJ. The Sydney System: a new classification of gastritis. Introduction. J Gastroenterol Hepatol, 1991; 6: 207-8.

8. Roitt I, Brostoff J, Male D. Immunology. Brema; Wydawnictwo Medyczne Słotwiński, Verlag: 1996.

9. Chmiela M, Czkwianianc E, Wadstrom T, Rudnicka W. Role of Helicobacter pylori surface structures in bacterial interaction with macrophages. Gut, 1997; 40: 20-4.

The activity and location of cathepsin D inhibitor in seeds of common vetch (*Vicia sativa* L.)

Roszkowska-Jakimiec W[1], Leśniewska J[2]

[1]Department of Instrumental Analysis, Medical University of Białystok, [2]Department of Botany, Institute of Biology, University of Białystok, Poland

Abstract

The activity of cathepsin D inhibitor is markedly higher in common vetch seed coat than in embryo cotyledons. The occurrence of considerable amounts of the inhibitor in the seed coat of vetch was confirmed by the fluorescent microscopic technique, with the use of fluorescein-marked cathepsin D.

Key words: cathepsin D inhibitor, fluorescein-marked cathepsin D, seed coat, common vetch (*Vicia sativa* L.).

Introduction

A peptide inhibitor of cathepsin D is present in common vetch seeds [1, 2]. However, it does not occur in the stem, roots, leaves, flowers, and pods of this plant. The vetch seeds are endosperm-free, they consist of an embryo and multilayer seed coat [3, 4].

The aim of the study was to compare the activity of cathepsin D inhibitor in seed coat and embryo cotyledons of common vetch.

Material and methods

The location of the inhibitor in cells of the seed coat and cotyledons was analysed by the fluorescent microscopic technique, using fluorescein-marked cathepsin D, capable of selective binding with the inhibitor.

Fluorescein isothiocyanate (FITC), cathepsin D, Bradford reagent and Folina and Ciocalteau reagent, Sigma, USA; haemoglobin, Difco, Laboratories, USA.

Seed coats of common vetch (*Vicia sativa* L.), cv. Szelejewska, were separated from the cotyledons, using the MF1 machine and shred in a mechanical mill. The seed coats and cotyledons were extracted. using distilled water in the 1:4 ratio of w/v. The extraction was carried out for 2 hours in laboratory temperature, while continuously stirring. In the supernatant, obtained in result of centrifugation (2700x g, 30 min, 4^{0}C), the activity of the inhibitor was determined, using cathepsin D and haemoglobin as substrates [5], as well as protein contents with the use of the Bradford method [6].

Fluorescent microscopic technique was incorporated to examine the location of the inhibitor at the level of the cells in seed coats and cotyledons, using fluorescein-marked cathepsin D [7]. Fragments of seed coats and cotyledons (7µm thick), obtained by a freezing microtome, were placed on microscope slides, covered with polylysine, stippled with marked cathepsin D (unmarked cathepsin D in the control) and incubated for 30 min. at 37^{0}C. Then, the slides were washed with phosphatic buffer, stippled with buffered glycerine, and closed with a cover glass. The preparations were evaluated, using a Nikon Eclipse E600 fluorescent microscope, at the excitation wave length of 450-490 nm, at which, fluorescein emits radiation of 520-550 wave length (green light).

Results and discussion

Approximately 70% of cathepsin D inhibitor activity occurs in the seed coat and the rest is present in the embryo cotyledons Table 1. The activity of cathepsin D inhibitor in seed coat is 1360.0 U/g of tissue and, in the cotyledons - 421.5 U/g. The protein content in the seed coat is 9.5 mg/g of tissue and that in the cotyledons - 53.5 mg/g. The inhibitor activity, expressed in pro-

ADDRESS FOR CORRESPONDENCE:
Wiesława Roszkowska-Jakimiec
Department of Instrumental Analysis
Medical University of Białystok
Mickiewicza 2c, 15-089 Białystok, Poland
e-mail: analinst@amb.edu.pl

Table 1. The activity of cathepsin D inhibitor and protein contents in extracts of seed coats and cotyledons of common vetch.

Extract	Protein, mg/g tissue	Activity of inhibitor		Inhibition, %
		u/g tissue	u/g protein	
Seed coat	**9.5**	**1360.0**	**143.1**	69
Cotyledons	**53.5**	**421.5**	**7.9**	22

Figure 1. Fragment of seed coat of common vetch, incubated with fluorescein-marked cathepsin D. L-light line, A-epidermis (palisade layer), B-osteosclereid layer, C-parenchymal cells. The arrows point to the sites of cathepsin D inhibitor occurrence. x 200.

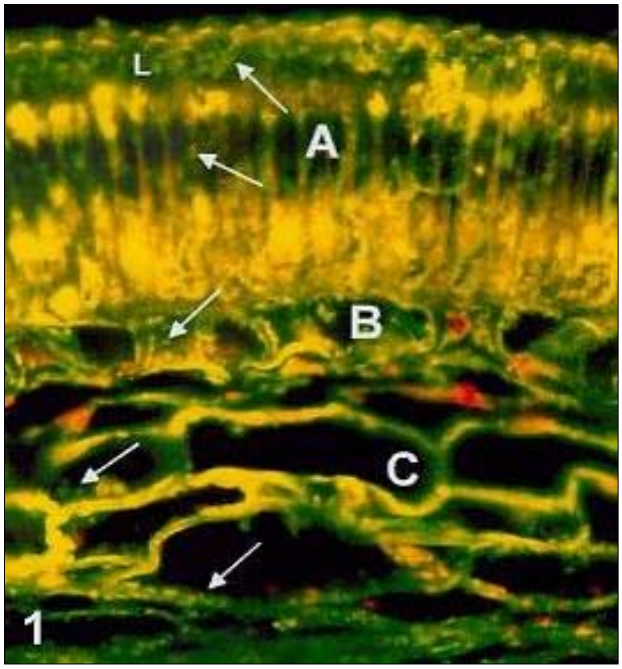

Figure 2. Fragment of seed coat of common vetch, incubated with cathepsin D, which was not marked with fluorescein. x 200.

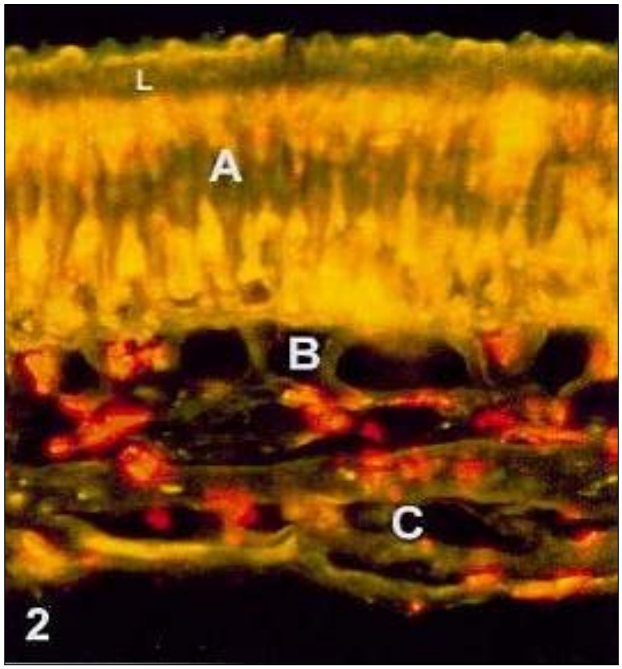

Figure 3. Fragment of embryo cotyledon tissue of common vetch, incubated with fluorescein-marked cathepsin D. S - starch grain. x 200.

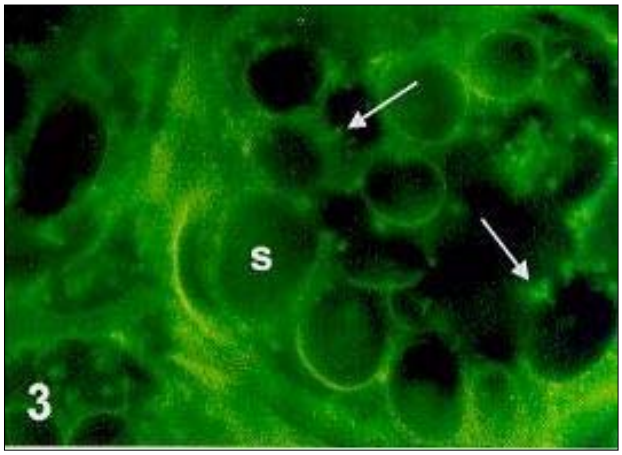

Figure 4. Fragment of embryo cotyledon tissue of common vetch, incubated with cathepsin D, which was not marked with fluorescein. x 200.

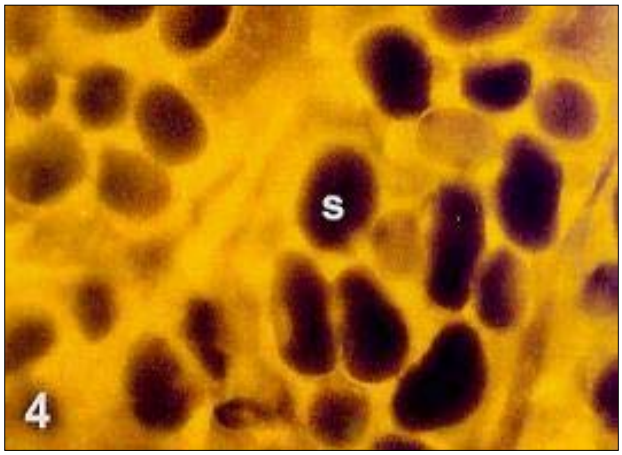

tein g, is 143.1 U/g in seed coat and 7.9 U/g of protein in cotyledons.

A similar distribution of the inhibitor was determined by the fluorescent microscopy technique. As it was observed (Fig. 1), the fragments, taken from the seed coat, incubated with fluorescein-marked cathepsin D, revealed a green signal, specific for this fluorochrome in the shape of small granules, occurring specifically in palisade cells of seed coat epidermis (A). The signal is markedly intensified in elongate protoplasts of these cells, as well as in the area of light line of the cell wall (L). The granules, emitting green light, occur close to cell walls in the cells, lying deeper in the seed coat, specifically in the parenchyma (B

and C). In the control preparations of the seed coat, there were no green light emitting granules (Fig. 2). The preparations of cotyledons, incubated with fluorescein-marked cathepsin D, revealed only few small clusters of granules of fluorochrome, emitting green light and located between starch grains in the cells of cotyledon (Fig. 3). However, the control cotyledons did not show any such granules (Fig. 4).

The study showed that the distribution inhibitor of cathepsin D in the seeds of common vetch is differentiated in particular types of its tissues. Proteolytic enzyme inhibitors, occurring in the seeds, protect reserve proteins during long (many months) storage against the activities of own proteases and the proteases of bacteria, mould, and insects that are present in the environment [8, 9]. Such a role is probably fulfilled by the cathepsin D inhibitor, which occurs mainly in the cells of the outer layer of seed coat in common vetch seeds.

References

1. Roszkowska-Jakimiec W. Peptide cathepsin D inhibit or from *Vicia sativa* L. seed hulls. XVII Polish Peptide Symposium, Łódź, 2003; 124.

2. Roszkowska-Jakimiec W, Bańkowska A. Cathepsin D inhibitor from *Vicia sativa* L. Ann AMB, 1998; 43: 245-49.

3. Johansson M, Walles B. Functional anatomy of the ovule in broad bean (*Vicia faba* L.): Ultrastructural seed development and nutrient pathways. Ann Bot, 1994; 74: 233-44.

4. Martin PD, Boža P, Merkulov LJ, Krstić B, Petković B, Veljić M, Pajević S. Seed sculpturing of selected European Vicia L. species (Fabaceae) and their taxonomical evaluation. Seed Sci Technol, 1998; 26: 17-32.

5. Greczaniuk A, Roszkowska-Jakimiec W, Gacko M, Worowska A. Determination of cathepsin D activity in blood plasma using hydrochloric acid denatured haemoglobin. Diagn Lab, 2000; 36: 97-101.

6. Bradford MM. A rapid and sensitive method for the quantitation of microgram quantities of protein utilizing the principle of protein - dye binding. Anal Biochem, 1976; 72: 248-54.

7. Haaijman JJ. Labeling of proteins with fluorescent dyes: Quantitative aspects of immunofluorescence microscopy. IBRO Hand, 1983.

8. Ryan CA. Protease inhibitors in plants: genes for improving defenses against insects and pathogenes. Ann Rev Phytophathol, 1990; 28: 245-9.

9. Senser F, Belitz HD, Kaiser KP, Santorius K. Seggestion of a protective function of proteinase inhibitors in potatoes: inhibition of proteolytic activity of microorganisms isolated from spoiled potato tubers. Z Lebensm Unters Forschung, 1974; 155: 10-4.

Effects of cathepsin D inhibitor from *Vicia sativa* L. seed hulls on human skin fibroblasts and breast cancer cells (*in vitro* studies)

Roszkowska-Jakimiec W[1], Wołczyński S[2], Chlabicz M[3]

[1] Department of Instrumental Analysis, [2] Department of Gynaecological Endocrinology,
[3] Department of Urology, Medical University of Białystok, Poland

Abstract

Cathepsin D is a lysosomal protease which plays an important role in cancer invasion and metastasis. There are known inhibitors of that enzyme, such as pepstatin and potato inhibitor. In this study, we examined effects of the cathepsin D inhibitor from *Vicia sativa* L. seed hulls on cell cultures of human skin fibroblasts and breast cancer cells. There is no effect of the D-cathepsin inhibitor from Vicia sativa L. seed hulls on the proliferative activity of either human skin fibroblasts or breast cancer cells, measured by the [3H] thymidine incorporation assay.

Key words: cathepsin D inhibitor, cathepsin D, fibroblasts, breast cancer cells, *Vicia sativa* L.

Introduction

Cathepsin D is ubiquitous lysosomal protease with important functions in protein catabolism. Three forms of the enzyme are known: 52 kDa procathepsin D, a 48-kDa intermediate form and stable cathepsin D with 34-kDa heavy and a 14-kDa light chain. Cathepsin D plays a key role in metastatic spread by promoting destruction of normal tissue architecture and in tumour growth by influencing of growth factors [1, 2]. There are known inhibitors of cathepsin D, such as pepstatin and potato inhibitor [3, 4].

ADDRESS FOR CORRESPONDENCE:
Marcin Chlabicz
Department of Urology
Medical University of Białystok
M. Skłodowskiej-Curie 24A, 15-276 Białystok Poland
e-mail: chlabicz@poczta.onet.pl

Material and methods

The specific objective of the studies was to examine the susceptibility of the cathepsin inhibitor D from seeds of *Vicia sativa* L. to the action of cathepsin D and its effect on DNA and cathepsin D activity in human skin fibroblasts and breast cancer cells MDA MB-231.

Peptide cathepsin D inhibitor was isolated from *Vicia sativa* L. seed hulls [5, 6]. Normal human skin fibroblasts were maintained in DMEM, supplemented with 10% FBS, 2 mmol glutamine, 50 U/ml penicillin and 50 µg/ml streptomycin at 37°C in 5% CO_2 in an incubator. The cells were used between 12th and 14th passages. The fibroblasts were subcultivated by tripsinization. Breast cancer cells were maintained in DMEM, supplemented with 10% FBS, 2 mmol glutamine, 50 U/ml penicillin and 50 µg/ml streptomycin at 37°C in 5% CO_2 in an incubator. The cells were cultured in Costar flasks and subconfluent cells were detached with 0.05% trypsin and 0,02% EDTA in calcium free PBS, plated at six-well plates (Nunc) in 2 ml of growth medium (DMEM without phenol red). The cells reached confluence at day 4 and, in most cases; such cells were used for the experiments.

In order to examine the effect of the studied inhibitor on cell proliferation, the fibroblasts were plated in 24-well tissue culture dishes at 1 x 10^5 cells/well and breast cancer cells at 1 x 10^6cells/well in 1 ml of growth medium. After 48h the cells were incubated at varying concentrations of the inhibitor (0.02, 0.2, 2.0 and 20 µmol/l) and 10 µl of 6.7 Ci/mM of [^{3}H] thymidine for 24 h at 37°C. The cells were rinsed three times with PBS, solubilized with 1 ml of 0.1 mol/l of sodium hydroxide, containing 1% SDS, scintillation fluid (3 ml) was added and radioactivity incorporation into DNA was measured in a scintillation counter. The activity of cathepsin D was determined, according to the used method [7]. Briefly, the monolayer was washed three times with 0.15 M NaCl. The cells were collected by scraping and suspended in 0.15 NaCl and centrifuged (2700 x g, 30 min) at 4°C. The cells were sonicated three times for 10 s at 0°C. The sam-

Table 1. Cathepsin D activity and protein concentration in supernatant and sediments of fibroblasts and breast cancer cells in presence of the inhibitor from *Vica sativa* L. seed hulls.

Cell inhibitor concentration	Supernatant		Sediments	
	Protein, mg/ml	Cathepsin D activity, Tyr, nmol/ml	Protein, mg/ml	Cathepsin D activity, Tyr, nmol/ml
Fibroblasts				
0.15 mol/l NaCl	4.64	2.4	0.098	24.8
0.02 ěmol/l	4.42	2.5	0.102	19.2
0.2 ěmol/l	4.47	2.4	0.102	19.2
2.0 ěmol/l	4.65	2.5	0.107	22.8
20 ěmol/l	4.69	2.4	0.118	24.8
MDA MB-231				
0.15 mol/l NaCl	4.65	5.3	0.103	80.0
0.02 ěmol/l	4.55	5.3	0.108	28.0
0.2 ěmol/l	4.58	5.3	0.108	28.8
2.0 ěmol/l	4.64	5.1	0.106	20.0
20 ěmol/l	4.61	5.2	0.104	12.8

ples were then centrifuged (16 000 x g, 30min) at 4°C. The sediment and the supernatant were used for protein determination by the Bradford method [8] and then by the cathepsin D activity assay.

Results and discussion

There is no antiproliferative activity of the cathepsin D inhibitor on human skin fibroblasts and breast cancer cells, measured by the [^{3}H] thymidine incorporation assay. D-cathepsin activity, measured in fibroblast supernatant, was 2.4 nmol Tyr/ml and, in breast cancer cells, it was 5.3 nmol Tyr/ml and there was no correlation between the activity and the inhibitor concentration Table 1. In the sediments of fibroblast homogenates, D-cathepsin activity in control without the inhibitor was 24.8 nmol/ml, while with the inhibitor, it ranged from 19.2 to 24.8 nmol/ml. In breast cancer cell sediments, the control activity was 80 nmol/ml and with the inhibitor activity, it was decreased to 12-28 nmol/ml, according to inhibitor concentration. The protein concentration in the supernatant fibroblast and breast cancer cells was 4.6 ng/ml and, in the sediments, it was 0.106 mg/ml.

There is no effect the D-cathepsin inhibitor from *Vicia sativa* L. seed hulls on the proliferative activity of human skin fibroblasts and breast cancer cells, measured by the [^{3}H] thymidine incorporation assay. The cathepsin D inhibitor from seeds of *Vicia sativa* L. does not penetrate into fibroblasts cells, but it penetrates inside breast cancer cells.

References

1. Westley BR, May FEB. Cathepsin D and breast cancer. Eur J Cancer, 1996; 32A: 15-24.

2. Rochefort H, Capony F, Garcia M. Estrogen induced lysosomal protease secreted by breast cancer cells: a role in carcinogenesis? J Cell Biochem 1987; 34: 17-29.

3. Worowski K. Izolowanie, właściwości fizykochemiczne i biologiczne inhibitorów enzymów proteolitycznych z ziemniaka. Rozprawa habilitacyjna. Akademia Medyczna w Białymstoku, 1976.

4. Worowski K, Ostrowska H. Katepsyna D. Post Biol Kom, 1980; 7: 119-47.

5. Roszkowska-Jakimiec W. Peptide cathepsin D inhibitor from *Vicia sativa* L. seed hulls. XVII Polish Peptide Symposium, Łódź, 2003: 124.

6. Roszkowska-Jakimiec W, Bańkowska A. Cathepsin D inhibitor from *Vicia sativa* L. Rocz AMB, 1998; 43: 245-9.

7. Greczaniuk A, Roszkowska-Jakimiec W, Gacko M, Worowska A. Determination of cathepsin D activity blood plasma using hydrochloric acid denatured haemoglobin. Diagn Lab, 2000; 36: 97-101.

8. Bradford MM. A rapid and sensitive metod for the quantitation of microgram quantities of protein utilizing the principle of protein - dye binding. Anal Biochem, 1976; 72: 248-54.

S-100 protein as marker of the blood-brain barrier disruption in children with internal hydrocephalus and epilepsy - a preliminary study

Sendrowski K[1], Sobaniec W[1], Sobaniec-Łotowska ME[2], Lewczuk P[1]

[1]Department of Child Neurology & Rehabilitation, [2]Department of Clinical Pathomorphology,
Medical University of Bialystok, Poland

Abstract

S-100 is a structural protein of the central nervous system. An elevated level of S-100 in CSF is generally considered to be a marker of nervous tissue damage. The presence of this protein in blood serum points to the functional and/or morphological disruption of the blood-brain barrier. We measured S-100 in the cerebrospinal fluid and blood of children with two of the most often observed pathological states in child neurology - internal hydrocephalus and epilepsy. High levels of S-100 in CSF were detectable in children with internal hydrocephalus. Increased blood levels of S-100 protein were detectable in both groups of paediatric patients. Our preliminary results indicate neuronal damage in internal hydrocephalus and morphological and/or functional disturbances of the blood-brain barrier (their increased permeability) in both above mentioned disabilities.

Key words: S-100 protein, blood-brain barrier, epilepsy, hydrocephalus.

Introduction

S-100 is a set of small, acidic, calcium-binding dimer proteins of approximately 20 kDa which are widely distributed in different tissues. The S-100 protein was first discovered by Moore in 1965 [1]. Dimeric combination of the α- and β-chain form three known subtypes: S-100ao (αα), S-100a (αβ) and S-100b (ββ). S-100b is regarded as nervous-system-specific protein and is present mainly in glial cells and Schwann cells [2]. The function of S-100 in the central nervous system (CNS) is only poorly understood. It is known that S-100 plays a role in neuronal plasticity and long-term potentiation processes [3, 4]. This protein is generally considered to be a marker of CNS damage [5]. Increased levels of S-100 in CSF or serum were measured after a variety of cerebral lesions and injuries, including stroke, severe head trauma, brain tumours, or multiple sclerosis.

Brain has its own unique and effective protective system that controls the process of active transport of chemical substances from blood to neurons and CSF. This system, known as the blood-brain barrier (BBB), is formed by complex tight junction of the brain capillary endothelial cells and segregates the circulating blood from interstitial fluid in the brain [6]. In normal conditions, S-100 does not cross the BBB. Levels of this protein in plasma are extremely low and approximately one third of the levels, found in the cerebrospinal fluid (CSF) [5]. Thus, opening the blood-brain barrier (BBB) would be expected to markedly increase plasma S-100 levels. Kapural et al. [7] suggest that S-100β is an early marker of BBB disruption that is not necessarily related to neuronal damage. We measured S-100 in children with two of the most often observed pathologic states in child neurology - internal hydrocephalus and epilepsy. Studies on the blood levels of S-100 protein in paediatric patients are very rare.

Material and methods

Two groups of patients: Group H - children with internal hydrocephalus and Group E - children with epilepsy were involved into the study.

Group H amounted to 4 patients in whom the shunt implantation was necessary. The CSF and blood samples were obtained just before the implantation. The control group included 5 healthy children, in whom only blood samples were taken to the study. Some level of S-100 protein has been detected at the Klinikum Grosshadern in Munich (Germany), using an

ADDRESS FOR CORRESPONDENCE:
Krzysztof Sendrowski
Department of Child Neurology & Rehabilitation
Medical University of Bialystok
Waszyngtona 17, 15-274 Bialystok, Poland
e-mail: krsen@mp.pl

Table 1. S-100 concentrations in CSF and serum in children with internal hydrocephalus.

Patient's number	S-100 in serum (μg/L)	S-100 in CSF (μg/L)
1.	0.065	0.790
2.	0.210	7.700
3.	0.140	11.500
4.	0.248	0.660

Table 2. S-100 concentrations in CSF and serum in children with epilepsy.

Patient's number	S-100 in serum (μg/L)	S-100 in CSF (μg/L)
1.	0.204	0.650
2.	0.280	0.620
3.	0.260	0.570
4.	0.230	0.340
5.	0.230	0.320
6.	0.134	0.300

immunofluorometric sandwich assay. Details of this method are described in [8]. In group E, there were 6 epileptic patients in whom lumbar puncture was performed to exclude infection of CNS. The CFS and blood samples were taken within 12 h after the seizure. The control group constituted 12 healthy children, in whom only blood samples were obtained. Levels of S-100 protein were measured, using the radioimmunometric assay (Sangtec, Sweden).

Results

Group H: The results, obtained Group E, are presented in Table 1. The range of S-100 concentration in CSF was 0.660-11.500 mg/ and. in blood serum - 0.065 - 0.248 μg/L respectively. In the healthy children, the median serum level of S-100 protein was 0.033 μg/L. The obtained data suggest that CSF levels of S-100 can be almost 8 times higher than those in serum of the same patients and that the concentration of S-100 in serum of children with hydrocephalus can be 8 times higher too than that in control group.

Group E: The results, obtained in Group E, are presented in Table 2. The range of S-100 concentration in CSF was 0.320 - 0.650 μg/L. In blood serum - 0.134 - 0.280 μg/L respectively. In all 12 cases of children in the control group, the level of S-100 in serum was lower than 0.010 μg/L. The obtained data suggest that CSF level of S-100 is 2-3 times higher than that in serum of the same epileptic children and that the concentration of S-100 in serum of epileptic children is15-20 times higher than that in control group.

Discussion

Several groups have reported increased CSF levels of S-100 protein in patients with lesions of the CNS [i.e. 9, 10] and a relationship between cell damage in the CNS and the concentration of S-100 in CSF [11]. There is evidence that CSF levels of S-100 may serve as quantitative markers of the extent of brain damage. However, especially in patients with intracranial pressure, lumbar puncture is contraindicated, due to the risk of transtentorial herniation. For these reasons, S-100 which is released from brain cells during brain damage, must be detectable in blood if it is to serve as a useful tool in clinical medicine. Otherwise, S-100 level in blood increased significantly when the BBB is disrupted and that is not necessarily related to neuronal damage [7]. Our study shows that CSF concentration of S-100 was only 2-3 times higher, compared to serum levels in the group of epileptic children. Similar results were found in healthy volunteers [5]. This fact does not point to any severe neuronal damage in epilepsy. Our results indicate an increased permeability of BBB in epilepsy and, in a less degree, in internal hydrocephalus. The obtained data can have practical meaning, especially in children affected by hydrocephalus [12]. Periodic controls of S-100 protein levels in blood may be a useful indicator of shunt function.

Conclusions

Increased blood levels of S-100 protein were detectable both in children with internal hydrocephalus and in those with epilepsy. Our results indicate morphological and/or functional disturbances of BBB (their increased permeability) in both above mentioned disabilities. Very high CSF levels of S-100 in Group H point to severe damage of the CNS tissues in children with internal hydrocephalus. There is no evidence of S-100 levels in CSF to the neuronal damage in epileptic children. We concluded that measuring the blood levels of S-100 protein may be a reproducible and less invasive method for determining the integrity of the BBB in children with internal hydrocephalus and epilepsy.

References

1. Moore BW. A soluble protein characteristic of the nervous system. Biochem Biophys Res Commun, 1965; 19: 739-44.
2. Isobe T, Takahashi K, Okuyama T. S-100a0 (alpha alpha) protein is present in neurons of the central nervous system. J Neurochem, 1984; 43: 1494-6.
3. Gerlai R, Wojtowicz JM, Marks A, Roder J. Overexpression of a calcium binding protein, S-100β, in astrocytes impairs synaptic plasticity and spatial learning in transgenic mice. Learn Mem, 1995; 2: 26-31.
4. Whitaker-Azmitia PM, Murphy R, Azmitia EC. Astroglial 5-HT1A receptors and S-100β in development and plasticity. Perspect Dev Neurobiol, 1994; 2: 233-8.
5. Grocott HP, Laskowitz DT, Newman MF. Markers of cerebral injury, In: The Brain and Cardiac Surgery, Newman SP, Harrison MJG [Eds] Harwood Academic Publishers, Amsterdam, 2001; pp. 113-42.
6. Reese TS, Karnovsky MJ. Fine structural localization

of a blood-brain barrier to exogenous peroxidase. J Cell Biol, 1967; 34: 207-17.

7. Kapural M, Krizanac-Bengez Lj, Barnett G, Perl J, Masaryk T, Apollo D, Rasmussen P, Mayberg MR, Janigro D. Serum S-100β as a possible marker of blood-brain barrier disruption. Brain Res, 2002; 940: 102-4.

8. Missler U, Wiesmann M. Measurement of S-100 protein in human blood and cerebrospinal fluid: analytical method and preliminary clinical results. Eur J Clin Chem Clin Biochem, 1995; 33: 743-8.

9. Mokuno K, Kato K, Kawai K, Matsuoka Y, Yanagi T, Sobue I. Neuron-specific enolase and S-100 protein levels in cerebrospinal fluid of patients with various neurological diseases. J Neurol Sci, 1983; 60: 443-51.

10. Persson L, Hardemark HG, Gustafsson J, Rundstrom G, Mendel-Hartvig I, Esscher T, Pahlman S. S-100 protein and neuron-specific enolase in cerebrospinal fluid and serum: markers of cell damage in human central nervous system. Stroke 1987; 18: 911-8.

11. Rosen H, Rosengren L, Herlitz J, Blomstrand C. Increased serum levels of the S-100 protein are associated with hypoxic brain damage after cardiac arrest. Stroke 1998; 29: 473-7.

12. Sendrowski K, Wiesmann M, Sobaniec W, Lewczuk P. The analysis of S-100 protein in CSF and serum in children with internal hydrocephalus (abstract). 71. Jahrestagung Deutsche Gesellschaft für Neurologie mit Fortbildungsakademie, München, 2-6 September 1998.

Attempts to detect Helicobacter pylori in atherosclerotic plaques

Sulewska A[1], Modrzejewski W[2], Kovalchuk O[3], Kasacka I[4], Jackowski R[5], Hirnle T[5], Musiał W[2], Chyczewski L[3]

[1]Clinic of Thoracic Surgery, [2]Clinic of Cardiology, [3]Department of Clinical Molecular Biology,
[4]Department of Histology and Embryology, [5]Clinic of Cardiosurgery, Medical University of Bialystok.

Abstract

Cardiovascular and cerebrovascular diseases are regarded to be the main causes of mortality in developed countries, atherosclerosis being at their pathological base. During the recent years, attention was paid to the role of bacterial infections, including Helicobacter pylori, in the process of atherogenesis and coronary heart disease development. The aim of the study was an evaluation of H. pylori presence - by means of PCR technique - in atherosclerotic changes, obtained by endarterectomy, performed during coronary artery bypass grafting (CABG). In the analysed group of patients, the following risk factors were found: hyperlipidaemia, smoking, hypertension, obesity, diabetes mellitus, cardiac infarction. No DNA of the bacteria was traced in any of the patients.

Key words: Helicobacter pylori, PCR technique, atherosclerotic plaques.

Introduction

Inflammatory factors play an important role in the pathogenesis of atherosclerosis. In patients with coronary heart disease, increased levels of C-reactive protein, TNF-α, interleukin 1, 6 and fibrinogen are observed. Since, in some patients with coronary heart disease, no common risk factors are reported (such as: hypertension, smoking, overweight, hypercholesterolaemia, genetic predispositions) viral (Cytomegalovirus, Hepatitis A, Herpes simplex type 1 and 2) and bacterial (Chlamydia pneumoniae and Helicobacter pylori) participation has been suggested in the development of atherosclerosis. These microorganisms can directly invade the vascular endothelium, inducing inflammatory response, or secrete endotoxins with either local or systemic impact [1]. The influence of infection with Helicobacetr pylori on the development of vascular diseases has not yet been explained. The results of serological analyses indicate bacterial presence in 50% of the adult population. The occurrence of antibodies in blood serum is not to be interpreted as a continuous infection or as a constant exposition of the cardiovascular system to pathogenic factors [2, 3, 4].

Our study attempted at finding DNA of Helicobacter pylori in atherosclerotic plaques, collected by endarterectomy, performed during coronary artery bypass grafting (CABG).

Material and methods

The material for the study (atherosclerotic plaques) was collected from twenty-one (21) patients (20 male and 1 female) in age between 42-73 years (the mean age: 57 years) with coronary heart disease, diagnosed by coronarography, operated at the Clinic of Cardiosurgery, Medical University of Bialystok between the years 1998-2003. Operated patients were seropositive for H. pylori and were determined risk factors of coronary heart disease. All of the patients were qualified to implantation of aortal-coronary bypasses because of extensive atherosclerotic changes in the coronary arteries and disqualification for transcutaneous interventions. In eighteen (18) patients, CABG was performed within schedule, while in the other three (3), the surgery was accelerated because of unstable course of the coronary heart disease. The decision about endarterectomy was intraoperatively made, on the basis of the coronary artery morphology and at the planned spot of distal bypass grafting. Cylinder-shaped atherosclerotic change was obtained by preparation, performed from the side of the adventitia, following a longitudinal incision of the artery. The collected material was placed

ADDRESS FOR CORRESPONDENCE:
Anetta Sulewska
Department of Clinical Molecular Biology,
Medical University of Bialystok
Waszyngtona 13, 15-269 Bialystok, Poalnd

in 10% solution of buffered formalin and transported to the Department of Clinical Molecular Biology at the Medical University of Bialystok. After 12-hour fixing, the material was routinely handled and embedded into paraffin blocks. For DNA isolation, 10 paraffin sections (5 µm thick) were placed in 1.5 ml Eppendorf tubes and deparaffinated in room temperature, using xylene - a mixture of xylene with chloroform (1:1) and absolute ethanol. DNA was isolated and purified by the phenolic-chloroform technique. The purified and dried DNA sediment was dissolved in 30 µl of elution buffer, incubated through the night in room temperature and then stored in -20^{0}C until further assay. During DNA isolation, also negative control was set up. PCR reaction was performed for a fragment of vacA Helicobacter pylori gene (specific vacuolating gene) of 229 bp in length, using a pair of primers: VAC3624F and VAC3853R (the sequence of the primers: VAC3624F GAG CGA GCT ATG GTT ATG AC; VAC3853R ACT CCA GCA TTC ATA TAG A). The obtained reaction mixture of 10 µl in volume contained: buffer x 10, dNTP (40 mM), the VACF primer (12 pmol/µl) the VACR primer (12 pmol/µl), Red polymerase (1U/µl), H_20_{dest}, DNA solution - 2ml. The thermal profile of the reaction was carried out for 40 cycles (94^{0}C - 30 s, 51^{0}C - 1 min, 72^{0}C - 30 s). The effectiveness of PCR technique was determined on the material from gastric biopsy specimens, fixed and embedded into paraffin blocks, identically as the atherosclerotic plaques, in which the presence of H. pylori had been found. Those samples stood for positive control. The PCR reaction was twice repeated. In order to visualise the product of PCR, electrophoresis was performed in 1.8% agarose gel with an addition of ethydine bromide (room temperature, voltage = 120V).

Results

Demographic data demonstrated that hyperlipidaemia was the most frequent risk factor (67%) of coronary heart disease, followed by smoking (62%) and hypertension (52%). In 25% of the patients, diabetes mellitus was diagnosed, while 20% of them revealed obesity. Two thirds of the patients had cardiac infarction in history. The above factors occurred, regardless of the presence of Helicobacter pylori in atherosclerotic changes, as no genome of the bacteria was traced in the analysed material (Fig.1).

Discussion

Infection with H. pylori may be associated with a number of parenteral diseases, including - among others - autoimmunising diseases, skin diseases, hepatic encephalopathy, the sudden infantile death syndrome and atherosclerosis of the coronary arteries [5]. Bacterial DNA can be detected in host's tissues by means of a very sensitive method - PCR.

In the performed studies, no presence of H. pylori genome was observed in any of the evaluated atherosclerotic change. The obtained results were concordant with some of the earlier reports. Neither Blasi et al. nor Dore et al. found the genome of H. pylori in any of their studied samples, collected from the aorta, the abdominal aorta, the carotid artery and the femoral

Figure 1. Amplification products of H. pylori control and negative samples in agarose gel.

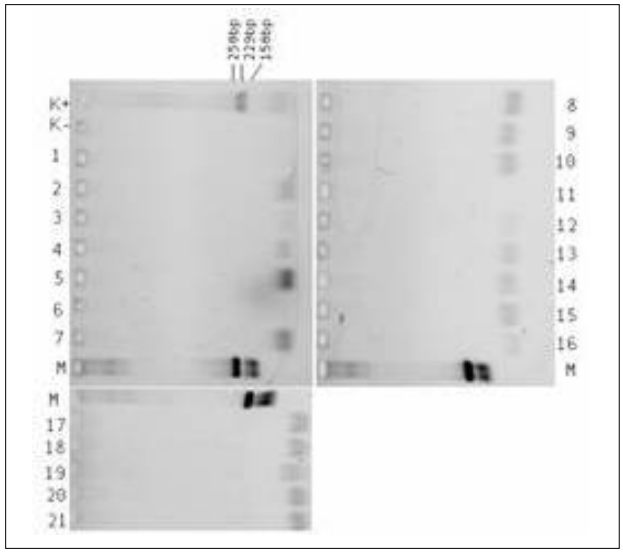

M - DNA molecular weight marker (250 bp and 150 bp),
K^+ positive control (229 bp),
K^- negative control, 1-21 negative samples.

artery [2, 3, 4]. Danesh et al. identified bacterial DNA in 1, out of 36 analysed cases only [6]. In turn, Farsak et al. obtained positive results in 37% of evaluated arteries [7].

Contradictory and discrepant results of studies, as presented in the reports, may have resulted from a focal localisation or periodical (transient) colonisation of tissues by H. pylori. The mechanism of blood vessel colonisation by this bacteria has not yet been unveiled. A finding of H. pylori DNA in the oral cavity, the liver, the bile tract or in atherosclerotic plaques may then turn out to be a false positive result. The bacteria is killed in blood serum, while free DNA in peripheral circulation may influence the false-positive results in tissues. Employing PCR for 16S rRNA and vacA genes, the presence of bacterial DNA in circulation was found in 65% and 50% of infected patients, respectively, while not a trace of that DNA was observed in the control group [8].

In the analysed group of patients (20 males and 1 female), we found the following risk factors of vascular diseases: hyperlipidaemia, smoking, hypertension, diabetes mellitus, obesity and cardiac infarction, while neither chronic peptide ulcer disease nor gastric carcinoma were noted in that reference. We cannot exclude an association of the above mentioned factors with H. pylori infection, although no bacterial DNA was found in any of the studied samples.

In 18 cross-sectional studies, each involving, at least, 500 persons, no unequivocal results were presented, either. The evaluation included, among others: systolic and diastolic blood pressure, the body mass index, plasma viscosity, total cholesterol concentration and the concentrations of glucose and C-reactive protein. The majority of the studied parameters did not show any statistically significant differences between the patients and the controls. Only a slight increase of plasma viscosity and glucose concentration was observed in the group of patients [9]. The participation of Helicobacter pylori in the ischaemic heart disease has not been unequivocally confirmed. The few reports,

which mention the presence of the bacterial genome in atherosclerotic changes, may not be regarded as evidence for a direct engagement of the bacteria in the pathogenic process - the bacteria in question may be, but a harmless commensal, localising itself in pathologically changed tissues.

References

1. Fong IW. Emerging relations between infectious disease and coronary artery disease and atherosclerosis. CMAJ, 2000; 163: 49-56.

2. Blasi F, Denti F, Erba M, Cosentini R, Raccanelli R, Rinaldi A, Fagetti L, Esposito G, Ruberti U, Allegra L. Detection of Chlamydia pneumoniae but not Helicobacter pylori in atherosclerotic plaques of aortic aneurysms. J Clin Microbiol, 1996; 34: 2766-9.

3. Dore MP, Sepulveda AR, Bacciu PP, Blasi F, Simula L, Marras L, Piccolo D, Cherchi GB, Graham DY, Realdi G. Detection of Chlamydia pneumoniae but not Helicobacter pylori DNA in atherosclerosis plaques. Dig Dis Sci, 2003; 48: 945-51.

4. Malnick SD, Goland S, Kaftoury A, Schwarz H, Pasik S, Mashiach A, Sthoeger Z. Evaluation of carotid arterial plaques after endarterectomy for Helicobacter pylori infection. Am J Cardiol, 1999; 83: 1586-7.

5. Realdi G, Dore MP, Fastame L. Extradigestive manifestations of Helicobacter pylori infection: fact and fiction. Dig Dis Sci, 1999; 44: 229-36.

6. Danesh J, Koreth J, Youngman L, Collins R, Arnold JR, Balarajan Y, McGee J, Roskell D. Is Helicobacter pylori a factor in coronary atherosclerosis? J Clin Microbiol, 1999; 37:1651.

7. Farsak B, Yildirir A, Akyön Y, Pinar A, Öç M, Böke E, Kes S, Tokgözoglu L. Detection of Chlamydia pneumoniae and Helicobacter pylori DNA in human atherosclerotic plaques by PCR. J Clin Microbiol, 2000; 38: 4408-11.

8. Dore MP, Realdi G, Sepulveda AR, Graham DY. Detection of genomic Helicobacter pylori DNA in the blood of patients positive for the infection. Dig Liver Dis, 2003; 35: 839-40.

9. Danesh J, Peto R. Risk factors for coronary heart disease and infection with Helicobacter pylori: meta-analysis of 18 studies. BMJ, 1998; 316: 1130-32.

Proliferative activity of chosen central nervous system (CNS) neoplasms

Lebelt A[1], Szkudlarek M[1], Guzińska-Ustymowicz K[2], Lemancewicz D[1], Zimnoch L[3], Dzięcioł J[1]

[1]Department of Human Anatomy, [2]Department of General Pathomorphology,
[3]Department of Medical Pathomorphology, Medical University of Białystok, Poland

Abstract

Gliomas are the most common neoplastic tumours of the central nervous system. The aim of the study was to evaluate the proliferative activity of chosen types of gliomas and to analyse their correlation with histological type, malignancy grade, location, size and clinical symptoms. The study involved patients with astrocytoma, anaplastic astrocytoma, glioblastoma, oligodendroglioma, anaplastic oligodendroglioma. The proliferative activity (the labelling index - LI) of glial cells was estimated, using immunohistochemistry. In studied groups, a positive correlation was noted between the proliferative activity and tumour size, but not between the proliferative activity and tumour location. The clinical symptoms were conditioned mainly by tumour location and, to a smaller extent, by its size.

Key words: proliferative activity, glioma, Ki-67, PCNA.

Introduction

Gliomas constitute approximately 50% of all brain tumours, showing a varied clinical course, depending on their histological type, grade and location. In case of many gliomas, the basic histopathological investigation requires the use of accessory diagnostic methods. One of them is the immunohistochemical examination which detects the presence of cycle phase-specific nuclear antigens to indicate the proliferative activity of tumours [1].

The aim of the study was to evaluate the proliferative activity of chosen brain gliomas and to analyse its correlation with histological type, grade, location, size and clinical symptoms.

ADDRESS FOR CORRESPONDENCE:
Agnieszka Lebelt
Department of Human Anatomy
Medical University of Białystok
Mickiewicza 2 A, 15-089 Białystok, Poland
Tel. (+48 85) 748 56 61

Material and Methods

The study involved 99 patients, aged 18-80 (54 women and 45 men) with clinically diagnosed brain tumour. Prior to surgery, all the patients had neurological examinations, revealing either symptomatic or asymptomatic focal CNS damage or intracranial hypertension. CT and/or MRI examination allowed determination of the location and size of the tumour. Group I consisted of patients with astrocytoma (22 patients), Group II - patients with anaplastic astrocytoma (31), Group III - patients with glioblastoma (23), Group IV - patients with oligodendroglioma (12) and Group V - patients with anaplastic oligodendroglioma (11). Ki-67 (clone MIB-1, DAKO): working dilution 1:50 and PCNA (clone PC 10, DAKO): working dilution 1:100 antibodies were used for immunohistochemical examinations. The proliferative activity was determined, based on the labelling index (LI), expressing the percentage of cells with Ki-67 and PCNA nuclear immunoreactivity, compared to the total cell count. The Statistica PL program with StatSoft was used for statistical analysis. For comparison of means, Student's 't' test was performed.

Results

In the presented study, the mean LI values differed among the groups, depending on the tumour histological grade. The highest proliferative activity, expressed by LI, was found in glioblastoma cells. Lower LI values were noted in anaplastic astrocytomas and oligodendrogliomas. Statistically significantly lower LI values were observed in astrocytomas and oligodendrogliomas. Detailed data are shown in Table 1.

Discussion and Conclusion

LI values in neoplastic glial cells, presented by other authors, show evident variations. Compared to the present study, lower Ki-67 LI values in anaplastic astrocytoma and glioblastoma were found

Table 1. Proliferative activity, size, location and clinical symptoms in the respective study groups.

Group	Histological type grading (G)	*number of cases*	Ki-67 – LI x (SD)	PCNA – LI x (SD)	diameter (cm)	Location of tumors (%)					Focal CNS damage of patients (%)				Intracranial hypertension of patients (%)			
						frontal lobe	temporal lobe	parietal lobe	motor and sensory area	area of posterior contact	aphasia	paresis	psychiatric disturbance	epilepsy	headache	vomiting	papilloedema	consciousness disturbance
I	Astrocytoma G2	*22*	1.52	2.42	4.96	18.2	40.9	9.1	18.2	13.6	9.1	50	13.6	27.3	63.6	9.1	18.2	4.5
II	Anaplastic astrocytoma G3	*31*	18.98	20.47	5.27	32.3	25.8	12.9	12.9	16.1	19.3	45.2	6.45	29	58.1	9.7	16.1	16.1
III	Glioblastoma G4	*23*	31.34	34.18	3.75	13	43.5	17.4	8.7	17.4	34.8	65.2	8.7	21.7	69.6	8.7	26.1	13
IV	Oligodendroglioma G2	*12*	2.25	3.14	3.63	50	25	0	25	0	8.3	33.3	25	50	25	0	8.3	0
V	Anaplastic G3 oligodendroglioma	*11*	14.72	17.02	4.69	45.5	27.3	18.2	9.1	0	0	36.4	18.2	54.5	63.6	0	18.2	9.1

by Eneström et al. [2] (13.3 and 24.3 respectively). However, LI values, detected in glioblastomas, are consistent with those, reported by Kayaselcuk et al. [3]. Considerably higher PCNA LI values, reaching 67 in glioblastoma and 48.57 in anaplastic astrocytoma, were noted by Korkolopoulou et al. [4]. The differences in LI values, presented by various authors, may have resulted from the use of different fixation methods and research procedures [5, 6]. However, despite LI variations, in all the reports, the proliferative activity of gliomas shows a correlation with tumour grade [1, 3, 7]. This seems to indicate that the proliferation index can be used as an accessory parameter to differentiate between border grades [8]. Many authors believe that LI value is a significant survival index [9, 10, 11] and can be used to assess the risk of recurrence [3]. The present analysis showed a positive correlation between the proliferative activity of the tumours and their diameters within respective histological types. The activity was most enhanced in glioblastomas, which demonstrated the highest LI level but were the smallest in diameter. No correlation was found between the proliferative activity and tumour location.

We observed that the clinical symptoms and their severity varied among patients. The prevailing symptoms were conditioned mainly by tumour location and concomitant swelling, rather than by glioma size. When tumour location was the same, the clinical symptoms, especially intracranial hypertension, were more enhanced in patients with higher proliferative activity of the neoplastic cells.

References

1. Zimnoch L, Kozielec Z, Lewko J, Cylwik B, Mariak Z. Badania aktywności proliferacyjnej glejowych nowotworów mózgu. Neur Neurochir Pol, 1999; 33: 89-96.
2. Eneström S, Vavruch L, Franlund B, Nordenskjöld B. Ki-67 antigen expression as a prognostic factor in primary and recurrent astrocytomas. Neurochirurgie, 1998; 44: 25-30.
3. Kayaselcuk F, Zorludemir S, Gumurdulu D, Zeren H, Erman T. PCNA and Ki-67 in central nervous system tumors: correlation with the histological type and grade. J Neur Onkol, 2002; 57: 115-21.
4. Korkolopoulou PI, Christodoulou P, Papanikolaou A, Thomas-Tsagli E. Proliferating cell nuclear antigen and nucleolar organizer regions in CNS tumors. Correlation with histological type and tumor grade. Am J Surg Pathol, 1993; 17: 912-9.
5. Sallinen PK, Haapasalo HK, Visakorpi T, Helen PT, Rantala IS, Helin HJ. Prognostication of astrocytoma patient survival by Ki-67 (MIB-1), PCNA, and S-phase fraction using archival paraffin-embedded samples. J Pathol, 1994; 174: 275-82.
6. Torp SH. Diagnostic and prognostic role of Ki67 immunostaining in human astrocytomas using four different antibodies. Clin Neuropathol, 2002; 21: 252-7.
7. Kordek R, Biernat W, Alwasiak J, Liberski P. Proliferating cell nuclear antigen PCNA and Ki-67 immunopositivity in human astrocytic tumors. Acta Neurochir, 1996; 138: 509-13.
8. Stupp R, Janzer RC, Hegi ME, Villemure JG, Mirimanoff RO. Prognostic factors for low-grade gliomas. Semin Oncol, 2003; 30: 23-8.
9. Ang LC, Plewes M, Tan L, Begley H, Agranovich A, Shul D. Proliferating cell nuclear antigen expression in the survival of astrocytoma patients. Can J Neurol Sci, 1994; 21: 306-10.
10. McKeever PE, Strawderman MS, Bakhtiar Y, Mikhail AA, Mila B. MIB-1 proliferation index predicts survival among patients with grade II astrocytoma. J Neuropathol Exp Neurol, 1998; 57: 931-6.
11. Zagzag D, Blanco C, Friedlander DR, Miller DC, Newcomb EW. Expression of p27KIP1 in human gliomas: relationship between tumor grade, proliferation index, and patient survival. Hum Pathol, 2003; 34: 4448-53.

Influence of thalidomide on megakaryocytes in multiple myeloma

Lemancewicz D[1,2], Dzięcioł J[1], Piszcz J[2], Kłoczko J[2], Lebelt A[1], Szkudlarek M[1]

[1]Department of Human Anatomy, [2]Department of Haematology, Medical University of Bialystok, Poland

Abstract

The aim of the study was to assess the influence of thalidomide on megakaryocytes (MK) in patients with multiple myeloma (MM). The study was based on bone marrow trephine biopsies from 12 patients with MM before initiation of thalidomide administration and after three months of its duration. The morphometric examinations were done, using image analysis (DP 12). Quantitative assessment of MK and the analysis of the morphological parameters of MK were performed. MK with features of dysplasia were more frequently observed before the treatment. Additionally, a greater number of the so-called 'naked nuclei' was noticed then. Due to the effect of thalidomide, the mean number of MK increased and so did their area. During the treatment, a more frequent presence of emperipolesis was observed. The observations confirm the fact that thalidomide may cause changes in MK.

Key words: multiple myeloma, thalidomide, trephine biopsy, megakaryocyte.

Introduction

Multiple myeloma (MM) is a malignant neoplasm, characterised by an increase of clonal plasma cells in the bone marrow. In the biology of MM, the process of angiogenesis in bone marrow stroma plays an important role and this phenomenon correlates with the activity and the clinical stage of the disease. About half of the patients exhibit resistance to the first choice treatment. The patients, who initially responded to therapy, showed an increased resistance in the course of the disease [1]. In order to assess the stage of the disease and the effectiveness of the applied treatment, bone marrow trephine biopsy (BMT) is recommended [2]. So far, there have not been any effective methods of MM treatment. During recent years, reports of thalidomide use in the therapy of MM have become available [1, 3]. Thalidomide affects HIM by inhibiting angiogenesis and induces apoptosis of newly generated vessels. It has a specific quality of regulating the secretion of many cytokines [4]. The cytokine-like Vascular Endothelial Growth Factor (VEGF), with other cytokines secreted by HIM cells, can be a stimulator of angiogenesis in the bone marrow [5, 6]. VEGF expression is particularly high in MK in some haematological malignancies [7]. MK of the bone marrow are not only the precursor cells for the platelets but they comprise an essential element of the bone marrow-blood barrier which regulates the release of other cells of the haematopoietic system into blood [8]. The aim of the study was to assess the influence of thalidomide on bone marrow MK in patients with MM.

Material and Methods

The study was based on bone marrow samples, collected from the posterior superior iliac spine of 12 patients (8 women and 4 men, aged from 44 to 73 years) in the 2nd and the 3rd clinical stage of MM, according to the classification of Durie and Salmon. in whom thalidomide was applied. The specimens were obtained by BMT before the treatment and after 3 months of its duration. Bone marrow tissue was carried out in Oxford solution and paraffin embedding. Thin sections of 5 μm were cut by the use of a microtome. Routine techniques staining, such as a hematoxylin and eosin, were applied. Morphometric examinations were done, using an image analysis set (DP12). A quantitative analysis of MK (nuclear megakaryocyte, MK; naked nuclei, NN; anuclear

ADDRESS FOR CORRESPONDENCE:
Dorota Lemancewicz
Department of Human Anatomy
Medical University of Bialystok
Mickiewicza 2A, 15-230 Bialystok
Tel. +48 85 748 56 61, fax +48 85 748 56 64,
e-mail: anatomia@amb.edu.pl

Table 1. Histomorphometric features (means±standard deviations) of megakaryocytes in bone marrow of patients with MM before and after three months of thalidomide treatment.

Patient No	BMT	MK	NN	AMK	N/C	CDMK	CDNMK
		x ± SD	x ± SD	x ± SD	x ± SD	x ± SD	x ± SD
1.	before	*1.08 ± 0.86	0.67 ± 0.58	86.00 ± 21.63	0.43 ± 0.21	0.78 ± 0.08	0.72 ± 0.13
	after	6.00 ± 1.80	1.67 ± 1.53	177.00 ± 32.51	0.33 ± 0.08	0.70 ± 0.10	0.52 ± 0.13
2.	before	4.33 ± 3.21	1.67 ± 1.53	*74.00 ± 19.08	0.50 ± 0.10	0.77 ± 0.08	0.89 ± 0.04
	after	5.98 ± 1.01	1.31 ± 1.14	167.67 ± 41.06	0.40 ± 0.05	0.72 ± 0.10	0.46 ± 0.17
3.	before	1.33 ± 1.15	0.67 ± 0.58	88.00 ± 20.66	* 0.68 ± 0.08	0.84 ± 0.07	*0.79 ± 0.05
	after	4.00 ± 2.00	1.67 ± 0.58	155.00 ± 37.75	0.50 ± 0.10	*0.73 ± 0.10	0.45 ± 0.05
4.	before	*2.67 ± 1.15	2.33 ± 0.58	96.33 ± 18.50	0.80 ± 0.05	0.89 ± 0.04	0.70 ± 0.13
	after	7.00 ± 1.00	1.15 ± 0.76	123.67 ± 32.87	0.86 ± 0.06	0.65 ± 0.05	0.76 ± 0.09
5.	before	*6.33 ± 2.08	1.33 ± 0.58	112.00 ± 20.42	0.62 ± 0.10	0.78 ± 0.08	0.70 ± 0.10
	after	1.15 ± 0.77	0.67 ± 0.58	168.33 ± 53.46	0.62 ± 0.10	0.72 ± 0.10	0.62 ± 0.10
6.	before	*10.67 ± 3.06	0.67 ± 0.58	106.33 ± 29.26	0.68 ± 0.08	0.78 ± 0.08	0.82 ± 0.08
	after	2.33 ± 1.53	1.67 ± 0.58	171.67 ± 40.10	0.53 ± 0.10	0.82 ± 0.04	0.70 ± 0.05
7.	before	3.13 ± 1.06	1.07 ± 0.87	118.67 ± 22.03	0.43 ± 0.08	0.86 ± 0.11	0.80 ± 0.05
	after	4.67 ± 2.08	1.33 ± 0.58	165.00 ± 47.70	0.62 ± 0.10	0.65 ± 0.13	0.67 ± 0.08
8.	before	1.67 ± 0.58	0.67 ± 0.58	*113.00± 5.94	0.62 ± 0.08	0.82 ± 0.09	0.54 ± 0.13
	after	3.67 ±1.53	1.33 ± 0.58	137.33 ± 25.01	0.47 ± 0.07	0.79 ± 0.06	0.82 ± 0.07
9.	before	3.33 ± 1.53	0.67 ± 0.58	119.33 ± 23.80	*0.50 ± 0.05	0.68 ± 0.16	0.81 ± 0.10
	after	3.00 ± 2.65	0.67 ± 0.58	156.67 ± 45.37	0.73 ± 0.08	0.80 ± 0.04	0.74 ± 0.09
10.	before	4.67 ± 3.06	1.33 ± 0.58	151.33 ± 29.37	*0.46 ± 0.08	*0.80 ± 0.03	0.74 ± 0.08
	after	2.15 ± 1.76	0.67 ± 0.58	162.67 ± 53.54	0.65 ± 0.11	0.71 ± 0.03	0.44 ± 0.06
11.	before	2.00 ± 0.87	0.67 ± 0.58	124.00 ± 34.70	0.82 ± 0.08	0.72 ± 0.13	0.73 ± 0.08
	after	4.67 ± 1.53	1.67 ± 0.58	166.0 ± 37.32	0.55 ± 0.07	0.78 ± 0.06	0.53 ± 0.08
12.	before	1.33 ± 1.15	1.00 ± 1.00	121.33 ± 31.07	*0.83 ± 0.08	*0.85 ± 0.09	0.82 ± 0.10
	after	2.67 ± 2.08	1.67 ± 0.58	168.33 ± 48.00	0.54 ± 0.06	0.73 ± 0.08	0.67 ± 0.16

* statistically significant differences
MK- nuclear megakaryocyte, NN- naked nuclei, AMK- area MK. N/C- nuclear/cytoplasmic ratio,
CDMK- circular deviation of cells, CDNMK- circular deviation of nuclei.

cytoplasmic fragments, CF) per square millimetre of bone marrow was done, taking into account the presence of the so-called cluster forms. The analysis of MK morphological features, such as the MK area (AMK), the nuclear/cytoplasmic ratio (N/C), circular deviation of cells (CDMK) and their nuclei (CDNMK), the analysis of emperipolesis incidence were also performed. The identification of MK immature forms was done, using CD61 monoclonal antibodies and the factor VIII. LSAB+HRP and DAB (DAKO) detection kits were used as the chromogen. Statistical analysis of the results was done, using the Statistica PL computer program.

Results

It has been observed that MK, with the features of dysplasia, were present in the majority of the patients, especially in cases of myeloma cell infiltration. MK of a small area were more often found either around or inside the infiltration. Under the influence of thalidomide, a decrease in infiltration was noticed and the mean number of MK increased, their area being enlarged as well. MK were disseminated and could be found around the walls of the cavity vessels. Before the treatment, an increased mean number of NN was assessed, in comparison to the mean number of NN during the treatment. While assessing the mean CDNMK, significant differences were observed before and after the treatment with thalidomide. In the majority of cases, the values were higher before the treatment and MK were rounder. During the treatment, the presence of single cluster forms and the phenomenon of emperipolesis were noticed (Table 1).

Discussion

The process of angiogenesis in the stroma of bone marrow is important in the pathogenesis of MM. This process correlates with myeloma cell proliferation [5]. In the present study, we noted that the presence of plasma cell infiltration affected the morphological changes in MK. The presence of dysplastic megakaryocytes was also confirmed. Dysmegakaryocytosis, which is manifested by the presence of micromegakaryocytes, micromegakaryoblasts, promegakaryoblasts, naked nuclei and promegakaryocytes, may lead to production of functionally impaired platelets [9].

Haemostasis disturbances may result from those changes. The disturbances of MK may strengthen the action of proangiogenic cytokines by release of the factors, stimulating angiogenesis, such as VEGF [6]. These cytokines show an association with the production of myeloma cells. Thus, an increased expression of the proangiogenic factors may take place. Thalidomide is an inhibitor of angiogenesis, although its exact mode of action has not been

well recognised yet [4]. It regulates the secretion of many cytokines and affects HIM. In the present study, quantitative and qualitative changes of MK were observed, due to thalidomide treatment. During the therapy, there was a shift of MK into the localisation around the cavity vessels. MK constitute a vital element of the marrow-blood barrier which, in normal conditions, releases only mature forms of the haematopoietic system into circulation [8]. In case of its impairment, immature cells may occur. The presence of emperipolesis should also be emphasised. It may be suggestive of still existing unfavourable conditions in HIM, which persist during treatment [10]. Differences in the extent of the disturbances to the mean shape of MK nuclei, before and during thalidomide treatment, may be connected to an increased proliferation of MK and the resulting dissociation of the nuclear and cytoplasmic maturation. The observed changes confirm the fact that thalidomide is a multidirectional agent, causing alterations in the marrow MK. The interest in this subject may be important, especially in comparison to recent reports, concerning the biology of the myeloma cell, its interaction with HIM and new possibilities of MM multidirectional treatment.

References

1. Dmoszyńska A. Rola Talidomidu w leczeniu szpiczaka plazmocytowego. Acta Heamatol Pol, 2001; 32, suppl 1: 56-9.

2. De Wolf-Peeters C. Bone marrow trephine interpretation: diagnostic utility and potential pitfalls. Histopathol, 1991; 18: 489-93.

3. Juliusson G, Celsing F, Turesson I, Lenhoff S, Adriansson M, Malm C. Frequent good partial remissions from thalidomide including best response ever in patients with advanced refractory and relapsed myeloma. Br J Haematol, 2000; 109: 88-96.

4. Jurczyszyn A, Wolska-Smoleń T, Skotnicki A. Szpiczak mnogi - rola angiogenezy i zastosowanie talidomidu. Przegl Lek, 2003; 60: 542-7.

5. Palmblad J. Angiogenesis in haematologic malignancies with focus on multiple myeloma. Haema, 2001; 4: 89-98.

6. Tefferi A. Myelofibrosis with myeloid metaplasia. N Engl J Med., 2000; 342: 1255-65.

7. Pruneri G, Bertolini F, Soligo D, Carboni N, Cortelezzi A, Ferrucci PF, Buffa R, Lambertenghi-Deliliers G, Pezzella F. Angiogenesis in myelodysplastic syndromes. Br J Cancer, 1999; 81: 1398-401.

8. Tavassoli M. Modulation of megakaryocyte emperipolesis by phlebotomy: megakaryocytes as a component of marrow-blood barrier. Blood Cells, 1986;12: 205-16.

9. Matolcsy A, Majdic O. Circulating megakaryoblasts in chronic myeloproliferative diseases. Acta Haematol, 1990; 84: 57-63.

10. Lee KP. Emperipolesis of hematopoietic cells within megakaryocytes in bone marrow of the rat. Vet Pathol, 1989; 26: 473-78.

Effects of endothelin-1 or of its receptor A a selective antagonist, on histological and ultrastructural patterns in experimental acute pancreatitis in rats

Andrzejewska A[1], Dlugosz JW[2]

[1]Department of Medical Pathomorphology, [2]Department of Gastroenterology and Internal Medicine,
Medical University of Bialystok, Poland

Abstract

The role of endothelin-1 (ET-1) and of its receptor A (ET_A) blockade in oedematous acute pancreatitis (AP) remains unclear. In 40 male Wistar rats with i.p. cerulein-induced AP, lasting 4 hours, ET-1 2x0.5 nmol/kg and 2x1.0 nmol/kg or selective ET_A antagonist LU 302146, 10 mg/kg and 20 mg/kg was given i.p. simultaneously with cerulein. Histological and ultrastructural studies of pancreatic specimens were done. ET-1 decreased the inflammatory infiltration, but not the mean scores of necrosis and vacuolization in AP. The ultrastructural damage of acinar cells was less evident after ET-1 than in untreated AP. Selective ET_A antagonist slightly aggravated the vacuolization and necrosis of acinar cells and some ultrastructural alterations in AP. In conclusion, ET-1, in contrast to selective ET_A antagonist, exerts some protective effect in the early course of oedematous cerulein-induced acute pancreatitis in rats.

Key words: acute pancreatitis, cerulein, endothelin-1, ETA antagonist, ultrastructure.

Introduction

The role of ET-1 and of its ET_A antagonists in acute pancreatitis remains controversial and not fully elucidated [1, 2]. In some experiments, a selective ET_A antagonist attenuated inflammatory changes in the pancreas with cerulein-induced AP, thus improving the course of the disease [3, 4, 5]. On the contrary, Kogire et al. [6] found that selective ET_A blockade worsened, whereas ET-1 improved histological changes in that model of AP. This problem has important clinical implications for either a possible treatment of AP or prevention of the disease progression from the oedematous stage to more severe, necrotic forms with poor prognosis, by early modification of ET-1 action.

Ultrastructural examination could be a reliable method for elucidation of this problem, however, such studies have not yet been conducted. Therefore, the aim of the present study was to assess and compare the effects ET-1 and of selective ET_A antagonist on ultrastructural and histological alterations in the pancreas in early cerulein-induced AP in rats.

Material and methods

The experiments, approved by the institutional Bioethical Commission, were carried out on 40 male, Wistar rats, 240 - 280 g of body weight (b.w.). AP was induced by two i.p. injections of cerulein (Sigma) at a dose of 40 µg/kg b.w. in 1 hour interval [7]. Group I. Control group (C) without AP (n=6). Group II. Rats with AP untreated (n=10). Group III and IV. Rats with AP treated with ET-1 (Sigma) i.p. 2 x 0.5 or 2 x 1.0 nmol/kg b.w., simultaneously with cerulein (n=6 in each group). Group V and VI. Rats with AP treated with LU 302146 (generously donated by Knoll AG) i.p. 10 or 20 mg/kg b.w. once, with the first i.p. cerulein injection (n=6 in each group). The rats were sacrificed in general anaesthesia by quick decapitation 4 hours after the first injection of cerulein. Pancreas specimens were taken for histological and ultrastructural examinations, performed as in our previous work, including a statistical analysis [8].

Results and discussion

The results of histological scoring of pancreatic changes are presented in Table 1. The ultrastructural patterns of acinar cells in the control group did not show any signs of damage. In

ADDRESS FOR CORRESPONDENCE:
Anna Andrzejewska
Department of Medical Pathomorphology
Medical University of Bialystok,
Waszyngtona 13, 15-269 Białystok, Poland
e-mail: anna.andrzejewska@poczta.fm

Table 1. Histological changes of the pancreas in cerulein acute pancreatitis (AP) in rats*.

No	Group	Oedema	PMN infiltration	Necrosis	Vacuolization
I	Control (n=6)	0-1 (0.12Ä0.03)	0-1 (0.06Ä0.02)	0-0 (0.00Ä0.00)	0-1 0.08Ä0.03
II	AP untreated (n=10)	1-3 (2.04Ä0.07)	0-3 (1.61Ä0.08)	0-2 (0.58Ä0.06)	1-3 (1.88Ä0.08)
III	AP + ET-1 2x0.5 nmol/kg (n=6)	2-3 (2.62Ä0.05)	0-3 (1.47Ä0.09)	0-2 (0.57Ä0.06)	1-3 (1.96Ä0.07)
IV	AP + ET-1 2x1.0 nmol/kg (n=6)	1-3 (2.12Ä0.08)	0-2 (1.04Ä0.05)	0-2 (0.54Ä0.06)	1-3 (1.92Ä0.08)
V	AP + LU 302146 10 mg/kg (n=6)	0-3 (1.96Ä0.09)	0-3 (1.43Ä0.09)	0-2 (0.86Ä0.07)	1-3 (1.91Ä0.09)
VI	AP + LU-302146 20 mg/kg (n=6)	0-3 (2.14Ä0.07)	0-3 (1.41Ä0.07)	0-2 (0.82Ä0.06)	1-3 (2.19Ä0.07)

*Values are expressed as the ranges of scores and means ± SEM.
Statistical significance of important differences:
Oedema: I / II, III, IV, V, VI $p < 0.001$; II / III $p < 0.001$; III / IV $p < 0.001$.
PMN infiltration: I / II, III, IV, V, VI $p < 0.001$; II / IV $p < 0.001$; II/VI $p < 0.05$.
Necrosis: I / II, III, IV, V, VI $p < 0.001$, II / V, VI $p < 0.01$.
Vacuolization: I / II, III, IV, V, VI $p < 0.001$, II / VI $p < 0.01$.

Figure 1. Part of acinar cell with dilated channels of RER and mitochondria with destruction of their cristae (arrow). Group II - AP untreated group. Original magnification x 3000.

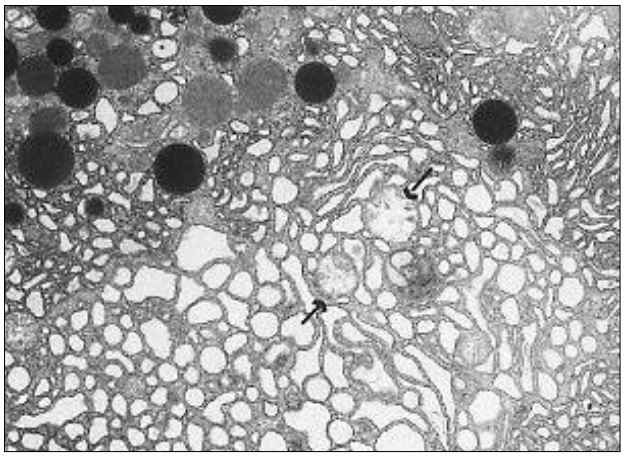

Figure 2. Vesicular transformation and circular arrangement of endoplasmic reticulum. Group III - AP, treated with the lower dose of ET-1. Original magnification x 7000.

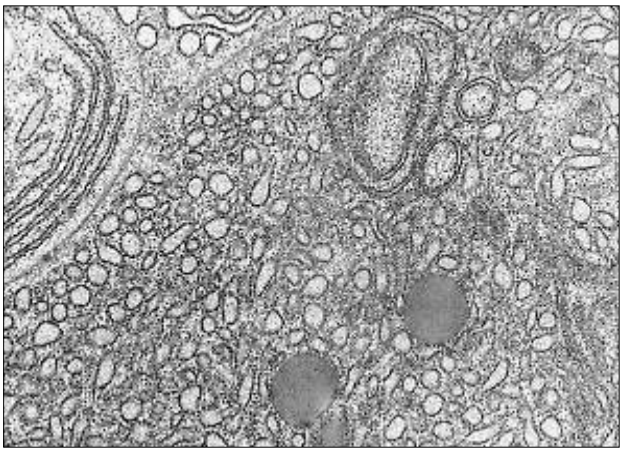

Figure 3. Nearly normal appearance of pancreatic acinar cells. Group. IV - AP, treated with the higher dose of ET-1. Original magnification x 3000.

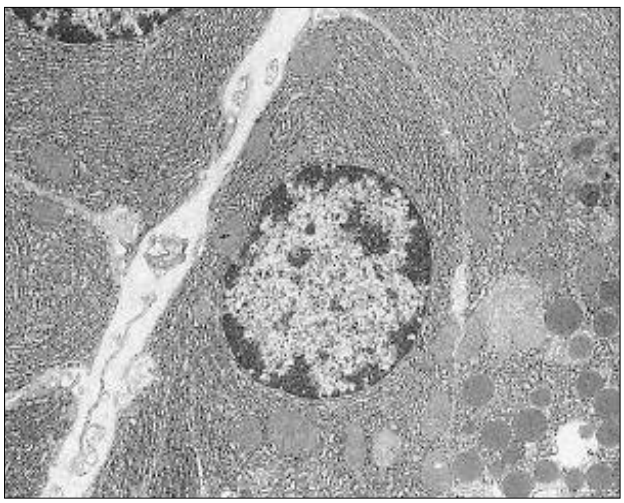

Figure 4. Numerous vacuoles in the cytoplasm of pancreatic acinar cell. Zymogen granules in one of them are seen (›). Group VI - AP, treated with the higher dose of ET_A antagonist. Original magnification x 3000.

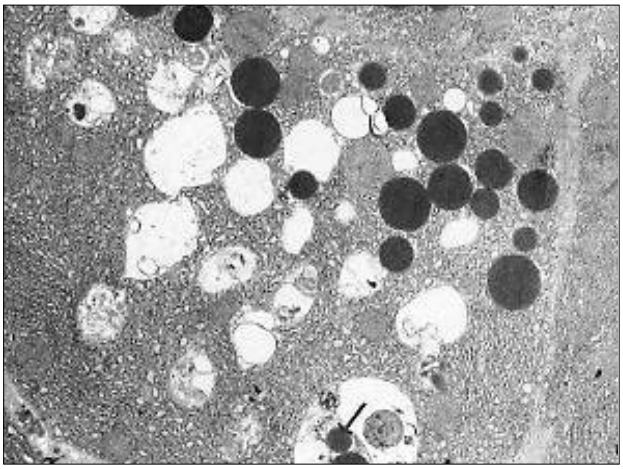

untreated AP, the majority of acinar cells contained quite numerous vacuoles. Zymogen granules were less numerous than those in the control group. The cisternae of Golgi apparatus were sometimes dilated. Channels of rough endoplasmic reticulum (RER) were usually dilated (Fig. 1) and disorganized. A necrosis of acinar cells was only sporadically observed. In the group, treated with a lower dose of ET-1, zymogen granules were scarce. The cytoplasm contained numerous phagosomes, autophagous vacuoles and vacuoles with amorphic content. Channels of RER were usually dilated and showed vesicular transformation or concentric arrangement (Fig. 2). Some of the mitochondria showed features of swelling. Necrosis of acinar cells was sporadic. In the group, treated with a higher dose of ET-1, those lesions were slightly less pronounced: phagosomes and vacuoles were less numerous, RER channels were dense and regularly arranged and mitochondria were normal (Fig. 3). The ultrastructural changes after the treatment with lower dose of selective ET_A antagonist resembled those, observed in the animals with untreated AP. However, after the treatment with higher dose, those lesions were more expressed. Many acinar cells showed features of total disintegration. The cytoplasm contained numerous autophagous vacuoles (Fig. 4). Zymogen granules had varied electron density; sometimes, they were found in autophagous vacuoles or were loosely spread in the interstitial space. The changes in RER, Golgi apparatus and mitochondria were similar to those, noted in the untreated group.

Summarizing our study, ET-1 exerted a distinct protective effect on histological changes in the pancreas, as evidenced by the decrease of inflammatory cells infiltration, more evident after the higher dose of this agent, despite of the slight increase of edema score after the lower dose of ET-1. On the contrary, a slight aggravating effect on the scores of necrosis and vacuolization could be observed after both doses of selective ETA antagonist. The ultrastructural examination supported less advanced alterations of pancreatic acinar cells in AP treated with ET-1, especially after the higher dose of this agent. It was manifested by a decreased number of phagosomes and autophagous vacuoles, as signs of focal degradation of the cytoplasm. The channels of RER were more regular and rarely dilated and the mitochondria were better preserved. Those findings indicate that ET-1 administration can partially ameliorate the course of early acute oedematous pancreatitis. The treatment with ET_A antagonist increased slightly the vacuolization of acinar cells but did not significantly affect the oedema. The score of necrosis was slightly increased after both ETA antagonist doses. The ultrastructural changes, such as: a decreased number of zymogen granules, disorganization of RER, autophagosomes and cytoplasmic vacuoles were also more prominent than those in the rats with untreated AP. Those observations did not support the assumption on the beneficial effect of ET_A blockade in cerulein-induced AP, while even suggesting some undesirable effects in the early course of oedematous AP, taking into account the investigated doses and the time of application. Generally, our results support and extent the observations of Kogire et al. [6] and Martignoni et al. [1].

In conclusion, our results indicate evident beneficial effects of ET-1 on histological and ultrastructural changes of the pancreas in the early course of cerulein-induced AP. On the other hand, treatment with selective ET_A antagonist in the investigated dosage exerted no alleviating influence on those changes, while the ultrastructural examination was even suggestive of its undesirable effects in early oedematous AP. Therefore, either in the prevention of oedematous pancreatitis (i.e., post-ERCP acute pancreatitis) or in the treatment of the early course of AP, ET-1, rather than its ET_A antagonists, is to be taken into consideration.

References

1. Martignoni ME, Ceyhan GO, Ayuni E, Kondo Y, Zimmermann A, Büchler MW, Friess H. Endothelin receptor antagonists are not beneficial in the therapy of acute experimental pancreatitis. Langenbeck's Arch Surg, 2004; 389: 184-92.

2. Dlugosz JW, Nowak K, Laszewicz W, Andrzejewska A, Wroblewski E. The effect of endothelin-1 receptor antagonists in acute pancreatitis in the rats. Exp Toxic Pathol, 2003; 55:137-45.

3. Eibl G, Hotz HG, Faulhaber J, Kirchengast M, Buhr HJ, Foitzik T. Effect of endothelin and endothelin receptor blockade on capillary permeability in experimental pancreatitis. Gut, 2000; 46: 390-4.

4. Foitzik T, Faulhaber J, Hotz HG, Kirchengast M, Buhr HJ. Endothelin mediates local and systemic disease sequelae in severe experimental pancreatitis. Pancreas, 2001; 22: 248-54.

5. Liu X, Nakano I, Ito T, Kimura T, Nawata H. Is endothelin-1 an aggravating factor in the development of acute pancreatitis? Chin Med J, 1999; 112: 603-7.

6. Kogire M, Inoue K, Higashide S-I, Takaori K, Echigo J, Gu Y-J, Sumi S, Uchida K, Imamura M. Protective effects of endothelin-1 on acute pancreatitis in rats. Dig Dis Sci, 1995; 40: 1207-12.

7. Yamaguchi H, Kimura T, Mimura K, Nawata H. Activation of proteases in cerulein-induced pancreatitis. Pancreas, 1989; 4: 565-71.

8. Andrzejewska A, Dlugosz JW. The endothelin-1 receptor antagonists ameliorate histology and ultrastructural alterations in the pancreas and decrease trypsinogen activation in severe taurocholate pancreatitis in rats. Int J Exp Path, 2003; 84: 221-9.

Amidolytic activity of plasma euglobulins

Jasielczuk J[1], Dąbrowka M[2], Gacko M[3], Jankiewicz M[1]

[1]Department of Instrumental Analysis, [2]Department of Hematological Diagnostics,
[3]Clinic of Vascular Surgery and Transplantation, Medical University of Bialystok, Poland

Abstract

Amidolytic activity of plasmin, produced in euglobulin fraction, does not correlate with the time of euglobulin fibrinolysis. It does not depend on fibrinogen concentration.

Key words: Euglobulin fibrinolysis time, fibrinogen concentration, plasmin amidolytic activity.

Introduction

Blood fibrinolytic activity is evaluated by the time of lysis of fibrin clot produced in the plasma euglobulin fraction [1, 2]. The time depends on two variables: different fibrinolytic activity and different fibrinogen concentration. It hinders a diagnostic interpretation of plasma euglobulin fibrinolysis time measurements.

Material and methods

The blood was taken from 74 patients and citrate plasma was obtained. Fibrinogen concentrations [3], fibrinolysis time [4], and amidolytic activity of the euglobulin fraction [5] were assessed. In order to determine amidolytic activity, 0.5ml 3 mmol/l of H-D-Val-Leu-Lys-pNA was added to 0.5ml of euglobulins dissolved in 0.5ml of borate buffer, containing 0.01mol/l of sodium citrate, and incubated for 30 min in 37^{0}C. The reaction was interrupted by adding 0.1ml of 50% acetic acid. The absorbance was measured in a cuvette with a 0.5 cm thick layer at 405 nm, as referred to the controls, in which acetic acid was added before the substrate was introduced. The results were read from a calibrated diagram, made with the use of model solutions of p-nitroaniline (pNa).

ADDRESS FOR CORRESPONDENCE:
Joanna Jasielczuk
Department of Instrumental Analysis
Medical University of Białystok
Mickiewicza 2 c, 15-089 Białystok, Poland
e-mail: analist @amb.edu.pl

Results

The time of euglobulin fibrinolysis was lengthened, together with an increase in fibrinogen concentrations (Table 1). However, there were no relationships observed between plasmin amidolytic activity and both the time of euglobulin fibrinolysis and fibrinogen concentrations.

Discussion

The results confirm the dependence of euglobulin fibrinolysis time on fibrinogen concentration [4, 6]. It debases the diagnostic value of euglobulin fibrinolysis time determination as a test, estimating plasma fibrinolytic activity. A reliable way of evaluation of plasmin activity, which is produced in plasma euglobulin fraction, is the measurement of its amidolytic activity. The activity depends on plasminogen activator tissue concentration, its inhibitor, and plasminogen [7, 8]. The measurement of amidolytic activity is thus an actual insight into the present status of plasma fibrinolytic activity. An additional advantage of amidolytic test is short determination time and measurement objectivism.

References

1. Chakrabarti R, Bielawiec M, Evans J F, Fearnley G R. Methological study and recomended technique for determining the euglobulin lysis time. J Clin Pathol, 1968; 21: 698-701.
2. Kowarzyk H, Buluk K. Advances in blood coagula-

Table 1. Fibrinogen concentration, euglobulin lysis time and amidolytic activity of plasma euglobulin.

Fibrinogen concentration, mg/dl	**Euglobulin lysis time, min**	**Amidolytic activity, pNA, nmol/ml**
195 ± 10,8 (n=22)	169 ± 17,9	47,1 ± 5,3
252 ± 34,0 (n=22)	286 ± 37,0	55,3 ± 4,1
364 ± 28,4 (n=18)	437 ± 54,6	41,3 ± 2,6
793 ± 82,9 (n=12)	936 ±128,0	50,2 ± 3,7

tion. Post Hig Med Dośw, 1950; 2: 1-13.

3. Quick A J. The physiology and pathology of haemostasis. Kimpton London, 1951; 156.

4. Kowalski E, Kopeć M, Niewiarowski S. An evaluation of the euglobulin method for the determination of fibrinolysis. J Clin Pathol, 1959; 12: 215-8.

5. Friberg P. Methods for the determination of plasmin, antiplasmin and plasminogen by mens of the substrate S-2251. Haemostasis, 1975; 7: 138-45.

6. Borawski J, Myśliwiec M. Plasma fibrinogen level is an important determinant of prolonged euglobulin clot lysis time in hemodialysis patints. Clin Appl Thrombos Hemostas, 2001; 7: 296-9.

7. Smith A A, Jacobson L J, Miller B I, Hathaway W E, Manco-Johnson M J. A new euglobulin clot lysis assay for global fibrynolysis. Thrombos Res, 2003; 112: 329-37.

8. Urano T, Nishikawa T, Nagai N, Takada Y, Takada A. Amounts of tPA and PAI-1 in the euglobulin fraction obtained at different pH: their relation to the euglobulin clot lysis time. Thrombos Res, 1997; 88: 75-80.

Changes in proteasome activity in the ischemic kidney of rat with experimental renovascular hypertension

Kruszewski K[1], Kalinowska J[1], Chabielska E[2], Kasacka I[3], Ostrowska H[1]

[1]Department of Biology, [2]Department of Biopharmacy, [3]Department of Histology and Embryology,
Medical University of Bialystok, Poland

Abstract

A long-lasting renal ischemia, followed by the left renal artery clipping (two-kidney, one clip Goldblatt model in rats) led to a marked decrease in proteasome chymotrypsin-like activity in the ischemic kidney. This activity was, however, significantly raised upon the stimulation with an artificial 20S proteasome activator SDS (0.025%). No changes were observed in either the levels of the constitutive 20S proteasome subunit (α5) or of its protein activator, PA28α, in the kidneys by Western blot. These preliminary results indicate that an inhibition of proteasome activity may result from a dissociation of the active proteasome complexes into the inactive 20S proteasome and its endogenous activators after a long-lasting renal ischemia.

Key words: proteasome, renal ischemia, rat.

Introduction

The proteasome-dependent proteolytic pathway is responsible for the degradation of damaged proteins, and many short-life regulatory proteins, involved in inflammatory processes, cell cycle regulation and gene expression [1, 2, 3]. In the living cell, proteasomes are present in a latent form (20S proteasome, 700kDa) and in active complexes with the protein regulators: PA28 and PA700 [4, 5]. PA700 enhances the ability of 20S proteasome to degrade the ubiquitinated proteins in an ATP-dependent manner, whereas PA28 regulator, in association with 20S proteasome, stimulates its capacity to the generation of antigen peptides, presented to the immune system on MHC class I molecules [1].

Alterations in proteasome activity have been demonstrated in a large number of pathological conditions, including cancer, neurodegenerative disorders, acute wasting conditions, ischemia-reperfusion injury and ischemic acute renal failure [3, 6, 7, 8]. In the present study, we investigated, whether a long-lasting renal ischemia, followed by the left renal artery clipping (two-kidney, one clip Godblatt model in rats), could influence the proteasome activity in the kidneys.

Material and methods

All the experimental procedures, involving animals and their care, were conducted in conformity with the national and international laws and with the Guidelines for the Use of Animals in Biochemical Research. Male Wistar rats (n=5), weighing 160 - 180 g each, were anesthetized with pentobarbital (40 mg/kg, i.p.). Two-kidney one clip (2K-1C) renovascular hypertension was induced by a partial, standardized clipping of the left renal artery (0.2-mm internal diameter) for 6 weeks [9]. Rat kidneys (unclipped and clipped) were placed in 50mmol/L Tris-HCl buffer at pH 8.0, containing a protease inhibitor cocktail, and were homogenized in ice with a Potter-Elvehjem homogenizer. The homogenates were then centrifuged for 60 minutes at 15000 x g +4^{0}C. The protein concentration of the supernatants was determined by the method of Bradford [10], using the Bio-Rad assay reagent with bovine serum albumin as a standard. The proteasome activity in kidney extracts (20µg of protein) was measured, using fluorogenic peptide Suc-Leu-Leu-Val-Tyr-AMC (100µmol/L) (Affinity, UK) in a 50mmol/L Tris-HCl buffer (pH 7.5), containing 5mmol/L EDTA, 1.0 mmol/L ATP and 15% glycerol, in either the absence or the presence of 20S proteasome activator 0.025% SDS [11]. For Western blot analysis, aliquots of the homogenates (20µg of protein per line) were

ADDRESS FOR CORRESPONDENCE:
Halina Ostrowska
Department of Biology
Medical University of Białystok,
ul. Kilinskiego 1, 15-089 Bialystok, Poland
Tel.: (+48) 85 74-85-460; Fax.: (+48) 85 74-85-461,
e-mail: halost@amb.edu.pl

Figure 1. Effects of left renal artery clipping on the chymotrypsin-like activity of proteasome in either the absence or the presence of SDS in clipped and unclipped rat kidneys.

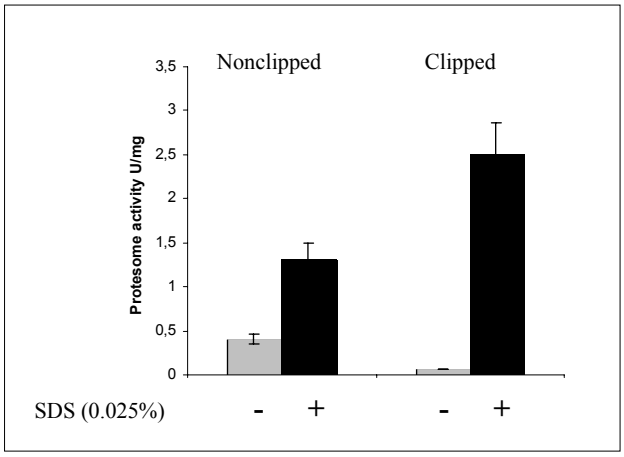

Figure 2. Effects of left artery clipping on the levels of constitutive proteasome subunit α5 and proteasome activator PA28α in clipped and unclipped rat kidneys.

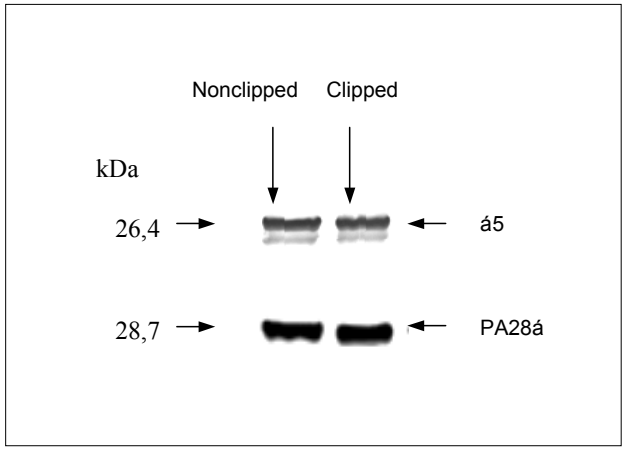

electrophoresed by SDS-PAGE on 10% gels under reducing conditions, according to Laemmli [12], and then the proteins were electroblotted onto nitrocellulose. The nitrocelluloses were incubated with anti-α5 (20S proteasome) and anti-PA28α antibodies (Affinity, UK). The proteasome subunits were identified, using the alkaline phosphate-conjugated anti-rabbit IgG as secondary antibody and visualized, using phosphatase substrate (Sigma, USA). The results are given as means ±SE of three independent measurements. Any value of $P<0.05$ was considered significant.

Results

The left renal artery clipping, lasting six weeks, led to a significant reduction in the clipped kidney mass (0,16g ±0,07), and statistically significant increases in the contralateral kidney mass, compared to respective values in the controls (1,35g ±0,13).

Proteasome activity, measured by the use of Suc-Leu-Leu-Val-Tyr-AMC substrate, clearly decreased in the clipped kidney, compared to that in the unclipped organ (*Fig. 1*). After the addition of 0.025% SDS, which is non-physiological activator of the latent 20S proteasome, that activity was significantly raised in the ischemic kidney (about 18 times).

No changes in the levels of the constitutive 20S proteasome subunit α5 were detected by Western blot in either the clipped or the non-clipped kidneys (*Fig. 2*). Likewise, the proteasome activator PA28α subunit was expressed at equally high levels in both kidneys.

Discussion

In the present study, we demonstrated that a long-lasting renal ischemia, followed by the left renal artery clipping, lead to a significant inhibition of proteasome activity in the ischemic kidney. As demonstrated by the Western blot analysis, the inhibition of the activity was not, however, accompanied by any reduction in 20S proteasome and its protein activator PA28 levels. Therefore, these data, together with the fact, that proteasome activity was significantly raised upon the addition of 0.025% SDS, a potent artificial activator of the latent 20S proteasome, indicate that the loss in proteasomal activity in the ischemic kidney could be due to irreversible dissociation of the active proteasome complexes into an inactive free 20S proteasome and its protein activators.

Ischemia leads to complex cellular events, which can affect proteasome function, including depletion of ATP and disturbances of intracellular calcium haemostasis. Several *in vitro* studies have demonstrated that ATP depletion causes an almost complete dissociation of active PA700-20S-PA700 and PA700-20S-PA28 complexes [4, 5, 13]. It has also been demonstrated that the binding of calcium ions to proteasome regulator PA28 inhibits the peptidase activity of PA28-20S proteasome complexes [14]. Therefore, it is likely that suppression of proteasome activity in the ischemic kidney may result from disturbances in the formation of active proteasome complexes, due to the depletion of ATP and/or increase in intracellular calcium levels during a long-lasting renal ischemia.

Acknowlegments

This work was supported by grants from the State Committee for Scientific Research (KBN) Nos 6PO5A03320 and 4-25747

References

1. Coux O, Tanaka K, Goldberg AL. Structure and functions of the 20S and 26 proteasomes. Annu Rev Biochem, 1996; 65: 801-47.

2. Adams J. The proteasome: structure, function and role in the cell. Cancer Treatment Reviews, 2003; 29: 3-9.

3. Gaczynska M, Osmulski PA, Ward WF. Caretaker or undertaker? The role of the proteasome in aging. Mech Ageing Dev, 2001; 122: 235-54.

4. DeMartino GM, Slaughter CA. The proteasome, a novel protease regulated by multiple mechanisms. J Biol Chem, 1999; 274: 22123-6.

5. Cascio P, Call M, Petre BM, Walz T, Goldberg AL. Properties of the hybrid form of the 26S proteasome containing both 19S and PA28 complexes. EMBO J, 2002; 21: 2636-45.

6. Ciechanover A. The ubiquitin-proteasome pathway: on protein death and cell life. EMBO J, 1998; 17: 7151-60.

7. Kukan M. Emerging roles of proteasomes in ischemia-reperfusion injury of organs. J Physiol Pharmacol, 2004; 55: 3-15.

8. Adams J. Proteasome inhibition: a novel approach to cancer therapy. Trends Mol Med, 2002; 8: 49-54.

9. Sigmon DH, Beierwaltes WH. Endothelium-derived constricting factor in renovascular hypertension. Hypertension, 1995; 25: 803-8.

10. Bradford MM. A rapid and sensitive method for the quantitation of microgram quantities of protein utilizing the principle of protein-dye binding. Anal Biochem, 1976; 72: 248-54.

11. Lightcap ES, McCormack TA, Pien CS, Chau V, Adams J, Elliott PJ. Proteasome inhibition measurements: clinical application. Clin Chem, 2000; 46: 673-83

12. Laemmli UK. Cleavage of structural proteins during the assembly of the head of bacteriophage T4. Nature, 1970; 227: 680-5.

13. Tanahashi N, Murakami Y, Minami Y, Shimbara N, Hendil KB, Tanaka K. Hybrid proteasomes. Induction by interferone-gamma and contribution to ATP-dependent proteolysis. J Biol Chem, 2000; 275: 14336-45.

14. Realini C, Rechsteiner M. A proteasome activator subunit binds calcium. J Biol Chem, 1995; 270: 29664-67.

Index of Authors

Annales Academiae Medicae Bialostocensis

http://www.roczniki-amb.com

Guest Editors: **L. Chyczewski (Bialystok, Poland)**
I. Kasacka (Bialystok, Poland)
W. Niklińska (Bialystok, Poland)
W. Pankiewicz (Bialystok, Poland)
E. Pluygers (Brassels, Belgium)

ISSN 0067-6489